Progress in the Chemistry of Organic Natural Products

A. Douglas Kinghorn
Heinz Falk
Simon Gibbons
Jun'ichi Kobayashi *Editors*

106

# Progress in the Chemistry of Organic Natural Products

Springer

# Progress in the Chemistry of Organic Natural Products

More information about this series at http://www.springer.com/series/10169

A. Douglas Kinghorn • Heinz Falk •
Simon Gibbons • Jun'ichi Kobayashi
Editors

# Progress in the Chemistry of Organic Natural Products

Volume 106

With contributions by

H.-P. Chen · J.-K. Liu

B. Amin · W. Voelter

L. Nahar · S.D. Sarker

Springer

*Editors*
A. Douglas Kinghorn
Division of Medicinal Chemistry & Pharmacognosy, College of Pharmacy
The Ohio State University
Columbus, Ohio
USA

Heinz Falk
Institute of Organic Chemistry
Johannes Kepler University Linz
Linz, Austria

Simon Gibbons
Research Department of Pharmaceutical and Biological Chemistry
UCL School of Pharmacy
London, United Kingdom

Jun'ichi Kobayashi
Graduate School of Pharmaceutical Science
Hokkaido University
Sapporo, Japan

ISSN 2191-7043 ISSN 2192-4309 (electronic)
Progress in the Chemistry of Organic Natural Products
ISBN 978-3-319-59541-2 ISBN 978-3-319-59542-9 (eBook)
DOI 10.1007/978-3-319-59542-9

Library of Congress Control Number: 2017948229



Printed on acid-free paper

This Springer imprint is published by Springer Nature
The registered company is Springer International Publishing AG
The registered company address is: Gewerbestrasse 11, 6330 Cham, Switzerland

# Contents

# Secondary Metabolites from Higher Fungi

**He-Ping Chen and Ji-Kai Liu**

## Contents



H.-P. Chen
State Key Laboratory of Phytochemistry and Plant Resources in West China, Kunming Institute of Botany, Chinese Academy of Sciences, Kunming 650201, People's Republic of China

J.-K. Liu (✉)
School of Pharmaceutical Sciences, South-Central University for Nationalities, No. 182 Minzu Road, Wuhan 430074, People's Republic of China
e-mail: liujikai@mail.scuec.edu.cn



A.D. Kinghorn, H. Falk, S. Gibbons, J. Kobayashi (eds.), *Progress in the Chemistry of Organic Natural Products, Vol. 106*, DOI 10.1007/978-3-319-59542-9_1

# 1 Introduction

Fungi are extremely abundant and globally diverse. They are the second largest group of organisms in the world only after insects. Recent estimates of the number of fungi on Earth are approximately 1.5 million. The total number of described fungi of all kinds is currently 100,000 species. The number of higher fungi (mushrooms) species on Earth is currently estimated at 150,000, yet perhaps only 10% (approximately 15,000 are named species) are known to science [1–4]. Higher fungi are currently being evaluated for their nutritional value and acceptability as well as for their pharmacological properties. They make up a vast and yet largely untapped source of potentially potent new pharmaceutical products [4]. In this contribution, a general overview of pigments, nitrogen-containing compounds, and terpenoids from higher fungi will be provided. Toxins are included in each section as they are encountered. Secondary metabolite structures and their biological activities, chemical synthesis, and biosynthesis will be discussed.

# 2 Pigments of Higher Fungi

## *2.1 Introduction*

This section, like previous reviews [5–10], surveys the chemical, biological, and mycological literature dealing with the isolation, structure elucidation, biological activities, and synthesis of pigments biosynthesized by those fungi that produce conspicuous fruiting bodies (macromycetes) or by fungi grown in mycelial cultures. Additionally, several colorless metabolites are included where they are significant or related to the pigments. However, unlike previous reviews, the pigments from slime molds (myxomycetes) are not included in this chapter. This chapter covers the literature from 2010 to 2016, and compounds are classified according to their perceived route of biosynthesis.

## *2.2 Pigments from the Shikimate-Chorismate Pathway*

### 2.2.1 Pigments Derived from Arylpyruvic Acids

Terphenylquinones

Terphenyls are a group of pigments consisting of a chain of three benzene rings. Almost all reported natural terphenyls are of the *p*-terphenyl type and have been found mainly in actinomycetes, lichens, and fungi. The structure elucidation, biological activities, transformation, and total synthesis as well as biosynthesis of

terphenyl derivatives from natural sources since 1877 have been reviewed in detail [11]. Mushroom-derived *p*-terphenyls were found in the genera *Sarcodon*, *Hydnellum*, *Boletopsis*, *Thelephora*, *Polyozellus*, and *Hypoxylon* (Table 1). Structurally, natural *p*-terphenyls are characterized by having various oxygenated substituents, such as hydroxy, methoxy, or acyloxy groups, and exhibit deceptively simple $^{1}$H NMR spectra, but complex $^{13}$C NMR spectra, with many olefinic quaternary carbons, which has made it difficult to determine the substitution positions of certain *p*-terphenyls.

**Table 1** Natural terphenyls discovered in recent years

| Compound[a] | | Origin | Biological activity | Refs. |
|---|---|---|---|---|
| Phellodonin (**1**) | | *Phellodon niger* | | [12] |
| Sarcoviolin β (**2**) | | *Sarcodon leucopus* | Antioxidative; α-glucosidase inhibition | [13] |
| Episarcoviolin β (**3**) | | *Sarcodon leucopus* | Antioxidative; α-glucosidase inhibition | [13] |
| 2′,3′,5′,6′-Tetracetoxy-4, 4″-dihydroxy-*p*-terphenyl | | *Sarcodon leucopus* | | [13] |
| Sarcoviolin ε (**29**) | | *Sarcodon scabrosus* | | [14] |
| Concrescenins A (**4**), B (**5**) | | *Hydnellum concrescens* | α-Glucosidase inhibition | [15] |
| Boletopsins A–C (**6**–**8**) | | *Boletopsis leucomelas* | KDR kinase inhibitor | [16] |
| Boletopsin 11 (**9**), 12 (**10**) | | *Boletopsis* sp. | | [17] |
| Boletopsin 13 (**11**), 14 (**12**) | | *Boletopsis* sp. | | [18] |
| Thelephantin O (**13**) | | *Thelephora aurantiotincta* | Antitumor (selective) | [19] |
| Vialinin A (**14**) | | *Thelephora aurantiotincta* | Antitumor (selective) | [19] |
| Vialinin C (**15**) | | *Thelephora vialis* | TNF-α production | [20] |
| Vialisyl A (**16**) | | *Thelephora vialis* | | [21] |
| Polyozellic acid (**17**) | | *Polyozellus multiplex* | Antiangiogenesis | [22] |
| Thelephoric acid (**18**) | | *Polyozellus multiplex* | Antiangiogenesis | [22] |
| Rickenyl A (**19**) | | *Hypoxylon rickii* | | [23] |
| Rickenyl B (**20**) | | *Hypoxylon rickii* | | [23] |
| Rickenyls C–E (**21**–**23**) | | *Hypoxylon rickii* | | [23] |

[a]Color of compound in adjoining column

The edible mushroom *Phellodon niger* has been investigated chemically infrequently. During a search for novel and secondary metabolites of mushrooms from Yunnan Province of the People's Republic of China, a nitrogenous *p*-terphenyl was reported by Fang et al. from *P. niger*, namely, phellodonin (**1**), along with sarcoviolin β (**2**) (Fig. 1) [12]. The EtOAc extract of the Tibetan wild mushroom *Sarcodon leucopus* showed a strong antioxidant activity. Bioactivity-guided fractionation of this extract resulted in the isolation of two red-colored sarcoviolin pigments, sarcoviolin β (**2**) and episarcoviolin β (**3**), and a green *p*-terphenyl pigment, 2′,3′,5′,6′-tetracetoxy-4,4″-dihydroxy-*p*-terphenyl, along with seven known *p*-terphenyls (Fig. 1). Episarcoviolin β is the N-1$\beta$ epimeric isomer of sarcoviolin β. All of the isolated compounds not only showed antioxidant effects in the DPPH radical-scavenging assay, but also mediated total antioxidant capacity, reducing power, and lipid peroxidation, and moreover displayed pronounced $\alpha$-glucosidase inhibitory activity. Among these compounds, sarcoviolin β exhibited the most pronounced $\alpha$-glucosidase inhibitory activity, with an $IC_{50}$ value of 0.58 μ$M$ [13]. Also, concrescenins A (**4**) and B (**5**) isolated from the consumed edible mushroom *Hydnellum concrescens* also exhibited potent inhibition of $\alpha$-glucosidase with $IC_{50}$ values of 0.99 and 3.11 μ$M$, respectively, in a non-competitive fashion (Fig. 1) [15]. It was established that the sarcodonins have a benzodioxazine core structure by X-ray crystallography [16].

Boletopsins A–C (**6**–**8**), along with the known compounds Bl-IV, Bl-V, cycloleucomelone, and cycloleucomelone-2-acetate, were isolated from an EtOAc-soluble fraction of the fruiting bodies of the mushroom *B. leucomelas* (Fig. 1). These compounds were evaluated with respect to their antiangiogenic acitivity by measuring their inhibitory effects on KDR kinase and proliferation of human umbilical vein endothelial cells (HUVECs). The results suggested that boletopsin C showed inhibitory acitivity against KDR kinase and proliferation of human umbilical vein endothelial cells with $IC_{50}$ values of 70.7 and 9.04 μ$M$ [14].

The mushroom *Boletopsis* sp. has been used traditionally by the Kiovi people in Papua New Guinea as a therapeutic agent for gastrointestinal complaints. Barrow et al. reported four *p*-terphenyl pigments, boletopsins 11–14 (**9**–**12**), from this fungus, and suggested a naming system for this type of compound based on chronological publication time (Fig. 1) [17, 18]. Boletopsins 11 (**9**) and 12 (**10**) showed moderate antibiotic activity against *Staphylococcus epidermidis* and *Pseudomonas aeruginosa*, while boletopsins 13 and 14 are two tri-/tetra-brominated *p*-terphenyls, which represent the first report of polybrominated fungal metabolites produced by a terrestrial macrofungus. The small sample quantities available were the main impediment in establishing unambiguously the structures of these molecules possessing bromine. Eventually, the structures of boletopsins 13 (**11**) and 14 (**12**) were established by synthesis unequivocally.

The genus *Thelephora* has proven to be a rich source of *p*-terphenyl pigments. In the course of screening food material for anticancer activity, the ethanol extract of *Thelephora aurantiotincta* was shown to decrease the viability of human

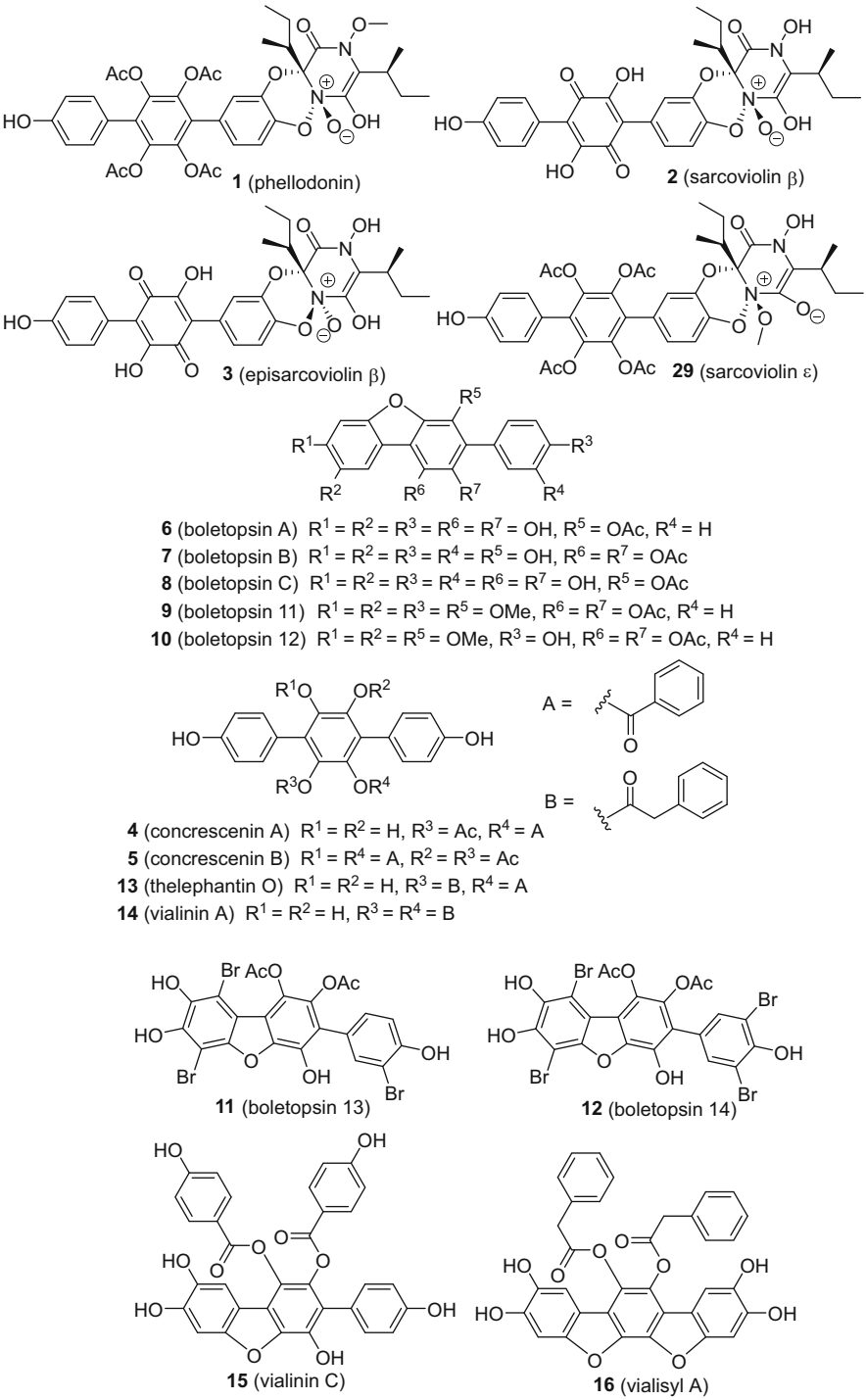


**Fig. 1** Structures of terphenyl derivatives

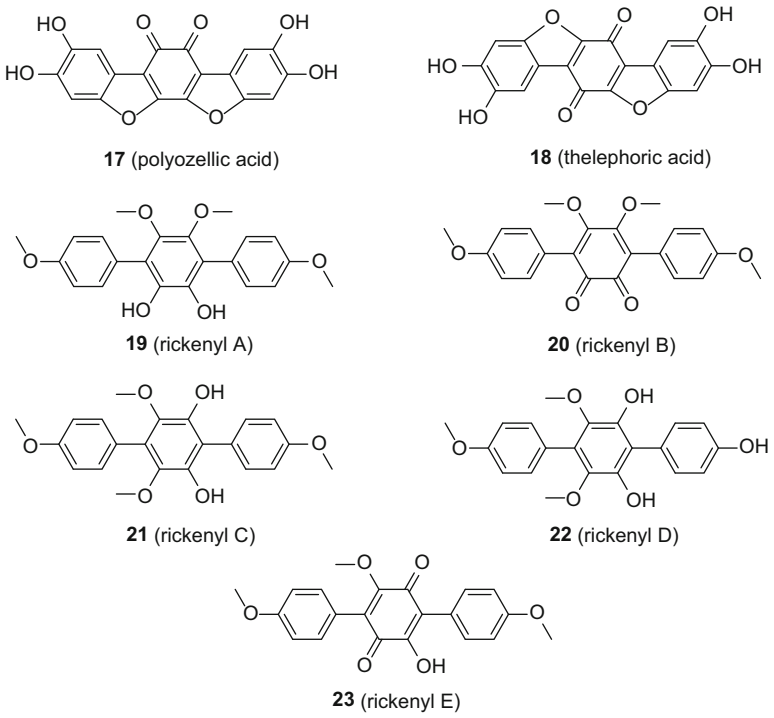


**Fig. 1** (continued)

hepatocellular carcinoma cells (HepG2). Further separation of this extract yielded thelephantin O (**13**) and the known compound vialinin A (**14**) (Fig. 1). These two compounds were tested for inhibitory activity against the cell viability of HepG2 and Caco2 cells, and non-cancerous human hepatocytes. The results demonstrated that both thelephantin O and vialinin A showed potent inhibitory activity against HepG2 and Caco2 in a dose-dependent manner but, notably, showed no cytotoxicity on non-cancerous human hepatocytes [19]. Vialinin C (**15**) was isolated from the fruiting bodies of *Thelephora vialis* and was successfully synthesized, adding to the list of dibenzofuran *p*-terphenyl derivatives with two *p*-hydroxybenzoyl substitutions (Fig. 1). Vialinin C showed an $IC_{50}$ value of 0.89 $\mu M$ when tested for inhibitory activity against TNF-$\alpha$ production [20]. The green pigment vialisyl A (**16**) was isolated from the same mushroom (*T. vialis*) and the structure was determined by 2D NMR spectroscopy, including a 2D-INADEQUATE experiment because an HMBC experiment was unsuitable for the unambiguous establishment of the structures due to the many contiguous quaternary carbons present (Fig. 1) [21].

The Japanese mushroom *Polyozellus multiplex* is an edible fungus with black-purple fruiting bodies. Polyozellic acid (**17**), a black powder with a symmetrical structure, was isolated from the fruiting bodies of *Polyzellus multiplex*, accompanied by the known compound thelephoric acid (**18**) (Fig. 1). The structure of **17** was established by NMR spectroscopic analysis and chemical modification. Biological evaluation of their effects on angiogenesis revealed that both **17** and **18** suppressed the formation of the tubule formation of HUVECs. Moreover, both strongly inhibited HUVECs in an invasion assay at a concentration of 2.5 μ*M* [22].

Not only are diverse *p*-terphenyls reported to have a basidiomycetous origin, but they are also represented in the ascomycete *Hypoxylon rickii*. Rickenyls A–E (**19**–**23**) are five pigments with a *p*-terphenyl backbone obtained from a mycelial extract of the fermentation of *H. rickii* (Fig. 1). These compounds are the first examples of *p*-terphenyls derived from the order Xylariales. Rickenyl A (**19**) exhibited strong antioxidative effects and moderate cytotoxic potencies against various cancer cell lines [23].

The *p*-terphenyls have long been attractive targets in terms of their total synthesis, not only because of the potential erroneous assignment of some of their structures, but also because of their interesting biological activities. Fujiwara and co-workers have accomplished the total synthesis of thelephantin O, vialinin A/terrestrin A, and terrestrins B–D in order to evaluate their biological activities (Scheme 1). The synthesis routes developed by Fujiwara were more efficient and practical and also applicable to symmetrical diesters, such as vialinin A, terrestrin A, and terrestrin B. All of the synthetic compounds, thelephantin O, vialinin A, terrestrin A, and terrestrins B, were evaluated for their inhibitory activities against HepG2 and Caco2 cells. The $IC_{50}$ values were found to be 16.3/24.1, 13.6/24.1, 15.5/26.5, 14.1/23.7, and 20.7/26.7 μ*M*, respectively [24].

The total synthesis of kynapcin-12 (**24**) was achieved by Takahashi and associates [25]. The key steps of the syntheses involved a double Suzuki-Miyaura coupling, CAN oxidation, and lead tetraacetate oxidation. However, total synthesis of the proposed structure of kynapcin-12 and its isomer suggested that the structure of kynapcin-12 should be revised to 2′,3′-diacetoxy-1,5′,6′,4″-tetrahydroxy-*p*-terphenyl (**25**), which was isolated from *Boletopsis grisea* (Scheme 2). Furthermore, the total synthesis of the proposed thelephantin D (**26**) also led to its structural revision, which proved to be identical with terrestrin C (**27**) (Scheme 2) [26].

Sarcodonins, sarcoviolins, hydnellins, and phellodonin are a group of *p*-terphenyls with a benzodioxazine core and an unprecedented *N*,*N*-dioxide ring junction, which were proposed by natural product chemists to be derived via a [4 +2] cycloaddition between the 3,4-benzoquinone of the terphenyl and the 1β–2β double bond of *N*-oxopyrazine. The instability and inaccessibility of crystals for X-ray structural analysis of these compounds has aroused suspicion as to their structural validity. Baran and co-workers reported the possibility of an alternative benzodioxane aminal core structure (**28**) for this family of compounds through

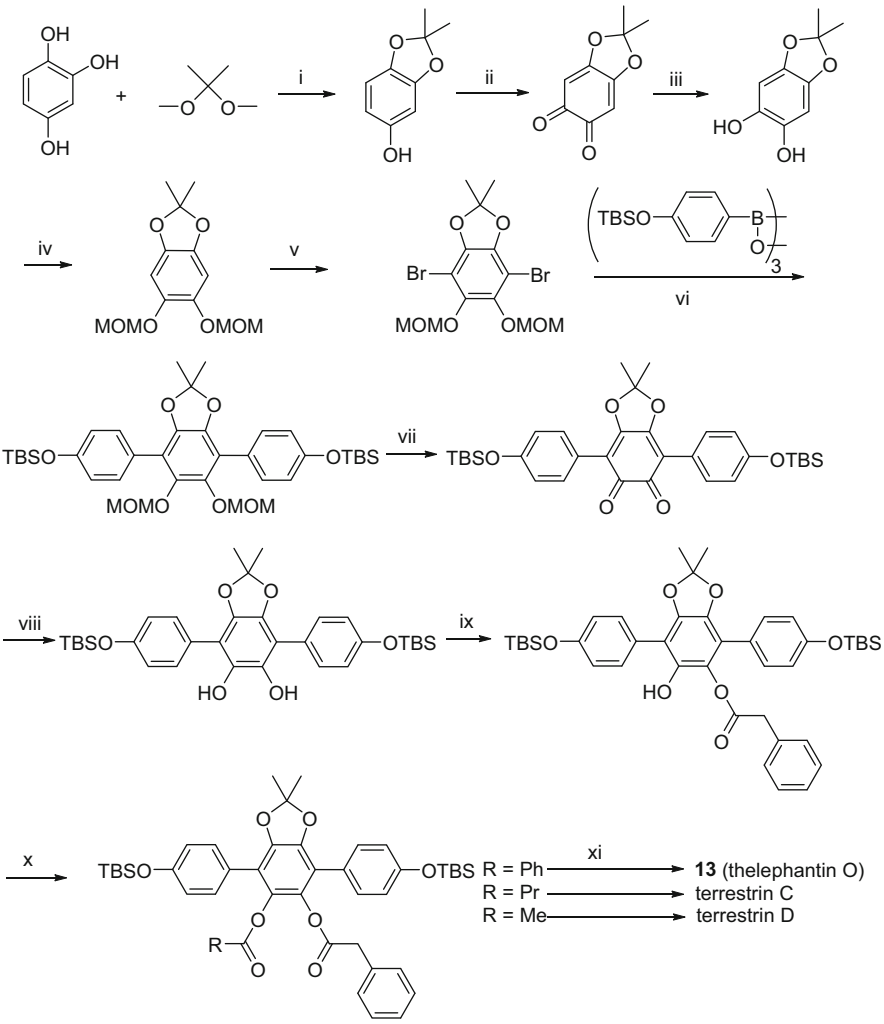


**Scheme 1** Total synthesis of thelephantin O (**13**), terrestrin C, and terrestrin D. Reagents and conditions: (i) PPTS (0.008 equiv), PhMe, reflux, 110 min; (ii) $K_2ON(SO_3)_2$, $KHPO_4$, $H_2O$, 0°C, 1 h; (iii) $H_2$, $PtO_2$, THF, 24°C, 2 h; (iv) NaH, DMF, 0°C, 1 h, then MOMBr, 0 → 24°C, 20 h; (v) BuLi, THF, 0°C, 1 h, then $CF_2BrCF_2Br$; (vi) $K_2CO_3$, $(Ph_3P)_4Pd$, 1,4-dioxane-$H_2O$ (3:1), reflux, 2 h; (vii) DDQ, TsOH·$H_2O$, PhH, 50°C, 24 min; (viii) $H_2$, $PtO_2$, THF, 24°C, 1 h; (ix) *n*-BuLi (1.2 equiv), THF, −78°C, 1 h, then $PhCH_2COCl$ (1.2 equiv), −78 → 24°C, 21 h; (x) NaH, THF, 0°C, 1 h, then RCOCl, 0 → 24°C, 18–22 h; (xi) $HSCH_2CH_2SH$, $AlCl_3$, $MeNO_2$, −20°C, 30 min

extensive synthesis studies (Scheme 3a) [27]. However, Fujimoto and co-workers isolated sarcodonin $\epsilon$ (**29**) from *S. scabrosus* in a sizable amount, which led to a crystal structure of the hydroxy-methylated derivative of compound **29** via $TMSCHN_2$ methylation. The X-ray crystallographic result provided solid evidence

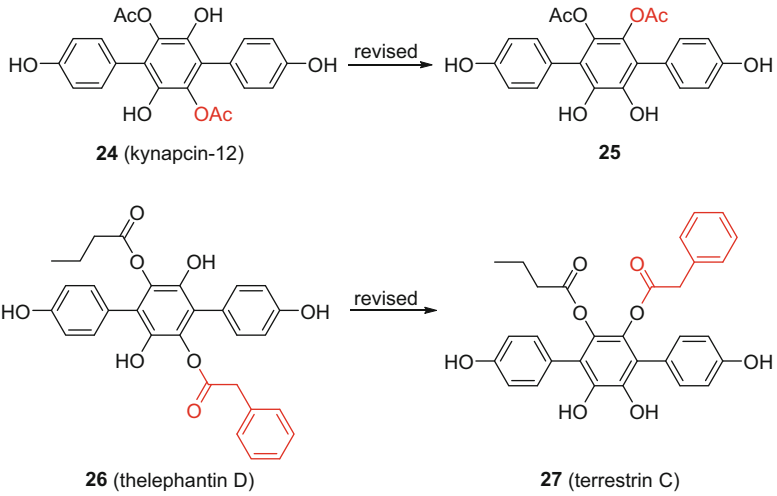


**Scheme 2** Structural revisions of kynapcin-12 (**24**) and thelephantin D (**26**)

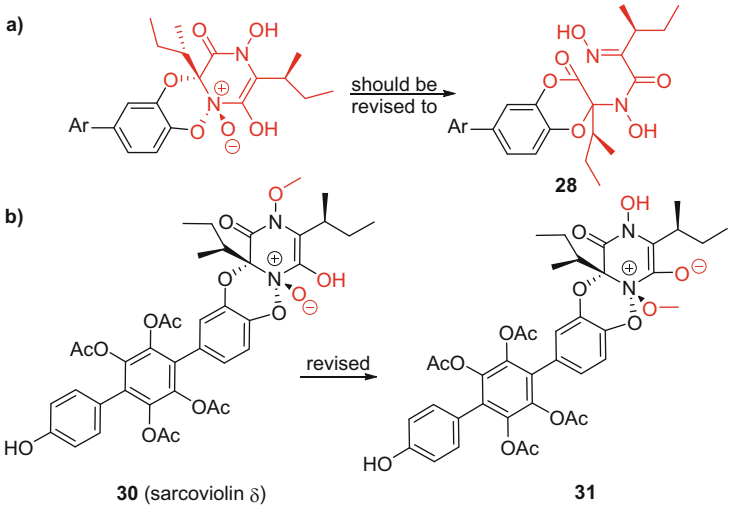


**Scheme 3** (**a**) Structural revisions of the sarcodonin, sarcoviolin, and the hydnellin natural product family as proposed by Baran et al. and (**b**) structural revision of sarcoviolin δ (**30**)

for the stable existence of the *N*,*N*-dioxide ring junction. By a methylation approach, Fujimoto and co-workers also revised the structure of the known compound sarcodonin δ from **30** to **31** (Scheme 3b) [16]. Later, the total syntheses of phellodonin and sarcodonin ε were accomplished by Baran and co-workers [28].

**Table 2** Pulvinic acids and related butenolides published in recent years

| Compound[a] | | Origin | Refs. |
|---|---|---|---|
| (±)-Tylopilusin A (**32**) | | *Tylopilus eximius* | [29] |
| (±)-Tylopilusin B (**33**) | | *Tylopilus eximius* | [29] |
| Tylopilusin C (**34**) | | *Tylopilus eximius* | [30] |
| Chromapedic acid (**37**) | | *Leccinum chromapes* | [31] |
| Isoxerocomic acid (**39**) | | *Leccinum chromapes* | [31] |
| Methyl isoxerocomate (**35**) | | *Leccinum chromapes* | [31] |
| Atromentic acid (**40**) | | *Leccinum chromapes* | [31] |
| Variegatorubin (**36**) | | *Leccinum chromapes* | [31] |

[a]Color of compound in adjoining column

## Pulvinic Acids and Related Butenolides

Inhibition of the yellow pigment produced by methicillin-resistant *Staphylococcus aureus* (MRSA) has been a new target for anti-MRSA agents. During the screening for these agents from a Japanese mushroom, (±)-tylopilusins A (**32**) and B (**33**) were isolated. These pulvinic acid-related compounds were obtained from the fruiting bodies of the mushroom *Tylopilus eximius* (Table 2, Fig. 2). Interestingly, these compounds were isolated as racemates, and were purified by enantioselective HPLC to afford their optically pure forms. During the isolation process, (±)-tylopilusin B (**33**) was crystallized and analyzed by X-ray crystallography. The absolute configurations of (+)- and (−)-tylopilusin A (**32**) were established by ECD calculations. A continuing study of this mushroom yielded tylopilusin C (**34**) (Table 2, Fig. 2). Biological testing suggested that the tylopilusins are inhibitors of a yellow pigment produced by pathogenic MRSA, but that they do not affect the growth of MRSA itself [29, 30].

Steglich et al. revealed that methyl isoxerocomate (**35**) was responsible for the bright-yellow color of the stalk bases of the American mushroom *Leccinum chromapes*, with variegatorubin (**36**) leading to the pink color of the cap skin (Table 2, Fig. 2). Moreover, chromapedic acid (**37**) was also isolated as a pale-yellow compound, which represents a new type of dimer formed from 4-hydroxyphenylpyruvic acid (Table 2, Fig. 2). When chromapedic acid was exposed to air, it transformed into 3-(3,4-dihydroxybenzyl)-4-(3,4-dihydroxyphenyl)furan-2,5-dione (**38**) [31].

Steglich et al. also proposed a possible biosynthesis pathway for the family of pyruvic acid derivatives. As depicted in Scheme 4, two molecules of 4-hydroxyphenylpyruvic acid react: (a) via the cyclization mode A to yield terphenylquinones, which, upon further oxidation, give pulvinic acids. Two molecules of pulvinic acids further dimerize to yield chalcitrin, norbadione A, and sclerocitrin; (b) via the cyclization mode B to yield tylopilusins, which further undergo decarboxylation to form cyclopentanoids; (c) via the cyclization mode C to

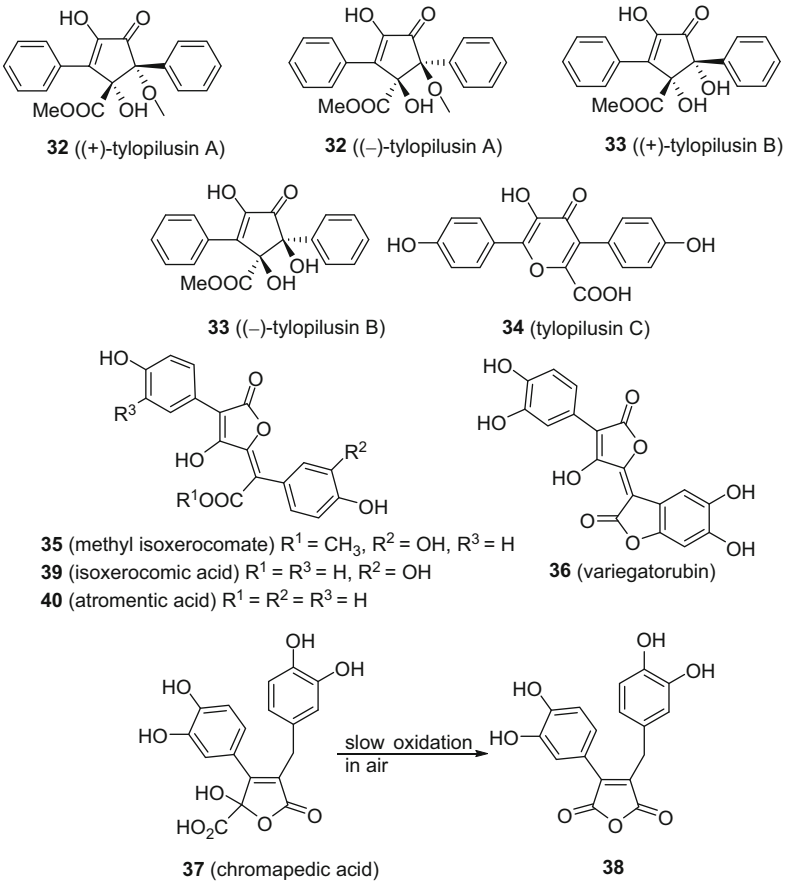


**Fig. 2** Pulvinic acids and related butenolides reported in recent years

give retipolides; (d) via the cyclization mode D to yield the aformentioned chromapedic acid; and (e) grevillins may be produced through the cyclization mode E [31].

### 2.2.2 Pigments Derived from Cinnamic Acids

Inonotusins A (**41**) and B (**42**) were isolated from the methanolic extract of the fruiting bodies of *Inonotus hispidus* (Fig. 3, Table 3). These compounds displayed significant scavenging activity against the 2,20-azinobis(3-ethylbenzthiazoline-6-sulfonate) radical cation. Inonotusin A (**41**) also exhibited moderate cytotoxicity against a human breast carcinoma cell line (MCF-7) with an $IC_{50}$ value of 19.6 μ*M*

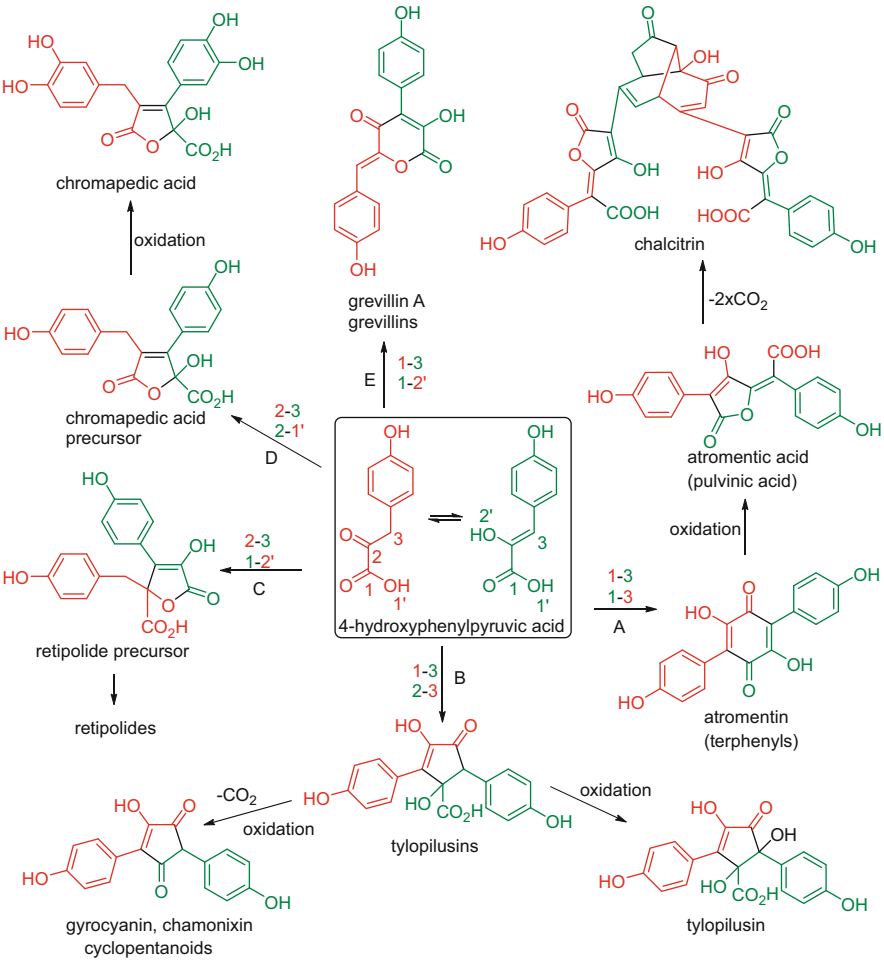


**Scheme 4** Postulated biosynthesis pathways for the pyruvic acid family

[32]. Phelliribsin A (**43**) is an orange pigment with an unprecedented spiroindene scaffold isolated from the medicinal fungus *Phellinus ribis* (Fig. 3, Table 3). The biosynthesis pathway of phelliribsin A is shown in Scheme 5 [33].

Phaeolschidins A–E (**44**–**48**), along with the known compound pinillidine (**49**), are five hispidin derivatives isolated from the fruiting bodies of the Tibetan mushroom *Phaeolus schweinitzii* (Fig. 3, Table 3). Phaeolschidins A–D (**44**–**47**) are bishispidin derivatives, which have rarely been found in Nature, with pinillidine originally isolated from the medicinal fungus *Phellinus pini* regarded as the first example. All of these compounds showed weak radical-scavenging activities [34].

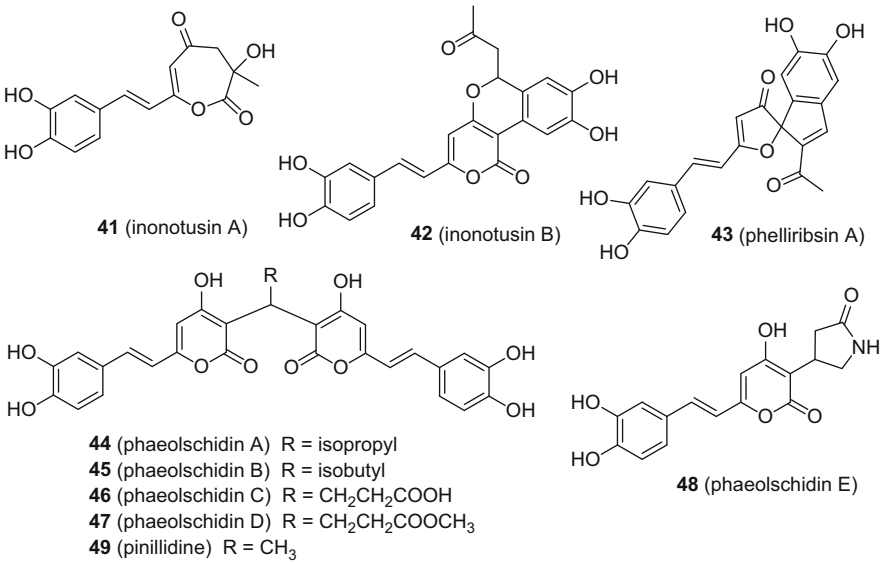


**Fig. 3** Compounds derived from cinnamic acids

**Table 3** Compounds derived from cinnamic acids

| Compound[a] | | Origin | Refs. |
|---|---|---|---|
| Inonotusins A (**41**), B (**42**) | | *Inonotus hispidus* | [32] |
| Phelliribsin A (**43**) | | *Phellinus ribis* | [33] |
| Phaeolschidins A–E (**41**–**48**) | | *Phaeolus schweinitzii* | [34] |
| Pinillidine (**49**) | | *Phaeolus schweinitzii* | [34] |

[a]Color of compound in adjoining column

### 2.2.3 Meroterpenoids Derived from Hydroquinone

In previous reviews, this section has been entitled "Compounds Derived from 4-Hydroxybenzoic Acid", referring to meroterpenoids derived from the shikimate-chorismate pathway. Biogenetically, as summarized in Scheme 6, the mevalonate pathway yields terpenoid precursors, while the shikimate pathway provides 4-hydroxybenzoic acid (**50**). Compound **50** undergoes two routes to produce hydroquinone and 4-(hydroxymethyl)phenol. A combination of these two pathways yields various meroterpenoids. Generally, this meroterpenoid category contains prenyl-/geranyl-/farnesyl-/geranylgeranyl-substituted benzoic acid or hydroquinone derivatives. Herein, these meroterpenoids are classified into four groups: prenylated benzene derivatives, meromonoquiterpenoids, merosesquiterpenoids, and meroditerpenoids, on the basis of the type of terpenoid moiety.

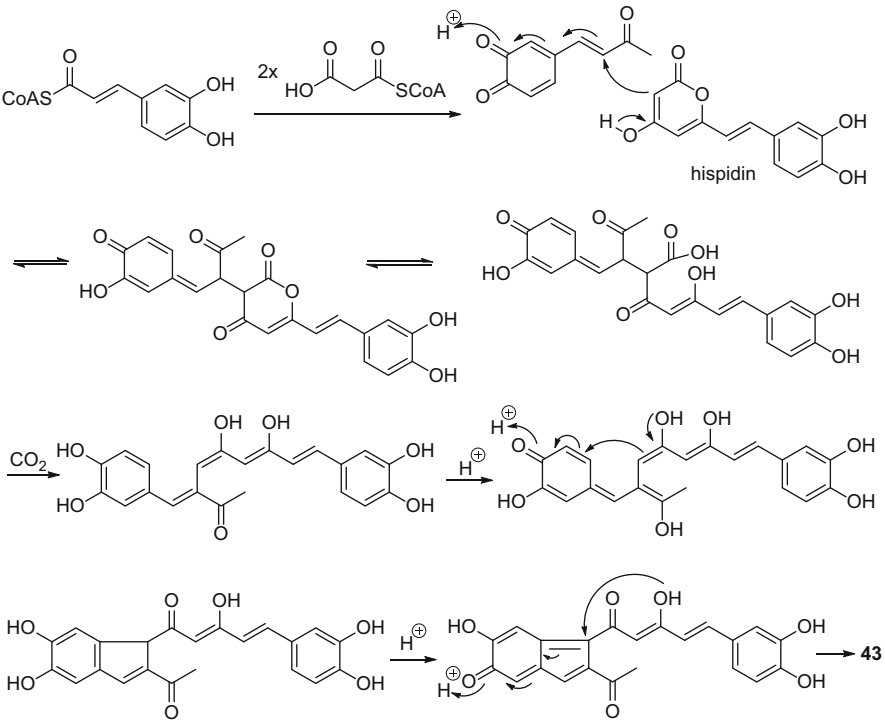


**Scheme 5** Postulated biosynthesis pathway of phelliribsin A (**43**)

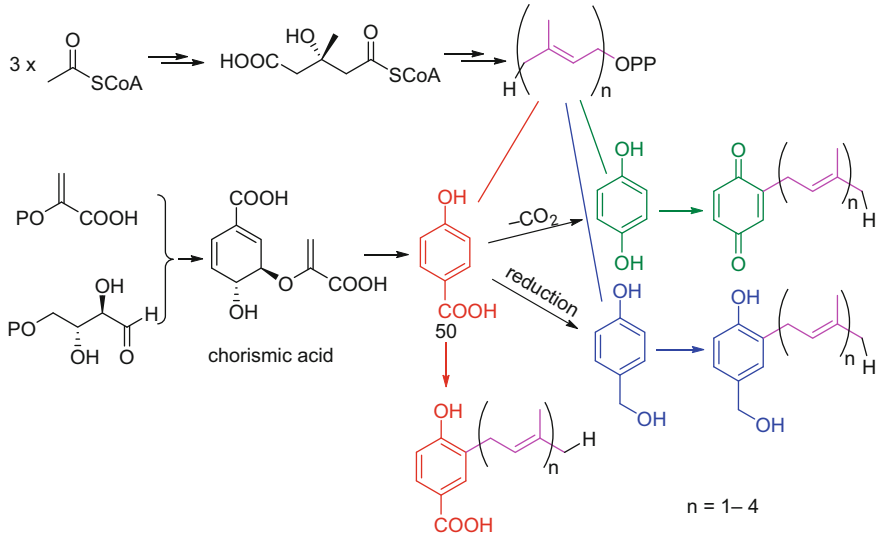


**Scheme 6** Biosynthesis pathway of hydroquinone meroterpenoids

Notably, in previous reviews, the meroterpenoids derived from the acetate-malonate pathway, of which the benzene ring typically is substituted with a methyl and a *p*-hydroxy group, are included in this section. In the present contribution, meroterpenoids derived from the acetate-malonate pathway are categorized in the Section entitled "Pigments from the Acetate-Malonate Pathway".

## Prenylated Benzene Derivatives

The genus *Stereum* is productive in accumulating prenylated benzene derivatives. Vibralactone (**51**) is a well-studied molecule featuring a β-lactone group and displaying pancreatic lipase inhibition [isolated from the culture broth of *Boreostereum vibrans* (syn. *Stereum vibrans*)] (Fig. 4) [35]. The biosynthesis pathway of vibralactone was elucidated and it was shown that the prenylated 4-hydroxybenzoic acid (**50**) is reduced to the prenylated 4-(hydroxymethyl)phenol (**52**), then cleavage of the benzene ring leads to the production of the key intermediate 1,5-*seco*-vibralactone (**53**), which further undergoes a 1,5-C—C bond formation to yield **51** (Scheme 7) [36]. Vibralactone derivatives were used as chemical probes to study the structure and activity of ClpP1P2 [37]. Interestingly, **51** was also encountered in another species of *Stereum* [38, 39]. Hoffmeister and co-workers found vibralactone and the co-isolates vibralactones R and S from a stereaceous fungus [39].

An in-depth study mainly by large-scale fermentation of *B. vibrans* resulted in the isolation of the vibralactone derivatives, vibralactones B–Q (**55**) [40–43], 1,5-*seco*-vibralactone (**53**) [40], and 10-lactyl vibralactone G (**54**) [44] (Table 4). Recently, several oximes and polyoxime esters with a vibralactone backbone, namely, vibralactoximes A–P (**56–59**), were reported to show more potent pancreatic lipase inhibitory activity than that of vibralactone (Table 4, Fig. 4). Moreover, most of these also exhibited cytotoxicity against five human cancer cell lines (HL-60, SMMC-7721, A-549, MCF-7, and SW480) [46].

A thorough analysis of the secondary metabolome of *B. vibrans* has resolved the divergent vibralactone biosynthesis pathways. Yang et al. proposed that prenylated 4-(hydroxymethyl)phenol (**52**) is a key intermediate for the generation of 20 analogues with different scaffolds, and confirmed this by feeding experiments with 3-allyl-4-hydroxybenzylalcohol, and the corresponding derivatives were obtained with allyl moieties rather than isoprenyl moieties [52]. In general, the secondary metabolome of *B. vibrans* is represented by five structural classes with the skeletons A–E, as depicted in Scheme 8. However, the isoprenyl moiety of those skeletons is conserved, while the benzene ring is present in various forms. In particular, **52** is at a junction of various biosynthesis routes. One proceeds by way of oxygenation and splitting of a benzene ring to give vibralactone J (**60**) with the scaffold type A. A second route involves a carbon–carbon formation reaction to yield vibralactone and its derivatives, representing scaffold type B. Third, an oxygenation and reduction on the benzene ring of **52** followed by a key ring contraction reaction yields vibralactone I (**61**), representing scaffold type C. On the other hand, oxygenation

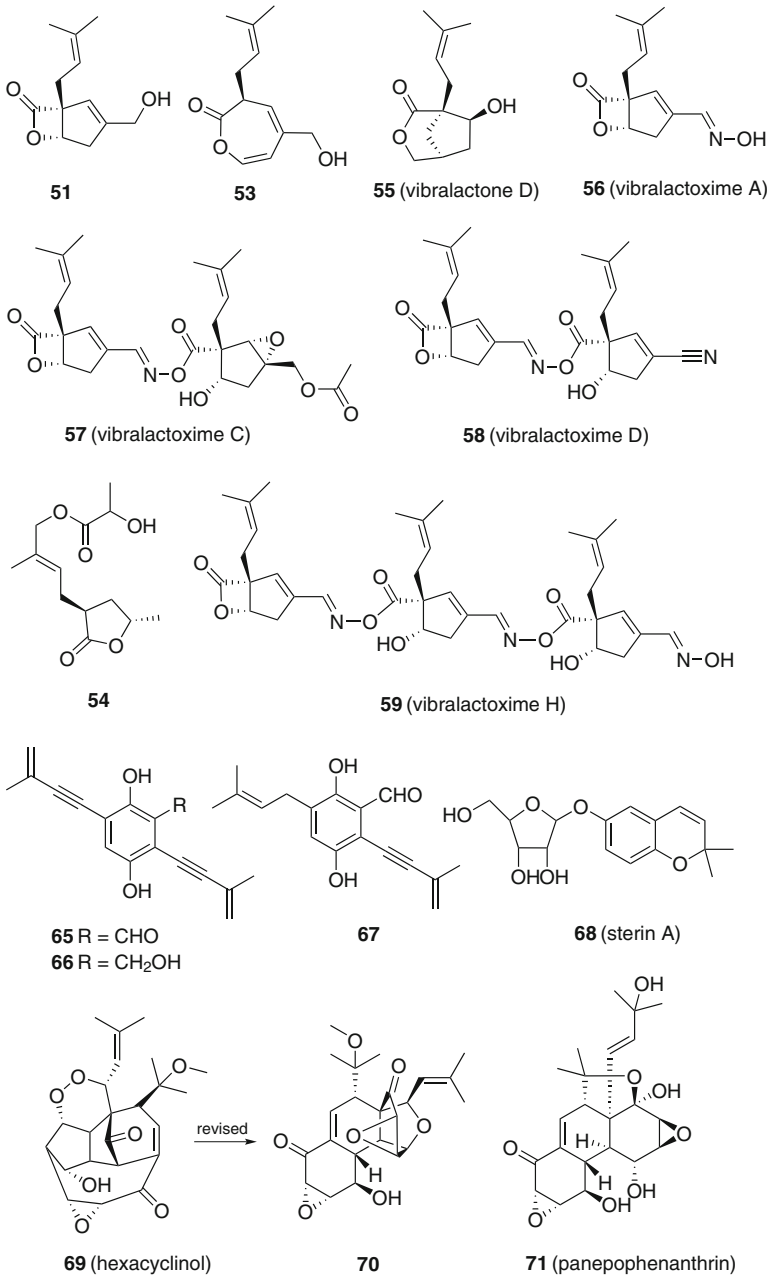


**Fig. 4** Prenylated benzene derivatives

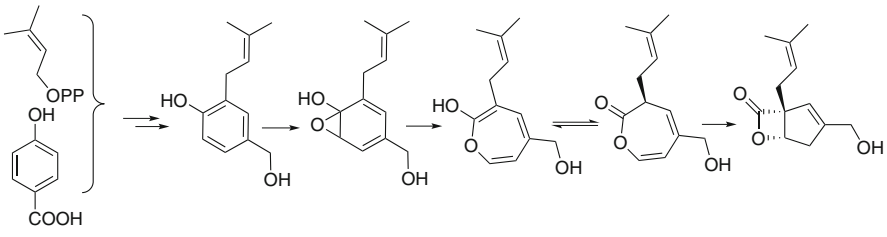


50 52 53 51

**Scheme 7** Biosynthesis pathway of vibralactone (**51**)

**Table 4** Prenylated benzene derivatives

| Compound[a] | | Origin | Refs. |
|---|---|---|---|
| Vibralactone (**51**) | | *Boreostereum vibrans* | [35] |
| Vibralactones B–Q (**55**) | | *Boreostereum vibrans* | [40–45] |
| Vibralactones R, S | | *Stereum* sp. | [39] |
| 10-Lactyl vibralactone G (**54**) | | *Boreostereum vibrans* | [44] |
| 1,5-*seco*-Vibralactone (**53**) | | *Boreostereum vibrans* | [40] |
| Vibralactoximes A–P (**56–59**) | | *Boreostereum vibrans* | [46] |
| Vibranether | | *Boreostereum vibrans* | [45] |
| 2,5-Dihydroxy-3,6-bis(3-methylbut-3-en-1-ynyl)benzaldehyde (**65**) | | *Stereum hirsutum* | [47] |
| 3-(Hydroxymethyl)-2,5-bis(3-methylbut-3-en-1-ynyl)benzene-1,4-diol (**66**) | | *Stereum hirsutum* | [47] |
| 2,5-Dihydroxy-3-iso-prenyl-6-(3-methylbut-3-en-1-ynyl)benzaldehyde (**67**) | | *Stereum hirsutum* | [47] |
| Sterins A–B (**68**) | | *Stereum hirsutum* | [48] |
| Sterin C | | *Stereum hirsutum* | [49] |
| Hexacyclinol (**69**) | | *Panus rudis* | [50] |
| Panepophenanthrin (**71**) | | *Panus rudis* | [51] |

[a]Color of compound in adjoining column

of the alcoholic hydroxy group leads to 3-prenyl-3-hydroxybenzoaldehyde (**62**). This intermediate undergoes a $C_2$ extension with pyruvate to give vibranether, based on skeleton D. Moreover, **62** may be further oxygenated to 3-prenyl-3-hydroxybenzoic acid (**63**). Decarboxylation of **63** followed by a cascade of oxygenation/decarboxylation reactions yields vibralactone G (**64**), representing skeleton E.

It is notable that Yang et al. also identified a FAD-dependent monooxygenase (VibMO1) that converts prenyl-4-hydroxybenzoate into prenylhydroquinone. Heterologous expression of VibMO1 confirmed this function. This finding provided

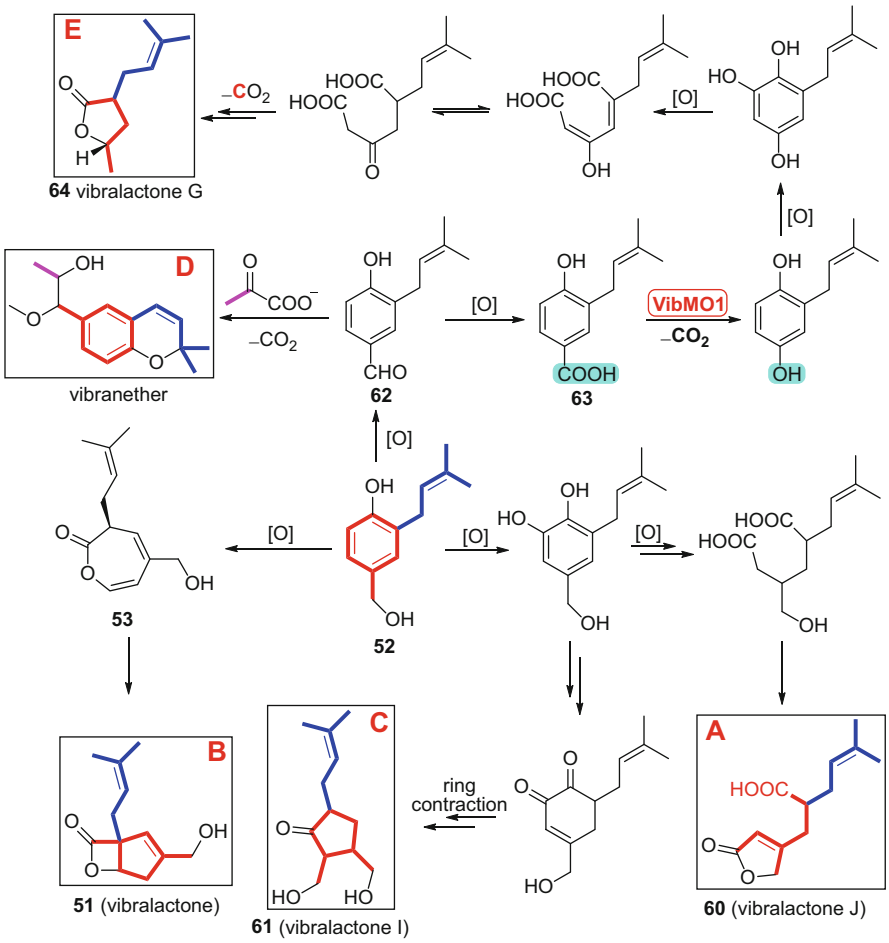


**Scheme 8** Proposed divergent biosynthesis pathways for five classes of secondary metabolites from *Boreostereum vibrans*

crucial information for the determination of enzymes essential for similar conversion steps in other organisms.

Compounds **65**–**67** were isolated from the cultures of the wood-decaying fungus *Stereum hirsutum*. These compounds feature a 3-methylbut-3-en-1-ynyl substituent, which originates from a prenyl group (Fig. 4) [47]. Sterins A–C were isolated from the same fungus by other research groups. The differences among sterins A–C is due to the form of the prenyl groups. In sterin A (**68**), the prenyl is cyclized with the phenolic hydroxy group to yield a 2*H*-chromene scaffold (Fig. 4) [48, 49].

Hexacyclinol (**69**) was isolated as a bioactive constituent from the culturing of the basidiomycete *Panus rudis* HKI 0254 (Fig. 4). This compound displayed inhibition of oxidant generation in zymosan-stimulated polymorphonuclear

neutrophil leukocytes. Furthermore, **69** also showed cytotoxicity against the L-929 murine fibroblast cell line and K562 cancer cell lines with $IC_{50}$ values of 1.4 and 0.4 μg/cm$^3$. Moreover, **69** exhibited inhibitory activity against *Plasmodium falciparum* with an $IC_{50}$ value of 2.49 μg/cm$^3$ [53]. Due to its diverse biological activities and intriguingly relatively complex structure, many research groups have been challenged to accomplish its total synthesis. However, it was proved that the structure of hexacyclinol was incorrectly assigned originally and this was revised to **70** [50]. Panepophenanthrin (**71**) is a similar type of meroterpenoid dimer isolated from the same fungus, *P. rudis* Fr. IFO8994, by a Japanese group (Fig. 4) [51]. The structure of **71** was established via NMR spectroscopic data interpretation and X-ray crystallographic analysis. This compound is an inhibitor of ubiquitin-activating enzyme, which is indispensable for the ubiquitin-proteasome pathway.

Interestingly, considering the high structural similarities between **69** and **71**, Rychnovsky reassigned the structure of **69** on the basis of $^{13}$C NMR chemical shifts derived by computational methods and proposed that **69** is an artefact, which arose from the acid-catalyzed rearrangement of **71** in the presence of methanol [54]. However, Porco et al. synthesized **71**, which was further exposed to various acidic conditions, but this treatment did not result in an observable conversion into **69** [55].

## Meromonoterpenoids

Meromonoterpenoids derived from the shikimate-chorismate pathway are a family of compounds in which the benzene ring is substituted by a geranyl residue. To the best of our knowledge, this family of compounds has only been found in the genera *Tricholoma*, *Lactarius*, *Clitocybe*, and *Ganoderma* (Table 5).

Tricholomenyns A–E (**72**–**76**) are five enyne-containing meromonoterpenoids isolated from the European mushroom *Tricholoma acerbum* (Fig. 5). Tricholomenyns A and B display antimitotic activity against T lymphocytes. Tricholomenyns C–E are dimers through an ester bond, and tricholomenyn C (**74**) is a useful chemotaxonomic marker for *Tricholoma* species since it is produced by *T. ustaloides*, *T. vaccinum*, *T. albobrunneum*, and *T. imbricatum* [56, 57]. Terreumols A–D (**77**–**80**) are four highly oxygenated meroterpenoids isolated from the fruiting bodies of the European gray knight mushroom *T. terreum* (Fig. 5). Structurally, all of these compounds contain two C–C bonds between the benzene ring and the terpenoid moieties to build a rare 10-membered ring. The absolute configurations of terreumols A (**77**) and C (**79**) were determined unambiguously by single-crystal X-ray crystallographic analysis. Terreumols A, C, and D exhibited cytotoxicity against five human cancer cell lines (HL-60, SMMC-7721, A-549, MCF-7, and SW480) with $IC_{50}$ values comparable to those of cisplatin [58]. The enantioselective total syntheses of **77** and **79** have been accomplished by Lindel and co-workers in 14 steps and with a 23% overall yield for terreumol A (**77**) [75]. The key step to (–)-terreumol C was a ring-closing metathesis to form a trisubstituted (*Z*) double bond embedded in the 10-membered ring of

**Table 5** Meromonoterpenoids

| Compound[a] | | Origin | Refs. |
|---|---|---|---|
| Tricholomenyns A–E (**72–76**) | | *Tricholoma acerbum* | [56, 57] |
| Terreumols A–D (**77–80**) | | *Tricholoma terreum* | [58] |
| Flavidulols A (**81**), C (**83**), D (**84**) | | *Lactarius flavidulus* | [59–61] |
| Flavidulol B (**82**) | | *Lactarius flavidulus* | [59] |
| Clavilactones A–E (**85–89**) | | *Clitocybe clavipes* | [62–64] |
| Petchienes A–E (**90**, **91**) | | *Ganoderma petchii* | [65] |
| Chizhines A–E | | *Ganoderma lucidum* | [66] |
| Spirolingzhines A–D (**92**) | | *Ganoderma lingzhi* | [67] |
| Lingzhines A–F (**93**) | | *Ganoderma lingzhi* | [67] |
| Applanatumols A (**94**), B (**95**) | | *Ganoderma applanatum* | [68] |
| (±)-Lingzhiol (**96**) | | *Ganoderma lucidum* | [69] |
| Applanatumin A (**98**) | | *Ganoderma applanatum* | [70] |
| (±)-Ganoapplanin (**99**) | | *Ganoderma applanatum* | [71] |
| (±)-Sinensilactam A (**97**) | | *Ganoderma sinensis* | [72] |
| Cochlearol A (**102**) | | *Ganoderma cochlear* | [73] |
| Cochlearines A (**100**), B (**101**) | | *Ganoderma cochlear* | [74] |

[a]Color of compound in adjoining column

the [8.4.0] bicyclic system. (–)-Terreumol A was obtained by diastereoselective epoxidation of terreumol C (Scheme 9).

Meroterpenoids with a rare 10-membered ring were also found in the genera *Lactarius* and *Clitocybe*. Flavidulols A–D (**81–84**) were isolated from the acetone extract of the edible mushroom *L. flavidulus* (Fig. 5). The 10-membered ring of flavidulol B was cleaved between C-4 and C-5 to give two terminal double bonds and connected between C-2 and C-7. Flavidulol C (**83**) is a meroterpenoid dimer through the C–C bond between the benzene rings. Flavidulol A (**81**) exhibited antibacterial activity against *Staphylococcus aureus* and *Bacillus subtilis* with the same *MIC* value of 6.2 μg/cm$^3$. Moreover, flavidulols A–C also displayed suppressive effects on the proliferation of murine lymphocytes stimulated by concanavalin A and lipopolysaccharide, with $IC_{50}$ values of 8.9, 4.9, and 36.3 μg/cm$^3$ against concanavalin A-induced proliferation and 6.7, 3.9, and 28.3 μg/cm$^3$ against lipopolysaccharide-induced proliferation, respectively [59–61]. Chemical investigation of solid medium (malt-peptone-glucose-agar) cultures of the basidiomycete *C. calvipes* led to the isolation of five ten-membered-ring meroterpenoids, designated as clavilactones A–E (**85–89**) (Fig. 5). Clavilactones A–C exhibited antimicrobial activity and inhibition of the germination of *Lepidium sativum*, while clavilactone D inhibited tyrosine kinase.

Recent years have been a time for the rapid discovery of meroterpenoids derived from the traditional Chinese medicinal mushroom genus *Ganoderma*. These

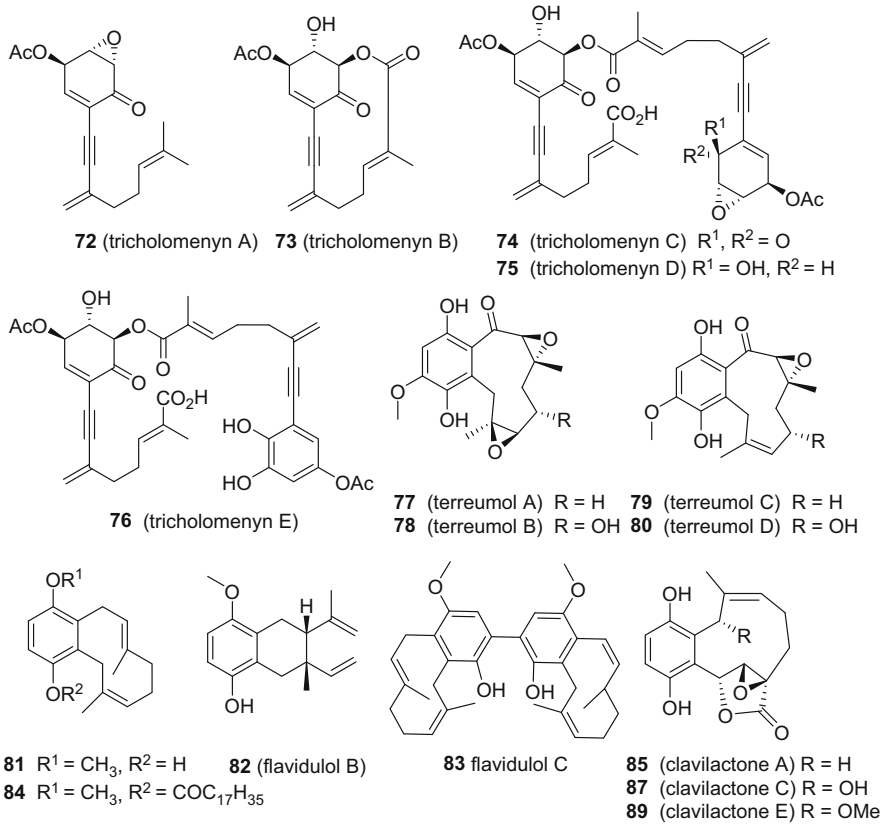


**Fig. 5** Structures of meromonoterpenoids

meroterpenoids with both intricate structures and promising bioactivities have attracted the interest of many research groups (Table 5).

Many meromonoterpenoids were isolated from different species of *Ganoderma*, such as petchienes A–E (**90**, **91**) [65], chizhines A–E [66], spirolingzhines A–D (**92**) [67], lingzhines A–F (**93**) [67], and applanatumols A (**94**) and B (**95**) [68]. Lingzhiol (**96**) was isolated as a racemate from the fruiting bodies of *G. lucidum* (Fig. 5). Structurally, lingzhiol (**96**), which bears an unusual 5/5/6/6 ring system, was characterized as sharing a C-3′–C-7′ axis. The absolute configuration of lingzhiol was established by X-ray diffraction analysis of (–)-lingzhiol, which was separated by chiral-phase HPLC. (+)- and (–)-Lingzhiol selectively inhibited the phosphorylation of Smad3 in TGF-$\beta$1-induced rat renal proximal tubular cells and activated Nrf2/Keap1 in mesangial cells [69]. The total synthesis of lingzhiol was achieved by Yang et al. [76], Qin et al. [77, 78], and Gautam and Birman [79].

(±)-Sinensilactam A (**97**) was isolated as colorless crystals from the fruiting bodies of *Ganoderma sinensis*, the structures of which were confirmed unambiguously by X-ray diffraction analysis (Fig. 5). Sinensilactam A is based on an

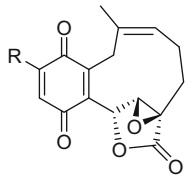


**86** (clavilactone B) R = H
**88** (clavilactone D) R = OH

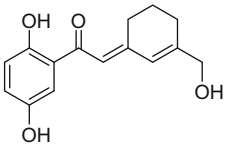


**90** (petchiene B)

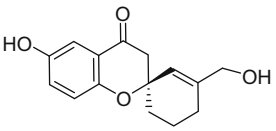


**91** ((–)-petchiene D)

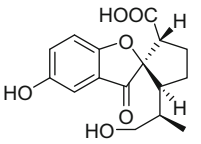


**92** ((–)-spirolingzhine A)

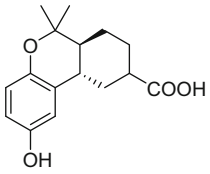


**93** (lingzhine A)

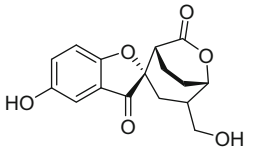


**94** (applanatumol A)

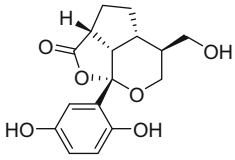


**95** (applanatumol B)

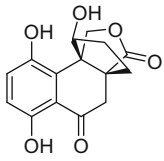


**96** ((–)-lingzhiol)

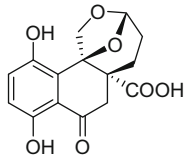


**102** (cochlearol A)

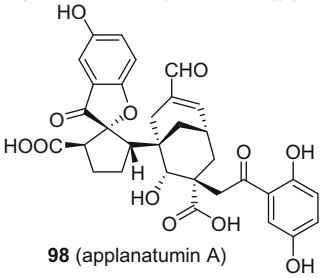


**98** (applanatumin A)

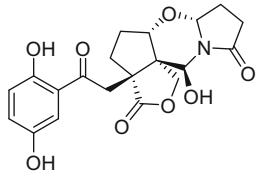


**97** ((–)-sinensilactam A)

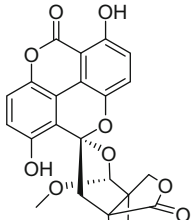


**99** ((+)-ganoapplanin)

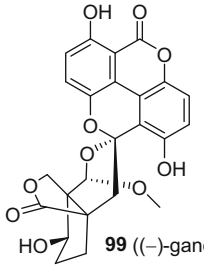


**99** ((–)-ganoapplanin)

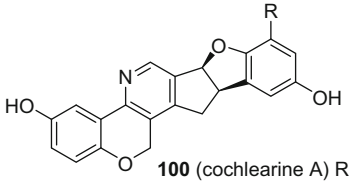


**100** (cochlearine A) R = A
**101** (cochlearine B) R = B

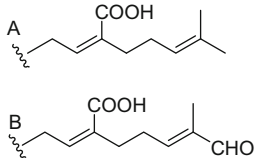


**Fig. 5** (continued)

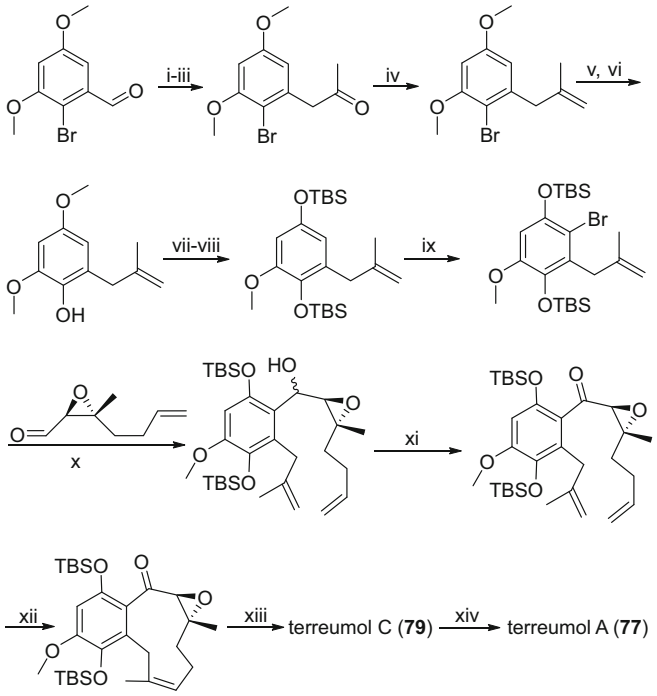


**Scheme 9** Total synthesis of terreumols A (**77**) and C (**79**).
Reagents and conditions: (i) $EtNO_2$ (2.0 equiv), $CyNH_2$ (1.0 equiv), HOAc, 100°C; (ii) Fe (6.0 equiv), HOAc, 100°C; (iii) 8% NaOH (aq.); (iv) $MePPh_3Br$ (3.0 equiv), KO*t*Bu (3.0 equiv), THF, 0°C → RT, 7h; (v) *n*BuLi (1.1 equiv), $B(OMe)_3$ (5.0 equiv), THF –78°C → RT, 6 h; (vi) $H_2O_2$, $Na_2CO_3$; (vii) CAN (2.5 equiv), MeCN/$H_2O$), 0°C, 20 min; (viii) $NaBH_4$ (2.0 equiv), THF, RT, 1 h; (ix) TBSOTf (3.0 equiv), $Et_3N$ (10.0 equiv), DCM, 0°C, 30 min; (x) *t*BuLi (2.0 equiv), $Et_2O$, −78°C; (xi) IBX (1.8 equiv), DMSO, RT, 4 h; (xii) Grubbs II (0.1 equiv), tetrafluoro-1,4-benzoquinone (0.8 equiv), PhMe, 100°C, 4 h; (xiii) $Et_3N{\cdot}3HF$ (10 equiv), THF, 60°C, 3 h; (xiv) *m*CPBA (1.2 equiv), DCM, RT, 6 h

unprecented 2*H*-pyrrolo[2,1-*b*][1,3]oxazin-6(7*H*)-one ring system, derived from the shikimate, mevalonate, and amino acid pathways. (–)-Sinensilactam exhibited inhibition of Smad3 phosphorylation in TGF-$\beta$1-induced human renal proximal tubular cells [72].

The dimeric meroterpenoid applanatumin A (**98**) was isolated from the mushroom *Ganoderma applanatum* (Fig. 5). Applanatumin A (**98**) possesses a hexacyclic skeleton containing a spiro[benzofuran-2,1′-cyclopentane] motif, which was established by extensive spectroscopic data interpretation supported by a computational approach. A plausible pathway was proposed to involve a Diels-Alder reaction as the key step. This compound exhibited potent antifibrotic activity in TGF-$\beta$1-induced human renal proximal tubular cells [70]. More recently, the compound ganoapplanin was also isolated from *G. applanatum* and is present as both enantiomers, but in unequal amounts (Fig. 5). The structure of (±)-

ganoapplanin (**99**), which bears an unprecedented dioxaspirocyclic skeleton constructed from a 6/6/6/6 tetracyclic system and an unusual tricyclo[4.3.3.$0^{3',7'}$] dodecane motif, was established by spectroscopic data interpretation and confirmed by single crystal X-ray diffraction analysis. Biological results suggested that the optically pure form and a racemic mixture displayed different potencies against the inhibition of T-type voltage-gated calcium channels (TTCCs). The maximum inhibition of (±)-ganoapplanin was 43%, while values of >80% were obtained for (+)- and (–)-ganoapplanin [71].

Cochlearines A (**100**) and B (**101**) are two examples of *Ganoderma* alkaloids bound with meromonoterpenoids through a C–C bond (Fig. 5). (±)-Cochlearine A significantly inhibited $Ca_v3.1$ T-type calcium channels and showed pronounced selectivity against $Ca_v1.2$, $Ca_v2.1$, $Ca_v2.2$, and $K_v11.1$ (hERG) channels [74].

## Merosesquiterpenoids

All merosesquiterpenoids reported in recent years have been obtained from species in the genus *Ganoderma*. The number of reports on both *Ganoderma* merosesquiterpenoids and the cyclization mode of the farnesyl unit have been less than those of the *Ganoderma* meromonoterpenoids and fewer structural types have been proposed. However, most of the terpenoid motifs of *Ganoderma* merosesquiterpenoids remain uncyclized, such as in zizhines A–F (**102**) [80], ganocalidins B–F [81], ganomycins E and F [82], fornicin E [82], and cochlearol D [83] (Table 6).

The total phenolic portion of an extract of *G. cochlear* yielded four pairs of polycyclic meroterpenoid enantiomers, namely, (±)-ganocins A–D (**103**–**106**) (Fig. 6). Their structures were established by extensive spectroscopic data analysis. The structure of ganocin A (**103**) was confirmed from the X-ray diffraction

**Table 6** Merosesquiterpenoids

| Compound[a] | | Origin | Refs. |
|---|---|---|---|
| Zizhines A–F (**102**) | | *Ganoderma sinensis* | [80] |
| Ganocalidins A–F (**111**) | | *Ganoderma calidophilum* | [81] |
| Ganocapensins A (**112**), B (**113**) | | *Ganoderma capense* | [82] |
| Ganomycins E, F | | *Ganoderma capense* | [82] |
| Fornicin E | | *Ganoderma capense* | [82] |
| (±)-Ganodilactone (**114**) | | *Ganoderma leucocontextum* | [84] |
| Cochlearols B–D (**107**, **115**) | | *Ganoderma cochlear* | [73, 83] |
| Ganocin A (**103**) | | *Ganoderma cochlear* | [85] |
| Ganocins B–D (**104**–**106**) | | *Ganoderma cochlear* | [85] |
| Cochlearoids A (**108**), B (**109**), E (**110**) | | *Ganoderma cochlear* | [74] |

[a]Color of compound in adjoining column

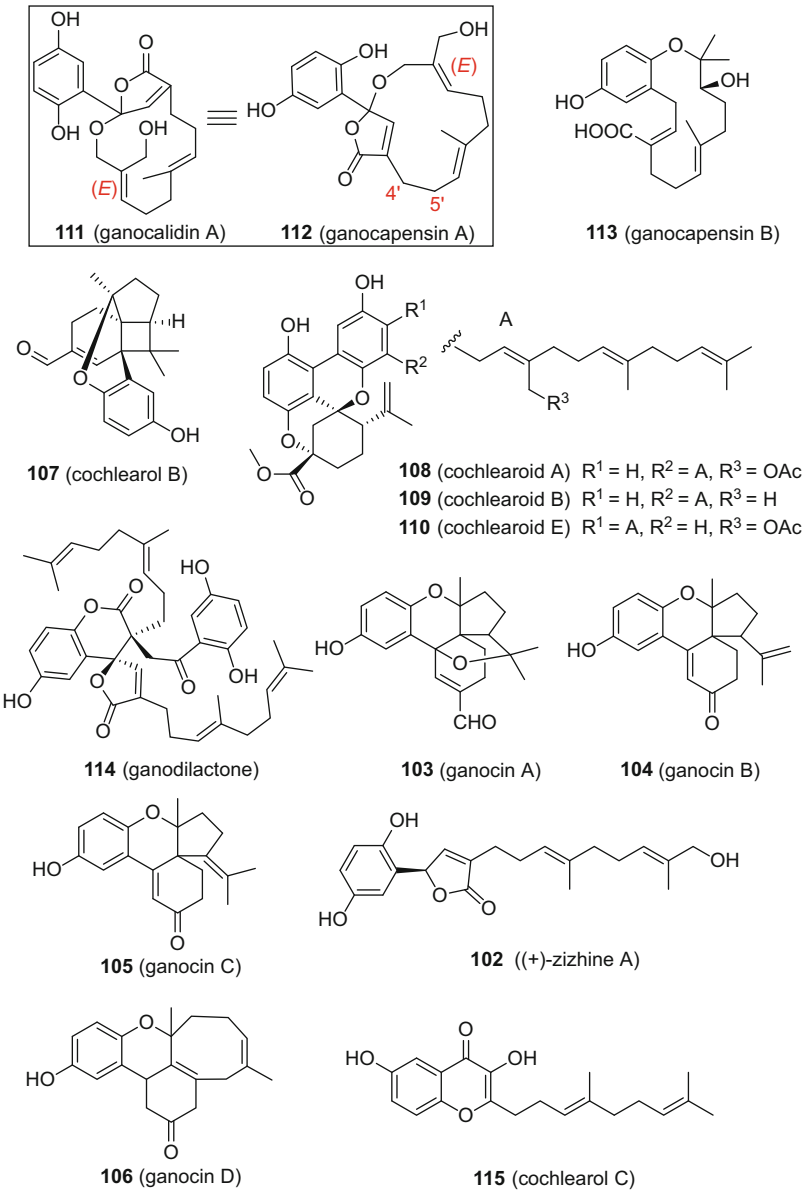


**Fig. 6** Structures of merosesquiterpenoids from *Ganoderma*

crystallographic data of its acetylated derivative. The possible biogenetic pathway of these compounds was also proposed. A chemical investigation of the same mushroom resulted in the isolation of the yellow amorphous solid cochlearol B (**107**), which is a 4/5/6/6/6 ring-fused meroterpenoid (Fig. 6). The structure of

cochlearol B also was established by extensive spectroscopic analysis. (–)-Cochlearol B potently disrupted Smad2 and Smad3 activation whereas (+)-cochlearol B showed no activity in this regard [73]. An in-depth investigation of the effect of a crude extract of *G. cochlear* on T-type calcium channels prompted the isolation of cochlearoids A (**108**), B (**109**), and E (**110**), which are three dimeric meroterpenoid enantiomers (Fig. 6). Their dimers are characterized by the C–C bond connection between two benzene rings resulting in a unique methanobenzo[*c*] oxocino[2,3,4-*ij*]-isochromene scaffold. Biological assays suggested that (+)-cochlearoid A has an effect on $Ca_v3.1$ similar to that of mibefradil [74].

Ganocalidin A (**111**) and ganocapensin A (**112**) are meroterpenoids with macrocycles. They were reported from different *Ganoderma* species by two different research groups (Fig. 6) [81, 82]. However, ganocalidin A and ganocapensin A proved to be the same molecule, based on a careful examination of their NMR data. Peng et al. misassigned the $^{13}C$ NMR chemical values between positions C-4′ and C-5′, but uncovered the racemic nature of ganocalidin A [82]. Ganocalidin A was reported to exhibit an inhibitory effect on $\beta$-hexosaminidase activity ($IC_{50}$ 9.44 $\mu M$) and reduced substantially the production of IL-4 and $LTB_4$ by RBL-2H3 cells in response to antigen stimulation, suggesting the potential antiallergic activity of this compound [81]. Ganocapensin B (**113**) is a meroterpenoid with a 14-membered macrocyclic ring, which is a rare feature in the *Ganoderma* meroterpenoid compound class (Fig. 6). The absolute configuration of OH-10′ was determined by a modified Mosher's method [82].

(±)-Ganodilactone (**114**) is a meroterpenoid dimer with a unique 5′*H*-spiro [chroman-4,2′-furan]-2,5′-dione ring system isolated from the Tibetan mushroom *G. leucocontextum* (Fig. 6). The (±)-, (+)-, and (–)-ganodilactones showed pancreatic lipase inhibitory activities with $IC_{50}$ values of 27.3, 4.0, and 2.5 $\mu M$, which were more active than that of vibralactone [84].

## Meroditerpenoids

Unlike the foregoing meroterpenoids, meroditerpenoids are found mainly in higher fungi and sponges. The terpenoid moiety of mushroom-derived meroditerpenoids always exhibits a linear geranyl moiety. Many compounds of this type were included as "Compounds Derived from 4-Hydroxybenzoic Acid" in previous reviews [1–6].

Cochlearoids C (**116**) and D (**117**) are two meroditerpenoids isolated from the medicinal fungus *G. cochlear*. The geranyl moiety of these two compounds remains uncyclized (Fig. 7) [74].

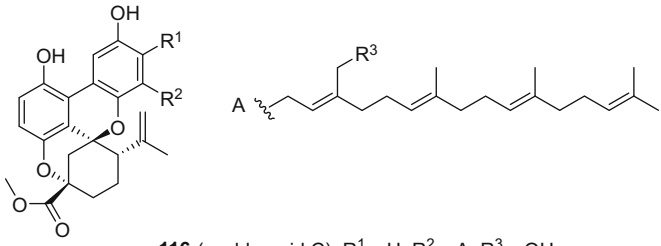


**116** (cochlearoid C) $R^1$ = H, $R^2$ = A, $R^3$ = OH
**117** (cochlearoid D) $R^1$ = A, $R^2$ = H, $R^3$ = OH

**Fig. 7** Structures of meroditerpenoids

## *2.3 Pigments from the Acetate-Malonate Pathway*

### 2.3.1 Pentaketides

A bioassay-guided isolation of the chloroform extract of the dried fruiting bodies of *Hypoxylon truncatum* gave hypoxylonols C–F (**120**–**123**), three reduced benzo[*j*] fluoranthene derivatives, together with hypoxylonols A (**118**) and B (**119**) (Fig. 8, Table 7) [86, 87]. Their structures were established by analysis of NMR spectroscopic data. The structures of hypoxylonols B, C, E, and F were confirmed by X-ray diffraction. Hypoxylonols D and E showed antiproliferative activity against human umbilical vein endothelial cells (HUVECs) with $IC_{50}$ values of 6.9 and 7.4 μ*M*, and against human umbilical artery endothelial cells (HUAECs) with $IC_{50}$ values of 6.1 and 4.1 μ*M*. A biological study suggested that hypoxylonol C has a dual effect against HUVECs. On the one hand, hypoxylonol C arrested the cell cycle at the G2/M phase by down-regulation of cell cycle-related gene expression, while, on the other hand, it inhibited angiogenesis of vascular endothelial cells by suppressing the expression of adhesion molecules [87].

In the form of a yellow powder, daldinone E (**124**) was isolated from the solid fermentation on "Cheerios™" breakfast cereal medium treated with the epigenetic modifier, suberoylanilide hydroxamic acid (SAHA), at a concentration of 800 μ*M*, and co-occurred with the known compound daldinone B (**125**) (Fig. 8). Interestingly, daldinone B appeared in both SAHA-treated and control cultures, while daldinone E could only be found from the SAHA-treated cultures. Their structures as well as their absolute configurations were established by spectroscopic methods and DFT calculations of specific rotations and ECD spectra. Structurally, daldinone E contains a chlorine atom. Daldinone B was proven to be established erroneously, and its structure was revised in this report (Fig. 8). Both compounds exhibited DPPH radical-scavenging activities with potencies comparable to the positive control ascorbic acid ($IC_{50}$ 3.2 μ*M*) [88].

A chemical study of the fruiting bodies of a mixture of *Annulohypoxylon* sp., *A. leptascum*, and *A.* cf. *truncatum*, which were collected from Argentina, Thailand, and the USA, led to the isolation of six benzo[*j*]fluoranthene pigments, truncatones

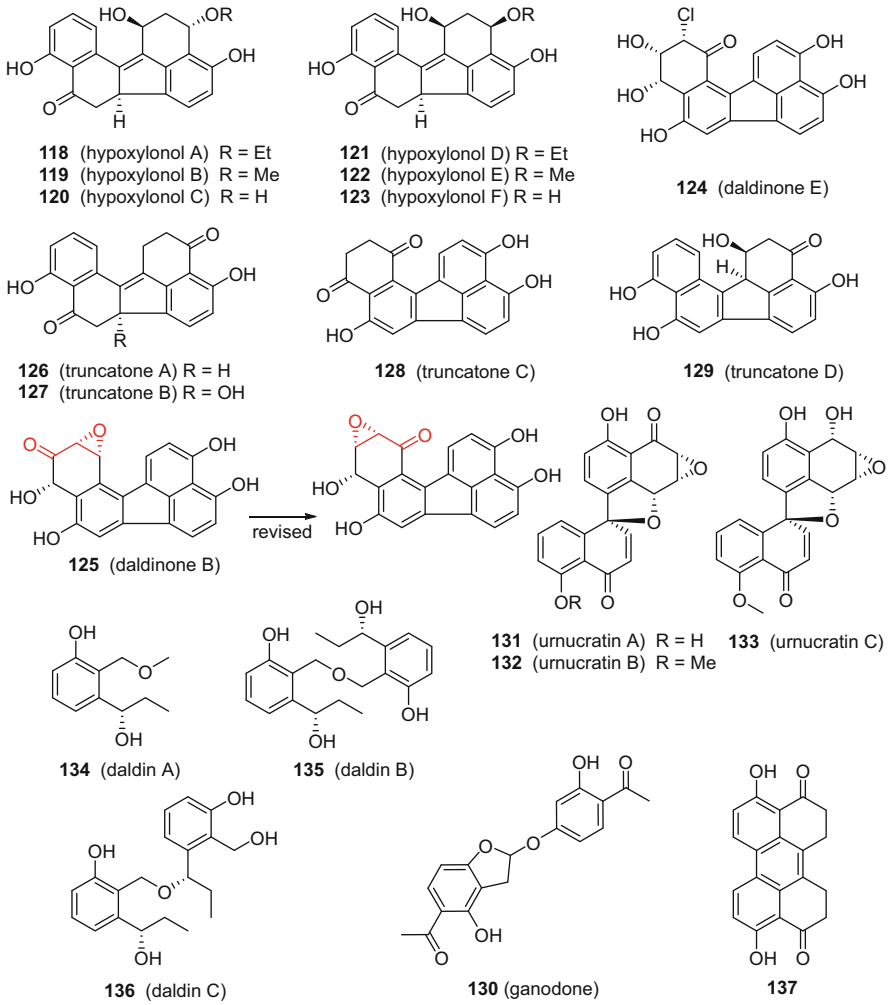


**Fig. 8** Structures of pentaketide pigments

B–D (**127**–**129**), along with the known compounds truncatone A (**126**), and hypoxylonols C and F (Fig. 8). The absolute configurations of truncatones A, B, and D were determined by CD spectroscopy. Truncatones A, C, and D showed moderate antiproliferative activities against the L-929 murine fibroblast cell line, with $IC_{50}$ values of 3.2, 7.0, and 1.1 $\mu M$, respectively [89].

Ganodone (**130**) is a benzofuran derivative isolated from the mature fruiting bodies of *Ganoderma tsugae* (Fig. 8). This compound possesses only one chiral carbon, and enantioselective HPLC analysis suggested its optically pure character on purification. The structural assignment of **130** was confirmed by chemical synthesis of racemic ganodone, while the absolute configuration remained

**Table 7** Pentaketide pigments

| Compound[a] | | Origin | Type | Refs. |
|---|---|---|---|---|
| Hypoxylonols C–F (**118–123**) | | *Hypoxylon truncatum* | Benzo[*j*]fluoranthene | [86, 87] |
| Daldinones B (**125**) and E (**124**) | | *Daldinia* sp. | Benzo[*j*]fluoranthene | [88] |
| Truncatones A–D (**126–129**) | | *Annulohypoxylon* sp.<br>*A. leptascum*<br>*A.* cf. *truncatum* | Benzo[*j*]fluoranthene | [89] |
| Ganodone (**130**) | | *Ganoderma tsugae* | Benzofuran | [90] |
| Urnucratins A–C (**131–133**) | | *Urnula craterium* | Spirobinaphthalene | [91] |
| Daldins A–C (**134–136**) | | *Daldinia concentrica* | Benzene derivative | [92] |
| 4,9-Dihydroxy-1,2,11, 12-tetrahydroperyl-ene-3, 10-quinone (**137**) | | *Bulgaria inquinans* | Perylenequinone | [93] |

[a]Color of compound in adjoining column

undetermined due to X-ray diffraction results conducted with an unsatisfactory Flack parameter value. Bioassay results using an MTT assay showed that **130** displayed potent cytostatic activity against the HCT-116, HeLa, and Neuro2a cell lines, with $IC_{50}$ values of 0.22 ± 0.01, 0.49 ± 0.03, and 0.081 ± 0.019 μ*M* [90].

A crude extract obtained from the saprobic North American cup fungus *Urnula craterium* exhibited promising antibacterial activity. A bioassay-guided isolation procedure used for this extract led to the discovery of three new spirobinaphthalenes, urnucratins A–C (**131–133**) (Fig. 8). Their structures were determined by means of spectroscopic data analysis and supported by quantum chemical CD calculations. Urnucratins A (**131**) and B (**132**) displayed the most promising antimicrobial potencies against the Gram-positive bacteria *Staphylococcus aureus* (ATCC 29213), methicillin-resistant *S. aureus* (MRSA), vancomycin-resistant *Enterococcus faecium* (ATCC), *E. faecalis* (ATCC 29212), and *Streptococcus pyogenes*, with an *MIC* value of 0.5 μg/cm$^3$ obtained for urnucratin A against both *E. faecalis* and *S. pyogenes*. However, none of these three compounds displayed inhibitory activities against Gram-negative bacteria [91].

The culture broth of *D. concentrica* yielded three new polyketides named daldins A–C (**134–136**), along with the known compound 2-hydroxymethyl-3-(1-hydroxypropyl)phenol (Fig. 8). The absolute configuration at a chiral oxygenated methine stereocenter in compounds **134–136** was established as (*S*) based on X-ray diffraction analysis, literature information, and comparison of optical rotation values [92].

Yellow needles of 4,9-dihydroxy-1,2,11,12-tetrahydroperyl-ene-3,10-quinone (**137**) were reported from the fungus *Bulgaria inquinans*, which is widely

distributed in the northern part of the People's Republic of China (Fig. 8). However, this perylenequinone pigment was not included in a previous review [93].

### 2.3.2 Hexaketides

Seven azaphilone pigments, lenormandins A–G (**138**–**144**), were isolated from the inedible fungus *Hypoxylon lenormandii* (Fig. 9, Table 8). Interestingly, HPLC analysis revealed that these compounds also occurred in herbarium specimens including various type materials collected in the nineteenth and early twentieth

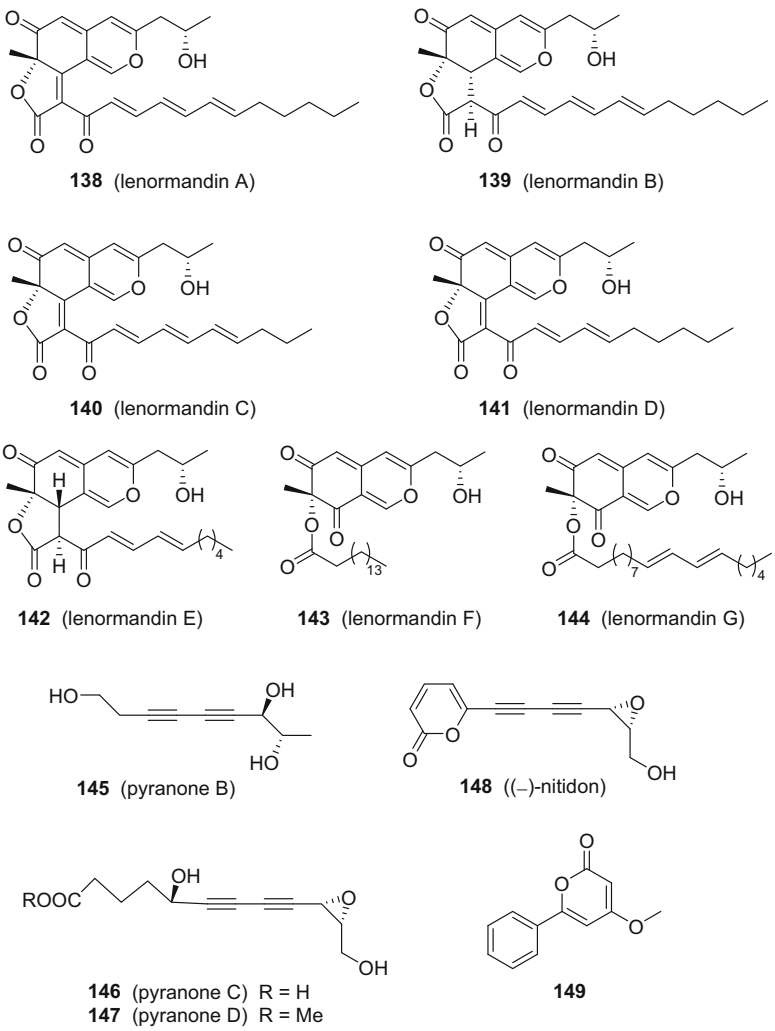


**Fig. 9** Structures of hexaketide pigments

**Table 8** Hexaketides

| Compound[a] | | Origin | Type | Refs. |
|---|---|---|---|---|
| Lenormandins A–G (**138–144**) | | *Hypoxylon lenormandii* | Azaphilone | [94] |
| Pyranones B–D (**145–147**) | | *Junghuhnia nitida* | Acetylene | [95] |
| (−)-Nitidon (**148**) | | *Junghuhnia nitida* | Acetylene | [95] |
| 4-Methoxy-6-phenyl-2*H*-pyran-2-one (**149**) | | *Sarcodon scabrosus* | Hexaketide | [96] |

[a]Color of compound in adjoining column

centuries, suggesting this group of pigments is specific for *H. lenormandii* from various geographic regions [94].

Pyranones B–D (**145–147**) and (–)-nitidon (**148**) are four highly unsaturated and conjugated compounds that were isolated from the culture broth of *Junghuhnia nitida* (Fig. 9). Their absolute configurations were determined by a matrix method or ECD calculations. Pyranones B–D were evaluated for their cytotoxicity against five human cancer cell lines (MCF-7, SMMC-7721, HL-60, SW480, and A-549), but none of them exhibited discernible inhibitory activity at the concentrations used [95].

The rare α-pyrone, 4-methoxy-6-phenyl-2*H*-pyran-2-one (**149**), was isolated from the bitter-tasting mushroom *Sarcodon scabrosus*, which was reported to afford mainly cyathane diterpenoids and terphenyl pigments (Fig. 9). This compound showed inhibition on lettuce seedling radicle growth with an $EC_{50}$ value of 0.446 μmol/cm$^3$ [96].

### 2.3.3 Octaketides

Azaphilone Pigments

Cohaerins G (**150**), H (**151**), I (**152**), and K (**153**) are yellowish azaphilone pigments isolated from the fruiting bodies of *Annulohypoxylon cohaerensi*. They were accompanied by the known azaphilones, cohaerins C–F. The absolute configurations were assigned by NOE experiments, CD spectroscopy, and use of a modified Mosher's method, which led to a revision of the absolute configurations of cohaerins C–F (Fig. 10) [97].

Anthraquinone and Anthraquinone Carboxylic Acids

The ascomycete *Bulgaria inquinans* is a wood-inhabiting fungus widely distributed in northern mainland China. After treatment with $Na_2CO_3$, the fruiting bodies are edible. A chemical investigation of the chloroform layer of a 70% ethanol extract of this fungus led to the isolation of the two anthraquinone derivatives bulgareone A

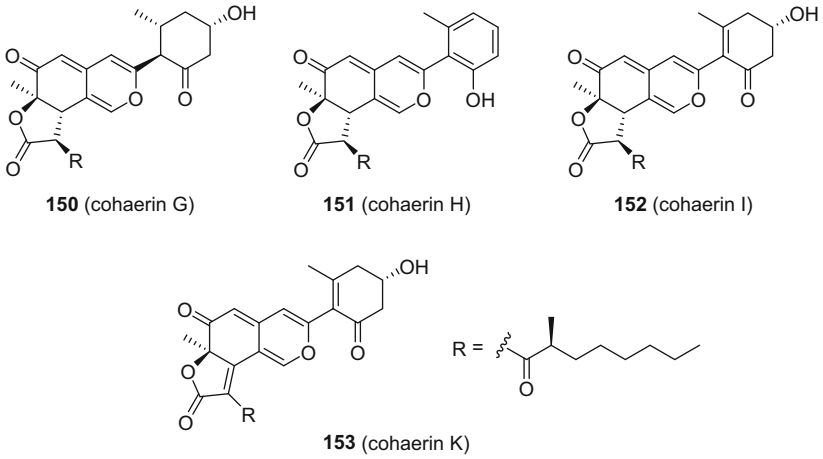


**Fig. 10** Octaketide azaphilone pigments

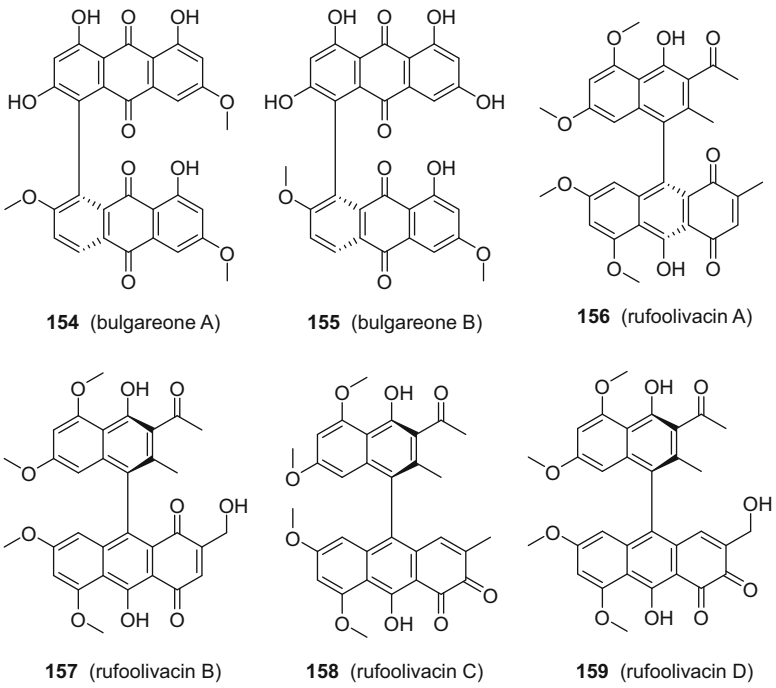


**Fig. 11** Structures of anthraquinones

(**154**) and B (**155**) (Fig. 11, Table 9). Both were purified as dark-red amorphous powders. The absolute configurations of the biphenyl bond were established as (*R*) in each case, based on the positive Cotton effect observed at 430 nm, corresponding

**Table 9** Anthraquinones

| Compound[a] | | Origin | Type | Refs. |
|---|---|---|---|---|
| Bulgareones A (**154**), B (**155**) | | *Bulgaria inquinans* | Anthraquinone | [98] |
| Rufoolivacins A–D (**156**–**159**) | | *Cortinarius rufo-olivaceus* | Anthraquinone | [99] |

[a]Color of compound in adjoining column

to an anticlockwise orientation of the two long axes of the anthraquinone backbone [98].

The macrofungal genus *Cortinarus* is a rich source of polyketide pigments. Rufoolivacins A–D (**156**–**159**) are polyketide-derived pigments isolated from the Chinese toadstool *Cortinarius rufo-olivaceus* (Fig. 11). Rufoolivacins C and D are unusual pigments incorporating an *ortho*-anthraquinone chromophore. Their structures as well as the axial chiralities were assigned through extensive spectroscopy and quantum calculations. All of these compounds proved to be toxic towards the brine shrimp [99].

## Coupled Pre-anthraquinones

The Tasmanian mushroom *Cortinatius vinpsipes* yielded a new violet-red 1,4-anthraquinone dimer, austrocolorone B (**160**), and a yellow dihydroanthracenone dimer, austrocolorin $B_1$ (**161**) (Fig. 12). In addition, **160** was assigned as the first naturally occurring 10,10′-coupled (or 9,9′-coupled) 1,4-anthracenedione dimer. The optical rotation value of austrocolorone B (–419 $cm^2/g$ (*c* 0.011, $CHCl_3$)) is due to the restricted rotation of the biaryl axis. The axial configurations of asymmetric bianthryls have been deduced from the shape of their CD spectra [10]. Based on this strategy, the absolute configuration of **160** was determined from its CD spectrum. Austrocolorone B and austrocolorin $B_1$ were evaluated against P388$D_1$ murine lymphoblast cells, and exhibited $IC_{50}$ values of 10 and 31 μg/$cm^3$ [100].

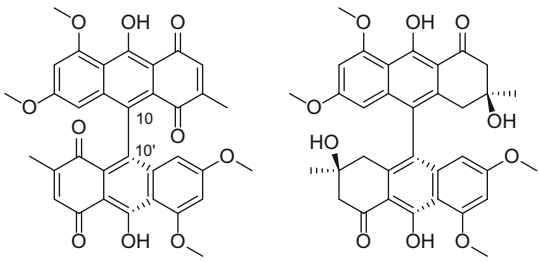


**160** (austrocolorone B) **161** (austrocolorin $B_1$)

**Fig. 12** Coupled pre-anthraquinones

### 2.3.4 Meroterpenoids Derived from the Acetate-Malonate Pathway

Meroterpenoids derived from mixed acetate–malonate and mevalonate pathways are structurally similar but less complex when compared to meroterpenoids derived from the shikimate pathway. This type of meroterpenoid was reported from various genera of Basidiomycetes, mainly *Stereum*, *Hericium*, and *Albatrellus* (Table 10). Biosynthesis considerations, as depicted in Scheme 10, suggested that four units of acetyl CoA undergo an aldol reaction and aromatization to yield the key intermediate, orsellinic acid thioester (**162**). Two molecules of orsellinic acid thioester could then dimerize through an intermolecular ester bond and become prenylated to give the *Stereum* meroterpenoids (pathway A). On the other hand, orsellinic acid can be directly geranylated and after further modifications could give *Hericium* meroterpenoids (pathway B). Through pathway C, orsellinic acid could become decarboxylated and further farnesylated to yield the *Albatrellus* meroterpenoids.

The edible Lion's Mane mushroom (*H. erinaceum*) has been used as a Traditional Chinese Medicine for a long time. Numerous publications have dealt with the secondary metabolites as well as their biological activities isolated from *H. erinaceum* (Table 10). Interestingly, most of the meroterpenoids derived from *H. erinaceum* display high structural similarities with mycophenolic acid (**163**), which is used as an immunosuppressant drug to prevent rejection in organ transplantation. The terpenoid parts of *Hericium*-derived meroterpenoids are farnesyl groups with oxygenated modifications. It should be pointed out that the meroterpenoids containing a nitrogen atom will be included in the next Section and classified as isoindolones.

Hericenone A (**164**) displayed growth inhibition of HeLa cells at a concentration of 100 μg/cm$^3$ (Fig. 13) [101]. Hericenones C–H (**165**–**170**), L (**171**), erinacene D (**172**), and 3-hydrohericenone F (**173**) are meroterpenoid fatty acid esters (Fig. 13). Their common fatty acid moieties are palmitoyl, stearoyl, and linoleoyl. Biological studies of these meroterpenoid fatty acid esters revealed that this type of compound possesses nerve growth factor (NGF)-stimulating activities depending on the chain length and nature of the double bond of the fatty acid moiety. Hericenones C, D, and E exhibited stimulatory activity on the synthesis of NGF in vitro. The activity level of hericenone D was almost at the same level as that of the potent stimulator epinephrine, while the activities of hericenone C (**172**) and E were weaker than that of hericenone D [102]. Structurally, hericenones F, G, and H possess a chroman scaffold formed by cyclization between the phenol group and C-3′ of the geranyl substituent, and all three were obtained as racemates. Hericenone H exhibited stimulant activity on the synthesis of NGF (45.1 ± 1.1 pg/cm$^3$ of NGF secreted into the medium in the presence of 33 μg/cm$^3$ of hericenone H), while hericenones F and G showed no activity under the same conditions [103].

3-Hydroxyhericenone F (**173**) was isolated from the mushroom *H. erinaceum* with the concomitant occurrence of hericenones I (**174**) and J (**175**) (Fig. 13). 3-Hydroxyhericenone F (**173**) was present in a racemic form as suggested by its CD spectroscopic data. These three isolates were subjected to testing in a protection

**Table 10** Meroterpenoids derived from the acetate-malonate pathway

| Compound[a] | | Origin | Refs. |
|---|---|---|---|
| Hericenones A (**164**), C-I (**165**–**170**), J (**175**), L (**171**) | | *Hericium erinaceum* | [101–105] |
| Isohericenone J (**176**) | | *Hericium erinaceum* | [106] |
| Erinacerin B (**178**) | | *Hericium erinaceum* | [107] |
| 3-Hydroxyhericenone F (**173**) | | *Hericium erinaceum* | [105] |
| Methyl 4-hydroxy-3-(3-methylbutanoyl)benzoate | | *Hericium erinaceum* | [108] |
| Erinacene D (**172**) | | *Hericium erinaceum* | [109] |
| Corallocin A (**177**) | | *Hericium coralloides* | [110] |
| Grifolin (**179**) | | *Albatrellus confluens* | [111] |
| Neoalbaconol (**180**) | | *Albatrellus confluens* | [112] |
| Albatrelins A–C (**181**–**183**) | | *Albatrellus ovinus* | [113] |
| Albatrelins D–F (**184**–**186**) | | *Albatrellus ovinus* | [113] |
| (*S*)-17-Hydroxy-18,20-ene-neogrifolin (**187**) | | *Albatrellus caeruleoporus* | [114] |
| (*S*)-18,19-Dihydroxyneogrifolin (**188**) | | *Albatrellus caeruleoporus* | [114] |
| (*S*)-9-Hydroxy-10,22-ene-neogrifolin (**189**) | | *Albatrellus caeruleoporus* | [114] |
| (9*S*,10*R*)-6,10-Epoxy-9-hydroxyneogrifolin (**190**) | | *Albatrellus caeruleoporus* | [114] |
| (9*S*,10*R*)-6,9-Epoxy-10-hydroxyneogrifolin (**191**) | | *Albatrellus caeruleoporus* | [114] |
| (−)-13,14-Dihydroxyneogrifolin (**192**) | | *Albatrellus caeruleoporus* | [114] |
| Albatrelins G (**193**) and H (**194**) | | *Albatrellus caeruleoporus* | [114] |
| (*S*)-10-Hydroxygrifolin (**195**) | | *Albatrellus caeruleoporus* | [114] |
| Cristatomentin (**196**) | | *Albatrellus cristatus* | [115] |
| Antroquinonol (**197**), antroquinonols B–D (**198**–**200**) | | *Antrodia cinnamomea* | [116–119] |

(continued)

**Table 10** (continued)

| Compound[a] | | Origin | Refs. |
|---|---|---|---|
| 4-Acetylantroquinonol B (**201**) | | *Antrodia cinnamomea* | [120] |
| Antrocamphins A (**202**), B (**203**) | | *Antrodia camphorata* | [121] |
| 2,3,4,5-Tetramethoxybenzoyl chloride (**213**) | | *Antrodia camphorata* | [121] |
| Antrodioxolanone (**207**) | | *Antrodia camphorata* | [121] |
| 2,2′,5,5′-Tetramethoxy-3,4,3′, 4′-bi-methylenedioxy-6,6′-dimethylbiphenyl (**208**) | | *Antrodia camphorata* | [122] |
| Benzocamphorins A (**204**), B (**205**) | | *Antrodia camphoratus* | [123] |
| Benzocamphorins C (**214**), D (**209**), E (**210**) | | *Antrodia camphoratus* | [123] |
| 4,7-Dimethoxy-5-methyl-1,3-benzodioxole (**215**) | | *Antrodia camphorata* | [124] |
| Antrocamphin O (**206**) | | *Antrodia camphorata* | [125] |
| 3-Isopropenyl-2-methoxy-6-methyl-4,5-methylenedioxyphenol (**216**) | | *Antrodia camphorata* | [126] |
| 2-Hydroxy-4,4′-dimethoxy-3,3′-dimethyl-5,6,5′, 6′-bimethylenedioxybiphenyl (**211**) | | *Antrodia camphorata* | [126] |
| 4,4′-Dihydroxy-3,3′-dimethoxy-2,2′-dimethyl-5,6,5′,6′-bimethylenedioxybiphenyl (**212**) | | *Antrodia camphorata* | [126] |
| Sterenins F (**217**) and G (**218**) | | *Stereum hirsutum* | [127] |
| Sterenins H–J (**219**–**221**) | | *Stereum hirsutum* | [127] |
| Compounds 1 (**222**), 2 (**223**) | | *Stereum hirsutum* | [128] |
| MS-3 (**224**) | | *Stereum hirsutum* | [128] |
| Hericenols A–D (**225**–**228**) | | *Stereum* sp. | [129] |
| 6-((2*E*,6*E*)-3,7-Dimethyldeca-2, 6-dienyl)-7-hydroxy-5-methoxy-4-methylphtanlan-1-one (**229**) | | *Laetiporus sulphureus* | [130] |

[a]Color of compound in adjoining column

assay targeted against endoplasmic reticulum (ER) stress-dependent cell death. 3-Hydroxyhericenone F showed dose-dependent and significant protective activity against both tunicamycin- and thapsigargin-induced toxicity, while hericenones I and J were inactive at concentrations of up to 10 μg/cm$^3$. However, the detailed mechanism of the effects of the compounds remained unresolved [105]. Kim et al. reported a molecule named isohericenone J (**176**) isolated from the fruiting bodies

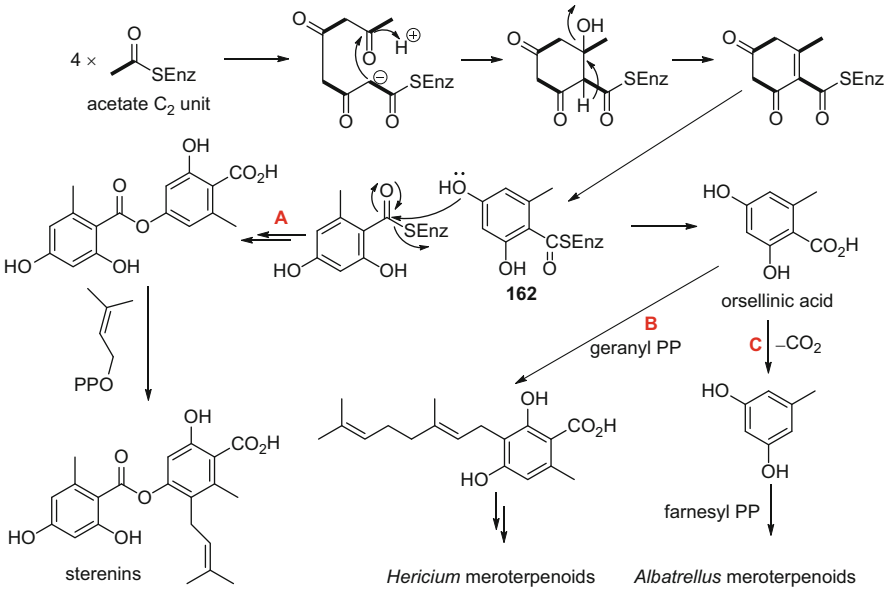


**Scheme 10** Biosynthesis pathways to the sterenins, and the *Hericium* and *Albatrellus* meroterpenoids

of *H. erinaceum*, although the NMR spectroscopic data were the same as those of hericenone J, suggesting the likelihood of structural misassignment of the latter compound [106].

Corallocin A (**177**) is a geranylated benzofuranone derivative isolated from the rarely investigated mushroom *H. coralloides* (Fig. 13). This compound was found to induce NGF and/or brain-derived neurotrophic factor expression in human 1321N1 astrocytes [110].

The inedible basidiomycetous genus *Albatrellus* produces nitrogen-free pigments (Table 10). The meroterpenoids derived from this genus are characterized by a farnesyl-substituted benzene ring. Among the reported pigments, grifolin (**179**) has been most studied meroterpenoid, and has proved to be a promising antitumor agent (Fig. 14). Grifolin (**179**) was isolated initially from the mushroom *Grifola confluens* and shown to act against the Gram-positive bacteria *Staphylococcus aureus* and *Bacillus subtilis* [131]. Later, in 2005, Liu and Cao et al. revealed the inhibitory activity of **179** against several tumor cell lines, including CNE1, HeLa, MCF-7, SW480, K562, Raji, and B95-8, by induction of apoptosis [132]. The natural abundance of **179** made it feasible to further study the molecular target and underlying mechanism of action of its cytotoxic activities. In-depth studies carried out by Liu and Cao et al. revealed that the ERK1/2 protein kinases are direct molecular targets of **179**, and that this molecule exerts its potential antitumor activity by epigenetic reactivation of metastasis inhibitory-related genes through ERK1/2-Elk1-DNMT1 signaling. This also suggests the role of **179** as an ERK1/2 kinase inhibitor as well as a useful epigenetic agent to further understand DNMT1

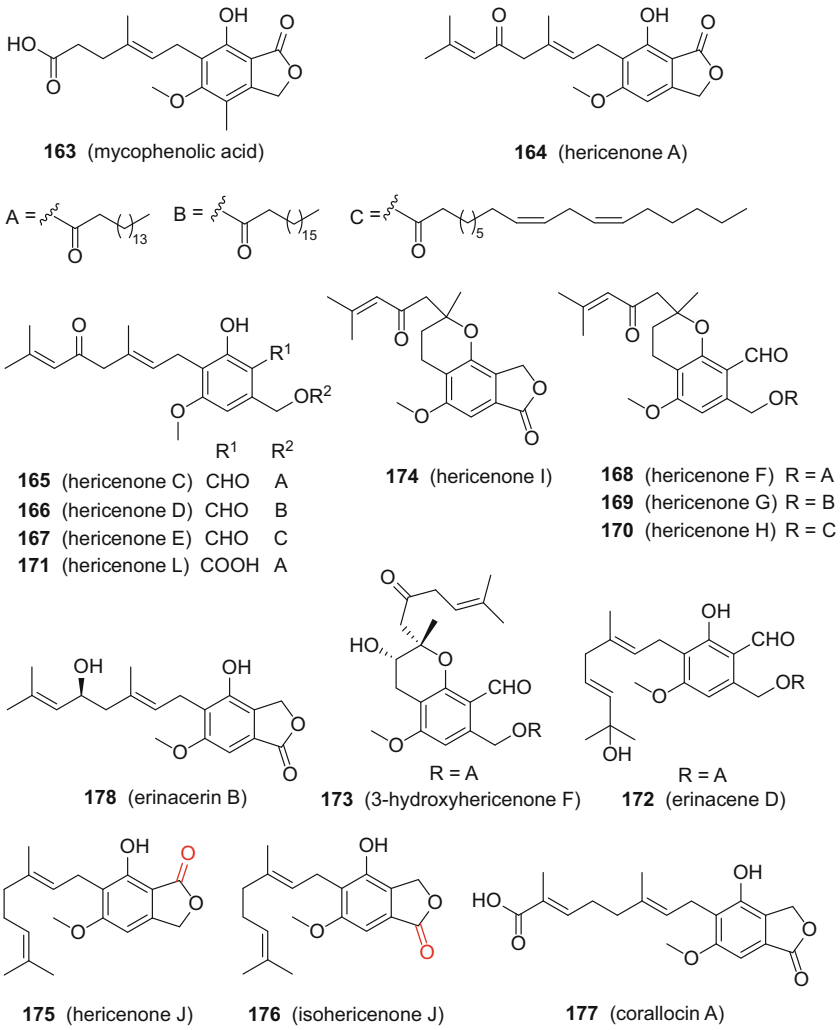


**Fig. 13** Meroterpenoids derived from the genus *Hericium*

function [133]. Moreover, **179** also decreased reactive oxygen species generation and intracellular ATP to suppress tumor cell adhesion/migration via impeding the interplay between peroxisome proliferator-activated receptor $\gamma$, coactivator $1\alpha$ (PGC1$\alpha$), and Fra-1/LSF-MMP2/CD33 axes [134]. Hence, grifolin (**179**) is a promising lead compound for further investigation of its antitumor potential.

Neoalbaconol (**180**) is a pigment isolated from the mushroom *A. confluens* (Fig. 14). Structurally, the terpenoid moiety of neoalbaconol can be regarded as a drimane rather than a linear farnesyl type. Biological investigations of this compound demonstrated that it can activate autophagy and cause apoptotic and necroptotic cell death by targeting 3-phosphoinositide-dependent protein kinase

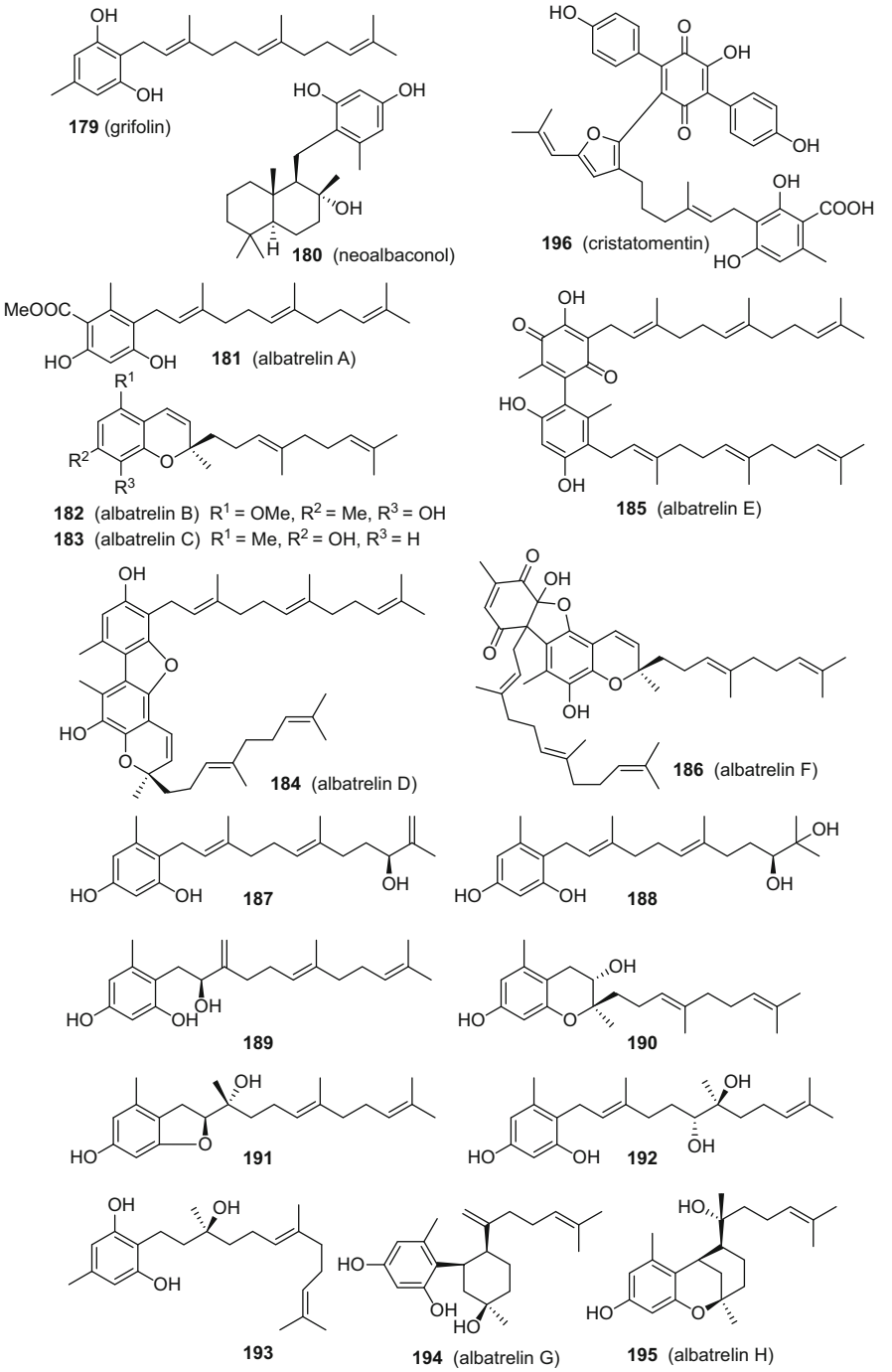


**Fig. 14** Meroterpenoids derived from the genus *Albatrellus*

1 (PDK1). It inhibited the downstream phosphoinositide-3 kinase (PI3-K)/Akt-hexokinase 2 (HK2) pathway, which eventually leads to energy depletion [135]. Further research suggested that neoalbaconol-induced cell death is partially dependent on TNF$\alpha$ feed-forward signaling. Moreover, neoalbaconol can abolish the ubiquitination of RIPK1 by down-regulating E3 ubiquitin ligases, cellular inhibitors of apoptosis protein 1/2 (cIAP1/2), and TNFα receptor-associated factors (TRAFs). Furthermore, this compound also causes RIPK3-mediated reactive oxygen species production and contributes to cell death [112].

Many grifolin derivatives were reported from the Basidiomycetes *A. ovinus* and *A. caeruleoporus*. Albatrelins A–F (**181**–**186**) were isolated from the fruiting bodies of *A. ovinus* collected in the eastern part of mainland China, of which albatrelins D–F are three novel dimers directly connected by two benzene rings (Fig. 14) [113].

A chemical investigation of the non-toxic but inedible mushroom *A. caeruleoporus* yielded various grifolin derivatives (**187**–**195**). All these isolated compounds were subjected to cytotoxicity assays against five human cancer cell lines (HL-60, SMMC-7721, A-549, MCF-7, and SW480). Of these substances, albatrelin G showed the most potent cytotoxicity against HL-60 cells, with an $IC_{50}$ value of 12.8 μ$M$ (Fig. 14) [114].

Cristatomentin (**196**) is a green pigment from the toadstool *A. cristatus*, and was proposed to be derived from the meroterpenoid cristatic acid and the terphenyl 2-*O*-acetlyatromentin, which co-occur with **196** in this mushroom (Fig. 14) [115].

The mushroom *Antrodia camphorata* is only found in Taiwan. Many publications have addressed the secondary metabolites of this medicinal species, which are mainly of the ergostane and lanostane triterpenoid types. Interestingly, merosesquiterpenoids were also found in this fungus but only in the cultured mycelium. So far, only five merosesquiterpenoids, namely, antroquinonol (**197**), antroquinonols B–D (**198**–**200**), and 4-acetylantroquinonol B (**201**), were reported (Table 10, Fig. 15). These antroquinonols display a chemical backbone similar to coenzyme Q and the plastoquinones, which are essential molecules for some life processes.

Antroquinonol (**197**) is the most abundant component from the mycelium of *A. camphorata*. It exhibits a broad spectrum of bioactivities, including anti-inflammatory and cytotoxic effects (Fig. 15). It was revealed that antroquinonol suppresses stem cell-like properties via targeting PI3K/AKT/$\beta$-catenin signaling [117]. Antroquinonol D (**200**) (3-demethoxyantroquinonol) is a DNA methyltransferase 1 inhibitor isolated from the mycelium of *A. camphorata* (Fig. 15). A thorough biological study suggested that **200** induces DNA demethylation and affects multiple tumor suppressor genes, while inhibiting breast cancer growth and migration potential [119]. The antiproliferative compound, 4-acetylantroquinonol B (**201**), was purified using antiproliferative activity toward HepG2 cells as a guide and was designated as the major potential antihepatoma constituent of *A. camphorata* (Fig. 15). The $EC_{50}$ value of this compound for HepG2 cells was 0.01±0.00 and 0.08±0.00 μg/cm$^3$ for 72 and 96 h treatments, respectively [120]. The biosynthesis pathways of antroquinonol and 4-acetylantroquinonol B were elucidated by Chou and co-workers [116]. The

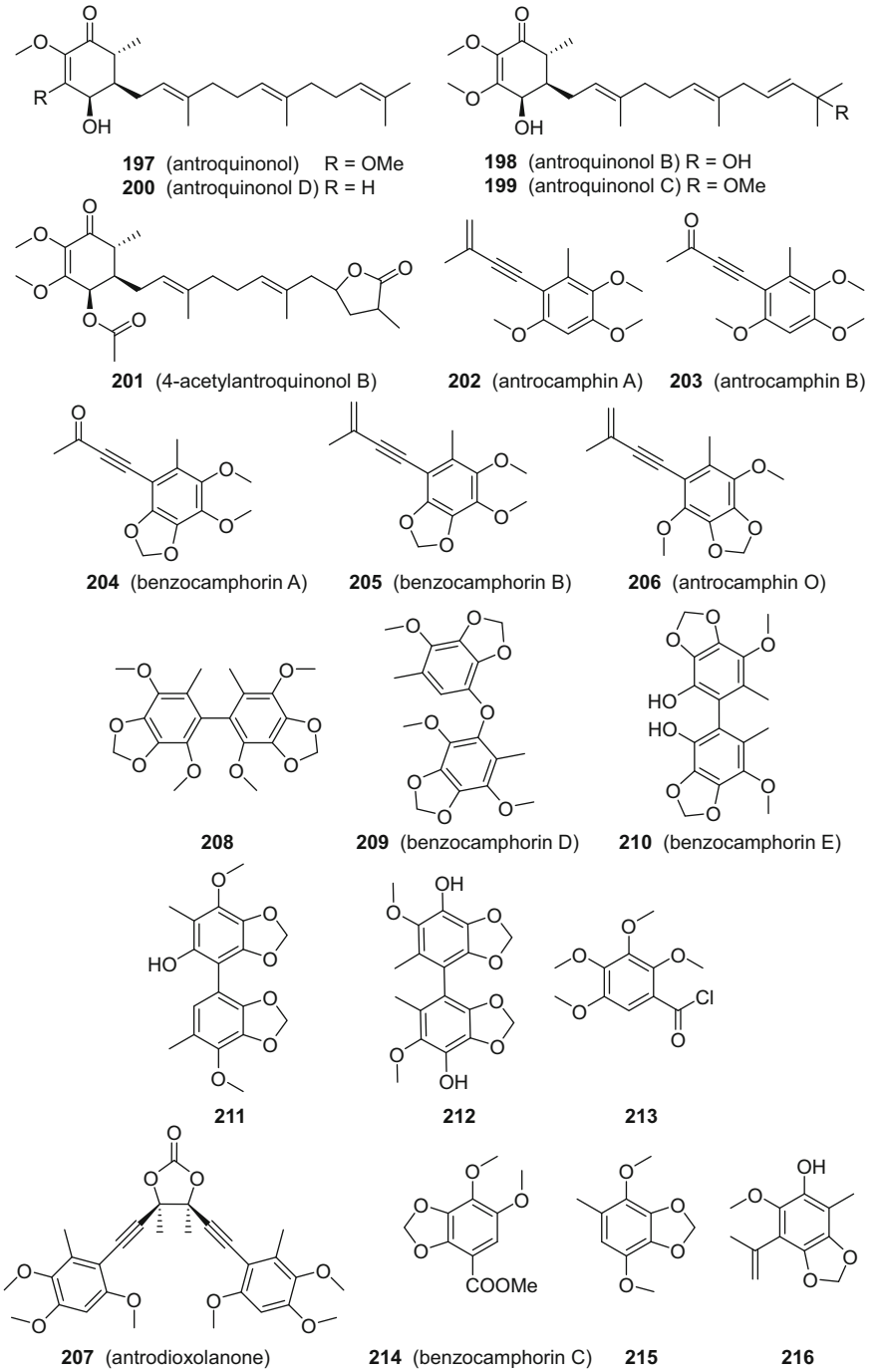


**Fig. 15** Meroterpenoids/benzenoids derived from *Antrodia camphorata*

total syntheses of antroquinonol (**197**) and antroquinonol D (**200**) were accomplished by Chen et al. via a route featuring an iridium-catalyzed olefin isomerization-Claisen rearrangement reaction, lactonization, and Grubbs olefin metathesis [118].

In addition to antroquinonol merosesquiterpenoids, *A. camphorata* has also been reported to produce benzenoid secondary metabolites. Some of these are prenylated benzene derivatives, while others are simple benzene derivatives or biphenyl compounds. Antrocamphins A (**202**) and B (**203**) [121], benzocamphorins A (**204**) and B (**205**) [123], and antrocamphin O (**206**) [125] are 3′-methylbut-3-en-1-ynyl or 3′-oxo-but-3-en-1-ynyl substituted benzenoids isolated from the fruiting bodies of *A. camphorata* (Fig. 15). These different substituents, which were recognized as arising from prenyl or *nor*-prenyl groups, play an important role in the mediation of their biological activities. Antrocamphin A (**202**) showed potent inhibition against *N*-formyl-methionyl-leucyl-phenylalanine-induced superoxide production with an $IC_{50}$ value of 9.33 ± 3.31 μ*M*, while antrocamphin B (**203**) was inactive in this regard [121]. Biological follow-up on the mechanism of the anti-inflammatory activity of compound **202** revealed that it suppresses pro-inflammatory molecular release via the down-regulation of iNOS and COX-2 expression through the NF-κB pathway [136]. Benzocamphorin B (**203**) also showed inhibition in relation to lipopolysaccharide-induced iNOS-dependent NO production with an $IC_{50}$ value of 12.1 ± 0 μ*M*, and NADPH oxidase (NOX)-dependent reactive oxygen species production with an $IC_{50}$ value of 14.4 ± 4.9 μ*M* [123]. Antrodioxolanone (**207**) is a rare carbonate-containing *meso* compound, which might be formed by intermolecular cyclization at the acetyl group of antrocamphin B (**203**) (Fig. 15) [121].

2,2′,5,5′-Tetramethoxy-3,4,3′,4′-bi-methylenedioxy-6,6′-dimethylbiphenyl (**208**) [122], benzocamphorins D (**209**) and E (**210**) [123], 2-hydroxy-4,4′-dimethoxy-3,3′-dimethyl-5,6,5′,6′-bimethylenedioxybiphenyl (**211**) [126], and 4,4′-dihydroxy-3,3′-dimethoxy-2,2′-dimethyl-5,6,5′,6′-bimethylenedioxybiphenyl (**212**) [126], are biphenyl compounds that were isolated from the fruiting bodies of *A. camphorata*. The benzene rings of **209** are connected via an ether bond, while the the other substituents are directly connected by carbon–carbon bonds (Fig. 15). Compound **212** inhibited LPS-induced NO production with an $IC_{50}$ value of 18.8 ± 0.6 μg/cm$^3$.

2,3,4,5-Tetramethoxybenzoyl chloride (**213**) [121], benzocamphorin C (**214**) [123], 4,7-dimethoxy-5-methyl-1,3-benzodioxole (**215**) [124], and 3-isopropenyl-2-methoxy-6-methyl-4,5-methylenedioxyphenol (**216**) [126] are four additional benzenoids obtained from the fruiting bodies of *A. camphorata* (Fig. 15). 2,3,4,5-Tetramethoxybenzoyl chloride was obtained as a natural product for the first time, and its structure was established via spectroscopic data interpretation and confirmed by a methanolysis experiment to give the corresponding benzoate. Compound **215** was isolated from three different sources of dried fruiting bodies of *A. camphorata*. Ho et al. have shown a potential role for compound **215** in cancer chemotherapy, which decreased tumor growth in a COLO-205 human colon cancer xenografted athymic nude mouse model, when injected intraperitoneally three times per week in the dose range 1–30 mg/kg body weight. Two mechanisms for the antitumor

activity of **215** were proposed: induction of p53-mediated p27/Kip1 protein levels, while not changing p21/Cip1 protein levels, and decreasing levels of the G0/G1 phase cell cycle regulators, cyclins D1, D3, and A. Compound **216** inhibited LPS-induced NO production in an in vitro bioassay, with an $IC_{50}$ value of 1.8 ± 0.2 μg/cm$^3$.

Sterenins E, and F–J (**217–221**) are meroterpenoids isolated from the solid fermentation of the fungus *Stereum hirsutum* (Fig. 16, Table 10). Salient structural differences between the sterenins and those of the above-mentioned meroterpenoids are the presence of additional orsellinic acid moieties and their shortened terpenoid moieties. Sterenins E–H showed inhibitory activities against yeast α-glucosidase with $IC_{50}$ values of 7.62, 3.06, 6.03, and 22.70 μ*M*, respectively, while sterenins I and J showed no activity of this type ($IC_{50}$ values of >50 μ*M*) [127]. Compounds 1 (**222**) and 2 (**223**) are two additional meroterpenoids isolated from another *S. hirsutum* strain collected on the Tibetan Plateau, along with the known compound, MS-3 (**224**) (Fig. 16). Both exhibited inhibitory activity against the

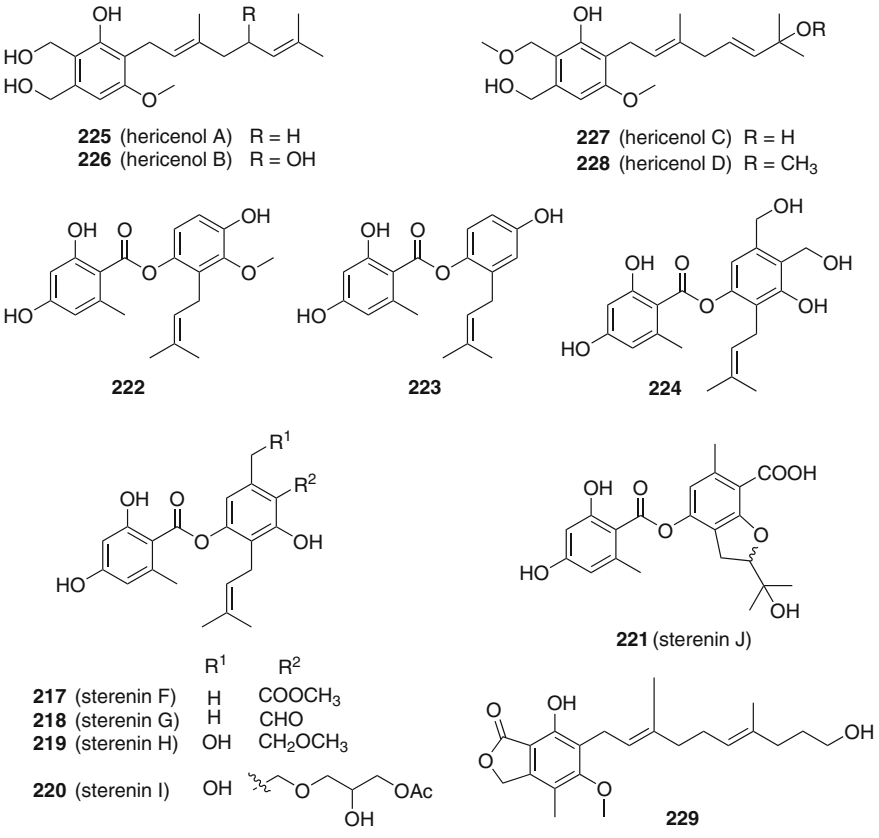


**Fig. 16** Meroterpenoids derived from the genus *Stereum* and the mushroom *Laetiporus sulphureus*

growth of *Staphylococcus aureus* and methicillin-resisitant *S. aureus* (MRSA) with the same *MIC* value of 25.0 μg/cm$^3$. Additionally, they also displayed antibacterial activities against *Bacillus subtilis*, with the respective *MIC* values of 25.0 and 50.0 μg/cm$^3$. Moreover, **222** displayed NO inhibitory activity in a LPS-induced macrophage in vitro bioassay with an $IC_{50}$ value of 19.17 ± 1.11 μ*M*. Compound **222** was evaluated for activity against A549 adenocarcinoma cells, and showed an $IC_{50}$ value of 13.14 ± 0.89 μ*M* [128].

Hericenols A–D (**225**–**228**) are *Stereum*-derived farnesyl-substituted benzene derivatives with structural similarities to those of the *Hericium*-derived meroterpenoids (Fig. 16). Hericenol A (**225**) showed weak antimicrobial activity, while hericenol C (**227**) exhibited cytotoxicity against COS-7 and COLO 320 cells, both with an $IC_{50}$ value of 5 μg/cm$^3$ [129].

Compound **229** is a mycophenolic acid analogue isolated from cultures of the mushroom *Laetiporus sulphureus*. This compound did not show any discernible cytotoxicity toward any of the HL-60, SMMC-7721, A-549, and MCF-7 cell lines at the concentration levels used (Fig. 16) [130].

### 2.3.5 Other Polyketides and Compounds of Fatty Acid Origin

As identified by large ribosomal subunit gene sequencing, a fungus designated BY1 was assigned to the Stereaceae family. When this fungus grown on a solid cultured medium was injured, the edges of the injured site turned to a yellow color 3–4 days after being wounded and the color remained unchanged for several weeks. HPLC-DAD analysis of an extract of the post-wounded BY1 mycelia revealed two major pigments. Their structures were established as (3*Z*,5*E*,7*E*,9*E*,11*E*,13*Z*,15*E*,17*E*)-18-methyl-19-oxoicosa-3,5,7,9,11,13,15,17-octaenoic acid (**230**) and (3*E*,5*Z*,7*E*,9*E*,11*E*,13*E*,15*Z*,17*E*,19*E*)-20-methyl-21-oxodocosa-3,5,7,9,11,13,15,17,19-nonaenoic acid (**231**), via extensive spectroscopic data acquisition and interpretation (Fig. 17). Anti-insect activity assays showed that these injury-elicited pigments may play a role in protecting the mycelium from feeding larvae. Both **230** and **231** showed selective antproliferative activities against K562 leukemia cells when compared with non-tumorigenic human umbilical vein epithelial cells (HUVECs). Thus, $GI_{50}$ values of 15.4 and 1.1 μ*M* were obtained for K-562 cells for **230** and **231**, respectively, compared with 71.6 and 17.4 μ*M* against HUVECs [137].

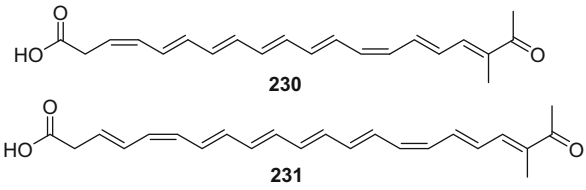


**Fig. 17** Pigments isolated from a wounded *Stereum* sp.

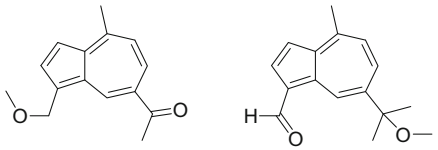


**232** (lactarioline A) **233** (lactarioline B)

**Fig. 18** Sesquiterpenoid pigments derived from the mushroom *Lactarius hatsudake*

## 2.4 Pigments from the Mevalonate Pathway

The edible mushroom *Lactarius hatsudake* yielded the blue and red guaiane sesquiterpene pigments lactariolines A (**232**) and B (**233**) (Fig. 18). Both were evaluated for their effects on the modulation of IFN-$\gamma$ in NK92 cells. The results showed that **232** and **255** inhibited IFN-$\gamma$ production in NK92 cells in a dose-dependent manner, corresponding to 56.7% inhibition at 400 μ*M* and 21.4% at 100 μ*M*, respectively, for **232**, and 80.9% inhibition at 400 μ*M* and 31.2% at 100 μ*M*, respectively, for **233** [138].

## 2.5 Pigments Containing Nitrogen

### 2.5.1 Indoles

Asterriquinones are members of tryptophan-derived indolyl benzoquinones that are found principally in Ascomycetes. This type of compound was shown to exhibit in vivo antitumor activities. The American fungus *Annulohypoxylon truncatum* collected in Texas yielded two deep-purple asterriquinone-type pigments, truncaquinones A (**234**) and B (**235**) as well as the known compound, truncatone (Fig. 19). The structures of compounds **234** and **235** were established by spectroscopic data analysis. The ambiguity of the position of a methoxy group in truncaquinone A was resolved using an HMBC experiment with extended long-range evolution delay times, which resulted in the appearance of $^4J_{CH}$ correlations from H-2″ to C-1 and C-3. Both compounds displayed weak activity against the

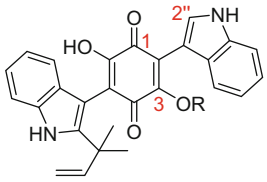


**234** (truncaquinone A) R = $CH_3$
**235** (truncaquinone B) R = H

**Fig. 19** Asterriquinone pigments isolated from *Annulohypoxylon truncatum*

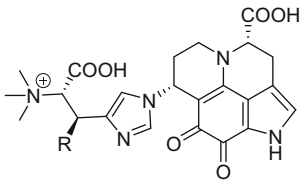


**236** (pelianthinarubin A) R = H
**237** (pelianthinarubin B) R = OH

**Fig. 20** Quinolines from the mushroom *Mycena pelianthina*

Gram-positive bacteria *Bacillus subtilis* and *Staphylococcus aureus*, with respective *MIC* values of 66.7 μg/cm$^3$ (for A and B) and 33.3/16.7 (for A and B). In addition, they were evaluated for their comparative cytotoxic effects against KB3.1 cancer cells ($IC_{50}$ 5.8 and 5.3 μ*M*, respectively) and the murine L-929 normal fibroblast cell line ($IC_{50}$ 17.3 and 16.0 μ*M*, respectively) [139].

### 2.5.2 Quinolines

The mushroom *Mycena pelianthina* is distributed widely in hardwood and mixed hardwood-conifer forests in Europe and North America. A chemical investigation of this mushroom furnished two previously unknown pyrroloquinoline pigments, pelianthinarubins A (**236**) and B (**237**). These contain a (*S*)-hercynine moiety, and differ considerably from other pyrroloquinoline alkaloids (Fig. 20). The planar structures of **236** and **237** were deduced from their NMR spectroscopic data, and their absolute configurations were established by comparison of CD spectra with those of synthesized standard samples, and by analysis of NOE effects and $^1$H NMR coupling constants. It was proposed that these two pigments might play an ecological role in chemical defense since they were not active in a panel of bioassays utilized [140].

### 2.5.3 β-Carbolines

The mushroom genus *Cortinarius* is a rich source of β-carboline alkaloids. Infractopicrin (**238**) and 10-hydroxy-infractopicrin (**239**) are two polycyclic β-carboline alkaloids isolated from the toadstool *C. infractus* (Fig. 21). Both exhibited AChE-inhibitory activity and displayed a higher selectivity than galanthamine, while neither showed inhibition of BChE up to a concentration of 100 μ*M*. The mode of action was also investigated by means of docking studies, suggesting that the lack of $\pi$-$\pi$-interactions in BChE is responsible for the selectivity. Moreover, studies on other Alzheimer's disease pathology-related targets showed an inhibitory effect on self-aggregation of Aβ-peptides but not on ACh-induced Aβ-peptide aggregation [141].

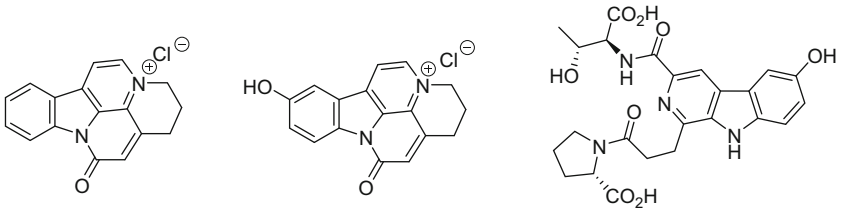


**238** (infractopicrin) **239** (10-hydroxy-infractopicrin) **240** (6-hydroxymetatacarboline D)

**Fig. 21** β-Carbolines from the mushroom *Cortinarius infractus* and *Mycena metata*

In the process of screening for β-carboline alkaloids using HR-MALDI-MS imaging of the mushroom *Mycena metata*, a series of alkaloids was detected and then isolated. 6-Hydroxymetatacarboline D (**240**) was the most abundant β-carboline alkaloid found, with its structure determined using 2D NMR spectroscopic methods and HR-ESIMS (Fig. 21). In order to determine its absolute configuration, 6-hydroxymetatacarboline D was hydrolyzed. The hydrolysis products were further derivatized to afford the resulting amino acids, for which their absolute configurations were determined by GC-MS comparison with authentic samples. Some minor constituents of *M. metata* were detected by application of LC-HR-ESIMS, LC-HR-ESIMS/MS, and LC-HR-ESIMS$^3$ techniques [142].

### 2.5.4 Polyenes with Tetramic Acid or Amino Acid End Groups

Mycenaaurin A (**241**) is an orange polyene pigment isolated from the fruiting bodies of the mushroom *Mycena aurantiomarginata* (Fig. 22). Structurally, mycenaaurin A consists of a tridecaketide and two amino acid moieties. The structure of mycenaaurin A was established from its 2D NMR spectroscopic data and by APCIMS. The absolute configuration was determined using chemical methods. Biological evaluation revealed **241** to show antimicrobial activity against *Bacillus pumilus* [143].

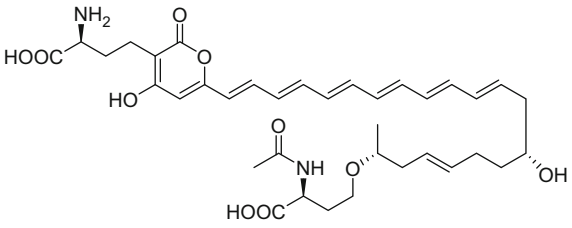


**241** (mycenaaurin A)

**Fig. 22** Structure of mycenaaurin A

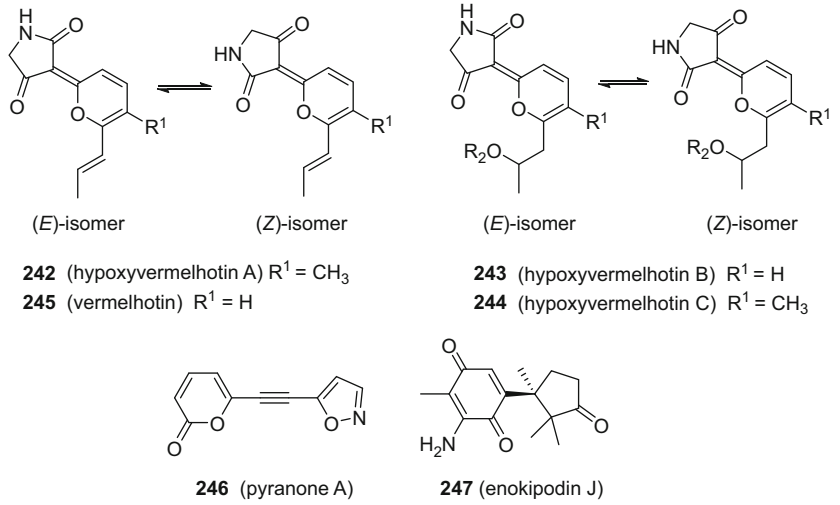


**Fig. 23** Structures of other pigments containing nitrogen

### 2.5.5 Other Pigments Containing Nitrogen

The four orange pigments, hypoxyvermelhotins A–C (**242**–**244**) and the known compound vermelhotin (**245**), were isolated from a newly classified species of the genus *Hypoxylon*, *H. lechatii* (Fig. 23). All four compounds were isolated as inseparable (*E*)/(*Z*) mixtures. When screened for cytotoxicity against the L-929 murine fibroblast cell line, of the compounds tested, **242** and **245** showed $IC_{50}$ values of 5.0 and 2.0 μg/cm$^3$. Additionally, **242** and **245** also displayed weak inhibition of *Mucor hiemalis* DSM 2656 and *Nematospora coryli* DSM 6981 [144].

The yellow oil pyranone A (**246**) is a pyranone- and isoxazole-containing compound isolated from a culture of the fungus *Junghuhnia nitida* (Fig. 23). Pyranone A was evaluated for cytotoxicity against five human cancer cell lines (MCF-7, SMMC-7721, HL-60, SW480, and A549) and showed comparable cytotoxic potencies to those of cisplatin [95]. Enokipodin J (**247**) was isolated as a purple powder from the rice fermentation of the edible mushroom *Flammulina velutipes* (Fig. 23). This compound represents the first example of a cuparane-type sesquiterpene containing an amino group [145].

## 3 Nitrogen-Containing Compounds of Higher Fungi

### *3.1 Introduction*

In this section, like in our previous reviews [146, 147], the chemical, biological, and mycological literature is covered dealing with the isolation, structure elucidation,

biological activities, and synthesis of nitrogen-containing compounds from the fruiting bodies or submerged cultures of macromycetes. The literature cited in this section covers reports that appeared in the years between 2010 and 2016.

## 3.2 Nitrogen Heterocycles

### 3.2.1 Indoles

Simple Indoles

It is well documented that the largest edible mushroom *Termitomyces titanicus* is always symbiotic with termites. Termites cultivate the mycelia in their nest and as a consequence the fruiting bodies arise on or near the mounds. The EtOAc- and EtOH-soluble extracts of this organism showed protective acitivity against endoplasmic reticulum stress-dependent cell death, leading to the isolation of the indole alkaloid termitomycamide B (**248**) from the EtOAc extract (Fig. 24) [148]. The structure of **248** was confirmed by the detection of linoleic acid and the corresponding amine. This compound was subjected to an evaluation of its protective activity against endoplasmic reticulum stress-dependent cell death caused by tunicamycin. It showed protective activity against tunicamycin-toxicity in a dose-dependent manner. A structure-activity relationship investigation revealed that the linoleic moiety of **248** is indispensable for this activity.

Three β-carboline alkaloids, cordysinins C–E (**249**–**251**), isolated from the medicinal fungus *Cordyceps sinensis*, were reported as new natural products (Fig. 24). Cordysinins C and D were obtained as enantiomers purified by chiral-phase HPLC and their absolute configurations were determined using the modified Mosher's method. The absolute configuration of cordysinin E (**251**) was established

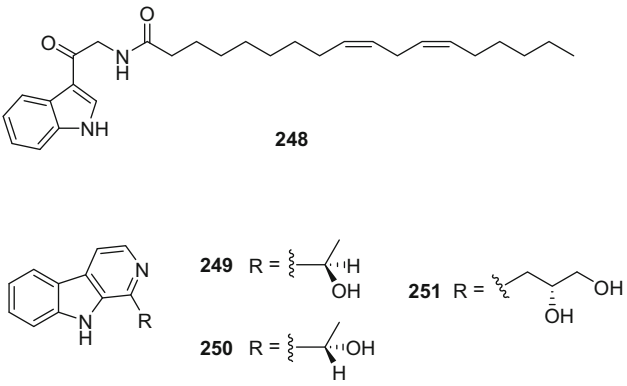


**Fig. 24** Structures of simple indoles

by comparison of its CD spectrum with those reported in the literature for related compounds [149].

## Isoindoles

Isoindoles account for the largest proportion of nitrogen-containing compounds derived from higher fungi. The edible mushroom *Hericium erinaceum* is a rich source of isoindoles both from its fruiting bodies and solid or liquid cultures (Table 11). Hericerin (**252**) was first isolated in 1991 from *H. erinaceum* (Fig. 25). It displayed significant inhibitory activity against pine pollen germination and tea pollen growth. However, the structure of **252** was established erroneously in the first report, and a structural revision was accomplished by total synthesis, showing that **252** should be revised to be the carbonyl regioisomer **253** [150, 151]. Indeed, Miyazawa et al. reported the same molecule and named it isohericerin [152], but with misassignments of the $^{13}C$ NMR data of C-3a and C-7a, which were corrected by Lee et al. [153].

Further investigation of the mushroom *H. erinaceum* led to the isolation of a series of isoindole compounds that differed in the substituents on the nitrogen atom and by varations of the geranyl side chain. Bioassay-guided isolation of an 80% aqueous MeOH extraction of the partially dried fruiting bodies of *H. erinaceum* led to the isolation of isohericenone (**255**) (Fig. 25). This compound showed cytotoxicity against the A549, SK-OV-3, SK-MEL-2, and HCT-15 cancer cell lines with respective $IC_{50}$ values of 2.6, 3.1, 1.9, and 2.9 μ*M* [153]. Hericerin A (**256**), isolated from the methanol extract of the fruiting bodies of *H. erinaceum* (Fig. 25), showed antiproliferative activity against HL-60 human acute promyelocytic leukemia cells with an $IC_{50}$ value of 3.06 μ*M* [106]. Fourteen new isoindole derivatives, namely, erinacerins C–L (**257–266**) and Q–T (**267–270**) as well as the known compound

**Table 11** Isoindoles isolated from the genus *Hericium*

| Compound | Origin | Refs. |
|---|---|---|
| Hericerin (**252**) | *Hericium erinaceum* | [150–152] |
| *N*-de-Phenylethyl isohericerin (**254**) | *Hericium erinaceum* | [152] |
| Isohericenone (**255**) | *Hericium erinaceum* | [153] |
| Hericerin A (**256**) | *Hericium erinaceum* | [106] |
| Erinacerins C–L (**257–266**), Q–T (**267–270**) | *Hericium erinaceum* | [154, 155] |
| Erinaceolactams A–E (**271–275**) | *Hericium erinaceum* | [156] |
| Corallocins B (**276**), C (**277**) | *Hericium coralloides* | [110] |
| Daldinan A (**278**) | *Daldinia concentrica* | [157] |
| Entonalactams A–C (**279–281**) | *Entonaema* sp. | [158] |
| 4,6-Dihydroxy-1*H*-isoindole-1,3(2*H*)-dione (**282**) | *Lasiosphaera fenzlii* | [159] |
| 4,6-Dihydroxy-2,3-dihydro-1*H*-isoindol-1-one (**283**) | *Lasiosphaera fenzlii* | [159] |
| Clitocybin A (**284**) | *Lasiosphaera fenzlii* | [159] |
| Sterenins K–M (**285–287**) | *Stereum hirsutum* | [127] |

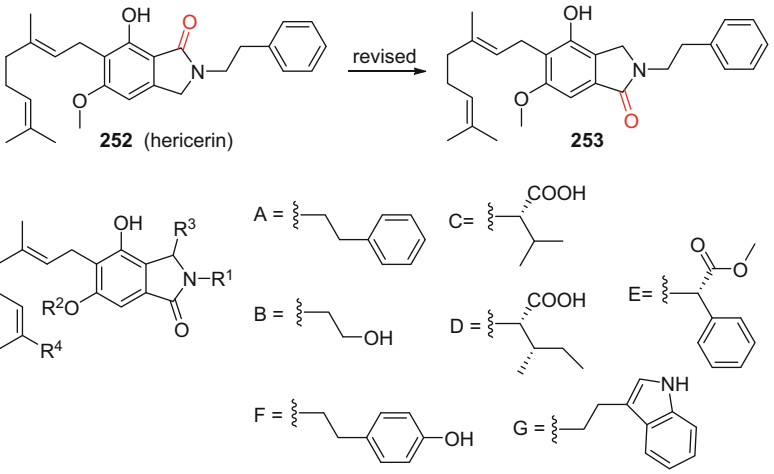


| | $R^1$ | $R^2$ | $R^3$ | $R^4$ | $R^5$ |
|---|---|---|---|---|---|
| **254** (N-de-phenylethyl isohericerin) | H | Me | H | H | H |
| **255** (isohericenone) | A | Me | H | H | =O |
| **256** (hericerin A) | B | Me | H | H | H |
| **257** (erinacerin C) | H | H | H | COOH | H |
| **258** (erinacerin D) | B | H | H | COOH | H |
| **259** (erinacerin E) | C | H | H | COOH | H |
| **260** (erinacerin F) | D | H | H | COOH | H |
| **267** (erinacerin Q) | A | H | H | COOH | H |
| **269** (erinacerin S) | H | H | =O | COOH | H |
| **271** (erinaceolactam A) | H | Me | H | H | =O |
| **272** (erinaceolactam B) | B | Me | H | H | =O |
| **276** (corallocin B) | F | Me | H | Me | H |
| **277** (corallocin C) | G | Me | H | Me | H |

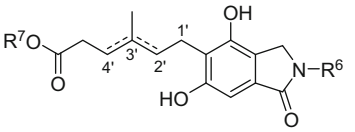


| | Δ | $R^6$ | $R^7$ |
|---|---|---|---|
| **261** (erinacerin G) | $\Delta^{2'}$ | H | Me |
| **262** (erinacerin H) | $\Delta^{3'}$ | H | Me |
| **263** (erinacerin I) | $\Delta^{2'}$ | B | Me |
| **264** (erinacerin J) | $\Delta^{3'}$ | B | Me |
| **265** (erinacerin K) | $\Delta^{2'}$ | E | Me |
| **266** (erinacerin L) | $\Delta^{3'}$ | E | Me |
| **268** (erinacerin R) | $\Delta^{2'}$ | H | Et |
| **270** (erinacerin T) | $\Delta^{2'}$ | H | Me |

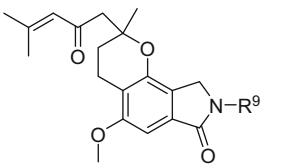


**273** (erinaceolactam C) $R^9$ = H

**274** (erinaceolactam D) $R^9$ = B

**275** (erinaceolactam E) $R^9$ =

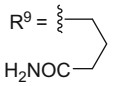


**Fig. 25** Structures of isoindoles isolated from the genus *Hericium*

hericerin (**252**) were isolated from the fermentation on rice of the mushroom *H. erinaceum* (Fig. 25) [154, 155]. Erinacerins E, F, K, and L were characterized by having amino acid moieties substituted on the nitrogen atom, of which the absolute configurations were established by comparing their specific rotation values with those of related synthetic phthalimidines. All compounds showed inhibitory activity against $\alpha$-glucosidase. The erinacerins displayed $IC_{50}$ values lower than 40 $\mu M$, with the exception of erinacerins G and I. Moreover, erinacerins Q–T exhibited inhibitory activity against protein tyrosine phosphatase-1B (PTP1B) with respective $IC_{50}$ values of 29.1, 42.1, 28.5, and 24.9 $\mu M$ [154].

Erinaceolactams A–E (**271**–**275**) were isolated from a 70% ethanol-soluble extract of the fruiting bodies of *H. erinaceum* (Fig. 25) [156]. It is noteworthy that erinaceolactams C–E were isolated as racemates since their specific rotations were nearly zero. This was verified by chiral-phase HPLC analysis and separation. Corallocins B (**276**) and C (**277**) are two isoindolinone derivatives isolated from the rarely investigated mushroom *H. coralloides* (Fig. 25). Both of these compounds induced nerve growth factor (NGF) and/or brain-derived neurotrophic factor expression in human 1321N1 astrocytes. Furthermore, **276** also showed antiproliferative activity against HUVECs and the MCF-7 and KB-3-1 human cancer cell lines [110].

The two genera *Daldinia* and *Entonaema* belonging to the family Xylariaceae were reported to produce isoindole alkaloids (Table 11). Daldinan A (**278**) is an isoindolinone isolated from a methanol extract of the fruiting bodies of *Daldinia concentrica*. However, its absolute configuration was not resolved [157]. Daldinan A (**278**) was judged as being inactive in a 1,1-diphenyl-2-picrylhydrazyl radical-scavenging assay, but active in a 2,2-azinobis(3-ethylbenzothiazoline-6-sulfonate) radical-scavenging assay with an $IC_{50}$ value of 10.4 $\mu M$, comparable to that of butylated hydroxyanisole ($IC_{50}$ 10.8 $\mu M$) (Fig. 26). A bioassay-guided fractionation of the Australian rainforest fungus *Entonaema* sp. resulted in the isolation of the three new isoindolinone derivatives, entonalactams A–C (**279**–**281**) (Fig. 26) [158]. All compounds were determined to be racemic based on specific rotation data and X-ray crystallographic analysis.

The fungus *Lasiosphaera fenzlii* is widely distributed in the People's Republic of China and is used in Traditional Chinese Medicine for the treatment of bleeding disorders. In an effort to search for tumor inhibitors from natural sources, three isoindole compounds were isolated from an EtOAc extract of this fungus [159]. They were identified as 4,6-dihydroxy-1*H*-isoindole-1,3(*2H*)-dione (**282**), 4,6-dihydroxy-2,3-dihydro-1*H*-isoindol-1-one (**283**), and clitocybin A (**284**) (Fig. 26). Compound **282** contains a phthalimide moiety with a similarity to that of thalidomide. All compounds were tested for their antiproliferative effects against the A549, PC-3, U87, and HeLa tumor cells and for in vitro antiangiogenic activity. The results showed that **282** displayed significant antiangiogenic activity, by inhibiting the secretion of vascular endothelial growth factor in A549 cells, and was more potent in this regard than thalidomide [159].

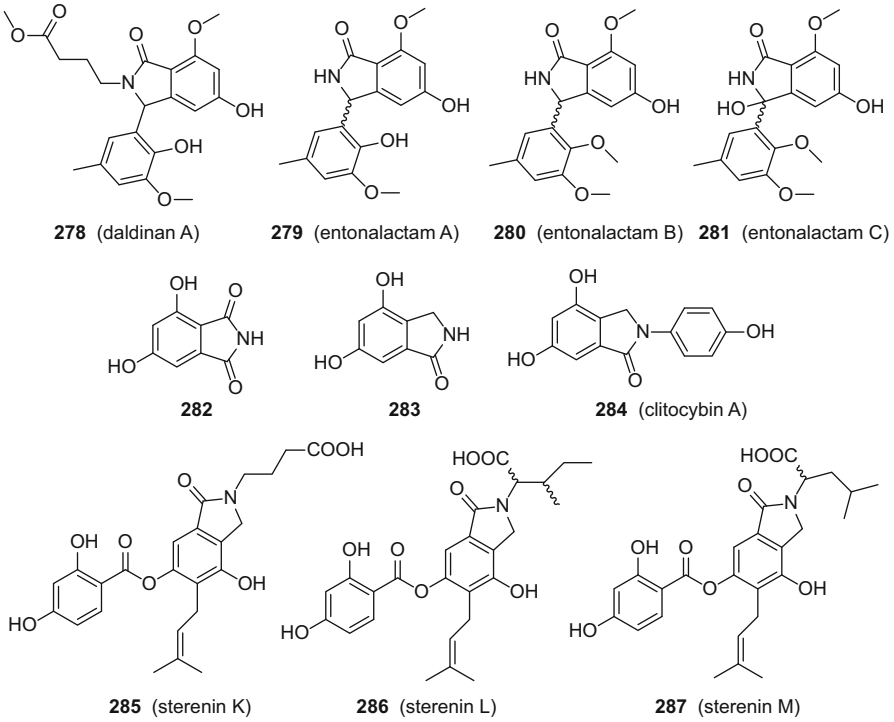


**Fig. 26** Structures of other isoindoles

Sterenins K–M (**285**–**287**) are three isoindole derivatives isolated from the fermentation on rice of the fungus *Stereum hirsutum* (Fig. 26). Sterenin L (**286**) showed $\alpha$-glucosidase inhibitory activity in vitro with an $IC_{50}$ value of 13.09 μ*M* [127].

### 3.2.2 Pyridines and Pyrroles

Several well-known medicinal fungi in the genus *Ganoderma* have been investigated extensively in terms of their secondary metabolites. The reported *Ganoderma* triterpenoids represent the largest group of such compounds that originate from higher fungi. Owing to the rapid development of experimental approaches and enhanced instrumentation used in natural products chemistry, many alkaloids, mainly pyridine-containing compounds, were characterized also from this genus (Table 12). Ganoine (**288**) and ganodine (**289**) represent the first examples of alkaloids containing a pyrrole ring isolated from the cultured mycelia of *G. capense* (Fig. 27) [160]. Sinensine (**290**) was the first pyridine-containing alkaloid isolated from the fruiting bodies of *G. sinense* (Fig. 27) [161]. This compound exhibited protective activity against hydrogen peroxide-mediated injury in HUVEC cells with an $EC_{50}$ value of 6.2 μ*M*. A further chemical investigation of

**Table 12** Pyridines and pyrroles

| Compound | Origin | Type | Refs. |
|---|---|---|---|
| Ganoine (**288**) | *Ganoderma capense* | Pyrrole-containing | [160] |
| Ganodine (**289**) | *Ganoderma capense* | Pyrrole-containing | [160] |
| Sinensine (**290**) | *Ganoderma sinense* | Pyridine-containing | [161] |
| Sinensines B–E (**291–294**) | *Ganoderma sinense* | Pyridine-containing | [162] |
| Lucidimines A–D (**295–298**) | *Ganoderma lucidum* | Pyridine-containing | [163] |
| Petchine (**299**) | *Ganoderma petchine* | Pyridine-containing | [164] |
| 3-Hydroxy-5-methyl-5,6-dihydro-7*H*-cyclopenta[*b*]pyridin-7-one (**300**) | *Ganoderma petchine* | Pyridine-containing | [164] |
| Termitomycamide C (**301**) | *Termitomyces titanicus* | Pyridine-containing | [148] |
| Sterostreins M–O (**302–304**) | *Stereumostrea* BCC22955 | Pyridine-containing | [165] |
| Divaricatines C (**305**), D (**306**) | *Clavicorona divaricata* | Pyridine-containing | [166] |
| Acuminatopyrone (**312**) | *Xylaria allantoidea* | Pyridine-containing | [167] |
| Erinacerins M–P (**313–316**) | *Hericium erinaceum* | Pyridine-containing | [154] |
| Pyristriatins A (**307**), B (**308**) | *Cyathus* cf. *striatus* | Pyridine-containing | [168] |
| Orellanine (**317**) ☠ | *Cortinarius orellanus* *Cortinarius rubellus* | Pyridine-containing | [169] |
| Orellanine-4-glucopyranoside (**318**) ☠ | *Cortinarius orellanus* *Cortinarius rubellus* | Pyridine-containing | [169] |
| Orellanine-4,4′-diglucopyranoside (**319**) ☠ | *Cortinarius orellanus* *Cortinarius rubellus* | Pyridine-containing | [169] |
| Radianspenes J–L (**309–311**) | *Coprinus radians* | Pyrrole-containing | [170] |
| Compound 1 (**320**) | *Flammulina velutipes* | Pyrrole-containing | [171] |
| 2-[2-Formyl-5-(methoxymethyl)-1*H*-pyrrol-1-yl] acetic acid (**321**) | *Leccinum extremiorientale* | Pyrrole-containing | [172] |
| (2*S*)-1-[2-(Furan-2-yl)-2-oxoethyl]-5-oxopyrrolidine-2-carboxylate (**322**) | *Armillaria mellea* | Pyrrole-containing | [173] |
| (2*S*)-1-[2-(Furan-2-yl)-2-oxoethyl]-5-oxopyrrolidine-2-carboxylic acid (**323**) | *Armillaria mellea* | Pyrrole-containing | [173] |
| 1-[2-(Furan-2-yl)-2-oxoethyl]pyrrolidin-2-one (**324**) | *Armillaria mellea* | Pyrrole-containing | [173] |

(continued)

**Table 12** (continued)

| Compound | Origin | Type | Refs. |
|---|---|---|---|
| (4*S*)-3,4-Dihydro-4-(4-hydroxybenzyl)-3-oxo-1*H*-pyrrolo[2,1-*c*][1,4]oxazine-6-carbaldehyde (**325**) | *Xylaria nigripes* | Pyrrole-containing | [174] |
| Methyl (2*S*)-2-[2-formyl-5-(hydroxymethyl)-1*H*-pyrrol-1-yl]-3-(4-hydroxyphenyl)propanoate (**326**) | *Xylaria nigripes* | Pyrrole-containing | [174] |
| Xylapyrrosides A (**327**), B (**328**) | *Xylaria nigripes* | Pyrrole-containing | [175] |
| Pollenopyrrosides A (**329**), B (**330**) | *Xylaria nigripes* | Pyrrole-containing | [175] |

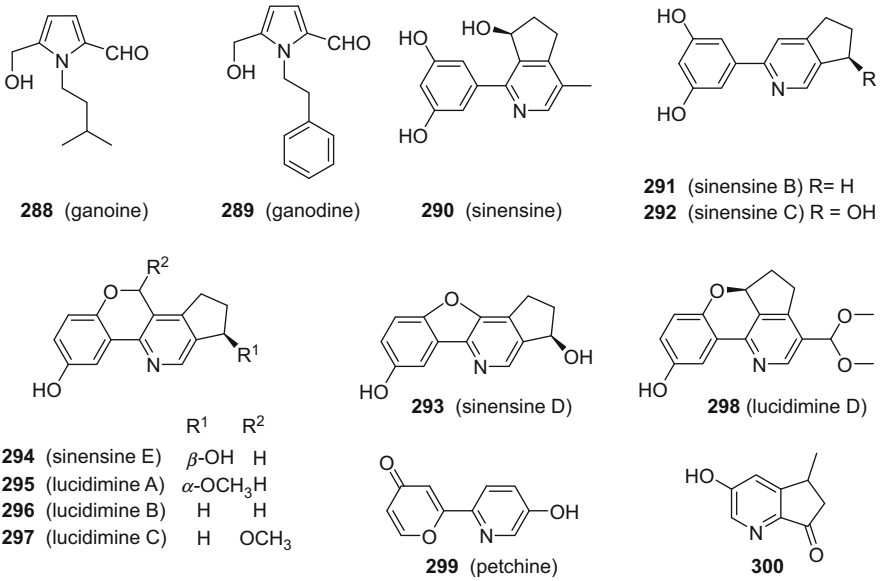


**Fig. 27** Structures of *Ganoderma* alkaloids

the fruiting bodies of *G. sinense* resulted in the discovery of four additional pyridine-containing alkaloids, sinensines B–E (**291**–**294**) (Fig. 27) [162]. The relative configuration of sinensine E (**294**) was determined by X-ray analysis of its acetylated product. Lucidimines A–D (**295**–**298**) are four pyridine alkaloids isolated from the fruiting bodies of *G. lucidum* [163]. Petchine (**299**) and 3-hydroxy-5-methyl-5,6-dihydro-7*H*-cyclopenta[*b*]pyridin-7-one (**300**) are alkaloids isolated from *G. petchii* (Fig. 27) [164].

Termitomycamide C (**301**) is a pyridine-containing amide from the edible very large mushroom *Termitomyces titanicus* (Fig. 28) [148]. Nitrogen-containing terpenoids are rarely encountered from organisms. Sterostreins M–O (**302**–**304**) and

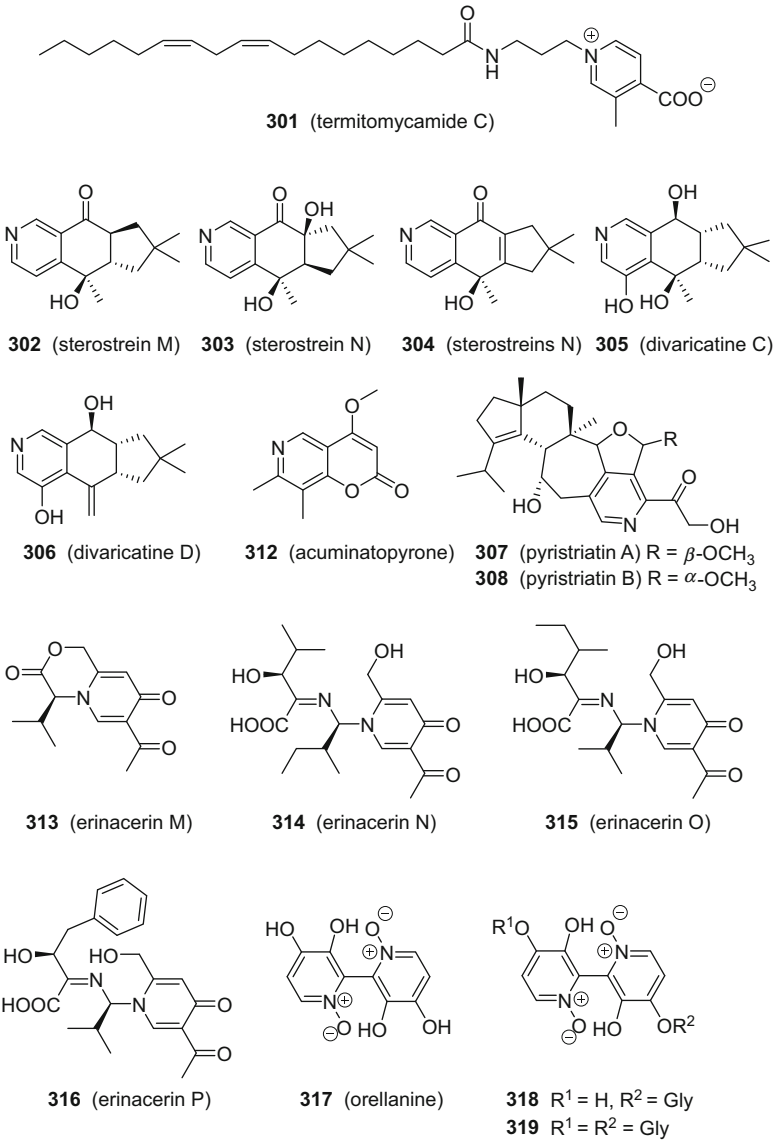


**Fig. 28** Structures of pyridine-containing compounds

divaricatines C (**305**) and D (**306**) are naturally pyridine ring-containing sesquiterpenoids (Fig. 28) [165, 166], while pyristriatins A (**307**), B (**308**), and radianspenes J–L (**309–311**) are pyridine or pyrrole ring-containing diterpenoids isolated from the cultures of the fungi *Cyathus* cf. *striatus* and *Coprinus radians*, respectively (Figs. 28 and 29) [168, 170]. Pyristriatins A (**307**) and B (**308**) were the first cyathane diterpenoids featuring a pyridine ring. These two compounds were

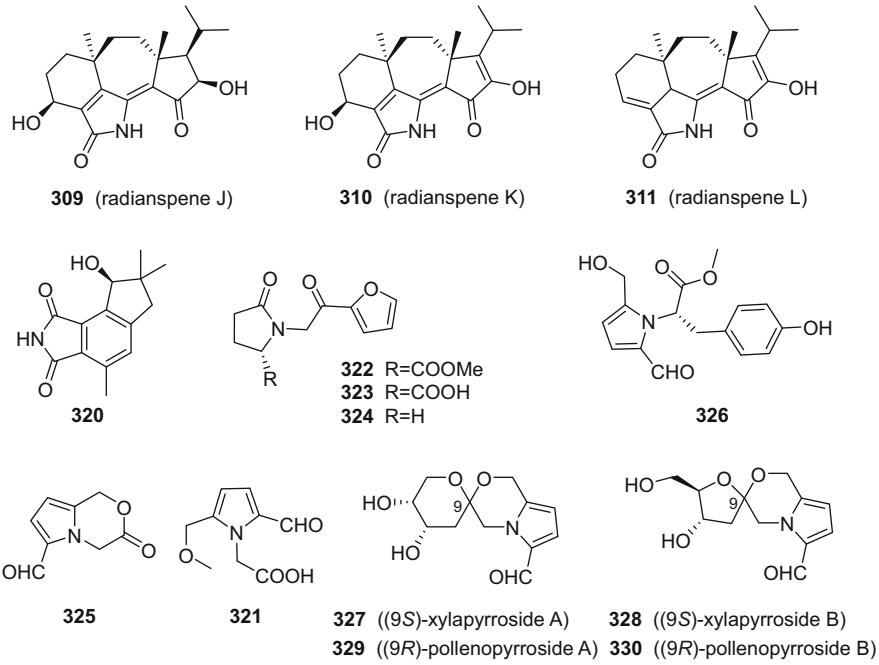


**Fig. 29** Structures of pyrrole-containing compounds

tested for their inhibitory activities against various bacteria, fungi, and three mammalian cell lines. Interestingly, both showed antibacterial activity exclusively against Gram-positive bacteria, exhibiting *MIC* values of 9.4 and 9.4 μg/cm$^3$ against *Bacillus subtilis* and *Staphylococcus aureus* for **307**, and 8.3 and 16.7 μg/cm$^3$ against *B. subtilis* and *S. aureus* for **308**. Additionally, **307** and **308** exhibited, in turn, $IC_{50}$ values of 12.7 and 14.7 μ*M* against KB 3.1 Hela cells [168].

Erinacerins M–P (**313–316**) are four pyridine-containing compounds that were isolated from a solid culture of the Lion's Mane mushroom, *H. erinaceum* (Fig. 28). A postulated biogenetic pathway proposed that the synthetic precursors are amino acids and that four molecules of acetyl CoA undergo cascade condensation reaction-dehydration or condensation reaction–decarboxylation–amination–dehydration processes to give erinacerins M (**313**) and N (**314**). Erinacerins M–P showed $IC_{50}$ values of 16.3, 18.2, 15.9, and 11.4 μ*M* against wild-type K562 cells [154].

Orellanine (**317**) is a nephrotoxic bipyridine *N*-dioxide toxin produced by various mushrooms in the family Cortinaceae. *Cortinarius orellanus* and *C. rubellus* are two of the world's most poisonous mushrooms, bearing striking similarities to those of the edible mushrooms *Cantharellus tubaeformis* and *Cantharellus cibarius*, which have led to several fatalities (Fig. 28). Orellanine poisoning is characterized by a latency period varying from 2 to 17 days before symptoms of acute renal failure occur. However, there is no cure for orellanine poisoning to date. Whereas **317** is selectively toxic to renal cells, it was tested as a

potential treatment for metastatic renal cancer. Herrmann and co-workers developed a quantitative and sensitive HPLC-ESI-MS/MS method for detecting **317** at a 4.9 ng/cm$^3$ level in all *Cortinarius* mushroom extracts that were investigated. They also identified orellanine mono- and diglucosides **318** and **319** that were rapidly hydrolyzed in a MeOH or acidified MeOH extract but not in a 3 *N* HCl extract. This research provided new approaches for food regulatory agencies to monitor food safety in terms of possible orellanine poisoning, in particular for suspected poisoning determination and detection of small amounts of orellanine in body fluids of tissues during the latency period of orellanine poisoning. Moreover, it also provided a method for maintaining the concentration of orellanine within a therapeutic range when conducting orellanine clinical trials for treating metastatic renal cancer [169].

A novel norsesquiterpene alkaloid was isolated from a solid culture of the edible fungus *Flammulina velutipes* (**320**) (Fig. 29). The absolute configuration of this compound was determined using the induced CD spectrum of the complex formed in situ with $Rh_2(OCOCF_3)_4$. This compound was evaluated against KB cells ($IC_{50}$ 16.6 μ*M*) [171].

A new pyrrole alkaloid, 2-[2-formyl-5-(methoxymethyl)-1*H*-pyrrol-1-yl]acetic acid (**321**), was isolated from the fruiting bodies of *Leccinum extremiorientale* (Fig. 29) [172]. Three γ-lactams, methyl (2*S*)-1-[2-(furan-2-yl)-2-oxoethyl]-5-oxopyrrolidine-2-carboxylate (**322**), (2*S*)-1-[2-(furan-2-yl)-2-oxoethyl]-5-oxopyrrolidine-2-carboxylic acid (**323**), and 1-[2-(furan-2-yl)-2-oxoethyl] pyrrolidin-2-one (**324**), were isolated from the culture broth of *Armillaria mellea* (Fig. 29). Their absolute configurations were established by computational methods [173].

The precious medicinal fungus *Xylaria nigripes* is called "Wuling Shen" in Chinese, and is used in Traditional Chinese Medicine for the treatment of insomnia and depression. From the fermented mycelia of *X. nigripes*, two pyrrole-containing alkaloids, (4*S*)-3,4-dihydro-4-(4-hydroxybenzyl)-3-oxo-1*H*-pyrrolo[2,1-*c*][1,4]oxazine-6-carbaldehyde (**325**) and methyl (2*S*)-2-[2-formyl-5-(hydroxymethyl)-1*H*-pyrrol-1-yl]-3-(4-hydroxyphenyl)propanoate (**326**), were obtained [174]. The absolute configurations of **325** and **326** were deduced from the observed Cotton effects of their CD spectra. Two pyrrole-containing compounds, xylapyrrosides A (**327**) and B (**328**), along with the known compounds pollenopyrrosides A (**329**) and B (**330**), were also isolated from this fungus (Fig. 29) [175]. Their structures were established based on spectroscopic and X-ray crystallographic analysis. Notably, the total syntheses of **327**, **328**, and **330** were also accomplished for the first time. Xylapyrrosides A (**327**) and B (**328**) are rare naturally spirocyclic pyrrole alkaloids.

## *3.3 Other Nitrogen Heterocycles*

The mushroom *Schizophyllum commune* is used as a food in Asia. A bioassay-guided chemical investigation of Danish *S. commune* led to the isolation of three heterocyclic compounds, schizines A (**331**), B (**332**), and epischizine A (**333**) (Fig. 30) [176], of which the latter might be an artifact with an inverted

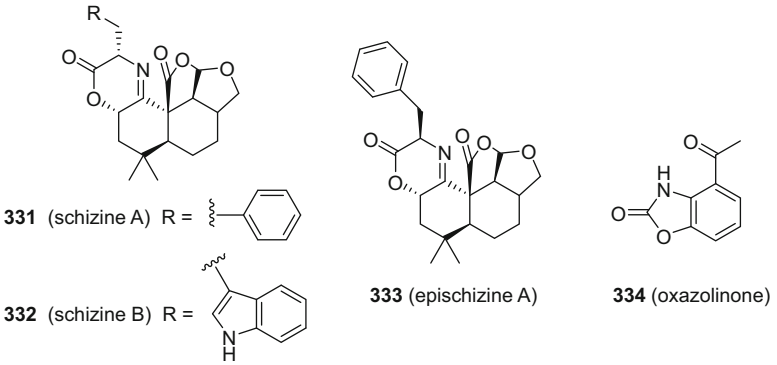


**Fig. 30** Structures of other nitrogen heterocycles

configuration at C-2′, when compared to **331**. These compounds contain an iminolactone (3,6-dihydro-2*H*-1,4-oxazin-2-one) group, which was encountered for the first time in Nature. The structure of **331** was confirmed by X-ray crystallographic analysis. With regard to the biosynthesis of these compounds, it was assumed that a reaction of the precursor amino acid with 2$\alpha$-hydroxy-1-ketomarasmone resulted in the formation of the iminolactone group (Scheme 11). Cytotoxicity assays revealed that **331** and **332** inhibited the growth of three tumor cancer cell lines, EL4 (leukemia), MCF-7 (breast), and PC3 (prostate), while **333** did not show any inhibition up to 200 μ*M* for any of these three cell lines.

Recently, during the preparation of an iminolactone assembly, an unexpected epimerization of the α-carbon atom of both D- and L-α-amino acids when esterified with (1*S*,2*S*,5*S*)-2-hydroxypinan-3-one was discovered. This led to a protocol in which iminolactones could be used as tools for conversion of the absolute configuration of α-amino acids [177]. Further bioassays on additional iminolactones showed considerable antiproliferative effects for some of these compounds toward three cancer cell lines (EL4, MCF-7, PC3), while having no inhibitory effects on non-malignant cell lines (McCoy, MCF10A, NIH3T3) [177].

A cancer cell line bioassay-guided separation of an EtOAc extract of the plant-associated fungus *Coprinus cinereus* led to the isolation of oxazolinone (**334**) [178].

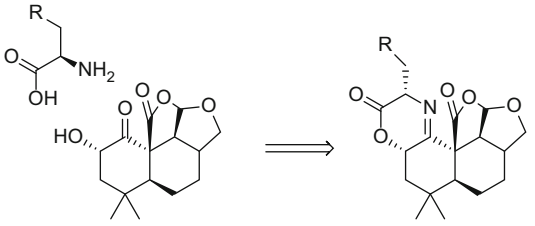

**Scheme 11** Plausible biosynthesis pathway for the schizines

## 3.4 Nucleosides and Non-protein Amino Acids

Bioactivity-guided fractionation using human peripheral blood mononuclear cells of the mushroom *Rubinoboletus ballouii* led to the isolation of 1-ribofuranosyl-s-triazin-2(1*H*)-one (**335**) (Fig. 31). This compound exhibited significant immunosuppressive effects on phytohemagglutinin (PHA)-stimulated human PBMCs by inhibiting [methyl-$^{3}$H]-thymidine uptake and inflammatory cytokine production [179]. 9*β*-D-Ribopyranosylpurine (**336**) was isolated from the edible mushroom *Tricholoma japonicum* (Fig. 31) [180]. Cordysinin B (**337**) was characterized as a new natural product from the the mycelia of *Cordyceps sinensis* (Fig. 31) [149].

Mushroom-derived non-protein amino acids are a class of compounds playing important roles both in allelopathic effects and as mushroom toxic principles. (2*S*,4*R*)-2-Amino-4-methyl-hex-5-enoic acid (**338**) is the major allelochemical isolated from the fruiting bodies of *Boletus fraternus* (Fig. 31). This non-protein amino acid caused 50% inhibition of lettuce seedling radicle growth at a concentration of 34 ppm [181]. Purpurolic acid (**339**) was obtained as a novel secondary metabolite from the sclerotia of *Claviceps purpurea*, which consists of proline and alanine moieties (Fig. 31). Purpurolic acid accumulates when *C. purpurea* parasitizes agricultural products. Its abundance is higher than those of the ergoline alkaloids, which suggests the use of **339** as a biomarker for detection of ergot contamination in agricultural products [182].

Myriocin (ISP-I) (**340**) is a crystalline compound first isolated from the thermophilic ascomycete *Myriococcum albomyces* and later re-encountered from the fermentation of *Cordyceps heteropoda* (Fig. 32) [183, 184]. Myriocin showed no antibacterial activity but was active against all the filamentous fungi tested to date. Moreover, **340** was shown by Fujita et al. to be five- to tenfold more potent than the immunosuppressant agent cyclosporine A. In order to simplify the structure and

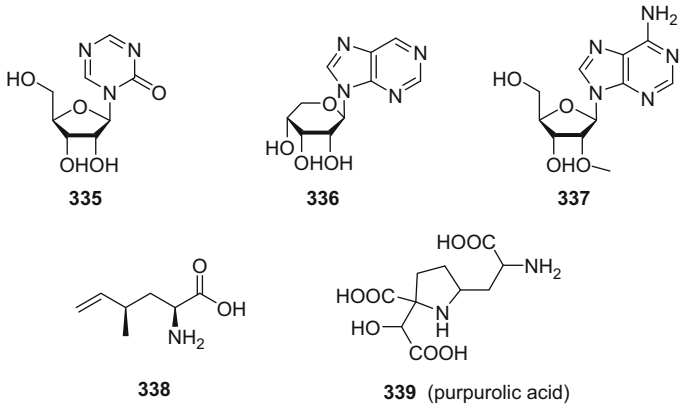


**Fig. 31** Structures of nucleosides **335–337**, (2*S*,4*R*)-2-amino-4-methyl-hex-5-enoic acid (**338**), and purpurolic acid (**339**)

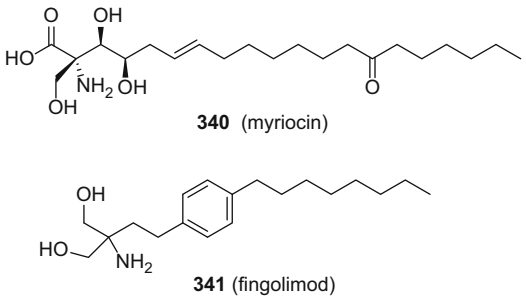


**Fig. 32** Structures of myriocin (**340**) and fingolimod (**341**)

improve the biological properties, many analogues of myriocin were synthesized. The introduction of an aromatic moiety, which could improve activity by restricting conformation, led to fingolimod (**341**) with improved biological activity, a more favorable toxicity profile, more desirable physical properties, and being devoid of chirality (Fig. 32). Ultimately, **341** was approved by the U.S. FDA as a new treatment for multiple sclerosis in September 2010 [185, 186].

The mushroom *Pleurocybella porrigens* is a species widespread in temperate forests of the Northern Hemisphere, which has been ingested for a long time all over the world. However, a mushroom intoxication incident occurred in Japan in 2004 with 55 people being poisoned, of which 17 died of acute encephalopathy. To elucidate the toxic properties of *P. porrigens*, Takata et al. conducted an oligosaccharide hydrolysis experiment to obtain saccharides from the fruiting bodies of this mushroom, leading to the isolation of the two neuraminic acids, *N*-acetylneuraminic acid (NeuAc) (**342**) and *N*-glycolylneuraminic acid (NeuGc) (**343**) (Table 13, Fig. 33). The more abundant **342** was found in both samples collected during the period of poisoning and in other years, while **343** could only be found in the samples collected in the period when the poisoning occurred, suggesting that **343** might be related to these incidents [187]. Moreover, Kawagishi and co-workers reported six unusual amino acids isolated from the lyophilized fruiting bodies of *P. porrigens* (**344**–**349**, Table 13, Fig. 33). Biological evaluation of these amino acids against mouse cerebrum glial cells revealed that **344** and **346**–**348** showed weak toxicity to the cells at 10 μg/cm$^3$, while **349** was inactive, indicative of the indispensable role of the 2-hydroxyvaline moiety for the mediation of their cytotoxicity [188].

A further inspection of these unusual amino acids suggested that all them share a β-hydroxyvaline unit, which inspired Kan and co-workers to propose the occurrence of a labile aziridine amino acid, namely, pleurocybellaziridine (**350**), as the common precursor (Table 13, Fig. 33). These authors then synthesized the proposed **350** and its esters. As shown in Scheme 12, the methyl ester **351** was synthesized via eight steps. Since **351** was unstable when hydrolyzed, the more stable compound **352** subsequently was synthesized as the diphenylmethyl (Dpm) ester (Scheme 12). The steric hindrance around the aziridine ring caused by the Dpm group made the

**Table 13** Nucleosides and non-protein amino acids

| Compound | Origin | Type | Refs. |
|---|---|---|---|
| 1-Ribofuranosyl-s-triazin-2(1*H*)-one (**335**) | *Rubinoboletus ballouii* | Nucleoside | [179] |
| 9$\beta$-D-Ribopyranosylpurine (**336**) | *Tricholoma japonicum* | Nucleoside | [180] |
| Cordysinin A (**337**) | *Cordyceps sinensis* | Nucleoside | [149] |
| (2*S*,4*R*)-2-Amino-4-methyl-hex-5-enoic acid (**338**) | *Boletus fraternus* | NAA | [181] |
| Purpurolic acid (**339**) | *Claviceps purpurea* | NAA | [182] |
| Myriocin (**340**) | *Cordyceps heteropoda* | NAA | [183, 184] |
| Fingolimod (**341**) | | | [185, 186] |
| *N*-Acetylneuraminic acid (**342**) | *Pleurocybella porrigens* | Saccharide | [187] |
| *N*-Glycolylneuraminic acid (**343**) | *Pleurocybella porrigens* | Saccharide | [187] |
| 2-Amino-3-ethoxy-3-methylbutanoic acid (**344**) | *Pleurocybella porrigens* | NAA | [188] |
| 2-Amino-3-(2,3-dihydroxypropoxy)-3,3-dimethylpropanoic acid (**345**) | *Pleurocybella porrigens* | NAA | [188] |
| Compound 3 (**346**) | *Pleurocybella porrigens* | NAA | [188] |
| 2-Amino-3-hydroxy-3-methylbutanoic acid (**347**) | *Pleurocybella porrigens* | NAA | [188] |
| 2-Amino-3-methoxy-3-methylbutanoic acid (**348**) | *Pleurocybella porrigens* | NAA | [188] |
| 3-Amino-2-hydroxy-3-methylbutanoic acid (**349**) | *Pleurocybella porrigens* | NAA | [188] |
| Pleurocybellaziridine (**350**) ☠ | *Pleurocybella porrigens* | NAA | [189] |
| (2*R*,4*S*)-Amino-hydroxy-5-hexynoic acid (**353**) ☠ | *Trogia venenata* | NAA | [190] |
| (2*R*)-Amino-5-hexynoic acid (**354**) ☠ | *Trogia venenata* | NAA | [190] |
| γ-Guanidinobutyric acid (**355**) ☠ | *Trogia venenata* | NAA | [190] |
| Cycloprop-2-ene carboxylic acid (**356**) ☠ | *Russula subnigricans* | Other | [191] |

Dpm ester **352** more stable than **351**. With these two esters in hand, the authors designed a sophisticated experimental procedure to confirm the presence of **350** in the mushroom extract. Thus, initially they treated the mushroom extract with $CH_2N_2$ or $Ph_2CN_2$, then purified the corresponding **350** ester with those synthesized as references, and achieved the expected results, which confirmed the natural existence of the labile amino acid, pleurocybellaziridine. Examination of the toxicity of both **350** and its methyl ester **351** showed that **350** significantly reduced

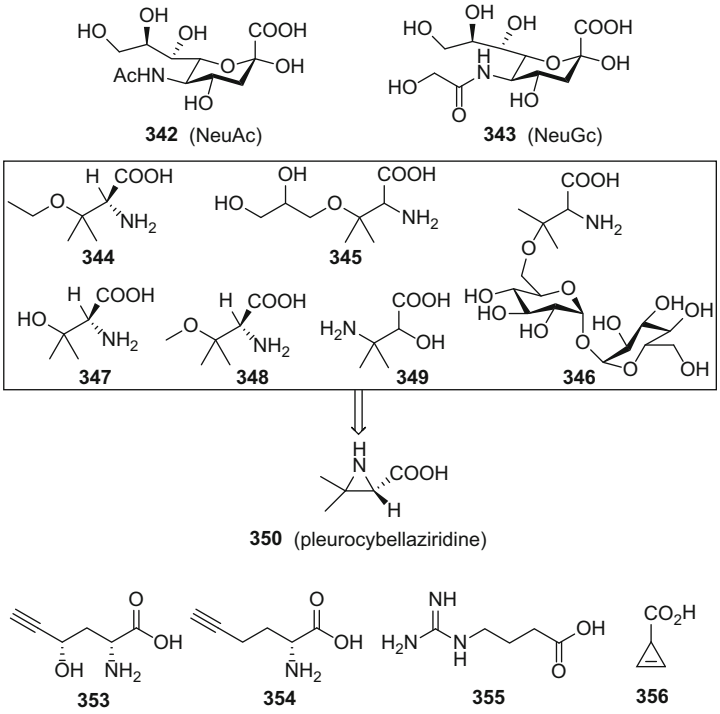


**Fig. 33** Structures of non-protein acid toxins from mushrooms *P. porrigens* and *T. venenata*

cell viability at concentrations of up to 10 μg/cm$^3$ (87 μ*M*), while its methyl ester demonstrated only weak cytotoxicity at 30 μg/cm$^3$ (233 μ*M*). These data suggested that **350** might be the actual compound causing the demyelinating symptoms, with its carboxylic acid residue and the aziridine skeleton being crucial for activity [189].

The mushroom *Trogia venenata* is a recently described species from Yunnan Province, southwest mainland China (Fig. 34). Epidemiological studies indicated that ingestion of this mushroom has been responsible for the sudden unexpected deaths of more than 260 people over the past 30 years. Liu and co-workers isolated and characterized three toxic non-protein amino acids from the fruiting bodies of this mushroom, namely, (2*R*)-amino-(4*S*)-hydroxy-5-hexynoic acid (**353**), (2*R*)-amino-5-hexynoic acid (**354**), and γ-guanidinobutyric acid (**355**), guided by oral toxicity tests in mice (Table 13, Fig. 33). The absolute configuration of **353** was determined as (2*R*,4*S*) by both matrix-mode and optical rotation computations based on DFT methods. This was also further confirmed by total synthesis (Scheme 13). Both **353** and **354** proved lethal for ICR mice with $LD_{50}$ values of 71 and 84 mg/kg, respectively. The total content of **353** and **354** in the fruiting bodies of *T. venenata* was 0.2%, equivalent to a lethal dose in a human (60 kg) if

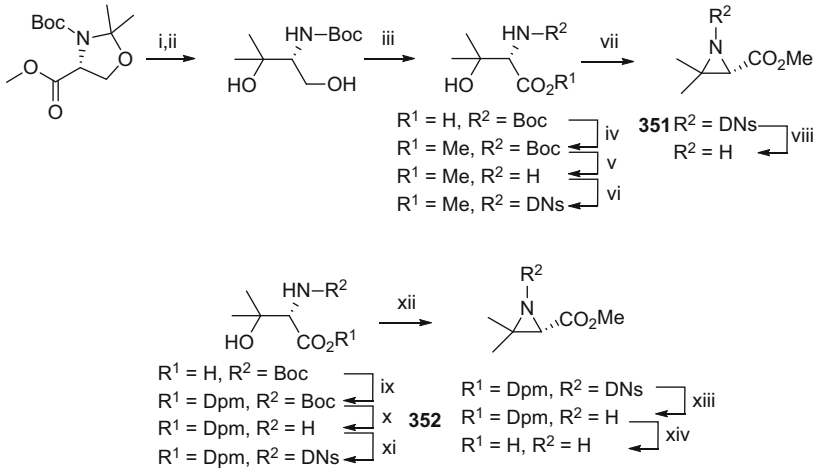


**Scheme 12** The total synthesis of pleurocybellaziridine and its esters **351** and **352**. Reagents and conditions: (i) MeMgBr, THF, −20°C; (ii) PPTS, MeOH, 96% (2 steps); (iii) TEMPO, $PhI(OAc)_2$, $NaClO_2$, MeCN, buffer pH 6.4, 96%; (iv) $CH_2N_2$, $Et_2O$ 87%; (v) HCl gas, MeOH; (vi) DNsCl, 2,6-lutidine, $CH_2Cl_2$, 72% (2 steps); (vii) DEAD, $Ph_3P$, toluene, 83%; (viii) *n*$PrNH_2$, $CH_2Cl_2$, 0°C → RT, 52%; (ix) $Ph_2CN_2$, $CH_2Cl_2$, 77%; (x) HCl gas, MeOH; (xi) DNsCl, $Na_2CO_3$, THF/$H_2O$ (2:1), 59% (2 steps); (xii) DIAD, $Ph_3P$, toluene, 70%; (xiii) *n*$PrNH_2$, $CH_2Cl_2$, 0°C → RT, 90%; (xiv) $H_2$, 5% Pd/C, MeOH, 67%. DNsCl = 2,3-dinitrobenzenesulfonyl, PPTS = pyridinium *p*-toluenesulfonate, TEMPO = 2,2,6,6-tetramethylpiperidine-1-oxyl, DIAD = diisopropyl azodicarboxylate, Dpm = diphenylmethyl

**Fig. 34** The toxic mushroom *Trogia venenata*

approximately 400 g of dried fruiting bodies were to be ingested. It is noteworthy that **353** was also detected in the cardiac blood of a mushroom poisoning victim in Yunnan Province [190].

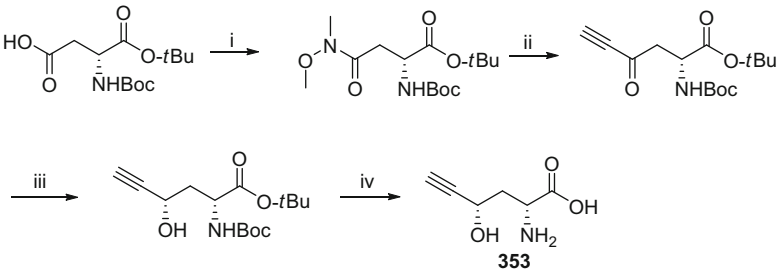


**Scheme 13** Total synthesis of **353**.
Reagents and conditions: (i) $Et_3N$, $CH_3ONHCH_3{\cdot}HCl$, $BOP{\cdot}PF_6$, $CH_2Cl_2$; (ii) HC≡CMgBr (5 equiv), $Et_2O$, −78°C, 78% yield; (iii) (*S*)-B-methyl Corey-Bakshi-Shibata (CBS) catalyst (2 equiv), $BH_3$-$SMe_2$ (2 equiv), toluene, 61% yield; (iv) $CF_3CO_2H$, 99% yield. BOP = benzotriazol-1-yl-oxy-tris-(dimethylamino)-phosphonium

The toxin of the mushroom *Russula subnigricans*, which caused several cases of fatal poisoning in Japan, was proven by Matsuura et al. to be the simple and unstable compound cycloprop-2-ene carboxylic acid (**356**) (Table 13, Fig. 33). While **356** is not a nitrogen-containing substance, this compound represents a new type of a mushroom toxin. Oral administration in mice with a synthetic sample of **356** caused tremor, hair erection, and decreased mobility within 3 h, and the mice died through collapse and tonic extension in the worst-affected cases. However, introduction of a methyl group into the skeleton of **356** considerably reduced the resultant toxicity. Preliminary biological testing revealed that **356** does not directly attack myocytes, but triggers rhabdomyolysis and subsequent lethal poisoning. Compound **356** showed no discernible general antibacterial acitivity nor cellular cytotoxicity. The $LD_{100}$ value of this compound in mice was 2.5 mg/kg, corresponding to a lethal dose of only a small amount of the mushrooms in humans, since the concentration level of this compound was 0.072% [191].

## 3.5 Cyclic Peptides

The basidiomycete *Lepista sordida* is an edible agaric species that belongs to the family Tricholomataceae. In the course of screening for bioactive metabolites from the macrofungi of southern mainland China, four diketopiperazines, lepistamides A–C (**357**–**359**) and diatretol (**360**), were isolated from a solid culture of *L. sordida* (Fig. 35). Lepistamide A (**357**) and **360** are C-3 epimers [192]. In the process of searching for anti-inflammatory principles from the mycelia of *Cordyceps sinensis*, a diketopiperazine was obtained and named cordysinin A (**361**) (Fig. 35). This compound showed inhibitory activities on superoxide anion generation and elastase release with respective $IC_{50}$ values of 11.34 and 13.03 μg/cm$^3$ [149]. Echinuline (**362**) is a cyclic dipeptide formed by triprenylated tryptophan and alanine. It was isolated from the Brazilian edible mushroom *Lentinus strigellus* (Fig. 35) [193].

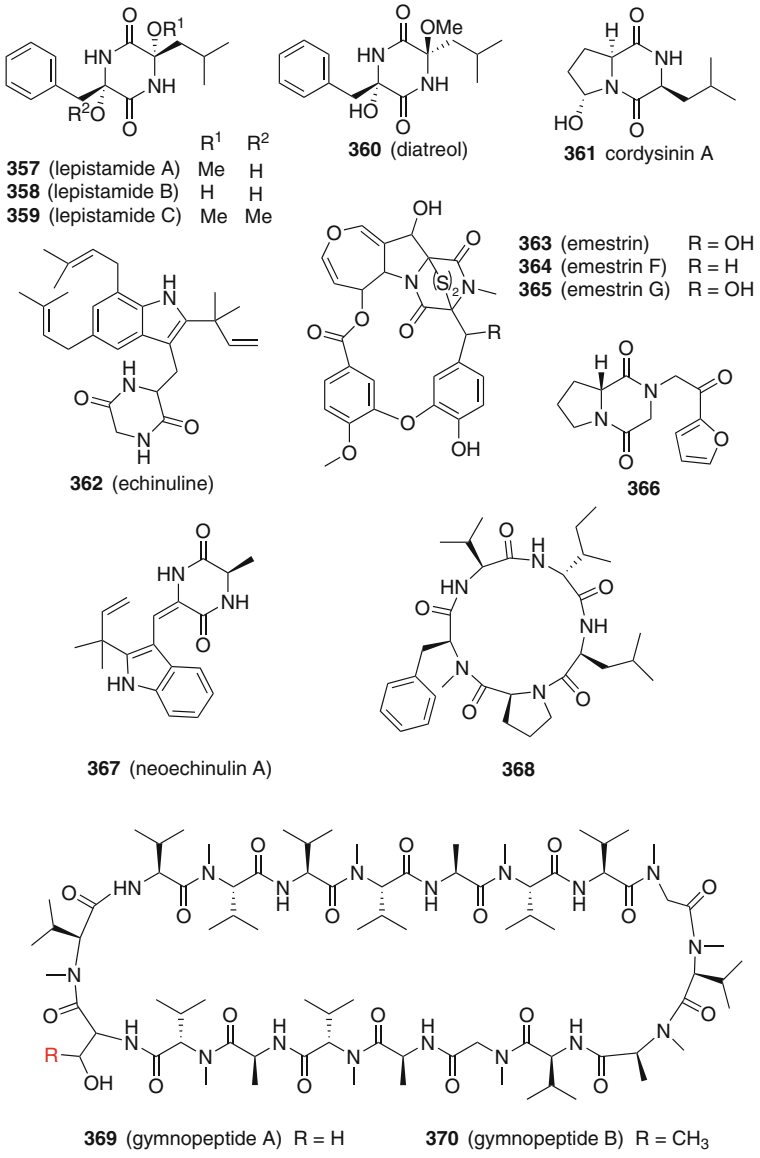


**Fig. 35** Structures of cyclic peptides

The macrofungal genus *Armillaria* is a rich source of protoilludane sesquiterpenoids with polyketide structural modifications. Furthermore, many cyclic peptides were isolated from cultures of *Armillaria* (Table 14). Three sulfur-containing diketopiperazines were isolated from EtOAc extracts of *A. tabescens* (JNB-OZ344), namely, emestrin (**363**), emestrin F (**364**), and emestrin

**Table 14** Cyclic peptides

| Compound | Origin | Type | Refs. |
|---|---|---|---|
| Lepistamides A–C (**357–359**) | *Lepista sordida* | Diketopiperazine | [192] |
| Diatretol (**360**) | *Lepista sordida* | Diketopiperazine | [192] |
| Cordysinin A (**361**) | *Cordyceps sinensis* | Diketopiperazine | [149] |
| Echinuline (**362**) | *Lentinus strigellus* | Diketopiperazine | [193] |
| Emestrin (**363**) | *Armillaria tabescens* | Diketopiperazine | [194] |
| Emestrins F (**364**), G (**365**) | *Armillaria tabescens* | Diketopiperazine | [194] |
| (*R*)-2-(2-(Furan-2-yl)-oxoethyl)-octahydropyrrolo [1,2-*a*]pyrazine-1,4-dione (**366**) | *Armillaria mellea* | Diketopiperazine | [195] |
| Neoechinulin A (**367**) | *Xylaria euglossa* | Diketopiperazine | [196] |
| Cyclo(*N*-methyl-L-Phe-L-Pro-L-Leu-D-Ile-L-Val) (**368**) | *Xylaria carpophila* | Macrocyclic peptide | [197] |
| Gymnopeptides A (**369**), B (**370**) | *Gymnopus fusipes* | Macrocyclic peptide | [198] |

G (**365**) (Fig. 35). Emestrin (**363**) exhibited antimicrobial activity against the fungi *Candida albicans* and *Cryptococcus neoformans* and the bacteria *Escherichia coli* and *Staphylococcus aureus*. The most significant inhibition was for *C. neoformans* with an $IC_{50}$ value of 0.6 μg/cm$^3$. Emestrin F (**364**) only showed activity against *C. neoformans* and *Mycobacterium intracellulare*, while **365** was inactive [194]. (*R*)-2-(2-(Furan-2-yl)-oxoethyl)-octahydropyrrolo[1,2-*a*]pyrazine-1,4-dione (**366**) is a furan-containing diketopiperazine isolated from the liquid fermentation broth of *A. mellea* (Fig. 35). Its absolute configuration was established by computational methods [195]. Neoechinulin A (**367**) is an indole-containing cyclic dipeptide isolated from the fruiting bodies of *Xylaria euglossa*, which is of chemotaxonomic relevance for this fungus (Fig. 35) [196].

Macrocyclic peptides are rarely encountered from higher fungi. A chemical study on the liquid cultures of the fungus *X. carpophila* resulted in the isolation of the cyclic pentadecapeptide cyclo(*N*-methyl-L-Phe-L-Pro-L-Leu-D-Ile-L-Val) (**368**) (Fig. 35). The absolute configutations of the amino acid units were established by the advanced Marfey's method [197]. Two additional cyclic octadecapeptides, gymnopeptides A (**369**) and B (**370**), were isolated from the Hungarian mushroom *Gymnopus fusipes* (syn. *Collybia fusipes*). They represent the largest cyclic peptides of mushroom origin (Fig. 35). The structures were established using extensive spectroscopic methods, such as from their $^1$H, $^{13}$C, 2D-TOCSY, and heteronuclear 2D NMR spectra, which revealed that these two compounds differ only in the presence of a single amino acid moiety. The absolute configurations of the amino acids except for the serine and threonine moieties, were determined by Marfey's derivatization in combination with HPLC-MS methods [198].

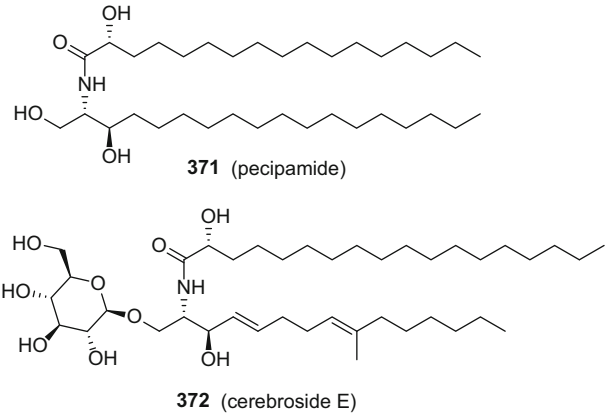


**Fig. 36** Strutures of sphingolipids

## *3.6 Sphingolipids*

The new $C_{18}$-ceramide, pecipamide (**371**), was isolated from the solid fermentation of the basidiomycetous fungus *Polyporus picipes* (Fig. 36). The structure of **371** was established as (2*S*,3*R*,2′*R*)-*N*-2′-hydroxyheptadecanoyl-2-amino-octadecane-1,3-diol [199]. Lee et al. reported the cerebroside, cerebroside E (**372**), from the well-known mushroom *Hericium erinaceus* (Fig. 36) [200]. Cerebroside E (**372**) was evaluated for its probable medicinal potential in several human diseases. The results showed that **372** attenuated cisplatin-induced nephrotoxicity in LLC-PK1 cells and exhibited a significant inhibitory activity on angiogenesis in HUVECs.

## *3.7 Miscellaneous*

Termitomycamides A (**373**), D (**374**), and E (**375**) are three linoleyl amides isolated from the very large edible mushroom *Termitomyces titanicus* (Fig. 37, Table 15). The structure of **375** was confirmed by synthesis [148]. The fruiting bodies of the mushroom *Lactarius vellereus* yielded leptosphaepin (**376**), a γ-lactone amide (Fig. 37). The structure of **376** was established through X-ray diffraction analysis [201].

Leccinine A (**377**) was isolated from the fresh fruiting bodies of the edible mushroom *Leccinum extremiorientale* (Fig. 37). The NMR data of **377** displayed pairs of signals both in the $^{1}H$ and $^{13}C$ NMR spectra. NMR data interpretation along with the MS data suggested that **377** consists of a pair of *N*-formyl rotational isomers in a ratio of 3:1 as determined from the integrated values of the $^{1}H$ NMR signals. Leccinine A (**377**) was subjected to evaluation in a bioassay concerning ER

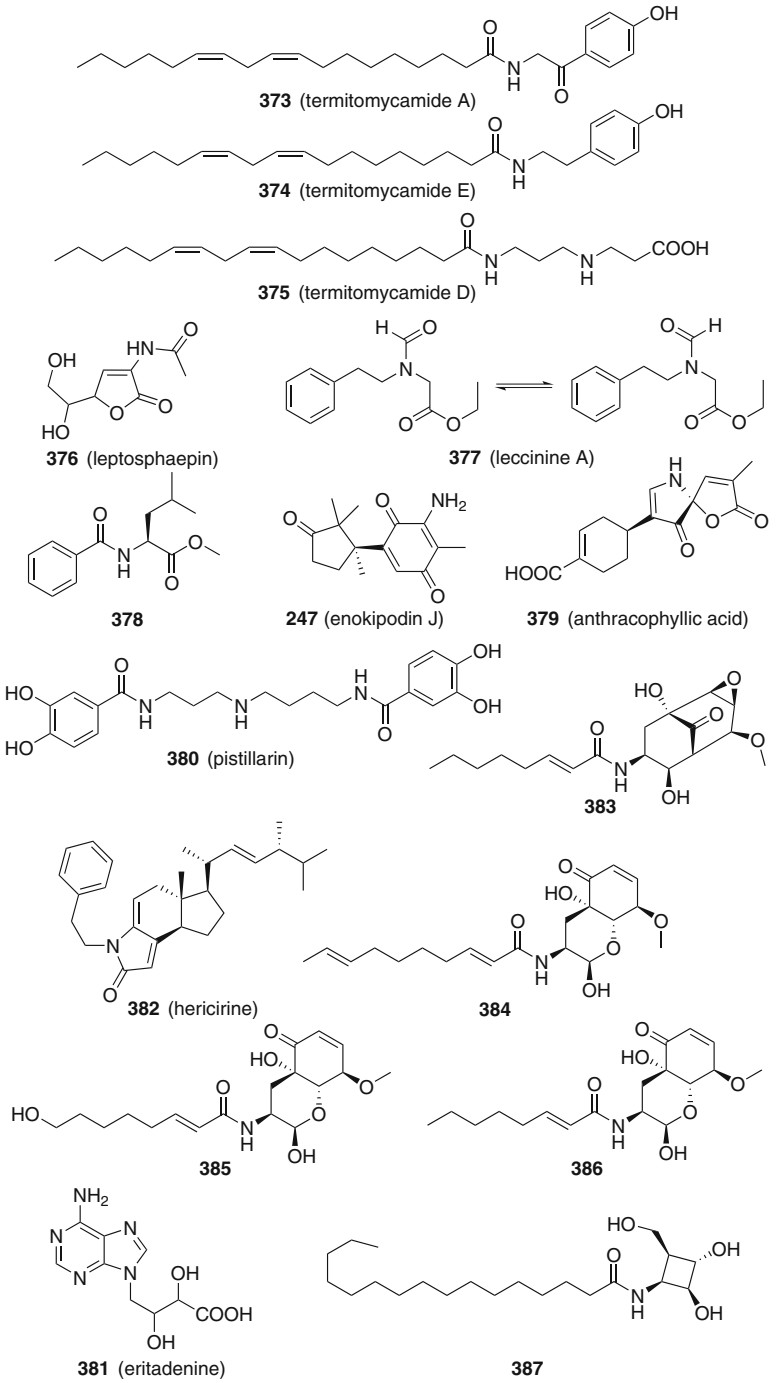


**Fig. 37** Structures of miscellaneous nitrogen-containing compounds

**Table 15** Miscellaneous nitrogen containing compounds

| Compound | Origin | Refs. |
|---|---|---|
| Termitomycamides A (**373**), D (**374**), and E (**375**) | *Termitomyces titanicus* | [148] |
| Leptosphaepin (**376**) | *Lactarius vellereus* | [201] |
| Leccinine A (**377**) | *Leccinum extremiorientale* | [202] |
| *N*-Benzoyl-L-leucine methyl ester (**378**) | *Agaricus blazei* | [203] |
| Enokipodin J (**247**) | *Flammulina velutipes* | [145] |
| Anthracophyllic acid (**379**) | *Anthracophyllum* sp. | [204] |
| Pistillarin (**380**) | *Rubinoboletus ballouii* | [179] |
| Eritadenine (**381**) | *Lentinus edodes* | [205] |
| Hericirine (**382**) | *Hericium erinaceum* | [206] |
| Compounds 1 (**383**), 2 (**384**) | *Ramaria madagascariensis* | [207] |
| Compounds 1 (**385**), 2 (**386**) | *Ramaria madagascariensis* | [208] |
| *N*-(3′$\alpha$,4′$\beta$-Dihydroxy-2′$\beta$-(hydroxymethyl)-1′$\beta$-(cyclobutyl) palmitamide (**387**) | *Ganoderma tsugae* | [209] |

stress-dependent cell death caused by tunicamycin (TM) and thapsigargin (TG). The results indicated that **377** exhibited significant dose-dependent protective activity against TG-toxicity, while no protective activity was observed using TM. Further structure-activity relationships of **377** were carried out by synthesizing analogues of leccinine A to test their activities. These results revealed that the formamide group is indispensable for such activity [202].

*N*-Benzoyl-L-leucine methyl ester (**378**) was isolated from the fruiting bodies of the medicinal fungus *Agaricus blazei* (Fig. 37) [203]. In turn, enokipodin J (**247**) was obtained from the solid fermentation of the edible mushroom *Flammulina velutipes* as a purple powder. This represents the first cuparane-type sesquiterpene containing an amino group to have been found (Fig. 37). Enokipodin J (**247**) exhibited cytotoxic effects against the HepG2, MCF-7, SGC7901, and A549 human tumor cell lines [145].

Crude extracts of the culture broth and cells of the basidiomycete *Anthracophyllum* sp. showed antimalarial activity against the K1 strain of *Plasmodium falciparum*, with $IC_{50}$ values varying from 1.563 to 3.125 μg/cm$^3$, while it showed no growth inhibitory activity against non-cancerous cells even at a concentration of 50 μg/cm$^3$. Further isolation work led to the purification of a nitrogen-containing bisabolane sesquiterpenoid containing a spiro-lactone group, anthracophyllic acid (**379**) (Fig. 37). The relative configuration of **379** was established by X-ray single-crystal diffraction analysis [204]. However, this compound was present as two isomers due to the spiro-lactone group. This epimerization phenomenon seems to be common when a compound contains such a spiro-lactone/lactam group [210].

Pistillarin (**380**) was obtained via the bioassay-guided isolation of the fruiting bodies of the wild mushroom *Rubinoboletus ballouii*. Biological testing indicated that pistillarin was responsible for the immunosuppressive activity demonstrated for an ethanol-soluble extract of this mushroom [179]. Eritadenine (**381**) is a purine alkaloid that was isolated from the shiitake mushroom, *Lentinus edodes*, which showed the highest concentration level of this compound among several edible mushrooms. Later, compound **381** was also isolated from *Agaricus bisporus*. This compound showed angiotensin-converting enzyme (ACE) inhibitory activity with an $IC_{50}$ of 0.091 $\mu M$, while the $IC_{50}$ of the positive control captopril was 0.025 $\mu M$. Further kinetic research of **381** revealed that this compound is a strong competitive inhibitor of ACE [205].

A chemical investigation on the dried fruiting bodies of the mushroom *Hericium erinaceum* yielded the norergosterol alkaloid hericirine (**382**). Its structure was elucidated after extensive spectroscopic analysis. Hericirine was found to inhibit protein expression of iNOS and COX-2 and also reduced NO, $PGE_2$, TNF-$\alpha$, IL-6, and IL-1$\beta$ production in RAW264.7 cells exposed to LPS. These inhibitory activities might be due to its ergosterol-related structure [206].

Four amide-group-containing alkaloids were isolated from a 95% ethanol-soluble extract of the mushroom *Ramaria madagascariensis* (**383**–**386**, Fig. 37) [207, 208]. *N*-(3′$\alpha$,4′$\beta$-Dihydroxy-2′$\beta$-(hydroxymethyl)-1′$\beta$-(cyclobutyl)palmitamide (**387**) was isolated from the fruiting bodies of *Ganoderma tsugae* (Fig. 37). The long-chain acyl moiety was determined as palmitoyl by acid hydrolysis of this compound to afford palmitic acid methyl ester and further characterized by GC-MS. This compound was found to contain a rare cyclobutyl ring [209].

# 4 Terpenoids of Higher Fungi

## *4.1 Sesquiterpenoids*

Among the secondary metabolites derived from higher fungi, the sesquiterpenoid family is undoubtedly the most diverse type of compound both in terms of their overall number and the range of structural scaffolds.

Farnesyl pyrophosphate (FPP, also known as farnesyl diphosphate, FDP) is a key intermediate for the divergent biosynthesis of sesquiterpenoids (Scheme 14). In turn, the key intermediates for humulane and germacrane are transformed enzymatically from FPP via 1,11- and 1,10-cyclizations. Additionally, through a 1,6-cyclization pathway, FPP produces the bisabolane skeleton, which further yields cuparane, chamigrane, and the rare spiro[4.5]decane (with only one example reported) scaffolds via 7,11-, 6,11-, and 6,10-cyclization modes. The cuparane backbone further affords the tricyclic gymnomitrane via methyl migrations and nucleophilic addition procedures (Scheme 15). Farnesyl pyrophosphate undergoes a 2,7-cyclization to yield the drimane sesquiterpenoids, which are a large group of sesquiterpenoid metabolites, while via 1,7-, 4,6-, and 6,11-cyclization cascades,

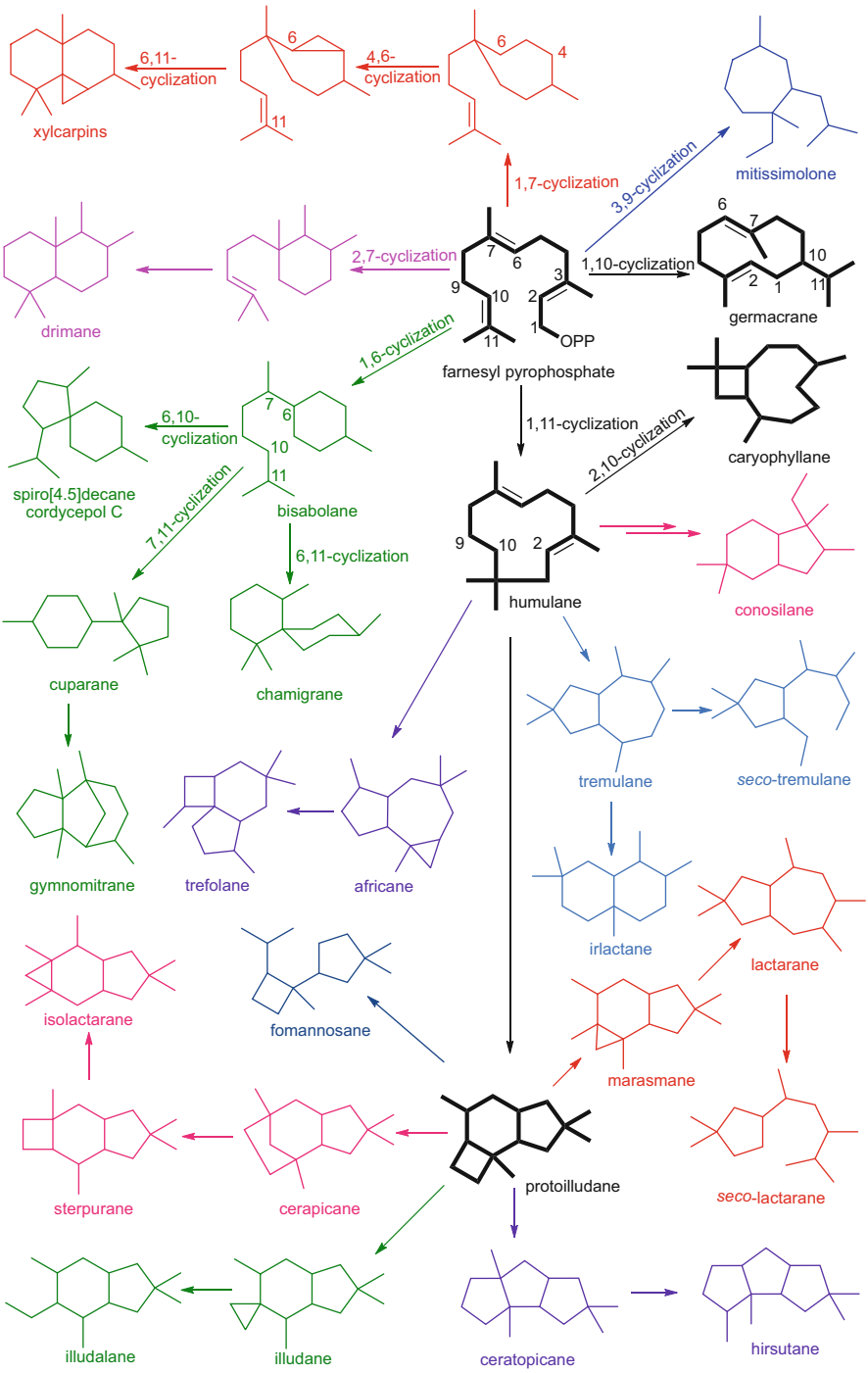


**Scheme 14** The biosynthesis of the tree of mushroom-derived sesquiterpenoid family (the FPP numbering is used throughout)

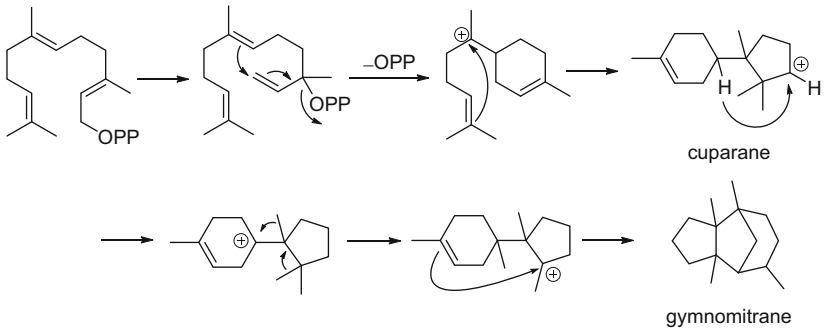


**Scheme 15** The biosynthesis pathway of gymnomitrane-type sesquiterpenoids

xylcarpin sesquiterpenoids are produced. Through a 3,9-cyclization, mitissimolone is obtained, which represents the only example of this mode of cyclization.

The FPP-humulane pathway is the most important for the formation of additional diverse sesquiterpenoids. Humulane yields the rare africane skeleton with a strained cyclopropane ring, which further produces a quaternary carbon-shared 4/6/5 tricyclic trefolane backbone. On the other hand, carbon–carbon bond formation between C-2 and C-9 with subsequent methyl migration of FPP yields the tremulane skeleton, which is converted via carbon–carbon bond cleavage and rearrangement to form the *seco*-tremulane and irlactane skeletons. Humulane produces the tricyclic protoilludane, a key intermediate for more than five subsequent pathways. One of them leads to illudane with a spiro-cyclopentane/cyclohexane scaffold. When the strained cyclopentane ring of illudane opens, this leads to the illudalane skeleton. The second pathway is the formation of the 3/6/5-fused tricyclic marasmane by arrangement of the cyclobutane ring of protoilludane. Marasmane proved to be the precursor of lactarane, which is converted to *seco*-lactarane via a carbon–carbon bond cleavage. Migration of the cyclobutane ring of protoilludane gives cerapicane. Cerapicane itself is the intermediate for sterpurane-type sesquiterpenoids, which further leads to the isolactarane scaffold. The fourth pathway with protoilludane as the precursor results in the cerapicane and hirsutane tricyclopentane skeletons, via ring rearrangements and methyl migrations. The last pathway constitutes a carbon–carbon bond cleavage in protoilludane, which leads to the fomannosane skeleton (Scheme 14).

The FPP-germacrane pathway further produces many sesquiterpenoid skeletons through no less than five branches (Scheme 16). Although only one germacrane-type of sesquiterpenoid has been reported among mushroom secondary metabolites, it is regarded as a key intermediate for many sesquiterpenoids that have retained isopropyl moieties. Germacrane, in a 1,11-cyclization manner, gives aristolane with a *geminal* methyl-substituted cyclopropane ring. Cleavage of the cyclopentane ring of aristolane gives nardosinane. Also, germacrane, when modified via a 1,6-cyclization pathway, produces cadinane. Ring reduction and carbon–carbon bond formation of cadinane lead to the spiroaxane and stereumane skeletons, respectively. In addition, eudesmane is formed by a 2,7-cyclization procedure; it

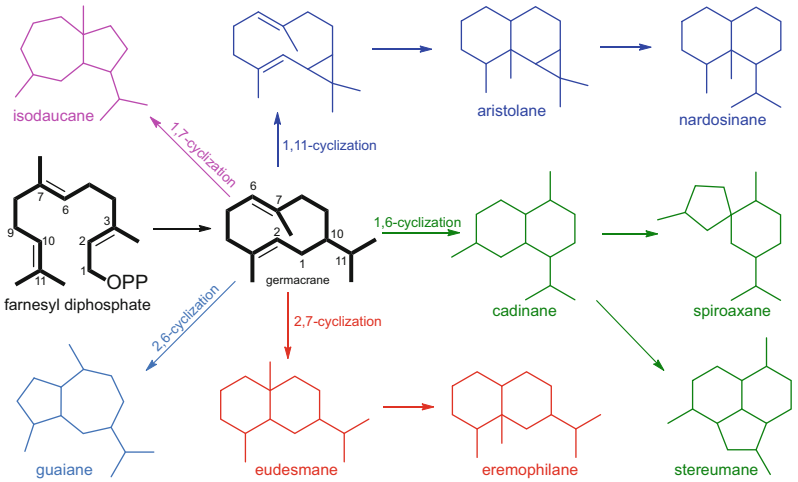


**Scheme 16** The sesquiterpenoid skeletons derived from the common precursor of germacrane

is converted into eremophilane via a methyl migration step. Moreover, germacrane yields the guaiane and isodaucane skeletons via 2,6- and 1,7-cyclization modes, respectively, of which the guaiane sesquiterpenoids are always aromatic and occur in the form of azulene pigments.

The pathway through which humulane, via 1,11-cyclization, gives *cis-*/*trans*-caryophyllanes, which subsequently produces a variety of sesquiterpenoids, is designated as the humulane–caryophyllane pathway (Scheme 17). These sesquiterpenoids are characterized by a retained *geminal* methyl substituted

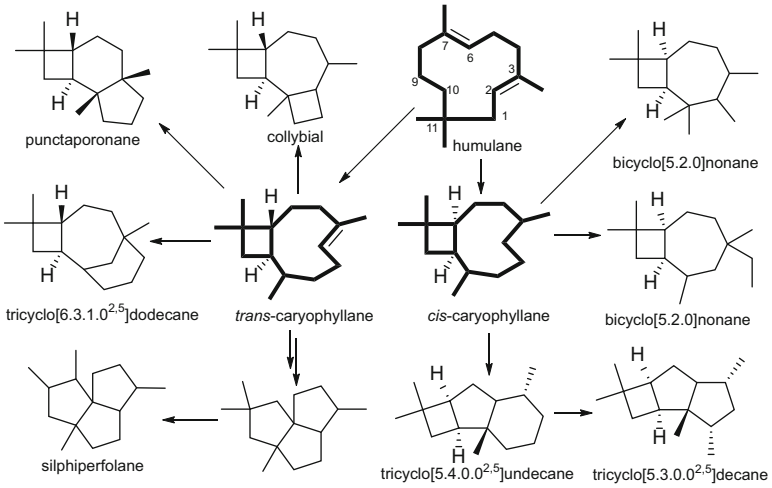


**Scheme 17** The sesquiterpenoid skeletons derived from the common precursors of *cis-*/*trans*-caryophyllane

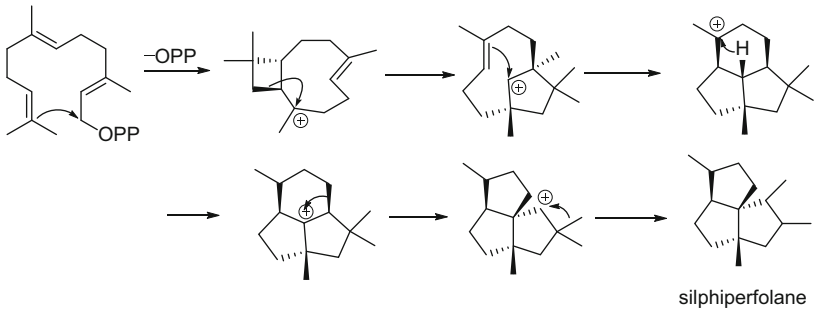


**Scheme 18** The biosynthesis pathway of silphiperfolane-type sesquiterpenoids

cyclobutane ring. Among them, the silphiperfolane type stems from *trans*-caryophyllane, but it is different from other caryophyllane-derived skeletons. The detailed biosynthesis pathway of silphiperfolane is shown in Scheme 18. The punctaporonane, collybial, and tricyclo[6.3.1.$0^{2.5}$]undecane skeletons are formed from the precursor *trans*-caryophyllane, while the tricyclo[5.4.0.$0^{2.5}$]undecane, tricyclo[5.3.0.$0^{2.5}$]decane, and bicyclo[5.2.0]nonane skeletons are derived from *cis*-caryophyllane.

### 4.1.1 Humulanes

Humulane-type sesquiterpenoids are found rarely in Nature. They have been recognized as being biogenetic precursors of many types of sesquiterpenoids (Schemes 14 and 17). Humulane-type sesquiterpenoids in mushrooms occur mainly in the genus *Lactarius* (Table 16). The macrocyclic nature of members of the humulane group has proved to be troublesome for the determination of their absolute configurations.

So far, only 13 humulanes were reported from higher fungi (Table 16). Antrodols A–C (**388–390**) were the first examples of humulanes isolated from fungal cultures, and the others were obtained from fruiting bodies of *Lactarius* mushrooms (Fig. 38) [211]. Mitissimols A–G (**391–397**) and mitissimol A oleate and linoleate (**398** and **399**) are humulanes isolated from the mushroom *L. mitissimus* (Fig. 38) [212–214]. The relative configuration of **391** was established by X-ray analysis, and the

**Table 16** Humulane sesquiterpenoids

| Compound | Origin | Type | Refs. |
|---|---|---|---|
| Antrodols A–C (**388–390**) | *Antrodiella albocinnamomea* | Humulane | [211] |
| Mitissimols A–G (**391–397**) | *Lactarius mitissimus* | Humulane | [212–214] |
| Mitissimol A oleate (**398**) | *Lactarius mitissimus* | Humulane | [212] |
| Mitissimol A linoleate (**399**) | *Lactarius mitissimus* | Humulane | [212] |
| (6*Z*,9*Z*)-2$\beta$,3$\alpha$-Epoxyhumula-6,9-dien-8$\alpha$-ol (**400**) | *Lactarius hirtipes* | Humulane | [215] |

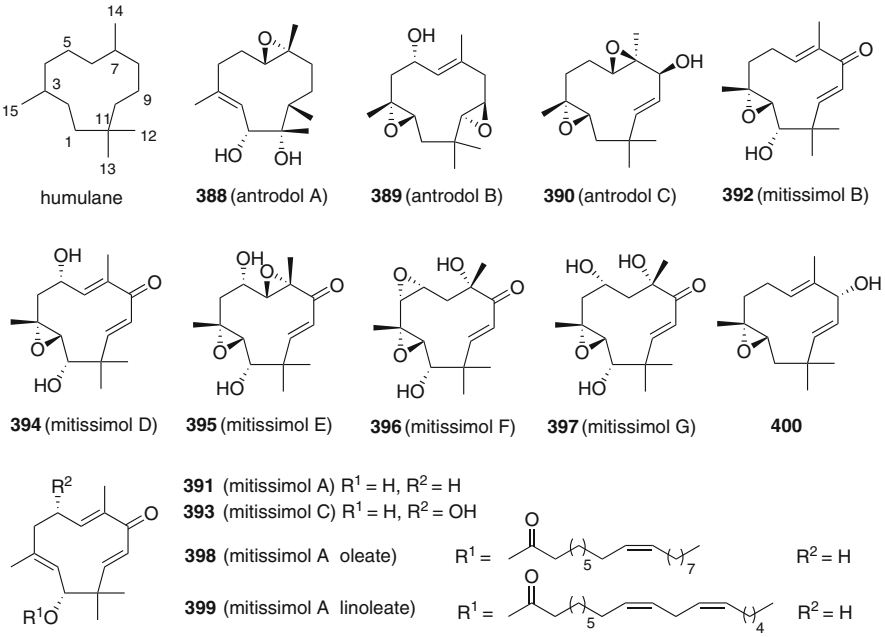


**Fig. 38** Structures of humulane and humulane-type sesquiterpenoids from higher fungi

absolute configuration of **395** was determined by means of the modified Mosher's method. Antrodol A (**388**) showed inhibitory activities against protein-tryosine phosphatase MEG2 and PTP1Bc with $IC_{50}$ values of 8.0 and 10.0 μg/cm$^3$. Antrodol C (**390**) showed a less potent inhibitory effect against protein-tyrosine phosphatase PTP1Bc, having an $IC_{50}$ value of 15.1 μg/cm$^3$ (Fig. 38) [211].

### 4.1.2 Africanes

Africane sesquiterpenoids are a class of 5/7/3 ring-fused sesquiterpenoids, which have been found to date mainly in marine soft corals and higher fungi. Species of the genera *Lemnalia* and *Sinularia* of the soft corals, *Leptographium* of the Ascomycetes, and *Omphalotus* and *Clavicorona* among the Basidiomycetes have been reported to produce africane-type sesquiterpenoids. So far, only three examples of this type of sesquiterpenoid were reported from higher fungal origin (Table 17, Fig. 39).

Omphadiol (**401**) is a sesquiterpenoid isolated from the basidiomycete *Omphalatus illudens*. This compound contains six contiguous stereogenic centers, which made it a challenging synthesis target. The total synthesis of omphadiol was achieved by Liu and Romo [219] and Liang and associates [220]. Liu and Romo developed a scaleable route to the key synthesis intermediate, the bicyclic β-lactone **404**, in three steps, and then achieved the total synthesis of (+)-omphadiol within ten steps (Scheme 19). This total synthesis was characterized by several efficient C–

**Table 17** Africane sesquiterpenoids

| Compound | Origin | Type | Refs. |
|---|---|---|---|
| Omphadiol (**401**) | *Omphalotus illudens* | Africane | [216, 217] |
| Isoomphadione (**402**) | *Omphalotus illudens* | Africane | [218] |
| Pyxidatol C (**403**) | *Clavicorona pyxidata* | Africane | [217] |

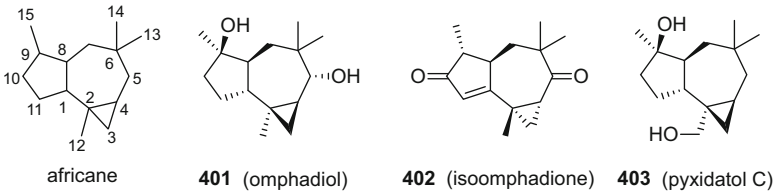


**Fig. 39** Structures of africane, omphadiol (**401**), isoomphadione (**402**), and pyxidatol C (**403**)

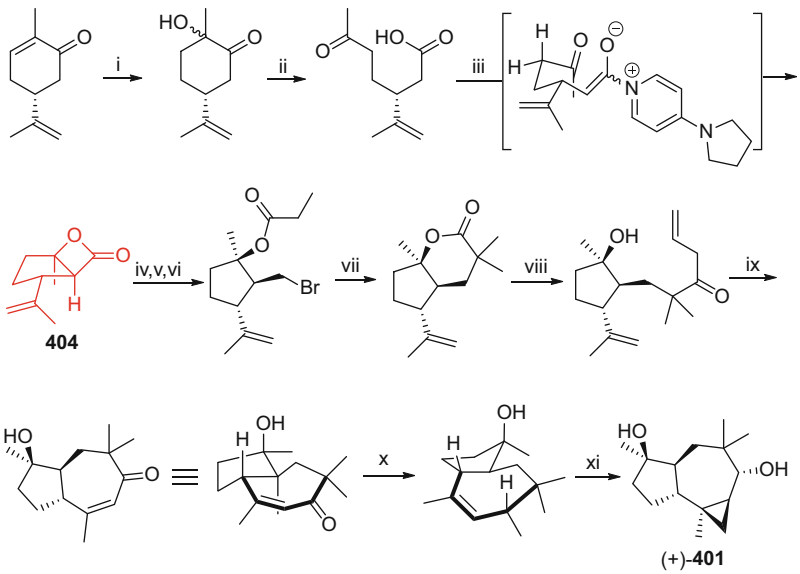


**Scheme 19** The total synthesis of (+)-omphadiol (**401**).
Reagents and conditions: (i) $[Mn(dpm)_3]$ (3 mol%), $PhSiH_3$ (1.5 equiv), *i*PrOH, $O_2$ (1 atm), 63% yield (d.r. 2:1); (ii) $H_5IO_6$, $Et_2O$, 95% yield; (iii) TsCl (1.5 equiv), 4-PPY (1 equiv), $K_2CO_3$ (3 equiv), DIPEA (4 equiv), $CH_2Cl_2$, 2 h, 83% yield (d.r. >19:1); (iv) DIBAI-H, $CH_2Cl_2$, −78 → 0°C, 99% yield; (v) TsCl, LiBr, py. 23 → 60°C, 3 h; (vi) $(EtCO)_2O$, $NEt_3$, DMAP, 23°C, 48 h, 79% yield; (vii) KHMDS (3 equiv), THF, −78°C 20 min, then MeI, 84% yield; (viii) $Ph_3SnCH_2CHCH_2PhLi$, $nBu_2O$, $Et_2O$, 0 → 23°C, then $Et_2O$, −78°C, 74% yield; (ix) Grubbs II (3 mol%), toluene, 90°C, 3 h, 95% yield; (x) *t*BuLi, DIBAI-H, toluene, −78°C, 86% yield (d.r. 14:1); (xi) diethyl zinc, $CH_2I_2$, $CH_2Cl_2$, 30 → 0°C, 83% yield (d.r. >19:1). dpm = dipivaloylmethanato; PPY = 4-pyrrolidinopyridine

C bond-forming reactions, novel single-pot, sequential, and tandem processes, and the highly stereocontrolled introduction of all six stereogenic centers [219].

### 4.1.3 Aristolanes

Most of the reported aristolane sesquiterpenoids are from the genus *Russula*. Recently, this type of sesquiterpenoid was also reported from the luminescent mushroom *Neomothopanus nambi* and the genus *Anthracophyllum* (Table 18). Nardosinane-type sesquiterpenoids are biogenetically related to the aristolanes.

The bright yellow compound, lepidamine (**405**), represented the first report of an aristolane-type sesquiterpene alkaloid from the basidiomycete *R. lepida* (Fig. 40) [224]. The configuration of C-2 of rulepidol (2-hydroxyaristolone) was corrected to (*S*) instead of (*R*) by a NOESY experiment together with calculations of the $^{1}$H and $^{13}$C NMR spectra based on the optimized geometries of C-2 (*S*)- and (*R*)-2-hydroxyaristolone diastereomers [221]. Ramarins A (**406**) and B (**407**) are two aristolanes isolated from the fruiting bodies of *Ramaria formosa*. Both showed

**Table 18** Aristolanes

| Compound | Origin | Type | Refs. |
|---|---|---|---|
| (+)-Aristolone | *Russula lepida* | Aristolane | [221–223] |
| Lepidamine (**405**) | *Russula lepida* | Aristolane | [224] |
| Rulepidol | *Russula lepida* | Aristolane | [221, 225] |
| (1*R*,2*S*)-1,2-Dihydroxyaristolone | *Russula lepida*<br>*Russula amarissima* | Aristolane | [221] |
| (2*S*,11*S*)-2,12-Dihydroxyaristolone | *Russula lepida*<br>*Russula amarissima* | Aristolane | [221] |
| (1*R*,2*S*,11*S*)-1,2,12-Trihydroxyaristolone | *Russula lepida*<br>*Russula amarissima* | Aristolane | [221] |
| (1*S*,2*S*,11*S*)-1,2,12-Trihydroxyaristolone | *Russula lepida*<br>*Russula amarissima* | Aristolane | [221] |
| Nambinones A, B, C (**410**) | *Neonothopanus nambi* | Aristolane | [226, 227] |
| 1-*epi*-Nambinone B | *Neonothopanus nambi* | Aristolane | [226] |
| Axinysone A | *Ramaria formosa* | Aristolane | [227] |
| Axinysone B | *Neonothopanus nambi* | Aristolane | [226] |
| Aurisins A (**408**), G, K (**409**) | *Neonothopanus nambi* | Dimeric aristolane | [226] |
| Ramarins A (**406**), B (**407**) | *Ramaria formosa* | Aristolane | [227] |
| *ent*-Aristolane | *Ramaria formosa* | Aristolane | [227] |
| (+)-1,2-Didehydro-9-hydroxyaristone | *Russula lepida* | Aristolane | [222] |
| (+)-12-Hydroxyaristolone | *Russula lepida* | Aristolane | [222] |
| Anthracophyllone | *Anthracophyllum* sp. | Aristolane | [204] |

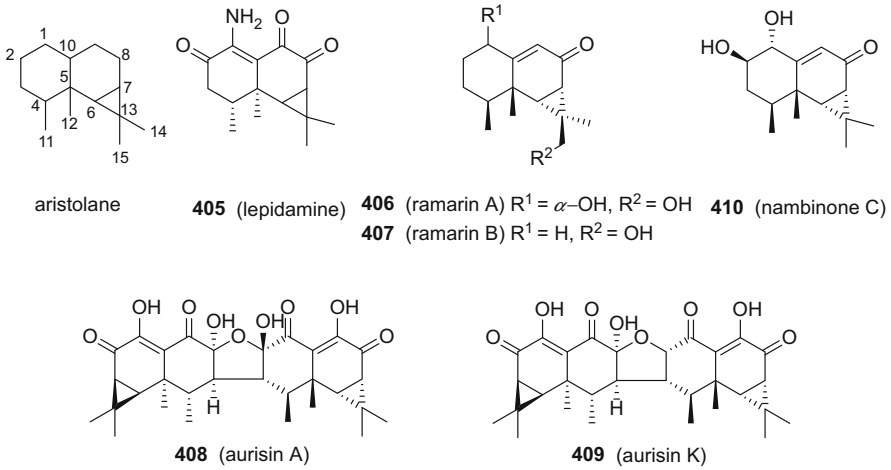


**Fig. 40** Structures of aristolane and selected derivatives

30–35% inhibitory acitivities against human neutrophil elastase (HNE) at a concentration of 100 μ*M*, whereas the positive control, epigallocatechin gallate, exhibited a 60% inhibition at 100 μ*M* [227].

A chemical investigation of the poisonous luminescent mushroom *N. nambi* yielded five aristolanes and the two aristolane dimers **408** and **409** (Table 18, Fig. 40). The relative configuration of aurisin A (**408**) was established by X-ray crystallographic analysis. Biological testing of aurisins A and K (**409**) showed antimalarial activity against *Plasmodium falciparum* ($IC_{50}$ 0.80 and 0.61 μ*M*, respectively) and antimycobacterial activity against *Mycobacterium tuberculosis* (*MIC* values of 92.55 and 23.94 μ*M*, respectively). Moreover, these two dimers also showed cytotoxicity against the NCI-H187 cancer cell line with $IC_{50}$ values of 1.55 and 1.45 μ*M*. Aurisin A also exhibited cytotoxicity against the BC1 cell line with an $IC_{50}$ value of 3.72 μ*M*, while aurisin K showed cytotoxicity against KB cells with an $IC_{50}$ value of 6.87 μ*M*. In addition, aurisin A displayed cytotoxic effects against several cholangiocarcinoma cell lines (KKU-100, KKU-139, KKU-156, and KKU-213) that were comparable in potency to the standard drug ellipticine. Nambinone C (**410**) was less active when evaluated against the NCI-H187 cell line, having an $IC_{50}$ value of 16.42 μ*M*. These data suggest that the dimerized products in this series produced improved bioactivities when compared to those of the monomers [226].

### 4.1.4 Aromadendranes

Aromadendrane-type sesquiterpenoids are a group of 5/7/3 ring-fused sesquiterpenoids that have been rarely reported from fungi (Table 19). With a *trans*-fused five- and seven-membered ring, the resultant skeleton is called

**Table 19** Aromadendranes

| Compound | Origin | Type | Refs. |
|---|---|---|---|
| Hebelodendrol | *Hebeloma longicaudum* | Alloaromadendrane | [228] |
| 2$\beta$,12-Dihydroxyledol | *Dichomitus squalens* | Aromadendrane | [229] |
| 2$\beta$,3$\beta$,12-Trihydroxyledol (**412**) | *Dichomitus squalens* | Aromadendrane | [230] |
| Dichomitone (**413**) | *Dichomitus squalens* | 1,10-*seco*-2,3-*seco*-Aromadendrane | [229] |
| (+)-Globulol (**411**) | *Quambalaria cyanescens* | Aromadendrane | [231] |
| Psilosamuiensins A, B | *Psilocybe samuiensis* | 2,3-*seco*-Aromadendrane | [232] |
| Compounds 1, 2 | *Agrocybe salicacola* | 2,3-*seco*-Aromadendrane | [233] |
| Inonotins A-L | *Inonotus* sp. BCC 23706 | Aromadendrane | [234] |

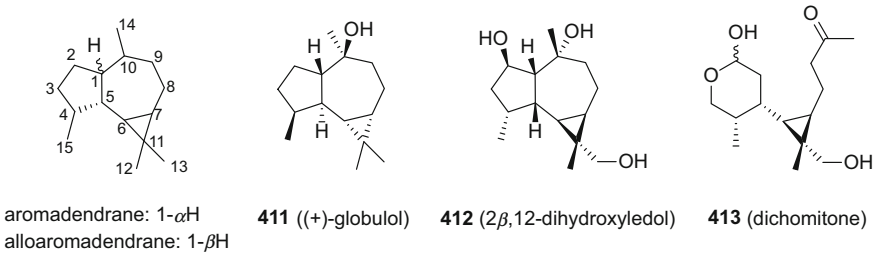


**Fig. 41** Structures of aromadendrane/alloaromadendrane, (+)-globulol (**411**), 2$\beta$,12-dihydroxyledol (**412**), and dichomitone (**413**)

aromadendrane, and with a *cis*-fused five- and seven-membered ring, alloaromadendrane. The carbon–carbon bonds between C-1 and C-3, C-1 and C-10 are vulnerable to being cleaved.

(+)-Globulol (**411**) is an aromadendrane sesquiterpenoid that was obtained from the mycelium of *Quambalaria cyanescens* in the form of needle-shaped crystals (Fig. 41) [231].

### 4.1.5 Bisabolanes

Bisabolane-type sesquiterpenoids occur both in the plant and fungal kingdoms (Table 20). However, Abraham did not cover this type of sesquiterpenoid in his review on fungal sesquiterpenes [251]. The side chain of bisabolanes is ususally oxygenated to ether or hemiacetal/acetal functionalities with the six-membered ring to produce complex polycyclic molecules. Many of these compounds display a range of biological activities.

**Table 20** Bisabolanes

| Compound | Origin | Type | Refs. |
|---|---|---|---|
| Lepistirone | *Lepista irina* | Bisabolane | [235] |
| Cheimonophyllons A–E (**414**) | *Cheimonophyllum candidissimum* | Bisabolane | [236, 237] |
| Cheimonophyllal | *Cheimonophyllum candidissimum* | Bisabolane | [236, 237] |
| (1*R*,7*S*)-15-Hydroxy-1-epi-*β*-bisabolol | *Aleuria aurantia* | Bisabolane | [238] |
| (6*S*,7*S*)-6,7-Dihydroxy-3,6-dimethyl-2-isovaleroyl-4,5,6,7-tetrahydrobenzofuran | *Lentinus squarrosulus* BCC 22366 | Bisabolane | [239] |
| Xylcarpins D, E | *Xylaria carpophila* | Bisabolane | [197] |
| Virgineol | *Amanita virgineoides* | Bisabolane | [240] |
| Anthracophyllic acid | *Anthracophyllum* sp. BCC18695 | Bisabolane | [204] |
| Armillariols A–C | *Armillaria* sp. | Bisabolane | [241] |
| ((6*S*,7*S*)-6,7-Dihydroxy-6-methyl-2-(3-methylbutanoyl)-4,5,6,7-tetrahydrobenzofuran-3-yl)methyl acetate | *Pleurotus eryngii* | Bisabolane | [242] |
| Polisins A–C | *Polyporus ellisii* | Norbisabolane | [243] |
| Pleurospiroketals A–E (**415**) | *Pleurotus cornucopiae* | Bisabolane | [244] |
| Inonolane A | *Inonotus vaninii* | Bisabolane | [245] |
| Daedatrin A | *Daedaleopsis tricolor* | Bisabolane | [246] |
| Daedatrins B, C | *Daedaleopsis tricolor* | Norbisabolane | [246] |
| Inonotic acids A, B | *Inonotus rickii* | Bisabolane | [247] |
| 3-*O*-Formyl inonotic acid A | *Inonotus rickii* | Bisabolane | [247] |
| Phelilane H | *Phellinus linteus* | Bisabolane | [248] |
| (2*E*,4*E*)-(+)-4′-Hydroxy-*γ*-ionylideneacetic acid | *Phellinus linteus* | Bisabolane | [248] |
| (2*E*,4*E*)-*γ*-Ionylideneacetic acid | *Phellinus linteus* | Bisabolane | [248] |
| Pleurotons A (**416**), B (**417**) | *Pleurotus cystidiosus* | Bisabolane | [249] |
| Gypseatriol | *Antrodiella gypsea* | Bisabolane | [250] |

A search for secondary metabolites with nematicidal activities from the culture broth of the basidiomycete *Cheimonophyllum candidissimum* resulted in the discovery of six bisabolane-type sesquiterpenoids, cheimonophyllons A–E (**414**) and cheimonophyllal (Fig. 42) [236, 237]. These compounds exhibited nematicidal and weak antifungal, antibacterial, and cytotoxic activities, which stimulated two research groups to accomplish the total synthesis of cheimonophyllon E and cheimonophyllal [252–254]. Arimillariol A, isolated from culture broth of *Arimillaria* sp., regulates hypocotyl and root growth of the lettuce [241]. Pleurospiroketals A–C (**415**), with a unique benzannulated 5,5-spiroketal skeleton obtained from the edible mushroom. *Pleurotus cornucopiae*, showed inhibitory activity against nitric oxide production in lipopolysaccharide-activated

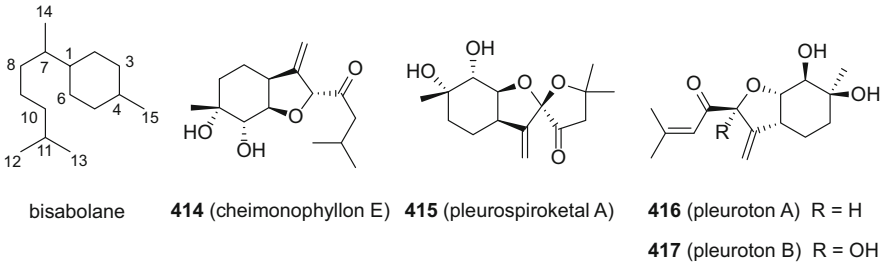


**Fig. 42** Structures of bisabolane, cheimonophyllon E (**414**), pleurospiroketal A (**415**), and pleurotons A (**416**), B (**417**)

macrophages with $IC_{50}$ values of 6.8, 12.6, and 20.8 μ*M*, respectively (Fig. 42) [244]. Pleurotons A (**416**) and B (**417**), from the edible mushroom *P. cystidiosus*, exhibited significant cytotoxicity against two human prostate cancer cell lines, with $IC_{50}$ values of 174 and 28 n*M*, respectively, against DU-145 cells, and 104 and 52 nM, against C42B cells (Fig. 42) [249].

### 4.1.6 Cadinanes

Mushroom-derived cadinane-type sesquiterpenoids are distributed in species of the genera *Stereum*, *Strobilurus*, *Lentinus*, *Tyromyces*, and *Phellinus* (Table 21). This type of compound has been reported to display diverse biological activities. Thus, (+)-10$\alpha$-hydroxy-4-muurolen-3-one (**418**) isolated from the basidiomycete *Favolaschia* sp. 87129 by Anke and colleagues, showed inhibition of leukotriene biosynthesis with $IC_{50}$ values between 5 and 10 μg/cm$^3$ (21.2–42.4 μ*M*) (Fig. 43) [260]. Stereumins C (**419**) and D exhibited potent activities comparable to that of a standard nematocide, avermectin, which killed 84.4 and 94.9% of *Panagrellus redivivus* at 400 mg/dm$^3$ in 48 h (Fig. 43) [268]. Stereumin T (**420**) exhibited antibacterial activity against *Bacillus cereus* with an *MIC* value of 3.97 μ*M*. 4$\beta$,14-Dihydroxy-6$\alpha$,7$\beta H$-1(10)-cadinene (**421**) inhibited HIV-1 with an $EC_{50}$ value of 3.0 μg/cm$^3$ (SI = 25.4) (Fig. 43) [266]. Strobilol H (**422**), an aromatic cadinane-type sesquiterpene from *Strobilurus ohshimae*, was evaluated against the YMB human breast cancer cell line, and gave an $IC_{50}$ value of 16 μ*M* (Fig. 43) [262, 263]. Both boreovibrin F (**423**) and trefoliol B (**424**) showed inhibitory effects against 11$\beta$-hydroxysteroid dehydrogenase-1 (11$\beta$-HSD1) (human $IC_{50}$ 46.7 μ*M*, mouse $IC_{50}$ 66.4 μ*M* for boreovibrin F, and human $IC_{50}$ 13.1 μ*M*, mouse $IC_{50}$ 91.8 μ*M* for trefoliol B) (Fig. 43) [271, 277].

**Table 21** Cadinanes

| Compound | Origin | Type | Refs. |
|---|---|---|---|
| δ-Cadinene | *Lentinus lepideus* | Cadinane | [255] |
| α-Muurolene | *Lentinus lepideus* | Cadinane | [255] |
| γ-Muurolene | *Lentinus lepideus* | Cadinane | [255] |
| Lentideus ether | *Lentinus lepideus* | Cadinane | [256] |
| Isolentideus ether | *Lentinus lepideus* | Cadinane | [256] |
| 10-Hydroxylentideus ether | *Lentinus lepideus* | Cadinane | [256] |
| (+)-Torreyol | *Xylobolus frustulatus* (synonym *Stereum frustulatus*) | Cadinane | [257] |
| Eleganthol | *Clitocybe elegans* | Cadinane | [258] |
| Ganomastenols A–D | *Ganoderma mastoporum* | Cadinane | [259] |
| (+)-10*α*-Hydroxy-4-muurolen-3-one (**418**) | *Favolaschia* sp. 87129 | Cadinane | [260] |
| 11-Desoxyeleganthol | *Limacella illinita* | Cadinane | [261] |
| Strobilols A–M (**422**) | *Strobilurus ohshimae* | Cadinane | [262–265] |
| 4*β*,14-Dihydroxy-6*α*,7*βH*-1(10)-cadinene (**421**) | *Tyromyces chioneus* | Cadinane | [266] |
| Stereumins A–E, G, K–U (**419**, **420**) | *Stereum* sp. CCTCC AF 207024 | Cadinane | [267–270] |
| Boreovibrins A–G (**423**) | *Boreostereum vibrans* | Cadinane | [271] |
| Lyophyllone A | *Lyophyllum transforme* | Cadinane | [272] |
| Lyophyllanetriol A | *Lyophyllum transforme* | Cadinane | [272] |
| Muurolane-10*β*,15-diol | *Ceriporia alachuana* | Cadinane | [273] |
| 2*β*-Hydroxy-*α*-cadinol | *Ceriporia alachuana* | Cadinane | [273] |
| 3*β*-Hydroxy-*δ*-cadinol | *Ceriporia alachuana* | Cadinane | [273] |
| Epicubenol | *Ceriporia alachuana* | Cadinane | [273] |
| 12-Hydroxy-*α*-cadinol | *Daedaleopsis tricolor* | Cadinane | [246] |
| (+)-(1*R*,3*R*,6*S*,7*S*,11*R*)-3,12-Dihydroxy-*α*-muurolene | *Trichaptum pargamenum* | Cadinane | [274] |
| (+)-(1*R*,3*R*,6*S*,7*S*,11*S*)-3,12-Dihydroxy-*α*-muurolene | *Trichaptum pargamenum* | Cadinane | [274] |
| (+)-(1*R*,3*R*,6*S*,7*S*,8*R*,11*R*)-3,8,12-Trihydroxy-*α*-muurolene | *Trichaptum pargamenum* | Cadinane | [274] |
| 3*α*-Hydroxyartemisinic acid | *Trichaptum pargamenum* | Cadinane | [274] |
| 3*α*,12-Dihydroxy-*δ*-cadinol | *Phellinus igniarius* | Cadinane | [275] |
| Tyromol B | *Tyromyces chioneus* | Cadinane | [276] |
| Agripilol C | *Tyromyces chioneus* | Cadinane | [276] |
| Trefoliol B (**424**) | *Tremella foliacea* | Cadinane | [277] |

### 4.1.7 Caryophyllanes and Caryophyllane-Related Sesquiterpenoids

Caryophyllane-type sesquiterpenoids, which have been reviewed previously [251], are found mainly in the plant kingdom. Caryophyllanes may be classified into two categories, *trans*- or *cis*- caryophyllanes, depending on the mode of fusion of the cyclobutane and nine-membered rings (Scheme 17). Further cyclization of the nine-

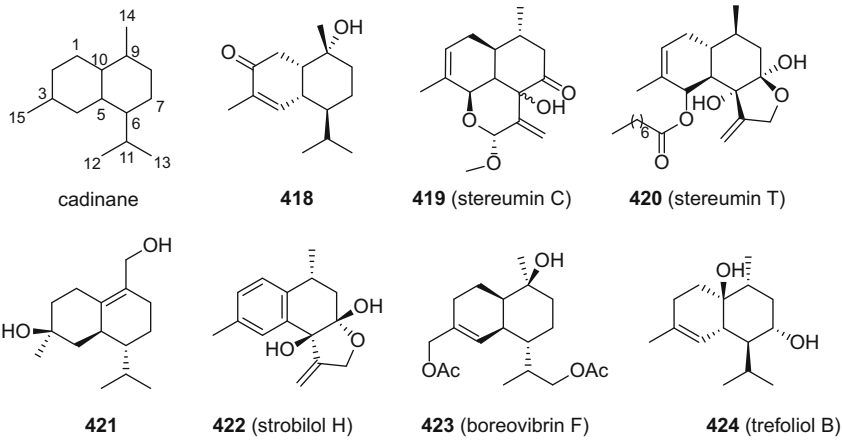


**Fig. 43** Structures of cadinane, (+)-10$\alpha$-hydroxy-4-muurolen-3-one (**418**), stereumins C (**419**) and T (**420**), 4$\beta$,14-dihydroxy-6$\alpha$,7$\beta H$-1(10)-cadinene (**421**), strobilol H (**422**), boreovibrin F (**423**), and trefoliol B (**424**)

membered ring leads to a series of "caryophyllane-related sesquiterpenoids". Herein, the "caryophyllane-related sesquiterpenoids" are defined as those with the features in common of having a *geminal* methyl-substituted cyclobutane ring and caryophyllane as the biogenetic precursor. Sesquiterpenoids based on the core structures tricyclo[5.4.0.0$^{2,5}$]undecane, tricyclo[5.3.0.0$^{2,5}$]decane, and bicyclo [5.2.0]nonane are classified as "caryophyllane-related sesquiterpenoids". Notably, the core tricyclo[5.4.0.0$^{2,5}$]undecane was assigned to a dehydrochlorination product of caryophyllene dihydrochloride [278]. Among fungi, it occurs naturally principally in the genera *Hebeloma*, *Naematoloma*, and *Hypholoma* (Table 22). Interestingly, almost all of the four-membered rings are *cis*-fused with other rings in the fungal caryophyllane-related compounds while *cis*-fused caryophyllanes have only accounted for a small proportion of the reported structures.

6,9-Dihydroxy-3(15)-caryophyllen-4,8-dione (**425**) displayed cytotoxic effects against the L1210 and HL60 cell lines with $IC_{50}$ values of 1.9 and 3.8 μ$M$ (Fig. 44) [279]. Hebelophyllenes G and H (**426**) are two 6,7-*seco*-caryophyllanes isolated from liquid cultures of *Hebeloma longicaudum* [228]. Fasciculares A–K (**427**, **428**) showed lettuce radicle elongation activities at a concentration of 100 ppm (Fig. 44) [285–287].

From a culture of the basidiomycete *Campanella junghuhnii*, a new sesquiterpene with a tricyclo[6.3.1.0$^{2,5}$]dodecane skeleton, 2,3,6-trihydroxycaryol-5-en-7-one (**429**), was obtained (Fig. 44). Comparative analysis between the structure of this compound and that of the cytotoxic sesquiterpene, caryo-7-en-6-ol, suggested that the precursor of this skeleton might be caryophyllane [288].

Compounds **430**–**432** are unusual sesquiterpenoids isolated from cultures of the tropical rainforest basidiomycete *Marasmiellus troyanus*. The absolute configuration of **430** was established by single-crystal X-ray structural analysis and the modified Mosher's method [281].

**Table 22** Caryophyllanes and related sesquiterpenoids

| Compound | Origin | Type | Refs. |
|---|---|---|---|
| 6,9-Dihydroxy-3(15)-caryophyllen-4,8-dione (**425**) | *Marasmius* sp. | Caryophyllane | [279] |
| Hebelophyllenes A–C | *Hebeloma longicaudum* | Caryophyllane | [280] |
| *β*-Caryophyllane | *Marasmiellus troyanus* | Caryophyllane | [281] |
| Hebelophyllenes E–H (**426**) | *Hebeloma longicaudum* | 6,7-*seco*-Caryophyllane | [228, 282] |
| Naematolins C, G | *Naematoloma fasciculare* | Tricyclo[5.4.0.0$^{2,5}$] undecane | [283] |
| Fascicularones A, C (**428**), D | *Naematoloma fasciculare* | Tricyclo[5.4.0.0$^{2,5}$] undecane | [284, 285] |
| Fascicularones E–H, J, K | *Hypholoma fasciculare* | Tricyclo[5.4.0.0$^{2,5}$] undecane | [286, 287] |
| Hebelophyllene D | *Hebeloma longicaudum* | Tricyclo[5.3.0.0$^{2,5}$] decane | [280] |
| Fascicularone B (**427**) | *Naematoloma fasciculare* | Tricyclo[5.3.0.0$^{2,5}$] decane | [284] |
| Fascicularone I | *Hypholoma fasciculare* | Tricyclo[5.3.0.0$^{2,5}$] decane | [286] |
| (2*S*,3*R*)-Dihydroxy-carophyllan-[5,8]-6,7-olide (**430**) | *Marasmiellus troyanus* | Bicyclo[5.2.0] nonane | [281] |
| (2*S*)-Hydroxy-3-oxo-carophyllan-[5,8]-6,7-olide (**431**) | *Marasmiellus troyanus* | Bicyclo[5.2.0] nonane | [281] |
| (2*S*,3*R*,7*S*)-Trihydroxy-carophyllan-[4,7]-6,8-oxide (**432**) | *Marasmiellus troyanus* | Bicyclo[5.2.0] nonane | [281] |
| 2,3,6-Trihydroxycaryol-5-en-7-one (**429**) | *Campanella junghuhnii* | Tricyclo[6.3.1.0$^{2,5}$] dodecane | [288] |
| Collybial | *Collybia confluens* | | [289] |

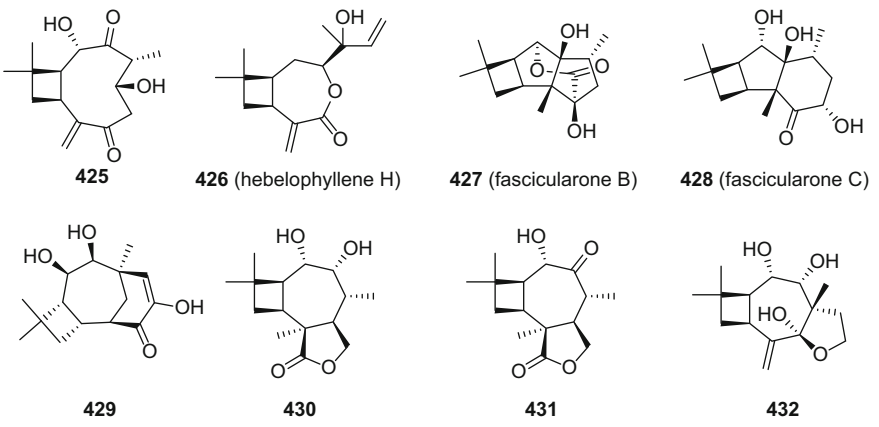


**Fig. 44** Selected examples of caryophyllane and caryophyllane-related sesquiterpenoids

### 4.1.8 Cuparanes

Cuparane-type sesquiterpenoids of fungal origin possess a skeleton with a six-membered ring connected to a five-membered ring, of which the six-membered ring is always aromatic (Table 23). This type of sesquiterpenoid was not covered in a previous review [251].

Isodeoxyhelicobasidin (**433**), isolated from the culture broth of *Volvariella bombycina*, dose-dependently inhibited human neutrophil elastase (HNE), with an $IC_{50}$ value of 9.0 μ*M*, which was comparable to the positive control, epigallocatechin gallate ($IC_{50}$ 12.9 μ*M*) (Fig. 45). This compound also exhibited antibacterial activity against a panel of Gram-positive bacteria with *MIC* values of 3.1 to 12.4 μg/cm$^3$ [294].

The highly oxygenated enokipodins A–D (**434**, **435**), isolated by Takahishi et al. from cultures of the edible mushroom *Flammulina velutipes*, exhibited antimicrobial activities against *Cladosporium herbarum* and *Bacillus subtilis* (Fig. 45). The sterically congested structures and the quaternary carbon stereocenters located on the cyclopentane ring of the enokopodins A–D have attracted considerable interest.

**Table 23** Cuparanes

| Compound | Origin | Type | Refs. |
|---|---|---|---|
| Enokipodins A–J (**434**, **435**) | *Flammulina velutipes* | Cuparane | [145, 290, 291] |
| Flamvelutpenoids A–D | *Flammulina velutipes* | Cuparane | [292] |
| 2,5-Cuparadiene-1,4-dione | *Flammulina velutipes* | Cuparane | [145] |
| Coprinol | *Coprinus* sp. | Cuparane | [293] |
| Isodeoxyhelicobasidin (**433**) | *Volvariella bombycina* | Cuparane | [294] |
| Deconins A–E (**436**) | *Deconica* sp. 471 | Cuparane | [295] |
| Spirobenzofuran | *Coprinus echinosporus* | Cuparane | [296] |
| Deoxyspirobenzofuran | *Coprinus echinosporus* | Cuparane | [296] |
| Methoxyspirobenzofuran | *Coprinus echinosporus* | Cuparane | [296] |

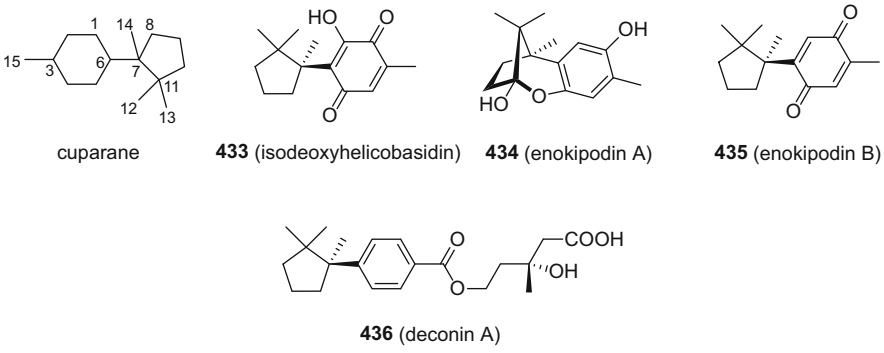


cuparane **433** (isodeoxyhelicobasidin) **434** (enokipodin A) **435** (enokipodin B)

**436** (deconin A)

**Fig. 45** Structures of cuparane, isodeoxyhelicobasidin (**433**), enokipodins A (**434**), B (**435**), and deconin A (**436**)

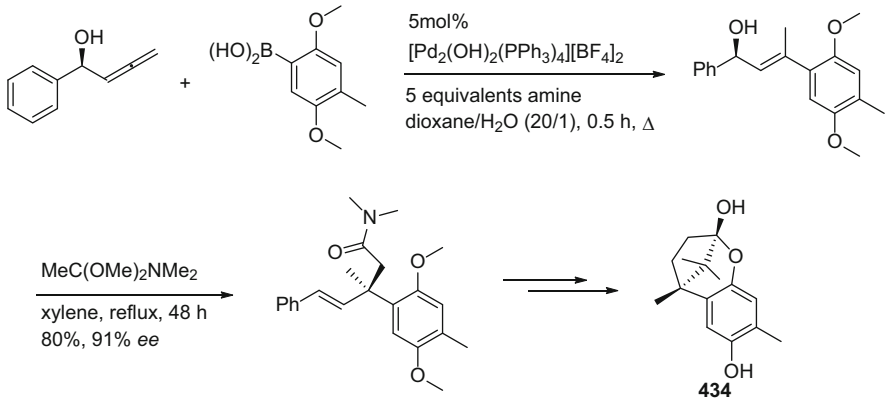


**Scheme 20** The key steps of the enantioselective total synthesis of enokipodin A (**434**) by Yoshida and co-workers

The total synthesis of enokipodins A–D was accomplished successfully by several groups [297–300]. For example, Yoshida et al. developed a strategy of a palladium-catalyzed addition of an arylboronic acid to an allene followed by an Eschenmoser-Claisen rearrangement with enantiospecific construction of the quaternary carbon atom (Scheme 20), leading to the enantioselective total syntheses of enokipodins A and B [300].

Deconins A–E (**436**) are the first cuparane sesquiterpenoids containing unmodified mevalonic acid residues, and were isolated from cultures of a Thai basidiomycete, *Deconica* sp. They showed weak antimicrobial activities [295].

### 4.1.9 Drimanes

Among the sesquiterpenoids of fungal origin, drimanes are one of the largest type of biologically active secondary metabolites. The first member of this group was reported from a higher fungus in 1980. Highly oxygenated drimane derivatives have been attributed with superoxide-release inhibition, insect antifeedant, platelet aggregation inhibition, antimicrobial, and cytotoxic biological activities (Table 24).

From the fermentation of *Kuehneromyces* sp., collected in Tasmania, drimane (kuehneromycin A) and 13-*nor*-drimane (kuehneromycin B, **437**) sesquiterpenoids were obtained. Kuehneromycin A proved to be a non-competitive inhibitor of the avian myeloblastosis virus and moloney murine leukemia virus reverse transcriptases. The 5$\beta$-H isomer of kuehneromycin B, panudial (**438**), which was obtained from a *Panus* sp., was found to be a potent inhibitor of platelet aggregation when stimulated with different inducers [311, 312].

It is noteworthy that within the large group of drimane derivatives, the cryptoporic acids, are a class of compounds linked to an isocitric acid moiety via an ether bond between C-11 and C-1′. They are only found in the genus

**Table 24** Drimane sesquiterpenoids

| Compound | Origin | Type | Refs. |
|---|---|---|---|
| Uvidins A-E | *Lactarius uvidus* | Drimane | [301, 302] |
| (–)-Drimenol | *Lactarius uvidus* | Drimane | [301] |
| Pereniporins A, B | *Perenniporia medullaepanis* | Drimane | [303] |
| Cryptoporic acids A–H (**442**) | *Cryptoporus volvatus* | Drimane | [304, 305] |
| Cryptoporic acids H, I | *Ganoderma neo-japonicum* | Drimane | [306] |
| Peniopholide | *Peniophora polygonia* | Drimane | [306] |
| 3*β*-Hydroxypeniopholide | *Peniophora polygonia* | Drimane | [306] |
| 3*α*-Hydroxypeniopholide | *Peniophora polygonia* | Drimane | [306] |
| 3*β*-Hydroxydihydroconfertifolin | *Peniophora polygonia* | Drimane | [306] |
| 6*β*-Hydroxycinnamolide | *Peniophora polygonia* | Drimane | [306] |
| 6*α*-Hydroxycinnamolide | *Peniophora polygonia* | Drimane | [306] |
| 7*α*-Hydroxyconfertifolin | *Peniophora polygonia* | Drimane | [306] |
| *cis*-Dihydroconfertifolin | *Peniophora polygonia* | Drimane | [306] |
| Cinnamolide | *Peniophora polygonia* | Drimane | [306] |
| 3*β*-Hydroxycinnamolide | *Peniophora polygonia* | Drimane | [306] |
| Roseolide A | *Roseoformes subflexibilis* | Dimeric drimane | [307] |
| Mniopetals A-F (**443**) | *Mniopetalum* sp. | Drimane | [308, 309] |
| Marasmal | *Mniopetalum* sp. | Drimane | [308, 309] |
| Anhydromarasmone | *Marasmius oreades* | Drimane | [310] |
| Marasmone (**444**) | *Marasmius oreades* | Drimane | [310] |
| Isomarasmone | *Marasmius oreades* | Drimane | [310] |
| Dihydromarasmone | *Marasmius oreades* | Drimane | [310] |
| Kuehneromycin A | *Kuehneromyces* sp. | Drimane | [311] |
| Kuehneromycin B (**437**) | *Kuehneromyces* sp. | 13-Nordrimane | [311] |
| Panudial (**438**) | *Panus* sp. 9096 | 13-Nordrimane | [312] |
| Haploporic acid A (**441**) | *Haploporus odorus* | Dimeric drimane | [313] |
| Isodrimenediol | *Polyporus arcularius* | Drimane | [314] |
| Isocryptoporic acids H, I | *Polyporus arcularius* | Drimane | [315] |
| 2′′-*O*-Methyl-cryptoporic acid H | *Polyporus cileates* | Drimane | [315] |
| Methoxylaricinolic acid (**445**) | *Stereum ostrea* | Drimane | [316] |
| Laricinolic acid | *Stereum ostrea* | Drimane | [316] |
| Nebularic acid A | *Lepista nebularis* | 11-Nordrimane | [317] |
| Nebularic acid B | *Lepista nebularis* | Drimane | [317] |
| Nebularilactones A, B | *Lepista nebularis* | Drimane | [317] |
| Strobilactones A, B | *Strobilurus ohshimae* | Drimane | [265] |
| 3-Keto-drimenol | *Clitocybe conglobata* | Drimane | [318] |
| 3*β*-Hydroxy-11-acetyldrimene | *Clitocybe conglobata* | Drimane | [318] |
| 3*β*-Hydroxydrimenol | *Clitocybe conglobata* | Drimane | [318] |
| 11,12-Dihydroxydrimene | *Clitocybe conglobata* | Drimane | [318] |

(continued)

**Table 24** (continued)

| Compound | Origin | Type | Refs. |
|---|---|---|---|
| 3*β*-Hydroxy-11,12-*O*-isopropyldrimene | *Clitocybe conglobata* | Drimane | [318] |
| Drimane-3,8,11,12-tetraol | *Marasmius cladophyllus* | Drimane | [319] |
| Cryptoporic acid J | *Marasmius cladophyllus* | Dimeric drimane | [319] |
| Cryptoporic acids J–O | *Cryptoporus sinensis* | Drimane | [320, 321] |
| Demethylcryptoporic acid D | *Cryptoporus sinensis* | Drimane | [321] |
| Arecoic acids A–F (**446**) | *Arecophila saccharicola* YMJ96022401 | Drimane | [322] |
| Marasmene B | *Marasmius* sp. | Drimane | [323] |
| Marasmals B, C | *Marasmius* sp. | Drimane | [323] |
| Funatrols A–D | *Funalia trogii* | Drimane | [324] |
| (2*S*)-Hydroxyalbicanol | *Polyporus arcularius* | Drimane | [325] |
| (2*S*)-Hydroxyalbicanol acetate | *Polyporus arcularius* | Drimane | [325] |
| 11,12-Epoxy-3*α*,6*β*,9*α*,11*α*-tetrahydroxydrimene | *Trichaptum biforme* | Drimane | [326] |
| 11,12-Epoxy-3*α*,9*α*,11*α*-trihydroxydrimene | *Trichaptum biforme* | Drimane | [326] |
| Cryptoporic acids P, Q | *Fomitella fraxinea* | Drimane | [327] |
| 11,12-Dihydroxy-15-drimeneoic acid | *Agaricus arvensis* | Drimane | [328] |
| 3*α*,11,15-Trihydroxydrimene | *Agaricus arvensis* | Drimane | [328] |
| 3*α*,6*β*-Dihydroxycinnamolide | *Inonotus rickii* | Drimane | [247] |
| 3*β*,6*β*-Dihydroxycinnamolide | *Fomitiporia punicata* | Drimane | [329] |
| Phellinuins A–G | *Phellinus tuberculosus* | Drimane | [330] |
| Porialbocin A | *Poria albocincta* BCC 26244 | Drimane | [331] |
| Inotolactone C | *Inonotus obliquus* | Drimane | [332] |
| 12-Hydroxy-3-oxodrimenol | *Phellinidium sulphurascens* | Drimane | [333] |
| 11-Hydroxyacetoxydrim-7-en-3*β*-ol | *Phellinidium sulphurascens* | Drimane | [333] |
| Cryptoporic acids R, S | *Cryptoporus volvatus* | Drimane | [334, 335] |
| 6′,6‴-Cryptoporic acid G dimethyl ester | *Cryptoporus volvatus* | Dimeric drimane | [335] |
| Sulphureuine B | *Laetiporus sulphureus* | Drimane | [336] |
| 15-Hydroxydrimenol | *Psathyrella candolleana* | Drimane | [337] |
| Cryptoporol A | *Cryptoporus volvatus* | Drimane | [338] |
| 6′-Cryptoporic acid E methyl ester | *Cryptoporus volvatus* | Dimeric drimane | [338] |

*Cryptoporus*. The terpenoid part of this type of compound is most often albicanol (**439**), but sometimes 15-hydroxyalbicanol (**440**), 3-hydroxyalbicanol, or (3-hydroxy-)drim-7-en-11-ol occur (Table 24). The position of dimerization of these compounds by ester bonds is either between C-15(C-15″) and C-4‴(C-4′),

or between C-15(C-15′) and C-5′′(C-5′), as for example in haploporic acid A (**441**). These compounds are responsible for the strong bitter taste of their mushrooms of origin, and show various other biological activities. For example, cryptoporic acid A (**442**) completely inhibited the germination of rice seeds at a concentration of 200 ppm (Fig. 46) [304]. Cryptoporic acids C–E showed superoxide releasing inhibitory activities (Fig. 46) [305]. Cryptoporic acid D exhibited inhibition against nitric oxide production in macrophages with an $IC_{50}$ value of 45.8 ± 3.6 μ$M$, which was comparable to that of the positive control used, hydrocortisone ($IC_{50}$ of 40.6 ± 2.5 μ$M$) (Fig. 46) [321]. Mniopetals A–F (**443**) are inhibitors of RNA-directed DNA-polymerases (Fig. 46) [308, 309].

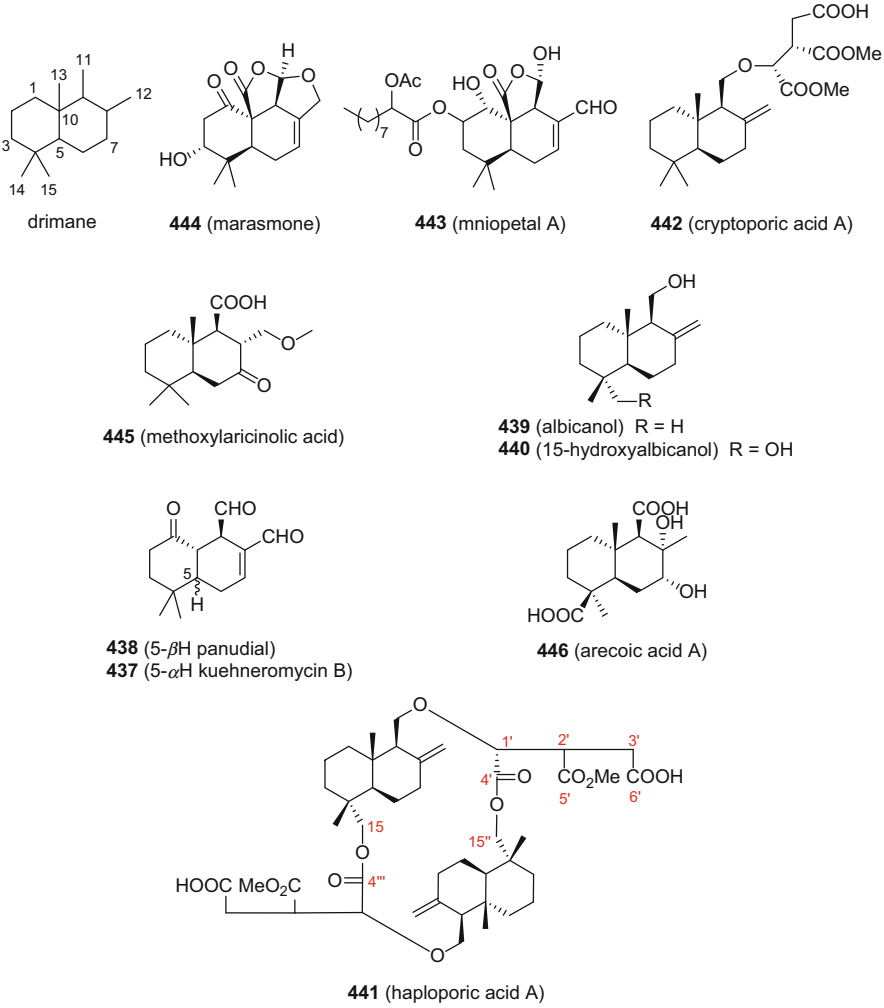


**Fig. 46** Structures of the drimane skeleton and selected drimane sesquiterpenoids

### 4.1.10 Eremophilanes and Eudesmanes

Eremophilane- and eudesmane-type sesquiterpenoids are representative of two skeletons having considerable similarities that often co-exist. These two types of sesquiterpenoids are mainly found in plants. In recent years, such compounds have been isolated and characterized frequently from fungi. Interestingly, nearly two-thirds of the fungal eremophilanes have been isolated from members of the genus *Xylaria* (Table 25).

**Table 25** Eremophilane and eudesmane sesquiterpenoids

| Compound | Origin | Type | Refs. |
|---|---|---|---|
| Hypodoratoxide (**447**) | *Hypomyces odoratus* | Eremophilane | [339, 340] |
| Integric acid (**448**) | *Xylaria* sp./*Xylaria feejeensis* 2FB-PPM08M | Eremophilane | [341–343] |
| Xylarenals A, B (**452**) | *Xylaria persicaria* | Eremophilane | [344] |
| Dacrymenone | *Dacrymyces* sp. | Eremophilane | [345] |
| 1$\beta$,7$\alpha$,10$\alpha$-Trihydroxyeremophil-11(13)-en-12,8$\beta$-olide | *Xylaria* sp. BCC 21097 | Eremophilane | [322, 346] |
| 7$\alpha$,10$\alpha$-Dihydroxy-1$\beta$-methoxyeremophil-11(13)-en-12,8$\beta$-olide | *Xylaria* sp. BCC 21097 | Eremophilane | [346] |
| 1$\alpha$,10$\alpha$-Epoxy-7$\alpha$-hydroxyeremophil-11(13)-en-12,8$\beta$-olide | *Xylaria* sp. BCC 21097 | Eremophilane | [346] |
| 1$\beta$,10$\alpha$,13-Trihydroxyeremophil-7(11)-en-12,8$\beta$-olide | *Xylaria* sp. BCC 21097 | Eremophilane | [322, 346] |
| 10$\alpha$,13-Dihydroxy-1$\beta$-methoxyeremophil-7(11)-en-12,8$\beta$-olide | *Xylaria* sp. BCC 21097 | Eremophilane | [346] |
| 1$\alpha$,10$\alpha$-Epoxy-13-hydroxyeremophil-7(11)-en-12,8$\beta$-olide | *Xylaria* sp. BCC 21097 | Eremophilane | [346] |
| 1$\alpha$,10$\alpha$-Epoxy-3$\alpha$-hydroxyeremophil-7(11)-en-12,8$\beta$-olide | *Xylaria* sp. BCC 21097 | Eremophilane | [346] |
| Mairetolide F | *Xylaria* sp. BCC 21097 | Eremophilane | [346] |
| Xylaranic acid | *Xylaria* sp. 101 | Eremophilane | [347] |
| 7$\beta$,8$\alpha$,12-Trihydroxyeremophila-9,11(13)-diene | *Xylaria* sp. BCC 5484 | Eremophilane | [348] |
| Arecolactone (**453**) | *Arecophila saccharicola* YMJ96022401 | Eremophilane | [322] |
| Polylisins A–D (**454**) | *Polyporus ellisii* | Eremophilane | [243] |
| Eremoxylarin C | *Xylaria allantoidea* BCC 23163 | Eremophilane | [167] |
| Eremoxylarin A | *Xylaria allantoidea* BCC 23163 | Eremophilane | [167] |

(continued)

**Table 25** (continued)

| Compound | Origin | Type | Refs. |
|---|---|---|---|
| 07H239-A | *Xylaria allantoidea* BCC 23163 | Eremophilane | [167] |
| Dictyophorines A (**449**), B | *Dictyophora indusiata* | Eudesmane | [349] |
| Teucrenone | *Dictyophora indusiata* | Eudesmane | [349] |
| (5$\beta$,6$\alpha$)-6,11-Dihydroxyeudesmane | *Sparassis crispa* | Eudesmane | [350] |
| 3$\alpha$,4-Epoxy-13-hydroxyeudesma-7 (11)-en-12,8$\alpha$-olide | *Xylaria* sp. BCC 5484 | Eudesmane | [348] |
| 3$\alpha$,4-Epoxyeudesma-7(11)-en-12,8$\alpha$-olide | *Xylaria* sp. BCC 5484 | Eudesmane | [348] |
| Flamvelutpenol A | *Flammulina velutipes* | Eudesmane | [351] |
| Eudesm-1$\beta$,6$\alpha$,11-triol (**450**) | *Phellinus ignarius* | Eudesmane | [352] |
| Hypoxylans A–C (**451**) | *Hypoxylon rickii* | 14-Noreudesmane | [353] |
| 14(10→1)*abeo*-Eudesm-11-ene-1,13-diol | *Marasmiellus ramealis* | 14(10→1)*abeo*-Eudesmane | [354] |
| 14(10→1)*abeo*-Eudesma-1,11,13-triol | *Marasmiellus ramealis* | 14(10→1)*abeo*-Eudesmane | [354] |

Hypodoratoxide (**447**), an eremophilane ether from *Hypomyces odoratus*, decreased germination rates and displayed potent antifungal activity against several organisms (Fig. 47) [339, 340]. Integric acid (**448**), an acyl eremophilane sesquiterpenoid, is an inhibitor of HIV-1 integrase (Fig. 47) [341]. Further biological evaluation revealed that integric acid exhibited inhibitory activity against the malarial parasite *Plasmodium falciparum* K1 strain with an $IC_{50}$ value of 6.91 $\mu M$ [342]. The SAR of derivatives of chemical and enzymatic modifications of integric acid were thoroughly investigated [355]. The biosynthesis pathway of integric acid was also elucidated.

Dictyophorines A (**449**) and B are eudesmane-type sesquiterpenoids first isolated from the mushrooms *Dictyophora indusiata* in 1997. They promote the synthesis of nerve growth factor (NGF)-synthesis in astroglial cells (Fig. 47) [349].

Eudesm-1$\beta$,6$\alpha$,11-triol (**450**) was isolated from cultures of *Phellinus ignarius* (Fig. 47). Its antiviral activity against the H5N1 influenza A virus was investigated using a MTT colorimetric assay system in Madin-Darby canine kidney cells. The results suggested that this compound significantly inhibited the influenza virus with an $EC_{50}$ value of $0.14 \pm 0.04$ $\mu M$. Molecular modeling revealed that the antiviral activity of compound **450** can be ascribed partially to the interactions of its hydroxy groups with an amino acid residue (Asn 170) of neuraminidase at the binding site [352].

Hypoxylans A–C (**451**) are three 14-noreudesmane sesquiterpenoids containing an aromatic ring, and were isolated from cultures of the ascomycete *Hypoxylon rickii* (Fig. 47). Biological evaluation showed that compound **451** has weak antibacterial activity against the Gram-positive bacterium *Staphylococcus aureus*

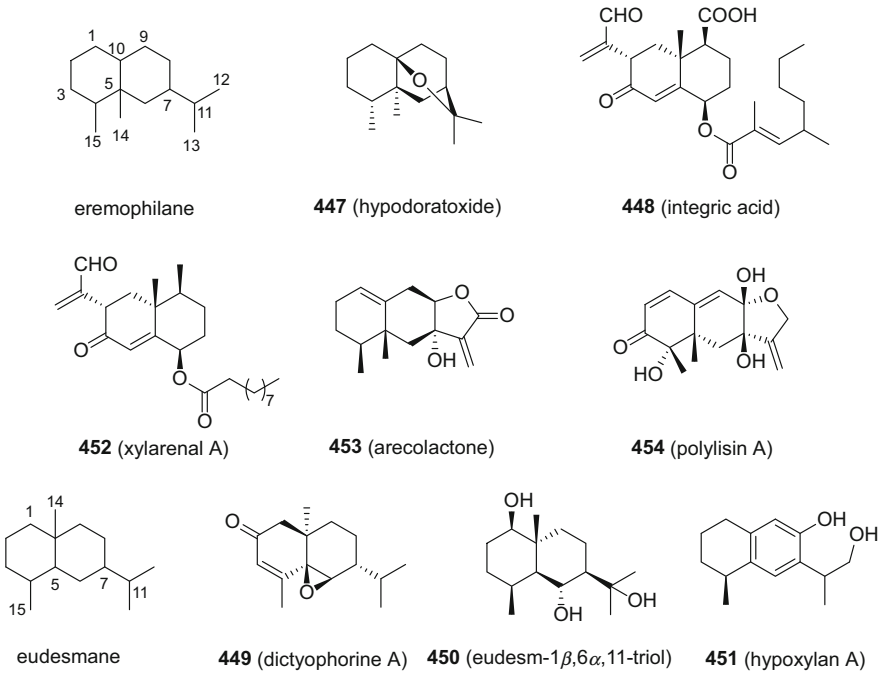


**Fig. 47** Structures of eremophilane, eudesmane, and selected examples of eremophilane and eudesmane sesquiterpenoids

DSM 346 with an *MIC* value of 67.0 μg/cm$^3$, and also it exhibited weak inhibitory activity against the L929 murine fibroblast cell line [353].

### 4.1.11 Hirsutanes and Related Triquinane Sesquiterpenoids

The protoilludane-derived triquinanes consist of at least six types of sesquiterpenoids, as depicted in Scheme 21. Hirsutanes are the most common and largest group of these structural types (Table 26). Notably, hirsutanes are invariably accompanied by compounds based on other carbon skeletons in many species. Hirsutanes were previously reviewed [251]. Hirsutanes are usually dimerized or trimerized via C–C or ester bonds and display diverse biological activities.

Sterhirsutins A-D (**455–458**) are heterodimeric sesquiterpenoids constructed by a Diels-Alder reaction of hirsutane on one side and humulane, hirsutane, and caryophyllane, on the other. They were isolated from the Tibetan fungus *Stereum hirsutum* (Fig. 48) [365, 366]. Sterhirsutin E (**459**) is a hirsutane homodimer via an ester bond, while sterhirsutin J (**460**) is a heterodimer constructed from a hirsutane sesquiterpenoid and a meroterpenoid. Sterhirsutins A and B showed cytotoxicity against the K562 cell line with $IC_{50}$ values of 12.97 and 16.29 μ*M*, and against the

**Scheme 21** The protoilludane-derived triquinane skeletons

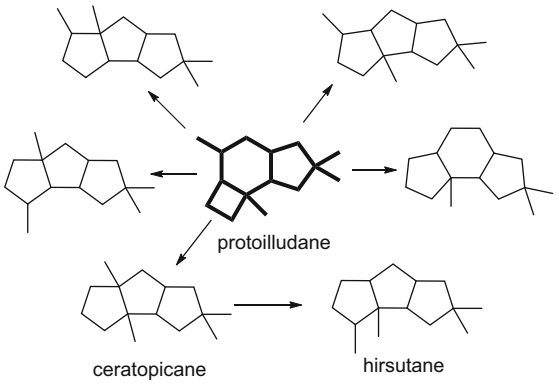


**Table 26** Hirsutanes and related sesquiterpenoids

| Compound | Origin | Type | Refs. |
|---|---|---|---|
| Phellodonic acid (**461**) | *Phellodon melaleucus* | Hirsutane | [356] |
| 1-Desoxyhypnophilin | *Lentinus crinitus* | Hirsutane | [357] |
| Hypnophilin | *Lentinus crinitus* | Hirsutane | [357, 358] |
| Hirsutenols A–C | *Stereum hirsutum* | Hirsutane | [359] |
| Dichomitol (**467**) | *Dichomitus squalens* | Hirsutane | [229] |
| Connatusins A, B | *Lentinus connatus* BCC 8996 | Hirsutane | [358] |
| Dihydrohypnophilin | *Lentinus connatus* BCC 8996 | Hirsutane | [358] |
| Hirsutenols D–F | *Stereum hirsutum* | Hirsutane | [360] |
| Creolophins A, C–E | *Creolophus cirrhatus* | 13-Norhirsutane | [361, 362] |
| Creolophin B | *Creolophus cirrhatus* | Hirsutane | [361, 362] |
| Xeromphalinones A–D | *Xeromphalina* sp. | Hirsutane | [363] |
| Xeromphalinones E (**463**), F | *Xeromphalina* sp. | Dimeric hirsutane | [363] |
| Chlorostereone | *Stereum* sp. | Hirsutane | [363] |
| Complicatic acid | *Stereum* sp. | Hirsutane | [363] |
| Pleurocybellone A (**462**) | *Pleurocybella porrigens* | | [363] |
| Coriolin C | *Pleurocybella porrigens* | Hirsutane | [363] |
| (−)-Hirsutanol A, C | *Gloeostereum incarnatum* | Hirsutane | [364] |
| (+)-Incarnal | *Gloeostereum incarnatum* | Hirsutane | [364] |
| Compounds 3–5 | *Stereum hirsutum* | Hirsutane | [128] |
| Sterhirsutins A (**444**), B (**456**) | *Stereum hirsutum* | Heterodimeric Hirsutane/humulane | [365] |
| Sterhirsutins C (**457**), D (**458**) | *Stereum hirsutum* | Heterodimeric Hirsutane/ caryophyllane | [366] |
| Hirsutic acids D, E | *Stereum hirsutum* | Hirsutane | [365] |
| Sterhirsutins E–G (**459**) | *Stereum hirsutum* | Dimeric hirsutane | [366] |
| Sterhirsutins H–I | *Stereum hirsutum* | Trimeric hirsutane | [366] |

(continued)

**Table 26** (continued)

| Compound | Origin | Type | Refs. |
|---|---|---|---|
| Sterhirsutins J–L (**460**) | *Stereum hirsutum* | Hirsutane | [366] |
| Antrodin A (**464**) | *Antrodiella albocinnamomea* | | [367] |
| Antrodin B (**465**) | *Antrodiella albocinnamomea* | Ceratopicane | [367] |
| Antrodin C (**466**) | *Antrodiella albocinnamomea* | | [367] |
| Antrodin D | *Antrodiella albocinnamomea* | Hirsutane | [367] |
| Trefoliol C | *Tremella foliacea* | | [277] |
| Flammulinol A | *Flammulina velutipes* | | [368] |

HCT116 cell line with $IC_{50}$ values of 10.74 and 16.35 μ*M*. From the same fungus, many hirsutane dimers and trimers have been isolated and they showed bioactivities in a panel of bioassays. Sterhirsutins E–G and I exhibited antiproliferative activity with $IC_{50}$ values in the range of 6–20 μ*M* (Fig. 48). Sterhirsutin K was found to possess autophagy-inducing activity at a concentration of 50 μ*M*, while sterhirsutins J and hirsutic acid E inhibited the growth of GFP-LC3 stable Hela cells at a dose of 50 μ*M* (inhibition rate 100%).

Phellodonic acid (**461**), the first bioactive metabolite from a culture of a species of the family Thelephoraceae, was found to display potent antibacterial activities against *Bacillus brevis* and *B. subtilis* with *MIC* values of 2 and 5 μg/cm$^3$ (Fig. 48). Pleurocybellone A (**462**) is a sesquiterpenoid with a fatty acid modification isolated from the mushroom *Pleurocybella porrigens*, which, as mentioned earlier in this chapter, was reported to produce toxic amino acids leading to several mushroom poisoning cases in Japan [187–189, 363]. The compound xeromphalinone E (**463**) is a hirsutane homodimer, in which two hirsutane units are directly connected by a carbon–carbon bond [363].

Antrodins A–C (**464**–**466**) are three novel triquinane sesquiterpenoids isolated from submerged cultures of the fungus *Antrodiella albocinnamomea*. The absolute configuration of **464** was determined using single-crystal X-ray diffraction analysis [367].

The structure of dichomitol (**467**) was isolated by Wei et al. from the cultures of the fungus *Dichomitus squalens* [229]. However, a total synthesis of the proposed structure led to distinctly different spectroscopic characteristics from those reported, indicative of the need to revise the structure of **467** [369].

Dihydrohypnophilin, isolated from *Lentinus conatus* BCC 8996, exhibited cytotoxic effects against the NCI-H187 and Vero cell lines with $IC_{50}$ values of 0.67 and 1.1 μg/cm$^3$. (–)-Hirsutanol A and (+)-incarnal, purified from *Gloeostereum incarnatum*, exhibited antiproliferative activity against murine B16 melanoma cells with $IC_{50}$ values of 25 and 14 μ*M*.

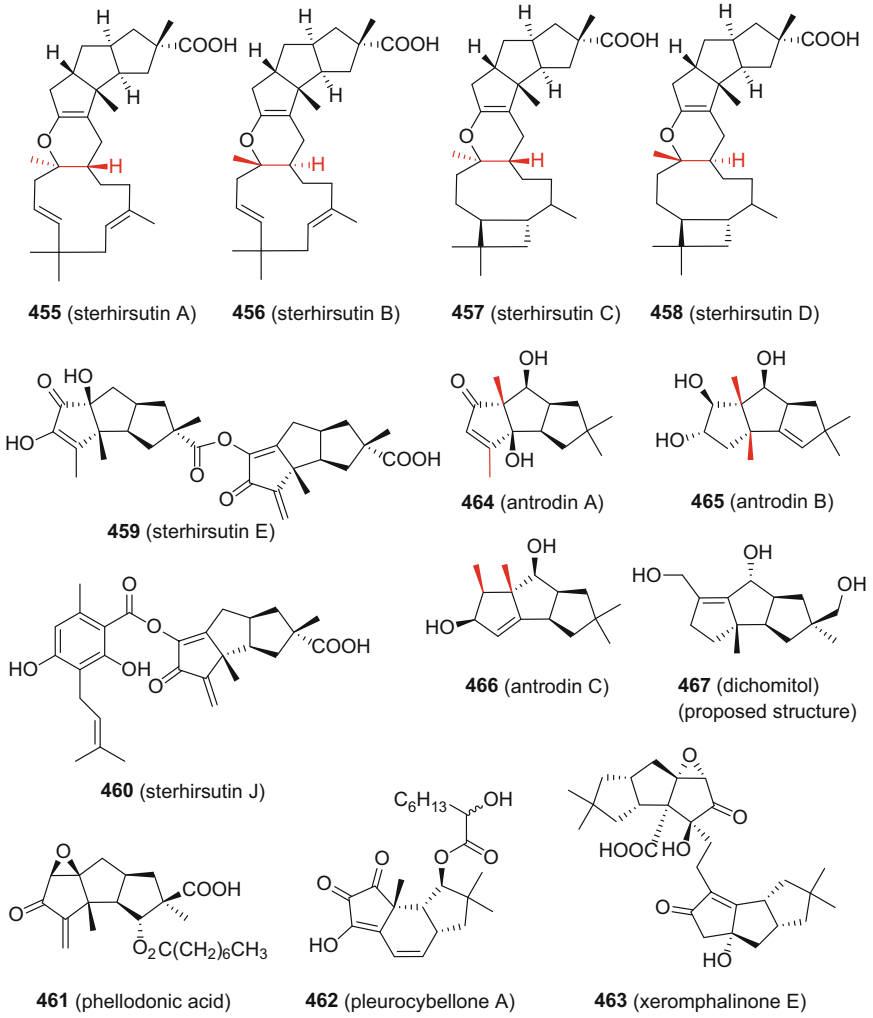


**Fig. 48** Selected compounds of hirsutane sesquiterpenes and related-triquinane skeletons

### 4.1.12 Protoilludanes and Cerapicanes

The 4/6/5 ring-fused protoilludane-type sesquiterpenoids are the precursors of many other sesquiterpenoids, representing the largest group of sesquiterpene metabolites of fungal origin. Among them, a large number of protoilludane orsellinates or everninates, which have been designated as protoilludane aryl esters, have been isolated only from the genus *Armillaria* (Table 27). Interestingly, the overall number and structural variety of these aryl esters varies among *Armillaria* species, but also within a given species, which is thought to be correlated with

**Table 27** Protoilludane sesquiterpenoids

| Compound | Origin | Type | Refs. |
|---|---|---|---|
| Armillaritin | *Armillaria mellea* | Protoilludane aryl ester | [370] |
| Armillarivin | *Armillaria mellea* | Protoilludane aryl ester | [370] |
| Armillyl orsellinate | *Armillaria mellea* | Protoilludane | [371] |
| Sulcatines C–E, G (**468**) | *Laurilia sulcata* | Norprotoilludane | [372, 373] |
| 7-*epi*-Sulcatine D | *Laurilia sulcata* | Norprotoilludane | [373] |
| Melleolides K–M | *Armillariella mellea* | Protoilludane aryl ester | [374] |
| Gloeophyllone | *Gloeophyllum* sp. 97022 | 15(11→10)-*abeo*-Protoilludane | [375] |
| Atlanticones A–D | *Lactarius altanticus* | Protoilludane | [376] |
| Illudiolone | *Omphalotus illudens* | Protoilludane | [218] |
| Tsugicoline A | *Clavicorona divaricata* | Protoilludane | [166, 377] |
| Tsugicoline E (**469**) | *Laurilia tsugicola* | Protoilludane | [378] |
| Repraesentin A | *Lactarius repraesentaneus* | Protoilludane | [379] |
| Repraesentins B (**472**), C | *Lactarius repraesentaneus* | Cerapicane | [379] |
| Riparol A | *Ripartites metrodii* 82136 | Protoilludane | [380] |
| Russujaponols A–D, G–H | *Russula japonica* | Protoilludane | [381, 382] |
| Pasteurestins A (**470**), B (**471**) | *Agrocybe cylindracea* | Protoilludane | [383, 384] |
| Pyxidatols A–C | *Clavaria pyxidata* | Protoilludane | [217] |
| Arnamial (**473**) | *Armillaria mellea* | Protoilludane aryl ester | [385] |
| Melledonol | *Armillaria mellea* | Protoilludane aryl ester | [385] |
| Melleolides C, D | *Armillaria mellea* | Protoilludane aryl ester | [385] |
| Melledonal A | *Armillaria mellea* | Protoilludane aryl ester | [385] |
| Melledonal C | *Armillaria mellea* | Protoilludane aryl ester | [385] |
| 10$\alpha$-Hydroxymelleolide | *Armillaria mellea* | Protoilludane aryl ester | [385] |
| 4,5-Dehydro-5-deoxyarimillol | *Coprinus cinereus* | Protoilludane | [386] |
| 5-Hydroxydichomitol | *Dichomitus squalens* | Protoilludane | [230] |
| Lentinellone | *Clavicorona divaricata* | Protoilludane | [166] |
| 10-Dehydroxymelleolide B | *Armillaria* sp. | Protoilludane aryl ester | [387] |
| 1-*O*-Formyl-10-dehydroxy-melleolide B | *Armillaria* sp. | Protoilludane aryl ester | [387] |
| 10-Oxo-melleolide B | *Armillaria* sp. | Protoilludane aryl ester | [387] |
| 2-Hydroxycoprinolone | *Granulobasidium vellereum* | Protoilludane | [388] |
| 8-Deoxy-4a-hydroxytsugicoline | *Granulobasidium vellereum* | Protoilludane | [388] |
| 8-Deoxydihydrotsugicoline | *Granulobasidium vellereum* | Protoilludane | [388] |

(continued)

**Table 27** (continued)

| Compound | Origin | Type | Refs. |
|---|---|---|---|
| Radulones A, B | *Granulobasidium vellereum* | Protoilludane | [388] |
| Coprinolone ketodiol | *Granulobasidium vellereum* | Protoilludane | [388] |
| 2a-Hydroxycoprinolone | *Granulobasidium vellereum* | Protoilludane | [389] |
| 3-Hydroxycoprinolone | *Granulobasidium vellereum* | Protoilludane | [389] |
| Coprinolone diol B | *Granulobasidium vellereum* | Protoilludane | [389] |
| Granulodienes A, B | *Granulobasidium vellereum* | Protoilludane | [389] |
| Granulone B | *Granulobasidium vellereum* | Protoilludane | [389] |
| 8-Deoxy-4a-hydroxytsugicoline B | *Granulobasidium vellereum* | Protoilludane | [389] |
| Demethylgranulone | *Granulobasidium vellereum* | Protoilludane | [389] |
| Cerapicolene (**476**) | *Granulobasidium vellereum* | Cerapicane | [389] |
| Melleolides N, Q, R | *Armillaria mellea* | Protoilludane aryl ester | [390] |
| 10-Dehydroxymelleolide D | *Armillaria* sp. | Protoilludane aryl ester | [391] |
| 13-Hydroxymelleolide K | *Armillaria* sp. | Protoilludane aryl ester | [391] |
| 5-*O*-Acetyl-7,14-dihydroxy-protoilludanol | *Conocybe siliginea* | Protoilludane | [392] |
| 5′-Methoxy-armillasin (**474**) | *Armillaria mellea* | Protoilludane aryl ester | [393] |
| 5-Hydroxyl-armillarivin (**475**) | *Armillaria mellea* | Protoilludane aryl ester | [393] |
| 6′-Dechloroarnamial | *Armillaria mellea* FR-P75 | Protoilludane aryl ester | [394] |
| 6′-Chloromelleolide F | *Armillaria mellea* FR-P75 | Protoilludane aryl ester | [394] |
| 10-Hydroxy-5′-methoxy-6′-chloroarmillane | *Armillaria mellea* FR-P75 | Protoilludane aryl ester | [394] |
| 13-Deoxyarmellides A, B | *Armillaria mellea* FR-P75 | Protoilludane aryl ester | [394] |

pathogenicity against their hosts or as a result of responding to the competitive growth of other antagonistic fungi [395].

This class of natural products is known to exhibit antimicrobial and cytotoxic activities. It was revealed that the $\Delta^{2,4}$-double bond of the protoilludane moiety is essential for antifungal activity against several fungi, e.g. *Aspergillus nidulans*, *Aspergillus flavus*, and *Penicillium notatum*, but did not result in cytotoxicity against human cancer cells [396]. Additionally, some other protoilludane aryl esters

displayed inhibition of lettuce growth and mycelial growth of *Coprinopsis cinerea* and/or *Flammulina velutipes*.

The biosynthesis pathway of the orsellinic acid moiety, a cross-coupling mechanism of the protoilludane moiety and orsellinic acid, and chlorination at C-6′ of some melleolides in vivo was clarified by Hoffmeister and associates. It was revealed that the non-reducing iterative type I polyketide synthase ArmB is responsible for the biosynthesis of orsellinic acid, and a transesterification reaction of orsellinic acid and the terpene moiety, and five flavin-dependent halogenases (ArmH1 to ArmH5), are responsible for catalyzing the transfer of a single chlorine atom to the melleolides [397, 398].

Protoilludanes, as well as their rearranged congeners, also have been isolated from other fungal genera, e.g. *Omphalotus*, *Coprinus*, *Lactarius*, and *Russula* (Table 27). Two compounds bearing rare skeletons, which are rearranged from protoilludane, sulcatine G (**468**), and cerapicane accompanied by several protoilludane sesquiterpenes, were purified from *Laurilia sulcata* (Fig. 49). The total synthesis of sulcatine G was accomplished by Mehta and Sreenivas and by Taber and Frankoski, leading to the establishment of the absolute configuration of the dextrorotatory isomer [399–401].

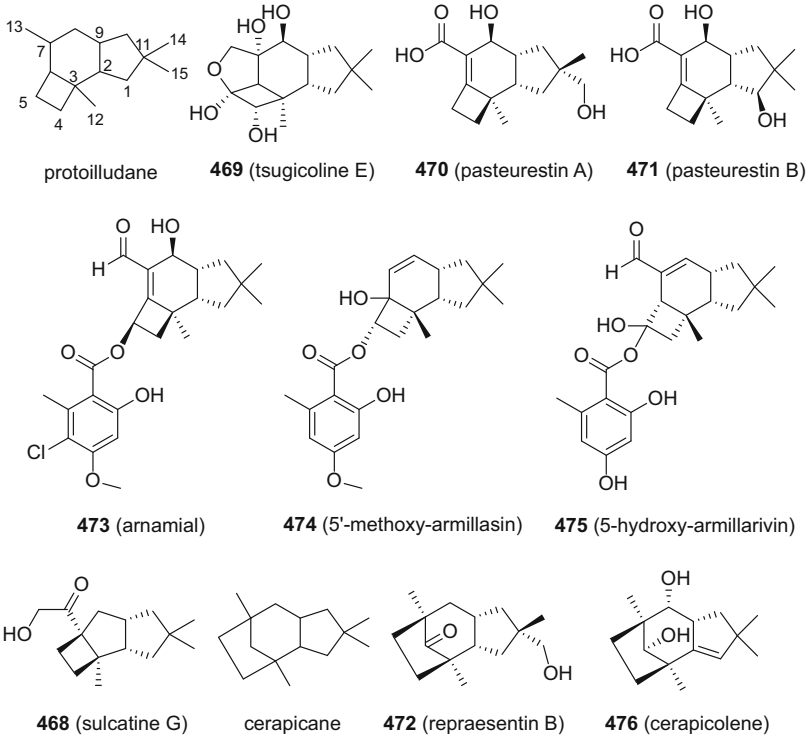


**Fig. 49** Structures of protoilludanes, cerapicanes, and selected compounds

(+)-Armillarivin was first discovered from an acetone extract of *Armillaria mellea* mycelia, but was not mentioned in a previous review [251]. The compounds 8-deoxydihydrotsugicoline and radudiol were isolated from the saprotrophic and rare wood-decaying fungus *Granulobasidium vellereum* [388, 389]. The chemoenzymatic total syntheses of (+)-armillarivin, 8-deoxydihydrotsugicoline, and radudiol were accomplished by Banwell's group [402, 403].

Tsugicoline E (**469**) is a polyoxygenated protoilludane sesquiterpene from the cultures of the fungus *Laurilia tsugicola* (Fig. 49). Its structure was established via NMR spectroscopic analysis and X-ray diffraction studies [378].

Pasteurestins A (**470**) and B (**471**), two protoilludane sesquiterpenoids from the basidiomycete *Agrocybe cylindracea*, are potential veterinary antibiotics, since they potently and selectively inhibited pathogens responsible for bovine respiratory disease, such as strains of *Mannheimia haemolytica* (Fig. 49). Unfortunately, they were reported in a patent application with neither their relative nor absolute configurations indicated [384]. The many contiguous stereocenters of pasteurestins A and B, and the lack of availability of the source material has posed challenges to the establishment of their absolute configurations. The total synthesis of **470** and **471** were conducted successfully by Kögl et al., involving key two step [2+2+2] $CpCo(CO)_2$-mediated Vollhardt cycloadditions in both syntheses, and a tin-mediated asymmetric Reformatsky-type condensation in the synthesis of **471** [383].

The variable structural features of this class of sesquiterpene has stimulated the testing of their activities in diverse types of bioassays, such as antifungal, radicle elongation promoting, and cytotoxicity determinations [390, 393]. Sulcatines C–E and G were active in an antifungal assay, and sulcatines C and E exhibited inhibition of *Cladosporium cladosporioides*, *C. cucumerinum*, and *Aspergillus niger* in amounts as low as 50 μg per plate in a bioautographic antifungal testing procedure [373]. Repraesentins A, B (**472**), and C promoted the radicle elongation of lettuce seedlings by 136, 118, and 184%, respectively, at 67 ppm [379]. Russujaponol A inhibited 63% of the invasion of the human HT1080 fibrosarcoma cell line to the reconstituted basal membrane at 3.73 μ*M* (positive control, doxorubicin 52% at 0.17 μ*M*) [381]. Russujaponols I–J promoted neurite outgrowth of cultured rat cortical neurons in a concentration range from 0.1 to 10 μ*M* [382]. Arnamial (**473**), a protoilludane everninate ester from the fungus *A. mellea*, showed cytotoxicity against Jurkat T, MCF-7 breast adenocarcinoma, CCRF-CEM lymphoblastic leukemia, and HCT-116 colorectal carcinoma cells, with $IC_{50}$ values of 3.9, 15.4, 8.9, and 10.7 μ*M* [385]. A SAR study of the melleolides revealed that hydroxylation of the terpenoid unit is of major relevance to the resultant cytotoxicity, while the position of the double bond and 6′-chlorination of the aromatic ring do not influence such activity [404]. Radulone A showed inhibition on spore germination of the competing fungi *Phlebiopsis gigantea*, *Coniophora puteana*, and *Heterobasidion occidentale* at 10, 500 and 100 μ*M* [388]. Melleolide K inhibited the growth of seveval

Gram-positive bacteria, yeasts, and fungi, but did not inhibit Gram-negative bacteria in this regard.

### 4.1.13 Fomannosanes

Fomannosane-type sesquiterpenoids possess *seco*-protoilludane skeletons and are rarely isolated from fungi. Only seven fomanosane-type sesquiterpenoids have been reported from mushrooms since an earlier review was published (Table 28) [251]. Illudosone hemiacetal (**477**) and illudosone (**478**) were isolated as a mixture of a hemiacetal and a free aldehyde (Fig. 50). 5-Desoxyilludosin (**479**) and 13-hydroxy-5-desoxyilludosin (**480**) were obtained from a fungal extract of *Bovista* sp. 96042 (Fig. 50). 5-Desoxyilludosin (**479**) was also found in the fungus *Ripartites metrodii* 93109. (2*S*,3*S*,9*R*)-5-Desoxy-14-hydroxyilludosin (**481**) was reported to exhibit inhibition of the murine P388 leukemia cell line with an $ED_{50}$ value of 5.3 μg/cm$^3$ (Fig. 50). The relative configuration of agrocybin H (**482**), isolated with the accompanying agrocybin I (**483**), was determined by single-crystal X-ray crystallographic diffraction analysis (Fig. 50).

**Table 28** Fomannosane sesquiterpenoids

| Compound | Origin | Type | Refs. |
|---|---|---|---|
| Illudosone hemiacetal (**477**) | *Omphalotus illudens* | Fomannosane | [218] |
| Illudosone (**478**) | *Omphalotus illudens*<br>*Agrocybe salicacola* | Fomannosane | [218, 405] |
| 5-Desoxyilludosin (**479**) | *Ripartites metrodii* 93109<br>*Bovista* sp. 96042 | Fomannosane | [380, 406] |
| 13-Hydroxy-5-desoxyilludosin (**480**) | *Bovista* sp. 96042 | Fomannosane | [406] |
| (2*S*,3*S*,9*R*)-5-Desoxy-14-hydroxyilludosin (**481**) | *Coprinus cinereus* | Fomannosane | [386] |
| Agrocybins H (**482**), I (**483**) | *Agrocybe salicacola* | Fomannosane | [405] |

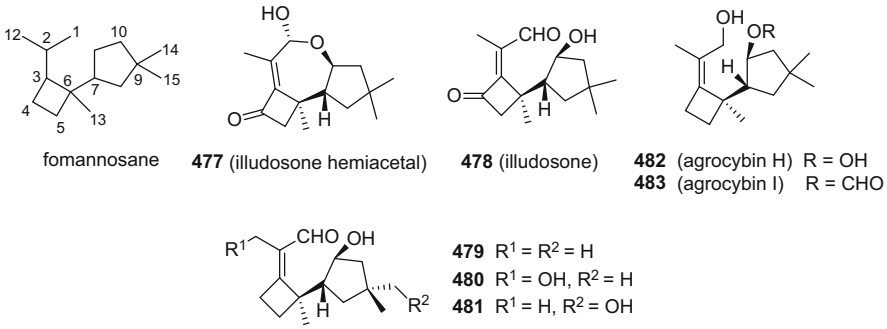


**Fig. 50** Structures of fomannosane and selected compounds

### 4.1.14 Illudanes and Illudalanes

Illudane-type sesquiterpenoids are derived biogenetically from the protoilludanes (Table 29), as verified from an experiment by feeding synthetic deuterium labeled *dl*-6-protoilludene to the illudin-producing fungus *Omphalotus olearius*. In this manner, illudins M (**484**) and S (**485**) were produced. Most illudanes exhibit cytotoxic effects toward many tumor cell lines and some are regarded as having a

**Table 29** Illudanes and illudalanes

| Compound | Origin | Type | Refs. |
|---|---|---|---|
| Psathyrellon B | *Bovista* sp. 96042 | Illudane | [406] |
| Bovistol (**494**) | *Bovista* sp. 96042 | Illudane-illudalane dimer | [406] |
| Illudane | *Bovista* sp. 96042<br>*Ripartites metrodii* 82136 | Illudane | [380, 406] |
| Illudins I, $I_2$, J, $J_2$ | *Coprinopsis episcopalis* (syn. *Coprinus episcopalis*) | Illudane | [407, 408] |
| Paneolic acid | *Panaeolus retirugis* | Illudane | [409] |
| Paneolilludinic acid | *Panaeolus retirugis* | Illudane | [409] |
| Riparol A | *Ripartites metrodii* 82136 | Illudane | [380] |
| Psathyrellon A | *Ripartites metrodii* 93109 | Illudane | [380] |
| Coprinastatin 1 (**487**) | *Coprinus cinereus* | Illudane | [178] |
| 7,7a-Diepicoprinastatin 1 | *Coprinus cinereus* | Illudane | [386] |
| Agrocybone (**495**) | *Agrocybe salicacola* | Illudane-illudalane dimer | [410] |
| Agrocybins A–G (**496**) | *Agrocybe salicacola* | Illudane | [411] |
| Illudin T | *Agrocybe salicacola* | Illudane | [411, 412] |
| Dichomilludol | *Dichomitus squalens* | Illudane | [230] |
| Phellinuin J | *Phellinus tuberculosus* | Illudane | [413] |
| Sulphureuine A | *Laetiporus sulphureus* | Illudane | [413] |
| (3*S*,7*R*)-Illudin M (**488**) | *Granulobasidium vellereum* | Illudane | [414] |
| (3*S*,7*S*)-Illudin M (**490**) | *Granulobasidium vellereum* | Illudane | [414] |
| (3*S*,4*S*,7*R*)-Dihydroilludin M (**491**) | *Granulobasidium vellereum* | Illudane | [414] |
| (3*S*,6*S*,7*R*)-Illudin S (**489**) | *Granulobasidium vellereum* | Illudane | [414] |
| Illudadiene A | *Granulobasidium vellereum* | Illudane | [414] |
| Illudadiene B | *Granulobasidium vellereum* | Illudane | [414] |
| Granuloinden B (**492**) | *Granulobasidium vellereum* | Illudalane | [414] |
| Granulodione (**493**) | *Granulobasidium vellereum* | 12-Norilludane | [415] |
| Gleophyllols A-D | *Gloeophyllum* sp. 97022 | 15(11→10)-*abeo*-Illudalane | [375] |

(continued)

**Table 29** (continued)

| Compound | Origin | Type | Refs. |
|---|---|---|---|
| Divaricatines A–D (**305**) | *Clavicorona divaricata* | Illudalane | [166, 377] |
| 7-*epi*-Tsugicoline H | *Clavicorona divaricata* | Illudalane | [377] |
| Tsugicoline M | *Clavicorona divaricata* | Illudalane | [377] |
| Echinolactones A, B | *Echinodontium japonicum* | Illudalane | [416] |
| Riparol B | *Ripartites metrodii* 82136 | Illudalane | [380] |
| Russujaponols E, F, I–L (**498–500**) | *Russula japonica* | Illudalane | [381, 382] |
| Coprinol | *Coprinus cinereus* | Illudalane | [178] |
| Epimer of coprinol | *Coprinus cinereus* | Illudalane | [178] |
| Sterostreins A–C, T (**497**) | *Stereum ostrea* BCC 22955 | Illudalane dimer | [417, 418] |
| Sterostreins D–I, M–S (**501**) | *Stereum ostrea* BCC 22955 | Illudalane | [165, 417–419] |
| Sterostreins J–L | *Stereum ostrea* BCC 22955 | 15-Norilludalane | [165] |
| Granulolactone | *Granulobasidium vellereum* | Illudalane | [415] |
| Puraquinoic acid (**502**) | *Mycena pura* | 12-Norilludalane | [420] |

high potential as anticancer drug lead compounds. Illudins M and S were isolated from the Jack-o'-Lantern mushroom, *Omphalotus illudens* (syn. *Clitocybe illudens*), in an attempt to discover antibiotics from Basidiomycetes at the New York Botanical Garden by Anchel et al. (Fig. 51) [421]. Illudin S showed potent antibiotic activity against *Staphylococcus aureus* but it was found to be extremely toxic to experimental animals. An investigation of the secondary metabolites of *O. illudens* indicated **485** to be the only constituent to exhibit antiviral activity [422]. Although illudins have been proven to be cytotoxic against various tumor cell types following extensive studies, their high toxicity and low therapeutic index has prevented their further development as anticancer agents to date. In order to improve on the therapeutic characteristics of illudins, hydroxymethylacylfulvene (irofulven, HMAF) (**486**) has been produced, with the acylfulvene core structure semi-synthesized from illudin S by treatment with dilute sulfuric acid and excess paraformaldehyde (Fig. 51). A phase I clinical trial revealed that **486** was more potent against gastrointestinal tumors and metastatic prostate cancer than mitomycin, cisplatin, and paclitaxel, and showed synergistic activity with conventional cancer chemotherapeutic agents. Hydroxymethylacylfulvene has reached phase III trial clinical testing [423, 424]. Certain urea, carbamate, and sulfonamide derivatives of acylfulvene were synthesized to evaluate their antitumor potential [425, 426]. As a result of their promising antitumor activity, illudins and acylfulvenes have long been an interesting synthesis targets for organic chemists. Several total racemic or enantioselective synthesis procedures for illudins and acylfulvenes have been reported [427–430].

The illudane-type sesquiterpenes paneolic acid and paneolilludinic acid exhibited antibacterial activity against *Staphylococcus aureus*. Paneolic acid gave

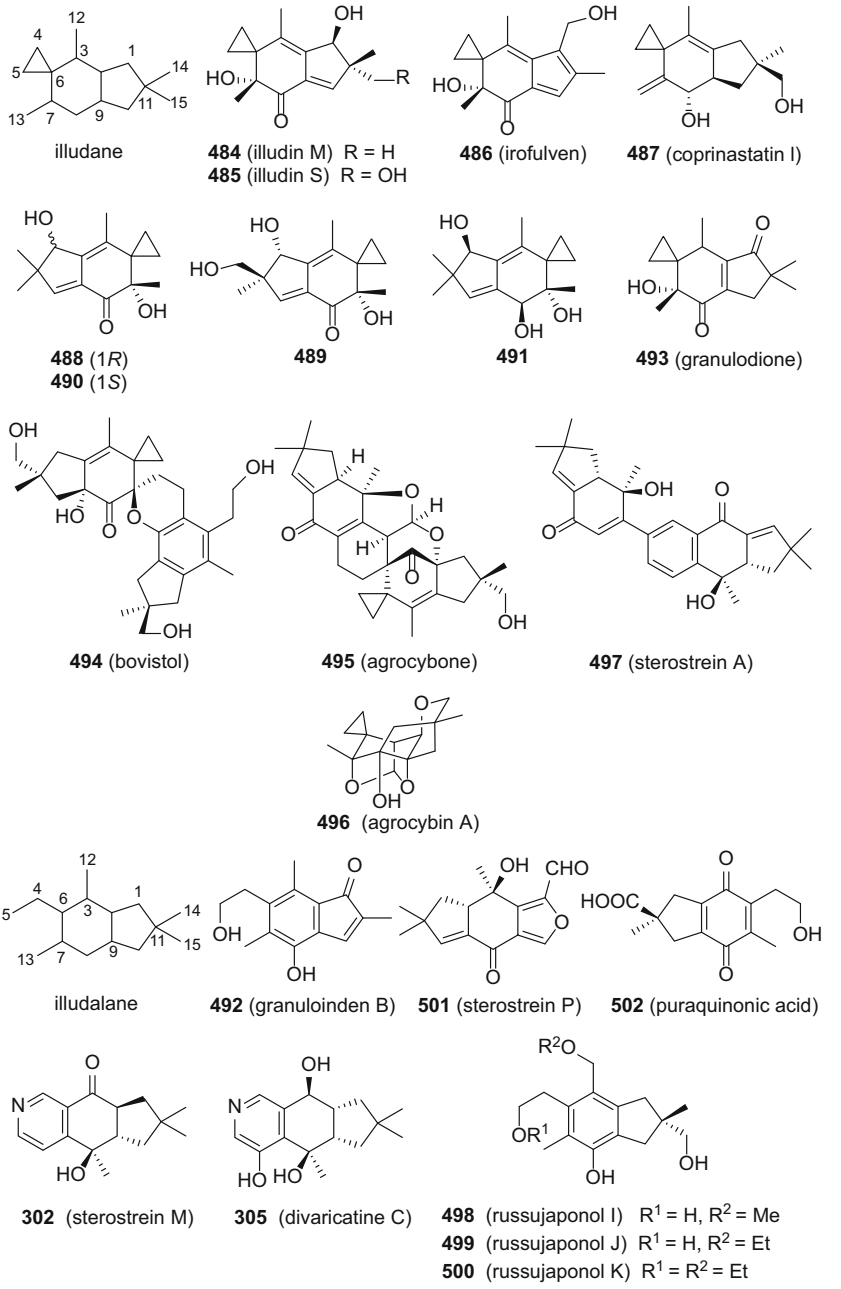


**Fig. 51** Structures of illudane and illudalane and selected derivatives

an $IC_{50}$ of 18.9 μg/cm$^3$ for HL-60 cells [409]. Coprinastatin 1 (**487**) showed both cytotoxicity against the P388 lymphocytic leukemia line ($ED_{50}$ of 5.3 μg/cm$^3$) and antibacterial activity against the pathogenic bacterium *Neisseria gonorrhoeae* (*MIC* value of 32–64 μg/cm$^3$) (Fig. 51) [178]. The saprotrophic wood-decaying fungus *Granulobasiodium vellereum* accumulates a variety of sesquiterpenoid metabolites. (3*S*,7*R*)-Illudin M (**488**) and (3*S*,4*S*,7*R*)-dihydroilludin M (**491**), enantiomers of illudin M and dihydroilludin M, respectively, and (3*S*,6*S*,7*R*)-illudin S (**489**) and (3*S*,7*S*)-illudin M (**490**), diastereomers of illudin M and illudin S, were isolated from cultures of *G. vellereum*. Compounds **488**–**490** were found to possess cytotoxic activities against two tumor cell lines (Huh7 and MT4), while **491** did not display such effects at concentrations up to 400 μ*M*. Both **489** and **490** showed ten times more potency than **488**. A chemical reactivity study revealed **489** to be more active than **488** when reacted with 2 *M* HCl and cysteine. These results might explain why **488**, **489**, and **490** displayed differential degrees of cytotoxicity [414]. From the same fungus, granuloinden B (**492**) was isolated and shown to be cytotoxic against the Huh7 and MT4 tumor cell lines, with $CC_{50}$ values of 6.7 and 0.15 μ*M* [431]. The 12-norilludane, granulodione (**493**), also isolated from the same fungus, caused an 83% mortality of *Tetranychus urticae* on exposure to this compound after 2 h (Fig. 51). The acaricidal activity of granulodione proved to be more potent than that of a known antifeedant plant compound, catechin [415].

Illudanes and illudalanes readily undergo dimerization via a Diels-Alder reaction to result in more complex molecules. For example, bovistol (**494**) is an illudane-illudalane dimer from *Bovista* sp. 96042 (Fig. 51) [406]. Agrocybone (**495**), with its structure determined by X-ray diffraction analysis, is an illudane-illudalane bis-sesquiterpene isolated from cultures of *Agrocybe salicacola*, and it displayed weak antiviral activity against respiratory syncytial virus (RSV) with an $IC_{50}$ value of 100 μ*M* [410]. Agrocybin A (**496**), a highly cyclized illudane sesquiterpenoid isolated from the same fungus, contains seven chiral stereocenters arranged compactly within six rings (Fig. 51). The relative configuration of agrocybin A was determined by X-ray diffraction analysis. Sterostreins A–C, and T are illudalane-norilludalane bis-sesquiterpenes obtained from *Stereum ostrea* BCC 22955 and *Stereum* sp. YMF1.1686, respectively [417, 418]. Sterostrein A (**497**) exhibited antimalarial activity against *Plasmodium falciparum* K1 cells ($IC_{50}$ value 2.3 μg/cm$^3$) as well as cytotoxicity against cancer cell lines (KB, MCF-7, and NCI-H187) and non-malignant Vero cells, with $IC_{50}$ values of 38, 7.2, 5.3, and 12 μg/cm$^3$, respectively (Fig. 51).

Compared to the large group of protoilludanes and illudanes, illudalanes have been encountered relatively rarely among higher fungi. Most of the reported illudalanes are active in biological assays. Russujaponols I–K (**498**–**500**), and L are aromatic illudalane sesquiterpenes from the fruiting bodies of *Russula japonica* (Fig. 51). When **498**–**500** were subjected to neurite outgrowth-promoting activity in primary neuronal cultures, they showed promotion of neurite outgrowth in cultured rat cortical neurons in a concentration range 0.1 to 10 μ*M* [382]. Sterostrein P (**501**) is an illudalane sesquiterpenoid with nematicidal activity, killing 72.4% of the *Caenorhabditis elegans* present at 500 mg/dm$^3$ in 72 h [419].

Sterostreins M–O (**302–304**), Q, divaricatines C (**305**), D (**306**), and illudinine are the only seven reported examples of aza-illudalanes found in the Basidiomycetes (Fig. 51) [165, 166, 419, 432]. More recently, it was revealed that the pyridyl moiety of these aza-illudanes arises from non-enzymatic condensation between the dione moiety and ammonia [433]. Divaricatines C and D showed weak antibacterial activity against *Bacillus cereus* and *Sarcinea lutea*, and inhibition of the root elongation *Lepidum sativum* of 85 and 72% after 48 h, respectively [166].

The 12-norilludalane sesquiterpene puraquinonic acid (**502**) was isolated from mycelial cultures of the basidiomycete *Mycena pura*, exhibiting induction of differentiation in HL-60 cells (Fig. 51) [420]. The challenging quaternary stereocenter (C-11) and the distal methyl and hydroxyethyl groups have increased the difficulties required to be overcome for its enantioselective total synthesis, although it appears to be a simple molecule at first glance. So far, a number of routes have dealt with the enantioselective total synthesis of **502**, which has been accomplished by several groups [434–439]. More recently, the first total synthesis of the illudalane sesquiterpene coprinol was achieved by Singh et al. [440].

### 4.1.15 Marasmanes

Marasmic acid was the first marasmane-type sesquiterpenoid to be isolated from the mushroom *Marasmius conigenus* nearly 70 years ago. However, not many marasmane metabolites have been reported from Basidiomycetes in the intervening period (Table 30, Fig. 52), and previous reviews have covered about 30 of these compounds. Interestingly, this type of sesquiterpenoid is found mainly among members of the family Russulaceae.

**Table 30** Marasmane sesquiterpenoids

| Compound | Origin | Type | Refs. |
|---|---|---|---|
| 7$\alpha$,8$\alpha$,13,14-Tetrahydroxy-marasm-5-γ-oic acid γ-lactone (**503**) | *Lactarius vellereus* | Marasmane | [441] |
| 10$\beta$-Hydroxy-lactarorufin A (**504**) | *Lactarius vellereus* | Marasmane | [441] |
| Lactapiperanols A–D (**505–508**) | *Lactarius piperatus* | Marasmane | [442] |
| Lactapiperanols E (**509**) | *Russula foetens* | Marasmane | [443] |
| 8$\alpha$,13-Dihydroxy-marasm-5-oic acid $\gamma$-lactone (**510**) | *Russula foetens* | Marasmane | [444] |
| 13-Hydroxy-marasm-7(8)-en-5-methoxy $\gamma$-acetal (**511**) | *Russula foetens* | Marasmane | [444] |
| 7$\alpha$,8$\alpha$,13-Trihydroxy-marasm-5-oic acid $\gamma$-lactone | *Russula foetens* | Marasmane | [444] |
| Pubescenone (**512**) | *Lactarius pubescens* | Marasmane | [445] |
| Russulfoen (**513**) | *Russula foetens* | Marasmane | [446] |

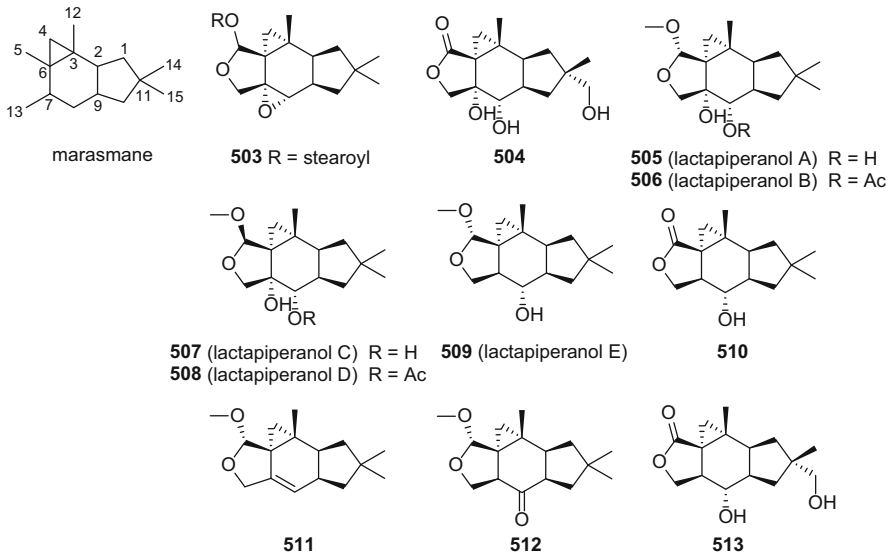


**Fig. 52** Structures of marasmane and selected derivatives

### 4.1.16 Lactaranes and *seco*-Lactaranes

Lactarane sesquiterpenoids also are derived mainly from the Russulaceae family (Table 31). A biomimetic transformation by heating isovelleral to yield the product pyrovellerofuran showed an interaction between the marasmanes and the lactaranes.

**Table 31** Lactarane and *seco*-lactarane sesquiterpenoids

| Compound | Origin | Type | Refs. |
|---|---|---|---|
| Cochleol (**522**) | *Lentinellus cochleatus* | Lactarane | [447] |
| 10*β*-Hydroxy-lactarorufin A (**523**) | *Lactarius vellereus* | Lactarane | [441] |
| Compound 1 | *Russula emetica* | Lactarane | [448] |
| Rufuslactone (**516**) | *Lactarius rufus* | Lactarane | [449] |
| 1,2-Dehydrolactarolide A (**517**) | *Lactarius vellereus* | Lactarane | [450] |
| Lactarorufin A | *Lactarius vellereus*/*L. subpiperatus* | Lactarane | [450] |
| 3-*O*-Ethyllactarolides A, B | *Lactarius vellereus* | Lactarane | [450] |
| Lactarolide A | *Lactarius subpiperatus* | Lactarane | [450] |
| Velleratretraol (**518**) | *Lactarius vellereus* | Lactarane | [451] |
| Subvellerolactones B–E (**519–521**) | *Lactarius subvellereus* | Lactarane | [452] |
| Sangusulactones A–C | *Russula sanguinea* | Lactarane | [453] |
| Blennin A | *Russula sanguinea* | Lactarane | [453] |
| 15-Hydroxyblennin A | *Russula sanguinea* | Lactarane | [453] |
| Russulanobilines A–C | *Russula nobilis* | Lactarane | [454] |
| Strobiluric acid (**524**) | *Strobilurus stephanocystis* | *seco*-Lactarane | [455] |

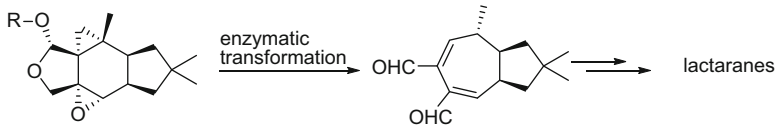


**514** (stearoylvelutinal)
R = $CH_3(CH_2)_{16}CO$
**515** (velutinal) R = H

(–)-velleral

**Scheme 22** The enzymatic transformation process of marasmanes to lactaranes

Results on the secondary metabolite differences between intact and injured *Russula* fruiting bodies have shed light on the biogenetic interrelationship between the marasmane and lactarane skeletons [456]. Thus, it was revealed that intact Russulaceae mushroom fruiting bodies produce inactive and tasteless fatty acid esters of sesquiterpenoid alcohols, e.g. stearoylvelutinal (**514**). When the fruiting bodies are injured, these fatty acid esters are transformed enzymatically into either tasteless or bitter, acrid components, with the latter responsible for the unfavorable taste of some *Russula* or *Lactarius* mushrooms, and are produced within a period varying from seconds to hours [447, 454, 457]. For example, stearoylvelutinal was transformed enzymatically to the dialdehyde velleral (**515**). Velleral is rapidly metabolized in injured specimens into many lactaranes (Scheme 22). These patterns constitute a chemical defense machinery, which protects mushrooms against predators, parasites, and microorganisms.

Compared to the illudanes, lactarane sesquiterpenes seem less promising in terms of drug discovery. However, several biological activities of lactaranes have been reported, which have involved assessments of antifungal, cytotoxic, and lettuce elongation growth promotion. Rufuslactone (**516**) not only displayed growth inhibition on the plant pathogenic fungus, *Alternaria brassicae*, with an inhibition rate of 68.3% at 100 μg/cm$^3$, but also negatively affected *A. alternata*, producing an inhibition rate of 38.9% at the same concentration level that growth was not affected by the positive control, carbendazim (Fig. 53), at 100 μg/cm$^3$ [449]. 1,2-Dehydrolactarolide A (**517**) exhibited growth promotion activities on radicle elongation in lettuce seedlings of 119, 152, and 162% at 3.6, 36, and 360 μ*M*, respectively (Fig. 53) [450]. Velleratretraol (**518**) is an unusual highly functionalized lactarane sesquiterpene obtained from *L. vellereus*. Its relative configuration was determined by X-ray diffraction analysis, while its absolute configuration was established by a computational method to calculate the optical rotation value (Fig. 53) [451]. Velleratretraol (**518**) showed weak activity against HIV-1 cells with an effective concentration of 68.0 μg/cm$^3$ and a selectivity index of 2.0. Subvellerolactones B–E (**519**–**521**), three lactarane lactones isolated from the inedible mushroom *L. subvellereus*, were evaluated in cytotoxicity assays using human cancer cell lines (Fig. 53). Subvellerolactone B (**520**) exhibited $IC_{50}$ values of 26.5, 18.3, and 14.2 μ*M*, respectively, when evaluated against the A549, SK-MEL-2, and HCT-15 cell lines. Subvellerolactones D and E were also tested

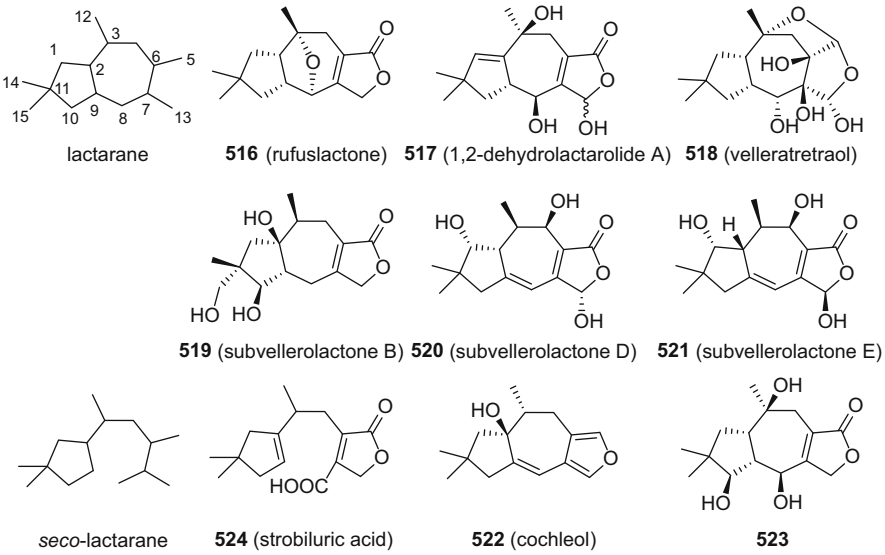


**Fig. 53** Structures of lactarane and *seco*-lactarane and selected derivatives

against the A549 and HCT-15 cell lines ($IC_{50}$ values for D: 25.1 and 17.8 μ*M*, and $IC_{50}$ values for E: 19.6 and 28.7 μ*M*, respectively) [452].

*Seco*-lactaranes are extremely rare in Nature (Table 31). Only one example of this type of sesquiterpenoid has been found since a previous review was published [251]. Strobiluric acid (**524**) was isolated from the fermentation broth of the basidiomycete *Strobilurus stephanocystis* and has displayed no discernible biological effect in studies conducted to date (Fig. 53).

### 4.1.17 Sterpuranes

Sterpurols A (**525**) and B (**526**) were obtained from the fermentation on rice of the edible fungus *Flammulina velutipes* (Fig. 54, Table 32). The absolute configuration of sterpurol A was established by circular dichroism of an in situ-formed complex with $[Rh_2(OCOCF_3)_4]$ [145].

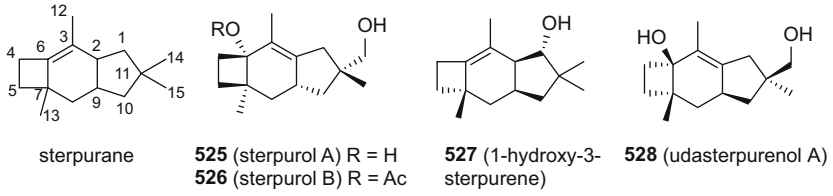


**Fig. 54** Structures of sterpuranes and selected compounds

**Table 32** Sterpurane sesquiterpenoids

| Compound | Origin | Type | Refs. |
|---|---|---|---|
| 1-Hydroxy-3-sterpurene (**527**) | *Gloeophyllum* sp. | Sterpurane | [375] |
| Udasterpurenol A (**528**) | *Phlebia uda* | Sterpurane | [458] |
| Sterpurols A (**525**), B (**526**) | *Flammulina velutipes* | Sterpurane | [145] |

### 4.1.18 Isolactaranes

Isolactaranes are 5/6/3 ring-fused sesquiterpenes, which were isolated initially from the genus *Lactarius*, and, to date, have been accompanied by lactaranes when purified. Isolactaranes and lactaranes are biogenetically different although they have similar names, which has created some confusion. Isolactaranes are thought to be derived from the sterpurane sesquiterpenoids, but not from the lactaranes or marasmanes (Table 33).

Hyphodontal (**529**) is a non-competitive inhibitor of the avian myeloblastosis virus ($K_i$ 346 μ*M*) and Moloney murine leukemia virus ($K_i$ 112 μ*M*) reverse transcriptases (Fig. 55) [459]. Sterelactones A–D (**530–533**) showed antibacterial, antifungal, and cytotoxic activities (Fig. 55). Udalactaranes A (**534**) and B (**536**) were isolated as mixtures with their repective epimeric acetals. They showed inhibition for spore germination of the plant pathogenic fungus *Fusarium graminearum* at 10 and 5 μg/cm$^3$, respectively (Fig. 55). Additionally, they also displayed cytotoxic effects against Jurkat cells with $IC_{50}$ values of 101 and 42 μ*M* [460]. Flammulinolides A–G (**538–544**) are isolactarane sesquiterpenes or isolactarane-related norsesquiterpenes obtained from the solid culture of the edible fungus *Flammulina velutipes* (Fig. 55). Flammulinolides A, B, and F showed cytotoxic properties against the KB cell line with $IC_{50}$ values of 3.9, 3.6, and 4.7 μ*M*, while flammulinolide exhibited cytotoxicity against the Hela cell line with an $IC_{50}$ value of 3.0 μ*M* [368].

**Table 33** Isolactarane sesquiterpenoids

| Compound | Origin | Type | Refs. |
|---|---|---|---|
| Udalactarane A (**534**) | *Phlebia uda* | Isolactarane | [458] |
| *epi*-Udalactarane A (**535**) | *Phlebia uda* | Isolactarane | [458] |
| Udalactarane B (**536**) | *Phlebia uda* | Isolactarane-sterpurane dimer | [458] |
| *epi*-Udalactarane B (**537**) | *Phlebia uda* | Isolactarane-sterpurane dimer | [458] |
| Hyphodontal (**529**) | *Hyphodontia* sp. | Isolactarane | [459] |
| Sterelactones A–D (**530–533**) | *Stereum* sp. IBWF01060 | Isolactarane | [460] |
| Flammulinolide A (**538**) | *Flammulina velutipes* | Isolactarane | [368] |
| Flammulinolides B–G (**539–544**) | *Flammulina velutipes* | 15-Norisolactarane | [368] |

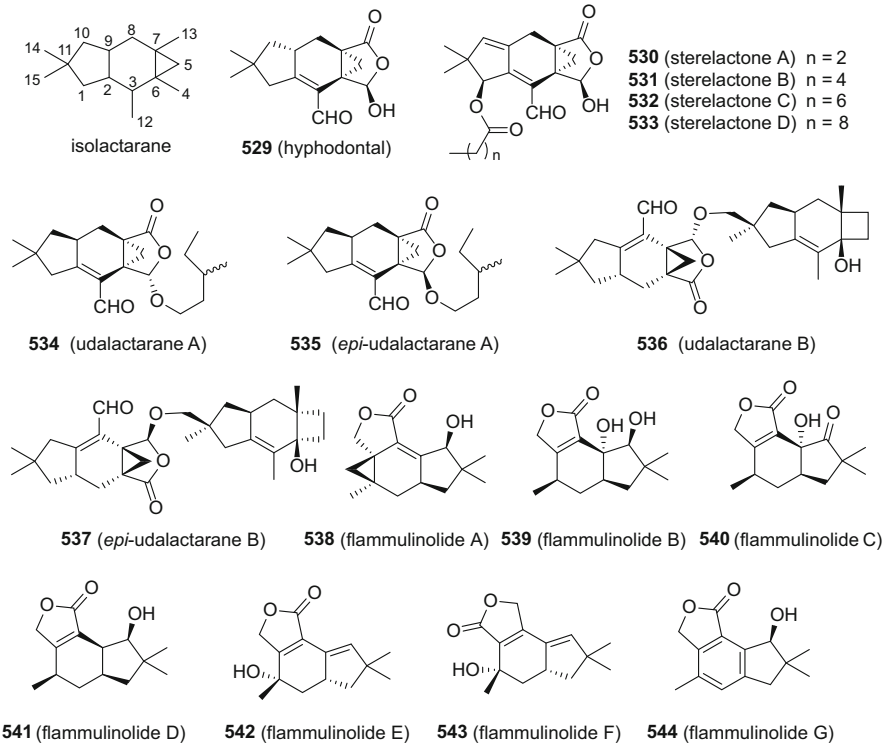


**Fig. 55** Structures of isolactarane sesquiterpenoids and related compounds

### 4.1.19 Tremulanes and *seco*-Tremulanes

Tremulane-type sesquiterpenoids are a class of sesquiterpenoids with a 5/7-ring-fused perhydroazulene carbon skeleton. In 1993, the first example of a tremulane was isolated from the wood-decaying fungus *Phellinus tremulae* by Ayer and Cruz [461]. Shortly after this, the biosynthesis pathway was elucidated by the same group through a $^{13}$C-labeled feeding experiment. This revealed that tremulanes are derived from *trans*,*trans*-farnesyl pyrophosphate via humulene and a key step of methyl migration (Scheme 14). In recent years, a number of tremulanes have been reported from mushrooms or wood-decaying fungi, mainly from the two species *Conocybe siliginea* and *Phellinus igniarius* (Table 34).

Tremulanes were reported to exhibit vascular-relaxing activities against phenylephrine-induced vasoconstriction as well as antiplasmodial activity [462, 465, 469]. Among these, 10$\beta$,12-dihydroxy-tremulene (**545**) exhibited vascular-relaxing activities against phenylephrine-induced vasoconstriction with a relaxing rate of 78.7% at a concentration of $3 \times 10^4$ *M*, and against KCl-induced vasoconstriction with a relaxing rate of 57.7% at the same concentration. The relaxing rate of tremulenediol B (**546**) was 59.3% against phenylephrine-induced

**Table 34** Tremulane and *seco*-tremulane sesquiterpenoids

| Compound | Origin | Type | Refs. |
|---|---|---|---|
| 10*β*,12-Dihydroxy-tremulene (**545**) | *Phellinus igniarius* | Tremulane | [462] |
| Tremulenediols A–C (**546**, **547**) | *Phellinus igniarius* | Tremulane | [462] |
| Conocenolides A (**548**), B (**549**) | *Conocybe siliginea* | *seco*-Tremulane | [463] |
| Conocenols A–D (**550**, **551**) | *Conocybe siliginea* | Tremulane | [463] |
| 11,12-Epoxy-12*β*-hydroxy-1-tremulen-5-one (**552**) | *Conocybe siliginea* | Tremulane | [464] |
| (−)-(2*S*,3*S*,6*S*,7*S*,9*R*)-Tremul-1(10)-ene-11,12,14-triol (**553**) | *Phellinus igniarius* | Tremulane | [465] |
| (−)-(2*S*,3*S*,6*S*,7*S*,9*S*)-Tremul-1(10)-ene-11,12,15-triol (**554**) | *Phellinus igniarius* | Tremulane | [465] |
| (+)-(1*R*,6*S*,7*S*)-Tremul-2-ene-12(11)-lactone (**555**) | *Phellinus igniarius* | Tremulane | [465] |
| 1*β*,12-Epoxy-14-hydroxy-2(11)-tremulene (**556**) | *Conocybe siliginea* | Tremulane | [466] |
| 1*β*,14-Epoxy-12-hydroxy-2(11)-tremulene (**557**) | *Conocybe siliginea* | Tremulane | [466] |
| 6*β*,12-Dihydroxy-tremulene (**558**) | *Phellinus igniarius* | Tremulane | [462] |
| 11,12-Epoxy-10*α*-hydroxy-5,6-*seco*-1,6(13)-tremuladien-5,12-olide (**559**) | *Conocybe siliginea* | *seco*-Tremulane | [467] |
| 11-Formyl-5,6-*seco*-1,6(13)-tremuladien-5,12-olide (**560**) | *Conocybe siliginea* | *seco*-Tremulane | [467] |
| 11-Acetyl-5,6-*seco*-1,6(13)-tremuladien-5,12-olide | *Conocybe siliginea* | *seco*-Tremulane | [467] |
| 11-Acetyl-10*α*-hydroxy-5,6-*seco*-1,6(13)-tremuladien-5,12-olide | *Conocybe siliginea* | *seco*-Tremulane | [467] |
| 12-Acetyl-5,6-*seco*-1,6(13)-tremuladien-5,11-olide | *Conocybe siliginea* | *seco*-Tremulane | [467] |
| 11,12-Dihydroxy-1-tremulen-5-one | *Conocybe siliginea* | Tremulane | [464] |
| 5*α*,12-Dihydroxy-1-tremulen-11-yl 2(*S*)-pyroglutamate | *Conocybe siliginea* | Tremulane | [464] |
| 2*α*,11-Dihydroxy-1(10)-tremulen-5,12-olide | *Conocybe siliginea* | Tremulane | [464] |
| 10*β*,11-Dihydroxy-5,6-*seco*-1,6(13)-tremuladien-5,12-olide | *Conocybe siliginea* | Tremulane | [464] |
| Tremulenediol A | *Conocybe siliginea* | Tremulane | [464] |
| Conocenolide A | *Conocybe siliginea* | Tremulane | [464] |
| 11-*O*-Acetyl-5*β*-11,12-trihydroxy-1-tremulene | *Conocybe siliginea* | Tremulane | [466] |
| 14-*O*-Acetyl-11,12,14-trihydroxy-1-tremulene | *Conocybe siliginea* | Tremulane | [466] |
| 15-*O*-Acetyl-11,12,15-trihydroxy-1-tremulene | *Conocybe siliginea* | Tremulane | [466] |
| 11-*O*-Acetyl-11,12,14-trihydroxy-1-tremulene | *Conocybe siliginea* | Tremulane | [466] |
| 1*β*,12-Epoxy-5*α*-hydroxy-3(11)-tremulene | *Conocybe siliginea* | Tremulane | [466] |
| 5*α*,11,12,14-Tetrahydroxy-1-tremulene | *Conocybe siliginea* | Tremulane | [392] |
| 4*α*,11,12,14-Tetrahydroxy-1-tremulene | *Conocybe siliginea* | Tremulane | [392] |
| (+)-(3*S*,6*R*,7*R*)-Tremulene-6,11,12-triol | *Phellinus igniarius* | Tremulane | [465] |
| (+)-(3*S*,6*S*,7*S*,10*S*)-Tremulene-10,11,12-triol | *Phellinus igniarius* | Tremulane | [465] |
| (+)-(3*S*,6*R*,7*R*,10*S*)-Tremulene-6,10,12-triol | *Phellinus igniarius* | Tremulane | [465] |
| (−)-(2*R*,3*S*,6*S*,7*S*,9*R*)-Tremul-1(10)-ene-11,12,14-triol | *Phellinus igniarius* | Tremulane | [465] |
| (−)-(2*S*,3*S*,4*S*,6S,7*S*)-Tremul-1(10)-ene-4,11,12-triol | *Phellinus igniarius* | Tremulane | [465] |

(continued)

**Table 34** (continued)

| Compound | Origin | Type | Refs. |
|---|---|---|---|
| (−)-(2*S*,3*R*,6S,7*S*)-Tremul-1(10)-ene-2,12-diol | *Phellinus igniarius* | Tremulane | [465] |
| 6*β*,11,12-Trihydroxy-tremul-1(10)-ene | *Phellinus igniarius* | Tremulane | [462] |
| 11,12-Dihydroxy-7*β*-peroxy-hydroxyl-tremul-1(10)-ene | *Phellinus igniarius* | Tremulane | [462] |
| 12,15-Dihydroxy-tremulene | *Phellinus igniarius* | Tremulane | [462] |
| (3*R**,3a*R**,4*R**,6*S**,6a*S**,7*S**)-6,8,8-Trimethyl-1,3,3a,4,5,6,6a,7,8,9-decahydroazuleno[4,5-*c*] furan-3,4,7-triol | *Marasmius cladophyllus* | Tremulane | [319] |
| Irlactin E | *Irpex lacteus* | Tremulane | [468] |
| Tremulenolide D | *Ceriporia alachuana* | Tremulane | [273] |
| 11,12-Epoxy-5,6-*seco*-tremula-1,6(13)-dien-5,12-olide | *Flavodon flavus* BCC17421 | *seco*-Tremulane | [469] |

vasoconstriction (Fig. 56) [462]. Tremulenediol A (**547**) showed antiplasmodial activity against *Plasmodium falciparum* (K1, multidrug resistant strain) with an $IC_{50}$ value of 8.6 μg/cm$^3$ (Fig. 56) [469].

*seco*-Tremulanes are derived biogenetically from tremulanes via a Baeyer-Villiger oxidation, leading to the cleavage of the C-5 to C-6 bond (Table 34). Conocenolides A (**548**) and B (**549**) are two inseparable *seco*-tremulanes that have been obtained from cultures of the mushroom *Conocybe siliginea* (Fig. 56) [463].

### 4.1.20 Alliacanes

Alliacane-type sesquiterpenes have been reported only rarely of mushroom origin. So far, only 18 members of this type of sesquiterpenoid were reported from four mushroom species (Table 35). Alliacols A (**561**) and B (**562**) not only showed antimicrobial activities, but also strongly inhibited DNA synthesis in cells of the ascetic form of Ehrlich carcinoma at concentrations of 2–5 μg/cm$^3$ (Fig. 57) [470]. The edible mushroom *Pleurotus cystidiosus* produces the alliacane-type clitocybulol sesquiterpenes, which possess some potent bioactivities (Fig. 57). Thus, clitocybulols D (**563**), E (**564**), and F (**565**) were reported to exhibit cytotoxicity against two human prostate cancer (DU-145 and C42B) cell lines (Fig. 57). The $IC_{50}$ values of clitocybulols D, E, and F were 233, 162, and 179 n*M*, respectively, against DU-145 cells, and were 163, 120, 119 n*M*, respectively, for C42B cells [249]. From the same edible fungus, clitocybulols G–O were obtained and their structures determined by spectroscopic data interpretation, inclusive of an analysis of their circular dichroism spectra (Fig. 57). Clitocybulols G (**566**), L (**567**) and C showed weak inhibitory activity against protein tyrosine phosphatase-1B (PTP1B), with $IC_{50}$ values of 49.5, 38.1, and 36.0 μ*M*, respectively [472].

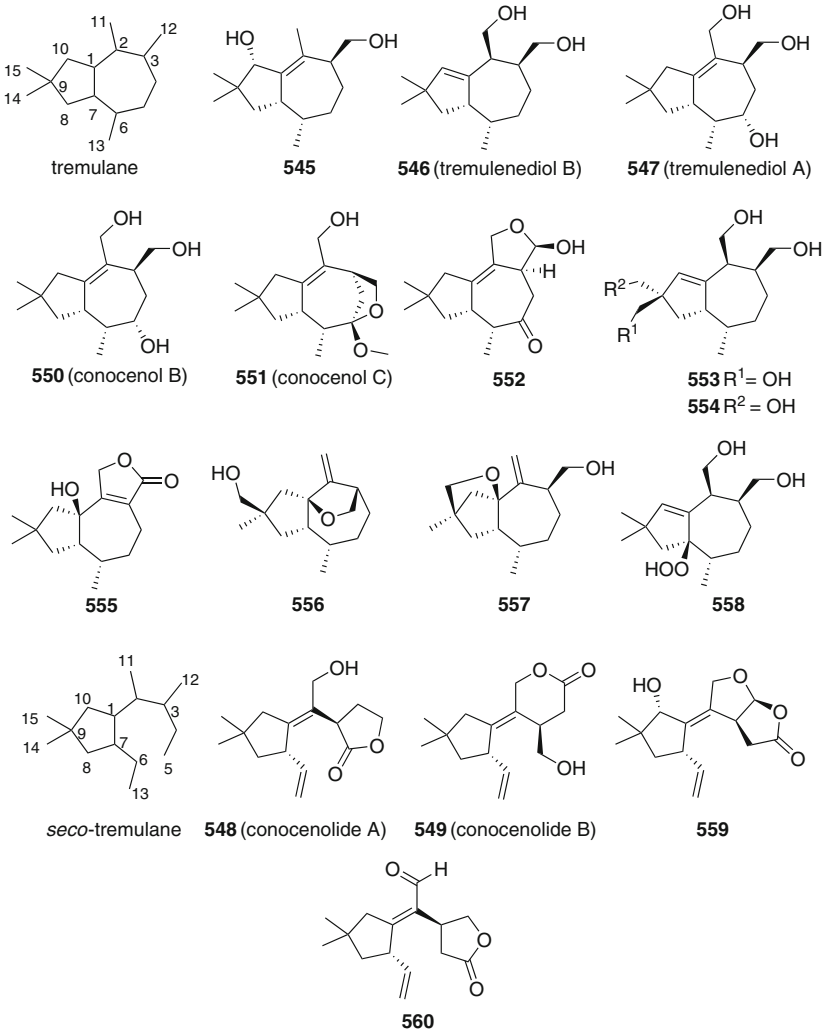


**Fig. 56** Structures of tremulanes and *seco*-tremulane derivatives

**Table 35** Alliacane sesquiterpenoids

| Compound | Origin | Type | Refs. |
|---|---|---|---|
| Alliacols A (**561**), B (**562**) | *Marasmius alliaceus* | Alliacane | [470] |
| Clitocybulols A–C (**568**–**570**) | *Clitocybula oculus* | Alliacane | [471] |
| Clitocybulols D–O (**563**–**567**) | *Pleurotus cystidiosus* | Alliacane | [249, 472] |
| Purpuracolide (**571**) | *Gomphus purpuraceus* | Alliacane | [473] |

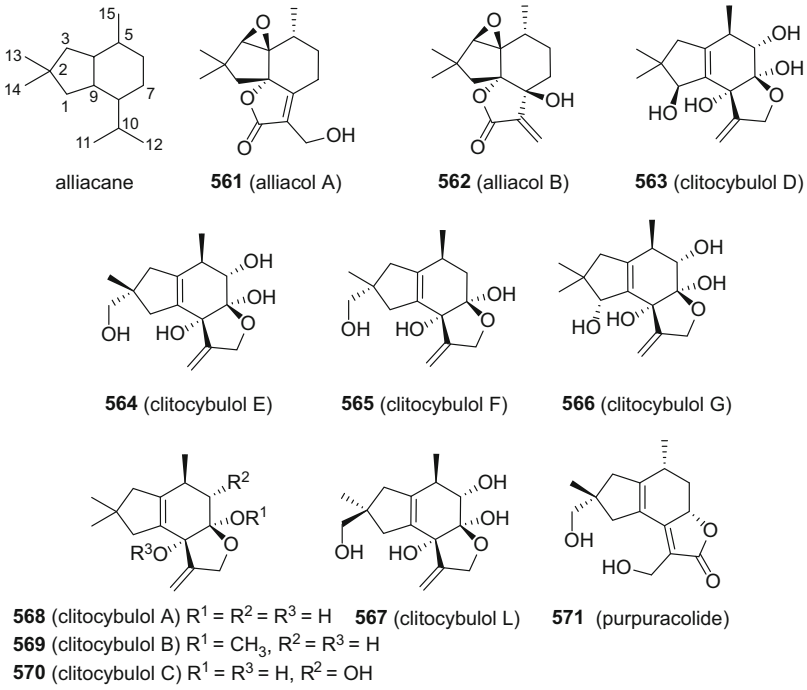


**Fig. 57** Structures of alliacane and selected derivatives

### 4.1.21 Botryanes

Botryane-type sesquiterpenoids have been encountered only rarely in mushrooms. Most of the reported botryanes were found in the ascomycetes *Daldinia concentrica* and *Hypoxylon rickii* (Table 36, Fig. 58). So far, no specific biological activity has been discerned for any member of the botryrane sesquiterpenoid class.

**Table 36** Botryane sesquiterpenoids

| Compound | Origin | Type | Refs. |
|---|---|---|---|
| Methyl-7*α*-acetoxydeacetylbotryoloate (**572**) | *Daldinia concentrica* | Botryane | [474] |
| 7*α*-Acetoxydeacetylbotryenedial | *Daldinia concentrica* | Botryane | [474] |
| 7*α*-Hydroxybotryenalol | *Daldinia concentrica* | Botryane | [474] |
| 7,8-Dehydronorbotryal | *Daldinia concentrica* | Botryane | [474] |
| 7*α*-Acetoxydehydrobotrydienal | *Daldinia concentrica* | Botryane | [474] |
| 7*α*-Acetoxy-15-methoxy-10-*O*-methyl-deacetyldihydrobotrydial (**573**) | *Daldinia concentrica* | Botryane | [474] |
| 7*α*-Hydroxy-10-*O*-ethyldihydrobotrydial | *Daldinia concentrica* | Botryane | [474] |
| 7-Hydroxy-16-*O*-methyldeacetyldihydrobotrydial | *Daldinia concentrica* | Botryane | [474] |
| 7-Hydroxy-16-*O*-methyldeacetyldihydrobotrydial-hydrate | *Daldinia concentrica* | Botryane | [474] |

(continued)

**Table 36** (continued)

| Compound | Origin | Type | Refs. |
|---|---|---|---|
| 7-Hydroxydeacetyl-botryenalol | *Daldinia concentrica* | Botryane | [474] |
| 7*α*-Hydroxydihydrobotrydial | *Daldinia concentrica* | Botryane | [474] |
| (1*S*)-7-[(2*E*)-But-2-enoyl]-1,3,3,6-tetramethyl-2,3-dihydro-1*H*-indene-1-carbaldehyde (**575**) | *Hypoxylon rickii* | Botryane | [353] |
| (3a*S*)-6-Hydroxy-3a,5,5,8-tetramethyl-3,3a,4,5-tetrahydro-1*H*-cyclopenta[*de*]isochromen-1-one (**576**) | *Hypoxylon rickii* | Botryane | [353] |
| (3a*S*)-7-Hydroxy-3a,5,5,8-tetramethyl-3,3a,4,5-tetrahydro-1*H*-cyclopenta[*de*]isochromen-1-one | *Hypoxylon rickii* | Botryane | [353] |
| (3a*S*)-3a,5,5,8-Tetramethyl-3,3a,4,5-tetrahydro-1*H*-cyclopenta[*de*]isochromen-1-one | *Hypoxylon rickii* | Botryane | [353] |
| (3a*S*,*8R*)-3a,5,5,8-Tetramethyl-3,3a,4,5,7,8-hexahydro-1*H*-cyclopenta[*de*]isochromen-1-one | *Hypoxylon rickii* | Botryane | [353] |
| Botryenanol | *Hypoxylon rickii* | Botryane | [353] |
| Boledulins A–C (**574**) | *Boletus edulis* | Botryane | [475] |

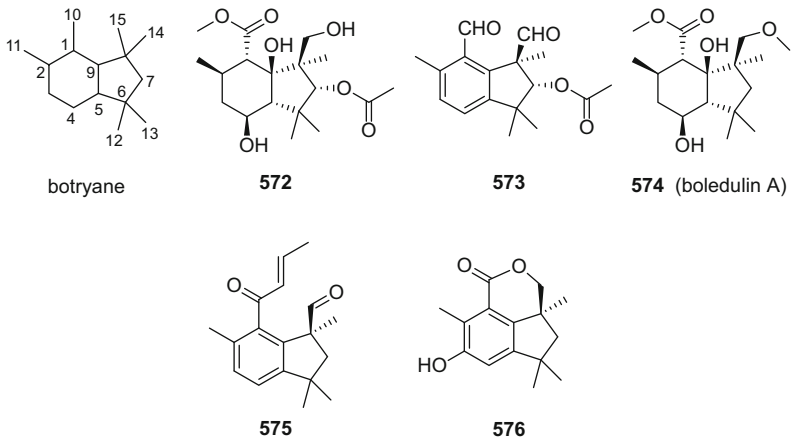


**Fig. 58** Structures of botryane and selected derivatives

### 4.1.22 Spiroaxanes

The spiroaxanes are a class of sesquiterpenoids with 5/6 spiro rings that were discovered initially from the marine sponge *Axinella cannabina*. To date, only 17 sesquiterpenes of this kind have been isolated from the Basidiomycetes, from the species *Pholiota adiposa*, *Phellinus igniarius*, *Tyromyces chioneus*, *Trametes versicolor*, and *Flammulina velutipes* (Table 37, Fig. 59). The structure of flammuspirone A (**577**) was determined by X-ray crystallographic analysis (Fig. 59). Biological testing revealed that flammuspirones A and C have weak

**Table 37** Spiroaxane sesquiterpenoids

| Compound | Origin | Type | Refs. |
|---|---|---|---|
| 15-Hydroxy-6$\alpha$,12-epoxy-7$\beta$,10$\alpha$H,11$\beta$H-spiroax-4-ene (**578**) | *Pholiota adiposa* | Spiroaxane | [476] |
| 3$\alpha$,6$\alpha$-Dihydroxyspiroax-4-ene (**580**) | *Phellinus igniarius* | Spiroaxane | [275] |
| Tyromol A (**579**) | *Tyromyces chioneus* | Spiroaxane | [276] |
| Tramspiroins A–D (**581**, **582**) | *Trametes versicolor* | Spiroaxane | [477] |
| Flammuspirones A–J (**577**) | *Flammulina velutipes* | Spiroaxane | [478] |

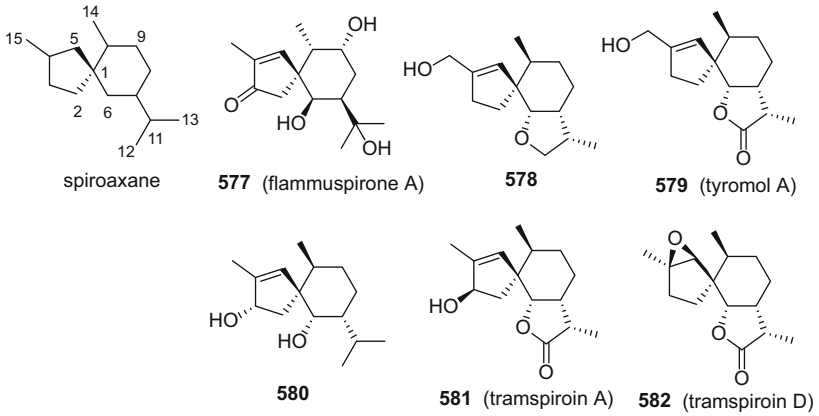


**Fig. 59** Structures of spiroaxane and selected compounds

HMG-CoA reductase activities and that flammuspirones C–E and H displayed marginal dipeptidyl peptidase-4 (DPP-4) inhibitory effects.

### 4.1.23 Other Skeletons

A summary of sesquiterpenoids from mushrooms bearing miscellaneous carbon skeletons is provided in Table 38.

Deoxycollybolidol (**583**) is a crystalline compound isolated from the fruiting bodies of *Collybia maculata*, and contains two lactone groups (Fig. 60) [479]. This species produces many types of sesquiterpenoids, including marasmanes and lactaranes. Two nardosinane sesquiterpenoids, rulepidanol (**584**) and rulepidadiene B, were isolated from the mushroom *Russula lepida* (Russulaceae). They were accompanied by two aristolanes, which has supported the hypothesis that nardosinane sesquiterpenes are derived from an aristolane precursor (Scheme 14, Fig. 60) [223].

**Table 38** Miscellaneous sesquiterpenoids

| Compound | Origin | Type | Refs. |
|---|---|---|---|
| Deoxycollybolidol (**583**) | *Collybia maculata* | | [479] |
| Rulepidanol (**584**) | *Russula lepida* | Nardosinane | [223] |
| Rulepidadiene B | *Russula lepida* | Nardosinane | [223] |
| Dictyopanines A-C (**585**) | *Dictyopanus* sp. HKI0181 | | [480] |
| 1(10),4-Germacradiene-2,6,12-triol (**586**) | *Resupinatus leightonii* | Germacrane | [481] |
| Russulanorol (**587**) | *Russula delica* | Russulane | [482] |
| Stereumone A (**588**) | *Stereum* sp. 8954 | | [483] |
| Stereumins H–J (**589**) | *Stereum* sp. CCTCC AF 207024 | Stereumane | [484] |
| Limacellone (**590**) | *Limacella illinita* | | [261] |
| Cyclopinol (**591**) | *Boletus calopus* | | [485] |
| Cyclocalopin A | *Boletus calopus* | | [485] |
| *O*-Acetylcyclocalopin A | *Boletus calopus* | | [485] |
| (3*R**,3a*S**,4*S**,8a*R**)-3-(1′-Hydroxy-1′-methylethyl)-5,8a-dimethyldecahydroazulen-4-ol (**592**) | *Sparassis crispa* | Isodaucane | [350] |
| Mitissimolone (**593**) | *Lactarius mitissimus* | | [486] |
| Sterperoxides A–D (**594**, **595**) | *Steccherinum ochraceum* | Chamigrane | [487, 488] |
| Xylaranols A, B (**596**) | *Xylaria* sp. 101 | Guaiane | [347] |
| Lactariolines A, B (**532**, **233**) | *Lactarius hatsudake* | Guaiane | [138] |
| Xylcarpins A–C (**597**) | *Xylaria carpophila* | Thujopsane | [197] |
| Trefolane A (**598**) | *Tremella foliacea* | Trefolane | [489] |
| Conosilane A (**599**) | *Conocybe siliginea* | Conosilane | [490] |
| Phellilins A–C (**600**, **601**) | *Phellinus linteus* | | [491] |
| Cordycepols A–C (**602**) | *Cordyceps ophioglossoides* | Spiro[4.5] decane | [492] |
| Cordycol | *Cordyceps ophioglossoides* | | [492] |
| Irlactins A–D (**603**) | *Irpex lacteus* | Irlactane | [468] |
| Postinins A (**604**), B (**605**) | *Postia* sp. | Ylangene | [493] |
| Brasilanes A–C (**606**) | *Coltricia sideroides* | Brasilane | [494] |
| Gymnomitrane-3$\alpha$,5$\alpha$,9$\beta$,15-tetraol (**607**) | *Ganoderma lucidum* | Gymnomitrane | [495] |

(continued)

**Table 38** (continued)

| Compound | Origin | Type | Refs. |
|---|---|---|---|
| Antrodin F | *Antrodiella albocinnamomea* | Gymnomitrane | [367] |
| Antrodin E (**610**) | *Antrodiella albocinnamomea* | Ventricosane | [367] |
| Penarines A–F (**608**, **609**) | *Hygrophorus penarius* | Ventricosane | [496] |
| 13-Hydroxysilphiperfol-6-ene (**611**) | *Hypoxylon rickii* | Silphiperfolane | [497] |
| 9-Hydroxysilphiperfol-6-en-13-oic acid (**612**) | *Hypoxylon rickii* | Silphiperfolane | [497] |
| 2-Hydroxysilphiperfol-6-en-13-oic acid | *Hypoxylon rickii* | Silphiperfolene | [497] |
| 15-Hydroxysilphiperfol-6-en-13-oic acid | *Hypoxylon rickii* | Silphiperfolene | [497] |

In the course of screening for new antibacterial compounds from the tropical mushroom, *Dictyopanus* sp. HKI0181, three sesquiterpenes, dictyopanines A (**585**), B, and C were obtained (Fig. 60). Structurally, these three sesquiterpenes are esterified by different fatty acids. Dictyopanines A–C were shown in an antibiotic assay using an agar well diffusion method to display antimicrobial activities against a small group of filamentous fungi and Gram-positive bacteria [480]. Bioactivity-guided isolation of submerged cultures of the basidiomycete *Resupinatus leightonii* led to the discovery of the macrocylic germacrane-type sesquiterpenoid 1(10),4-germacradiene-2,6,12-triol (**586**), which activated cAMP-mediated signal transduction in the formation of melanized appressoria for the invasion of host plants by the plant pathogenic fungus *Magnaporthe grisea* (Fig. 60) [481]. The norsesquiterpenoid russulanorol (**587**), based on the russulane skeleton, was isolated from the mushroom *Russula delica* (Fig. 60). The structure of **587** was elucidated by interpretation of its spectroscopic data and by chemical transformations. The analytical data obtained suggested that russulanorol occurs as two co-existing isomers [482].

The genus *Stereum* produces many different sesquiterpenoid classes, including cadinanes, drimanes, hirsutanes, illudalanes, isolactaranes, and sterpuranes, suggesting that different terpenoid cyclase enzymes are also produced. Stereumone A (**588**) possesses an unusual 4*H*-naphtho[2,3-*b*]furan skeleton, which has not previously been found among the sesquiterpenoids to date [483]. Stereumins H–J (**589**) were isolated from the culture broth of the basidiomycete *Stereum* sp. CCTCC AF 207024, and possess a stereumane-type backbone. Their structures were determined unambiguously with the involvement of X-ray crystallographic and computional methods [484].

Limacellone (**590**) obtained from the fermentation broth of *Limacella illinita*, is a cage-like sesquiterpene having a $C_{15}$ carbon skeleton (Fig. 60). Limacellone was evaluated for cytotoxicity against the L1210 cell line ($IC_{50}$ value of 90 μg/cm$^3$) and it affected the shoot growth both *Setaria italica* and *Lepidium sativum* [261]. Cyclopinol (**591**), isolated from the mushroom *Boletus calopus*, is a spiro-sesquiterpene containing lactone and hemiacetal groups (Fig. 60) [485]. The edible

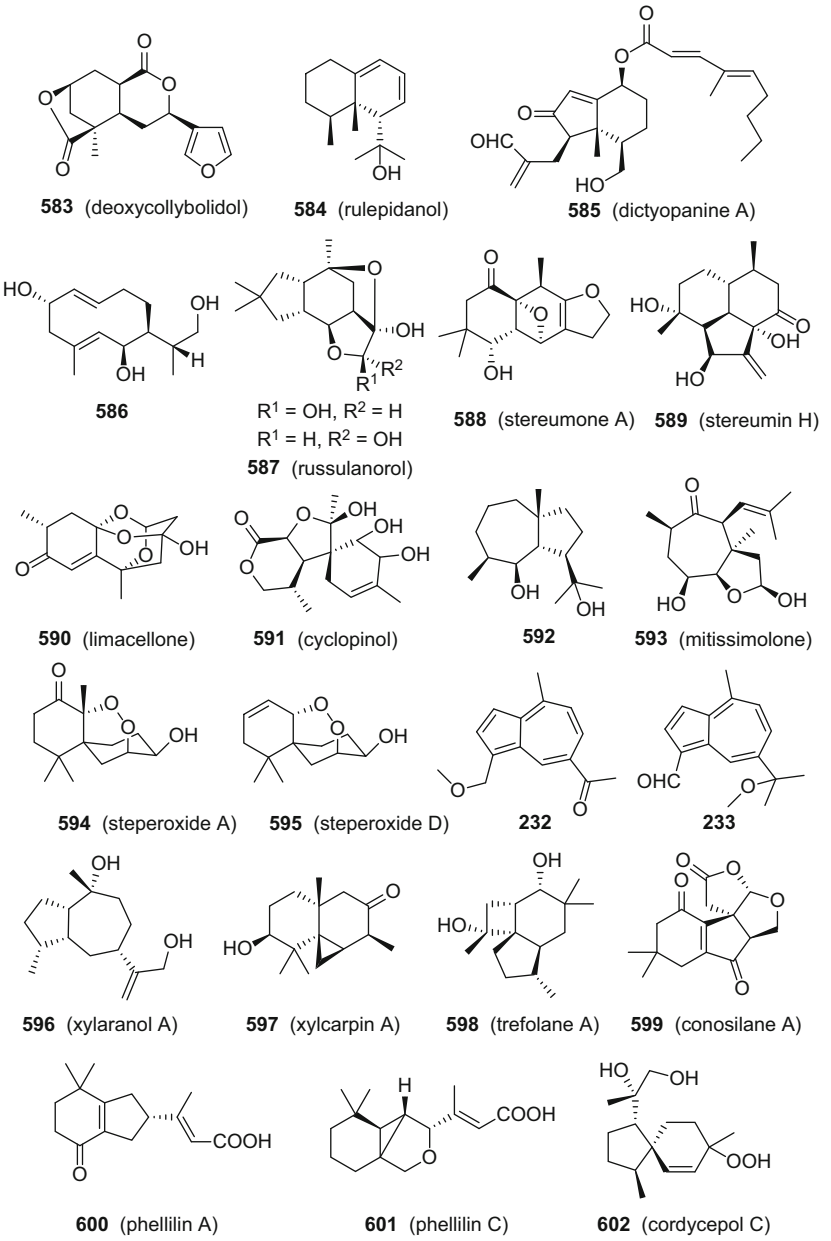


**Fig. 60** Structures of miscellaneous sesquiterpenoids

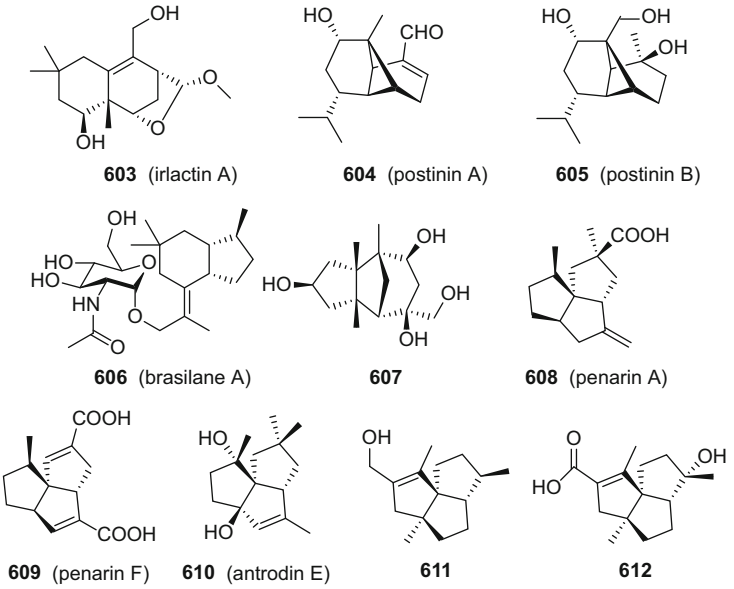


**Fig. 60** (continued)

cauliflower mushroom *Sparassis crispa* is used as a Chinese medicinal species and/or a functional food. The chemical investigation of this mushroom led to the isolation of the initial isodaucane-type sesquiterpenod (3*R**,3a*S**,4*S**,8a*R**)-3(1′-hydroxy-1′-methylethyl)-5,8a-dimethyldecahydroazulen-4-ol (**592**) [350].

Mitissimolone (**593**) was obtained as a cytotoxic sesquiterpenoid from an ethanol extract of the fruiting bodies of *Lactarius mitissimus*. The $IC_{50}$ value was 29.8 μg/cm$^3$ for this compound against the HeLa cell line (Fig. 60) [486]. During a search for bioactive compounds from the basidiomycete *Steccherinum ochraceum*, four chamigrane sesquiterpenoids with an endoperoxide function, namely, steperoxides A-D (**594**, **595**) were obtained (Fig. 60). The chamigranes have mainly been found to be derived from marine organisms and they are halogenated. This was the first time that chamigranes were reported to be of mushroom origin. Sterperoxide D (**595**) showed antimicrobial activity against *Staphylococcus aureus* with inhibition zones of 22 and 19 mm at 10 and 5 μg/disk, respectively [487, 488].

Four guaiane-type sesquiterpenoids, xylaranols A (**596**) and B, and lactariolines A (**232**) and B (**233**), were isolated from the fruiting bodies of *Xylaria* sp. and *Lactarius hatsudake* [138, 347]. Lactariolines A and B are two azulene sesquiterpene pigments bearing a conjugated 5/7-ring-fused system (Fig. 60). Lactarioline A (**232**) displays a blue color while lactarioline B is red. Lactarioline A inhibited IFN-$\gamma$ production in NK92 cells in a dose-dependent manner, corresponding to 56.7% inhibiton at 400 μ*M* and 21.4% at 100 μ*M*, respectively. Similarly, lactarioline B also exhibited inhibitory activity in a dose-dependent manner with 80.9% inhibition at 400 μ*M* and 31.2% at 100 μ*M* [138].

Fungi belonging to the genus *Xylaria* are known to produce a variety of bioactive compounds, varying from sesquiterpenoids to diterpenoids. A phytochemical study of the fermentation broth of the fungus *Xylaria carpophila* led to the isolation of three thujopsane sesquiterpenoids, xylcarpins A–C (**597**) (Fig. 60) [197]. Thujopsane sesquiterpenoids have been found only in plants previously and this was the first report of their occurrence among the fungi.

Trefolane A (**598**) and conosilane A (**599**), isolated from the culture broth of the Basidiomycetes *Tremella foliacea* and *Conocybe siliginea*, respectively, were found to produce novel sesquiterpenoids based on additional skeletons (Fig. 60) [489, 490]. Their structures were elucidated using spectroscopic methods and confirmed by single-crystal X-ray diffraction analysis. Of these, trefolane possesses a 5/6/4 tricyclic ring system, representing a 4(6→7)*abeo*-africane skeleton. In turn, conosilane possesses a 6/5/5/5 tetracyclic ring system, in which two pentacyclic rings are formed through acetal bonds. The precursor of trefolane and conosilane is humulane, which is produced by fanesyl pyrophosphate (FPP). Conosilane A (**598**) was tested against human and mouse 11$\beta$-HSD1 (hydroxysteroid dehydrogenase-1), with inhibition rates of 53.3 and 70.0%, respectively, at a concentration of 10 μg/cm$^3$.

In the course of discovering new anti-inflammatory lead drugs from higher fungi, three sesquiterpenoids, phellilins A–C (**600**, **601**), were isolated from the cultured mycelium of *Phellinus linteus* (Fig. 60). The biogenetic interrelationships of these three compounds were also discussed [491].

The fungus *Cordyceps ophioglossoides* is a parasite of certain types of *Elaphomyces* species and it was used in traditional Chinese medicine as a tonic. A chemical investigation of this fungicolous fungus resulted in the purification of three unusual spiro[4.5]decane sesquiterpenes, namely, cordycepols A–C, as well as the known compound, cordycol (Fig. 60). A preliminary cytotoxicity determination of these compounds revealed that cordycepol C (**602**) and cordycol showed inhibitory activities in a dose- and time-dependent manner [492]. Mechanistically, cordycepol C induced apoptosis of HepG2 hepatoma cells without affecting the L-02 normal liver cell line, and also caused poly(ADP-ribose) polymerase-1 (PARP-1) cleavage and triggered the loss of mitochondrial membrane potential in HepG2 cells in a time- and dose-dependent manner. It also induced the expression of the Bax protein, followed by its translocation from the cytosol to mitochondria in both wild type and p53 knockdown HepG2 cells [498].

*Irpex lacteus* is a pathogenic wood-decaying fungus belonging to the family Polyporaceae. Irlactins A–D (**603**) isolated from the culture broth of this fungus were characterized as sesquiterpenoids having a rearranged 6/6 bicyclic system. Their absolute configurations were established by single-crystal X-ray diffraction analysis. Irlactins B–D were obtained as a mixture in solution, while a co-crystal of irlactins C and D was obtained in methanol [468].

Postinins A (**604**) and B (**605**) are two ylangene-type sesquiterpenoids isolated from cultures of the fungus *Postia* sp. (Fig. 60). They possess a rigid core structure that was found previously only in soft corals. Both postinins A and B showed inhibitory activities against protein-tryosine phosphatase 1 and SH2-containing cytoplasmic tyrosine phosphatase-1 (SHP1) and -2 (SHP2), with $IC_{50}$ values in the range 1.6–6.2 μg/cm$^3$ [493].

Three new brasilane-type sesquiterpenes, brasilanes A–C (**606**), were found in a culture of *Coltricia sideroides* and they represent the first representatives of this class to have been isolated from the Basidiomycetes (Fig. 60). This rare type of sesquiterpenoid was isolated previously only from various liverworts, red algae, and endophytic fungi [494].

Antrodin F is a gymnomitrane-type sesquiterpenoid isolated initially from a culture of the basidiomycete *Antrodiella albocinnamomea* (Fig. 60). Its structure was established unambiguously by X-ray diffraction analysis. Furthermore, gymnomitrane-3$\alpha$,5$\alpha$,9$\beta$,15-tetrol (**607**) was isolated from the fruiting bodies of the medicinal fungus *Ganoderma lucidum*. Gymnomitrane-3$\alpha$,5$\alpha$,9$\beta$,15-tetrol (**607**) inhibited the growth of the epidermal growth factor receptor-tyrosine kinase inhibitor EGFR-TKI-resistant A549 human lung cancer and PC3 human prostate cancer cell lines with inhibition rates of 18.8 and 52.5%, respectively, at a concentration of 30 μ*M* [495].

The ventricosane- and silphiperfolene-type sesquiterpenoids are very rare in Nature, and only several examples are known as the secondary metabolites of higher fungi. The ventricosanes have been reported primarily from liverworts, and silphiperfolenes from the plant family Asteraceae. Penarines A–F (**608**, **609**) are ventricosane-type sesquiterpenes isolated from the basidiomycete *Hygrophorus penarius*, but did not show any discernible types of activity when evaluated in a panel of bioassays (Fig. 60) [496]. Four silphiperfolene derivatives (as e.g. **611**, **612**) were isolated from a culture of the ascomycete *Hypoxylon rickii*, and represent the first examples of this kind of sesquiterpene isolated from the fungi (Fig. 60) [497].

## *4.2 Diterpenoids*

Among the terpenoids biosynthesized by higher fungi, the diterpenoid class is less varied than the sesquiterpenoids both with respect to their structural diversity and the overall number of representatives (Fig. 61). The diterpenoids derived from

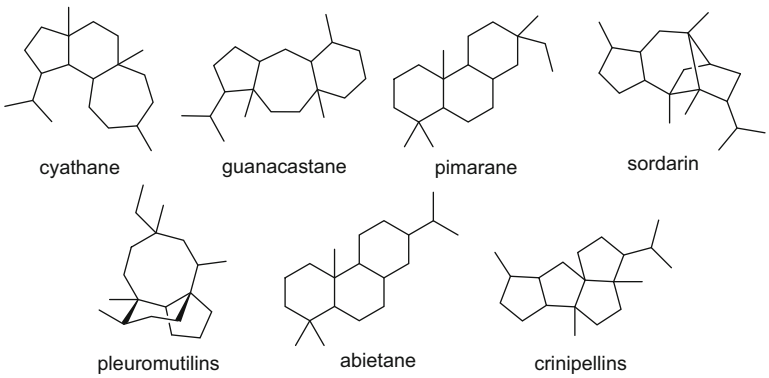


**Fig. 61** The primary skeletons of fungal-originated diterpenoids

macromycetes, and specifically, the cyathanes from the mushroom *Hericium erinaceum* as well as their bioactivities, were reviewed previously [499, 500]. This chapter does not include those compounds covered in these two reviews and only covers the literature dealing with the isolation, structural elucidation, and biological evaluation of fungal diterpenoids reported during the period 2008–2016.

### 4.2.1 Cyathanes

The 5/6/7 ring-fused cyathane-type of diterpenes, including the cyathane-xylosides, is the largest group of diterpenoids from higher fungi. Cyathanes have been isolated mainly from the three genera *Cyathus*, *Hericium*, and *Sarcodon*, and the three particular species, *Phellodon niger*, *Laxitextum incrustatum*, and *Strobilurus tenacellus* (Table 39).

**Table 39** Cyathane diterpenoids

| Compound | Origin | Type | Refs. |
|---|---|---|---|
| 11-*O*-Acetylcyathin $A_3$ | *Hericium erinaceum* | Cyathane | [501] |
| Erinacine A (**613**) | *Hericium erinaceum* | Cyathane | [502, 503] |
| (12*S*)-11$\alpha$,14$\beta$-Epoxy-13a,14b,15-trihydroxycyath-3-ene | *Strobilurus tenacellus* | Cyathane | [504] |
| (12*R*)-11$\alpha$,14$\beta$-Epoxy-13a,14b,15-trihydroxycyath-3-ene | *Strobilurus tenacellus* | Cyathane | [504] |
| Nigernins A–F (**616**, **617**) | *Phellodon niger* | Cyathane | [12, 505] |
| Scabronines G (**614**), H (**615**), K, L, M | *Sarcodon scabrosus* | Cyathane | [506–508] |
| Secoscabronine M | *Sarcodon scabrosus* | Cyathane | [509] |
| Cyrneine E | *Sarcodon cyrneus* | Cyathane | [510] |
| Cyathins D–H (**618**, **619**), W, V, T, Q (**620**) | *Cyathus africanus* | Cyathane | [511–513] |
| Cyathin I (**621**) | *Cyathus hookeri* | Cyathane | [514] |
| Cyathins J–P | *Cyathus gansuensis* | Cyathane | [515] |
| Striatoids A–F (**622**) | *Cyathus striatus* | Cyathane xyloside | [516] |
| Pyristriatins A, B (**624**) | *Cyathus* cf. *striatus* | Cyathane | [168] |
| Compound 1 | *Hericium erinaceus* | Cyathane | [517] |
| Laxitextines A, B (**623**) | *Laxitextum incrustatum* | Cyathane xyloside | [518] |

It is noteworthy that the cyathane-xylosides were only reported from liquid cultures of the fungal strains, and not from the fruiting bodies or rice cultures, while cyathane-non-xyloside analogs were reported from liquid/solid cultures and fruiting bodies. Structurally, among the total of 107 reported cyathanes, 93 contain a C-2–C-3 double bond, accounting for 87% of this group. Three of these are 2,3-*seco*, six are 2,3-epoxidized, and five are non-C-2–C-3 olefinic, which attests to the highly conserved double bond between C-2 and C-3.

Nerve growth factor (NGF) is a member of small secreted proteins known as neurotrophins, which are vital signaling molecules for the growth and maintenance of neural cells. Intake of exogenous NGF stimulates the outgrowth of neuritic projections, and may have applications in the treatment of neurodegenerative disorders, such as Alzheimer's disease. However, a drawback is that NGF is not able to cross the blood-brain barrier and is rapidly metabolized in vivo. Therefore, the search for natural products with the potential to stimulate the endogenous production of NGF is of potential importance in drug discovery. Cyathanes were proven to exhibit diverse biological activities, including neurite outgrowth-stimulating/neurotrophic, anti-inflammation, antimicrobial, and antitumor-related effects. However, it is due to their NGF-stimulating activity, that cyathanes have attracted considerable attention both in terms of drug discovery and compound total synthesis.

Erinacine A (**613**), a potent stimulator of NGF synthesis, was obtained from mycelia of the monkey head mushroom, *Hericium erinaceum* (Fig. 62). This has become a compound of great interest in recent years. It was shown that erinacine A increases catecholamine and NGF content in the central nervous system as demonstrated in an in vivo experiment in rats [503]. Very recently, several papers have dealt with *Hericium erinaceum* mycelia and/or erinacine A, including their role in protecting against ischemia-injury-induced neuronal cell death, their toxicological safety evaluation by a feeding study in mice, the molecular mechanism in the protection of MPTP-induced neurotoxicity, as well as the amelioration of Alzheimer's disease-related pathologies [519–524].

Scabronines G (**614**) and H (**615**) are two C-11 epimers isolated from the fruiting bodies of the mushroom *Sarcodon scabrosus* (Fig. 62). In vitro antimicrobial studies showed that the antibacterial potencies of scabronines G and H were almost the same as that of streptomycin at concentrations of 1 mg/cm$^3$ and 100 μg/cm$^3$ against *Staphylococcus aureus*, *Bacillus thuringiensis*, *B. megaterium*, *B. subtilis*, and *Escherichia coli*. However, at a concentration of 10 μg/cm$^3$, only *E. coli* and *B. megaterium* were sensitive to these two compounds while streptomycin was still effective against all of the bacteria. Scabronines G and H also displayed inhibitory activity against *Gibberella zeae*, *Sclerotinia sclerotiorum*, *Fusarium moniliforme*, and *F. oxysporum* at a concentration of 1 mg/cm$^3$ [507].

In the course of investigating the secondary metabolites from the edible mushroom, *Phellodon niger*, six cyathane diterpenoids, nigernins A–F (**616**, **617**), including four with a rare aromatic acyl group modification, were isolated (Fig. 62). Position C-15 is oxygenated in all six compounds in the form of a carboxylic acid group [12, 505].

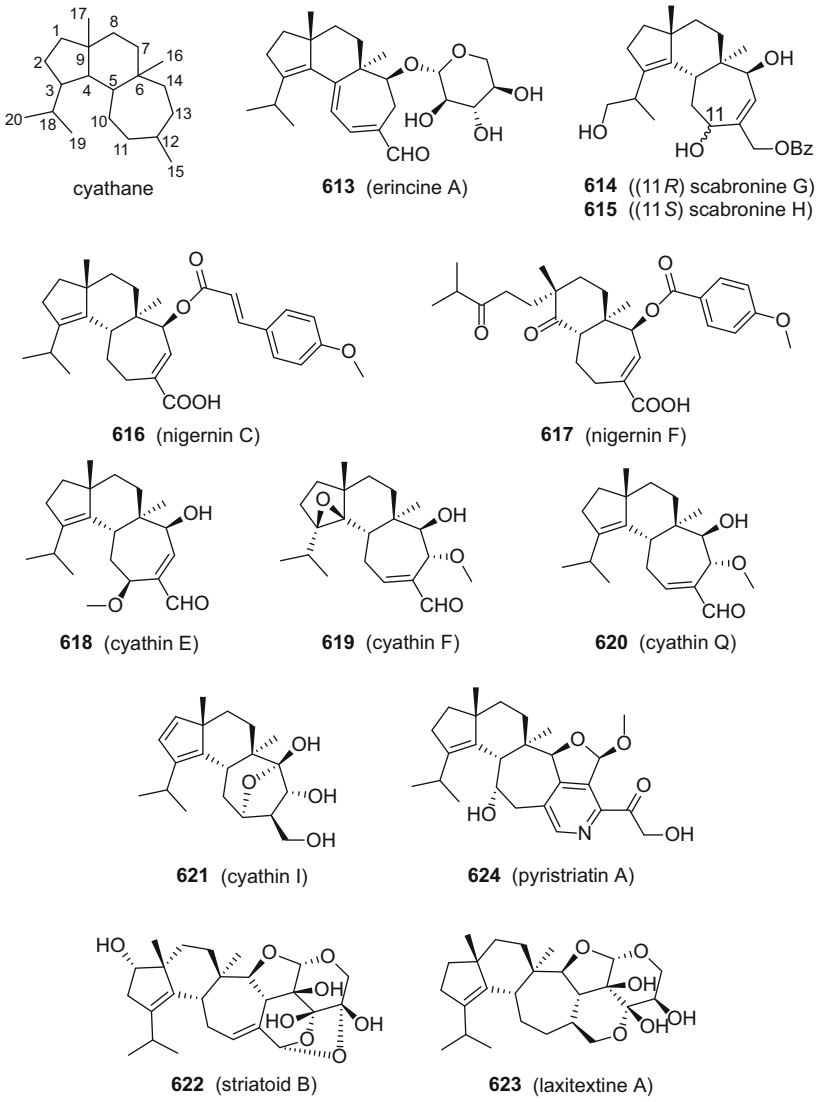


**Fig. 62** Structures of cyathane and selected derivatives

The rice fermentation of the fungus *Cyathus africanus* is a good source of cyathane diterpenoids [511–513]. The structure of cyathin E (**618**) was confirmed by single-crystal X-ray crystallographic analysis (Fig. 62). Cyathins F (**619**) and H showed potent inhibition against nitric oxide production in lipopolysaccharide-activited macrophages with $IC_{50}$ values of 2.57 and 1.45 μ*M*, respectively (Fig. 62). Neosarcodonin O and 11-*O*-acetylcyathatriol were assessed for cytotoxicity against the Hela and K562 cell lines and gave $IC_{50}$ values of $<10$ μ*M* [511].

In turn, cyathine W showed an $IC_{50}$ value of 12.1 μ*M* against the K562 cell line [512]. Cyathin Q (**620**), a cyathane diterpene that was obtained by bioactivity-guided purification, exhibited inhibitory activity against HCT116 colon cancer cells and Bax-deficient HCT116 cells in vitro and in vivo (Fig. 62). A mechanism-of-action study showed that cyathin Q exerted induction of mitochondrial and autophagy-dependent apoptosis in HCT116 cells [513].

The fungus *Cyathus hookeri* is close taxonomically to *C. africanus*. It is characterized by a campanulate peridium covered with wool-like hairs and a broadly ovoid basidiospore. A chemical investigation on this fungus led to the isolation of cyathin I (**621**) as well as two known compounds, including erinacine I. Cyathin I (**621**) and erinacine I showed inhibitory effects against nitric oxide production in macrophages with $IC_{50}$ values of 15.5 and 16.8 μ*M*, respectively (Fig. 62) [514].

From a submerged culture of the bird's nest fungus, *Cyathus striatus*, six highly oxygenated cyathane-xylosides, striatoids A–F (**622**) (Fig. 62) were isolated. These compounds enhanced NGF-induced neutrite outgrowth using rat pheochromocytoma cells as a model system of neuronal differentiation. It was revealed that these diterpenoid derivatives dose-dependently enhanced NGF-mediated neurite outgrowth in rat pheochromocytoma cells [516].

A bioassay-guided isolation procedure of the mycelial culture of *Laxitextum incrustatum*, collected in Kenya, led to the purification of the two cyathanes, laxitextines A (**623**) and B (Fig. 62). Laxitextine A showed inhibition of *Staphylococcus aureus* at 7.8 μg/cm$^3$ and also anti-MRSA activity with an *MIC* value of 7.8 μg/cm$^3$. Furthermore, both showed inhibitory activities against the MCF-7 cell line with $IC_{50}$ values of 2.3 and 2.0 μ*M*, respectively [518].

A phytochemical investigation of the cultures of the Thai fungus *Cyathus* cf. *striatus* led to the isolation of two pyridine ring-containing cyathane derivatives, which were named pyristriatins A (**624**) and B (Fig. 62). These compounds demonstrated antibacterial activity against Gram-positive bacteria. They also showed antifungal activity against some filamentous fungi as well as yeasts [168].

Owing to the documented biological activity of the cyathane diterpenoids, this group of compounds have been of considerable interest in terms of their total synthesis. Several total syntheses of cyathanes have been reported, including those of cyathin $A_3$ [525, 526], cyathin $B_2$ [525], (–)-scabronine A [527], (–)-scabronine G [527, 528], and (–)-erinacine E [529], to name just a few. Nakada et al. have accomplished the total synthesis of eight cyathanes [530, 531].

(–)-Scabronine A (**625**), one of the most potent NGF synthesis stimulators, contains six contiguous stereogenic centers in its seven-membered ring, which has increased the difficulty of its total synthesis. The first enantioselective total synthesis of (–)-scabronines A and G was achieved by Kobayakawa and Nakada in 2013 [527]. It was shown that **626** is a key intermediate for the synthesis of (–)-scabronines A and G, and was constructed by a step involving an oxidative dearomatization/intramolecular IEDDA reaction cascade (Scheme 23). This

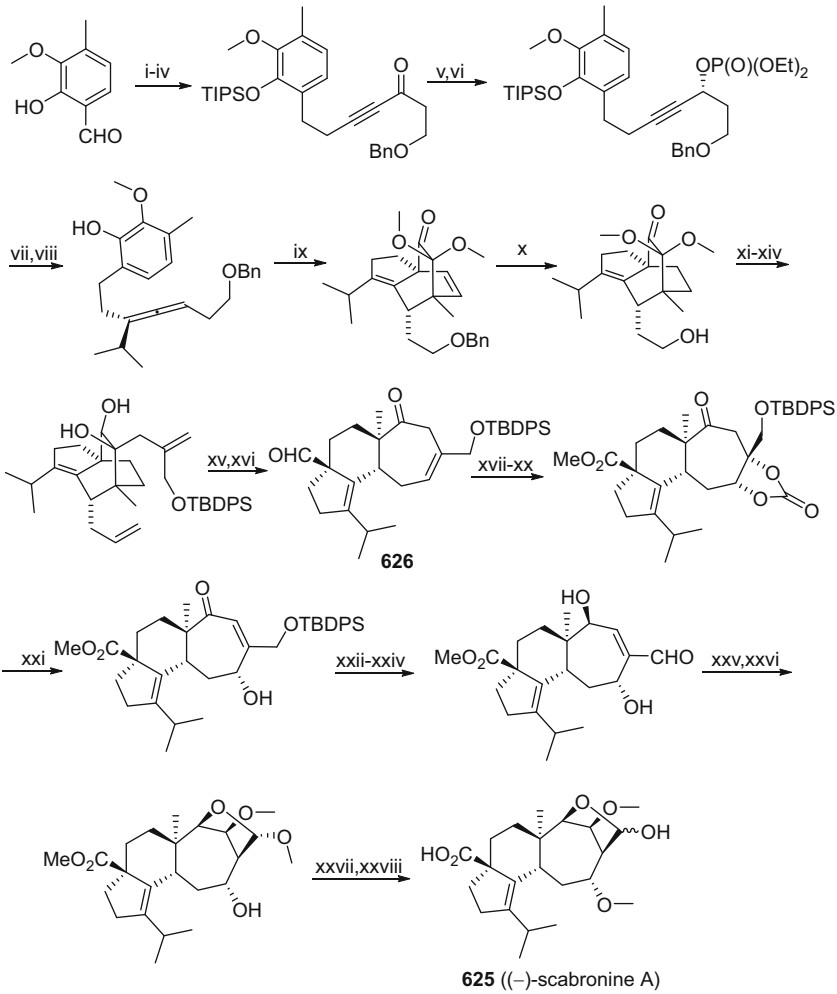


**Scheme 23** Total synthesis of (−)-scabronine A (**625**).
Reagents and conditions: (i) TIPSCl, imidazole, DMF, 40°C, 83%. (ii) propargyl bromide, Zn, $TiCl_4$ (5 mol%), THF, 0°C. (iii) $Et_3SiH$, $BF_3{\cdot}OEt_2$, $CH_2Cl_2$, 0°C, 84% (2 steps). (iv) *n*BuLi, BnO$(CH_2)_2$CON(OMe)Me, THF, −78°C to RT, 89%. (v) Ru[(*R*,*R*)-Tsdpen]( *p*-cymene) (6 mol%), *i*PrOH, RT, 92% (95% *ee*). (vi) $(EtO)_2P(O)Cl$, DMAP, $Et_3N$, $CH_2Cl_2$, RT, 97%. (vii) *i*PrMgCl, CuCN·2 LiCl, THF, −78°C, quant. (viii) TBAF, THF, 0°C, 97% (95% *ee*). (ix) PIDA, MeOH, RT, 7 days, 97%. (x) $H_2$, Pd/C (5 mol%), EtOAc, RT, 92% [95% *ee*, >99% *ee* (recryst.)]. (xi) $(COCl)_2$, DMSO, $Et_3N$, $CH_2Cl_2$, −78 to 0°C, 98%. (xii) $Ph_3PCH_3Br$, *t*BuOK, THF, 0°C, 99%. (xiii) $NaBH_4$, MeOH, 0°C; then, 3*N* HCl (aq.), 95%. (xiv) $H_2C{=}C(CH_2Br)(CH_2OTBDPS)$, Zn, THF, RT, 91%. (xv) PIDA, $CH_2Cl_2$, RT, 90%. (xvi) Grubbs II (2.5 mol%), $CH_2Cl_2$, reflux, 89%; (xvii) $NaClO_2$, $NaH_2PO_4$, 2-methyl-2-butene, THF, *t*BuOH, $H_2O$, RT. (xviii) MeI, $K_2CO_3$, DMF, RT, 74% (2 steps). (xix) $OsO_4$ (2.5 mol%), NMO, THF, *t*BuOH, $H_2O$, RT. (xx) triphosgene, pyridine, DMAP, $CH_2Cl_2$, 0°C to RT, 66% ($\alpha$), 20% ($\beta$) (2 steps). (xxi) DBU, PhH, RT, quant.; (xxii) (*R*)-CBS, $BH_3{\cdot}SMe_2$, THF, 0°C. (xxiii) TBAF, THF, 0°C to RT, 90% (2 steps). (xxiv) TEMPO (20 mol %), PIDA, $CH_3CN$, $CH_2Cl_2$, $KPB_7$, 80%. (xxv) NaOMe, MeOH, 0 to 15°C. (xxvi) HCl, MeOH, 0°C to RT, 82% (15$\alpha$), 7% (15$\beta$). (xxvii) MeI, NaH, THF, RT, 99%. (xxviii) 2 *N* NaOH (aq.), MeOH, 70°C, then, 3 *N* HCl (aq.), 94%. NMO = *N*-methylmorpholine *N*-oxide

approach enabled the total synthesis of (–)-scabronine G in 19 steps with a 21% overall yield. Additionally, a highly stereoselective oxa-Michael/protonation/acetalization cascade enabled the completion of the first total synthesis of (–)-scabronine A [527].

### 4.2.2 Guanacastanes

The 5/7/6 ring-fused guanacastane-type of diterpenoid is rarely encountered in the secondary metabolites of macromycetes. Recent years have been a period for the rapid discovery of this kind of diterpenoid, mainly from the genus *Coprinus*. So far, about 35 examples of the guanacastanes have been isolated from higher fungi, including six reviewed previously (Table 40) [500]. Most members of this compound type contain large conjugated systems, which leads to the observation of maxima at long-wavelengths in their UV absorption spectra.

A strain of *Coprinus radians* was isolated from the spore suspension of an *Amanita* sp. Thirteen guanacastane-type diterpenoids were obtained from the PDA solid medium (Table 40). Radianspenes J–L (**309–311**) are three lactam group-containing guanacastane diterpenoids, and radianspene M (**627**) is a guanacastane dimer (Fig. 63) [170].

Guanacastanes were reported to possess cancer cell cytotoxic effects and 11$\beta$-HSD1 inhibitory activity. Radianspene C (**628**) exhibited growth inhibitory activity against the MDA-MB-435 cell line with an $IC_{50}$ value of 0.91 $\mu M$ [170]. Plicatilisin A (**629**) was reported to exhibit cytotoxic effects against the HepG2, HeLa, MDA-MB-231, BGC-823, HCT 116, and U2OS human cancer cell lines with $IC_{50}$ values ranging from 1.2 to 6.0 $\mu M$ [535]. Plicatilisin F (**630**), isolated from *C. plicatilis*, was obtained as two inseparable tautomers in a 1:1 ratio [534]. Guanacastepene R (**631**) displayed inhibitory activities against the human and mouse isozymes of 11$\beta$-HSD1 with $IC_{50}$ values of 6.2 and 13.9 $\mu M$ (Fig. 63) [536].

The complex polycyclic rings of the guanacastanes have attracted some attention with respect to their total synthesis [537–540].

**Table 40** Guanacastane diterpenoids

| Compound | Origin | Type | Refs. |
|---|---|---|---|
| 2,5-Epoxy-5,13-dihydroxyneodolast-3-en-14-one | *Trametes corrugata* | Guanacastane | [532] |
| Lacrymarone | *Lacrymaria velutina* | Guanacastane | [533] |
| Radianspenes A–M (**309–311**, **627**, **628**) | *Coprinus radians* | Guanacastane | [170] |
| Plicatilisins A–H (**629–630**) | *Coprinus plicatilis* | Guanacastane | [534, 535] |
| Guanacastepenes P–T (**631**) | *Psathyrella candollana* | Guanacastane | [536] |

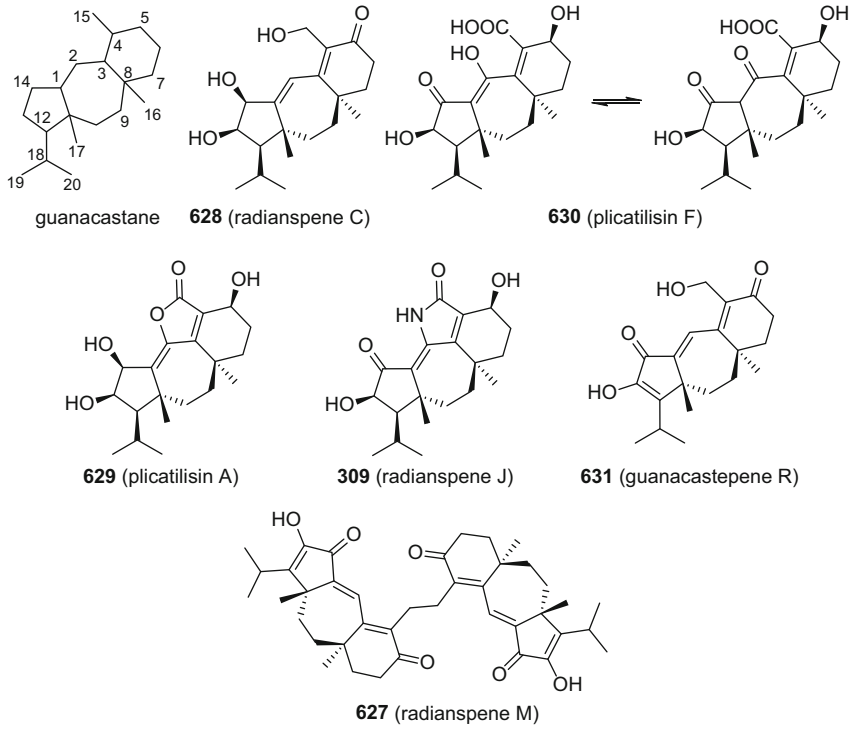


**Fig. 63** Structures of guanacastane and selected compounds

### 4.2.3 Isopimaranes

Almost all of the reported mushroom isopimarane-type diterpenes have been found either in the fruiting bodies or the cultures of the ascomycete genus *Xylaria* (Table 41). The isopimarane skeleton has a tendency to be oxygenated, and, among the reported isopimaranes, the C-19 methyl group is often oxygenated to a carboxylic acid group. *Xylaria*-derived isopimaranes have shown cytotoxic effects against many different cancer cell line types.

The fungus *Xylaria polymorpha* is a copious secondary metabolite-producing strain. A rice fermentation of this species led to the isolation of three isopimarane diterpene glycosides and three unusual compunds of this class (**632**) (Fig. 64). The sugar moieties of these glycosides are either D-mannose or D-glucose and the absolute configurations of the sugar moieties were established by comparison of their optical rotation values with those of authentic samples. The sugars were obtained by enzymatic hydrolysis of the original isolated samples [541]. A 6,7-*seco*-isopimarane, spiropolin A (**633**), and a cyclopropane-bearing compound, myrocin E (**634**), were also isolated from the rice fermentation of *X. polymorpha* (Fig. 64). The structure of spiropolin A was established unequivocally by single-

**Table 41** Isopimarane diterpenoids

| Compound | Origin | Type | Refs. |
|---|---|---|---|
| 16$\alpha$-D-Mannopyranosyloxyisopimar-7-en-19-oic acid (**632**) | *Xylaria polymorpha* | Isopimarane | [541] |
| 15-Hydroxy-16$\alpha$-D-mannopyranosyloxyisopimar-7-en-19-oic acid | *Xylaria polymorpha* | Isopimarane | [541] |
| 16$\alpha$-D-Glucopyranosyloxyisopimar-7-en-19-oic acid | *Xylaria polymorpha* | Isopimarane | [541] |
| Spiropolin A (**633**) | *Xylaria polymorpha* | 6,7-Isopimarane | [542] |
| Myrocins D, E (**634**) | *Xylaria polymorpha* | Isopimarane | [542] |
| Xylarenolide | *Xylaria* sp. 101 | Isopimarane | [347] |
| Xylopimarane (**635**) | *Xylaria* sp. BCC4297 | 20-Norisopimarane | [543] |
| Sphaeropsidin C | *Xylaria* sp. BCC4297 | Isopimarane | [543] |
| Compound 4 | *Xylaria* sp. BCC5484 | Isopimarane | [348] |
| Hymatoxin E | *Xylaria* sp. BCC5484 | Isopimarane | [348] |
| Xylallantins A, B (**636**, **637**), C | *Xylaria allantoidea* BCC23163 | Isopimarane | [167] |
| Xylarianes A, B | *Xylaria* sp. 290 | Isopimarane | [544] |

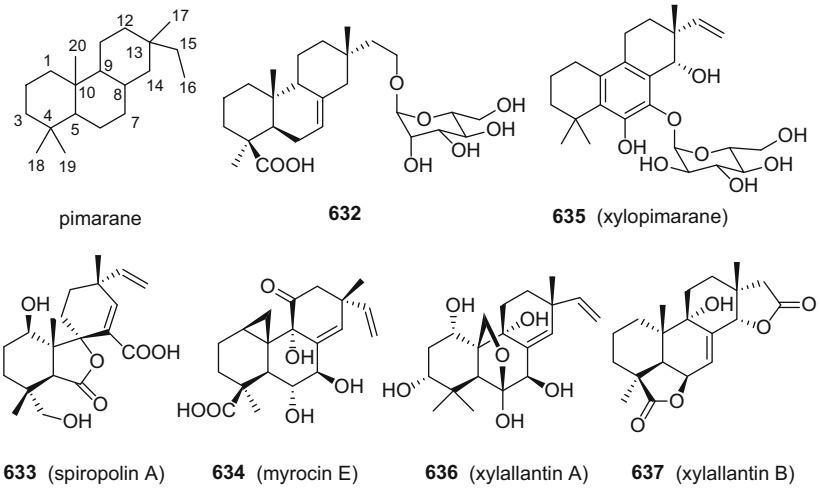


**Fig. 64** Structures of pimarane and selected derivatives

crystal X-ray diffraction analysis. Spiropolin A (**633**) represents the first example of a naturally occurring 6,7-secopimarane (Fig. 64). A bioassay used demonstrated that spiropolin A restores the growth inhibition caused by hyperactivated $Ca^{2+}$-signaling in a mutant yeast strain [542].

*Xylaria* species also play an important role in wood decomposition. A chemical investigation of the wood-decaying fungus *Xylaria* sp. BCC4297 led to the

discovery of a ring B aromatic 20-norisopimarane glucoside, namely, xylopimarane (**635**), along with the known compound sphaeropsidin C (Fig. 64). Xylopimarane was evaluated for cytotoxicity against the KB, MCF-7, and NCI-H187 cancer cell lines, and exhibited $IC_{50}$ values of 1.0, 12, and 65 μ*M*, respectively. It was assumed that sphaeropsidin C is a precursor of xylopimarane via a decarboxylation-aromatization process followed by glycosidation [543].

The first chemical study of the wood-decaying fungus *Xylaria allantoidea* BCC23163 led to the isolation of four isopimarane diterpenoids. Xylallantin A (**636**) was found to be highly oxygenated with five hydroxy groups, of which one is formed by a hemiacetal structure between the hydroxy group of C-20 and the ketone carbonyl on C-6 (Fig. 64). This compound gave an $IC_{50}$ value of 17 μg/cm$^3$ when evaluated against NCI-H187 cells. Xylallantins B (**637**) and C were characterized as possessing an ester bond between C-19 and C-6 (Fig. 64) [167].

### 4.2.4 Sordarins

Sordarins are a group of diterpenoids with a bridged ring and are distributed mainly in the family Xylariaceae. However, this type of diterpene is often found in filamentous fungi. Only two reports on the isolation of sordarins have been published, from the wood-decaying fungi *Xylaria* sp. and *Xylotumulus gibbisporus* (Fig. 65).

Xylarin (**638**), with a tricyclic uronic acid moiety, is an antifungal metabolite from the liquid culture of a wood-decaying *Xylaria* species (Fig. 65). It showed inhibition of fungal growth, and the *MIC* values for **638** against *Nematospora coryli*

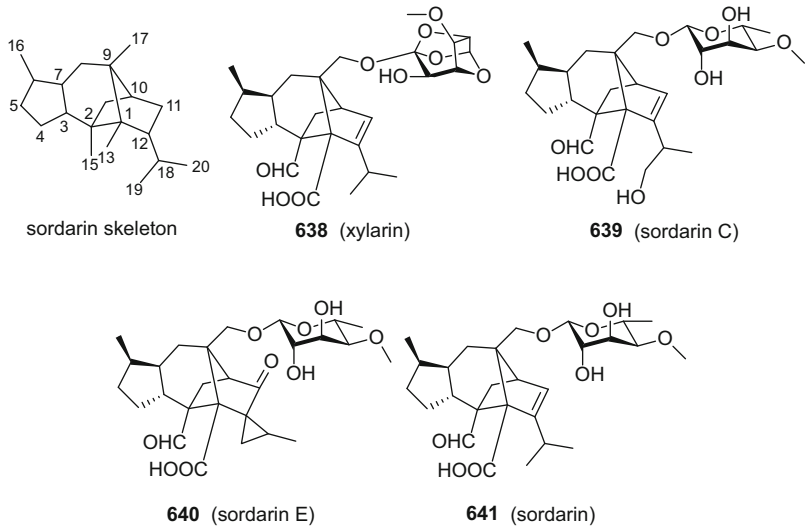


**Fig. 65** Structures of the sordarins

and *Saccharomyces cerevisiae* were 0.5 and 5 μg/cm$^3$, respectively. However, **638** did not exhibit discernible antibacterial activity [545].

The fungus *Xylotumulus gibbisporus* was described for the first time in 2006 from dead angiosperm wood collected from the Bird Park area in the Hawaii Volcanoes National Park. Sordarins C–F (**639**, **640**) are diterpene glycosides, and, along with sordarin (**641**), were isolated from the fermented broth of *X. gibbisporus* (Fig. 65). These compounds were evaluated for their antifungal and NO production inhibition activities. Compound **641** exhibited antifungal activities against *Candida albicans* ATCC 18804, *C. albicans* ATCC MYA-2876, and *Saccharomyces cerevisiae* ATCC 2345, with $IC_{50}$ values of 64.0, 32.0, and 32.0 μg/cm$^3$. Sordarin and sordarin D also displayed weak inhibition of NO production [546].

### 4.2.5 Pleuromutilins

The fungal secondary metabolite pleuromutilin (**642**) was first reported in 1951 from the two basidiomycete species *Pleurotus passeckerianus* and *Pleurotus mutilus* (now known as *Clitopilus scyphoides*), by Kavanagh and co-workers (Fig. 66) [547].

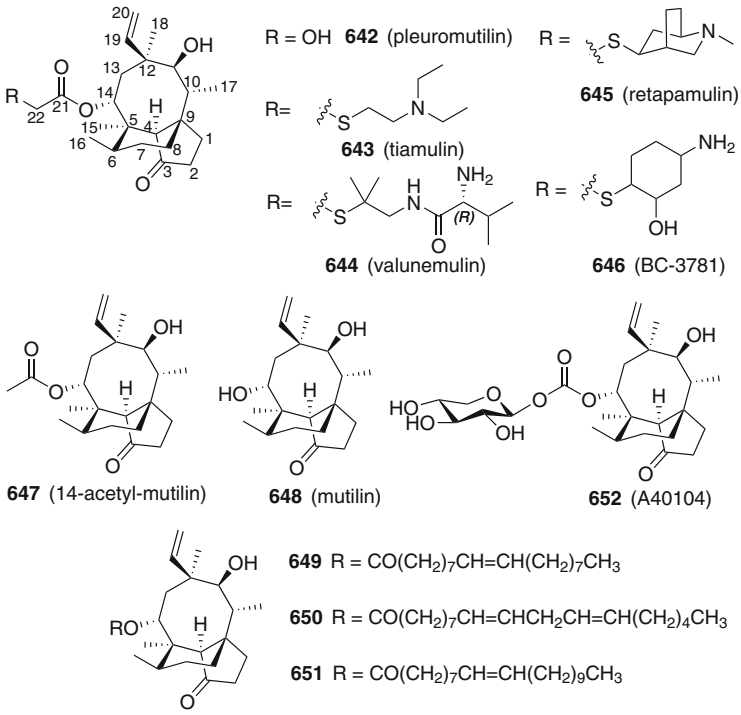


**Fig. 66** Structures of pleuromutilin (**642**), its optimized compounds, and pleuromutilin derivatives

Antimicrobial testing revealed that **642** is highly active against Gram-positive cocci, but an in vivo experiment in mice using *Streptococcus hemolyticus* resulted in the low rate of survival of the test animals, a finding that led to less attention being placed on pleuromutilin subsequently. In the early 1960s, pleuromutilin was re-encountered from a culture of *Clitopilus passeckeranius* and it demonstrated enhanced inhibitory activity against both penicillin- and streptomycin-resistant *Staphylococcus* and *Mycoplasma* spp. In order to improve on their antimicrobial activity, many pleuromutilin derivatives have been synthesized, mainly to introduce structural variations of the C-14 side chain. Up to the present, tamulin (**643**) and valunemulin (**644**) have been developed successfully as veterinary antibiotics (Fig. 66) [548, 549].

Pleuromutilins appear to exert their antimicrobial activity by inhibition of prokaryotic protein synthesis through an interaction with the 50S ribosomal subunit. This antibacterial mechanism has enhanced the development of pleuromutilin derivatives for human use, and as might be expected, considerable attention has been given to the synthesis of pleuromutilin derivatives to explore their potential for humans. Retapamulin (**645**) was approved by the U.S. FDA for the topical treatment of impetigo and traumatic lesions of skin infections, but has limited water solubility (Fig. 66). Compound BC-3781 (**646**) is a synthesized pleuromutilin thioether derivative which entered Phase II clinical studies (Fig. 66) [548, 549].

The development of improved pleuromutilin derivatives with the potiential for human use is ongoing. A structure-activity relationship study revealed that the C-14 side chain functionality is the key determinant for properties driving systemic efficacy. However, additional evidence is needed to support a direct link between the putative antimicrobial target, the peptidyl transferase center (PTC) of the 50S ribosomal subunit and its substrate, and the pleuromutilin derivatives [549–552].

Owing to the excellent antimicrobial activity of pleuromutilins, much work on their biosynthesis as well as total synthesis has been undertaken in recent years. For example, seven gene clusters responsible for pleuromutilin biosynthesis were identified, and heterologous expression within the ascomycete *Aspergillus oryzae* successfully improved the production of pleuromutilin by tenfold [553].

In addition, efforts in searching for new pleuromutilins from natural sources have continued. In 1976, Knauseder et al. isolated several pleuromutilin derivatives from a culture of *Clitopilus passeckerianus* (**647–651**) (Fig. 66) [554]. A40104A (**652**), pleuromutilin $\beta$-D-xylopyranoside, has been reported to exhibit antibiotic activity that is fivefold greater than that of pleuromutilin (Fig. 66) [555].

### 4.2.6 Abietanes

Abietane-type diterpenoids occur mainly as plant-derived secondary metabolites. However, some examples of this type of diterpene have been isolated from fungi. So far, only seven abietanes, of which the C rings are all aromatic, are of mushroom origin (Table 42).

**Table 42** Abietane diterpenoids

| Compound | Origin | Type | Refs. |
|---|---|---|---|
| 12-Hydroxy-7-oxo-5,8,11,13-tetraene-18,6-abitanolide (**653**) | *Phellinus igniarius* | Abietane | [556] |
| Dehydroabietic acid (**654**) | *Phellinus pini* | Abietane | [557] |
| Rickitin A(**655**) | *Hypoxylon rickii* | Abietane | [353] |
| Perenacidins A–D (**656–659**) | *Perenniporia subacida* | Abietane | [558] |

From two *Phellinus* fruiting bodies, *P. igniarius* and *P. pini*, the two abietanes, 12-hydroxy-7-oxo-5,8,11,13-tetraene-18,6-abitanolide (**653**) and dehydroabietic acid (**654**) were obtained (Fig. 67) [556, 557]. Dehydroabietic acid showed very weak inhibition of NO production with an $IC_{50}$ value of 98.9 μ*M*, while L-NMMA, the positive control, gave an $IC_{50}$ value of 15.7 μ*M*. The ascomycete *Hypoxylon rickii* has been found to produce different types of secondary metabolites, including the abietane diterpenoid, rickitin A (**655**) (Fig. 67). Rickitin A displayed weak antibacterial activity against *Staphylococcus aureus* DSM 346, with an *MIC* value of 33.3 μg/cm$^3$, and was evaluated for cytotoxic effects against the KB3.1 cervical carcinoma cell line and L929 mouse fibroblast cells, with $IC_{50}$ values of 18.0 and 23.0 μg/cm$^3$, respectively [353].

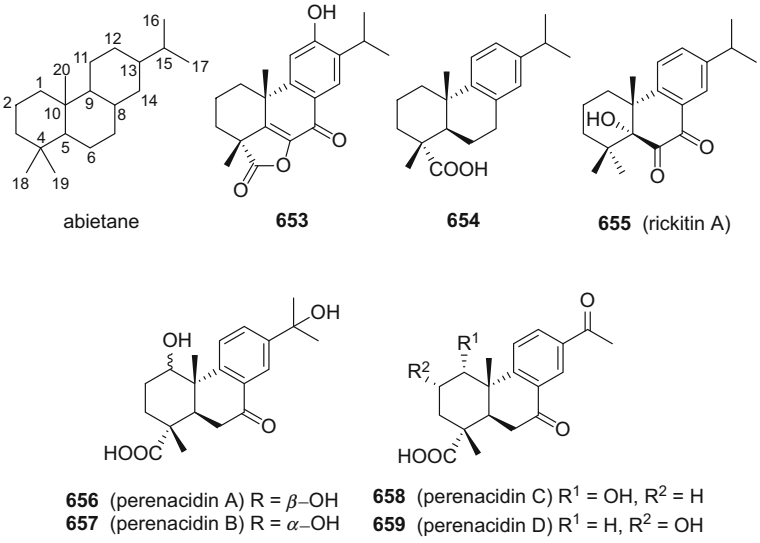


**Fig. 67** Structures of abietane and selected compounds

### 4.2.7 Crinipellins

Crinipellins are a class of diterpenoids possessing a tetraquinane skeleton, and these compounds are produced by the basidiomycetous genus *Crinipellis* (Table 43). Culturing of the fungus *Crinipellis stipitaria* led to the the isolation of a crystalline substance with antibiotic properties, named crinipellin. However, later on the structure of this substance was determined to be 9-*O*-acetylcrinipellin A (**660**) (Fig. 68) [559, 560]. The structure of crinipellin remained undetermined until 1985. Four related diterpenes were obtained from several strains of this fungus, namely, crinipellins A (**661**), B (**662**), dihydrocrinipellin B (**663**), and tetrahydrocrinipellin A (**664**) (Fig. 68). The absolute configuration of crinipellin B was established by single-crystal X-ray diffraction analysis [559]. Crinipellin derivatives were found in a fungus collected in Yunnan Province, People's Republic of China, and partial sequence analysis of the internal transcribed spacers (ITS1 and ITS2) and the 5.8S rDNA gene were supportive of the organism being investigated as belonging to the genus *Crinipellis*. Four additional crinipellin derivatives **665–668** were isolated from an agar culture of this fungus. All showed moderate growth-inhibitory activities against HeLa cells [561].

More recently, four potentially anti-inflamatory crinipellin analogues, crinipellins E–H (**669–672**), were isolated from the liquid culture of a *Crinipellis* species (Fig. 68). Structurally, the C-14 isopropyl moiety is modified as terminal double bonds in crinipellins G and H. Biological testing revealed that crinipellins E, F, and G dose-dependently inhibited LPS/IFN-$\gamma$ induced CXCL10 promoter activity in transiently transfected human MonoMac6 cells, with $IC_{50}$ values of 15, 1.5, and 3.15 μ$M$, respectively. Moreover, the aforementioned three crinipellins also reduced mRNA levels and the synthesis of pro-inflammatory mediators, while crinipellin H was devoid of these types of biological activities [562].

Although the crinipellins were discovered in 1985, reports dealing with their isolation and characterization have been limited to only three research articles,

**Table 43** Crinipellins

| Compound | Origin | Type | Refs. |
|---|---|---|---|
| Crinipellins A (**661**), B (**662**) | *Crinipellis stipitaria* | Crinipellin | [559] |
| 9-*O*-Acetylcrinipellin A(**660**) | *Crinipellis stipitaria* | Crinipellin | [559, 560] |
| Dihydrocrinipellin B (**663**) | *Crinipellis stipitaria* | Crinipellin | [559] |
| Tetrahydrocrinipellin A (**664**) | *Crinipellis stipitaria* | Crinipellin | [559] |
| (4$\beta$)-4,4-*O*-Dihydrocrinipellin A (**665**) | *Crinipellis* sp. 113 | Crinipellin | [561] |
| (4$\beta$,8$\alpha$)-4,4-*O*-8,8-*O*-Tetrahydrocrinipellin B (**666**) | *Crinipellis* sp. 113 | Crinipellin | [561] |
| Crinipellins C (**667**), D (**668**) | *Crinipellis* sp. 113 | Crinipellin | [561] |
| Crinipellins E–H (**669–672**) | *Crinipellis* sp. | Crinipellin | [562] |

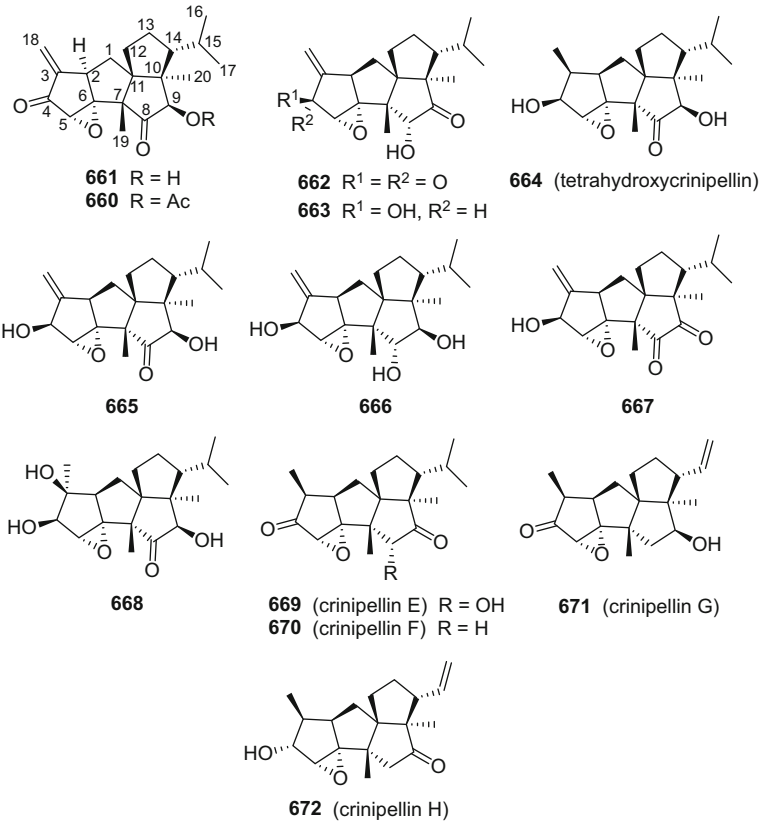


**Fig. 68** Structures of crinipellins

including one that was just published very recently. For some time, their interesting tetraquanane structures and promising bioactivities have made the crinipellins appealing synthetic targets [563, 564].

### 4.2.8 Miscellaneous Diterpenoids

Macromycetes species have yielded several other types of diterpenoids, such as cleistanthanes, labdanes and rosanes. Many of these diterpenoids were reported in recent years, which has expanded the known chemical diversity of terpenoids produced by fungi.

A culture of the basidiomycetous fungus *Albatrellus confluens* yielded two cleistanthane-type diterpenes, 3*α*,5*α*,8*β*-trihydroxycleistanth-13(17),15-dien-18-oic acid (**673**) and 8*β*-hydroxy-18-norcleistanth-4(5),13(17),15-trien-3-one (**674**) (Fig. 69) [565]. Gleromycenolic acid A (**675**) is a cleistanthane-type diterpene isolated from the medicinal fungus *Engleromyces goetzii*. This species is distributed widely in the Tibetan plateau and in Sichuan and Yunnan provinces of

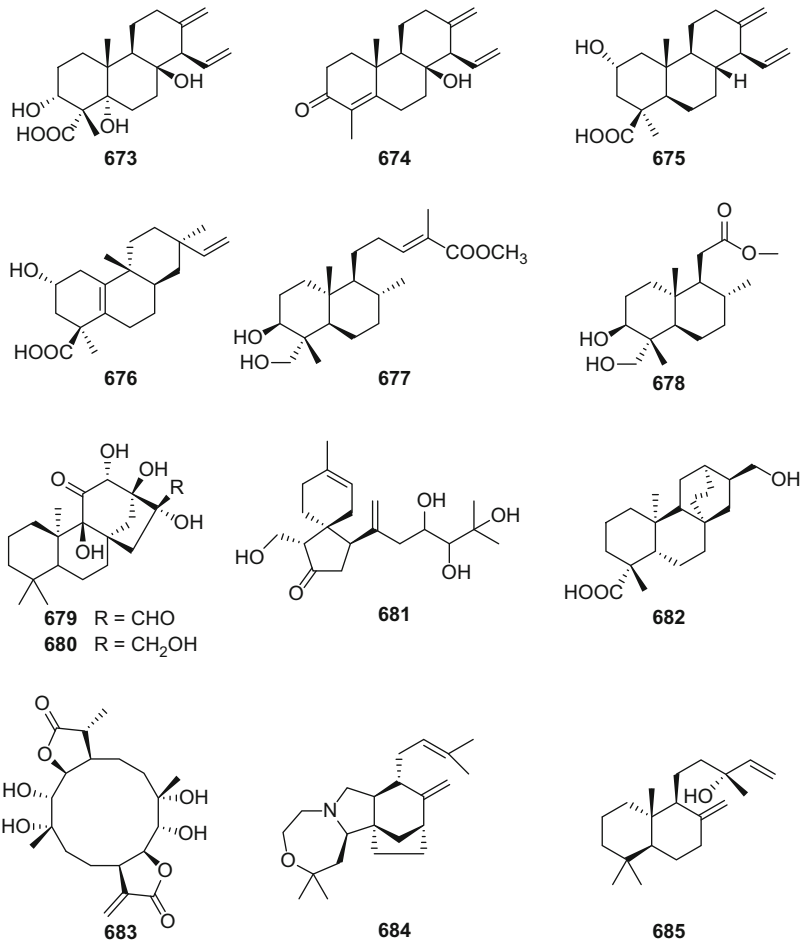


**Fig. 69** Structures of miscellaneous diterpenoids

mainland China, and is used to treat infections, inflammation, and cancer (Fig. 69). Gleromycenolic acid A (**675**) inhibited the activity of the cholesterol ester transfer protein (CETP) with an $IC_{50}$ value of 7.55 μ*M* [566]. Moreover, five additional rosane-type diterpenoids (**676**) were also obtained from cultures of *Engleromyces goetzii*, but they were devoid of discernible CETP inhibitory activity.

In the course of searching for novel inhibitors of human neutrophil elastase (HNE), two labdane diterpenes, **677** and **678**, were isolated from the fruiting bodies of *Ramaria formosa* (Table 44). Both exhibited moderate inhibition of HNE. Other types of diterpenoids, such as kauranes (**679**, **680**), a viscidane (**681**), an atisane (**682**), the macrocyclic eryngiolide A (**683**), and the diterpenoid alkaloid concavine, represent a miscellanous group of diterpenoids isolated from mushrooms.

Tricholomalides A–C (**686**, **687**) are three γ-lactone group-containing diterpenoids isolated from a methanol extract of the fruiting bodies of *Tricholoma*

**Table 44** Miscellaneous diterpenoids

| Compound | Origin | Type | Refs. |
|---|---|---|---|
| 3$\alpha$,5$\alpha$,8$\beta$-Trihydroxycleistanth-13(17),15-dien-18-oic acid (**673**) | *Albatrellus confluens* | Cleistanthane | [565] |
| 8$\beta$-Hydroxy-18-norcleistanth-4(5),13(17),15-trien-3-one (**674**) | *Albatrellus confluens* | Cleistanthane | [565] |
| Gleromycenolic acid A (**675**) | *Engleromyces goetzii* | Cleistanthane | [566] |
| Engleromycenolic acid B | *Engleromyces goetzii* | Rosane | [566] |
| Engleromycenol (**676**) | *Engleromyces goetzii* | Rosane | [566] |
| Rosololactone | *Engleromyces goetzii* | Rosane | [566] |
| Rosenonolactone | *Engleromyces goetzii* | Rosane | [566] |
| 7-Deoxyrosenonolactone | *Engleromyces goetzii* | Rosane | [566] |
| 8,14-Labdadien-13-ol (**685**) | *Phellinus pini* | Labdane | [557] |
| 3$\beta$,18-Dihydroxy-8*S*-labd-13*E*-en-16-oate (**677**) | *Ramaria formosa* | Labdane | [567] |
| 3$\beta$,18-Dihydroxy-8*S*-tetra-*nor*-labdan-12-oate (**678**) | *Ramaria formosa* | Norlabdane | [567] |
| Phlebiakauranol aldehyde (**679**) | *Punctularia atropurpurascens* | Kaurane | [568] |
| Phlebiakauranol alcohol (**680**) | *Punctularia atropurpurascens* | Kaurane | [568] |
| 8-Oxoviscida-2,11(18)-diene-13,14,15,19-tetraol (**681**) | *Hypsizygus marmoreus* | Viscidane | [569] |
| 17-Hydroxy-*ent*-atisan-19-oic acid (**682**) | *Inonotus obliquus* | Atisane | [332] |
| Eryngiolide A (**683**) | *Pleurotus eryngii* | | [570] |
| Concavine (**684**) | *Clitocybe concava* | Diterpenoid alkaloid | [571] |

sp. These three compounds were evaluated for the induction of neurite outgrowth in rat pheochromocytoma cells at a concentration of 100 μ*M* [572]. A total synthesis of tricholomalides A and B led to a revision of their structures (Scheme 24) [573].

**Scheme 24** Structural revisions of tricholomalides A (**686**) and B (**687**)

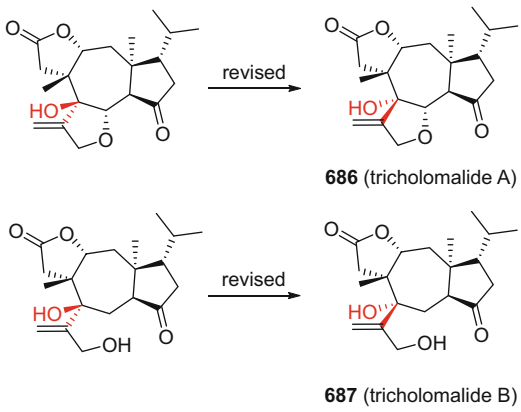


**686** (tricholomalide A)

**687** (tricholomalide B)

## 4.3 Triterpenoids

Triterpenoids are a major group of secondary metabolites from mushrooms, especially from their fruiting bodies. Triterpenoids are composed of six isoprene units represented by acyclic, mono-, di-, tri-, tetra-, and pentacyclic carbon skeletons. So far, a total of four types of polycyclic triterpenoids have been isolated from higher fungi, namely, those of the lanostane-, ergostane-, cucurbitane-, and saponaceolide types (Fig. 70). Among them, the lanostanes account for the largest proportion of mushroom triterpenoids. In turn, the *Ganoderma*-derived lanostanes have been investigated to the greatest extent thus far. Some fungal-derived lanostanes are considered to be potential anticancer compounds [574]. Ergostane-type triterpenoids have been found mainly in the medicinal fungus *Antrodia cinnamomea*.

### 4.3.1 *Ganoderma* Lanostanes

The genus *Ganoderma* comprises more than 300 species that are distributed mostly in tropical regions [575]. *Ganoderma* species are a group of medicinal fungi that have been used as remedies for the treatment of many different types of disease for thousands of years in China. A literature survey revealed that except for the extensively studied species *Ganoderma lucidum*, a further 23 species of *Ganoderma* have been subjected to phytochemical investigation. These are: *G. amboinense*, *G. annulare*, *G. applanatum* (synonym *G. lipsiense*), *G. australe*, *G. boninense*, *G. capense*, *G. carnosum*, *G. cochlear*, *G. colossum*, *G. concinna*, *G. curtisii*, *G. fornicatum*, *G. hainanense*, *G. leucocontextum*, *G. mastoporum*, *G. neo-japonicum*, *G. orbiforme*, *G. pfeifferi*, *G. resinaceum*, *G. sinense*,

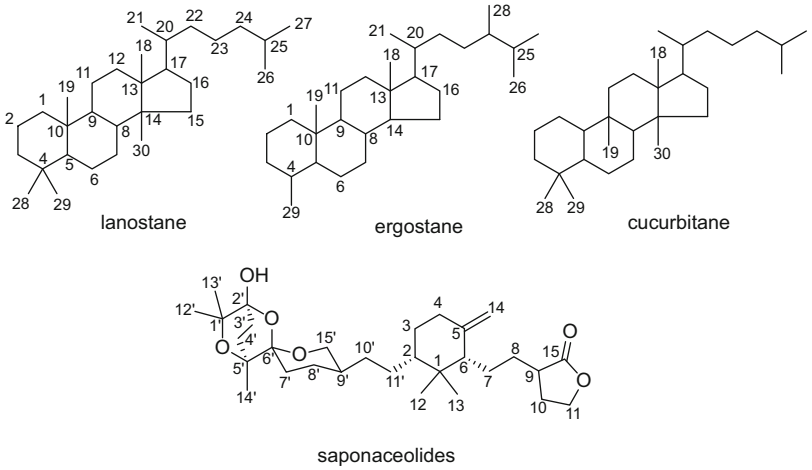


**Fig. 70** Triterpenoid skeletons from higher fungi

*G. theaecolum*, *G. tropicum*, and *G. tsugae*. The secondary metabolites of *Ganoderma* species comprise (nor-)lanostanes, $C_{30}$ pentacyclic triterpenes, meroterpenoids, sesquiterpenoids, alkaloids, steroids, and benzenoids. Baby et al. have published a systematic review of the secondary metabolites from *Ganoderma* [576]. However, this review highlighted the structural classification of the *Ganoderma* triterpenoids, while the biological activities of these triterpenes were only discussed briefly. Therefore, those *Ganoderma* triterpenes with distinctive structures and/or significant and promising bioactivities are highlighted in the present section (Table 45).

Lanostane triterpenoids from the genus *Ganoderma* have been classified into four groups based on the carbon number of the lanostane skeleton as follows: (a) $C_{30}$ lanostanes including ganoderic acids and other functionalized lanostanes, such as aldehydes, alcohols, esters, glycosides, lactones, and ketones; (b) $C_{27}$ lanostanes with the C-25, C-26, C-27 carbon atoms degraded, including lucidenic acids, alcohols, lactones, and esters; (c) $C_{24}$ and $C_{25}$ lanostanes, and (d) $C_{30}$ pentacyclic triterpenes. Almost half of the lanostanes have been reported from the medicinal fungus *G. lucidum*.

*Ganoderma* triterpenoids display diverse biological activities, such as having anti-inflammatory, antitumor, antiviral, and antiplasmodial effects (Table 45). Many biological studies on *Ganoderma* triterpenoids have focused on their effects on the proliferation of tumor cells and their potential anti-inflammatory activity. Additionally, *Ganoderma* triterpenoids also exhibit the inhibition of many enzymes.

Ganoderic acid Df as well as its methyl ester were isolated from *G. lucidum*. A biological study revealed ganoderic acid Df to have human aldose reductase inhibitory activity in vitro, with an $IC_{50}$ value of 22.8 $\mu M$, while its methyl ester derivative was much less active. Therefore, it was suggested that the carboxylic acid group of the side chain is essential for aldose reductase inhibitory activity [582]. A similar general observation was made for ganoderic acid C2 and ganoderenic acid A (**693**) (Fig. 71), using the same type of biological test system [609]. Moreover, ganoderenic acid A is a potent inhibitor of $\beta$-glucuronidase, which is associated with liver injury [610]. $\alpha$-Glucosidase inhibitors prevent the digestion of carbohydrates and some have use as potential drug leads for the treatment of diabetes mellitus type-2. A bioguided-isolation procedure of the chloroform extract of *G. lucidum* resulted in the isolation of ganoderol B. Ganoderol B displayed $\alpha$-glucosidase inhibitory activity with an $IC_{50}$ value of 48.5 $\mu g/cm^3$ (119.8 $\mu M$) [625]. Lucidenic acid O and lucidenic lactone are trinorlanostanes isolated from *G. lucidum*. Both these compounds were found to inhibit calf DNA polymerase $\alpha$, rat DNA polymerase $\beta$, and human immunodeficiency virus type 1 reverse transcriptase at a concentration of 100 $\mu M$ [619].

The activity of *Ganoderma* triterpenoids against the source of malaria infection, *Plasmodium falciparum*, and against the pathogenic bacterium, *Mycobacterium tuberculosis*, have also been reported. Ganoderic acid S, 23-hydroxyganoderic acid S, ganoderic aldehyde TR, and ganoboinketals A–C were reported to exhibit antiplasmodial activity [592, 630]. Ganoderic aldehyde TR possesses an aldehyde

**Table 45** Selected *Ganoderma* lanostanes

| Compound | Origin | Type | Biological activity | Refs. |
|---|---|---|---|---|
| Ganoderic acid A (**688**) | *G. lucidum* | C30 | a, b | [577–579] |
| Ganoderic acid B | *G. lucidum* | C30 | a | [577, 578] |
| Ganoderic acids C, D (C1) | *G. lucidum* | C30 | c, d | [580, 581] |
| Ganoderic acid Df | *G. lucidum* | C30 | e | [582] |
| Ganoderic acid F (**689**) | *G. lucidum* | C30 | f1, g | [583, 584] |
| Ganoderic acid G, H | *G. lucidum* | C30 | a | [577] |
| Ganoderic acid Me (**690**) | *G. lucidum* | C30 | f2, h, i, j, f3 | [585–590] |
| Ganoderic acid Mf | *G. lucidum* | C30 | j | [588, 591] |
| Ganoderic acid S | *G. lucidum* | C30 | j, k | [583, 591, 592] |
| 23-Hydroxy-ganoderic acid S | *G. lucidum* | C30 | k | [592] |
| Ganoderic acid T | *G. lucidum* | C30 | f3 | [593, 594] |
| Ganoderic acid X | *G. amboinense* | C30 | f4 | [595] |
| Ganoderic acid Y | *G. lucidum* | C30 | l1 | [596] |
| Ganoderic acid β | *G. lucidum* | C30 | l2 | [597] |
| Ganoderic acids γ, δ, ε, ζ, η, θ | *G. lucidum* | C30 | f5 | [598] |
| Ganodermic acids T-Q | *G. lucidum* | C30 | l3 | [599] |
| Ganodermanondiol (**691**) | *G. lucidum* | C30 | m, n1 | [600–602] |
| Ganodermanontriol (**692**) | *G. lucidum* | C30 | n2, f | [600, 603–607] |
| Ganodermatetraol | *G. sinense* | C30 | o | [608] |
| Ganoderenic acid A (**693**) | *G. lucidum* | C30 | e, p1 | [609–611] |
| Ganoderic aldehyde A | *G. lucidum* | C30 | f | [612, 613] |
| Ganoderic aldehyde TR | *G. lucidum* | C30 | k | [592] |
| Ganolucidic acid A | *G. lucidum* | C30 | l2 | [597, 614] |
| Ganolucidic acids B, C | *G. lucidum* | C30 | o | [608, 614, 615] |
| Lucidenic acid A (**694**) (Lucidenated A) | *G. lucidum* | C27 | l3 | [599, 616] |

(continued)

**Table 45** (continued)

| Compound | Origin | Type | Biological activity | Refs. |
|---|---|---|---|---|
| Lucidenic acid B | *G. lucidum* | C27 | f6 | [616, 617] |
| Lucidenic acid C | *G. lucidum* | C27 | l3 | [616] |
| Lucidenic acid D2, E2, F | *G. lucidum* | C27 | l3 | [599] |
| 20-Hydroxylucidenic acid N | *G. lucidum* | C27 | f | [618] |
| Lucidenic acid O and lactone | *G. lucidum* | C27 | q, l4 | [619] |
| Ganoderiol A | *G. lucidum* | C30 | r | [620, 621] |
| Ganoderiol F | *G. lucidum* | C30 | f8, l, k | [622–624] |
| Ganoderol B | *G. lucidum* | C30 | p2, s | [625, 626] |
| Lucidimol B | *G. lucidum* | C30 | f | [627] |
| Ganoderal A (**695**) | *G. lucidum* | C30 | g | [583] |
| Butyl ganoderates A, B | *G. lucidum* | C30 | t | [628] |
| Butyl lucidenates A, N | *G. lucidum* | C27 | t | [628] |
| 3-Oxo-5$\alpha$-lanosta-8,24-dien-21-oic acid | *G. tsugae* | C30 | u | [629] |
| 15,16-Dihydroxy-lanosta-7,9(11),24-trien-3-one | *G. lucidum* | C30 | l1 | [596] |
| Ganoboninketals A–C (**696**, **697**) | *G. boninense* | 3,4-*seco*-27-Norlanostane | k | [630] |
| Cochlates A–C (**698**) | *G. cochlear* | 3,4-*seco*-C27 | v | [631, 632] |
| Fornicatins A, D, F | *G. cochlear* | 3,4-*seco*-C30 | v | [631] |
| 3$\alpha$,12$\beta$,15$\alpha$-Triacetoxy-5$\alpha$-lanosta-7,9(11),24-trien-26-oic acid | *G. lucidum* | C30 | f7 | [633] |
| Ganocochlearic acid A (**699**) | *G. cochlear* | Hexanorlanstane | y | [632] |
| Ganoleucoins A–P (**700**) | *G. leucocontextum* | C30 | w, p2 | [634] |
| (22*Z*,24*Z*)-13-Hydroxy-3-oxo-14(13→12)*abeo*-lanosta-8,22,24-trien-26,23-olide (**701**) | *G. lucidum* | 14(13→12)*abeo*-Lanostane | y | [635] |
| (24*E*)-3$\beta$,15$\alpha$-Diacetoxy-7$\alpha$-hydroxylanosta-8,24-dien-26-oic acid (**702**) | *G.* sp. BCC 16642 | C30 | x | [636] |
| 3$\beta$,15$\alpha$-Diacetoxylanosta-8,24-dien-26-oic acid | *G.* sp. BCC 16642 | C30 | x | [636, 637] |

| | | | | |
|---|---|---|---|---|
| (22*S*,24*E*)-3$\beta$,15$\alpha$,22-Triacetoxylanosta-7,9 (11),24-trien-26-oic acid | *G.* sp. BCC 16642 | C30 | x | [636] |
| Leucocontextins A–X (**703**) | *G. leucocontextum* | C30 | y | [638, 639] |
| Colossolactones A–G (**704**, **705**, **706**) | *G. colossum* | C30 | u, f | [640, 641] |
| Colossolactones I–VIII | *G. colossum* | C30 | l | [642, 643] |
| Ganodermalactones A–G (**708**, **709**) | *G.* sp. | C30 | k | [641] |
| Ganodermadiol | *G. pfeifferi* | C30 | l5 | [644] |
| Ganoderone A | *G. pfeifferi* | C30 | l5 | [645] |
| Lucialdehyde B | *G. pfeifferi* | C30 | l5 | [645] |

Biological activities: a: antinoceptive effect; b: farnesyl protein transferase inhibition; c: histamine release inhibition; d: TNF-$\alpha$ production reducing activity; e: human aldose reductase inhibition; f: antitumor; f1: cytotoxicity against HeLa human cervical carcinoma cells; f2: human colon carcinoma cell apoptosis-inducing activity; f3: tumor invasion inhibition; f4: inhibition on topoisomerase of cancer cells; f5: cytotoxicity against Meth-A and LLC tumor cells; f6: human-leukemia cell apoptosis-inducing activity; f7: cytotoxicity against PC-3 cells; f8: induction of senescence in hepatoma HepG2 cells; g: anti-ACE (angiotensin converting enzyme); h: immune function-increasing activity; i: multidrug resistance inhibition; j: cell cycle of tumor cell-arresting; k: antiplasmodial/antimalarial; l: anti-HIV activity; l1: antiviral against EV71; l2: HIV-1 protease inhibition; l3: inhibitory for EBV-EA induction by TPA; l4: inhibition on HIV reverse transcriptase; l5: antiviral activity against herpes simplex virus; m: melanogenesis inhibition; n1: protection on *t*-butyl hydroperoxide-induced hepatotoxicity; n2: hepatoprotective; o: induction of hPXR-mediated CYP3A4 expression; p1: $\beta$-glucuronidase-inhibitory activity; p2: $\alpha$-glucosidase inhibitory activity; q: eukaryotic DNA polymerase inhibition; r: suppression on migration and adhesion of MDA-MB231 cell; s: anti-androgenic activity; t: antiobesity; u: anti-inflammatory; v: inhibitory on increase of ALT and AST level in HepG2 cells treated by $H_2O_2$; w: inhibition on HMG-CoA reductase; x: antitubercular activity; y: no (obvious) activity

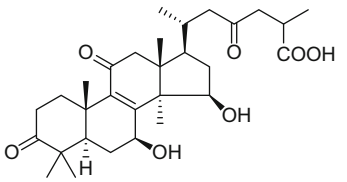


**688** (ganoderic acid A)

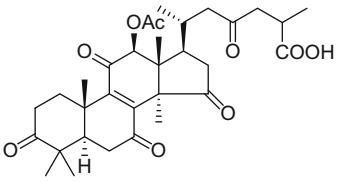


**689** (ganoderic acid F)

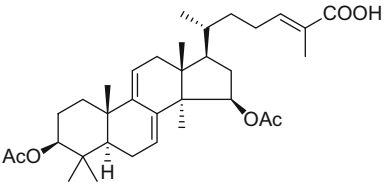


**690** (ganoderic acid Me)

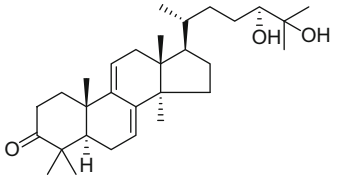


**691** (ganodermanondiol)

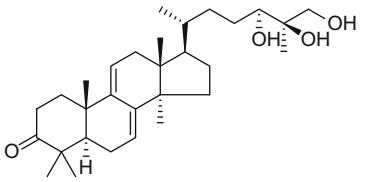


**692** (ganodermanontriol)

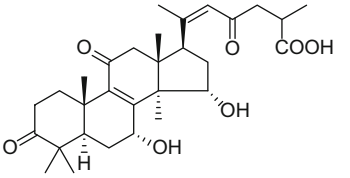


**693** (ganoderenic acid A)

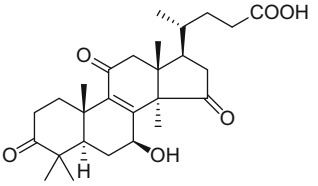


**694** (lucidenic acid A)

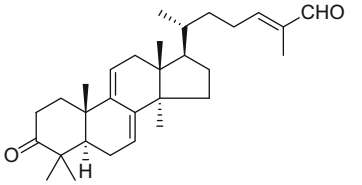


**695** (ganoderal A)

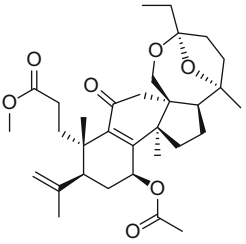


**696** (ganoboninketal A)

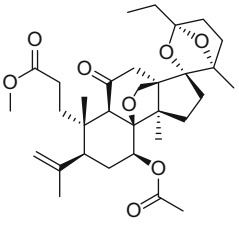


**697** (ganoboninketal C)

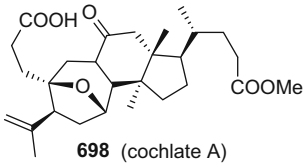


**698** (cochlate A)

**Fig. 71** Selected structures of *Ganoderma* lanostanes

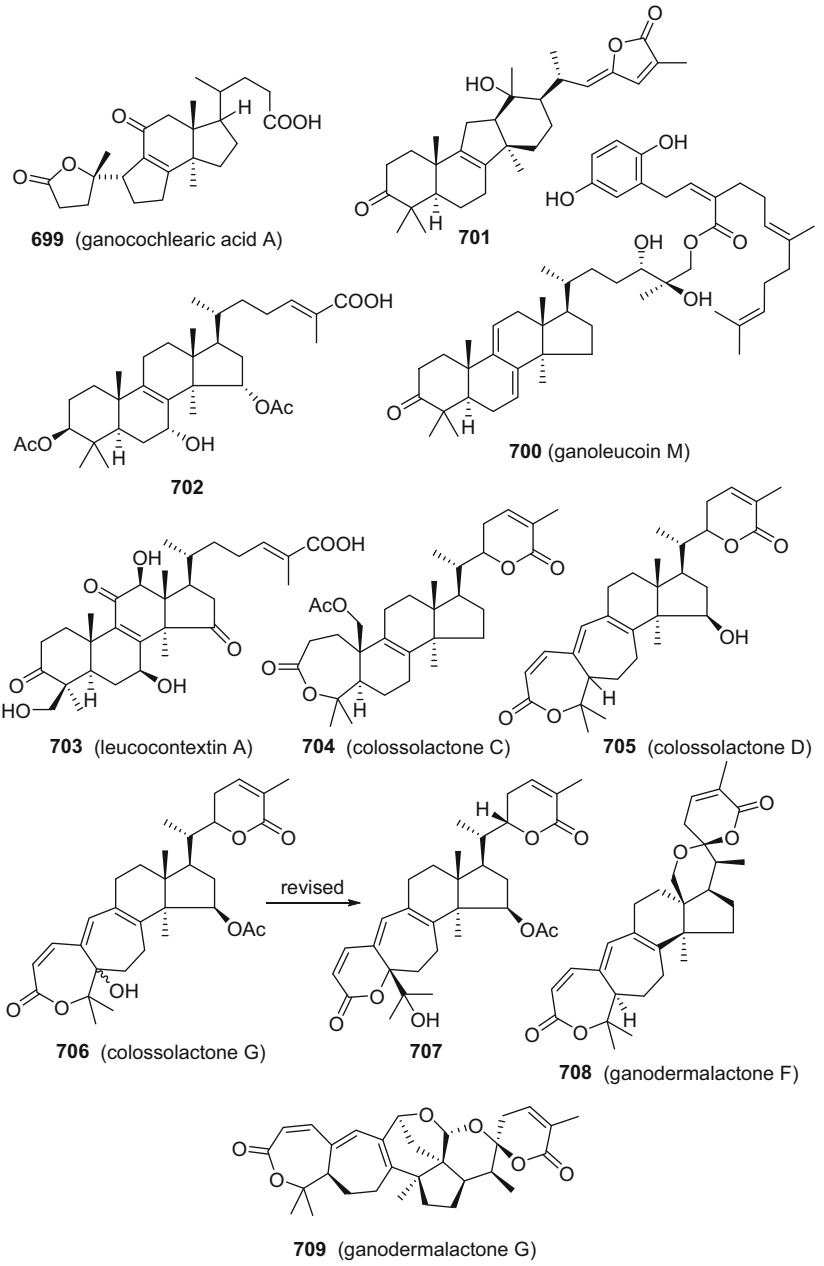


**Fig. 71** (continued)

group and proved to be more active than 23-hydroxyganoderic acid S, which contains a carboxylic acid group. The $IC_{50}$ values of ganoderic aldehyde TR, ganoderic acid S, and 23-hydroxyganoderic acid S were 6, 11, 11 μ*M*, respectively, while the co-occurring compound ganoderic acid DM showed no antiplasmodial activity in vitro at 20 μ*M*. In contrast to its biologically active structural analogs, ganoderic acid DM lacks a 7,9(11)-diene moiety, which is regarded as an essential functional group for their conferment of antiplasmodial activity [592]. This same conclusion could also be drawn from the anti-HIV-1 efffects of ganoderic acid B and ganoderiol B, and the antitubercular effect of 3$\beta$,15$\alpha$,22$\beta$-triacetoxy-lanosta7,9 (11),24-trien-26-oic acid (Fig. 71) [646, 647]. Both ganoderic acid B and ganoderiol B, are more active against HIV-1 protease than triterpenoids that are devoid of a $\Delta^{7,9(11)}$ substructure [646].

Ganoboninketals A–C (**696–697**), isolated from *G. boninense*, are three nortriterpenes with a rearranged 3,4-*seco*-norlanostane skeleton (Fig. 71). All showed antiplasmodial activity against *Plasmodium falciparum*, with $IC_{50}$ values of 4.0, 7.9, and 1.7 μ*M*, respectively [630].

A series of lanostanes varying in the presence of acetoxy groups was isolated from *Ganoderma* sp. BCC 16642. Most displayed growth inhibitory activities against *Mycobacterium tuberculosis* H37Ra, with the *MIC* value of the most active compound being 0.781 μg/cm$^3$. Structure-activity relationships of these lanostanes were proposed, which suggested that a 3$\beta$-OAc group is crucial for antitubercular activity. Moreover, lanostanes containing a 7,9(11)-diene motif showed higher antitubercular activity than their 8-ene congeners [636].

The lanostane skeletons of *Ganoderma* species tend to undergo carbon bond cleavage and rearrangement, and the C-3–C-4 bond may be cleaved to form a 3,4-*seco*-lanostane skeleton. Other rearrangements of the lanostanes lead to the 14 (13→12)*abeo*-lanostane and 9(10→19)*abeo*-lanostane skeletons [635, 640, 641]. The side chains of lanostane skeletons readily form lactone groups or spiroketal lactone groups, and then result in the formation of more complex polycyclic triterpenoids. Colossolactones and ganodermalactones are unusual tritepenoids isolated from the mushrooms *G. colossum* and *Ganoderma* spp., respectively, and feature an α,β-unsaturaed-δ-lactone group and have structural similarities to those of triterpenoid lactones isolated from the medicinal plant genera *Schisandra* and *Kadsura* (Fig. 71) [648–651].

### 4.3.2 *Antrodia cinnamomea* Ergostanes and Lanostanes

The medicinal fungus *Antrodia cinnamomea* (synonyms *A. camphorata*, *Taiwanofungus camphorata*, and *Ganoderma camphoratum*) is a rare and valuable fungus indigenous to Taiwan. The Chinese name of this fungus is "Chang-Kun" or "Niu-Chang-Chih". This fungus has been used traditionally as an antidote as well as anticancer and anticnesmatic agent. The first study of the chemical constituents of this fungus was conducted in 1995, and, after this, more and more attention has been paid to the constituents of *A. cinnamomea* and their biological evaluation. Tzeng et al. have

**Table 46** Ergostanes and lanostanes from *A. cinnamomea*

| Compound | Origin | Type | Refs. |
|---|---|---|---|
| Zhankuic acid C (**710**) | *T. camphoratus* | Ergostane | [653, 654] |
| Zhankuic acids D, E | *A. cinnamomea* | Ergostane | [655] |
| 15$\alpha$-Acetyl-dehydrosulphurenic acid | *A. cinnamomea* | Lanostane | [655] |
| Eburicoic acid (**712**) | *A. camphorata* | Lanostane | [656] |
| Dehydroeburicoic acid (**713**) | *A. cinnamomea* | Lanostane | [655, 657–661] |
| Dehydrosulphurenic acid | *A. cinnamomea* | Lanostane | [655] |
| Antcinate A | *A. camphorata* | Ergostane | [662] |
| (25*R*/*S*)-Antcin C | *A. cinnamomea* | Ergostane | [663] |
| Methyl antcinate A | *A. camphorata* | Ergostane | [664, 665] |
| Methyl antcinate B | *A. camphorata* | Ergostane | [122, 666] |
| Methyl antcinate K | *A. salmonea* | Ergostane | [667] |
| Methyl antcinate L | *A. salmonea* | Ergostane | [667] |
| Antcin K (**711**) | *A. cinnamomea* | Ergostane | [668, 669] |
| Antcin M | *A. salmonea* | Ergostane | [667] |
| Camphoratins A–J | *T. camphoratus* | Ergostane | [123, 670] |
| 3,7,11-Trioxo-5$\alpha$-lanosta-8,24(*E*)-dien-26-oic acid | *A. camphorata* | Lanostane | [671] |
| Methyl 11$\alpha$-3,7-dioxo-5$\alpha$-lanosta-8,24(*E*)-dien-26-oate | *A. camphorata* | Lanostane | [671] |
| Methyl 3,7,11,12,15,23-hexaoxo-5$\alpha$-lanost-8-en26-oate | *A. camphorata* | Lanostane | [671] |
| Ethyl 3,7,11,12,15,23-hexaoxo-5$\alpha$-lanost8-en-26-oate | *A. camphorata* | Lanostane | [671] |
| Ethyl lucidenate A | *A. camphorata* | Lanostane | [672] |
| Ethyl lucidenate F | *A. camphorata* | Lanostane | [672] |
| 15-*O*-Acetylganolucidate A | *A. camphorata* | Lanostane | [672] |
| 3,11,15,23-Tetraoxo-27$\xi$-lanosta-8,16-dien-26-oic acid | *A. camphorata* | Lanostane | [672] |

published a systematic review of the bioactive compounds and the pharmacological effects of *A. camphorata* [652]. However, this review did not include all triterpenoids that were reported before 2009. Therefore, such compounds will be included in the present chapter, which also covers the triterpenoids from *A. camphorata* as well as their biological activities reported from 2009 to 2016 (Table 46).

The triterpenoids found in the fruiting bodies, submerged cultures, and wood or solid-state culturess of *A. camphorata* are only representative of the ergostane and lanostane types. Due to the high structural and stereochemical similarities of the ergostanes isolated from *A. camphorata*, which has made their purification process difficult, most have been obtained as (25*R*/*S*) epimeric mixtures. Several new approaches were applied to successfully separate the (25*R*/*S*) ergostanes, for example, by employing supercritical-fluid chromatography [673]. Interestingly, using a MTT assay it was shown that (25*S*)-antcin C exhibited cytotoxicity against Hep G2

and MCF-7 cells with $IC_{50}$ values of 14.5 and 12.8 μg/cm$^3$, while (25*R*)-antcin C did not show significant cytotoxic effects [663].

Many of the isolated triterpenoids from *A. camphorata* have been reported to display potential antitumor and anti-inflammatory activities [670, 672, 674]. Methyl antcinate L, antcin M, and methyl antcinate K inhibited NO production with $IC_{50}$ values around 1.7–16.5 μ*M* [667]. Zhankuic acid C (**710**) exhibited an immunosuppressive effect on dendritic cell activation and the contact hypersensitivity response. This suggested that this compound may be a promising agent for use in treating chronic inflammation and autoimmune diseases (Fig. 72) [654]. Antcin K (**711**) is the most abundant ergostane tritepenoid from the fruiting bodies of basswood-cultivated *A. cinnamomea* (Fig. 72). Biological studies showed that compound **711** can reduce the protein expression of integrins $\beta$1, $\beta$3, $\alpha$5, and $\alpha$v and suppress phosphorylation of FAK, Src, PI3K, AKT, MEK, ERK, and JNK, so as to inhibit the adhesion, migration, and invasion of Hep 3B human hepatoma cells. Moreover, antcin K can induce mitochondrial and endoplasmic reticulum stress-mediated apoptosis in this same type of cells. These results suggested that antcin K could be used as an adjuvant in liver cancer therapy [668, 669].

Further studies have revealed that other lanostane-related triterpenoids, C-24 methyl lanostane (which was also named eburicane), eburicoic acid (**712**) and dehydroeburicoic acid (**712**) isolated from this medicinal fungus, display several biological activities (Fig. 72). Eburicoic acid and dehydroeburicoic acid inhibited acetic acid-induced writhing responses and formalin-induced pain in the late phase in mice. They also displayed potential anti-inflammatory activity and thus might decrease inflammatory cytokines and increase antioxidant enzyme activity [658]. Dehydroeburicoic acid (**712**) induced G2/M phase arrest in a dose-dependent

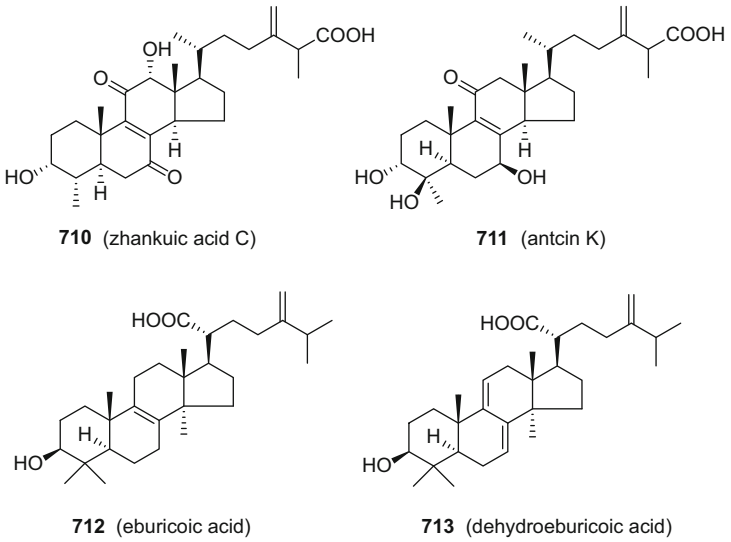


**Fig. 72** Selected structures of ergostane and lanostane triterpenoids from *Antrodia cinnamomea*

manner in HL 60 cells. In xenograft animal model work, it was revealed that dehydroeburicoic acid reduced tumor weight and size [659, 661]. Further studies have shown that **712** also displayed antidiabetic and antihyperlipidemic-related activities [660].

### 4.3.3 *Poria cocos* Lanostanes

*Poria cocos* is a saprophytic fungus that parasitizes the roots of many *Pinus* species. The sclerotia of *P. cocos* have been used as a traditional Chinese medicine for their diuretic, sedative, and tonic effects. Pharmacological investigations have revealed that *P. cocos*-derived polysaccharides are related to observed immune-stimulating effects, while the lanostane triterpenoids are responsible for anti-inflammatory and cytotoxic activities evident in laboratory studies. Lanostanes as well as eburicanes originating from *P. cocos* were fully reviewed in previous accounts [574, 675]. Herein are covered the triterpenoids isolated from *P. cocos* between the years 2012 and 2016 as well as the newly reported biological activities of several triterpenoids (Table 47).

Pachymic acid (**714**) is one of the predominant and most well-studied eburicane triterpenoids isolated from *P. cocos* (Fig. 73). Previous investigations have shown that pachymic acid can stimulate glucose uptake through enhanced GLUT4 expression and translocation [679], inhibit cell growth, modulate arachidonic acid metabolism in A549 non-small cell lung cancer cells [680], and damage breast cancer cell

**Table 47** Selected compounds from *P. cocos*

| Compound | Origin | Type | Refs. |
|---|---|---|---|
| 3-*epi*-Benzoyloxy-dehydrotumulosic acid | *Poria cocos* | Eubricane | [676] |
| 3-*epi*-(3′-*O*-Methylmalonyloxy)-dehydrotumulosic acid | *Poria cocos* | Eubricane | [676] |
| 3-*epi*-(3′-Hydroxy-3′-methylglutaryloxyl)-dehydrotumulosic acid | *Poria cocos* | Eubricane | [676] |
| 16$\alpha$-Hydroxy-3-oxo-24-methyllanosta-5,7,9(11),24(31)-tetraen-21-oic acid (**715**) | *Poria cocos* | Eubricane | [677] |
| 3$\beta$,16$\alpha$,29-Trihydroxy-24-methyllanosta-7,9(11),24(31)-trien-21-oic acid | *Poria cocos* | Eubricane | [677] |
| 3$\beta$,16$\alpha$,30-Trihydroxy-24-methyllanosta-7,9(11),24(31)-trien-21-oic acid | *Poria cocos* | Eubricane | [677] |
| 3$\beta$-Acetoxy-16$\alpha$,24$\beta$-dihydroxylanosta-7,9(11),25-trien-21-oic acid | *Poria cocos* | Lanostane | [677] |
| 3$\beta$,16$\alpha$-Dihydroxy-7-oxo-24-methyllanosta-8,24(31)-dien-21-oic acid | *Poria cocos* | Eubricane | [677] |
| 3$\alpha$,16$\alpha$-Dihydroxy-7-oxo-24-methyllanosta-8,24(31)-dien-21-oic acid | *Poria cocos* | Eubricane | [677] |
| 3-(2-Hydroxyacetoxy)-5$\alpha$,8$\alpha$-peroxydehydrotumulosic acid (**716**) | *Poria cocos* | Eubricane | [678] |

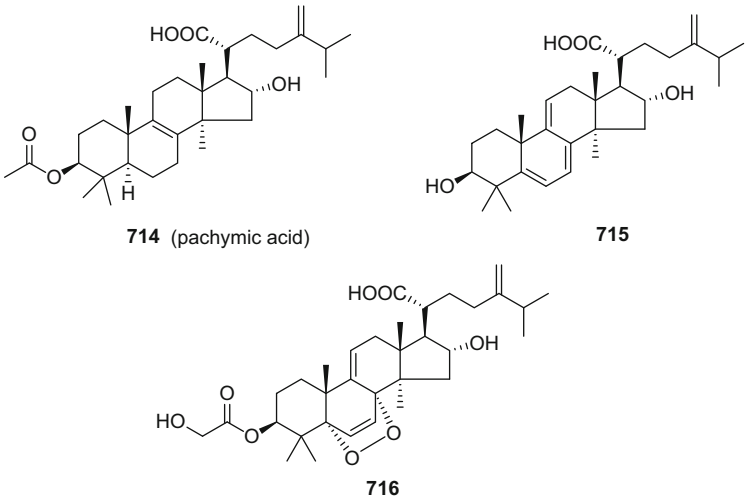


**Fig. 73** Selected structures of eburicanes from *P. cocos*

invasion by suppressing nuclear factor-κB-dependent matrix metalloproteinase-9 expression [681]. Moreover, pachymic acid remains a molecule of interest with potential for treating many other diseases.

In the course of a pharmacological investigation of compound **714**, oral administration in mice prolonged sleeping time and suppressed locomotion activity, suggestive of sedative-hypnotic effects. Moreover, **714** increased protein level expression of $GAD_{65/67}$ over a broad dose range, and increased $\alpha$- and $\beta$-subunit protein levels, but decreased $\gamma$-subunit protein levels in $GABA_A$ receptors. This experimental work suggested that pachymic acid has potential for the treatment of insomnia [682].

Other bioassays on pachymic acid have focused mainly on its potential antitumor activity. Chen et al. reported that **714** significantly reduced cell growth in a dose- and time-dependent manner, arrested the $G_0$ phase of the cell cycle in gallbladder cells, and affected the AKT and ERK signaling pathways [683]. Moreover, **714** exerted antitumor-related activity in other in vitro and in vivo bioassays [684–687].

### 4.3.4 Lanostanes from Other Mushrooms

Lanostanes are widely distributed secondary metabolites of additional mushrooms, and the majority are found in their fruiting bodies (Tables 48, 49, and 50). Due to the shortages of their organisms of origin and the consequent difficulty in obtaining sufficient quantities of fruiting bodies, only a small number of these mushrooms have been investigated chemically and reported to produce triterpenoids.

**Table 48** Lanostane triterpenoids reported from other mushrooms (1)

| Compound | Origin | Type | Biological activity | Refs. |
|---|---|---|---|---|
| Astrapteridone | *A. pteridis* | Lanostane | | [688] |
| Astrapteridiol | *A. pteridis* | Lanostane | | [688] |
| 3-*epi*-Astrapteridiol (**717**) | *A. pteridis* | Lanostane | a | [688] |
| Astraodoric acids A–D | *A. odoratus* | Lanostane | a, b | [689] |
| Astraeusins A–L | *A. odoratus* | Lanostane | | [690] |
| Astrakurkurol | *A. hygrometricus* | Lanostane | c1 | [691] |
| Astrakurkurone (**718**) | *A. hygrometricus* | Lanostane | c1, d | [691, 692] |
| Astrasiaone | *A. asiaticus* | Lanostane | | [693] |
| Astrasiate | *A. asiaticus* | Lanostane | b | [693] |
| Carboxyacetylquercinic acid | *D. quercina* | Lanostane | | [694] |
| Polyporenic acid C | *D. dickinsii* | Lanostane | e | [695] |
| Compound 2 | *D. dickinsii* | Lanostane | | [695] |
| 31-Hydroxycarboxyacetylquercinic acid (**719**) | *D. dickinsii* | Lanostane | c | [696] |
| Daedaleanic acid A (**720**) | *D. dickinsii* | 19(10→5)*abeo*-4,5-*seco*-Lanostane | | [697] |
| Daedaleanic acids B, C | *D. dickinsii* | Lanostane | | [697] |
| Daedaleaside A (**721**) | *D. dickinsii* | 19(10→5)*abeo*-4,5-*seco*-Lanostane | | [697] |
| Daedaleasides B–E | *D. dickinsii* | Lanostane | b | [697] |
| Daedalols A–C | *Daedalea* sp. | Lanostane | f | [698] |
| Fomitellic acid A–D | *Fomitella fraxinea* | Lanostane | g | [699, 700] |
| Fomlactones A–C | *Fomes cajanderi* | Lanostane | | [701] |
| Fomitopsins A–C (**722**) | *Fomitopsis spraguei* | Lanostane | | [702] |
| Fomitopinic acids A, B | *Fomitopsis pinicola* | Lanostane | | [703] |
| Fomitosides A–J (**723**) | *Fomitopsis pinicola* | Lanostane glycoside | h | [703] |
| Fomitoside K (**724**) | *Fomitopsis nigra* | Lanostane glycoside | b | [704, 705] |
| 3$\alpha$-(3′-Butylcarboxyacetoxy)-oxepanoquercinic acid C | *Fomitopsis rosea* | Lanostane | c2 | [706] |

(continued)

**Table 48** (continued)

| Compound | Origin | Type | Biological activity | Refs. |
|---|---|---|---|---|
| 3$\alpha$-Hydroxy-24-methylene-23-oxolanost-8-en-26-carboxylic acid | *Fomitopsis rosea* | Lanostane | c2 | [706] |
| Fomiroid A | *Fomitopsis nigra* | Lanostane | i | [707] |
| Fomefficinin | *Fomes officinalis* | Lanostane | b | [708] |
| Officimalonic acid A (**725**) | *Fomes officinalis* | 7(8→9)*abeo*-Lanostane | | [709] |
| Officimalonic acids B–H | *Fomes officinalis* | Lanostane | b,j | [709] |

Biological activities: a: antituberculosis; b: cytotoxicity; c: antimicrobial; c1: antifungal; c2: antibacterial; d: leishmanicidal; e: collagenase inhibition; f: aspartic protease BACE1 inhibition; g: DNA polymerase inhibition; h: COX-2 inhibition; i: Cholesterol uptake inhibition; j: NO production inhibition

**Table 49** Lanostane triterpenoids reported from other mushrooms (2)

| Compound | Origin | Type | Refs. |
|---|---|---|---|
| (3′*S*)-3*β*-Acetyl-2*α*-(3′-hydroxy-3′-methyl)glutarylcrustulinol (HS-A) | *Hebeloma crustuliniforme* | Lanostane | [710, 711] |
| HS-A (**726**), B, C | *H. spoliatum* | Lanostane | [711] |
| Hebelomic acids A–F, H–I (**727**) | *H. senescens* | Lanostane | [712–714] |
| 24(*E*)-3*β*-Hydroxylanosta-8,24-dien-26-al-21-oic acid | *H. versipelle* | Lanostane | [715] |
| Inonotsuoxides A, B | *I. obliquus* | Lanostane | [716] |
| Inotodiol (**728**) | *I. obliquus* | Lanostane | [717] |
| Inonotsutriols A–C (**729**) | *I. obliquus* | Lanostane | [718] |
| (3*β*,22*R*,23*E*)-Lanosta-8,23-diene-3,22,25-triol | *I. obliquus* | Lanostane | [719] |
| (3*β*,22*R*,23*E*)-Lanosta-7,9(11),23-triene-3,22,25-triol | *I. obliquus* | Lanostane | [719] |
| Inoterpenes A-F | *I. obliquus* | Lanostane | [720] |
| Spiroinonotsuoxodiol (**731**) | *I. obliquus* | 7(8→9)*abeo*-Lanostane | [721] |
| Inonotusols A–G (**730**) | *I. obliquus* | Lanostane | [722] |
| Inotolactones A (**732**), B (**733**) | *I. obliquus* | Lanostane | [332] |
| Inonotusanes A, B | *I. obliquus* | Lanostane | [723] |
| Inonotusane C | *I. obliquus* | 3-Norlanostane | [723] |

**Table 50** Lanostane triterpenoids reported from other mushrooms (3)

| Compound | Origin | Type | Refs. |
|---|---|---|---|
| Fasciculols A–F (**734**), H–M | *Neamatoloma fasciculare* | Lanostane | [724–727] |
| Fasciculic acids A–C (**735**) | *Neamatoloma fasciculare* | Lanostane | [728, 729] |
| Clavaric acid | *Clavariadelphus truncates* | Lanostane | [730] |
| Elfvingic acids A–H (**739**) | *Elfvingia applanata* | Lanostane | [731] |
| Tyromycin A | *Tyromyces lacteus* | Lanostane | [732] |
| Thyromycic acids B–G (**737**) | *Tyromyces fissilis* | Lanostane | [733, 734] |
| Blazeispirol A (**736**) | *Agaricus blazei* | Nor-lanostane | [735] |
| Hexatenuins A–C (**738**) | *Hexagonia tenuis* | Lanostane | [736] |
| Hexagonins A–E | *Hexagonia apiaria* | Lanostane | [737] |
| Gloeophyllins A–J | *Gloeophyllum abietinum* | Lanostane | [738] |
| Phellibarins A–C (**740**) | *Phellinus rhabarbarinus* | Lanostane | [739] |
| Saponaceols A–C (**741**) | *Tricholoma saponaceum* | Lanostane | [740] |

Fruiting bodies from the genus *Astraeus* have a star-like structure and are thus sometimes called earth-star fungi. Most mushrooms belonging to this genus are edible. A bioassay-guided fractionation of an EtOH extract of the mushroom *A. pteridis* led to the isolation of three lanostane triterpenoids with intramolecular hemiacetal groups, astrapteridone, astrapteridiol, and 3-*epi*-astrapteridiol (**717**) (Fig. 74) [688]. The absolute configuration of astrapteridone was established by

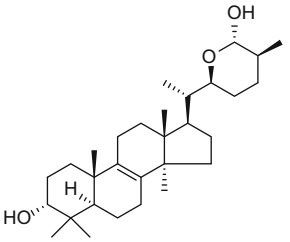

**717** (3-*epi*-astrapteridiol)

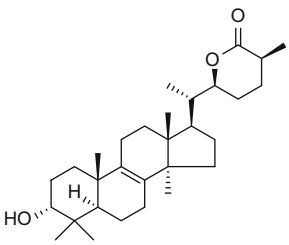

**718** (astrakurkurone)

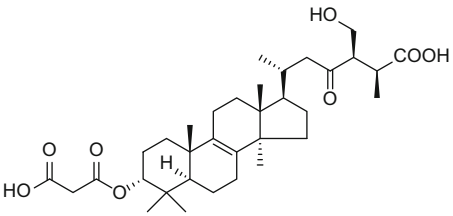

**719** (31-hydroxycarboxyacetylquercinic acid)

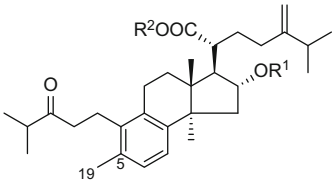

**720** (daedaleanic acid A) $R^1$ = H, $R^2$ = H
**721** (daedaleaside A) $R^1$ = Ac, $R^2$ = Glc

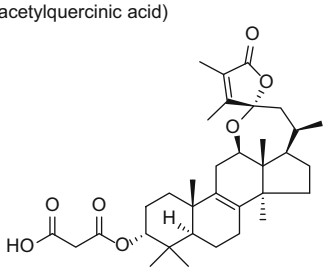

**722** (fomitopsin B)

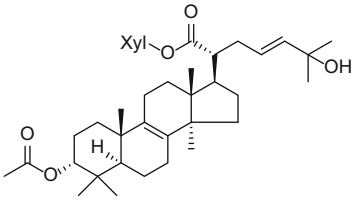

**723** (fomitoside E)

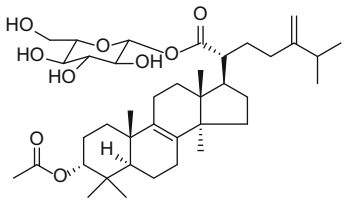

**724** (fomitoside K)

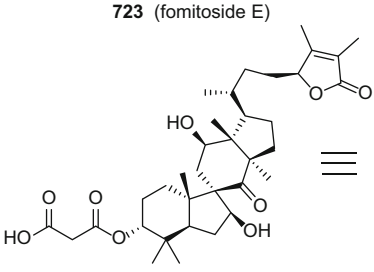

**725** (officimalonic acid A)

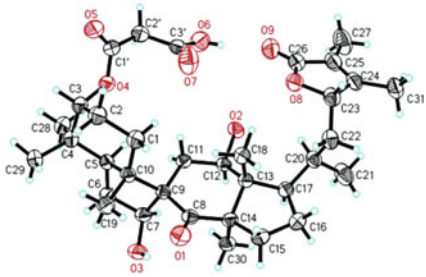

**Fig. 74** Structures of lanostane triterpenoids isolated from other mushrooms (1)

single-crystal X-ray diffraction analysis. All compounds were evaluated for antituberculosis activity against *M. tuberculosis*. 3-*epi*-Astrapteridiol showed moderate activity with a *MIC* value of 34.0 μg/cm$^3$. From the popular Thai edible mushroom *A. odoratus*, five lanostane triterpenes, astraodorol and astraodoric acids A–D, were obtained. Astrodoric acids A and B exhibited antituberculosis activities in vitro with respective *MIC* values of 50 and 25 μg/cm$^3$, and exhibited cytotoxic effects against the KB and NCI-H187 cell lines [689]. The predominant compound, astraodorol, was used as a template to synthesize ten derivatives, which showed promising antimalarial activities [741]. Astrakurkurol and astrakurkurone (**718**) are two crystalline triterpenes reported from the Indian edible mushroom *A. hygrometricus* (Fig. 74). Both showed inhibition of the growth of *Candida albicans*, and were comparable in potency to the standard antifungal antibiotics used. Additionally, **718** also inhibited the growth of *Leishmania donovani* promastigotes [691].

The fungus *Daedalea dickinsii* is a wood-decaying fungus that is distributed widely in East Asia. This organism produces lanostane triterpenes with particular structural modifications, such as esterification by malonic acid at C-3 and glucosidation at the C-21 carboxylic acid group. 31-Hydroxycarboxyacetylquercinic acid (**719**) was isolated from the fruiting bodies of *D. dickinsii*. It showed antimicrobial activities against human pathogenic fungi and bacteria [696]. Daedaleanic acid A (**720**) and daedaleaside A (**721**) display a rare rearrangement of the lanostane skeleton, 19(10→5)*abeo*-4,5-*seco*-lanostane, of which ring A is cleaved between C-4 and C-5, and ring B is aromatic (Fig. 74). Other triterpenes obtained this study showed induction activity on internucleosomal DNA fragmentation characteristic of apoptotic cell death in the HL-60 cell line [697].

The genus *Fomitopsis* belongs to the family Polyporaeae and has proven to be a good source of triterpenes. Many such species were investigated phytochemically, including *F. nigra*, *F. pinicola*, *F. rosea*, and *F. spragei*. For example, fomitopsin B (**722**) is a triterpenoid with an intramolecular spiro-acetal group isolated from the fruiting bodies of *F. spraguei* (Fig. 74) [702]. In the course of a chemical study of the wood-decaying fungus *F. pinicola*, two lanostane triterpenoids and ten lanostane triterpenoid glycosides were obtained from the fruiting bodies. Fomitopinic acid A, and fomitosides E (**723**) and F displayed inhibition of the COX-2 enzyme with $IC_{50}$ values in the range 0.15–1.15 μ*M*, with the positive control being indomethacin ($IC_{50}$ 0.60 μ*M*) [703]. Fomitoside K (**724**) is a bioactive lanostane triterpenoid glycoside isolated from the fruiting bodies of *F. nigra*. Fomitoside K induced apoptosis in YD-10B cells through the ROS-dependent mitochondrial dysfunction pathway [704, 705].

Officimalonic acid A (**725**), isolated from the ethnomedicinal fungus *F. officinalis*, is an unusual triterpenoid with a 7(8→9)*abeo*-lanostane skeleton. Its absolute configuration was established by X-ray diffraction analysis (Fig. 74) [709].

Lanostane triterpenoids from the genus *Hebeloma* were proven to be toxic metabolites (Table 49). The three triterpenoids HS-A (**726**), B, and C were isolated from the Japanese mushroom *H. spoliatum* (Fig. 75). They showed a papaverine-

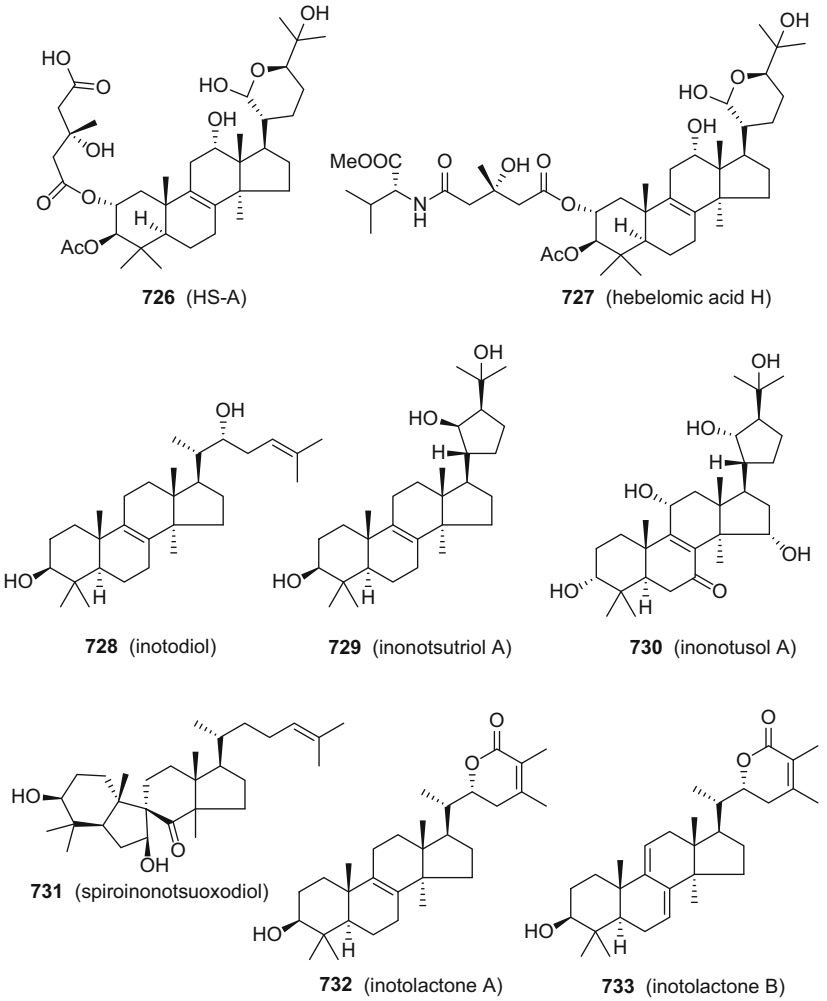


**Fig. 75** Structures of lanostane triterpenoids isolated from other mushrooms (2)

like relaxation effect in mice. Intraperitoneal administration of HS-A, B, and C caused death after paralysis of the limbs in mice at a dose 100 mg/kg [711]. Several hebelomic acids were isolated also from this genus. Interestingly, most of these isolated triterpenoids contain a 3-hydroxy-3-methylglutaric acid (HMG) acyl moiety, of which the absolute configuration was established by chemical methods [714]. Moreover, hebelomic acids H (**727**) and I from the fruiting bodies of *H. senescens* are two triterpene depsipeptides containing valine and isoleucine units. The absolute configurations of the HMG residue and amino acids were determined by chemical methods [713].

The fungus *Inonotus obliquus* is called "Kabanoanatake" in Japan, and "Chaga" in Russia. This fungus has been used as a Russian folk medicine for treating cancer since at least the sixteenth century. Investigation of the secondary metabolites of *I. obliquus* has been a topic of extensive interest for some time. The major group of metabolites, which are lanostane triterpenoids, turned out to be bioactive constituents of *I. obliquus* (Table 49). Inotodiol (**728**) is a C-3,C-22-dihydroxy substituted lanostane triterpene and it is also the most abundant triterpene isolated from the fruiting bodies of *I. obliquus* (Fig. 75). Inotodiol displayed potent anti-tumor-promoting activity in an in vivo model, and mechanistically it induces DNA fragmentation and increases caspase-3/7 activity [716, 717]. Notably, lanostane triterpenoids with a five-membered ring between C-20 and C-24 located in the side chain have been found only from this fungus, namely, inonotsutriols A–C (**729**) [718], inoterpene F [720], and inonotusols A–G (**730**) [722]. Spiroinonotsuoxodiol (**731**) represents the first compound with a 7(8→9)*abeo*-lanostane skeleton isolated from the higher fungi (Fig. 75). Other reports describing this kind of skeleton refer to species in the plant genus *Abies* [742–744]. Spiroinonotsuoxodiol was evaluated for cytotoxicity against the P388, L1210, HL-60, and KB cell lines, demonstrating respective $IC_{50}$ values of 29.5, 12.5, 30.1, 21.2 μ*M* [721]. Inotolactones A (**732**) and B (**733**) are α,β-unsaturated δ-lactone-bearing lanostane-type triterpenoids isolated from a submerged culture of *I. obliquus*. They exhibited more potent $\alpha$-glucosidase inhibitory activities than the positive control acarbose, attesting to the potential antihyperglycemic properties of this fungus (Fig. 75) [332].

Lanostane triterpenoids were also found in other mushrooms, such as the genera *Clavariadelphus*, *Elfvingia*, *Gloeophyllum*, *Hexagonia*, *Neamatoloma*, *Phellinus*, and *Tyromyces* (Table 50). The triterpenoids from the bitter mushroom *N. fasciculare* were reported to exhibit plant growth inhibition [724], and are toxic to humans, and inhibit calmodulin. Fasciculols E (**734**) and F have been shown to cause paralysis and death in mice, with $LD_{50}$ values of 50 mg/kg and 168 mg/kg, respectively (Fig. 76) [727]. Fasciculic acids A–C (**735**) and F are calmodulin antagonists [726, 729]. Clavaric acid isolated from the fungus *Clavariadelphus truncatus* is an inhibitor of human farnesyl-protein transferase (FPT) [745].

Blazeispirol A (**736**) is a hexanor-lanostane isolated from the fermentation of the mushroom *Agaricus blazei* (Fig. 76). A biological study showed that blazeispirol A induces cell death in Hep 3B human hepatoma cells through caspase-dependent and caspase-independent pathways, suggesting its potential for cancer chemopreventive and chemotherapeutic use [735]. The genus *Hexagonia* accumulates lanostane triterpenoids with a spiro-lactone group in the side chain, forming some rigid lanostanes. Hexatenuins A–C and hexagonins A–E showed anti-inflammatory and antitrypanosomal activities [736, 737].

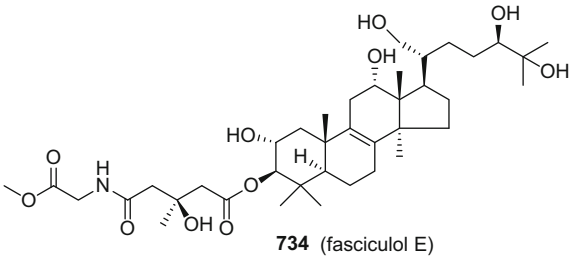

**734** (fasciculol E)

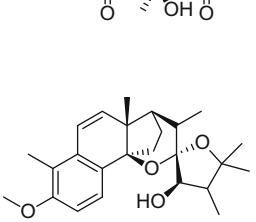

**736** (blazeispirol A)

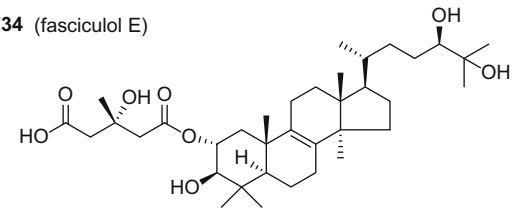

**735** (fasciculic acid A)

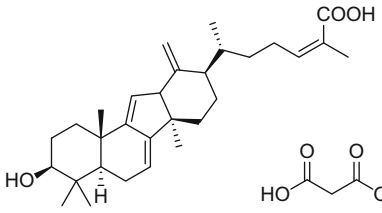

**737** (tyromycic acid E)

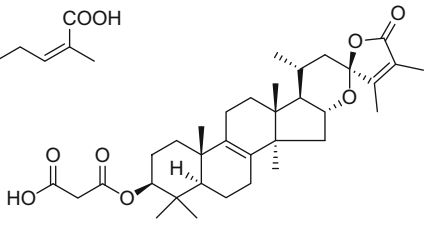

**738** (hexatenuin A)

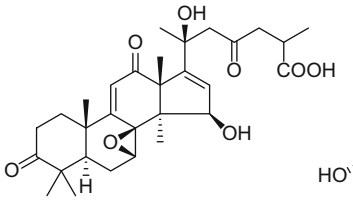

**739** (elfvingic acid D)

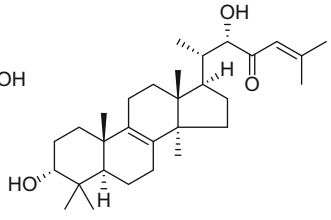

**740** (phellibarin A)

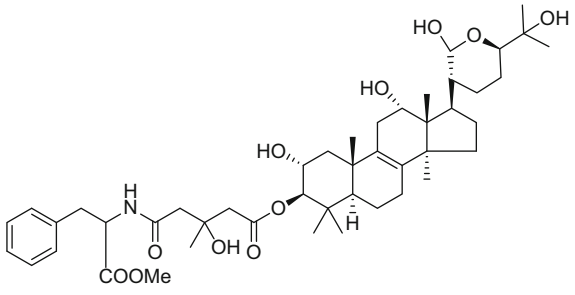

**741** (saponaceol A)

**Fig. 76** Structures of lanostane triterpenoids isolated from other mushrooms (3)

### 4.3.5 Cucurbitanes

Cucurbitane triterpenoids are a group of usually bitter-tasting constituents produced mainly by members of the plant families Cucurbitaceae [746], Cruciferae, and Primulaceae. However, this type of triterpenoid has been found also in mushrooms, specifically the two species *Hebeloma vinosophyllum* and *Leucopaxillus gentianeus* and the genus *Russula* (Table 51).

Twelve cucurbitane triterpenoids, hebevinosides I–XII (**742**) were isolated from the mushroom *H. vinosophyllum* (Fig. 77). These cucurbitanes were purified as toxic principles of this mushroom [747–749]. A bitter component of the mushroom *L. gentianeus* is cucurbitacin B, which has been investigated extensively biologically as a common higher plant constituent.

The genus *Russula* affords lactarane-type sesquiterpenoids, which have been mentioned previously. Many cucurbitane triterpenoids were also found in this genus (Table 51).

**Table 51** Cucurbitane triterpenoids

| Compound | Origin | Type | Refs. |
|---|---|---|---|
| Hebevinosides I–XIV (**742**) | *Hebeloma vinosophyllum* | Cucurbitane | [747–749] |
| Cucurbitacin B | *Leucopaxillus gentianeus* | Cucurbitane | [750] |
| Leucopaxillones A (**743**), B (**744**) | *Leucopaxillus gentianeus* | Cucurbitane | [750] |
| Cucurbitacin D | *Leucopaxillus gentianeus* | Cucurbitane | [751] |
| 16-Deoxycucurbitacin B | *Leucopaxillus gentianeus* | Cucurbitane | [751] |
| Rosacea acids A, B | *Russula rosacea* | Cucurbitane | [752] |
| Lepida acid A (**745**) | *Russula lepida* | Cucurbitane | [753] |
| (24*E*)-3$\beta$-Hydroxycucurbita-5,24-diene-26-oic acid | *Russula lepida* | Cucurbitane | [754] |
| (24*E*)-3,4-*seco*-Cucurbita-4,24-diene-3,26-dioic acid (**746**) | *Russula lepida* | 3,4-*seco*-Cucurbitane | [754] |
| (24*E*)-3,4-*seco*-Cucurbita-4,24-diene-3,26,29-trioic acid (**747**) | *Russula lepida* | 3,4-*seco*-Cucurbitane | [754] |
| Lepidolide (**748**) | *Russula lepida* | Cucurbitane | [755] |
| (24*E*)-3,4-*seco*-Cucurbita-4,24-diene-3-hydroxy-26,29-dioic acid | *Russula lepida* | Cucurbitane | [222] |
| Roseic acid (**749**) | *Russula aurora*/ *Russula minutula* | Cucurbitane | [756] |
| Roseolactones A, B | *Russula aurora*/ *Russula minutula* | Cucurbitane | [756] |

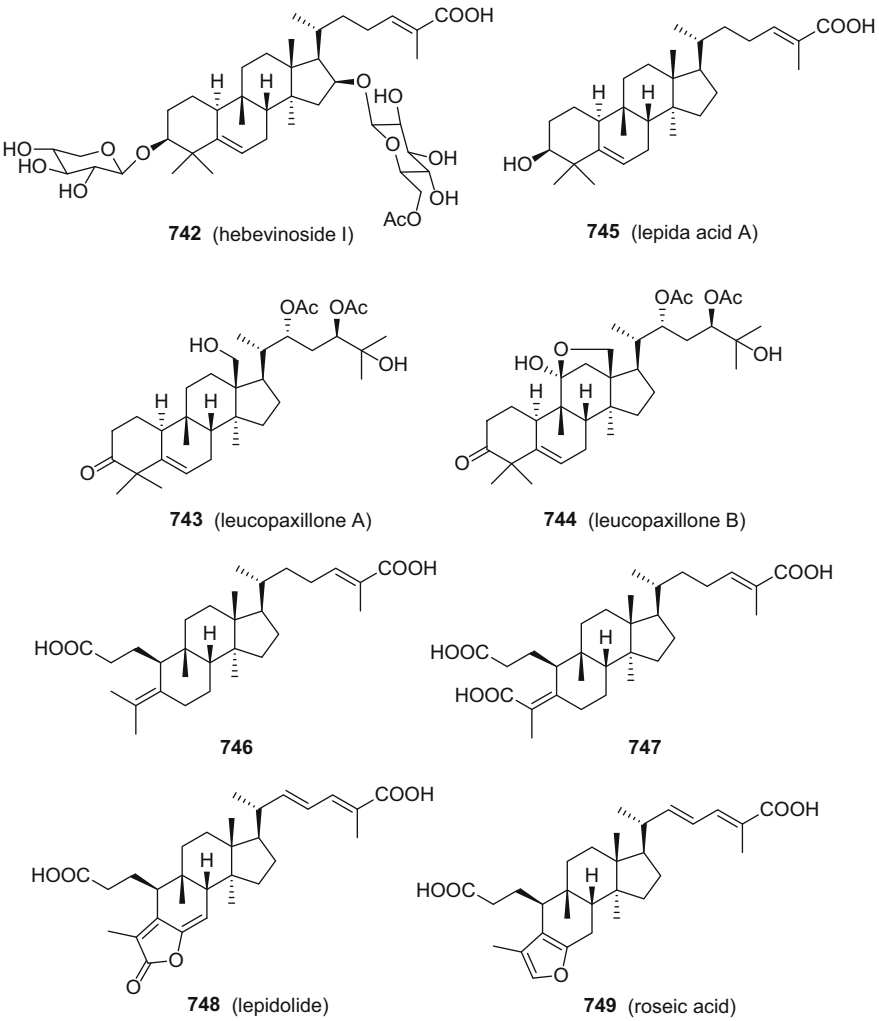


**Fig. 77** Selected structures of cucurbitane derivatives

### 4.3.6 Saponaceolides

Saponaceolides are a group of triterpenoids isolated from the genus *Tricholoma*, with there having been 25 examples reported so far. The spiro and bridged structural features of saponaceolides are vulnerable to rearrangement, which has led to the formation of terreolides A–F (Table 52, Fig. 78) [760].

Repeated ingestion of the wild mushroom *T. equestre* caused rhabdomyolysis in France [762]. The mushroom *T. terreum* is a co-occurring species of *T. equestre* in southwestern France (Fig. 79). The crude extracts ($CHCl_3$-MeOH, 1:1) of these two mushrooms were found to be toxic to mice, while only the non-polar fraction (ethyl

**Table 52** Saponaceolides from mushroom *T. saponaceum*, and *T. terreum*

| Compound | Origin | Type | Refs. |
|---|---|---|---|
| Saponaceolides A–G | *Tricholoma saponaceum* | Saponaceolides | [757–759] |
| Terreolides A–F (**753**, **754**) | *Tricholoma terreum* | Saponaceolides | [760] |
| Saponaceolides H–L, N–S | *Tricholoma terreum* | Saponaceolides | [760, 761] |
| Saponaceolides B (**751**), M (**752**) ☠ | *Tricholoma terreum* | Saponaceolides | [760] |

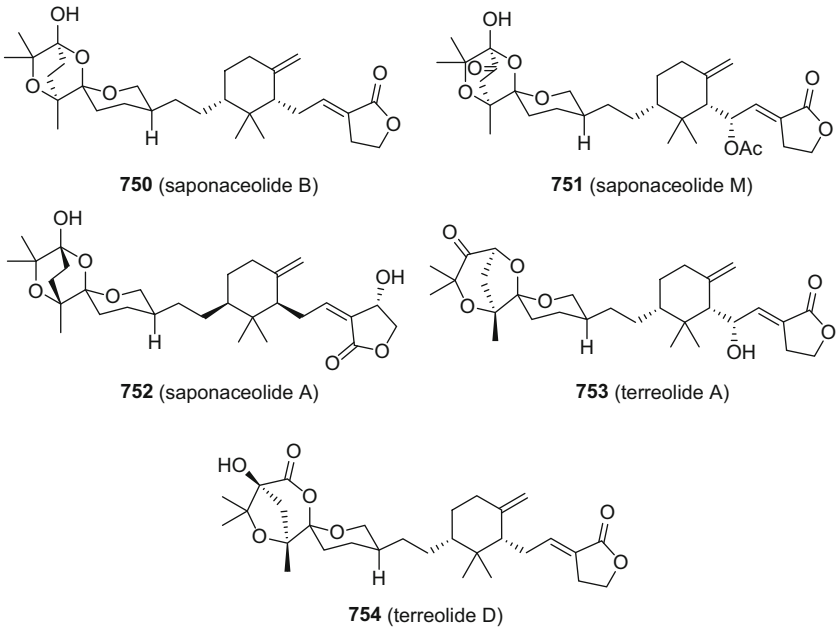


**Fig. 78** Structures of saponaceolides A (**752**), B (**750**), M (**751**), and terreolides A (**753**) and D (**754**)

**Fig. 79** The mushroom *Tricholoma terreum*

acetate layer) was toxic when the extract of *T. terreum* was partitioned between water and ethyl acetate. Further chemical investigation of the secondary metabolites of *T. terreum* led to the isolation of 15 triterpenoids, namely, terreolides A–F and saponaceolides H–P. Acute toxicity and the serum creatine kinase (CK) assays in mice treated with these compounds revealed that saponaceolides B (**751**) and M (**752**) were toxic principles, with $LD_{50}$ values of 88.3 and 63.7 mg/kg. They caused a 1.52- to 1.65-fold increase in serum CK levels relative to mice that received either water or 1% Tween-80 alone. This investigation documented a hitherto unknown poisonous European mushroom, *T. terreum* [760].

## 5 Conclusions

The first systematic investigations of secondary metabolites from higher fungi originated after the discovery and introduction of penicillin into clinical practice. From 1940 until the early 1950s mycelial cultures or fruiting bodies of more than 2000 higher fungi were screened for the production of antibiotics [763]. These investigations resulted in the discovery of pleuromutilin (**642**), the lead compound for the semisynthetic tiamulin (**643**) used in veterinary practice and recently also in humans [764]. It is also of significance that a synthetic analog of illudin S (**485**), (–)-irofulven (**486**), has entered clinical trials and demonstrated activity against ovarian, gastrointestinal, and non-small cell lung forms of cancer. As compared to the natural product, **486** has a much better therapeutic index and pharmacological profile [765].

As can be deduced from the numerous new structures described recently and documented in this chapter, interest in the secondary metabolism of higher fungi has gained momentum. The biological activities are interesting and may help to define new lead compounds offering structures not easily detected by the random screening of compound assemblies derived from combinatorial chemical synthesis procedures. The availability of secondary metabolites from higher fungi is facilitated by progress made in fermentation technologies and genetics, opening up access to novel templates for chemical syntheses and providing new chemical approaches to probe as yet unexplored biological targets [763]. The higher fungi should continue to attract the interest of natural products chemists and other investigators well into the future as a source not only of potential drugs, but also of toxins, hallucinogens, and pigments.

## References

1. Wasser SP (2011) Current findings, future trends, and unsolved problems in studies of medicinal mushrooms. Appl Microbiol Biotechnol 89:1323
2. Hawksworth DL (2001) Mushrooms: the extent of the unexplored potential. Int J Med Mushrooms 3:5

3. Mueller GM, Schmit JP (2007) Fungal biodiversity: what do we know? What can we predict? Biodivers Conserv 16:1
4. Kirk PM, Cannon PF, Minter DW, Stalpers JA (2008) Ainsworth and Bisby's Dictionary of the Fungi, 10th edn. CABI International, Wallingford, CT, USA
5. Gill M (1994) Pigments of fungi (macromycetes). Nat Prod Rep 11:67
6. Gill M (1996) Pigments of fungi (macromycetes). Nat Prod Rep 13:513
7. Gill M (1999) Pigments of fungi (macromycetes). Nat Prod Rep 16:301
8. Gill M (2003) Pigments of fungi (macromycetes). Nat Prod Rep 20:615
9. Gill M, Steglich W (1987) Pigments of fungi (macromycetes). Prog Chem Org Nat Prod 51:1
10. Zhou ZY, Liu JK (2010) Pigments of fungi (macromycetes). Nat Prod Rep 27:1531
11. Liu JK (2006) Natural terphenyls: developments since 1877. Chem Rev 106:2209
12. Fang ST, Zhang L, Li ZH, Li B, Liu JK (2010) Cyathane diterpenoids and nitrogenous terphenyl derivative from the fruiting bodies of basidiomycete *Phellodon niger*. Chem Pharm Bull 58:1176
13. Ma K, Han JJ, Bao L, Wei TZ, Liu HW (2014) Two sarcoviolins with antioxidative and $\alpha$-glucosidase inhibitory activity from the edible mushroom *Sarcodon leucopus* collected in Tibet. J Nat Prod 77:942
14. Kaneko A, Tsukada M, Fukai M, Suzuki T, Nishio K, Miki K, Kinoshita K, Takahashi K, Koyama K (2010) KDR kinase inhibitor isolated from the mushroom *Boletopsis leucomelas*. J Nat Prod 73:1002
15. Wang SM, Han JJ, Ma K, Jin T, Bao L, Pei YF, Liu HW (2014) New $\alpha$-glucosidase inhibitors with *p*-terphenyl skeleton from the mushroom *Hydnellum concrescens*. Fitoterapia 98:149
16. Masubuti H, Endo Y, Araya H, Uekusa H, Fujimoto Y (2013) Establishment of benzodioxazine core structure for sarcodonin class of natural products by X-ray analysis. Org Lett 15:2076
17. Wossa SW, Beekman AM, Ma P, Kevo O, Barrow RA (2013) Identification of boletopsin 11 and 12, antibiotics from the traditionally used fungus *Boletopsis* sp. Asian J Org Chem 2:565
18. Beekman AM, Wossa SW, Kevo O, Ma P, Barrow RA (2015) Discovery and synthesis of boletopsins 13 and 14, brominated fungal metabolites of terrestrial origin. J Nat Prod 78:2133
19. Norikura T, Fujiwara K, Narita T, Yamaguchi S, Morinaga Y, Iwai K, Matsue H (2011) Anticancer activities of thelephantin O and vialinin A isolated from *Thelephora aurantiotincta*. J Agric Food Chem 59:6974
20. Ye YQ, Negishi C, Hongo Y, Koshino H, Onose J, Abe N, Takahashi S (2014) Structural elucidation and synthesis of vialinin C, a new inhibitor of TNF-$\alpha$ production. Bioorg Med Chem 22:2442
21. Liu R, Wang YN, Xie BJ, Pan Q (2015) A new *p*-terphenyl derivative from the mushroom *Thelephora vialis*. Helv Chim Acta 98:1075
22. Nagasawa I, Kaneko A, Suzuki T, Nishio K, Kinoshita K, Shiro M, Koyama K (2014) Potential anti-angiogenesis effects of *p*-terphenyl compounds from *Polyozellus multiplex*. J Nat Prod 77:963
23. Kuhnert E, Surup F, Herrmann J, Huch V, Muller R, Stadler M (2015) Rickenyls A-E, antioxidative terphenyls from the fungus *Hypoxylon rickii* (Xylariaceae, Ascomycota). Phytochemistry 118:68
24. Fujiwara K, Sato T, Sano Y, Norikura T, Katoono R, Suzuki T, Matsue H (2012) Total synthesis of thelephantin O, vialinin A/terrestrin A, and terrestrins B–D. J Org Chem 77:5161
25. Takahashi S, Yoshida A, Uesugi S, Hongo Y, Kimura K, Matsuoka K, Koshino H (2014) Structural revision of kynapcin-12 by total synthesis, and inhibitory activities against prolyl oligopeptidase and cancer cells. Bioorg Med Chem Lett 24:3373
26. Fujiwara K, Kushibe K, Sato T, Norikura T, Matsue H, Iwai K, Katoono R, Suzuki T (2015) Synthesis of ganbajunins D and E and the proposed structure of thelephantin D. Eur J Org Chem:5798
27. Lin DW, Masuda T, Biskup MB, Nelson JD, Baran PS (2011) Synthesis-guided structure revision of the sarcodonin, sarcoviolin, and hydnellin natural product family. J Org Chem 76:1013

28. Usui I, Lin DW, Masuda T, Baran PS (2013) Convergent synthesis and structural confirmation of phellodonin and sarcodonin ε. Org Lett 15:2080
29. Fukuda T, Nagai K, Tomoda H (2012) (±)-Tylopilusins, diphenolic metabolites from the fruiting bodies of *Tylopilus eximius*. J Nat Prod 75:2228
30. Fukuda T, Tomoda H (2013) Tylopilusin C, a new diphenolic compound from the fruiting bodies of *Tylopilus eximinus*. J Antibiot 66:355
31. Gruber G, Kerschensteiner L, Steglich W (2014) Chromapedic acid, pulvinic acids and acetophenone derivatives from the mushroom *Leccinum chromapes* (Boletales). Z Naturforsch B 69:432
32. Zan LF, Qin JC, Zhang YM, Yao YH, Bao HY, Li X (2011) Antioxidant hispidin derivatives from medicinal mushroom *Inonotus hispidus*. Chem Pharm Bull 59:770
33. Kubo M, Liu YH, Ishida M, Harada K, Fukuyama Y (2014) A new spiroindene pigment from the medicinal fungus *Phellinus ribis*. Chem Pharm Bull 62:122
34. Han JJ, Bao L, He LW, Zhang XQ, Yang XL, Li SJ, Yao YJ, Liu HW (2013) Phaeolschidins A–E, five hispidin derivatives with antioxidant activity from the fruiting body of *Phaeolus schweinitzii* collected in the Tibetan plateau. J Nat Prod 76:1448
35. Liu DZ, Wang F, Liao TG, Tang JG, Steglich W, Zhu HJ, Liu JK (2006) Vibralactone: a lipase inhibitor with an unusual fused β-lactone produced by cultures of the basidiomycete *Boreostereum vibrans*. Org Lett 8:5749
36. Zhao PJ, Yang YL, LC D, Liu JK, Zeng Y (2013) Elucidating the biosynthetic pathway for vibralactone: a pancreatic lipase inhibitor with a fused bicyclic β-lactone. Angew Chem Int Ed 52:2298
37. Zeiler E, Braun N, Böttcher T, Kastenmüller A, Weinkauf S, Sieber SA (2011) Vibralactone as a tool to study the activity and structure of the ClpP1P2 complex from *Listeria monocytogenes*. Angew Chem Int Ed 50:11001
38. Aqueveque P, Cespedes CL, Becerra J, Davila M, Sterner O (2015) Bioactive compounds isolated from submerged fermentations of the Chilean fungus *Stereum rameale*. Z Naturforsch C 70:97
39. Schwenk D, Brandt P, Blanchette RA, Nett M, Hoffmeister D (2016) Unexpected metabolic versatility in a combined fungal fomannoxin/vibralactone biosynthesis. J Nat Prod 79:1407
40. Jiang MY, Wang F, Yang XL, Fang LZ, Dong ZJ, Zhu HJ, Liu JK (2008) Derivatives of vibralactone from cultures of the basidiomycete *Boreostereum vibrans*. Chem Pharm Bull 56:1286
41. Jiang MY, Zhang L, Dong ZJ, Yang ZL, Leng Y, Liu JK (2010) Vibralactones D-F from cultures of the basidiomycete *Boreostereum vibrans*. Chem Pharm Bull 58:113
42. Wang GQ, Wei K, Feng T, Li ZH, Zhang L, Wang QA, Liu JK (2012) Vibralactones G–J from cultures of the basidiomycete *Boreostereum vibrans*. J Asian Nat Prod Res 14:115
43. Wang GQ, Wei K, Zhang L, Li ZH, Wang QA, Liu JK (2014) Three new vibralactone-related compounds from cultures of basidiomycete *Boreostereum vibrans*. J Asian Nat Prod Res 16:447
44. Chen HP, Zhao ZZ, Yin RH, Yin X, Feng T, Li ZH, Wei K, Liu JK (2014) Six new vibralactone derivatives from cultures of the fungus *Boreostereum vibrans*. Nat Prod Bioprospect 4:271
45. Wang GQ, Wei K, Li ZH, Feng T, Ding JH, Wang QA, Liu JK (2013) Three new compounds from the cultures of basidiomycete *Boreostereum vibrans*. J Asian Nat Prod Res 15:950
46. Chen HP, Zhao ZZ, Li ZH, Dong ZJ, Wei K, Bai X, Zhang L, Wen CN, Feng T, Liu JK (2016) Novel natural oximes and oxime esters with a vibralactone backbone from the basidiomycete *Boreostereum vibrans*. Chemistry Open 5:142
47. Dubin GM, Fkyerat A, Tabacchi R (2000) Acetylenic aromatic compounds from *Stereum hirsutum*. Phytochemistry 53:571
48. Yun BS, Cho Y, Lee IK, Cho SM, Lee TH, Yoo ID (2002) Sterins A and B, new antioxidative compounds from *Stereum hirsutum*. J Antibiot 55:208
49. Yoo NH, Yoo ID, Kim JW, Yun BS, Ryoo IJ, Yoon ES, Chinh NT, Kim JP (2005) Sterin C, a new antioxidant from the mycelial culture of the mushroom *Stereum hirsutum*. Agric Chem Biotechnol 48:38

50. Saielli G, Bagno A (2009) Can two molecules have the same NMR spectrum? Hexacyclinol revisited. Org Lett 11:1409
51. Sekizawa R, Ikeno S, Nakamura H, Naganawa H, Matsui S, Iinuma H, Takeuchi T (2002) Panepophenanthrin, from a mushroom strain, a novel inhibitor of the ubiquitin-activating enzyme. J Nat Prod 65:1491
52. Yang YL, Zhou H, Du G, Feng KN, Feng T, Fu XL, Liu JK, Zeng Y (2016) A monooxygenase from *Boreostereum vibrans* catalyzes oxidative decarboxylation in a divergent vibralactone biosynthesis pathway. Angew Chem Int Ed 55:5463
53. Schlegel B, Hartl A, Dahse HM, Gollmick FA, Grafe U, Dorfelt H, Kappes B (2002) Hexacyclinol, a new antiproliferative metabolite of *Panus rudis* HKI 0254. J Antibiot 55:814
54. Rychnovsky SD (2006) Predicting NMR spectra by computational methods: structure revision of hexacyclinol. Org Lett 8:2895
55. Porco JA, Su S, Lei XG, Bardhan S, Rychnovsky SD (2006) Total synthesis and structure assignment of (+)-hexacyclinol. Angew Chem Int Ed 45:5790
56. Garlaschelli L, Magistrali E, Vidari G, Zuffardi O (1995) Tricholomenyn A and tricholomenyn B, novel antimitotic acetylenic cyclohexenone derivatives from the fruiting bodies of *Tricholoma acerbum*. Tetrahedron Lett 36:5633
57. Garlaschelli L, Vidari G, Vitafinzi P (1996) Tricholomenyns C, D, and E, novel dimeric dienyne geranyl cyclohexenones from the fruiting bodies of *Tricholoma acerbum*. Tetrahedron Lett 37:6223
58. Yin X, Feng T, Li ZH, Dong ZJ, Li Y, Liu JK (2013) Highly oxygenated meroterpenoids from fruiting bodies of the mushroom *Tricholoma terreum*. J Nat Prod 76:1365
59. Fujimoto H, Nakayama Y, Yamazaki M (1993) Identification of immunosuppressive components of a mushroom, *Lactarius flavidulus*. Chem Pharm Bull 41:654
60. Takahashi A, Kusano G, Ohta T, Nozoe S (1988) The constituents of *Lactarius flavidulus* IMAI. Chem Pharm Bull 36:2366
61. Takahashi A, Kusano G, Ohta T, Nozoe S (1993) Revised structures of flavidulols, constituents of *Lactarius flavidulus* IMAI, and the structure of flavidulol D. Chem Pharm Bull 41:2032
62. Arnone A, Cardillo R, Meille SV, Nasini G, Tolazzi M (1994) Isolation and structure elucidation of clavilactones A–C, new metabolites from the fungus *Clitocybe clavipes*. J Chem Soc Perkin Trans 1:2165
63. Cassinelli G, Lanzi C, Pensa T, Gambetta RA, Nasini G, Cuccuru G, Cassinis M, Pratesi G, Polizzi D, Tortoreto M, Zunino F (2000) Clavilactones, a novel class of tyrosine kinase inhibitors of fungal origin. Biochem Pharmacol 59:1539
64. Merlini L, Nasini G, Scaglioni L, Cassinelli G, Lanzi C (2000) Structure elucidation of clavilactone D: an inhibitor of protein tyrosine kinases. Phytochemistry 53:1039
65. Gao QL, Guo PX, Luo Q, Yan H, Cheng YX (2015) Petchienes A-E, meroterpenoids from *Ganoderma petchii*. Nat Prod Commun 10:2019
66. Luo Q, Wang XL, Di L, Yan YM, Lu Q, Yang XH, Hu DB, Cheng YX (2015) Isolation and identification of renoprotective substances from the mushroom *Ganoderma lucidum*. Tetrahedron 71:840
67. Yan YM, Wang XL, Luo Q, Jiang LP, Yang CP, Hou B, Zuo ZL, Chen YB, Cheng YX (2015) Metabolites from the mushroom *Ganoderma lingzhi* as stimulators of neural stem cell proliferation. Phytochemistry 114:155
68. Luo Q, Di L, Yang XH, Cheng YX (2016) Applanatumols A and B, meroterpenoids with unprecedented skeletons from *Ganoderma applanatum*. RSC Adv 6:45963
69. Yan YM, Ai J, Zhou LL, Chung ACK, Li R, Nie J, Fang P, Wang XL, Luo J, Hu Q, Hou FF, Cheng YX (2013) Lingzhiols, unprecedented rotary door-shaped meroterpenoids as potent and selective inhibitors of *p*-smad3 from *Ganoderma lucidum*. Org Lett 15:5488
70. Luo Q, Di L, Dai WF, Lu Q, Yan YM, Yang ZL, Li RT, Cheng YX (2015) Applanatumin A, a new dimeric meroterpenoid from *Ganoderma applanatum* that displays potent antifibrotic activity. Org Lett 17:1110

71. Li L, Li H, Peng XR, Hou B, Yu MY, Dong JR, Li XN, Zhou L, Yang J, Qiu MH (2016) (±)-Ganoapplanin, a pair of polycyclic meroterpenoid enantiomers from *Ganoderma applanatum*. Org Lett 18:6078
72. Luo Q, Tian L, Di L, Yan YM, Wei XY, Wang XF, Cheng YX (2015) (±)-Sinensilactam A, a pair of rare hybrid metabolites with smad3 phosphorylation inhibition from *Ganoderma sinensis*. Org Lett 17:1565
73. Dou M, Di L, Zhou LL, Yan YM, Wang XL, Zhou FJ, Yang ZL, Li RT, Hou FF, Cheng YX (2014) Cochlearols A and B, polycyclic meroterpenoids from the fungus *Ganoderma cochlear* that have renoprotective activities. Org Lett 16:6064
74. Zhou FJ, Nian Y, Yan YM, Gong Y, Luo Q, Zhang Y, Hou B, Zuo ZL, Wang SM, Jiang HH, Yang J, Cheng YX (2015) Two new classes of T-type calcium channel inhibitors with new chemical scaffolds from *Ganoderma cochlear*. Org Lett 17:3082
75. Frichert A, Jones PG, Lindel T (2016) Enantioselective total synthesis of terreumols A and C from the mushroom *Tricholoma terreum*. Angew Chem Int Ed 55:2916
76. Long R, Huang J, Shao WB, Liu S, Lan Y, Gong JX, Yang Z (2014) Asymmetric total synthesis of (–)-lingzhiol via a Rh-catalysed [3+2] cycloaddition. Nat Commun 5:5707
77. Chen D, Liu HM, Li MM, Yan YM, Xu WD, Li XN, Cheng YX, Qin HB (2015) Concise synthesis of (±)-lingzhiol via epoxy-arene cyclization. Chem Commun 51:14594
78. Chen D, Xu WD, Liu HM, Li MM, Yan YM, Li XN, Li Y, Cheng YX, Qin HB (2016) Enantioselective total synthesis of (+)-lingzhiol via tandem semipinacol rearrangement/Friedel-Crafts type cyclization. Chem Commun 52:8561
79. Gautam KS, Birman VB (2016) Biogenetically inspired synthesis of lingzhiol. Org Lett 18:1499
80. Cao WW, Luo Q, Cheng YX, Wang SM (2016) Meroterpenoid enantiomers from *Ganoderma sinensis*. Fitoterapia 110:110
81. Huang SZ, Cheng BH, Ma QY, Wang Q, Kong FD, Dai HF, Qiu SQ, Zheng PY, Liu ZQ, Zhao YX (2016) Anti-allergic prenylated hydroquinones and alkaloids from the fruiting body of *Ganoderma calidophilum*. RSC Adv 6:21139
82. Peng XR, Li L, Wang X, Zhu GL, Li ZR, Qiu MH (2016) Antioxidant farnesylated hydroquinones from *Ganoderma capense*. Fitoterapia 111:18
83. Dou M, Li RT, Cheng YX (2016) Minor compounds from fungus *Ganoderma cochlear*. Chin Herb Med 8:85
84. Chen HP, Zhao ZZ, Zhang Y, Bai X, Zhang L, Liu JK (2016) (+)- and (–)-Ganodilactone, a pair of meroterpenoid dimers with pancreatic lipase inhibitory activities from the macromycete *Ganoderma leucocontextum*. RSC Adv 6:64469
85. Peng XR, Liu JQ, Wan LS, Li XN, Yan YX, Qiu MH (2014) Four new polycyclic meroterpenoids from *Ganoderma cochlear*. Org Lett 16:5262
86. Fukai M, Tsukada M, Miki K, Suzuki T, Sugita T, Kinoshita K, Takahashi K, Shiro M, Koyama K (2012) Hypoxylonols C-F, benzo[*j*]fluoranthenes from *Hypoxylon truncatum*. J Nat Prod 75:22
87. Fukai M, Suzuki T, Nagasawa I, Kinoshita K, Takahashi K, Koyama K (2014) Antiangiogenic activity of hypoxylonol C. J Nat Prod 77:1065
88. Du L, King JB, Cichewicz RH (2014) Chlorinated polyketide obtained from a *Daldinia* sp. treated with the epigenetic modifier suberoylanilide hydroxamic acid. J Nat Prod 77:2454
89. Sudarman E, Kuhnert E, Hyde KD, Sir EB, Surup F, Stadler M (2016) Truncatones A-D, benzo[*j*]fluoranthenes from *Annulohypoxylon* species (Xylariaceae, Ascomycota). Tetrahedron 72:6450
90. La Clair JJ, Rheingold AL, Burkart MD (2011) Ganodone, a bioactive benzofuran from the fruiting bodies of *Ganoderma tsugae*. J Nat Prod 74:2045
91. Liu XT, Schwan WR, Volk TJ, Rott M, Liu MM, Huang P, Liu Z, Wang Y, Zitomer NC, Sleger C, Hartsel S, Monte A, Zhang LX (2012) Antibacterial spirobisnaphthalenes from the North American cup fungus *Urnula craterium*. J Nat Prod 75:1534

92. Feng T, Li ZH, Yin X, Dong ZJ, Wang GQ, Li XY, Li Y, Liu JK (2013) New benzene derivatives from cultures of ascomycete *Daldinia concentrica*. Nat Prod Bioprospect 3:150
93. Xian LPZ, Jing XNL, Meng DL, Sha Y (2006) A new perylenequinone from the fruit bodies of *Bulgaria inquinans*. J Asian Nat Prod Res 8:743
94. Kuhnert E, Surup F, Sir EB, Lambert C, Hyde KD, Hladki AI, Romero AI, Stadler M (2015) Lenormandins A–G, new azaphilones from *Hypoxylon lenormandii* and *Hypoxylon jaklitschii* sp. nov., recognised by chemotaxonomic data. Fungal Divers 71:165
95. Hu DB, Li WX, Zhao ZZ, Feng T, Yin RH, Li ZH, Liu JK, Zhu HJ (2014) Highly unsaturated pyranone derivatives from the basidiomycete *Junghuhnia nitida*. Tetrahedron Lett 55:6530
96. Endo Y, Minowa A, Kanamori R, Araya H (2012) A rare α-pyrone from bitter tooth mushroom, *Sarcodon scabrosus* (Fr.) Karst. Biochem Syst Ecol 44:286
97. Surup F, Mohr KI, Jansen R, Stadler M (2013) Cohaerins G–K, azaphilone pigments from *Annulohypoxylon cohaerens* and absolute stereochemistry of cohaerins C–K. Phytochemistry 95:252
98. Li N, Xu J, Li X, Zhang P (2013) Two new anthraquinone dimers from the fruit bodies of *Bulgaria inquinans*. Fitoterapia 84:85
99. Gao JM, Qin JC, Pescitelli G, Di PS, Ma YT, Zhang AL (2010) Structure and absolute configuration of toxic polyketide pigments from the fruiting bodies of the fungus *Cortinarius rufo-olivaceus*. Org Biomol Chem 8:3543
100. Beattie KD, Thompson DR, Tiralongo E, Ratkowsky D, May TW, Gill M (2011) Austrocolorone B and austrocolorin $B_1$, cytotoxic anthracenone dimers from the Tasmanian mushroom *Cortinarius vinosipes* Gasparini. Tetrahedron Lett 52:5448
101. Kawagishi H, Ando M, Mizuno T (1990) Hericenone A and hericenone B as cytotoxic principles from the mushroom *Hericium erinaceum*. Tetrahedron Lett 31:373
102. Kawagishi H, Ando M, Sakamoto H, Yoshida S, Ojima F, Ishiguro Y, Ukai N, Furukawa S (1991) Hericenone C, hericenone D and hericenone E, stimulators of nerve growth-factor (NGF)-synthesis, from the mushroom *Hericium erinaceum*. Tetrahedron Lett 32:4561
103. Kawagishi H, Ando M, Shinba K, Sakamoto H, Yoshida S, Ojima F, Ishiguro Y, Ukai N, Furukawa S (1993) Chromans, hericenone F, hericenone G, and hericenone H from the mushroom *Hericium erinaceum*. Phytochemistry 32:175
104. Ma BJ, Ma JC, Ruan Y (2012) Hericenone L, a new aromatic compound from the fruiting bodies of *Hericium erinaceum*s. Chin J Nat Med 10:363
105. Ueda K, Tsujimori M, Kodani S, Chiba A, Kubo M, Masuno K, Sekiya A, Nagai K, Kawagishi H (2008) An endoplasmic reticulum (ER) stress-suppressive compound and its analogues from the mushroom *Hericium erinaceum*. Bioorg Med Chem 16:9467
106. Li W, Zhou W, Kim EJ, Shim SH, Kang HK, Kim YH (2015) Isolation and identification of aromatic compounds in Lion's Mane mushroom and their anticancer activities. Food Chem 170:336
107. Yaoita Y, Danbara K, Kikuchi M (2005) Two new aromatic compounds from *Hericium erinaceum* (Bull.:Fr.) Pers. Chem Pharm Bull 53:1202
108. Ueda K, Kodani S, Kubo M, Masuno K, Sekiya A, Nagai K, Kawagishi H (2009) Endoplasmic reticulum (ER) stress-suppressive compounds from scrap cultivation beds of the mushroom *Hericium erinaceum*. Biosci Biotechnol Biochem 73:1908
109. Li W, Sun YN, Zhou W, Shim SH, Kim YH (2014) Erinacene D, a new aromatic compound from *Hericium erinaceum*. J Antibiot 67:727
110. Wittstein K, Rascher M, Rupcic Z, Löwen E, Winter B, Köster RW, Stadler M (2016) Corallocins A–C, nerve growth and brain-derived neurotrophic factor inducing metabolites from the mushroom *Hericium coralloides*. J Nat Prod 79:2264
111. Ye M, Luo XJ, Li LL, Shi Y, Tan M, Weng XX, Li W, Liu JK, Cao Y (2007) Grifolin, a potential antitumor natural product from the mushroom *Albatrellus confluens*, induces cell-cycle arrest in G1 phase via the ERK1/2 pathway. Cancer Lett 258:199
112. Yu XF, Deng QP, Li W, Xiao LB, Luo XJ, Liu XL, Yang LF, Peng SL, Ding ZH, Feng T, Zhou J, Fan J, Bode AM, Dong ZG, Liu JK, Cao Y (2015) Neoalbaconol induces cell death through necroptosis by regulating RIPK-dependent autocrine TNFα and ROS production. Oncotarget 6:1995

113. Liu LY, Li ZH, Ding ZH, Dong ZJ, Li GT, Li Y, Liu JK (2013) Meroterpenoid pigments from the basidiomycete *Albatrellus ovinus*. J Nat Prod 76:79
114. Liu LY, Li ZH, Wang GQ, Wei K, Dong ZJ, Feng T, Li GT, Li Y, Liu JK (2014) Nine new farnesylphenols from the basidiomycete *Albatrellus caeruleoporus*. Nat Prod Bioprospect 4:119
115. Koch B, Kilpert C, Steglich W (2010) Cristatomentin, a green pigment of mixed biogenetic origin from *Albatrellus cristatus* (Basidiomycetes). Eur J Org Chem:359
116. Chou KCC, Yang SH, Wu HL, Lin PY, Chang TL, Sheu F, Chen KH, Chiang BH (2017) Biosynthesis of antroquinonol and 4-acetylantroquinonol B via a polyketide pathway using orsellinic acid as a ring precursor in *Antrodia cinnamomea*. J Agric Food Chem 65:74
117. Lin HC, Lin MH, Liao JH, Wu TH, Lee TH, Mi FL, CH W, Chen KC, Cheng CH, Lin CW (2017) Antroquinonol, a ubiquinone derivative from the mushroom *Antrodia camphorata*, inhibits colon cancer stem cell-like properties: insights into the molecular mechanism and inhibitory targets. J Agric Food Chem 65:51
118. Sulake RS, Chen CP (2015) Total synthesis of (+)-antroquinonol and (+)-antroquinonol D. Org Lett 17:1138
119. Wang SC, Lee TH, Hsu CH, Chang YJ, Chang MS, Wang YC, Ho YS, Wen WC, Lin RK (2014) Antroquinonol D, isolated from *Antrodia camphorata*, with DNA demethylation and anticancer potential. J Agric Food Chem 62:5625
120. Lin YW, Pan JH, Liu RH, Kuo YH, Sheen LY, Chiang BH (2010) The 4-acetylantroquinonol B isolated from mycelium of *Antrodia cinnamomea* inhibits proliferation of hepatoma cells. J Sci Food Agric 90:1739
121. Chen JJ, Lin WJ, Liao CH, Shieh PC (2007) Anti-inflammatory benzenoids from *Antrodia camphorata*. J Nat Prod 70:989
122. Geethangili M, Fang SH, Lai CH, Rao YK, Lien HM, Tzeng YM (2010) Inhibitory effect of *Antrodia camphorata* constituents on the *Helicobacter pylori*-associated gastric inflammation. Food Chem 119:149
123. Shi LS, Chao CH, Shen DY, Chan HH, Chen CH, Liao YR, SJ W, Leu YL, Shen YC, Kuo YH, Lee EJ, Qian KD, Wu TS, Lee KH (2011) Biologically active constituents from the fruiting body of *Taiwanofungus camphoratus*. Bioorg Med Chem 19:677
124. Tu SH, Wu CH, Chen LC, Huang CS, Chang HW, Chang CH, Lien HM, Ho YS (2012) In vivo antitumor effects of 4,7-dimethoxy-5-methyl-1,3-benzodioxole isolated from the fruiting body of *Antrodia camphorata* through activation of the p53-mediated p27/kip1 signaling pathway. J Agric Food Chem 60:3612
125. Chen PY, Wu JD, Tang KY, CC Y, Kuo YH, Zhong WB, Lee CK (2013) Isolation and synthesis of a bioactive benzenoid derivative from the fruiting bodies of *Antrodia camphorata*. Molecules 18:7600
126. Chen YC, Chiu HL, Chao CY, Lin WH, Chao LK, Huang GJ, Kuo YH (2013) New anti-inflammatory aromatic components from *Antrodia camphorata*. Int J Mol Sci 14:4629
127. Wang BT, Qi QY, Ma K, Pei YF, Han JJ, Xu W, Li EW, Liu HW (2014) Depside $\alpha$-glucosidase inhibitors from a culture of the mushroom *Stereum hirsutum*. Planta Med 80:918
128. Ma K, Bao L, Han JJ, Jin T, Yang XL, Zhao F, Li SF, Song FH, Liu MM, Liu HW (2014) New benzoate derivatives and hirsutane type sesquiterpenoids with antimicrobial activity and cytotoxicity from the solid-state fermented rice by the medicinal mushroom *Stereum hirsutum*. Food Chem 143:239
129. Omolo JO, Anke H, Sterner O (2002) Hericenols A-D and a chromanone from submerged cultures of a *Stereum* species. Phytochemistry 60:431
130. Fan QY, Yin X, Li ZH, Li Y, Liu JK, Feng T, Zhao BH (2014) Mycophenolic acid derivatives from cultures of the mushroom *Laetiporus sulphureus*. Chin J Nat Med 12:685
131. Hirata Y, Nakanishi K (1950) Grifolin, an antibiotic from a basidiomycete. J Biol Chem 184:135
132. Ye M, Liu JK, Lu ZX, Zhao Y, Liu SF, Li LL, Tan M, Weng XX, Li W, Cao Y (2005) Grifolin, a potential antitumor natural product from the mushroom *Albatrellus confluens*, inhibits tumor cell growth by inducing apoptosis in vitro. FEBS Lett 579:3437

133. Luo XJ, Yang LF, Xiao LB, Xia XF, Dong X, Zhong JF, Liu Y, Li NM, Chen L, Li HD, Li W, Liu WB, Yu XF, Chen HY, Tang M, Weng XX, Yi W, Bode A, Dong ZG, Liu JK, Cao Y (2015) Grifolin directly targets ERK1/2 to epigenetically suppress cancer cell metastasis. Oncotarget 6:42704
134. Luo XJ, Li NM, Zhong JF, Tan ZQ, Liu Y, Dong X, Cheng C, Xu ZJ, Li HD, Yang LF, Tang M, Weng XX, Yi W, Liu JK, Cao Y (2016) Grifolin inhibits tumor cells adhesion and migration via suppressing interplay between PGC1α and Fra-1/LSF-MMP2/CD44 axes. Oncotarget 7:68708
135. Deng Q, Yu X, Xiao L, Hu Z, Luo X, Tao Y, Yang L, Liu X, Chen H, Ding Z, Feng T, Tang Y, Weng X, Gao J, Yi W, Bode AM, Dong Z, Liu J, Cao Y (2013) Neoalbaconol induces energy depletion and multiple cell death in cancer cells by targeting PDK1-PI3-K/Akt signaling pathway. Cell Death Dis 4:e804
136. Hsieh YH, Chu FH, Wang YS, Chien SC, Chang ST, Shaw JF, Chen CY, Hsiao WW, Kuo YH, Wang SY (2010) Antrocamphin A, an anti-inflammatory principle from the fruiting body of *Taiwanofungus camphoratus*, and its mechanisms. J Agric Food Chem 58:3153
137. Schwenk D, Nett M, Dahse HM, Horn U, Blanchette RA, Hoffmeister D (2014) Injury-induced biosynthesis of methyl-branched polyene pigments in a white-rotting basidiomycete. J Nat Prod 77:2658
138. Xu GH, Kim JW, Ryoo IJ, Choo SJ, Kim YH, Seok SJ, Ahn JS, Yoo ID (2010) Lactariolines A and B: New guaiane sesquiterpenes with a modulatory effect on interferon-γ production from the fruiting bodies of *Lactarius hatsudake*. J Antibiot 63:335
139. Surup F, Wiebach V, Kuhnert E, Stadler M (2016) Truncaquinones A and B, asterriquinones from *Annulohypoxylon truncatum*. Tetrahedron Lett 57:2183
140. Pulte A, Wagner S, Kogler H, Spiteller P (2016) Pelianthinarubins A and B, red pyrroloquinoline alkaloids from the fruiting bodies of the mushroom *Mycena pelianthina*. J Nat Prod 79:873
141. Geissler T, Brandt W, Porzel A, Schlenzig D, Kehlen A, Wessjohann L, Arnold N (2010) Acetylcholinesterase inhibitors from the toadstool *Cortinarius infractus*. Bioorg Med Chem 18:2173
142. Jaeger RJR, Lamshoft M, Gottfried S, Spiteller M, Spiteller P (2013) HR-MALDI-MS imaging assisted screening of β-carboline alkaloids discovered from *Mycena metata*. J Nat Prod 76:127
143. Jaeger RJR, Spiteller P (2010) Mycenaaurin A, an antibacterial polyene pigment from the fruiting bodies of *Mycena aurantiomarginata*. J Nat Prod 73:1350
144. Kuhnert E, Heitkamper S, Fournier J, Surup F, Stadler M (2014) Hypoxyvermelhotins A–C, new pigments from *Hypoxylon lechatii* sp. nov. Fungal Biol 118:242
145. Wang YQ, Bao L, Yang XL, Li L, Li SF, Gao H, Yao XS, Wen HA, Lie HW (2012) Bioactive sesquiterpenoids from the solid culture of the edible mushroom *Flammulina velutipes* growing on cooked rice. Food Chem 132:1346
146. Jiang MY, Feng T, Liu JK (2011) N-containing compounds of macromycetes. Nat Prod Rep 28:783
147. Liu JK (2005) N-containing compounds of macromycetes. Chem Rev 105:2723
148. Choi JH, Maeda K, Nagai K, Harada E, Kawade M, Hirai H, Kawagishi H (2010) Termitomycamides A to E, fatty acid amides isolated from the mushroom *Termitomyces titanicus*, suppress endoplasmic reticulum stress. Org Lett 12:5012
149. Yang ML, Kuo PC, Hwang TL, TS W (2011) Anti-inflammatory principles from *Cordyceps sinensis*. J Nat Prod 74:1996
150. Gomez-Prado RA, Miranda LD (2013) Concise total synthesis of hericerin natural product. Tetrahedron Lett 54:2131
151. Kobayashi S, Inoue T, Ando A, Tamanoi H, Ryu I, Masuyama A (2012) Total synthesis and structural revision of hericerin. J Org Chem 77:5819
152. Miyazawa M, Takahashi T, Horibe I, Ishikawa R (2012) Two new aromatic compounds and a new D-arabinitol ester from the mushroom *Hericium erinaceum*. Tetrahedron 68:2007

153. Kim KH, Noh HJ, Choi SU, Lee KR (2012) Isohericenone, a new cytotoxic isoindolinone alkaloid from *Hericium erinaceum*. J Antibiot 65:575
154. Wang K, Bao L, Ma K, Liu N, Huang Y, Ren JW, Wang WZ, Liu HW (2015) Eight new alkaloids with PTP1B and $\alpha$-glucosidase inhibitory activities from the medicinal mushroom *Hericium erinaceus*. Tetrahedron 71:9557
155. Wang K, Bao L, Qi QY, Zhao F, Ma K, Pei YF, Liu HW (2015) Erinacerins C–L, isoindolin-1-ones with $\alpha$-glucosidase inhibitory activity from cultures of the medicinal mushroom *Hericium erinaceus*. J Nat Prod 78:146
156. Wang XL, Xu KP, Long HP, Zou H, Cao XZ, Zhang K, JZ H, He SJ, Zhu GZ, He XA, PS X, Tan GS (2016) New isoindolinones from the fruiting bodies of *Hericium erinaceum*. Fitoterapia 111:58
157. Lee IK, Kim SE, Yeom JH, Ki DW, Lee MS, Song JG, Kim YS, Seok SJ, Yun BS (2012) Daldinan A, a novel isoindolinone antioxidant from the Ascomycete *Daldinia concentrica*. J Antibiot 65:95
158. Choomuenwai V, Beattie KD, Healy PC, Andrews KT, Fechner N, Davis RA (2015) Entonalactams A–C: isoindolinone derivatives from an Australian rainforest fungus belonging to the genus *Entonaema*. Phytochemistry 117:10
159. Lu WW, Gao YJ, Su MZ, Luo Z, Zhang W, Shi GB, Zhao QC (2013) Isoindolones from *Lasiosphaera fenzlii* REICH. and their bioactivities. Helv Chim Acta 96:109
160. Yu JG, Chen RY, Yao ZX, Zhai YF, Yang SL, Ma JL (1990) Studies on constituents of *Ganoderma capense* IV. The chemical structures of ganoine, ganodine and ganoderpurine. Acta Pharm Sin 25:612
161. Liu C, Zhao F, Chen RY (2010) A novel alkaloid from the fruiting bodies of *Ganoderma sinense* Zhao, Xu et Zhang. Chin Chem Lett 21:197
162. Liu JQ, Wang CF, Peng XR, Qiu MH (2011) New alkaloids from the fruiting bodies of *Ganoderma sinense*. Nat Prod Bioprospect 1:93
163. Zhao ZZ, Chen HP, Feng T, Li ZH, Dong ZJ, Liu JK (2015) Lucidimine A-D, four new alkaloids from the fruiting bodies of *Ganoderma lucidum*. J Asian Nat Prod Res 17:1160
164. Dai WF, Guo PX, ZC T, Li RT, Cheng YX (2015) Five new compounds from the fungus *Ganoderma petchii*. Fitoterapia 106:68
165. Isaka M, Srisanoh U, Sappan M, Supothina S, Boonpratuang T (2012) Sterostreins F–O, illudalanes and norilludalanes from cultures of the basidiomycete *Stereumostrea* BCC 22955. Phytochemistry 79:116
166. Nasini G, Arnone A, Bava A, Musso L (2012) Isolation and structure elucidation of aza-sesquiterpenoids of protoilludane origin formed by shaken cultures of the fungus *Clavicorona divaricata*. Phytochem Lett 5:224
167. Isaka M, Yangchum A, Supothina S, Chanthaket R, Srikitikulchai P (2014) Isopimaranes and eremophilanes from the wood-decay fungus *Xylaria allantoidea* BCC 23163. Phytochem Lett 8:59
168. Richter C, Helaly SE, Thongbai B, Hyde KD, Stadler M (2016) Pyristriatins A and B: pyridino-cyathane antibiotics from the basidiomycete *Cyathus* cf. *striatus*. J Nat Prod 79:1684
169. Herrmann A, Hedman H, Rosen J, Jansson D, Haraldsson B, Hellenas KE (2012) Analysis of the mushroom nephrotoxin orellanine and its glucosides. J Nat Prod 75:1690
170. Ou YX, Li YY, Qian XM, Shen YM (2012) Guanacastane-type diterpenoids from *Coprinus radians*. Phytochemistry 78:190
171. Xu ZY, Wu ZA, Bi KS (2013) A novel norsesquiterpene alkaloid from the mushroom-forming fungus *Flammulina velutipes*. Chin Chem Lett 24:57
172. Yang NN, Huang SZ, Ma QY, Dai HF, Guo ZK, Yu ZF, Zhao YX (2015) A new pyrrole alkaloid from *Leccinum extremiorientale*. Chem Nat Compd 51:730
173. Wang YC, Zhang YW, Zheng LH, Bao YL, Wu Y, Yu CL, Huang YX, Sun LG, Zhang Y, Jia XJ, Li YX (2013) Four new alkaloids from the fermentation broth of *Armillaria mellea*. Helv Chim Acta 96:330

174. Xiong J, Huang Y, Wu XY, Liu XH, Fan H, Wang W, Zhao Y, Yang GX, Zhang HY, Hu JF (2016) Chemical constituents from the fermented mycelia of the medicinal fungus *Xylaria nigripes*. Helv Chim Acta 99:83
175. Li M, Xiong J, Huang Y, Wang LJ, Tang Y, Yang GX, Liu XH, Wei BG, Fan H, Zhao Y, Zhai WZ, Hu JF (2015) Xylapyrrosides A and B, two rare sugar-morpholine spiroketal pyrrole-derived alkaloids from *Xylaria nigripes*: isolation, complete structure elucidation, and total syntheses. Tetrahedron 71:5285
176. Liu XM, Frydenvang K, Liu HZ, Zhai L, Chen M, Olsen CE, Christensen SB (2015) Iminolactones from *Schizophyllum commune*. J Nat Prod 78:1165
177. Jensen CM, Chow HQ, Chen M, Zhai L, Frydenvang K, Liu HZ, Franzyk H, Christensen SB (2016) Iminolactones as tools for inversion of the absolute configuration of α-amino acids and as inhibitors of cancer cell proliferation. Eur J Med Chem 114:118
178. Pettit GR, Meng YH, Pettit RK, Herald DL, Cichacz ZA, Doubek DL, Richert L (2010) Isolation and structure of coprinastatin 1 from *Coprinus cinereus*. J Nat Prod 73:388
179. Li LF, Chan BCL, Yue GGL, Lau CBS, Han QB, Leung PC, Liu JK, Fung KP (2013) Two immunosuppressive compounds from the mushroom *Rubinoboletus ballouii* using human peripheral blood mononuclear cells by bioactivity-guided fractionation. Phytomedicine 20:1196
180. Haraguchi A, Kinoshita K, Fukai M, Koyama K (2015) A novel nucleoside from the edible mushroom, *Tricholoma japonicum*. J Nat Med 69:584
181. Araya H, Nagai Y, Otaka J (2014) Isolation of (2*S*,4*R*)-2-amino-4-methyl-hex-5-enoic acid, a nonprotein amino acid, as an allelochemical from the fruiting bodies of *Boletus fraternus* Peck. J Plant Interact 9:627
182. Roberts A, Beaumont C, Manzarpour A, Mantle P (2016) Purpurolic acid: a new natural alkaloid from *Claviceps purpurea* (Fr.) Tul. Fungal Biol 120:104
183. Kluepfel D, Vezina C, Sehgal SN, Kudelski A, Charest MP, Bagli J (1972) Myriocin, a new antifungal antibiotic from *Myriococcum albomyces*. J Antibiot 25:109
184. Krasnoff SB, Reategui RF, Wagenaar MM, Gloer JB, Gibson DM (2005) Cicadapeptins I and II: new Aib-containing peptides from the entomopathogenic fungus *Cordyceps heteropoda*. J Nat Prod 68:50
185. Chiba K, Adachi K (2012) Discovery of fingolimod, the sphingosine 1-phosphate receptor modulator and its application for the therapy of multiple sclerosis. Future Med Chem 4:771
186. Strader CR, Pearce CJ, Oberlies NH (2011) Fingolimod (FTY720): a recently approved multiple sclerosis drug based on a fungal secondary metabolite. J Nat Prod 74:900
187. Takata T, Hasegawa T, Tatsuno T, Date J, Ishigaki Y, Nakamura Y, Tomosugi N, Takano F, Ohta T (2009) Isolation of *N*-acetylneuraminic acid and *N*-glycolylneuraminic acid from *Pleurocybella porrigens*. J Health Sci 55:373
188. Kawaguchi T, Suzuki T, Kobayashi Y, Kodani S, Hirai H, Nagai K, Kawagishi H (2010) Unusual amino acid derivatives from the mushroom *Pleurocybella porrigens*. Tetrahedron 66:504
189. Wakimoto T, Asakawa T, Akahoshi S, Suzuki T, Nagai K, Kawagishi H, Kan T (2011) Proof of the existence of an unstable amino acid: pleurocybellaziridine in *Pleurocybella porrigens*. Angew Chem Int Ed 50:1168
190. Zhou ZY, Shi GQ, Fontaine R, Wei K, Feng T, Wang F, Wang GQ, Qu Y, Li ZH, Dong ZJ, Zhu HJ, Yang ZL, Zeng G, Liu JK (2012) Evidence for the natural toxins from the mushroom *Trogia venenata* as a cause of sudden unexpected death in Yunnan Province, China. Angew Chem Int Ed 51:2368
191. Matsuura M, Saikawa Y, Inui K, Nakae K, Igarashi M, Hashimoto K, Nakata M (2009) Identification of the toxic trigger in mushroom poisoning. Nat Chem Biol 5:465
192. Chen XL, Wu M, Ti HH, Wei XY, Li TH (2011) Three new 3,6-dioxygenated diketopiperazines from the basidiomycete *Lepista sordida*. Helv Chim Acta 94:1426
193. Barros BA, De Oliveira MCF, Mafezoli J, Barbosa FG, Rodrigues E (2012) Secondary metabolite production by the basidiomycete, *Lentinus strigellus*, under different culture conditions. Nat Prod Commun 7:771

194. Herath HMTB, Jacob M, Wilson AD, Abbas HK, Nanayakkara NPD (2013) New secondary metabolites from bioactive extracts of the fungus *Armillaria tabescens*. Nat Prod Res 27:1562
195. Wang YC, Zhang YW, Zheng LH, Bao YL, Wu Y, Yu CL, Sun LG, Zhang Y, Huang YX, Sun Y, Li YX (2013) A new compound from liquid fermentation broth of *Armillaria mellea* and the determination of its absolute configuration. J Asian Nat Prod Res 15:203
196. Wang XN, Huang WY, Du JC, Li CY, Liu JK (2014) Chemical constituents from the fruiting bodies of *Xylaria euglossa* Fr. and its chemotaxonomic study. Biochem Syst Ecol 54:157
197. Yin X, Feng T, Li ZH, Su J, Li Y, Tan NH, Liu JK (2011) Chemical investigation on the cultures of the fungus *Xylaria carpophila*. Nat Prod Bioprospect 1:75
198. Vanyolos A, Dekany M, Kovacs B, Kramos B, Berdi P, Zupko I, Hohmann J, Beni Z (2016) Gymnopeptides A and B, cyclic octadecapeptides from the mushroom *Gymnopus fusipes*. Org Lett 18:2688
199. Li Y, Ma YT, Kuang Y, Gao JM, Qin JC (2010) Pecipamide, a new sphingosine derivative from the cultures of *Polyporus picipes* (Basidiomycetes). Lipids 45:457
200. Lee SR, Jung K, Noh HJ, Park YJ, Lee HL, Lee KR, Kang KS, Kim KH (2015) A new cerebroside from the fruiting bodies of *Hericiumerinaceus* and its applicability to cancer treatment. Bioorg Med Chem Lett 25:5712
201. Zhao LY, Zuo W, Fu QB, Zhao LJ, Zhu WL, Luo DQ (2010) Chemical constituents from fruit body of *Lactarius vellereus*. Chin Tradit Herb Drugs 10:5
202. Choi JH, Ozawa N, Yamakawa Y, Nagai K, Hirai H, Kawagishi H (2011) Leccinine A, an endoplasmic reticulum stress-suppressive compound from the edible mushroom *Leccinum extremiorientale*. Tetrahedron 67:6649
203. Ueguchi Y, Matsunami K, Otsuka H, Kondo K (2011) Constituents of cultivated *Agaricus blazei*. J Nat Med 65:307
204. Intaraudom C, Boonyuen N, Supothina S, Tobwor P, Prabpai S, Kongsaeree P, Pittayakhajonwut P (2013) Novel spiro-sesquiterpene from the mushroom *Anthracophyllum* sp. BCC18695. Phytochem Lett 6:345
205. Afrin S, Rakib MA, Kim BH, Kim JO, Ha YL (2016) Eritadenine from edible mushrooms inhibits activity of angiotensin-converting enzyme in vitro. J Agric Food Chem 64:2263
206. Li W, Zhou W, Lee DS, Shim SH, Kim YC, Kim YH (2014) Hericirine, a novel anti-inflammatory alkaloid from *Hericium erinaceum*. Tetrahedron Lett 55:4086
207. Liu DZ, Li JG, Zhang MW, Liu G (2014) Two new alkaloids from the edible macrofungus *Ramaria madagascariensis*. J Basic Microbiol 54:S70
208. Liu DZ, Li JG, Zhang MW, Liu G (2015) New bicyclic hemiacetals from the edible mushroom *Ramaria madagascariensis*. J Antibiot 68:137
209. Lin KW, Maitraie D, Huang AM, Wang JP, Lin CN (2016) Triterpenoids and an alkamide from *Ganoderma tsugae*. Fitoterapia 108:73
210. Zhang LH, Feng BM, Chen G, Li SG, Sun Y, Wu HH, Bai J, Hua HM, Wang HF, Pei YH (2016) Sporulaminals A and B: a pair of unusual epimeric spiroaminal derivatives from a marine-derived fungus *Paraconiothyrium sporulosum* YK-03. RSC Adv 6:42361
211. Chen ZM, Fan QY, Yin X, Yang XY, Li ZH, Feng T, Liu JK (2014) Three new humulane sesquiterpenes from cultures of the fungus *Antrodiella albocinnamomea*. Nat Prod Bioprospect 4:207
212. Luo DQ, Gao Y, Gao JM, Wang F, Yang XL, Liu JK (2006) Humulane-type sesquiterpenoids from the mushroom *Lactarius mitissimus*. J Nat Prod 69:1354
213. Luo DQ, Gao Y, Yang XL, Tang JG, Liu JK (2007) Highly oxidized humulane sesquiterpenes from the basidiomycete *Lactarius mitissimus*. J Antibiot 60:162
214. Luo DQ, Gao Y, Yang XL, Tang JG, Zhao LY, Liu JK (2007) Two new highly oxidized humulane sesquiterpenes from the basidiomycete *Lactarius mitissimus*. Helv Chim Acta 90:1112
215. Hu L, Liu JK (2002) The first humulene type sesquiterpene from *Lactarius hirtipes*. Z Naturforsch C 57:571

216. McMorris TC, Lira R, Gantzel PK, Kelner MJ, Dawe R (2000) Sesquiterpenes from the basidiomycete *Omphalotus illudens*. J Nat Prod 63:1557
217. Zheng YB, Lu CH, Zheng ZH, Lin XJ, Su WJ, Shen YM (2008) New sesquiterpenes from edible fungus *Clavicorona pyxidata*. Helv Chim Acta 91:2174
218. McMorris TC, Kashinatham A, Lira R, Rundgren H, Gantzel PK, Kelner MJ, Dawe R (2002) Sesquiterpenes from *Omphalotus illudens*. Phytochemistry 61:395
219. Liu G, Romo D (2011) Total synthesis of (+)-omphadiol. Angew Chem Int Ed 50:7537
220. Zhou LL, Yao YM, Xu WB, Liang GX (2014) Total syntheses of (±)-omphadiol and (±)-pyxidatol C through a *cis*-fused 5,7-carbocyclic common intermediate. J Org Chem 79:5345
221. Clericuzio M, Cassino C, Corana F, Vidari G (2012) Terpenoids from *Russula lepida* and *R. amarissima* (Basidiomycota, Russulaceae). Phytochemistry 84:154
222. Lee JS, Maarisit W, Abdjul DB, Yamazaki H, Takahashi O, Kirikoshi R, Kanno SI, Namikoshi M (2016) Structures and biological activities of triterpenes and sesquiterpenes obtained from *Russula lepida*. Phytochemistry 127:63
223. Vidari G, Che ZL, Garlaschelli L (1998) New nardosinane and aristolane sesquiterpenes from the fruiting bodies of *Russula lepida*. Tetrahedron Lett 39:6073
224. Tan JW, Dong ZJ, Hu L, Liu JK (2003) Lepidamine, the first aristolane-type sesquiterpene alkaloid from the basidiomycete *Russula lepida*. Helv Chim Acta 86:307
225. Tan JW, Dong ZJ, Liu JK (2000) A new sesquiterpenoid from *Russula lepida*. Acta Bot Sin 43:329
226. Kanokmedhakul S, Lekphrom R, Kanokmedhakul K, Hahnvajanawong C, Bua-Art S, Saksirirat W, Prabpai S, Kongsaeree P (2012) Cytotoxic sesquiterpenes from luminescent mushroom *Neonothopanus nambi*. Tetrahedron 68:8261
227. Kim KC, Lee IS, Yoo ID, Ha BJ (2015) Sesquiterpenes from the fruiting bodies of *Ramaria formosa* and their human neutrophil elastase inhibitory activity. Chem Pharm Bull 63:554
228. Wichlacz M, Ayer WA, Trifonov LS, Chakravarty P, Khasa D (1999) Two 6,7-*seco*-caryophyllenes and an alloaromadendrane from liquid cultures of *Hebeloma longicaudum*. Phytochemistry 52:1421
229. Huang ZL, Dan Y, Huang YC, Lin LD, Li TH, Ye WH, Wei XY (2004) Sesquiterpenes from the mycelial cultures of *Dichomitus squalens*. J Nat Prod 67:2121
230. Xie HH, Xu XY, Dan Y, Wei XY (2011) Novel sesquiterpenes from the mycelial cultures of *Dichomitus squalens*. Helv Chim Acta 94:868
231. Stodulkova E, Sulc M, Cisarova I, Novak P, Kolarik M, Flieger M (2008) Production of (+)-globulol needle crystals on the surface mycelium of *Quambalaria cyanescens*. Folia Microbiol 53:15
232. Pornpakakul S, Suwancharoen S, Petsom A, Roengsumran S, Muangsin N, Chaichit N, Piapukiew J, Sihanonth P, Allen JW (2009) A new sesquiterpenoid metabolite from *Psilocybe samuiensis*. J Asian Nat Prod Res 11:12
233. Zhu YC, Wang G, Liu JK (2010) Two new sesquiterpenoids from basidiomycete *Agrocybe salicacola*. J Asian Nat Prod Res 12:464
234. Isaka M, Yangchum A, Supothina S, Boonpratuang T, Choeyklin R, Kongsaeree P, Prabpai S (2015) Aromadendrane and cyclofarnesane sesquiterpenoids from cultures of the basidiomycete *Inonotus* sp. BCC 23706. Phytochemistry 118:94
235. Abraham WR, Hanssen HP, Urbasch I (1991) Lepistirones, major volatile metabolites from liquid cultures of *Lepista irina* (Basidiomycotina). Z Naturforsch C 46:169
236. Stadler M, Anke H, Sterner O (1994) New nematocidal and antimicrobial compounds from the basidiomycete *Cheimonophyllum candidissimum* (Berk & Curt.) Sing. 1. Producing organism, fermentation, isolation, and biological activities. J Antibiot 47:1284
237. Stadler M, Anke H, Sterner O (1994) Six new antimicrobial and nematocidal bisabolanes from the basidiomycete *Cheimonophyllum candidissimum*. Tetrahedron 50:12649
238. Zhang L, Wang F, Dong ZJ, Liu JK (2008) New bisabolane sesquiterpene from culture broth of the fungus *Aleuria aurantia* (Pezizaceae). Acta Bot Yunnan 30:611

239. Isaka M, Sappan M, Rachtawee P, Boonpratuang T (2011) A tetrahydrobenzofuran derivative from the fermentation broth of *Lentinus squarrosulus* BCC 22366. Phytochem Lett 4:106
240. Asano M, Yamada K, Tanaka T, Matsuo Y, Kouno I (2013) New bisabolane sesquiterpene from the mycelia of *Amanita virgineoides*. Chem Pharm Bull 61:366
241. Kobori H, Sekiya A, Yasuda N, Noguchi K, Suzuki T, Choi JH, Hirai H, Kawagishi H (2013) Armillariols A to C from the culture broth of *Armillaria* sp. Tetrahedron Lett 54:5481
242. Liu S, Dong YA, Li YX, Bao L, Liu HW, Li HR (2013) Chemical constituents from the rice fermented with the edible mushroom *Pleurotus eryngii* and their quinone oxidoreductase 1 inducing effect. Fitoterapia 91:9
243. Wang S, Li ZH, Dong ZJ, Liu JK, Feng T (2013) Norbisabolane and eremophilane sesquiterpenoids from cultures of the basidiomycete *Polyporus ellisii*. Fitoterapia 91:194
244. Wang SJ, Bao L, Han JJ, Wang QX, Yang XL, Wen HA, Guo LD, Li SJ, Zhao F, Liu HW (2013) Pleurospiroketals A–E, perhydrobenzannulated 5,5-spiroketal sesquiterpenes from the edible mushroom *Pleurotus cornucopiae*. J Nat Prod 76:45
245. Yang J, Wang N, Yuan HS, Hu JC, Dai YC (2013) A new sesquiterpene from the medicinal fungus *Inonotus vaninii*. Chem Nat Compd 49:261
246. Zhao JY, Feng T, Li ZH, Dong ZJ, Zhang HB, Liu JK (2013) Sesquiterpenoids and an ergosterol from cultures of the fungus *Daedaleopsis tricolor*. Nat Prod Bioprospect 3:271
247. Chen HP, Dong WB, Feng T, Yin X, Li ZH, Dong ZJ, Li Y, Liu JK (2014) Four new sesquiterpenoids from fruiting bodies of the fungus *Inonotus rickii*. J Asian Nat Prod Res 16:581
248. Lee MS, Hwang BS, Lee IK, Seo GS, Yun BS (2015) Chemical constituents of the culture broth of *Phellinus linteus* and their antioxidant activity. Mycobiology 43:43
249. Zheng YB, Pang HY, Wang JF, Shi GW, Huang JZ (2015) New apoptosis-inducing sesquiterpenoids from the mycelial culture of Chinese edible fungus *Pleurotus cystidiosus*. J Agric Food Chem 63:545
250. Zhao ZZ, He LQ, Chen HP, Li ZH, Dong ZJ, Feng T, Liu JK (2016) A new bisabolane-type sesquiterpenoid from the fermentation broth of fungus *Antrodiella gypsea*. J Asian Nat Prod Res 18:184
251. Abraham WR (2001) Bioactive sesquiterpenes produced by fungi: are they useful for humans as well. Curr Med Chem 8:583
252. Brocksom TJ, Zanotto PR, Brocksom U (2005) The enantioselective syntheses of bisabolane sesquiterpenes lepistirone and cheimonophyllon E. Tetrahedron Lett 46:2397
253. Takao K, Hara M, Tsujita T, Yoshida K, Tadano K (2001) Total synthesis of (+)-cheimonophyllon E, a bisabolane sesquiterpenoid. Tetrahedron Lett 42:4665
254. Takao K, Tsujita T, Hara M, Tadano K (2002) Asymmetric total syntheses of (+)-cheimonophyllon E and (+)-cheimonophyllal. J Org Chem 67:6690
255. Hanssen HP (1982) Sesquiterpene hydrocarbons from *Lentinus lepideus*. Phytochemistry 21:1159
256. Abraham WR, Hanssen HP, Mohringer C (1988) Novel sesquiterpene ethers from liquid cultures of the wood-rotting fungus *Lentinus lepideus*. Z Naturforsch C 43:24
257. Vaneijk GW, Roeijmans HJ, Verwiel PEJ (1984) Isolation and identification of the sesquiterpenoid (+)-torreyol from *Xylobolus frustulatus*. Exp Mycol 8:273
258. Arnone A, Colombo A, Nasini G, Meille SV (1993) Eleganthol, a sesquiterpene from *Clitocybe elegans*. Phytochemistry 32:1493
259. Hirotani M, Ino C, Hatano A, Takayanagi H, Furuya T (1995) Ganomastenol A, ganomastenol B, ganomastenol C and ganomastenol D, cadinene sesquiterpenes, from *Ganoderma mastoporum*. Phytochemistry 40:161
260. Zapf S, Wunder A, Anke T, Klostermeyer D, Steglich W, Shan R, Sterner O, Scheuer W (1996) (+)-10$\alpha$-Hydroxy-4-muurolen-3-one, a new inhibitor of leukotriene biosynthesis from a *Favolaschia* species. Comparison with other sesquiterpenes. Z Naturforsch C 51:487
261. Gruhn N, Schoettler S, Sterner O, Anke T (2007) Biologically active metabolites from the basidiomycete *Limacella illinita* (Fr.) Murr. Z Naturforsch C 62:808

262. Hiramatsu F, Murayama T, Koseki T, Funakoshi T, Shiono Y (2011) Cadinane sesquiterpenoids, strobilols L and M, from *Strobilurus ohshimae*. Nat Prod Res 25:781
263. Hiramatsu F, Murayama T, Koseki T, Okada K, Shiono Y (2008) Cadinane-type sesquiterpenoids, strobilols E-K, from the liquid culture of *Strobilurus ohshimae*. Helv Chim Acta 91:1595
264. Hiramatsu F, Murayama T, Koseki T, Shiono Y (2007) Strobilols A-D: four cadinane-type sesquiterpenes from the edible mushroom *Strobilurus ohshimae*. Phytochemistry 68:1267
265. Shiono Y, Hiramatsu F, Murayama T, Koseki T, Funakoshi T, Ueda K, Yasuda H (2007) Two drimane-type sesquiterpenes, strobilactones A and B, from the liquid culture of the edible mushroom *Strobilurus ohshimae*. Z Naturforsch B 62:1585
266. Liu DZ, Wang F, Yang LM, Zheng YT, Liu JK (2007) A new cadinane sesquiterpene with significant anti-HIV-1 activity from the cultures of the basidiomycete *Tyromyces chioneus*. J Antibiot 60:332
267. Bunyapaiboonsri T, Yoiprommarat S, Nopgason R, Komwijit S, Veeranondha S, Puyngain P, Boonpratuang T (2014) Cadinane sesquiterpenoids from the basidiomycete *Stereum* cf. *sanguinolentum* BCC 22926. Phytochemistry 105:123
268. Li GH, Duan M, Yu ZF, Li L, Dong JY, Wang XB, Guo JW, Huang R, Wang M, Zhang KQ (2008) Stereumin A–E, sesquiterpenoids from the fungus *Stereum* sp. CCTCC af 207024. Phytochemistry 69:1439
269. Liu FF, Li GH, Yang ZS, Zheng X, Yang Y, Zhang KQ (2010) Two new sesquiterpenes from the fungus *Stereum* sp. Helv Chim Acta 93:1737
270. Zheng X, Li GH, Xie MJ, Wang X, Sun R, Lu H, Zhang KQ (2013) Stereumins K-P, sesquiterpenes from the fungus *Stereum* sp. CCTCC AF 2012007. Phytochemistry 86:144
271. Ding JH, Feng T, Li ZH, Li L, Liu JK (2012) Twelve new compounds from the basidiomycete *Boreostereum vibrans*. Nat Prod Bioprospect 2:200
272. Clericuzio M, Negri R, Cossi M, Gilardoni G, Gozzini D, Vidari G (2013) Cadinane sesquiterpenes from the mushroom *Lyophyllum transforme*. Phytochemistry 93:192
273. Liu LY, Li ZH, Si J, Dong ZJ, Liu JK (2013) Two new sesquiterpenoids from the fungus *Ceriporia alachuana*. J Asian Nat Prod Res 15:300
274. Yang XY, Feng T, Wang GQ, Ding JH, Li ZH, Li Y, He SH, Liu JK (2014) Chemical constituents from cultures of the basidiomycete *Trichaptum pargamenum*. Phytochemistry 104:89
275. Yin RH, Zhao ZZ, Ji X, Dong ZJ, Li ZH, Feng T, Liu JK (2014) Steroids and sesquiterpenes from cultures of the fungus *Phellinus igniarius*. Nat Prod Bioprospect 5:17
276. Guo H, Feng T, Li ZH, Liu JK (2014) Two new sesquiterpenoids from basidiomycete *Tyromyces chioneus*. Acta Pharm Sin 49:1578
277. Ding JH, Li ZH, Wei K, Dong ZJ, Ding ZH, Feng T, Liu JK (2016) Two new sesquiterpenoids from cultures of the basidiomycete *Tremella foliacea*. J Asian Nat Prod Res 18:46
278. Gollnick K, Schade G, Cameron AF, Hannaway C, Robertson JM (1971) The structure of a hydrocarbon, 2,6,10,10-tetramethyltricyclo[7,2,0,$0^{2,7}$]undec-5-ene, obtained from caryophyllene dihydrochloride: X-ray analysis of the dibromo-derivative. J Chem Soc D Chem Commun 3:46
279. Fabian K, Anke T, Sterner O (1999) 6,9-Dihydroxy-3(15)-caryophyllen-4,8-dione – a new antibiotic from a *Marasmius* species. Z Naturforsch C 54:469
280. Wichlacz M, Ayer WA, Trifonov LS, Chakravarty P, Khasa D (1999) *cis*-Fused caryophyllenes from liquid cultures of *Hebeloma longicaudum*. Phytochemistry 51:873
281. Evans L, Hedger J, O'Donnell G, Skelton BW, White AH, Williamson RT, Gibbons S (2010) Structure elucidation of some highly unusual tricyclic *cis*-caryophyllane sesquiterpenes from *Marasmiellus troyanus*. Tetrahedron Lett 51:5493
282. Wichlacz M, Ayer WA, Trifonov LS, Chakravarty P, Khasa D (1999) A caryophyllene-related sesquiterpene and two 6,7-*seco*-caryophyllenes from liquid cultures of *Hebeloma longicaudum*. J Nat Prod 62:484

283. Doi K, Shibata T, Yokoyama N, Terasawa H, Matsuda O, Kashino S (1990) Structure of naematolin C and naematolin G, novel 4,8,11,11-tetramethyltricyclo[5.4.0.$0^{2,3}$]undecane sesquiterpenoids. J Chem Soc Chem Commun 10:725
284. Shiono Y, Matsuzaka R, Wakamatsu H, Muneta K, Murayama T, Ikeda M (2004) Fascicularones A and B from a mycelial culture of *Naematoloma fasciculare*. Phytochemistry 65:491
285. Shiono Y, Wakamatsu H, Murayama T, Ikeda M (2004) Fascicularones C and D, tricyclo [5.4.0.$0^{2,5}$]undecane sesquiterpenoids from the liquid culture of *Naematoloma fasciculare*. Z Naturforsch B 59:119
286. Akasaka F, Shiono Y, Murayama T, Ikeda M (2005) Fascicularones H-K, four new sesquiterpenoids from the cultured mycelia of the fungus *Hypholoma fasciculare*. Helv Chim Acta 88:2944
287. Shiono Y, Akasaka H, Hiramatsu F, Sato K, Murayama T, Ikeda M (2005) Three sesquiterpenoids, fascicularones E, F, and G produced by the fungus *Hypholoma fasciculare*. Z Naturforsch B 60:880
288. Liu R, Zhou ZY, Xu D, Wang F, Lin JK (2009) A new tricyclo[6.3.1.$0^{2,5}$]dodecane sesquiterpene from cultures of the basidiomycete *Campanella junghuhnii*. Helv Chim Acta 92:375
289. Simon B, Anke T, Anders U, Neuhaus M, Hansske E (1995) Collybial, a new antibiotic sesquiterpenoid from *Collybia confluens* (Basidiomycetes). Z Naturforsch C 50:173
290. Ishikawa NK, Fukushi Y, Yamaji K, Tahara S, Takahashi K (2001) Antimicrobial cuparene-type sesquiterpenes, enokipodins C and D, from a mycelial culture of *Flammulina velutipes*. J Nat Prod 64:932
291. Ishikawa NK, Yamaji K, Tahara S, Fukushi Y, Takahashi K (2000) Highly oxidized cuparene-type sesquiterpenes from a mycelial culture of *Flammulina velutipes*. Phytochemistry 54:777
292. Wang YQ, Bao L, Yang XL, Dai HQ, Guo H, Yao XS, Zhang LX, Liu HW (2012) Four new cuparene-type sesquiterpenes from *Flammulina velutipes*. Helv Chim Acta 95:261
293. Johansson M, Sterner O, Labischinski H, Anke T (2001) Coprinol, a new antibiotic cuparane from a *Coprinus* species. Z Naturforsch C 56:31
294. Xu GH, Kim YH, Choo SJ, Ryoo IJ, Zheng CJ, Seok SJ, Kim WG, Yoo ID (2009) Isodeoxyhelicobasidin, a novel human neutrophil elastase inhibitor from the culture broth of *Volvariella bombycina*. J Antibiot 62:333
295. Surup F, Thongbai B, Kuhnert E, Sudarman E, Hyde KD, Stadler M (2015) Deconins A-E: cuparenic and mevalonic or propionic acid conjugates from the basidiomycete *Deconica* sp. 471. J Nat Prod 78:934
296. Ki DW, Kim DW, Hwang BS, Lee SW, Seok SJ, Lee IK, Yun BS (2015) New antioxidant sesquiterpenes from a culture broth of *Coprinus echinosporus*. J Antibiot 68:351
297. Kuwahara S, Saito M (2004) Enantioselective total synthesis of enokipodins A-D. Tetrahedron Lett 45:5047
298. Saito M, Kuwahara S (2005) Enantioselective total synthesis of enokipodins A-D, antimicrobial sesquiterpenes produced by the mushroom, *Flammulina velutipes*. Biosci Biotechnol Biochem 69:374
299. Srikrishna A, Srinivasa Rao M (2004) The first total synthesis of the antimicrobial sesquiterpenes (±)-enokipodins A and B. Synlett 2004:374
300. Yoshida M, Shoji Y, Shishido K (2009) Total syntheses of enokipodins A and B utilizing palladium-catalyzed addition of an arylboronic acid to an allene. Org Lett 11:1441
301. Maria DB, Giorgio M, Giovanni V, Paola VF, Giovanni F (1980) Uvidins, new drimane sesquiterpenes from *Lactarius uvidus* Fries. J Chem Soc Perkin Trans 1:221
302. Debernardi M, Mellerio G, Vidari G, Vitafinzi P, Fronza G (1983) Structure and chemical correlations of uvidin C, uvidin D, and uvidin E, new drimane sesquiterpenes from *Lactarius uvidus* Fries. J Chem Soc Perkin Trans 1:2739
303. Kida T, Shibai H, Seto H (1986) Structure of new antibiotics, pereniporins A and B, from a basidiomycete. J Antibiot 39:613

304. Hashimoto T, Tori M, Mizuno Y, Asakawa Y (1987) Cryptoporic acids A and B, novel bitter drimane sesquiterpenoid ethers of isocitric acid, from the fungus *Cryptoporus volvatus*. Tetrahedron Lett 28:6303
305. Hashimoto T, Tori M, Mizuno Y, Asakawa Y, Fukazawa Y (1989) The superoxide release inhibitors, cryptoporic acids C, D, and E: dimeric drimane sesquiterpenoid ethers of isocitric acid from the fungus *Cryptoporus volvatus*. J Chem Soc Chem Commun 4:258
306. Hirotani M, Furuya T, Shiro M (1991) Cryptoporic acid H and acid I, drimane sesquiterpenes from *Ganoderma neo-japonicum* and *Cryptoporus volvatus*. Phytochemistry 30:1555
307. Nozoe S, Agatsuma T, Takahashi A, Ohishi H, In Y, Kusano G (1993) Roseolide A, a novel dimeric drimane sesquiterpenoid from the basidiomycete *Roseoformes subflexibilis*. Tetrahedron Lett 34:2497
308. Kuschel A, Anke T, Velten R, Klostermeyer D, Steglich W, Konig B (1994) The mniopetals, new inhibitors of reverse transcriptases from a *Mniopetalum* species (Basidiomycetes). 1. Producing organism, fermentation, isolation and biological activities. J Antibiot 47:733
309. Velten R, Klostermeyer D, Steffan B, Steglich W, Kuschel A, Anke T (1994) The mniopetals, new inhibitors of reverse transcriptases from a *Mniopetalum* species (Basidiomycetes). 2. Structure elucidation. J Antibiot 47:1017
310. Ayer WA, Craw PC, Stout TJ, Clardy JC (1989) Novel sesquiterpenoids from the fairy ring fungus, *Marasmius oreades*. Can J Chem 67:773
311. Erkel G, Lorenzen K, Anke T, Velten R, Gimenez A, Steglich W (1995) Kuehneromycins A and B, two new biological active compounds from a Tasmanian *Kuehneromyces* sp. (Strophariaceae, Basidiomycetes). Z Naturforsch C 50:1
312. Lorenzen K, Anke T, Anders U, Hindermayr H, Hansske F (1994) Two inhibitors of platelet-aggregation from a *Panus* species (Basidiomycetes). Z Naturforsch C 49:132
313. Morita Y, Hayashi Y, Sumi Y, Kodaira A, Shibata H (1995) Haploporic acid A, a novel dimeric drimane sesquiterpenoid from the basidiomycete *Haploporus odorus*. Biosci Biotechnol Biochem 59:2008
314. Fleck WF, Schlegel B, Hoffmann P, Ritzau M, Heinze S, Gräfe U (1996) Isolation of isodrimenediol, a possible intermediate of drimane biosynthesis from *Polyporus arcularius*. J Nat Prod 59:780
315. Cabrera GM, Roberti MJ, Wright JE, Seldes AM (2002) Cryptoporic and isocryptoporic acids from the fungal cultures of *Polyporus arcularius* and *P. ciliatus*. Phytochemistry 61:189
316. Kim YH, Yun BS, Ryoo IJ, Kim JP, Koshino H, Yoo ID (2006) Methoxylaricinolic acid, a new sesquiterpene from the fruiting bodies of *Stereum ostrea*. J Antibiot 59:432
317. Wangun HVK, Dorfelt H, Hertweck C (2006) Nebularic acids and nebularilactones, novel drimane sesquiterpenoids from the fungus *Lepista nebularis*. Eur J Org Chem:1643
318. Xu D, Sheng Y, Zhou ZY, Liu R, Leng Y, Liu JK (2009) Sesquiterpenes from cultures of the basidiomycete *Clitocybe conglobata* and their 11$\beta$-hydroxysteroid dehydrogenase inhibitory activity. Chem Pharm Bull 57:433
319. Meng J, Li YY, Ou YX, Song LF, Lu CH, Shen YM (2011) New sesquiterpenes from *Marasmius cladophyllus*. Mycology 2:30
320. Wu W, Zhao F, Bao L, Lu JC, Liu HW (2011) Two new cryptoporic acid derivatives from the fruiting bodies of *Cryptoporus sinensis*. Helv Chim Acta 94:2020
321. Wu W, Zhao F, Ding R, Bao L, Gao H, Lu JC, Yao XS, Zhang XQ, Liu HW (2011) Four new cryptoporic acid derivatives from the fruiting bodies of *Cryptoporus sinensis*, and their inhibitory effects on nitric oxide production. Chem Biodivers 8:1529
322. Lee LW, Wang GJ, Lin MH, Ju YM, Lin YW, Chen FY, Lee TH (2013) Isolation and characterization of sesquiterpenes from *Arecophila saccharicola* YMJ96022401 with NO production inhibitory activity. Phytochemistry 85:129
323. Liermann JC, Thines E, Opatz T, Anke H (2012) Drimane sesquiterpenoids from *Marasmius* sp. inhibiting the conidial germination of plant-pathogenic fungi. J Nat Prod 75:1983
324. Ding JH, Feng T, Li ZH, Si J, Yu HY, Zhang HB, Liu JK (2013) Four new sesquiterpenoids from cultures of the fungus *Funalia trogii*. J Asian Nat Prod Res 15:828

325. Otaka J, Araya H (2013) Two new isodrimene sesquiterpenes from the fungal culture broth of *Polyporus arcularius*. Phytochem Lett 6:598
326. Yang XY, Feng T, Ding JH, Li ZH, Li Y, Fan QY, Liu JK (2013) Two new drimane sesquiterpenoids from cultures of the basidiomycete *Trichaptum biforme*. Nat Prod Bioprospect 3:154
327. Yoshikawa K, Koso K, Shimomura M, Tanaka M, Yamamoto H, Imagawa H, Arihara S, Hashimoto T (2013) Yellow pigments, fomitellanols A and B, and drimane sesquiterpenoids, cryptoporic acids P and Q, from *Fomitella fraxinea* and their inhibitory activity against COX and 5-LO. Molecules 18:4181
328. Zhao JY, Ding JH, Li ZH, Dong ZJ, Feng T, Zhang HB, Liu JK (2013) Two new sesquiterpenes from cultures of the basidiomycete *Agaricus arvensis*. J Asian Nat Prod Res 15:305
329. Guo HY, Lu YD, Li ZH, Wang G, Liu JK (2014) A new drimane-type sesquiterpenoid from fermentation broth of *Fomitiporia punicata*. Nat Prod Res Dev 26:6
330. He JB, Feng T, Zhang S, Dong ZJ, Li ZH, Zhu HJ, Liu JK (2014) Seven new drimane-type sesquiterpenoids from cultures of fungus *Phellinus tuberculosus*. Nat Prod Bioprospect 4:21
331. Isaka M, Chinthanom P, Danwisetkanjana K, Choeyklin R (2014) A new cryptoporic acid derivative from cultures of the basidiomycete *Poria albocincta* BCC 26244. Phytochem Lett 7:97
332. Ying YM, Zhang LY, Zhang X, Bai HB, Liang DE, Ma LF, Shan WG, Zhan ZJ (2014) Terpenoids with $\alpha$-glucosidase inhibitory activity from the submerged culture of *Inonotus obliquus*. Phytochemistry 108:171
333. Zhao ZZ, Chen HP, Feng T, Li ZH, Dong ZJ, Liu JK (2014) Four new sesquiterpenoids from cultures of the fungus *Phellinidium sulphurascens*. Nat Prod Bioprospect 5:23
334. Wang JC, Li GZ, Lv N, Shen LG, Shi LL, Si JY (2016) Cryptoporic acid S, a new drimane-type sesquiterpene ether of isocitric acid from the fruiting bodies of *Cryptoporus volvatus*. J Asian Nat Prod Res 19:719
335. Wang J, Li G, Gao L, Cao L, Lv N, Shen L, Si J (2015) Two new cryptoporic acid derivatives from the fruiting bodies of *Cryptoporus volvatus*. Phytochem Lett 14:63
336. Zhang JW, Wen GL, Zhang L, Duan DM, Ren ZH (2015) Sulphureuine B, a drimane type sesquiterpenoid isolated from *Laetiporus sulphureus* induces apoptosis in glioma cells. Bangladesh J Pharmacol 10:844
337. Li XM, Yin X, Li ZH, Feng T, Liu JK (2015) A new drimane sesquiterpenoid from cultures of fungus *Psathyrella candolleana*. Nat Prod Res Dev 27:1131
338. Wang J, Li G, Lv N, Gao L, Cao L, Shen L, Si JY (2016) Chemical constituents from the fruiting bodies of *Cryptoporus volvatus*. Arch Pharm Res 39:747
339. Kuhne B, Hanssen HP, Abraham WR, Wray V (1991) A phytotoxic eremophilane ether from *Hypomyces odoratus*. Phytochemistry 30:1463
340. Urbasch I, Kühne B, Hanssen HP, Abraham WR (1991) Fungicidal activity of hypodoratoxide from *Hypomyces odoratus*. Planta Med 57:A18
341. Singh SB, Zink D, Polishook J, Valentino D, Shafiee A, Silverman K, Felock P, Teran A, Vilella D, Hazuda DJ, Lingham RB (1999) Structure and absolute stereochemistry of HIV-1 integrase inhibitor integric acid. A novel eremophilane sesquiterpenoid produced by a *Xylaria* sp. Tetrahedron Lett 40:8775
342. Srisapoomi T, Ichiyanagi T, Nakajima H, Aimi T, Boonlue S (2015) Biological activities of integric acid isolated from the wood-decay fungus *Xylaria feejeensis* 2FB-PPM08M. Chiang Mai J Sci 42:70
343. Srisapoomi T, Ichiyanagi T, Nakajima H, Aimi T, Boonlue S (2015) Biosynthesis of integric acid isolated from the wood-decay fungus *Xylaria feejeensis* 2FB-PPM08M. Curr Microbiol 70:550
344. Smith CJ, Morin NR, Bills GF, Dombrowski AW, Salituro GM, Smith SK, Zhao A, MacNeil DJ (2002) Novel sesquiterpenoids from the fermentation of *Xylaria persicaria* are selective ligands for the NPY Y5 receptor. J Org Chem 67:5001

345. Mierau V, Anke T, Sterner O (2003) Dacrymenone and VM 3298-2 – new antibiotics with antibacterial and antifungal activity. Z Naturforsch C 58:541
346. Isaka M, Chinthanom P, Boonruangprapa T, Rungjindamai N, Pinruan U (2010) Eremophilane-type sesquiterpenes from the fungus *Xylaria* sp. BCC 21097. J Nat Prod 73:683
347. Li YY, Hu ZY, Lu CH, Shen YM (2010) Four new terpenoids from *Xylaria* sp. 101. Helv Chim Acta 93:796
348. Isaka M, Srisanoh U, Sappan M, Kongthong S, Srikitikulchai P (2012) Eremophilane and eudesmane sesquiterpenoids and a pimarane diterpenoid from the wood-decay fungus *Xylaria* sp. BCC 5484. Phytochem Lett 5:78
349. Kawagishi H, Ishiyama D, Mori H, Sakamoto H, Ishiguro Y, Furukawa S, Li JX (1997) Dictyophorines A and B, two stimulators of NGF-synthesis from the mushroom *Dictyophora indusiata*. Phytochemistry 45:1203
350. Kodani S, Hayashi K, Hashimoto M, Kimura T, Dombo M, Kawagishi H (2009) New sesquiterpenoid from the mushroom *Sparassis crispa*. Biosci Biotechnol Biochem 73:228
351. Wang YQ, Yang XL, Bao L, Gao H, Yao XS, Liu HW (2012) Isolation and identification of secondary metabolites from the solid culture of *Flammulina velutipes*. Mycosystema 31:127
352. Song AR, Sun XL, Kong C, Zhao C, Qin D, Huang F, Yang S (2014) Discovery of a new sesquiterpenoid from *Phellinus ignarius* with antiviral activity against influenza virus. Arch Virol 159:753
353. Kuhnert E, Surup F, Wiebach V, Bernecker S, Stadler M (2015) Botryane, noreudesmane and abietane terpenoids from the ascomycete *Hypoxylon rickii*. Phytochemistry 117:116
354. Yang NN, Ma QY, Huang SZ, Dai HF, Guo ZK, XH L, Wang YG, ZF Y, Zhao YX (2015) Chemical constituents from cultures of the fungus *Marasmiellus ramealis* (Bull.) Singer. J Braz Chem Soc 26:9
355. Singh SB, Felock P, Hazuda DJ (2000) Chemical and enzymatic modifications of integric acid and HIV-1 integrase inhibitory activity. Bioorg Med Chem Lett 10:235
356. Stadler M, Anke T, Dasenbrock J, Steglich W (1993) Phellodonic acid, a new biologically-active hirsutane derivative from *Phellodon melaleucus* (Thelephoraceae, Basidiomycetes). Z Naturforsch C 48:545
357. Abraham WR, Abate D (1995) Chromanones from *Lentinus crinitus* (Basidiomycetes). Z Naturforsch C 50:748
358. Rukachaisirikul V, Tansakul C, Saithong S, Pakawatchai C, Isaka M, Suvannakad R (2005) Hirsutane sesquiterpenes from the fungus *Lentinus connatus* BCC 8996. J Nat Prod 68:1674
359. Yun BS, Lee IK, Cho Y, Cho SM, Yoo ID (2002) New tricyclic sesquiterpenes from the fermentation broth of *Stereum hirsutum*. J Nat Prod 65:786
360. Yoo NH, Kim JP, Yun BS, Ryoo IJ, Lee IK, Yoon ES, Koshino H, Yoo ID (2006) Hirsutenols D, E and F, new sesquiterpenes from the culture broth of *Stereum hirsutum*. J Antibiot 59:110
361. Birnbacher J, Schueffler A, Deininger F, Opatz T, Anke T (2008) Isolation and biological activity of new norhirsutanes from *Creolophus cirrhatus*. Z Naturforsch C 63:203
362. Opatz T, Kolshorn H, Birnbacher J, Schüffler A, Deininger F, Anke T (2007) The creolophins: a family of linear triquinanes from *Creolophus cirrhatus* (basidiomycete). Eur J Org Chem 2007:5546
363. Liermann JC, Schuffler A, Wollinsky B, Birnbacher J, Kolshorn H, Anke T, Opatz T (2010) Hirsutane-type sesquiterpenes with uncommon modifications from three Basidiomycetes. J Org Chem 75:2955
364. Asai R, Mitsuhashi S, Shigetomi K, Miyamoto T, Ubukata M (2011) Absolute configurations of (–)-hirsutanol A and (–)-hirsutanol C produced by *Gloeostereum incarnatum*. J Antibiot 64:693
365. Qi QY, Bao L, Ren JW, Han JJ, Zhang ZY, Li Y, Yao YJ, Cao R, Liu HW (2014) Sterhirsutins A and B, two new heterodimeric sesquiterpenes with a new skeleton from the culture of *Stereum hirsutum* collected in Tibet plateau. Org Lett 16:5092

366. Qi QY, Ren JW, Sun LW, He LW, Bao L, Yue W, Sun QM, Yao YJ, Yin WB, Liu HW (2015) Stucturally diverse sesquiterpenes produced by a Chinese Tibet fungus *Stereum hirsutum* and their cytotoxic and immunosuppressant activities. Org Lett 17:3098
367. Chen ZM, Chen HP, Wang F, Li ZH, Feng T, Liu JK (2015) New triquinane and gymnomitrane sesquiterpenes from fermentation of the basidiomycete *Antrodiella albocinnamomea*. Fitoterapia 102:61
368. Wang Y, Bao L, Liu D, Yang X, Li S, Gao H, Yao XS, Wen HA, Liu HW (2012) Two new sesquiterpenes and six norsesquiterpenes from the solid culture of the edible mushroom *Flammulina velutipes*. Tetrahedron 68:3012
369. Mehta G, Pallavi K (2006) Total synthesis of the putative structure of the novel triquinane based sesquiterpenoid natural product dichomitol. Tetrahedron Lett 47:8355
370. Yang JS, Wang YL, Feng XZ, Yu DQ, Liang XT (1991) Chemical constituents of *Armillaria mellea*. VII. Isolation and characterization of chemical constituents of the acetone extract. Acta Pharm Sin 26:117
371. Donnelly D, Sanada S, O'Reilly J, Polonky J, Prange T, Pascard C (1982) Isolation and structure (X-ray analysis) of the orsellinate of armillol, a new antibacterial metabolite from *Armillaria mellea*. J Chem Soc Chem Commun:135
372. Arnone A, Nasini G, Depava OV (1993) Isolation and structure elucidation of sulcatine G, a novel sesquiterpene from *Laurilia sulcata*. J Chem Soc Perkin Trans 1:2723
373. Arnone A, Nasini G, Depava OV, Assante G (1992) Isolation and structure elucidation of sulcatine C, sulcatine D and sulcatine E, novel norsesquiterpenes from *Laurilia sulcata*, and 7-*epi*-sulcatine D. J Chem Soc Perkin Trans 1:615
374. Momose I, Sekizawa R, Hosokawa N, Iinuma H, Matsui S, Nakamura H, Naganawa H, Hamada M, Takeuchi T (2000) Melleolides K, L and M, new melleolides from *Armillaria mellea*. J Antibiot 53:137
375. Rasser F, Anke T, Sterner O (2000) Secondary metabolites from a *Gloeophyllum* species. Phytochemistry 54:511
376. Clericuzio M, Mella M, Toma L, Finzi PV, Vidari G (2002) Atlanticones, new protoilludane sesquiterpenes from the mushroom *Lactarius atlanticus* (Basidiomycetes). Eur J Org Chem 2002:988
377. Arnone A, Candiani G, Nasini G, Sinisi R (2003) Isolation and structure elucidation of new sesquiterpenes of protoilludane origin from the fungus *Clavicorona divaricata*. Tetrahedron 59:5033
378. Arnone A, Gregorio DC, Meille SV, Nasini G, Sidoti G (1999) Tsugicoline E, a new polyoxygenated protoilludane sesquiterpene from the fungus *Laurilia tsugicola*. J Nat Prod 62:51
379. Hirota M, Shimizu Y, Kamo T, Makabe H, Shibata H (2003) New plant growth promoters, repraesentins A, B and C, from *Lactarius repraesentaneus*. Biosci Biotechnol Biochem 67:1597
380. Weber D, Erosa G, Sterner O, Anke T (2006) New bioactive sesquiterpenes from *Ripartites metrodii* and *R. tricholoma*. Z Naturforsch C 61:663
381. Yoshikawa K, Kaneko A, Matsumoto Y, Hama H, Arihara S (2006) Russujaponols A–F, illudoid sesquiterpenes from the fruiting body of *Russula japonica*. J Nat Prod 69:1267
382. Yoshikawa K, Matsumoto Y, Hama H, Tanaka M, Zhai HF, Fukuyama Y, Arihara S, Hashimoto T (2009) Russujaponols G-L, illudoid sesquiterpenes, and their neurite outgrowth promoting activity from the fruit body of *Russula japonica*. Chem Pharm Bull 57:311
383. Kogl M, Brecker L, Warrass R, Mulzer J (2008) Novel protoilludane lead structure for veterinary antibiotics: total synthesis of pasteurestins A and B and assignment of their configurations. Eur J Org Chem 16:2714
384. Tomio T, Hironobu I, Isao M, Susumu M (2002) New antibiotics pasteurestin A and B, and method for producing the same. Jap Pat 2002:212137
385. Misiek M, Williams J, Schmich K, Huttel W, Merfort I, Salomon CE, Aldrich CC, Hoffmeister D (2009) Structure and cytotoxicity of arnamial and related fungal sesquiterpene aryl esters. J Nat Prod 72:1888

386. Pettit GR, Meng YH, Pettit RK, Herald DL, Hogan F, Cichacz ZA (2010) Isolation and structure of a cyclobutane-type sesquiterpene cancer cell growth inhibitor from *Coprinus cinereus* (Coprinaceae). Bioorg Med Chem 18:4879
387. Yin X, Feng T, Liu JK (2012) Structures and cytotoxicities of three new sesquiterpenes from cultures of *Armillaria* sp. Nat Prod Bioprospect 2:245
388. Nord CL, Menkis A, Vasaitis R, Broberg A (2013) Protoilludane sesquiterpenes from the wood decomposing fungus *Granulobasidium vellereum* (Ellis & Cragin) Jülich. Phytochemistry 90:128
389. Nord CL, Menkis A, Lendel C, Vasaitis R, Broberg A (2014) Sesquiterpenes from the saprotrophic fungus *Granulobasidium vellereum* (Ellis & Cragin) Jülich. Phytochemistry 102:197
390. Chen CC, Kuo YH, Cheng JJ, Sung PH, Ni CL, Chen CC, Shen CC (2015) Three new sesquiterpene aryl esters from the mycelium of *Armillaria mellea*. Molecules 20:9994
391. Kobori H, Sekiya A, Suzuki T, Choi JH, Hirai H, Kawagishi H (2015) Bioactive sesquiterpene aryl esters from the culture broth of *Armillaria* sp. J Nat Prod 78:163
392. Yang XY, Li ZH, Dong ZJ, Feng T, Liu JK (2015) Three new sesquiterpenoids from cultures of the basidiomycete *Conocybe siliginea*. J Asian Nat Prod Res 17:1
393. Li Z, Wang Y, Jiang B, Li W, Zheng L, Yang X, Bao Y, Sun L, Huang Y, Li Y (2016) Structure, cytotoxic activity and mechanism of protoilludane sesquiterpene aryl esters from the mycelium of *Armillaria mellea*. J Ethnopharmacol 184:119
394. Bohnert M, Nutzmann HW, Schroeckh V, Horn F, Dahse HM, Brakhage AA, Hoffmeister D (2014) Cytotoxic and antifungal activities of melleolide antibiotics follow dissimilar structure-activity relationships. Phytochemistry 105:101
395. Misiek M, Hoffmeister D (2008) Processing sites involved in intron splicing of *Armillaria* natural product genes. Mycol Res 112:216
396. Bohnert M, Scherer O, Wiechmann K, Konig S, Dahse HM, Hoffmeister D, Werz O (2014) Melleolides induce rapid cell death in human primary monocytes and cancer cells. Bioorg Med Chem 22:3856
397. Lackner G, Bohnert M, Wick J, Hoffmeister D (2013) Assembly of melleolide antibiotics involves a polyketide synthase with cross-coupling activity. Chem Biol 20:1101
398. Wick J, Heine D, Lackner G, Misiek M, Tauber J, Jagusch H, Hertweck C, Hoffmeister D (2016) A fivefold parallelized biosynthetic process secures chlorination of *Armillaria mellea* (honey mushroom) toxins. Appl Environ Microbiol 82:1196
399. Mehta G, Sreenivas K (2001) Total synthesis of the novel tricyclic sesquiterpene sulcatine G. Chem Commun:1892
400. Mehta G, Sreenivas K (2002) Enantioselective total synthesis of the novel tricyclic sesquiterpene (–)-sulcatine G. Absolute configuration of the natural product. Tetrahedron Lett 43:3319
401. Taber DF, Frankowski KJ (2005) Synthesis of (+)-sulcatine G. J Org Chem 70:6417
402. Chang EL, Bolte B, Lan P, Willis AC, Banwell MG (2016) Chemoenzymatic total syntheses of the enantiomers of the protoilludanes 8-deoxydihydrotsugicoline and radudiol. J Org Chem 81:2078
403. Schwartz BD, Matousova E, White R, Banwell MG, Willis AC (2013) A chemoenzymatic total synthesis of the protoilludane aryl ester (+)-armillarivin. Org Lett 15:1934
404. Bohnert M, Miethbauer S, Dahse HM, Ziemen J, Nett M, Hoffmeister D (2011) In vitro cytotoxicity of melleolide antibiotics: structural and mechanistic aspects. Bioorg Med Chem Lett 21:2003
405. Liu LY, Li ZH, Dong ZJ, Li XY, Su J, Li Y, Liu JK (2012) Two novel fomannosane-type sesquiterpenoids from the culture of the basidiomycete *Agrocybe salicacola*. Nat Prod Bioprospect 2:130
406. Rasser F, Anke T, Sterner O (2002) Terpenoids from *Bovista* sp. 96042. Tetrahedron 58:7785
407. del Val AG, Platas G, Arenal F, Orihuela JC, Garcia M, Hernandez P, Royo I, De Pedro N, Silver LL, Young K, Vicente MF, Pelaez F (2003) Novel illudins from *Coprinopsis episcopalis* (syn. *Coprinus episcopalis*), and the distribution of illudin-like compounds among filamentous fungi. Mycol Res 107:1201

408. Reina M, Orihuela JC, González-Coloma A, de Inés C, de la Cruz M, del Val AG, Torno JR, Fraga BM (2004) Four illudane sesquiterpenes from *Coprinopsis episcopalis*. Phytochemistry 65:381
409. Ma WZ, Huang YC, Lin LD, Zhu XF, Chen YZ, Xu HH, Wei XY (2004) Two new biologically active illudane sesquiterpenes from the mycelial cultures of *Panaeolus redrugis*. J Antibiot 57:721
410. Zhu YC, Wang G, Yang XL, Luo DQ, Zhu QC, Peng T, Liu JK (2010) Agrocybone, a novel bis-sesquiterpene with a spirodienone structure from basidiomycete *Agrocybe salicacola*. Tetrahedron Lett 51:3443
411. Liu LY, Zhang L, Feng T, Li ZH, Dong ZJ, Li XY, Su J, Li Y, Liu JK (2011) Unusual illudin-type sesquiterpenoids from cultures of *Agrocybe salicacola*. Nat Prod Bioprospect 1:87
412. Wang G, Liu LY, Zhu YC, Liu JK (2011) Illudin T, a new sesquiterpenoid from basidiomycete *Agrocybe salicacola*. J Asian Nat Prod Res 13:430
413. He JB, Tao J, Miao XS, Feng YP, Bu W, Dong ZJ, Li ZH, Feng T, Liu JK (2015) Two new illudin type sesquiterpenoids from cultures of *Phellinus tuberculosus* and *Laetiporus sulphureus*. J Asian Nat Prod Res 17:1054
414. Nord C, Menkis A, Broberg A (2015) Cytotoxic illudane sesquiterpenes from the fungus *Granulobasidium vellereum* (Ellis & Cragin) Jülich. J Nat Prod 78:2559
415. Kokubun T, Scott-Brown A, Kite GC, Simmonds MSJ (2016) Protoilludane, illudane, illudalane, and norilludane sesquiterpenoids from *Granulobasidium vellereum*. J Nat Prod 79:1698
416. Suzuki S, Murayama T, Shiono Y (2005) Illudalane sesquiterpenoids, echinolactones A and B, from a mycelial culture of *Echinodontium japonicum*. Phytochemistry 66:2329
417. Isaka M, Srisanoh U, Choowong W, Boonpratuang T (2011) Sterostreins A–E, new terpenoids from cultures of the basidiomycete *Stereum ostrea* BCC 22955. Org Lett 13:4886
418. Tian MQ, Liu R, Li JF, Zhang KQ, Li GH (2016) Three new sesquiterpenes from the fungus *Stereum* sp. YMF1.1686. Phytochem Lett 15:186
419. Li JF, Qin YK, Tian MQ, Zhang KQ, Li GH (2014) Two new sesquiterpenes from the fungus *Stereum* sp. NN048997. Phytochem Lett 10:32
420. Becker U, Erkel G, Anke T, Sterner O (1997) Puraquinonic acid, a novel inducer of differentiation of human HL-60 promyelocytic leukemia cells from *Mycena pura* (Pers. ex Fr.) Nat Prod Lett 9:229
421. Anchel M, Hervey A, Robbins WJ (1950) Antibiotic substances from Basidiomycetes. VII. *Clitocybe illudens*. Proc Natl Acad Sci U S A 36:300
422. Lehmann VKB, Huang A, Ibanez-Calero S, Wilson GR, Rinehart KL (2003) Illudin S, the sole antiviral compound in mature fruiting bodies of *Omphalotus illudens*. J Nat Prod 66:1257
423. McMorris TC (1999) Discovery and development of sesquiterpenoid derived hydroxymethylacylfulvene: a new anticancer drug. Bioorg Med Chem 7:881
424. Tanasova M, Sturla SJ (2012) Chemistry and biology of acylfulvenes: sesquiterpene-derived antitumor agents. Chem Rev 112:3578
425. McMorris TC, Chimmani R, Alisala K, Staake MD, Banda G, Kelner MJ (2010) Structure-activity studies of urea, carbamate, and sulfonamide derivatives of acylfulvene. J Med Chem 53:1109
426. Staake MD, Kashinatham A, McMorris TC, Estes LA, Kelner MJ (2016) Hydroxyurea derivatives of irofulven with improved antitumor efficacy. Bioorg Med Chem Lett 26:1836
427. Gong JC, Neels JF, Yu X, Kensler TW, Peterson LA, Sturla SJ (2006) Investigating the role of stereochemistry in the activity of anticancer acylfulvenes: synthesis, reductase-mediated bioactivation, and cellular toxicity. J Med Chem 49:2593
428. McMorris TC, Staake MD, Kelner MJ (2004) Synthesis and biological activity of enantiomers of antitumor irofulven. J Org Chem 69:619
429. Movassaghi M, Piizzi G, Siegel DS, Piersanti G (2006) Enantioselective total synthesis of (–)-acylfulvene and (–)-irofulven. Angew Chem Int Ed 45:5859

430. Siegel DS, Piizzi G, Piersanti G, Movassaghi M (2009) Enantioselective total synthesis of (–)-acylfulvene and (–)-irofulven. J Org Chem 74:9292
431. Nord CL, Menkis A, Broberg A (2014) Cytotoxic illudalane sesquiterpenes from the wood-decay fungus *Granulobasidium vellereum* (Ellis & Cragin) Jülich. Molecules 19:14195
432. Nair MSR, Takeshita H, McMorris TC, Anchel M (1969) Metabolites of *Clitocybe illudens*. IV. Illudalic acid, a sesquiterpenoid, and illudinine, a sesquiterpenoid alkaloid. J Org Chem 34:240
433. Yan YJ, Yang J, Yu ZY, Yu MM, Ma YT, Wang L, Su C, Luo JY, Horsman GP, Huang SX (2016) Non-enzymatic pyridine ring formation in the biosynthesis of the rubrolone tropolone alkaloids. Nat Commun 7:13083
434. Clive DLJ, Sannigrahi M, Hisaindee S (2001) Synthesis of (±)-puraquinonic acid: an inducer of cell differentiation. J Org Chem 66:954
435. Clive DLJ, Yu ML (2002) Synthesis of (+)-puraquinonic acid. Chem Commun:2380
436. Clive DLJ, Yu ML, Sannigrahi M (2004) Synthesis of optically pure (+)-puraquinonic acid and assignment of absolute configuration to natural (–)-puraquinonic acid. Use of radical cyclization for asymmetric generation of a quaternary center. J Org Chem 69:4116
437. Hisaindee S, Clive DLJ (2001) A synthesis of puraquinonic acid. Tetrahedron Lett 42:2253
438. Kraus GA, Choudhury PK (2002) Synthesis of puraquinonic acid ethyl ester and deliquinone via a common intermediate. J Org Chem 67:5857
439. Tiong EA, Rivalti D, Williams BM, Gleason JL (2013) A concise total synthesis of (*R*)-puraquinonic acid. Angew Chem Int Ed 52:3442
440. Suresh M, Kumar N, Veeraraghavaiah G, Hazra S, Singh RB (2016) Total synthesis of coprinol. J Nat Prod 79:2740
441. Daniewski WM, Gumuika M, Skibicki P, Anczewski W, Jacobsson U, Norin T (1994) New constituents of *Lactarius vellereus*. Nat Prod Lett 5:123
442. Yaoita Y, Machida K, Kikuchi M (1999) Structures of new marasmane sesquiterpenoids from *Lactarius piperatus* (Scop. ex Fr.) SF Gray. Chem Pharm Bull 47:894
443. Wang XN, Wang F, JC D, Ge HM, Tan RX, Liu JK (2005) A new marasmane sesquiterpene from the basidiomycete *Russula foetens*. Z Naturforsch B 60:1065
444. Wang XN, Shen JH, MC D, Liu JK (2006) Marasmane sesquiterpenes isolated from *Russula foetens*. J Antibiot 59:669
445. Shao HJ, Wang CJ, Dai Y, Wang F, Yang WQ, Liu JK (2007) Pubescenone, a new marasmane sesquiterpenoid from the mushroom *Lactarius pubescens*. Heterocycles 71:1135
446. Kim KH, Noh HJ, Choi SU, Park KM, Seok SJ, Lee KR (2010) Russulfoen, a new cytotoxic marasmane sesquiterpene from *Russula foetens*. J Antibiot 63:575
447. Pang ZJ, Bocchio F, Sterner O (1992) The isolation of a new lactarane furan from injured fruit bodies of *Lentinellus cochleatus*. Nat Prod Lett 1:65
448. Kobata K, Kano S, Shibata H (1995) New lactarane sesquiterpenoid from the fungus *Russula emetica*. Biosci Biotechnol Biochem 59:316
449. Luo DQ, Wang F, Bian XY, Liu JK (2005) Rufuslactone, a new antifungal sesquiterpene from the fruiting bodies of the basidiomycete *Lactarius rufus*. J Antibiot 58:456
450. Kamo T, Matsue M, Kashiwabara M, Hirota M (2006) 1,2-Dehydrolactarolide A, a new plant growth regulatory lactarane sesquiterpene from *Lactarius vellereus*. Biosci Biotechnol Biochem 70:2307
451. Luo DQ, Zhao LY, Shi YL, Tang HL, Li YY, Yang LM, Zheng YT, Zhu HJ, Liu JK (2009) Velleratretraol, an unusual highly functionalized lactarane sesquiterpene from *Lactarius vellereus*. J Antibiot 62:129
452. Kim KH, Noh HJ, Choi SU, Park KM, Seok SJ, Lee KR (2010) Lactarane sesquiterpenoids from *Lactarius subvellereus* and their cytotoxicity. Bioorg Med Chem Lett 20:5385
453. Yaoita Y, Hirao M, Kikuchi M, Machida K (2012) Three new lactarane sesquiterpenoids from the mushroom *Russula sanguinea*. Nat Prod Commun 7:1133
454. Malagon O, Porta A, Clericuzio M, Gilardoni G, Gozzini D, Vidari G (2014) Structures and biological significance of lactarane sesquiterpenes from the European mushroom *Russula nobilis*. Phytochemistry 107:126

455. Hiramatsu F, Murayama T, Koseki T, Shiono Y (2008) A new secolactarane-type sesquiterpene from *Strobilurus tephanocystis*. Nat Prod Res 22:1007
456. Froborg J, Magnusson G (1978) On the biogenetic interrelationship between the marsmane- and vellerane sesquiterpene skeletons. Tetrahedron 34:2027
457. Gilardoni G, Malagon O, Tosi S, Clericuzio M, Vidari G (2014) Lactarane sesquiterpenes from the European mushrooms *Lactarius aurantiacus*, *L. subdulcis*, and *Russula sanguinaria*. Nat Prod Commun 9:319
458. Schuffler A, Wollinsky B, Anke T, Liermann JC, Opatz T (2012) Isolactarane and sterpurane sesquiterpenoids from the basidiomycete *Phlebia uda*. J Nat Prod 75:1405
459. Erkel G, Anke T, Velten R, Gimenez A, Steglich W (1994) Hyphodontal, a new antifungal inhibitor of reverse transcriptases from *Hyphodontia* sp. (Corticiaceae, Basidiomycetes). Z Naturforsch C 49:561
460. Opatz T, Kolshorn H, Anke H (2008) Sterelactones: new isolactarane type sesquiterpenoids with antifungal activity from *Stereum* sp. IBWF 01060. J Antibiot 61:563
461. Ayer WA, Cruz ER (1993) The tremulanes, a new group of sesquiterpenes from the aspen rotting fungus *Phellinus tremulae*. J Org Chem 58:7529
462. Yin RH, Zhao ZZ, Chen HP, Yin X, Ji X, Dong ZJ, Li ZH, Feng T, Liu JK (2014) Tremulane sesquiterpenes from cultures of the fungus *Phellinus igniarius* and their vascular-relaxing activities. Phytochem Lett 10:300
463. Liu DZ, Wang F, Liu JK (2007) Sesquiterpenes from cultures of the basidiomycete *Conocybe siliginea*. J Nat Prod 70:1503
464. Zhou ZY, Tang JG, Wang F, Dong ZJ, Liu JK (2008) Sesquiterpenes and aliphatic diketones from cultures of the basidiomycete *Conocybe siliginea*. J Nat Prod 71:1423
465. Wu XL, Lin S, Zhu CG, Yue ZG, Yu Y, Zhao F, Liu B, Dai JG, Shi JG (2010) Homo- and heptanor-sterols and tremulane sesquiterpenes from cultures of *Phellinus igniarius*. J Nat Prod 73:1294
466. Yang XY, Feng T, Yin X, Li ZH, Zhang L, Liu JK (2012) Seven new sesquiterpenes from cultures of the basidiomycete *Conocybe siliginea*. Chin J Chem 30:1231
467. Yang XY, Feng T, Ding JH, Yin X, Guo H, Li ZH, Liu JK (2013) Five new 5,6-*seco*-tremulane sesquiterpenoids from the basidiomycete *Conocybe siliginea*. Nat Prod Bioprospect 3:48
468. Ding JH, Feng T, Cui BK, Wei K, Li ZH, Liu JK (2013) Novel sesquiterpenoids from cultures of the basidiomycete *Irpex lacteus*. Tetrahedron Lett 54:2651
469. Isaka M, Palasarn S, Supothina S, Srichomthong K, Choeyklin R (2016) *seco*-Tremulanes from cultures of the basidiomycete *Flavodon flavus* BCC 17421. Helv Chim Acta 99:232
470. Anke T, Watson WH, Giannetti BM, Steglich W (1981) The alliacols A and B from *Marasmius alliaceus* (Jacq. ex Fr.) Fr. J Antibiot 34:1271
471. Ayer WA, Shan RD, Trifonov LS, Hutchison LJ (1998) Sesquiterpenes from the nematicidal fungus *Clitocybula oculus*. Phytochemistry 49:589
472. Tao QQ, Ma K, Bao L, Wang K, Han JJ, Zhang JX, Huang CY, Liu HW (2016) New sesquiterpenoids from the edible mushroom *Pleurotus cystidiosus* and their inhibitory activity against $\alpha$-glucosidase and PTP1B. Fitoterapia 111:29
473. Jiang MY, Yang XL, Fang LZ, Dong ZJ, Liu JK (2008) Purpuracolide: a new alliacane sesquiterpene from the basidiomycete *Gomphus purpuraceus*. Z Naturforsch B 63:1012
474. Qin XD, Shao HJ, Dong ZJ, Liu JK (2008) Six new induced sesquiterpenes from the cultures of ascomycete *Daldinia concentrica*. J Antibiot 61:556
475. Feng T, Li ZH, Dong ZJ, Su J, Li Y, Liu JK (2011) Non-isoprenoid botryane sesquiterpenoids from basidiomycete *Boletus edulis* and their cytotoxic activity. Nat Prod Bioprospect 1:29
476. Liu DZ, Jia RR, Wang F, Liu JK (2008) A new spiroaxane sesquiterpene from cultures of the basidiomycete *Pholiota adiposa*. Z Naturforsch B 63:111
477. Wang SR, Zhang L, Chen HP, Li ZH, Dong ZJ, Wei K, Liu JK (2015) Four new spiroaxane sesquiterpenes and one new rosenonolactone derivative from cultures of basidiomycete *Trametes versicolor*. Fitoterapia 105:127

478. Tao QQ, Ma K, Yang YL, Wang K, Chen BS, Huang Y, Han JJ, Bao L, Liu XB, Yang ZL, Yin WB, Liu HW (2016) Bioactive sesquiterpenes from the edible mushroom *Flammulina velutipes* and their biosynthetic pathway confirmed by genome analysis and chemical evidence. J Org Chem 81:9867
479. Fogedal M, Norberg T (1986) Deoxycollybolidol, a sesquiterpene from *Collybia peronata*. Phytochemistry 25:2661
480. Dörfelt H, Schlegel B, Gräfe U (2000) Dictyopanines A, B and C, new bicyclic sesquiterpene esters from *Dicotyopanus* sp. HKI 0181. J Antibiot 53:839
481. Eilbert F, Engler-Lohr M, Anke H, Sterner O (2000) Bioactive sesquiterpenes from the basidiomycete *Resupinatus leightonii*. J Nat Prod 63:1286
482. Yaoita Y, Ono H, Kikuchi M (2003) A new norsesquiterpenoid from *Russula delica* Fr. Chem Pharm Bull 51:1003
483. Li GH, Zhang KQ (2005) A novel sesquiterpene isolated from *Stereum* sp. 8954. Chin Chem Lett 16:1615
484. Li GH, Liu FF, Shen L, Zhu HJ, Zhang KQ (2011) Stereumins H–J, stereumane-type sesquiterpenes from the fungus *Stereum* sp. J Nat Prod 74:296
485. Liu DZ, Wang F, Jia RR, Liu JK (2008) A novel sesquiterpene from the basidiomycete *Boletus calopus*. Z Naturforsch B 63:114
486. Luo DQ, Liang SJ, Shi YL, Tang HL (2009) Mitissimolone, a new sesquiterpene with a novel carbon skeleton from the basidiomycete *Lactarius mitissimus*. Helv Chim Acta 92:2082
487. Liu DZ, Dong ZJ, Wang F, Liu JK (2010) Two novel norsesquiterpene peroxides from basidiomycete *Steccherinum ochraceum*. Tetrahedron Lett 51:3152
488. Liu DZ, Luo MH (2010) Two new chamigrane metabolites from fermentation broth of *Steccherinum ochraceum*. Fitoterapia 81:1205
489. Ding JH, Feng T, Li ZH, Yang XY, Guo H, Yin X, Wang GQ, Liu JK (2012) Trefolane A, a sesquiterpenoid with a new skeleton from cultures of the basidiomycete *Tremella foliacea*. Org Lett 14:4976
490. Yang XY, Feng T, Li ZH, Sheng Y, Yin X, Leng Y, Liu JK (2012) Conosilane A, an unprecedented sesquiterpene from the cultures of basidiomycete *Conocybe siliginea*. Org Lett 14:5382
491. Huang SC, Kuo PC, Hwang TL, Chan YY, Chen CH, TS W (2013) Three novel sesquiterpenes from the mycelium of *Phellinus linteus*. Tetrahedron Lett 54:3332
492. Sun YS, Zhao Z, Feng QS, Xu QQ, Lu LX, Liu JK, Zhang L, Wu B, Li YQ (2013) Unusual spirodecane sesquiterpenes and a fumagillol analogue from *Cordyceps ophioglossoides*. Helv Chim Acta 96:76
493. Fan QY, Dong ZJ, Li ZH, Yin X, Yang XY, Feng T, Wei K, Liu JK, Zhao BH (2014) Two new ylangene-type sesquiterpenoids from cultures of the fungus *Postia* sp. J Asian Nat Prod Res 16:254
494. Hu DB, Zhang S, He JB, Dong ZJ, Li ZH, Feng T, Liu JK (2015) Brasilane sesquiterpenoids and alkane derivatives from cultures of the basidiomycete *Coltricia sideroides*. Fitoterapia 104:50
495. Pham TB, Descoutures D, Nguyen HD, Nguyen PDN, Nguyen TD (2015) A new cytotoxic gymnomitrane sesquiterpene from *Ganoderma lucidum* fruiting bodies. Nat Prod Commun 10:1911
496. Otto A, Porzel A, Schmidt J, Wessjohann L, Arnold N (2014) Penarines A-F, (*nor*-)sesquiterpene carboxylic acids from *Hygrophorus penarius* (Basidiomycetes). Phytochemistry 108:229
497. Surup F, Kuhnert E, Liscinskij E, Stadler M (2015) Silphiperfolene-type terpenoids and other metabolites from cultures of the tropical Ascomycete *Hypoxylon rickii* (Xylariaceae). Nat Prod Bioprospect 5:167
498. Sun YS, Lv LX, Zhao Z, He X, You L, Liu JK, Li YQ (2014) Cordycepol C induces caspase-independent apoptosis in human hepatocellular carcinoma HepG2 cells. Biol Pharm Bull 37:608

499. Ma BJ, Shen JW, Yu HY, Ruan Y, Wu TT, Zhao X (2010) Hericenones and erinacines: stimulators of nerve growth factor (NGF) biosynthesis in *Hericium erinaceus*. Mycology 1:92
500. Shen JW, Ruan Y, Ma BJ (2009) Diterpenoids of macromycetes. J Basic Microbiol 49:242
501. Kenmoku H, Tanaka K, Okada K, Kato N, Sassa T (2004) Erinacol (cyatha-3,12-dien-14$\beta$-ol) and 11-*O*-acetylcyathin $A_3$, new cyathane metabolites from an erinacine Q-producing *Hericium erinaceum*. Biosci Biotechnol Biochem 68:1786
502. Kawagishi H, Shimada A, Shirai R, Okamoto K, Ojima F, Sakamoto H, Ishiguro Y, Furukawa S (1994) Erinacine A, erinacine B and erinacine C, strong stimulators of nerve growth-factor (NGF)-synthesis, from the mycelia of *Hericium erinaceum*. Tetrahedron Lett 35:1569
503. Shimbo M, Kawagishi H, Yokogoshi H (2005) Erinacine A increases catecholamine and nerve growth factor content in the central nervous system of rats. Nutr Res 25:617
504. Shiono Y, Hiramatsu F, Murayama T, Koseki T, Funakoshi T (2008) Two cyathane-type diterpenoids from the liquid culture of *Strobilurus tenacellus*. Chem Biodivers 5:1811
505. Fang ST, Feng T, Zhang L, Dong ZJ, Li ZH, Liu JK (2011) Cyathane diterpenoids from fruiting bodies of *Phellodon niger*. Nat Prod Bioprospect 1:37
506. Liu L, Shi XW, Zong SC, Tang JJ, Gao JM (2012) Scabronine M, a novel inhibitor of NGF-induced neurite outgrowth from PC12 cells from the fungus *Sarcodon scabrosus*. Bioorg Med Chem Lett 22:2401
507. Ma BJ, TT W, Ruan Y, Shen JW, Zhou H, HY Y, Zhao X (2010) Antibacterial and antifungal activity of scabronine G and H in vitro. Mycology 1:200
508. Shi XW, Liu L, Gao JM, Zhang AL (2011) Cyathane diterpenes from Chinese mushroom *Sarcodon scabrosus* and their neurite outgrowth-promoting activity. Eur J Med Chem 46:3112
509. Shi XW, Zhang AL, Pescitelli G, Gao JM (2012) Secoscabronine M, a novel diterpenoid from the Chinese bitter mushroom *Sarcodon scabrosus*. Chirality 24:386
510. Marcotullio MC, Rosati O, Maltese F, Messina F (2013) Cyrneine E, a new cyathane diterpene from *Sarcodon cyrneus*. Rec Nat Prod 7:239
511. Han JJ, Chen YH, Bao L, Yang XL, Liu DL, Li SJ, Zhao F, Liu HW (2013) Anti-inflammatory and cytotoxic cyathane diterpenoids from the medicinal fungus *Cyathus africanus*. Fitoterapia 84:22
512. Han JJ, Zhang L, JK X, Bao L, Zhao F, Chen YH, Zhang WK, Liu HW (2015) Three new cyathane diterpenoids from the medicinal fungus *Cyathus africanus*. J Asian Nat Prod Res 17:541
513. He LW, Han JJ, Li BW, Huang L, Ma K, Chen Q, Liu XZ, Bao L, Liu HW (2016) Identification of a new cyathane diterpene that induces mitochondrial and autophagy-dependent apoptosis and shows a potent in vivo anti-colorectal cancer activity. Eur J Med Chem 111:183
514. Xu ZY, Yan S, Bi KS, Han JJ, Chen YH, Wu ZA, Chen YH, Liu HW (2013) Isolation and identification of a new anti-inflammatory cyathane diterpenoid from the medicinal fungus *Cyathus hookeri* Berk. Fitoterapia 86:159
515. Wang BT, Han JJ, Xu W, Chen YH, Liu HW (2014) Production of bioactive cyathane diterpenes by a bird's nest fungus *Cyathus gansuensis* growing on cooked rice. Food Chem 152:169
516. Bai R, Zhang CC, Yin X, Wei J, Gao JM (2015) Striatoids A–F, cyathane diterpenoids with neurotrophic activity from cultures of the fungus *Cyathus striatus*. J Nat Prod 78:783
517. Zhang Z, Liu RN, Tang QJ, Zhang JS, Yang Y, Shang XD (2015) A new diterpene from the fungal mycelia of *Hericium erinaceus*. Phytochem Lett 11:151
518. Mudalungu CM, Richter C, Wittstein K, Abdalla MA, Matasyoh JC, Stadler M, Süssmuth RD (2016) Laxitextines A and B, cyathane xylosides from the tropical fungus *Laxitextum incrustatum*. J Nat Prod 79:894
519. Kuo HC, Lu CC, Shen CH, Tung SY, Hsieh MC, Lee KC, Lee LY, Chen CC, Teng CC, Huang WS, Chen TC, Lee KF (2016) *Hericium erinaceus* mycelium and its isolated erinacine

A protection from MPTP-induced neurotoxicity through the ER stress, triggering an apoptosis cascade. J Transl Med 14:78
520. Lee KC, Kuo HC, Shen CH, Lu CC, Huang WS, Hsieh MC, Huang CY, Kuo Y, Hsieh YY, Teng CC, Lee LY, Tung SY (2016) A proteomics approach to identifying novel protein targets involved in erinacine A-mediated inhibition of colorectal cancer cells' aggressiveness. J Cell Mol Med 21:588
521. Lee KF, Chen JH, Teng CC, Shen CH, Hsieh MC, Lu CC, Lee KC, Lee LY, Chen WP, Chen CC, Huang WS, Kuo HC (2014) Protective effects of *Hericium erinaceus* mycelium and its isolated erinacine A against ischemia-injury-induced neuronal cell death via the inhibition of iNOS/p38 MAPK and nitrotyrosine. Int J Mol Sci 15:15073
522. Li IC, Chen YL, Lee LY, Chen WP, Tsai YT, Chen CC, Chen CS (2014) Evaluation of the toxicological safety of erinacine A-enriched *Hericium erinaceus* in a 28-day oral feeding study in Sprague-Dawley rats. Food Chem Toxicol 70:61
523. Lu CC, Huang WS, Lee KF, Lee KC, Hsieh MC, Huang CY, Lee LY, Lee BO, Teng CC, Shen CH, Tung SY, Kuo HC (2016) Inhibitory effect of erinacine A on the growth of DLD-1 colorectal cancer cells is induced by generation of reactive oxygen species and activation of p70s6K and p21. J Funct Foods 21:474
524. Tzeng TT, Chen CC, Lee LY, Chen WP, Lu CK, Shen CC, Huang FCY, Chen CC, Shiao YJ (2016) Erinacine A-enriched *Hericium erinaceus* mycelium ameliorates Alzheimer's disease-related pathologies in APPswe/PS1dE9 transgenic mice. J Biomed Sci 23:49
525. Kim K, Cha JK (2009) Total synthesis of cyathin $A_3$ and cyathin $B_2$. Angew Chem Int Ed 48:5334
526. Ward DE, Shen JH (2007) Enantioselective total synthesis of cyathin $A_3$. Org Lett 9:2843
527. Kobayakawa Y, Nakada M (2013) Total syntheses of (–)-scabronines G and A, and (–)-episcabronine A. Angew Chem Int Ed 52:7569
528. Waters SP, Tian Y, Li YM, Danishefsky SJ (2005) Total synthesis of (–)-scabronine G, an inducer of neurotrophic factor production. J Am Chem Soc 127:13514
529. Watanabe H, Nakada M (2008) Biomimetic total synthesis of (–)-erinacine E. J Am Chem Soc 130:1150
530. Kobayakawa Y, Nakada M (2014) Enantioselective total synthesis of (–)-cyathin $B_2$. J Antibiot 67:483
531. Nakada M (2014) Enantioselective total syntheses of cyathane diterpenoids. Chem Rec 14:641
532. Liu R, Liu JK (2009) A new neodolastane diterpene from cultures of the basidiomycete *Trametes corrugata*. Heterocycles 78:2565
533. Ju YM, Wang GJ, Chen CY, Tsau YJ, Chou CH, Lee TH (2010) Chemical constituents from fermented broth and mycelium of the basidiomycete *Lacrymaria velutina*. Bot Stud 51:311
534. Liu YZ, Lu CH, Shen YM (2014) Guanacastane-type diterpenoids from *Coprinus plicatilis*. Phytochem Lett 7:161
535. Liu YZ, Li YY, Ou YX, Xiao SY, Lu CH, Zheng ZH, Shen YM (2012) Guanacastane-type diterpenoids with cytotoxic activity from *Coprinus plicatilis*. Bioorg Med Chem Lett 22:5059
536. Yin X, Feng T, Li ZH, Leng Y, Liu JK (2014) Five new guanacastane-type diterpenes from cultures of the fungus *Psathyrella candolleana*. Nat Prod Bioprospect 4:149
537. Brummond KM, Gao D (2003) Unique strategy for the assembly of the carbon skeleton of guanacastepene A using an allenic Pauson-Khand-type reaction. Org Lett 5:3491
538. Gampe CM, Carreira EM (2011) Total syntheses of guanacastepenes N and O. Angew Chem Int Ed 50:2962
539. Iimura S, Overman LE, Paulini R, Zakarian A (2006) Enantioselective total synthesis of guanacastepene N using an uncommon 7-*endo* Heck cyclization as a pivotal step. J Am Chem Soc 128:13095
540. Miller AK, Hughes CC, Kennedy-Smith JJ, Gradl SN, Trauner D (2006) Total synthesis of (–)-heptemerone B and (–)-guanacastepene E. J Am Chem Soc 128:17057

541. Shiono Y, Motoki S, Koseki T, Murayama T, Tojima M, Kimura K (2009) Isopimarane diterpene glycosides, apoptosis inducers, obtained from fruiting bodies of the ascomycete *Xylaria polymorpha*. Phytochemistry 70:935
542. Shiono Y, Matsui N, Imaizumi T, Koseki T, Murayama T, Kwon E, Abe T, Kimura KI (2013) An unusual spirocyclic isopimarane diterpenoid and other isopimarane diterpenoids from fruiting bodies of *Xylaria polymorpha*. Phytochem Lett 6:439
543. Isaka M, Yangchum A, Auncharoen P, Srichomthong K, Srikitikulchai P (2011) Ring B aromatic norpimarane glucoside from a *Xylaria* sp. J Nat Prod 74:300
544. Xu PP, You HC, Hu ZY, Li YY, Shen YM (2013) Two new pimarane-type diterpenes from the metabolites of *Xylaria* sp. 290. Chin J Org Chem 33:2618
545. Schneider G, Anke H, Sterner O (1995) Xylarin, an antifungal *Xylaria* metabolite with an unusual tricyclic uronic acid moiety. Nat Prod Lett 7:309
546. Chang YC, Lu CK, Chiang YR, Wang GJ, Ju YM, Kuo YH, Lee TH (2014) Diterpene glycosides and polyketides from *Xylotumulus gibbisporus*. J Nat Prod 77:751
547. Kavanagh F, Hervey A, Robbins WJ (1951) Antibiotic substances from Basidiomycetes VIII. *Pleurotus multilus* (Fr.) Sacc. and *Pleurotus passeckerianus* Pilat. Proc Natl Acad Sci U S A 37:570
548. Novak R (2011) Are pleuromutilin antibiotics finally fit for human use? Ann N Y Acad Sci 1241:71
549. Wang XY, Ling Y, Wang H, Yu JH, Tang JM, Zheng H, Zhao X, Wang DG, Chen GT, Qiu WQ, Tao JH (2012) Novel pleuromutilin derivatives as antibacterial agents: synthesis, biological evaluation and molecular docking studies. Bioorg Med Chem Lett 22:6166
550. Fu LQ, Ling CY, Guo XS, He HL, Yang YS (2012) Synthesis and antibacterial activity of pleuromutilin derivatives with novel C(14) side chain. Chin Chem Lett 23:9
551. Ling CY, Fu LQ, Gao S, Chu WJ, Wang H, Huang YQ, Chen XY, Yang YS (2014) Design, synthesis, and structure-activity relationship studies of novel thioether pleuromutilin derivatives as potent antibacterial agents. J Med Chem 57:4772
552. Lotesta SD, Liu JJ, Yates EV, Krieger I, Sacchettini JC, Freundlich JS, Sorensen EJ (2011) Expanding the pleuromutilin class of antibiotics by de novo chemical synthesis. Chem Sci 2:1258
553. Bailey AM, Alberti F, Kilaru S, Collins CM, De Mattos-Shipley K, Hartley AJ, Hayes P, Griffin A, Lazarus CM, Cox RJ, Willis CL, O'Dwyer K, Spence DW, Foster GD (2016) Identification and manipulation of the pleuromutilin gene cluster from *Clitopilus passeckerianus* for increased rapid antibiotic production. Sci Rep 6:25202
554. Knauseder F, Brandl E (1976) Pleuromutilins – fermentation, structure and biosynthesis. J Antibiot 29:125
555. Boeck LD, Reynolds PA, Wetzel RW (1981) Regulation of the A40104 fermentation-production of A40104A, a pleuromutilin glycoside antibiotic. In: Vezina C, Singh K (eds) Fermentation Products. Pergamon, Willowdale, Ont, Canada, p 187
556. Wang Y, Wang SJ, Mo SY, Li SH, Yang YC, Shi JG (2006) An abietane diterpene and a sterol from fungus *Phellinus igniarius*. Chin Chem Lett 17:481
557. Jang HJ, Yang KS (2011) Inhibition of nitric oxide production in RAW 264.7 macrophages by diterpenoids from *Phellinus pini*. Arch Pharm Res 34:913
558. Wen CN, Hu DB, Bai X, Wang F, Li ZH, Feng T, Liu JK (2016) Chemical constituents from fruiting bodies of basidiomycete *Perenniporia subacida*. Fitoterapia 109:179
559. Anke T, Heim J, Knoch F, Mocek U, Steffan B, Steglich W (1985) Crinipellins, the first natural products with a tetraquinane skeleton. Angew Chem Int Ed 24:709
560. Kupka J, Anke T, Oberwinkler F, Schramm G, Steglich W (1979) Crinipellin, a new antibiotic from the basidiomycetous fungus *Crinipellis stipitaria* (Fr.) Pat. J Antibiot 32:130
561. Li YY, Shen YM (2010) Four novel diterpenoids from *Crinipellis* sp. 113. Helv Chim Acta 93:2151
562. Rohr M, Oleinikov K, Jung M, Sandjo LP, Opatz T, Erkel G (2017) Anti-inflammatory tetraquinane diterpenoids from a *Crinipellis* species. Bioorg Med Chem 25:514

563. Kang T, Song SB, Kim WY, Kim BG, Lee HY (2014) Total synthesis of (–)-crinipellin A. J Am Chem Soc 136:10274
564. Schwartz CE, Curran DP (1990) New tandem radical cyclizations directed toward the synthesis of crinipellin A. J Am Chem Soc 112:9272
565. Zhou ZY, Liu R, Jiang MY, Zhang L, Niu Y, Zhu YC, Dong ZJ, Liu JK (2009) Two new cleistanthane diterpenes and a new isocoumarin from cultures of the basidiomycete *Albatrellus confluens*. Chem Pharm Bull 57:975
566. Wang Y, Zhang L, Wang F, Li ZH, Dong ZJ, Liu JK (2015) New diterpenes from cultures of the fungus *Engleromyces goetzii* and their CETP inhibitory activity. Nat Prod Bioprospect 5:69
567. Lee IS, Kim KC, Yoo ID, Ha BJ (2015) Inhibition of human neutrophil elastase by labdane diterpenes from the fruiting bodies of *Ramaria formosa*. Biosci Biotechnol Biochem 79:1921
568. Anke H, Casser I, Steglich W, Pommer EH (1987) Phlebiakauranol aldehyde an antifungal and cytotoxic metabolite from *Punctularia atropurpurascens*. J Antibiot 40:443
569. Zhang L, Li ZH, Dong ZJ, Yan L, Liu JK (2015) A viscidane diterpene and polyacetylenes from cultures of *Hypsizygus marmoreus*. Nat Prod Bioprospect 5:99
570. Wang SJ, Li YX, Bao L, Han JJ, Yang XJ, Li HR, Wang YQ, Li SJ, Liu HW (2012) Eryngiolide A, a cytotoxic macrocyclic diterpenoid with an unusual cyclododecane core skeleton produced by the edible mushroom *Pleurotus eryngii*. Org Lett 14:3672
571. Arnone A, Bava A, Fronza G, Nasini G, Ragg E (2005) Concavine, an unusual diterpenic alkaloid produced by the fungus *Clitocybe concava*. Tetrahedron Lett 46:8037
572. Tsukamoto S, Macabalang AD, Nakatani K, Obara Y, Nakahata N, Ohta T (2003) Tricholomalides A–C, new neurotrophic diterpenes from the mushroom *Tricholoma* sp. J Nat Prod 66:1578
573. Wang Z, Min SJ, Danishefsky SJ (2009) Total synthesis and structural revision of (±)-tricholomalides A and B. J Am Chem Soc 131:10848
574. Rios JL, Andujar I, Recio MC, Giner RM (2012) Lanostanoids from fungi: a group of potential anticancer compounds. J Nat Prod 75:2016
575. Richter C, Wittstein K, Kirk PM, Stadler M (2015) An assessment of the taxonomy and chemotaxonomy of *Ganoderma*. Fungal Divers 71:1
576. Baby S, Johnson AJ, Govindan B (2015) Secondary metabolites from *Ganoderma*. Phytochemistry 114:66
577. Koyama K, Imaizumi T, Akiba M, Kinoshita K, Takahashi L, Suzuki A, Yano S, Horie S, Watanabe K, Naoi Y (1997) Antinociceptive components of *Ganoderma lucidum*. Planta Med 63:224
578. Kubota T, Asaka Y, Miura I, Mori H (1982) Structures of ganoderic acid A and acid B, two new lanostane type bitter triterpenes from *Ganoderma lucidum* (Fr.) Karst. Helv Chim Acta 65:611
579. Lee S, Park S, Oh JW, Yang CH (1998) Natural inhibitors for protein prenyltransferase. Planta Med 64:303
580. Kohda H, Tokumoto W, Sakamoto K, Fujii M, Hirai Y, Yamasaki K, Komoda Y, Nakamura H, Ishihara S, Uchida M (1985) The biologically active constituents of *Ganoderma lucidum* (Fr.) Karst. Histamine release-inhibitory triterpenes. Chem Pharm Bull 33:1367
581. Liu CD, Yang N, Song Y, Wang LX, Zi JC, Zhang SW, Dunkin D, Busse P, Weir D, Tversky J, Miller RL, Goldfarb J, Zhan JX, Li XM (2015) Ganoderic acid C1 isolated from the anti-asthma formula, Ashmi™ suppresses TNF-$\alpha$ production by mouse macrophages and peripheral blood mononuclear cells from asthma patients. Int Immunopharmacol 27:224
582. Fatmawati S, Shimizu K, Kondo R (2010) Ganoderic acid Df, a new triterpenoid with aldose reductase inhibitory activity from the fruiting body of *Ganoderma lucidum*. Fitoterapia 81:1033
583. Morigiwa A, Kitabatake K, Fujimoto Y, Ikekawa N (1986) Angiotensin-converting enzyme-inhibitory triterpenes from *Ganoderma lucidum*. Chem Pharm Bull 34:3025

584. Yue QX, Song XY, Ma C, Feng LX, Guan SH, WY W, Yang M, Jiang BH, Liu X, Cui YJ, Guo DA (2010) Effects of triterpenes from *Ganoderma lucidum* on protein expression profile of Hela cells. Phytomedicine 17:606
585. Chen NH, Liu JW, Zhong JJ (2008) Ganoderic acid Me inhibits tumor invasion through down-regulating matrix metalloproteinases 2/9 gene expression. J Pharm Sci 108:212
586. Chen NH, Zhong JJ (2009) Ganoderic acid Me induces $G_1$ arrest in wild-type p53 human tumor cells while $G_1$/S transition arrest in p53-null cells. Process Biochem 44:928
587. Jiang ZJ, Jin TT, Gao F, Liu JW, Zhong JJ, Zhao H (2011) Effects of ganoderic acid Me on inhibiting multidrug resistance and inducing apoptosis in multidrug resistant colon cancer cells. Process Biochem 46:1307
588. Nishitoba T, Sato H, Shirasu S, Sakamura S (1987) Novel triterpenoids from the mycelial mat at the previous stage of fruiting of *Ganoderma lucidum*. Agric Biol Chem 51:619
589. Wang G, Zhao J, Liu JW, Huang YP, Zhong JJ, Tang W (2007) Enhancement of IL-2 and IFN-γ expression and NK cells activity involved in the anti-tumor effect of ganoderic acid Me in vivo. Int Immunopharmacol 7:864
590. Zhou L, Shi P, Chen NH, Zhong JJ (2011) Ganoderic acid Me induces apoptosis through mitochondria dysfunctions in human colon carcinoma cells. Process Biochem 46:219
591. Liu RM, Zhong JJ (2011) Ganoderic acid Mf and S induce mitochondria mediated apoptosis in human cervical carcinoma Hela cells. Phytomedicine 18:349
592. Adams M, Christen M, Plitzko I, Zimmermann S, Brun R, Kaiser M, Hamburger M (2010) Antiplasmodial lanostanes from the *Ganoderma lucidum* mushroom. J Nat Prod 73:897
593. Chen NH, Zhong JJ (2011) p53 is important for the anti-invasion of ganoderic acid T in human carcinoma cells. Phytomedicine 18:719
594. Xu K, Liang X, Gao F, Zhong JJ, Liu JW (2010) Antimetastatic effect of ganoderic acid T in vitro through inhibition of cancer cell invasion. Process Biochem 45:1261
595. Li CH, Chen PY, Chang UM, Kan LS, Fang WH, Tsai KS, Lin SB (2005) Ganoderic acid X, a lanostanoid triterpene, inhibits topoisomerases and induces apoptosis of cancer cells. Life Sci 77:252
596. Zhang W, Tao J, Yang X, Yang Z, Zhang L, Liu H, Wu K, Wu J (2014) Antiviral effects of two *Ganoderma lucidum* triterpenoids against enterovirus 71 infection. Biochem Biophys Res Commun 449:307
597. Min BS, Nakamura N, Miyashiro H, Bae KW, Hattori M (1998) Triterpenes from the spores of *Ganoderma lucidum* and their inhibitory activity against HIV-1 protease. Chem Pharm Bull 46:1607
598. Min BS, Gao JJ, Nakamura N, Hattori M (2000) Triterpenes from the spores of *Ganoderma lucidum* and their cytotoxicity against Meth-A and LLC tumor cells. Chem Pharm Bull 48:1026
599. Iwatsuki K, Akihisa T, Tokuda H, Ukiya M, Oshikubo M, Kimura Y, Asano T, Nomura A, Nishino H (2003) Lucidenic acids P and Q, methyl lucidenate P, and other triterpenoids from the fungus *Ganoderma lucidum* and their inhibitory effects on Epstein-Barr virus activation. J Nat Prod 66:1582
600. Fujita A, Arisawa M, Saga M, Hayashi T, Morita N (1986) Two new lanostanoids from *Ganoderma lucidum*. J Nat Prod 49:1122
601. Kim JW, Kim HI, Kim JH, Kwon OC, Son ES, Lee CS, Park YJ (2016) Effects of ganodermanondiol, a new melanogenesis inhibitor from the medicinal mushroom *Ganoderma lucidum*. Int J Mol Sci 17:1798
602. Li B, Lee DS, Kang Y, Yao NQ, An RB, Kim YC (2012) Protective effect of ganodermanondiol isolated from the Lingzhi mushroom against *tert*-butyl hydroperoxide-induced hepatotoxicity through Nrf2-mediated antioxidant enzymes. Food Chem Toxicol 53:317
603. Ha DT, Oh J, Khoi NM, Dao TT, Dung LV, Do TN, Lee SM, Jang TS, Jeong GS, Na M (2013) In vitro and in vivo hepatoprotective effect of ganodermanontriol against *t*-BHP-induced oxidative stress. J Ethnopharmacol 150:875

604. Jedinak A, Jiang JH, Harvey K, Sliva D (2007) Ganodermanontriol: novel antitumor agent against colon cancer. Cancer Res 67(Suppl 9):1524
605. Jedinak A, Thyagarajansahu A, Jiang J, Sliva D (2011) Ganodermanontriol, a lanostanoid triterpene from *Ganoderma lucidum*, suppresses growth of colon cancer cells through $\beta$-catenin signaling. Int J Oncol 38:761
606. Jiang J, Jedinak A, Sliva D (2011) Ganodermanontriol (GDNT) exerts its effect on growth and invasiveness of breast cancer cells through the down-regulation of CDC20 and uPA. Biochem Biophys Res Commun 415:325
607. Kennedy EM, P'pool SJ, Jiang JH, Sliva DD, Minto RE (2011) Semisynthesis and biological evaluation of ganodermanontriol and its stereoisomeric triols. J Nat Prod 74:2332
608. Liu JQ, Wang CF, Li Y, Luo HR, Qiu MH (2012) Isolation and bioactivity evaluation of terpenoids from the medicinal fungus *Ganoderma sinense*. Planta Med 78:368
609. Fatmawati S, Shimizu K, Kondo R (2010) Inhibition of aldose reductase in vitro by constituents of *Ganoderma lucidum*. Planta Med 76:1691
610. Kim DH, Shim SB, Kim NJ, Jang IS (1999) $\beta$-Glucuronidase-inhibitory activity and hepatoprotective effect of *Ganoderma lucidum*. Biol Pharm Bull 22:162
611. Komoda Y, Nakamura H, Ishihara S, Uchida M, Kohda H, Yamasaki K (1985) Structures of new terpenoid constituents of *Ganoderma lucidum* (Fr.) Karst. (Polyporaceae). Chem Pharm Bull 33:4829
612. Lin CN, Tome WP, Won SJ (1990) A lanostanoid of Formosan *Ganoderma lucidum*. Phytochemistry 29:673
613. Lin CN, Tome WP, Won SJ (1991) Novel cytotoxic principles of Formosan *Ganoderma lucidum*. J Nat Prod 54:998
614. Kikuchi T, Matsuda S, Murai Y, Ogita Z (1985) Ganoderic acid G and I and ganolucidic acid A and B, new triterpenoids from *Ganoderma lucidum*. Chem Pharm Bull 33:2628
615. Nishitoba T, Sato H, Sakamura S (1985) New terpenoids, ganoderic acid J and ganolucidic acid C, from the fungus *Ganoderma lucidum*. Agric Biol Chem 49:3637
616. Nishitoba T, Sato H, Kasai T, Kawagishi H, Sakamura S (1985) New bitter $C_{27}$ and $C_{30}$ terpenoids from the fungus *Ganoderma lucidum* (Reishi). Agric Biol Chem 49:1793
617. Hsu CL, Yu YS, Yen GC (2008) Lucidenic acid B induces apoptosis in human leukemia cells via a mitochondria-mediated pathway. J Agric Food Chem 56:3973
618. Akihisa T, Nakamura Y, Tagata M, Tokuda H, Yasukawa K, Uchiyama E, Suzuki T, Kimura Y (2007) Anti-inflammatory and anti-tumor-promoting effects of triterpene acids and sterols from the fungus *Ganoderma lucidum*. Chem Biodivers 4:224
619. Mizushina Y, Takahashi N, Hanashima L, Koshino H, Esumi Y, Uzawa J, Sugawara F, Sakaguchi K (1999) Lucidenic acid O and lactone, new terpene inhibitors of eukaryotic DNA polymerases from a basidiomycete, *Ganoderma lucidum*. Bioorg Med Chem 7:2047
620. Sato H, Nishitoba T, Shirasu S, Oda K, Sakamura S (1986) Ganoderiol A and B, new triterpenoids from the fungus *Ganoderma lucidum* (Reishi). Agric Biol Chem 50:2887
621. Wu GS, Song YL, Yin ZQ, Guo JJ, Wang SP, Zhao WW, Chen XP, Zhang QW, Lu JJ, Wang YT (2013) Ganoderiol A-enriched extract suppresses migration and adhesion of MDA-MB-231 cells by inhibiting FAK-SRC-paxillin cascade pathway. PLoS One 8:e76620
622. Chang UM, Li CH, Lin LI, Huang CP, Kan LS, Lin SB (2006) Ganoderiol F, a *Ganoderma* triterpene, induces senescence in hepatoma HepG2 cells. Life Sci 79:1129
623. Levita J, Chao KH, Mutakin M (2014) Interactions of ganoderiol F with aspartic proteases of HIV and plasmepsin for anti-HIV and anti-malarial discovery. Int J Pharm Pharm Sci 6:561
624. Zhang Q, Zuo F, Nakamura N, Ma CM, Hattori M (2009) Metabolism and pharmacokinetics in rats of ganoderiol F, a highly cytotoxic and antitumor triterpene from *Ganoderma lucidum*. J Nat Med 63:304
625. Fatmawati S, Shimizu K, Kondo R (2011) Ganoderol B: a potent $\alpha$-glucosidase inhibitor isolated from the fruiting body of *Ganoderma lucidum*. Phytomedicine 18:1053

626. Liu J, Shimizu K, Konishi F, Kumamoto S, Kondo R (2007) The anti-androgen effect of ganoderol B isolated from the fruiting body of *Ganoderma lucidum*. Bioorg Med Chem 15:4966
627. Tung NT, Trang Tran TT, Cuong TD, Thu NV, Woo Mi H, Min BS (2014) Cytotoxic triterpenoids from the fruiting bodies of *Ganoderma lucidum*. Nat Prod Sci 20:7
628. Lee I, Seo J, Kim J, Kim H, Youn U, Lee J, Jung H, Na M, Hattori M, Min B, Bae K (2010) Lanostane triterpenes from the fruiting bodies of *Ganoderma lucidum* and their inhibitory effects on adipocyte differentiation in 3T3-L1 cells. J Nat Prod 73:172
629. Ko HH, Hung CF, Wang JP, Lin CN (2008) Antiinflammatory triterpenoids and steroids from *Ganoderma lucidum* and *G. tsugae*. Phytochemistry 69:234
630. Ma K, Ren JW, Han JJ, Bao L, Li L, Yao YJ, Sun C, Zhou B, Liu HW (2014) Ganoboninketals A–C, antiplasmodial 3,4-*seco*-27-norlanostane triterpenes from *Ganoderma boninense* Pat. J Nat Prod 77:1847
631. Peng XR, Liu JQ, Wang CF, Li XY, Shu Y, Zhou L, Qiu MH (2014) Hepatoprotective effects of triterpenoids from *Ganoderma cochlear*. J Nat Prod 77:737
632. Peng XR, Wang X, Zhou L, Hou B, Zuo ZL, Qiu MH (2015) Ganocochlearic acid A, a rearranged hexanorlanostane triterpenoid, and cytotoxic triterpenoids from the fruiting bodies of *Ganoderma cochlear*. RSC Adv 5:95212
633. Nguyen VT, Tung NT, Cuong TD, Hung TM, Kim JA, Woo MH, Choi JS, Lee JH, Min BS (2015) Cytotoxic and anti-angiogenic effects of lanostane triterpenoids from *Ganoderma lucidum*. Phytochem Lett 12:69
634. Wang K, Bao L, Xiong WP, Ma K, Han JJ, Wang WZ, Yin WB, Liu HW (2015) Lanostane triterpenes from the Tibetan medicinal mushroom *Ganoderma leucocontextum* and their inhibitory effects on HMG-CoA reductase and $\alpha$-glucosidase. J Nat Prod 78:1977
635. Zhao ZZ, Yin RH, Chen HP, Feng T, Li ZH, Dong ZJ, Cui BK, Liu JK (2015) Two new triterpenoids from fruiting bodies of fungus *Ganoderma lucidum*. J Asian Nat Prod Res 17:750
636. Isaka M, Chinthanom P, Sappan M, Danwisetkanjana K, Boonpratuang T, Choeyklin R (2016) Antitubercular lanostane triterpenes from cultures of the basidiomycete *Ganoderma* sp. BCC 16642. J Nat Prod 79:161
637. Lin LJ, Shiao MS, Yeh SF (1988) Seven new triterpenes from *Ganoderma lucidum*. J Nat Prod 51:918
638. Zhao ZZ, Chen HP, Huang Y, Li ZH, Zhang L, Feng T, Liu JK (2016) Lanostane triterpenoids from fruiting bodies of *Ganoderma leucocontextum*. Nat Prod Bioprospect 6:103
639. Zhao ZZ, Chen HP, Li ZH, Dong ZJ, Xue B, Zhou ZY, Feng T, Liu JK (2016) Leucocontextins A-R, lanostane-type triterpenoids from *Ganoderma leucocontextum*. Fitoterapia 109:91
640. Kleinwachter P, Anh N, Kiet TT, Schlegel B, Dahse HM, Hartl A, Grafe U (2001) Colossolactones, new triterpenoid metabolites from a Vietnamese mushroom *Ganoderma colossum*. J Nat Prod 64:236
641. Lakornwong W, Kanokmedhakul K, Kanokmedhakul S, Kongsaeree P, Prabpai S, Sibounnavong P, Soytong K (2014) Triterpene lactones from cultures of *Ganoderma* sp. KM01. J Nat Prod 77:1545
642. El Dine RS, El Halawany AM, Ma CM, Hattori M (2008) Anti-HIV-1 protease activity of lanostane triterpenes from the Vietnamese mushroom *Ganoderma colossum*. J Nat Prod 71:1022
643. El Dine RS, El Halawany AM, Nakamura N, Ma CM, Hattori M (2008) New lanostane triterpene lactones from the Vietnamese mushroom *Ganoderma colossum* (Fr.) C.F. Baker. Chem Pharm Bull 56:642
644. Mothana RA, Awadh Ali NA, Jansen R, Wegner U, Mentel R, Lindequist U (2003) Antiviral lanostanoid triterpenes from the fungus *Ganoderma pfeifferi*. Fitoterapia 74:177
645. Niedermeyer Timo HJ, Lindequist U, Mentel R, Gördes D, Schmidt E, Thurow K, Lalk M (2005) Antiviral terpenoid constituents of *Ganoderma pfeifferi*. J Nat Prod 68:1728

646. El-Mekkawy S, Meselhy Meselhy R, Nakamura N, Tezuka Y, Hattori M, Kakiuchi N, Shimotohno K, Kawahata T, Otake T (1998) Anti-HIV-1 and anti-HIV-1-protease substances from *Ganoderma lucidum*. Phytochemistry 49:1651
647. Shiao MS, Lin LJ, Yeh SF (1988) Triterpenes from *Ganoderma lucidum*. Phytochemistry 27:2911
648. Chen DF, Zhang SX, Wang HK, Zhang SY, Sun QZ, Cosentino LM, Lee KH (1999) Novel anti-HIV lancilactone C and related triterpenes from *Kadsura lancilimba*. J Nat Prod 62:94
649. Chen YP, Lin ZW, Zhang HJ, Sun HD (1990) A triterpenoid from *Kadsura heteroclita*. Phytochemistry 29:3358
650. Liu JS, Huang MF (1983) Schisanlactone B, a new triterpenoid from a *Schisandra* sp. Tetrahedron Lett 24:2355
651. Liu JS, Huang MF, Arnold GF, Arnold E, Clardy J, Ayer WA (1983) Schisanlactone A, a new type of triterpenoid from a *Schisandra* sp. Tetrahedron Lett 24:2351
652. Geethangili M, Tzeng YM (2011) Review of pharmacological effects of *Antrodia camphorata* and its bioactive compounds. Evid-Based Complement Alternat Med 2011:212641
653. Chen CH, Yang SW, Shen YC (1995) New steroid acids from *Antrodia cinnamomea*, a fungal parasite of *Cinnamomum micranthum*. J Nat Prod 58:1655
654. Lin MK, Lee MS, Chang WT, Chen HY, Chen JF, Li YR, Lin CC, Wu TS (2015) Immunosuppressive effect of zhankuic acid C from *Taiwanofungus camphoratus* on dendritic cell activation and the contact hypersensitivity response. Bioorg Med Chem Lett 25:4637
655. Yang SW, Shen YC, Chen CH (1996) Steroids and triterpenoids of *Antodia cinnamomea* – a fungus parasitic on *Cinnamomum micranthum*. Phytochemistry 41:1389
656. Su YC, Liu CT, Chu YL, Raghu R, Kuo YH, Sheen LY (2012) Eburicoic acid, an active triterpenoid from the fruiting bodies of basswood cultivated *Antrodia cinnamomea*, induces ER stress-mediated autophagy in human hepatoma cells. J Tradit Complement Med 2:312
657. Deng JY, Chen SJ, Jow GM, Hsueh CW, Jeng CJ (2009) Dehydroeburicoic acid induces calcium- and calpain-dependent necrosis in human U87MG glioblastomas. Chem Res Toxicol 22:1817
658. Deng JS, Huang SS, Lin TH, Lee MM, Kuo CC, Sung PJ, Hou WC, Huang GJ, Kuo YH (2013) Analgesic and anti-inflammatory bioactivities of eburicoic acid and dehydroeburicoic acid isolated from *Antrodia camphorata* on the inflammatory mediator expression in mice. J Agric Food Chem 61:5064
659. Du YC, Chang FR, Wu TY, Hsu YM, El-Shazly M, Chen CF, Sung PJ, Lin YY, Lin YH, Wu YC, Lu MC (2012) Antileukemia component, dehydroeburicoic acid from *Antrodia camphorata* induces DNA damage and apoptosis in vitro and in vivo models. Phytomedicine 19:788
660. Kuo YH, Lin CH, Shih CC (2015) Antidiabetic and antihyperlipidemic properties of a triterpenoid compound, dehydroeburicoic acid, from *Antrodia camphorata* in vitro and in streptozotocin-induced mice. J Agric Food Chem 63:10140
661. Lai KH, Du YC, Lu MC, Wu TY, Hsu YM, Lin YC, El-Shazly M, Chu TS, Chen CF, Chang FR, Wu YC (2012) Dehydroeburicoic acid, an antileukemic triterpene from the fruiting bodies of dish-cultured *Antrodia cinnamomea*. Planta Med 78:1084
662. Lu ZM, Xu ZH (2011) Antcin A contributes to anti-inflammatory effect of Niuchangchih (*Antrodia camphorata*). Acta Pharm Sin 32:981
663. Lin TY, Chien SC, Kuo YH, Wang SY (2012) Distinguishing between *R*- and *S*-antcin C and their cytotoxicity. Nat Prod Commun 7:835
664. Hsieh YC, Rao Yerra K, Wu CC, Huang CYF, Geethangili M, Hsu SL, Tzeng YM (2010) Methyl antcinate A from *Antrodia camphorata* induces apoptosis in human liver cancer cells through oxidant-mediated Cofilin-and Bax-triggered mitochondrial pathway. Chem Res Toxicol 23:1256
665. Tsai WC, Rao YK, Lin SS, Chou MY, Shen YT, Wu CH, Geethangili M, Yang CC, Tzeng YM (2010) Methylantcinate A induces tumor specific growth inhibition in oral cancer cells via Bax-mediated mitochondrial apoptotic pathway. Bioorg Med Chem Lett 20:6145

666. Hsieh YC, Rao YK, Whang-Peng J, Huang CYF, Shyue SK, Hsu SL, Tzeng YM (2011) Antcin B and its ester derivative from *Antrodia camphorata* induce apoptosis in hepatocellular carcinoma cells involves enhancing oxidative stress coincident with activation of intrinsic and extrinsic apoptotic pathway. J Agric Food Chem 59:10943
667. Shen CC, Wang YH, Chang TT, Lin LC, Don MJ, Hou YC, Lious KT, Chang S, Wang WY, Ko HC, Shen YC (2007) Anti-inflammatory ergostanes from the basidiomata of *Antrodia salmonea*. Planta Med 73:1208
668. Huang YL, Chu YL, Ho CT, Chung JG, Lai CI, YC S, Kuo YH, Sheen LY (2015) Antcin K, an active triterpenoid from the fruiting bodies of basswood-cultivated *Antrodia cinnamomea*, inhibits metastasis via suppression of lntegrin-mediated adhesion, migration, and invasion in human hepatoma cells. J Agric Food Chem 63:4561
669. Lai CI, Chu YL, Ho CT, Su YC, Kuo YH, Sheen LY (2016) Antcin K, an active triterpenoid from the fruiting bodies of basswood cultivated *Antrodia cinnamomea*, induces mitochondria and endoplasmic reticulum stress-mediated apoptosis in human hepatoma cells. J Tradit Complement Med 6:48
670. Wu SJ, Leu YL, Chen CH, Chao CH, Shen DY, Chan HH, Lee EJ, Wu TS, Wang YH, Shen YC, Qian KD, Bastow KF, Lee KH (2010) Camphoratins A-J, potent cytotoxic and anti-inflammatory triterpenoids from the fruiting body of *Taiwanofungus camphoratus*. J Nat Prod 73:1756
671. Huang HC, Liaw CC, Yang HL, Hseu YC, Kuo HT, Tsai YC, Chien SC, Amagaya S, Chen YC, Kuo YH (2012) Lanostane triterpenoids and sterols from *Antrodia camphorata*. Phytochemistry 84:177
672. Liaw CC, Chen YC, Huang GJ, Tsai YC, Chien SC, Wu JH, Wang SY, Chao LK, Sung PJ, Huang HC, Kuo YH (2013) Anti-inflammatory lanostanoids and lactone derivatives from *Antrodia camphorata*. J Nat Prod 76:489
673. Qiao X, An R, Huang Y, Ji S, Li L, Tzeng YM, Guo DA, Ye M (2014) Separation of (25*R*/*S*)-ergostane triterpenoids in the medicinal mushroom *Antrodia camphorata* using analytical supercritical-fluid chromatography. J Chromatogr A 1358:252
674. Kuo YH, Huang GJ (2012) New anti-inflammatory aromatic and triterpene components from *Antrodia camphorata*. Planta Med 78:1190
675. Rios JL (2011) Chemical constituents and pharmacological properties of *Poria cocos*. Planta Med 77:681
676. She GM, Zhu NL, Wang S, Liu Y, Ba YY, Sun CQ, Shi RB (2012) New lanostane-type triterpene acids from *Wolfiporia extensa*. Chem Cent J 6:39
677. Lai K, Lu MC, Du YC, El-Shazly M, Wu TY, Hsu YM, Henz A, Yang JC, Backlund A, Chang FR, Wu YC (2016) Cytotoxic lanostanoids from *Poria cocos*. J Nat Prod 79:2805
678. Li SP, Wang ZX, Gu R, Zhao YW, Huang WZ, Wang ZZ, Xiao W (2016) A new epidioxy-tetracyclic triterpenoid from *Poria cocos* Wolf. Nat Prod Res 30:1712
679. Huang YC, Chang WL, Huang SF, Lin CY, Lin HC, Chang TC (2010) Pachymic acid stimulates glucose uptake through enhanced GLUT4 expression and translocation. Eur J Pharmacol 648:39
680. Ling H, Jia XB, Zhang YC, Gapter LA, Lim YS, Agarwal R, Ng KY (2010) Pachymic acid inhibits cell growth and modulates arachidonic acid metabolism in nonsmall cell lung cancer A549 cells. Mol Carcinog 49:271
681. Ling H, Zhang YC, Ng KY, Chew EH (2011) Pachymic acid impairs breast cancer cell invasion by suppressing nuclear factor-κB-dependent matrix metalloproteinase-9 expression. Breast Cancer Res Treat 126:609
682. Shah VK, Choi JJ, Han JY, Lee MK, Hong JT, Oh KW (2014) Pachymic acid enhances pentobarbital-induced sleeping behaviors via $GABA_A$-ergic systems in mice. Biomol Ther 22:314
683. Chen YG, Lian PL, Liu YF, Xu KS (2015) Pachymic acid inhibits tumorigenesis in gallbladder carcinoma cells. Int J Clin Exp Med 8:17781
684. Cheng S, Swanson K, Eliaz I, McClintick JN, Sandusky GE, Sliva D (2015) Pachymic acid inhibits growth and induces apoptosis of pancreatic cancer in vitro and in vivo by targeting ER stress. PLoS One 10:e0122270

685. Jeong JW, Lee WS, Go SI, Nagappan A, Baek JY, Lee JD, Lee SJ, Park C, Kim GY, Kim HJ, Kim GS, Kwon TK, Ryu CH, Shin SC, Choi YH (2015) Pachymic acid induces apoptosis of EJ bladder cancer cells by DR5 up-regulation, ROS generation, modulation of BCL-2 and IAP family members. Phytother Res 29:1516
686. Li FF, Yuan Y, Liu Y, Wu QQ, Jiao R, Yang Z, Zhou MQ, Tang QZ (2015) Pachymic acid protects H9C2 cardiomyocytes from lipopolysaccharide-induced inflammation and apoptosis by inhibiting the extracellular signal-regulated kinase 1/2 and p38 pathways. Mol Med Rep 12:2807
687. Ma J, Liu J, Lu CW, Cai DF (2015) Pachymic acid induces apoptosis via activating ROS-dependent JNK and ER stress pathways in lung cancer cells. Cancer Cell Int 15:78
688. Stanikunaite R, Radwan MM, Trappe JM, Fronczek F, Ross SA (2008) Lanostane-type triterpenes from the mushroom *Astraeus pteridis* with antituberculosis activity. J Nat Prod 71:2077
689. Arpha K, Phosri C, Suwannasai N, Mongkolthanaruk W, Sodngam S (2012) Astraodoric acids A-D: new lanostane triterpenes from edible mushroom *Astraeus odoratus* and their anti-*Mycobacterium tuberculosis* H37RA and cytotoxic activity. J Agric Food Chem 60:9834
690. Isaka M, Palasarn S, Srikitikulchai P, Vichai V, Komwijit S (2016) Astraeusins A–L, lanostane triterpenoids from the edible mushroom *Astraeus odoratus*. Tetrahedron 72:3288
691. Lai TK, Biswas G, Chatterjee S, Dutta A, Pal C, Banerji J, Bhuvanesh N, Reibenspies JH, Acharya K (2012) Leishmanicidal and anticandidal activity of constituents of Indian edible mushroom *Astraeus hygrometricus*. Chem Biodivers 9:1517
692. Mallick S, Dey S, Mandal S, Dutta A, Mukherjee D, Biswas G, Chatterjee S, Mallick S, Lai TK, Acharya K, Pal C (2015) A novel triterpene from *Astraeus hygrometricus* induces reactive oxygen species leading to death in *Leishmania donovani*. Future Microbiol 10:763
693. Pimjuk P, Phosri C, Wauke T, McCloskey S (2015) The isolation of two new lanostane triterpenoid derivatives from the edible mushroom *Astraeus asiaticus*. Phytochem Lett 14:79
694. Adam HK, Bryce TA, Campbell IM, NJ MC, Gaudemer A, Gmelin R, Polonsky J (1967) Metabolites of the Polyporaceae II. Carboxyacetylquercinic acid – a novel triterpene conjugate from *Daedalea quercina*. Tetrahedron Lett:1461
695. Kawagishi H, Li H, Tanno O, Inoue S, Ikeda S, Ohnishi-Kameyama M, Nagata T (1997) A lanostane-type triterpene from a mushroom *Daedalea dickinsii*. Phytochemistry 46:959
696. Bae KG, Min TJ (2000) The structure and antibiotic activities of hydroxy acid of lanostenol compound in *Daedalea dickinsii*. Bull Kor Chem Soc 21:1199
697. Yoshikawa K, Kouso K, Takahashi J, Matsuda A, Okazoe M, Umeyama A, Arihara S (2005) Cytotoxic constituents of the fruit body of *Daedalea dickisii*. J Nat Prod 68:911
698. Sorribas A, Jimenez JI, Yoshida WY, Williams PG (2011) Daedalols A–C, fungal-derived BACE1 inhibitors. Bioorg Med Chem 19:6581
699. Mizushina Y, Tanaka N, Kitamura A, Tamai K, Ikeda M, Takemura M, Sugawara F, Arai T, Matsukage A, Yoshida S, Sakaguchi K (1998) The inhibitory effect of novel triterpenoid compounds, fomitellic acids, on DNA polymerase $\beta$. Biochem J 330:1325
700. Tanaka N, Kitamura A, Mizushina Y, Sugawara F, Sakaguchi K (1998) Fomitellic acids, triterpenoid inhibitors of eukaryotic DNA polymerases from a basidiomycete, *Fomitella fraxinea*. J Nat Prod 61:193
701. He J, Feng XZ, Lu Y, Zhao B (2003) Fomlactones A-C, novel triterpene lactones from *Fomes cajanderi*. J Nat Prod 66:1249
702. Quang DN, Arakawa Y, Hashimoto T, Asakawa Y (2005) Lanostane triterpenoids from the inedible mushroom *Fomitopsis spraguei*. Phytochemistry 66:1656
703. Yoshikawa K, Inoue M, Matsumoto Y, Sakakibara C, Miyataka H, Matsumoto H, Arihara S (2005) Lanostane triterpenoids and triterpene glycosides from the fruit body of *Fomitopsis pinicola* and their inhibitory activity against COX-1 and COX-2. J Nat Prod 68:69
704. Bhattarai G, Lee YH, Lee NH, Lee IK, Yun BS, Hwang PH, Yi HK (2012) Fomitoside-K from *Fomitopsis nigra* induces apoptosis of human oral squamous cell carcinomas (YD-10B) via mitochondrial signaling pathway. Biol Pharm Bull 35:1711

705. Lee IK, Jung JY, Yeom JH, Ki DW, Lee MS, Yeo WH, Yun BS (2012) Fomitoside K, a new lanostane triterpene glycoside from the fruiting body of *Fomitopsis nigra*. Mycobiology 40:76
706. Popova M, Trusheva B, Gyosheva M, Tsvetkova I, Bankova V (2009) Antibacterial triterpenes from the threatened wood-decay fungus *Fomitopsis rosea*. Fitoterapia 80:263
707. Chiba T, Sakurada T, Watanabe R, Yamaguchi K, Kimura Y, Kioka N, Kawagishi H, Matsuo M, Ueda K (2014) Fomiroid A, a novel compound from the mushroom *Fomitopsis nigra*, inhibits NPC1L1-mediated cholesterol uptake via a mode of action distinct from that of ezetimibe. PLoS One 9:e116162
708. Feng W, Yang JS (2015) A new drimane sesquiterpenoid and a new triterpene lactone from fungus of *Fomes officinalis*. J Asian Nat Prod Res 17:1065
709. Han J, Li L, Zhong J, Tohtaton Z, Ren Q, Han L, Huang X, Yuan T (2016) Officimalonic acids A−H, lanostane triterpenes from the fruiting bodies of *Fomes officinalis*. Phytochemistry 130:193
710. De Bernardi M, Fronza G, Gianotti MP, Mellerio G, Vidari G, Vita-Finzi P (1983) Fungal metabolites XIII: new cytotoxic triterpene from *Hebeloma* species (Basidiomycetes). Tetrahedron Lett 24:1635
711. Fujimoto H, Takano Y, Yamazaki M (1992) Isolation, identification and pharmacological studies on three toxic metabolites from a mushroom, *Hebeloma spoliatum*. Chem Pharm Bull 40:869
712. Bocchi M, Garlaschelli L, Vidari G, Mellerio G (1992) New farnesane sesquiterpenes from *Hebeloma senescens*. J Nat Prod 55:428
713. Dossena A, Lunghi A, Garlaschelli L, Vidari G (1996) The structure and absolute configuration of two novel triterpene depsipeptides from the fruiting bodies of *Hebeloma senescens*. Tetrahedron-Asymmetry 7:1911
714. Garlaschelli L, Vidari G, Virtuani M, Vitafinzi P, Mellerio G (1995) The structures of new lanostane triterpenes from the fruiting bodies of *Hebeloma senescens*. J Nat Prod 58:992
715. Shao HJ, Qing C, Wang F, Zhang YL, Luo DQ, Liu JK (2005) A new cytotoxic lanostane triterpenoid from the basidiomycete *Hebeloma versipelle*. J Antibiot 58:828
716. Nakata T, Yamada T, Taji S, Ohishi H, Wada SI, Tokuda H, Sakuma K, Tanaka R (2007) Structure determination of inonotsuoxides A and B and in vivo anti-tumor promoting activity of inotodiol from the sclerotia of *Inonotus obliquus*. Bioorg Med Chem 15:257
717. Nomura M, Takahashi T, Uesugi A, Tanaka R, Kobayashi S (2008) Inotodiol, a lanostane triterpenoid, from *Inonotus obliquus* inhibits cell proliferation through caspase-3-dependent apoptosis. Anticancer Res 28:2691
718. Taji S, Yamada T, Tanaka R (2008) Three new lanostane triterpenoids, inonotsutriols A, B, and C, from *Inonotus obliquus*. Helv Chim Acta 91:1513
719. Taji S, Yamada T, Wada S, Tokuda H, Sakuma K, Tanaka R (2008) Lanostane-type triterpenoids from the sclerotia of *Inonotus obliquus* possessing anti-tumor promoting activity. Eur J Med Chem 43:2373
720. Nakamura S, Iwami J, Matsuda H, Mizuno S, Yoshikawa M (2009) Absolute stereostructures of inoterpenes A–F from sclerotia of *Inonotus obliquus*. Tetrahedron 65:2443
721. Handa N, Yamada T, Tanaka R (2010) An unusual lanostane-type triterpenoid, spiroinonotsuoxodiol, and other triterpenoids from *Inonotus obliquus*. Phytochemistry 71:1774
722. Liu C, Zhao C, Pan HH, Kang J, Yu XT, Wang HQ, Li BM, Xie YZ, Chen RY (2014) Chemical constituents from *Inonotus obliquus* and their biological activities. J Nat Prod 77:35
723. Zhao F, Mai Q, Ma J, Xu M, Wang X, Cui T, Qiu F, Han G (2015) Triterpenoids from *Inonotus obliquus* and their antitumor activities. Fitoterapia 101:34
724. Ikeda M, Sato Y, Izawa M, Sassa T, Miura Y (1977) Isolation and structure of fasciculol A, a new plant growth inhibitor from *Neamatoloma fasciculare*. Agric Biol Chem 41:1539
725. Kim KH, Moon E, Choi SU, Kim SY, Lee KR (2013) Lanostane triterpenoids from the mushroom *Naematoloma fasciculare*. J Nat Prod 76:845

726. Kubo I, Matsumoto A, Kozuka M, Wood WF (1985) Calmodulin inhibitors from the bitter mushroom *Naematoloma fasciculare* (Fr.) Karst. (Strophariaceae) and absolute configuration of fasciculols. Chem Pharm Bull 33:3821
727. Suzuki K, Fujimoto H, Yamazaki M (1983) The toxic principles of *Naematoloma fasciculare*. Chem Pharm Bull 31:2176
728. Nozoe S, Takahashi A, Ohta T (1993) Chirality of the 3-hydroxy-3-methylglutaric acid moiety of fasciculic acid A, a calmodulin antagonist isolated from *Naematoloma fasciculare*. Chem Pharm Bull 41:1738
729. Takahashi A, Kusano G, Ohta T, Ohizumi Y, Nozoe S (1989) Fasciculic acids A, B and C as calmodulin antagonists from the mushroom *Naematoloma fasciculare*. Chem Pharm Bull 37:3247
730. Jayasuriya H, Silverman KC, Zink DL, Jenkins RG, Sanchez M, Pelaez F, Vilella D, Lingham RB, Singh SB (1998) Clavaric acid: a triterpenoid inhibitor of farnesyl-protein transferase from *Clavariadelphus truncatus*. J Nat Prod 61:1568
731. Yoshikawa K, Nishimura N, Bando S, Arihara S, Matsumura E, Katayama S (2002) New lanostanoids, elfvingic acids A−H, from the fruit body of *Elfvingia applanata*. J Nat Prod 65:548
732. Weber W, Semar M, Anke T, Bross M, Steglich W (1992) Tyromycin A: a novel inhibitor of leucine and cysteine aminopeptidases from *Tyromyces lacteus*. Planta Med 58:56
733. Quang DN, Hashimoto T, Tanaka M, Asakawa Y (2003) Tyromycic acids F and G: two new triterpenoids from the mushroom *Tyromyces fissilis*. Chem Pharm Bull 51:1441
734. Quang DN, Hashimoto T, Tanaka M, Takaoka S, Asakawa Y (2004) Tyromycic acids B–E, new lanostane triterpenoids from the mushroom *Tyromyces fissilis*. J Nat Prod 67:148
735. Su ZY, Tung YC, Hwang LS, Sheen LY (2011) Blazeispirol A from *Agaricus blazei* fermentation product induces cell death in human hepatoma Hep 3B cells through caspase-dependent and caspase-independent pathways. J Agric Food Chem 59:5109
736. Umeyama A, Ohta C, Shino Y, Okada M, Nakamura Y, Hamagaki T, Imagawa H, Tanaka M, Ishiyama A, Iwatsuki M, Otoguro K, Omura S, Hashimoto T (2014) Three lanostane triterpenoids with antitrypanosomal activity from the fruiting body of *Hexagonia tenuis*. Tetrahedron 70:8312
737. Thang TD, Kuo PC, Ngoc NTB, Hwang TL, Yang ML, Ta SH, Lee EJ, Kuo DH, Hung NH, Tuan NN, Wu TS (2015) Chemical constituents from the fruiting bodies of *Hexagonia apiaria* and their anti-inflammatory activity. J Nat Prod 78:2552
738. Han JJ, Bao L, Tao QQ, Yao YJ, Liu XZ, Yin WB, Liu HW (2015) Gloeophyllins A–J, cytotoxic ergosteroids with various skeletons from a Chinese Tibet fungus *Gloeophyllum abietinum*. Org Lett 17:2538
739. Feng T, Cai JL, Li XM, Zhou ZY, Li ZH, Liu JK (2016) Chemical constituents and their bioactivities of mushroom *Phellinus rhabarbarinus*. J Agric Food Chem 64:1945
740. Yoshikawa K, Kuroboshi M, Ahagon S, Arihara S (2004) Three novel crustulinol esters, saponaceols A-C, from *Tricholoma saponaceum*. Chem Pharm Bull 52:886
741. Nasomjai P, Arpha K, Sodngam S, Brandt SD (2014) Potential antimalarial derivatives from astraodorol. Arch Pharm Res 37:1538
742. Tanaka R, Usami Y, In Y, Ishida T, Shingu T, Matsunaga S (1992) The structure of spiroveitchionolide, an unusual lanostane-type triterpene lactone from *Abies veitchii*. J Chem Soc Chem Commun:1351
743. Tanaka R, Wada SI, Aoki H, Matsunaga S, Yamori T (2004) Spiromarienonols A and B: two new 7(8→9)*abeo*-lanostane-type triterpene lactones from the stem bark of *Abies mariesii*. Helv Chim Acta 87:240
744. Zhao QQ, Song QY, Jiang K, Li GD, Wei WJ, Li Y, Gao K (2015) Spirochensilides A and B, two new rearranged triterpenoids from *Abies chensiensis*. Org Lett 17:2760
745. Lingham RB, Silverman KC, Jayasuriya H, Kim BM, Amo SE, Wilson FR, Rew DJ, Schaber MD, Bergstrom JD, Koblan KS, Graham SL, Kohl NE, Gibbs JB, Singh SB (1998) Clavaric acid and steroidal analogues as Ras- and FPP-directed inhibitors of human farnesyl-protein transferase. J Med Chem 41:4492

746. Zhou Y, Ma Y, Zeng J, Duan L, Xue X, Wang H, Lin T, Liu Z, Zeng K, Zhong Y, Zhang S, Hu Q, Liu M, Zhang H, Reed J, Moses T, Liu X, Huang P, Qing Z, Liu X, Tu P, Kuang H, Zhang Z, Osbourn A, Ro DK, Shang Y, Huang S (2016) Convergence and divergence of bitterness biosynthesis and regulation in Cucurbitaceae. Nat Plants 2:16183
747. Fujimoto H, Suzuki K, Hagiwara H, Yamazaki M (1986) New toxic metabolites from a mushroom, *Hebeloma vinosophyllum*. 1. Structures of hebevinoside-I, hebevinoside-II, hebevinoside-III, hebevinoside-IV, and hebevinoside-V. Chem Pharm Bull 34:88
748. Fujimoto H, Hagiwara H, Suzuki K, Yamazaki M (1987) New toxic metabolites from a mushroom, *Hebeloma vinosophyllum*. 2. Isolation and structures of hebevinoside-VI, hebevinoside-VII, hebevinoside-VIII, hebevinoside-IX, hebevinoside-X, and hebevinoside-XI. Chem Pharm Bull 35:2254
749. Fujimoto H, Maeda K, Yamazaki M (1991) New toxic metabolites from a mushroom, *Hebeloma vinosophyllum*. 3. Isolation and structures of 3 new glycosides, hebevinoside-XII, hebevinoside-XIII and hebevinoside-XIV, and productivity of the hebevinosides at 3 growth-stages of the mushroom. Chem Pharm Bull 39:1958
750. Clericuzio M, Mella M, Vita-Finzi P, Zema M, Vidari G (2004) Cucurbitane triterpenoids from *Leucopaxillus gentianeus*. J Nat Prod 67:1823
751. Clericuzio M, Tabasso S, Bianco MA, Pratesi G, Beretta G, Tinelli S, Zunino F, Vidari G (2006) Cucurbitane triterpenes from the fruiting bodies and cultivated mycelia of *Leucopaxillus gentianeus*. J Nat Prod 69:1796
752. Wang HB, Yang GH, Wu SH, Wang SF, Li GY, Xu WK, Meng LS, Li ZY (1994) Chemical studies on *Russula rosacea*. Acta Pharm Sin 29:43
753. Tan JW, Liu JK, Dong ZJ, Liu PG, Ji DG (1999) Lepida acid A from Basidiomycetes *Russula lepida*. Chin Chem Lett 10:297
754. Tan JW, Dong ZJ, Liu JK (2000) New terpenoids from Basidiomycetes *Russula lepida*. Helv Chim Acta 83:3191
755. Tan JW, Dong ZJ, Ding ZH, Liu JK (2002) Lepidolide, a novel *seco*-ring-A cucurbitane triterpenoid from *Russula lepida* (Basidiomycetes). Z Naturforsch C 57:963
756. Clericuzio M, Vidari G, Cassino C, Legnani L, Toma L (2014) Roseic acid and roseolactones A and B, furan-cucurbitane triterpenes from *Russula aurora* and *R. minutula* (Basidiomycota). Eur J Org Chem 5462
757. De Bernardi M, Garlaschelli L, Gattl G, Vidari G, Finzi PV (1988) The unprecedented structure of saponaceolide A, a cytotoxic C-30 terpenoid from *Tricholoma saponaceum*. Tetrahedron 44:235
758. De Bernardi M, Garlaschelli L, Toma L, Vidari G, Vita-Finzi P (1991) The structure of saponaceolides B, C, and D, new C-30 terpenoids from *Tricholoma saponaceum*. Tetrahedron 47:7109
759. Yoshikawa K, Kuroboshi M, Arihara S, Miura N, Tujimura N, Sakamoto K (2002) New triterpenoids from *Tricholoma saponaceum*. Chem Pharm Bull 50:1603
760. Yin X, Feng T, Shang JH, Zhao YL, Wang F, Li ZH, Dong ZJ, Luo XD, Liu JK (2014) Chemical and toxicological investigations of a previously unknown poisonous European mushroom *Tricholoma terreum*. Chem Eur J 20:7001
761. Feng T, He J, Ai HL, Huang R, Li ZH, Liu JK (2015) Three new triterpenoids from European mushroom *Tricholoma terreum*. Nat Prod Bioprospect 5:205
762. Bedry R, Baudrimont I, Deffieux G, Creppy EE, Pomies JP, Ragnaud JM, Dupon M, Neau D, Gabinski C, De Witte S, Chapalain JC, Beylot J, Godeau P (2001) Wild-mushroom intoxication as a cause of rhabdomyolysis. New Engl J Med 345:798
763. Schüffler A, Anke T (2009) Secondary Metabolites of Basidiomycetes. In: Anke T, Weber D (eds) Physiology and Genetics XV: Selected Basic and Applied Aspects. Springer, Berlin, p 209
764. Daum RS, Kar S, Kirkpatrick P (2007) Retapamulin. Nat Rev Drug Discov 6:865
765. Paci A, Rezai K, Deroussent A, De Valeriola D, Re M, Weill S, Cvitkovic E, Kahatt C, Sha A, Waters S, Weems G, Vassal G, Lokiec F (2006) Pharmacokinetics, metabolism, and routes of excretion of intravenous irofulven in patients with advanced solid tumors. Drug Metab Dispos 34:1918

**He-Ping Chen** was born in Anhui Province, People's Republic of China, in 1990. After receiving his B.Sc. degree in the Pharmacy of Chinese Medicine from Anhui Medical University in 2011, he joined Professor Ji-Kai Liu's group at Kunming Institute of Botany, Chinese Academy of Sciences, as a postgraduate student (2011–2014). He is currently carrying out his doctoral research in the field of isolation, structure elucidation, bioactivity determination, and chemical modification of mushroom natural products at this same institution (2014–present).

**Ji-Kai Liu** is a full-time Professor and Dean at the School of Pharmaceutical Sciences, South-Central University for Nationalities, Wuhan, People's Republic of China. He acquired his Ph.D. degree at Lanzhou University in 1988, specializing in Organic Chemistry. Following this, he served at Sun Yat-sen University as a faculty member until 1995, where he worked on natural products chemistry. During the period 1993–1994, he was an Alexander von Humboldt Research Fellow at the University of the Saarland in Germany. From 1996–1997 he worked as a Senior Scientist at the Pharmaceutical Research Center of Bayer AG in Wuppertal, Germany. In 1997, he was appointed as Professor of Natural Products Chemistry at the Kunming Institute of Botany (KIB), Chinese Academy of Sciences, and served as a Vice President of KIB and Director of the State Key Laboratory of Phytochemistry and Plant Resources in West China during the period 2006–2014. He has published over 200 scientific papers in many leading internationally recognized peer-reviewed journals in his field. He is the author of a book entitled "Mycochemistry", and has been named as a co-inventor for more than ten patents. Professor Liu has received an array of honors and awards, such as the Hundred Talent Program of CAS (1995), the Bayer-CAS Award (2002), the National Natural Science Prize (2003, 2nd Class; the Central People's Government of China), and was named as Chief Scientist of the 973 program. He currently serves as Editor-in-Chief of "Natural Products and Bioprospecting", Associate Editor of the "Journal of Ginseng Research", and is an Editorial Board member for six other international journals. His research field focuses on bioactive compounds obtained from higher fungi, and includes aspects of natural product chemical biology, total synthesis, and biosynthesis.

# Human Deiminases: Isoforms, Substrate Specificities, Kinetics, and Detection

**Bushra Amin and Wolfgang Voelter**

## Contents



## 1 Introduction

Devastating neurodegenerative and autoimmune disorders, such as Alzheimer's disease, multiple sclerosis, rheumatoid arthritis, various cardiomyopathies, and diversified cancers have been repeatedly promulgated with common evidence of

B. Amin (✉)
Department of Chemistry, University of Pittsburgh, Pittsburgh 15260, PA, USA
e-mail: bua4@pitt.edu

W. Voelter
Interfacultary Institute of Biochemistry, University of Tübingen, Hoppe-Seyler-Str. 4, 72076 Tübingen, BW, Germany
e-mail: wolfgang.voelter@uni-tuebingen.de



A.D. Kinghorn, H. Falk, S. Gibbons, J. Kobayashi (eds.), *Progress in the Chemistry of Organic Natural Products, Vol. 106*, DOI 10.1007/978-3-319-59542-9_2

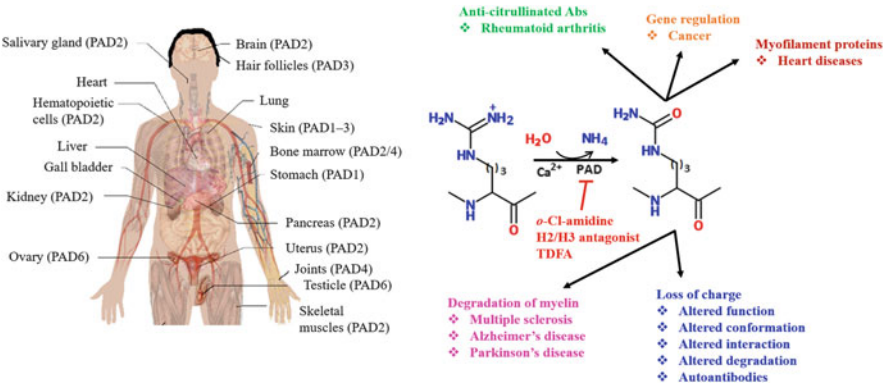


**Fig. 1** Graphical illustration of the organ-specific expression of peptidylarginine deiminase isoforms in humans. Conversion of positively-charged arginine to neutral citrulline in a protein influences structure and function of these molecules and plays a central role in pathogenesis of many diseases. Selective PAD inhibitors may antagonize its hyperactivity

accumulation of citrullinated proteins, autoantibody generation, and expression of peptidylarginine deiminase (PAD). Peptidylarginine deiminase (EC 3.5.3.15) belongs to a Ca(II)-dependent group of enzymes. It catalyzes a particular post-translational modification called "citrullination" or "deimination" to create novel epitopes on common proteins providing "neoantigens", which are now known to be characteristic for autoimmune and neurodegenerative diseases [1]. By irreversible removal of the imine group from the protein-embedded arginine side chain at neutral pH [2], peptidylarginine deiminase consequently induces an uncharged citrulline residue into a protein chain (Fig. 1). Although a tRNA for citrulline does not exist [3–5], several proteins are known to contain citrulline. The first example was described by Rogers and Simmonds as "trichohyalin" in hair follicles [6]. Selective expression of peptidylarginine deiminase isoforms in neurons and astrocytes and accompanying citrullinated proteins within and surrounding PAD-expressing cells is predominant in neurodegenerative changes typical of the respective pathology of multiple sclerosis and Alzheimer's disease.

In recent years it has become obvious that myelin basic protein, histones, collagen, fibronectin, as well as other cellular proteins can be modified by peptidylarginine deiminases during epigenetic regulation in the cell. Conversion of the arginyl residue plays a key role in the molecular mechanism that contributes to protein degradation, traumatic brain injuries, and cardiomyopathies in neurodegenerative and autoimmune diseases [7, 8]. Disease-associated neuronal loss results in the release of cellular contents, including citrullinated proteins and their degradation fragments, into the brain interstitium [9]. Once they have entered the blood and the lymphatic circulation, these neo-antigens may elicit an immune response resulting in the production of autoantibodies.

At physiological activity levels, peptidylarginine deiminases regulate many cell signaling pathways including differentiation, apoptosis, and gene transcription

[10]. Increased research efforts over the past few decades have helped to advance an understanding of the pathological events associated with PAD. In addition, while linked to several human pathologies (see Fig. 1), the properties of peptidylarginine deiminases has demonstrated their importance as unique therapeutic targets [11] and for antioxidation [12]. However, little is known about the underlying mechanisms of peptidylarginine deiminase involved in the initiation of pathologies such as in Alzheimer's disease, multiple sclerosis, sepsis, and tumorigenesis. Herein, a detailed survey is presented on deiminase enzymes, their regulation, homeostasis, selective inhibitors, and common detection assays, which is intended to collate widely dispersed knowledge in the field to channel future studies in the direction of the research areas to be explored.

## 2 Isozymes of Peptidylarginine Deiminase

Peptidylarginine deiminase-encoding genes are localized at chromosome 1p35–36 (Fig. 2) in humans as a well-organized cluster within a 350 kilobase-pair (kb) region [13, 14]. Peptidylarginine deiminases are unable to convert free L-arginine to L-citrulline, while this can be done by nitric oxide synthase (EC 1.14.13.39) in eukaryotes and arginine deiminase (EC 3.5.3.6) in bacteria, independent from the Ca(II) concentration, yielding nitric oxide instead of ammonia as a by-product of the conversion [15]. To date, only a single prokaryotic enzyme, AAF06719, identified in *Porphyromonas gingivalis* [16] can convert both L-arginine and peptide-bound arginine into citrulline, independent of Ca(II) ions [17].

Currently, five family members of PAD enzymes (PAD1–4 and PAD6) have been discovered, cloned, and characterized in mammals [18, 19], and they display 50–70% sequence similarity [19–22]. Each isotype has a tissue-specific expression pattern and is distributed over a wide range of cells and tissues throughout the body [23–26]. All known hPAD isozymes, their tissue distribution, cellular localization, and a few of their known substrates are summarized in Table 1.

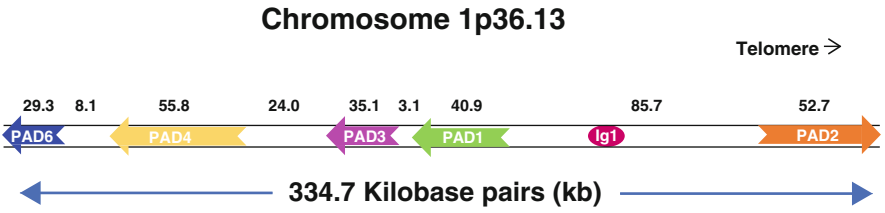


**Fig. 2** Schematic representation of the human peptidylarginine deiminase gene locus on chromosome 1p36.13. Scheme of human peptidylarginine deiminase genes at the p-arm on chromosome one (1p36.13). The transcribed regions of the genes are represented by colors and the transcription orientations are illustrated by arrowheads

**Table 1** Cellular localization, substrates, and conserved active site residues of peptidylarginine deiminase isozymes[a]

| | Tissue distribution | Cellular localization | Mass/ kDa | Substrates | Physiological functions | | Pathology |
|---|---|---|---|---|---|---|---|
| PAD1 | Epidermis, stomach | Cytoplasmic | 74.6 | Keratin, filaggrin | Skin keratinization | | Psoriasis |
| | D352 | R374 | R376 | H472 | D474 | L639 | C645 |
| PAD2 | Brain, skeletal muscles, salivary glands, uterus, ovary, kidney, spleen, pancreas, hematopoietic lineage | Cytoplasmic | 75.3 | MBP, MOG, GFAP, vimentin | Gene regulation, myelin formation in CNS, immunity | | Multiple sclerosis, prion disease, Alzheimer's disease |
| | D351 | R373 | G375 | H471 | D473 | F641 | C647 |
| PAD3 | Hair folicles, epidermis | Cytoplasmic | 74.6 | Tricohyalin, filaggrin | Epidermal barrier functions regulation | | |
| | D350 | R372 | G374 | H470 | D472 | L640 | C646 |
| PAD4 | Haematopoietic cells including eosinophils, neutrophils | Cytoplasmic and nuclear | 74 | Histone H2A, H3, H4, vimentin, fibrin, antithrombin | Gene regulation, NET formation, immunity | | Rheumatoid arthritis, multiple sclerosis, cancer |
| | A350 | R372[b] | R374[b] | H471 | D473 | R639[b] | C645 |
| PAD6 | Oocytes, early cleavage-stage embryo, ovary, testis, peripheral leucocytes | Cytoplasmic | 77.7 | Keratin-containing intermediate filaments | Embryonic development | | |
| | D359 | Q381 | A383 | H480 | D482 | E670 | A676 |

[a]Human PAD1 to 4 and 6 correspond to EMBL accession numbers AB033768 (Q9ULC6), AB030176 (Q9Y2J8), AB026831 (Q9ULW8), AB017919 (Q9UM07), and AY422079 (Q6TGC4). In parentheses the corresponding UniProtKB accession numbers are given. The D, H, and C residues are highly conserved and can be well-aligned in all peptidylarginine deiminase isoforms, while residues at positions 372[b], 374[b], and 639[b] may play a role in substrate specificity

[b]Amino acids are numbered according to human peptidylarginine deiminase type 4

## *2.1 Peptidylarginine Deiminase Type 1*

Peptidylarginine deiminase type 1 (PAD1) is encoded by the 40.9 kb region localized in between the PADI-2 and PADI-3 genes that span at the p-arm of chromosome 1 (1p36.13) (see Fig. 2). While available RT-PCR and EST data suggest a broader tissue distribution of peptidylarginine deiminase type 1 (PAD1) [18, 27, 28], it is primarily expressed in the epidermis and uterus [29, 30] where it citrullinates keratinocytes, keratins (K1, K10), and keratin-associated filaggrin protein [15]. The loss of charge following citrullination alters inter- and intra-molecular interactions leading to partial protein unfolding and modulating the cornification of epidermis [21]. The disassembly of the filaggrin-cytokeratin complex makes it susceptible to cleavage by proteases like calpain [31, 32] that converts pro-filaggrin into mature filaggrin [33], which can aggregate with keratin filaments

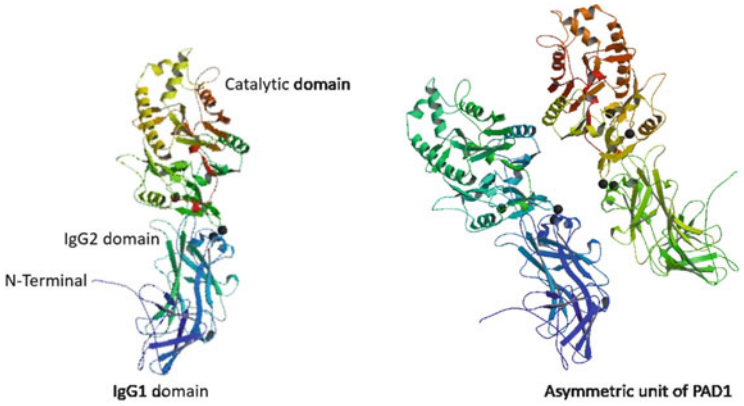


**Fig. 3** Ribbon representation of X-ray structure and asymmetric unit of peptidylarginine deiminase type 1. The PAD1 contains three main domains, i.e. the catalytic, IgG1, and IgG2 domains. In an asymmetric crystal, PAD1 exists in its monomeric form, as recently revealed by small-angle X-ray scattering analysis [40] (PDBID: 5HP5)

by ionic interactions that enhance the physical resistance of the epidermis by protecting keratin from proteolytic cleavage [34–36].

Among the five known isozymes, PAD1, exhibits the broadest substrate specificity [37, 38], when incubated with S100A3 protein, as compared to PAD2 and PAD3. An X-ray structure can be used to elucidate both the catalytic mechanism and the broad substrate precision. Recently, hexagonal bipyramidal crystals of full-length hPAD1 (663 amino acids, UniProt No. Q9ULC6) have been obtained with unit-cell parameters of $a = b = 90.3$ and $c = 372.3$ Å, belonging to the p61 space group [39, 40]. Human PAD isozymes exist as head-to-tail homodimers in solution [41, 42]. The asymmetric crystal of PAD1 (Fig. 3) contains two monomers. Also, small-angle X-ray scattering analysis has revealed PAD1 as a monomer in solution [40].

## *2.2 Peptidylarginine Deiminase Type 2*

The gene encoding for peptidylarginine deiminase type 2 (PAD2) is large (52.7 kb), and is localized about 85.7 kilobase pairs away from the other members (see Fig. 2) of the family and is transcribed in the direction of telomere [30]. Peptidylarginine deiminase type 2 is distributed in common tissues including those in the central nervous system, skeletal muscles, spleen, secretory glands, uterus, kidney, female reproductive organs, and hematopoietic systems (see Table 1), where its expression is regulated at both the mRNA splicing and protein translation levels [43]. The gray matter of the brain and hypothalamus have higher expression levels of peptidylarginine deiminase type 2 compared to the cerebellum [15]. Myelin basic protein, the major protein component of myelin sheathes that helps to cover the

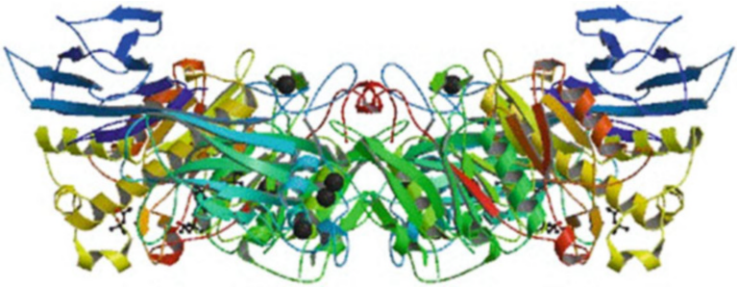

**Fig. 4** Ribbon representation of the crystal structure of peptidylarginine deiminase type 2. An X-ray diffraction study of PAD2 has revealed that PAD2 preferentially exists in a head-to-head homo-2-meric form in the presence of 10 m*M* Ca(II) ions [48] (PDBID: 4N2B)

axons of nerve cells, and the glial fibrillary acidic protein are the two major targets of PAD2 in the brain [21], whereas in the skeletal muscles and macrophages, the intermediate filament "vimentin" is a well-known PAD2 substrate [25]. The physio-pathological aspects of citrullination of these natural substrates of peptidylarginine deiminase are discussed later in this contribution. Peptidylarginine deiminase type 2 mainly resides in the cytoplasm, but in epithelial cells of human and canine mammary glands it has been reported to exhibit nuclear translocation, where it binds directly to chromatin [44, 45] and citrullinates of histones H3 and H4. Thus, PAD2 may regulate gene activity of the estrogen receptor alpha [29, 46].

Beta- and gamma-actin were described also as substrates for PAD2 in neutrophils [47]. Recently, X-ray crystallographic details of the head-to-head homo-2-mer PAD2 (Fig. 4) with 10 m*M* calcium ions were reported [48]. However, a full-length cDNA profile of 2348 base pairs encoding a 665 amino acid sequence of PAD2 with a predicted molecular mass of 75 kDa was cloned some years ago [49]. In vitro kinetic properties of human peptidylarginine deiminase isoform 2 (hPAD2) show a twofold reduction in Ca(II) dependence due to phosphatidylserine and phosphatidylcholine [50], while it generally requires about 1–100 μ*M* Ca(II) for activity (as described in Sect. 4).

## *2.3 Peptidylarginine Deiminase Type 3*

Peptidylarginine deiminase type 3 expresses exclusively in the inner and outer root sheathes of hair follicles and the epidermis [42, 49, 51–53]. The encoding 35.1 kilo base pair (kb) genes are localized in close proximity (i.e. about 3.1 kb) to the PADI-1 genes, as illustrated in Fig. 2. Trichohyalin, a major structural protein of the hair follicle, is a natural substrate of PAD3 [54]. Citrullination affects the alpha-helical structure of trichohyalin and helps it to crosslink with keratin filaments by transglutaminase-3 [15, 55]. In the presence of Ca(II) ions, citrullination mediates

the aggregation of keratin filaments to form a solid matrix contributing to the directional hair growth [56–58].

In addition, PAD3 is co-localized with profilaggrin and filaggrin in granular keratinocytes and the lower stratum spinosum of the epidermis [43]. The ionic interactions of the positively-charged filaggrin can bundle negatively-charged keratin intermediate filaments into tight arrays [59]. A decrease in the net positive charge as a consequence of filaggrin deimination may induce its dissociation and subsequent degradation. Due to this phenomenon, the skin produces a natural moisturizing factor [52, 60, 61], which is necessary for epidermal barrier functions [62, 63]. Peptidylarginine deiminases of types 1–3 are reported to be expressed in normal human keratinocytes (NHKs) with an increased level of mRNA when exposed to vitamin D, but the amount of proteins remains unaffected [52]. The EF-hand type Ca(II)-binding protein is a member of S100 family. This protein S100A3 is co-localized with PAD3 in hair cuticles. Peptidylarginine deiminase type 3 catalyzes the conversion of a symmetric pair of R51 at the surface of the S100A3 dimer and promotes its assembly as a homo-tetramer [38, 64]. At this stage PAD1 and PAD2 convert R3, R22, R51, and R77 to citrulline at the surface of the S100A3 protein [37, 39]. The recognition mechanism of sheltered R51 by PAD3 remains unclear. Moreover, these different substrate specificities among PAD isozymes affirm the need to determine the X-ray structure of all isozymes [65].

In 2012 a research group from Japan has reported the crystal structure and some preliminary X-ray analytical data of human PAD3 [66]. This comprised hexagonal pyramidal crystals containing two hPAD3 molecules as a putative dimeric biological unit. It belongs to space group R3 with unit cell parameters $a$ and $b = 114.97$, and $c = 332.49$ Å, $\alpha = \beta = 90$, and $\gamma = 120°$ [66].

## *2.4 Peptidylarginine Deiminase Type 4*

Human PAD4 was named initially PAD5 (or PAD V in some literature reports). For its slightly different reaction kinetics when compared to mouse PAD4 [67], human peptidylarginine deiminase type 4 was thought to be novel, but its genomic organization, expression data and amino acid sequence corresponded to those of rodent PAD4 [3, 68]. Thus, the HUGO Gene Nomenclature Committee (HGNC) has renamed it human PAD4 [15, 30]. It is mainly expressed by cells of the hematopoietic lineage [43, 51, 69] and can be detected in various tissues [21, 43, 54]. Human myeloid leukemia HL-60 cells were first reported to contain PAD4, when induced to differentiate into granulocytes [70]. PAD4 encoding genes (55.8 kb) span at chromosome 1p35–36 in between PADI3 and PADI6 (see Fig. 2). Nucleophosmin/B23 and core histones (H2A, H3, and H4) are the reported substrates of PAD4 in calcium ionophore-stimulated granulocytes and HL-60 cells [3, 67, 70, 71].

The X-ray crystal structure of human PAD4 was reported by Arita and colleagues in 2003 [70] who demonstrated that binding of different substrates (benzoyl-L-arginine amide or histone N-terminal peptides) does not change the crystal

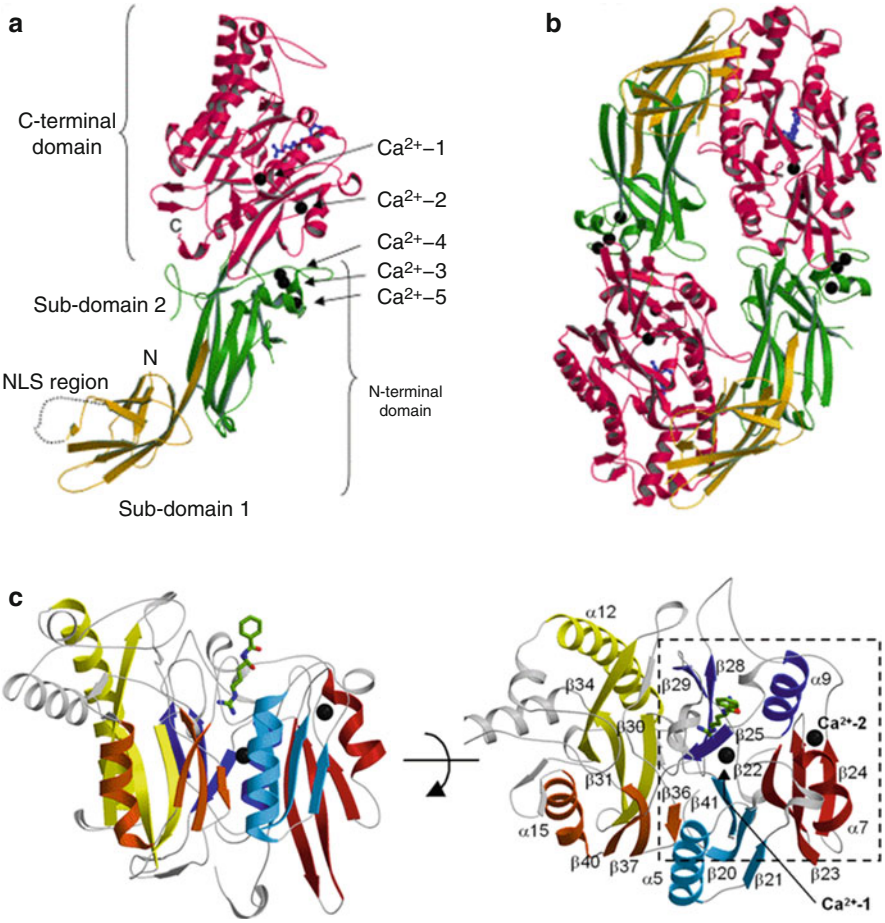


**Fig. 5** Structure of peptidylarginine deiminase type 4. (**a**) Ribbon representation of the monomeric PAD4. Five Ca(II) ions (Ca1–Ca5) are shown as black balls, and the substrate, benzoyl-L-arginine amide, is illustrated as dark blue ball-and-stick model. Subdomains 1 and 2 and the C-terminal domain are marked in color. The nuclear localization signal (NLS) region is shown by a dotted line; (**b**) head-to-tail dimer of PAD4; (**c**) the C-terminal domain of PAD4. Five ββαβ modules are light blue, red, dark blue, yellow, and orange. The substrate, benzoyl-L-arginine amide, is a green stick model. The right panel provides a top-down view of the left panel (printed with permission from Ref. [22])

structure of Ca(II)-bound PAD4 [22, 72]. The molecular weight of human PAD4 is 74.079 kDa (663 amino acids) and contains two N-terminal immunoglobulin-like subdomains (Fig. 5). Subdomain 1, extending from residue M1 to C118, contains nine β-strands and a classic nuclear localization sequence (NLS, 56-PPAKKKST-63) at the molecular surface. This unique NLS translocates human PAD4 to the nucleus during cell activation as PAD4 is predominantly localized in the cytoplasm [41]. Subdomain 2 (A119 to P300) is constituted of ten β-strands and four short α-helices [42].

The C-terminal catalytic domain (N301 to P663) is highly conserved among all PAD isozymes [15, 21, 73, 74]. It has a structure of five circularly arranged ββαβ modules that make a pseudo 5-fold symmetric structure called an α/β propeller, a characteristic of the deiminase superfamily [17, 22, 42, 72]. The first β-strand of each individual module (β41, β22, β25, β30, β36) forms an active site cleft of the enzyme to bind with the substrate [22]. Based on crystallographic data, PAD4 has five calcium-binding motifs, which are highly conserved among all PAD isozymes except for PAD6 [56, 74]. The N-terminal subdomain 2 occupies three calcium ions (Ca3–Ca5) while the other two calcium ions (Ca1 and Ca2) bind to the C-terminal catalytic domain. The binding of calcium ions occurs in a cooperative manner and induces conformational changes leading to the activation of the enzyme [48, 51, 42, 75]. Binding of calcium ions is one of the factors discussed extensively in enzyme regulation [51, 76].

Although it is unknown whether all PAD isoforms can multimerize, human PAD4 exists as a head-to-tail dimer with an elongated rubber boot structure [20, 22, 42, 41, 77]. The N-terminal domain of one monomer binds to the C-terminal domain [4] by hydrophobic interactions and salt bridges between the adjacent monomers [20, 42]. A crystallographic two-fold axis runs vertically through the center of the dimer [22]. Dimerization of PAD4 has been suggested to be required for its regulatory mechanism. The kinetic studies of hPAD4 indicate that the disruption of the dimer interface does not only decrease the enzymatic activity, but also affects the cooperative binding of calcium ions [20, 48]. Among the residues R8, Y237, D273, E281, Y435, R544, and D547, located at the surface of the dimer, R8, D547, and Y435 mediate hydrophobic interactions, imperative for dimerization [20]. Peptidylarginine deiminase type 4 appears to play an important role in gene regulation, inflammatory diseases, and neurodegeneration.

## *2.5 Peptidylarginine Deiminase Type 6*

Some years ago, the identification of highly abundant, zona-free metaphase II mouse egg-protein, revealed the existence of this novel PAD isotype [78, 79]. The amplified mouse ovarian adapter-ligated cDNA library encodes for 681 amino acids that exhibit 40% homology with the calcium-dependent peptidylarginine deiminase family [78]. Based on its homology with the PAD family and its expression in egg cells [79], embryos [51], oocytes [4, 80], and ovaries [69, 80], the protein was designated as ePAD (egg- and embryo-abundant peptidylarginine deiminase). Later on, in a large-scale sequencing project, new human cDNA was constructed from a fetal brain cDNA library. The putative protein encoded by this cDNA was found to be orthologous to ePAD, and was thus renamed as hPAD6 by the HUGO Gene Nomenclature Committee (HGNC) [15, 81].

The peptidylarginine deiminase type 6-encoding gene is an about 29.3 kb region at chromosome 1p36.13, containing 16 exons (see Fig. 2) and expressing the 77.7 kDa (694 amino acids, pI 5.13) cytoplasmic PAD6 protein [43, 81, 82]. It

contains a short lysine-rich motif (139-SDKQAKKK-147) in its N-terminal domain, but it remains to be tested if it is involved in nuclear translocation [83]. Peptidylarginine deiminase type 6 has been reported to be essential for female fertility [84, 85] and lattice formation within oocytes and early embryos [86], where citrullination of epithelial cell keratin results in cytoskeletal reorganization during the early stages of development [87]. Peptidylarginine deiminase type 6 associates with α-tubulin at lattices to stabilize microtubule formation, while in PAD6-null mice, a defective organelle repositioning has been reported [84, 87]. Additionally, immunohistochemical data suggest the presence of PAD6 in cortical granules of mouse oocytes, released extracellularly during oocyte fertilization to associate with blastomeric surfaces as a peripheral membrane protein. This indicates the extracellular functions of PAD6 in preimplantation development [82].

In contrast to the other family members, the biochemical properties, regulation, and functions of PAD6 are poorly understood so far [88, 89]. Interestingly, the sequence alignment of all PAD isozymes reveals the loss of a conserved active-site cysteine residue and acidic residues in PAD6 (see Table 1) which are involved in Ca(II) binding [22, 43, 89], suggesting a possible need of further factors or scaffolds for enzymatic activity. Fluorescence polarization and X-ray crystallography have confirmed (Fig. 6) the two binding sites at PAD6 for the 4-3-3 protein, a

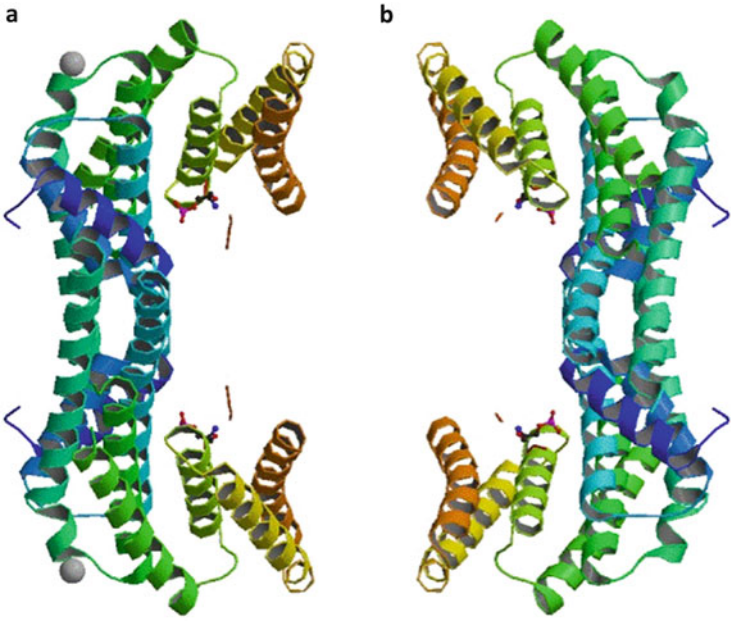


**Fig. 6** Binding sites of peptidylarginine deiminase type 6 for the 14-3-3 protein. Using X-ray crystallography two binding motifs of PAD6 are revealed for the eukaryotic adaptor protein 14-3-3 that binds to PAD6 with two binding motifs: (**a**) Binding motif I and (**b**) Binding motif II during the cell cycle in a phosphorylation-dependent manner suggested to play a part in the regulation of its activity [88] (PDBID: 4DAT(a), 4DAU(b))

member of a class of highly conserved and abundant eukaryotic adapter proteins that influence a plethora of physiological processes in a phosphorylation-dependent manner [88, 90]. Peptidylarginine deiminase type 6, purified from the mouse ovary, showed no enzymatic activity, but interestingly the isozyme has the potential to constitute a hexameric structure rather than being a dimer like other members of the family [89].

## 3 Isolation and Sequence Determination of Peptidylarginine Deiminase

The presence of a non-ribosomal-encoded citrulline amino acid in a variety of protein substrates is a consequence of enzyme-catalyzed post-translational modification (PTM). Citrulline was first described in *Citrullus vulgaris* (water melon) by Fearon and colleagues in 1939 [91], whereas Rogers and coworkers have reported the presence of an arginine-converting enzyme in crude extracts of hair follicles that catalyze the conversion of arginyl residues of the insoluble trichohyalin to citrulline [92]. Later, this enzyme was purified from the stratum corneum of calf's snouts [93] and described as an epidermal arginine-converting enzyme that is active at neutral pH and dependent on the presence of Ca(II) ions for activity. A partially purified enzyme using ammonium sulfate precipitation, ion-exchange, and size-exclusion chromatography exhibited a molecular weight of 69 kDa [93]. The occurrence of the enzyme in the epidermis was further confirmed by Fujisaki and Sugawara [94], who proposed the name "peptidylarginine deiminase (PAD)", and extracted this enzyme from the epidermis of a newborn rat. An enhanced activity of peptidylarginine deiminase was recorded in the presence of the reducing agent dithiothreitol towards N-substituted L-arginine derivatives. Fujisaki and Sugawara further suggested that peptidylarginine deiminase is an SH-enzyme, for which the activity is affected by the nature of the neighboring arginyl residues [94].

An 115 kDa peptidylarginine deiminase isotype was partially extracted from rabbit skeletal muscles [95], kidney, lung, and brain [96] for which protamine, histone, and ribonuclease A were reported to be the better substrates when compared to small synthetic peptides [95]. The isoelectric point (pI) and amino acid composition of PAD were determined, respectively, as 5.3 and $\geq$663 amino acids. Soybean trypsin inhibitor-affinity chromatography was used to improve peptidylarginine deiminase purification [97]. Combined biochemical and immunochemical investigations of peptidylarginine deiminase in various tissues have suggested the occurrence of three PAD isotypes (muscle type, hair follicle type, and epidermal type) in mammals [98]. The tissue distribution of peptidylarginine deiminase was described by activity monitoring in various mouse organs [99]. The salivary glands, pancreas, and uterus were observed to exhibit higher

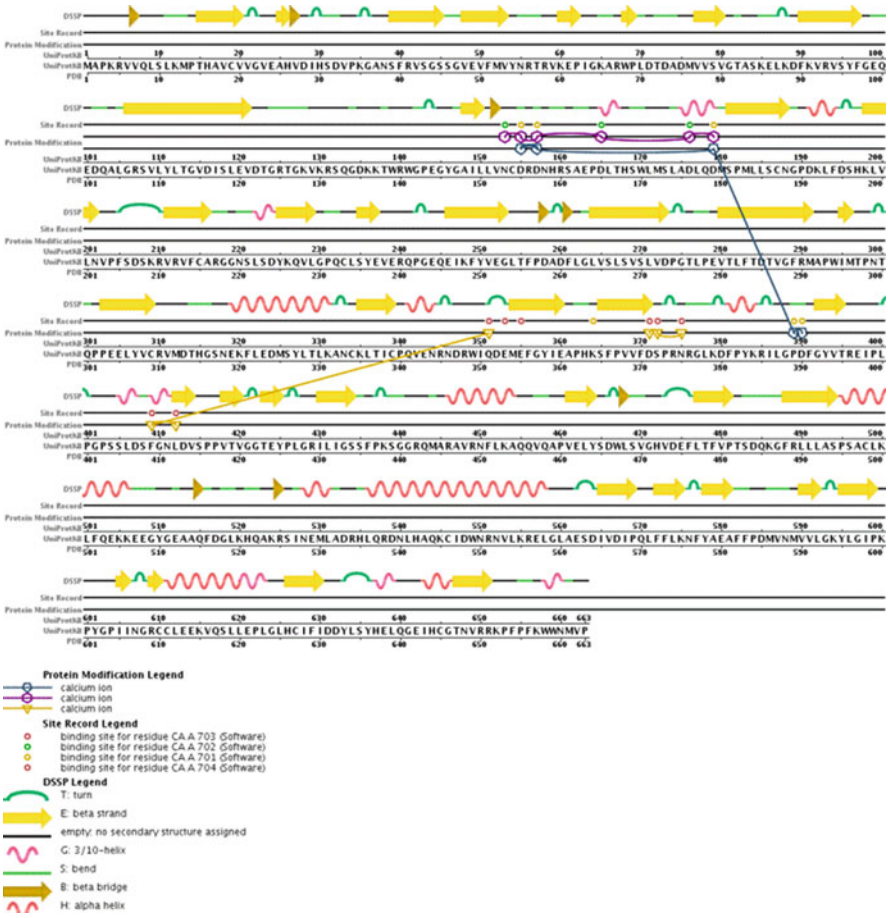


**Plate 1** Graphical representation of full-length human peptidylarginine deiminase type 1 sequence as reported in UniprotKB accession number Q9ULC6. Human peptidylarginine deiminase type 1 is composed of 663 amino acids. A digital solid state propulsion (DSSP) algorithm suggests the secondary structure of PAD1 is 16% helical (18 helices of 113 residues) and 32% β-sheets (48 strands made up of 219 residues). The remaining 331 residues are either a part of β-bridges, turns, or bends, or have no secondary structure. Three to four calcium-binding sites are also predicted as indicated with colored circles (PDBID: 5HP5)

peptidylarginine deiminase activity with sex- and estrous cycle-related differences [100].

The primary structure of rat muscle-type PAD was determined partially by subjecting peak fractions of lysyl endopeptidase digests from a high-performance liquid chromatography column to an amino acid analyzer [101]. The entire sequence of peptidylarginine deiminase was deduced from the sequences of three overlapping cDNA clones synthesized using total RNA from various organs of the

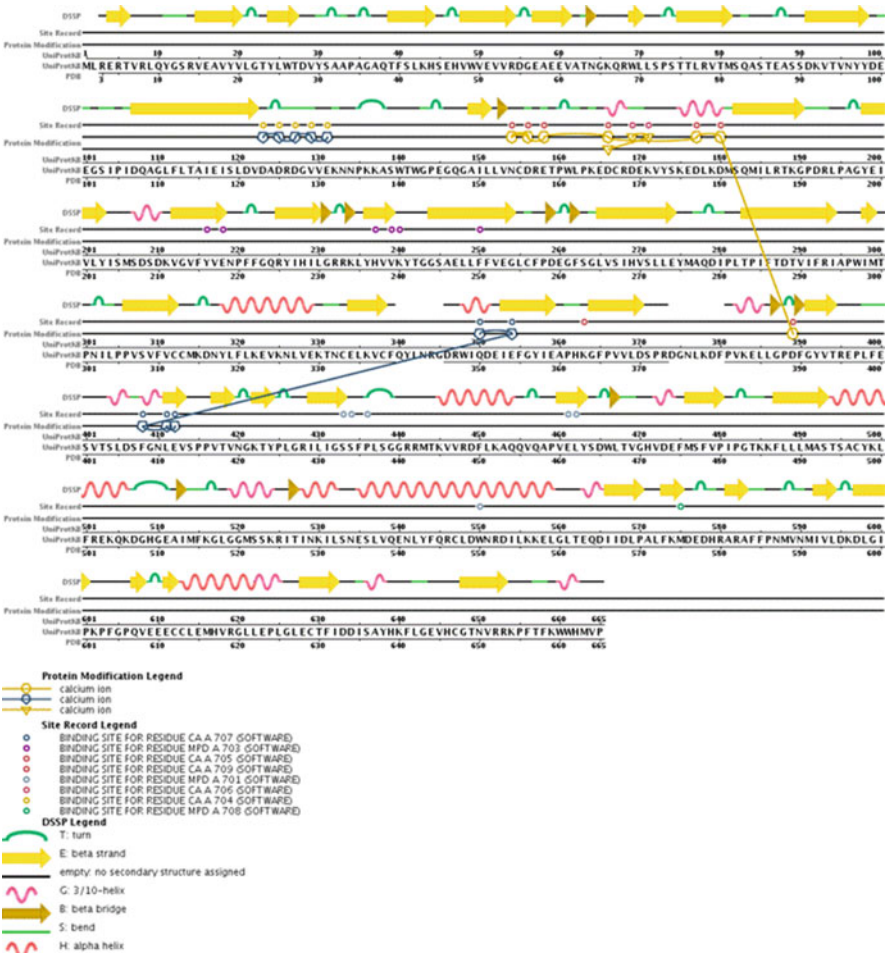


**Plate 2** Graphical representation of full-length human peptidylarginine deiminase type 2 sequence as reported in UniprotKB accession number Q9Y2J8. PAD2 contains 665 amino acids. A DSSP algorithm suggests a secondary structure of PAD2 that is 17% helical (19 helices of 123 residues) and contains 34% β-sheets (52 strands made up of 239 residues). The remaining 303 residues are either a part of β-bridges, turns, or bends, or have no secondary structure. Three calcium-binding sites are also predicted as indicated with colored circles (PDBID: 4N2B)

rat [98, 101, 102]. Epidermal and hair follicle-specific rat PAD3 was later cloned and sequenced using full-length cDNA by RT-PCR [2]. Plates 1–3 show the full-length sequence and calcium-binding sites of human peptidylarginine deiminases types 1, 2, and 4 (PDBID: 5HPH, 4N2N, and 1DW9). No matching entry was found in the RCSB Protein Data Bank for PAD types 3 and 6.

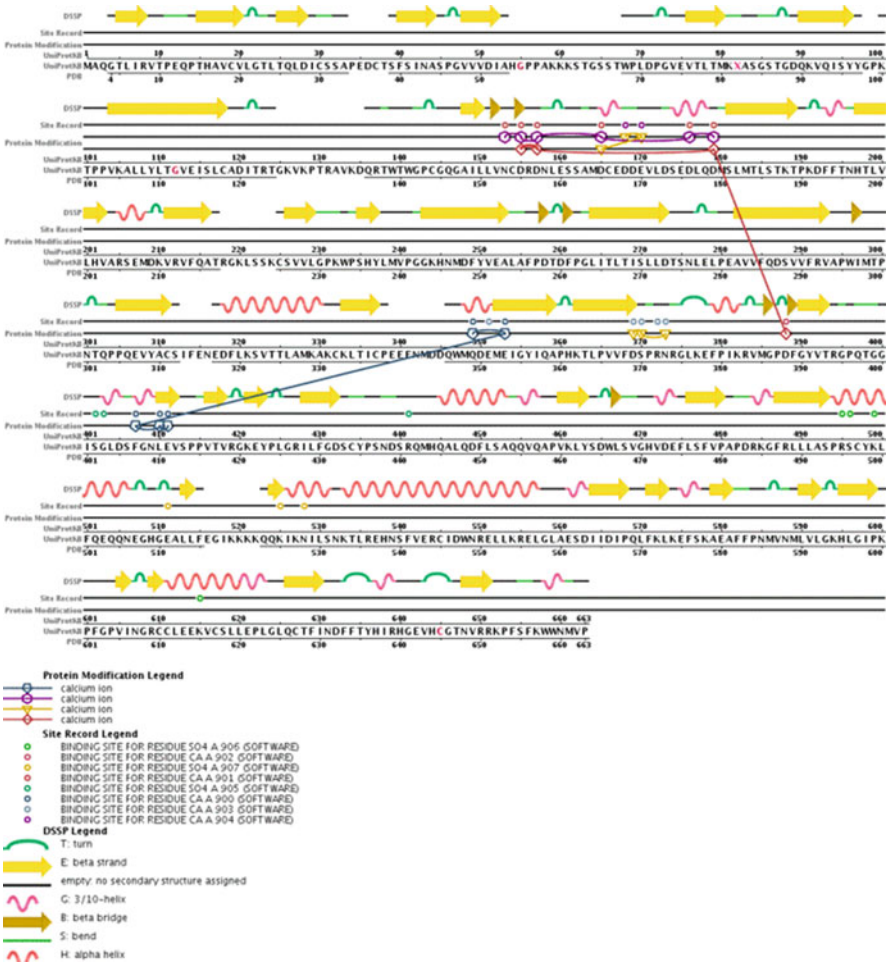


**Plate 3** Graphical representation of the sequence of human peptidylarginine deiminase type 4 as reported in UniprotKB accession number Q9UM07. PAD4 contains 663 amino acids. The predicted secondary structure of PAD2 is 19% helical (22 helices of 129 residues) and contains 33% β-sheets (48 strands made up of 222 residues). The other 312 residues are either a part of β-bridges, turns, or bends, or have no secondary structure. Three to four calcium-binding sites are also predicted as indicated with colored circles (PDBID: 1WD9)

## 4 Ca(II) and pH-Dependence of Peptidylarginine Deiminase

Calcium is an essential cofactor for deiminase activity [15]. The cytosolic concentration of Ca(II) is relatively low under physiological conditions (about $10^{-7}$ M) that keeps peptidylarginine deiminase from being active [25, 103, 104], and a 100-fold higher concentration (approximately 1–100 μ*M*) of Ca(II) is generally

required by all enzyme isoforms for conversion of their substrates [74, 105]. Modification of the peptidylarginine side chain influences the movement of Ca(II) ions from the extracellular to intracellular milieu [15]. Calcium sensitivity varies among PAD isozymes, depending on the nature of the substrate [63, 83]. For peptidylarginine deiminase type 2, a half-maximal activity was reported at 40–60 μ*M* Ca(II) concentrations [97]. In terms of the catalysis and regulation of the deiminase enzymes, pH optimum and Ca(II) ion concentration are the two crucial factors, as discussed below.

Five to six Ca(II) ions are required per enzyme monomer [48, 51, 42], as revealed during the detailed crystallographic analysis of peptidylarginine deiminase type 1 [40], type 2 [48], type 3 [75], type 4 [22, 70, 72], and peptidylarginine deiminase type 6 [88]. Two of the 5/6 calcium ions (Ca1 and Ca2) bind to the C-terminal catalytic domain, inducing a major conformational change and generating the active site cleft, competent for catalysis [74, 75]. The remaining three calcium ions (Ca3 to Ca5) bind to the N-terminal subdomain 2 and promote the formation of an α-helix between residues 158–171 [106], which is disordered in the apoenzyme [22, 42]. The newly discovered sixth calcium-binding site (Ca6) is not detected in PAD4, although it is conserved in peptidylarginine deiminase type 2 [48].

The dependence of enzyme activity on binding of calcium ions leads to the rearrangement and stabilization of the immunoglobulin-like N-terminal domain. This IgG-like domain acts as a regulatory mechanism for the enzyme [22, 51]. Calcium ions bind in a cooperative manner [20], and once they are in loco, induce marked structural changes in the enzyme to arrange the distances and conformations of the ten major amino acids of the active site, i.e. R346, R372, W347, D350, D472, G374, V468, H470, L640, and C646 [75].

Calcium-binding motifs are highly conserved among all peptidylarginine deiminase isoforms except for PAD6 [56, 107], which is probably a possible explanation for its inadequate detectable activity [89]. An artificial increase of cytosolic Ca(II) concentrations using a calcium ionophore leads macrophages to apoptosis and exhibits only a selective citrullination of vimentin [25, 103]. Although all PAD isotypes are highly specific to calcium ions, peptidylarginine deiminase type 1 and type 3 have been also reported to exhibit, in turn, up to 15 and 2.5% activity in the presence of Ba(II), a group II divalent metal ion [107]. Other bivalent cations, e.g. Zn(II), Mg(II), Mn(II), Co(II), Ni(II), Cu(II), and Sr(II) are not able generate any activity in PAD isozymes. Instead, at a concentration of 1 mM along with 1 mM calcium, an inhibition of PAD activity was recorded with Mn(II) (80% inhibition), Ni(II) (65% inhibition), and Co(II) (25% inhibition) for rabbit skeletal muscle peptidylarginine deiminase type 2 [83, 108].

Additionally, all isoforms of PAD require an optimal pH (between 7.2–7.6) for catalysis [4, 94]. Measurements of pH and p$K_a$ of active site residues are used to describe the catalytic mechanism of the enzyme [109]. Kinetic values ($K_{cat}$ and $K_m$), when plotted against the pH profile, give a bell-shaped curve with p$K_a$ 7.3 and 8.2 for the ascending and descending limbs of the curve, which corresponds to the

p$K_a$ values of the active site of cysteine and histidine residues [74, 109]. The active site residues, C645 and H471, deprotonate and protonate subsequently prior to the substrate binding, suggesting a reverse protonation mechanism of catalysis [110]. Human peptidylarginine deiminases type 2 and type 4 exhibit a decreasing trend of activity beyond the optimal pH to pH 9.5, and thereafter no or negligible activity is reported [4]. The pH profile of *Porphyromonas gingivalis* PAD (about 51 kDa) indicated pH 9.5 as the optimal pH for maximum activity, while the enzyme exhibited 38.5 and 3.4% activity at pH 6 and 11 [111].

## 5 Mechanism of Catalysis and Active-Site Cleft

Structural and mechanistic studies with peptidylarginine deiminase type 4 indicate that four key catalytic residues (D350, H471, D372, and C645) are involved in substrate binding [22, 74, 105, 107, 109]. As mentioned earlier, the amino acids of the C-terminal catalytic domain and the acidic residues involved in Ca(II) binding are highly conserved among all deiminase isozymes [13, 15, 107] except for peptidylarginine deiminase type 6 [22, 83, 89], which exhibits a few variations (see Table 1).

Among these major residues of the active site, C645 exists as a thiolate in the active form of the enzyme [109] and is known to act as a nucleophile at the guanidinium carbon of the protein-embedded arginine leading to the formation of a tetrahedral intermediate [22, 30, 74]. Residue H471 stabilizes the charge of the thiolate through an ion pair, while the guanidine side chain is held by hydrogen-bonding interactions with two conserved aspartate residues, i.e. D350 and D473 [110]. After formation of a transition state intermediate, H471 acts as a general acid to eliminate ammonia causing the transition state intermediate to collapse and forming an *S*-alkylthiouronium intermediate. It ultimately hydrolyzes to generate citrulline and evacuate thiolate for further catalysis. The remaining active site residues at positions 372, 374, and 639 (R or other amino acids in hPAD1–4 and 6 as summarized in Table 1) do not play a role in enzyme catalysis, but are thought to be involved in substrate specificity by forming a kind of filter for substrates at the entry of the active site cleft [83].

As suggested by reaction simulations, the thiouronium intermediate is attacked by an ordered water molecule, activated through H471, forming another tetrahedral intermediate before the generation of citrulline as the second product [17, 22, 112]. Some other mechanisms have also been proposed with arginine [113] or ammonia [105] acting as the general base. However, the available data are most consistent with H471 acting as the general base [22, 105, 109]. As most mechanistic studies on peptidylarginine deiminases have been performed with PAD4, it will be of interest to determine if other deiminases can catalyze their substrates following similar mechanisms or if they are distinct from PAD4 [110].

## 6 Substrate Specificity of Peptidylarginine Deiminase

Initially, the specificity of peptidylarginine deiminases towards protein substrates has not been investigated, except for the dermal type and human PAD4 [72, 83]. Thus, understanding of the natural and preferential substrate selection of peptidylarginine deiminase isozymes remains quite narrow [4, 30, 104, 107]. It has been reported that peptidylarginine deiminase binds with the substrates when present in the ES-$H^+$ form, where E is the enzyme, $S^-$ represents the negatively-charged thiolate and $H^+$ is the positively-charged imidazolonium ion at the active site center of peptidylarginine deiminase [107, 109]. Due to the surplus of acidic residues, all human peptidylarginine deiminase isoforms have a low calculated p*I* value (about 5.8), resulting in net negative charge under physiological conditions (on average –14), which is favorable for the interaction with positively charged arginines of the substrates [15].

Peptidylarginine deiminase activity has been monitored in many organs, tissues, and cells, particularly in relation to their physiological substrates, i.e., structural proteins like keratin, alpha-tubulin, vimentin, glial fibrillary acidic protein, myelin basic protein [63, 73, 84, 87, 114–116], intermediate filaments-associated proteins like trichohyalin, filaggrin [59, 117], nuclear proteins such as histones and nucleophosmin [71, 118, 119], as well as some extracellular proteins like fibrin, fibronectin, and others [14, 120].

In vitro studies suggest that peptidylarginine deiminase isoforms have broader specificity and rely mainly on the accessibility of arginine [4, 15, 42] in the unstructured regions of the substrates [42, 107]. Purified or recombinant peptidylarginine deiminase types 1–4 exhibited different relative activities and citrullination patterns with benzoylarginine [83], histone peptides [72], and HL-60 cell lysate [47], where certain proteins were citrullinated more rapidly than others by individual deiminase isotypes [15]. The substrate specificities of human peptidylarginine deiminase types 2 and 4 were recently mapped using assemblies of synthetic peptides and heterogeneous protein samples [11]. Evaluation of the flanking amino acids by amino acid substitutions (Fig. 7) depicted a higher substrate specificity for human peptidylarginine deiminase type 4 than type 2 [104]. Certain amino acids flanking the targeted arginine and the conformation of the substrate's secondary structure were reported to influence the PAD activity [30, 59, 83, 121, 122]. A summary of specificity of peptidylarginine deiminase towards the primary and secondary structure of substrates is provided in Table 2.

Although the consensus amino acid sequences for the targets against all PAD isotypes remain obscure [4], subcellular localization of the enzyme, its micro environment, e.g. inter- and intracellular Ca(II) concentrations as well as the physiochemical features like structure, charge, size, and flexibility of the target protein, are reported to be important for in vivo substrate selection [15].

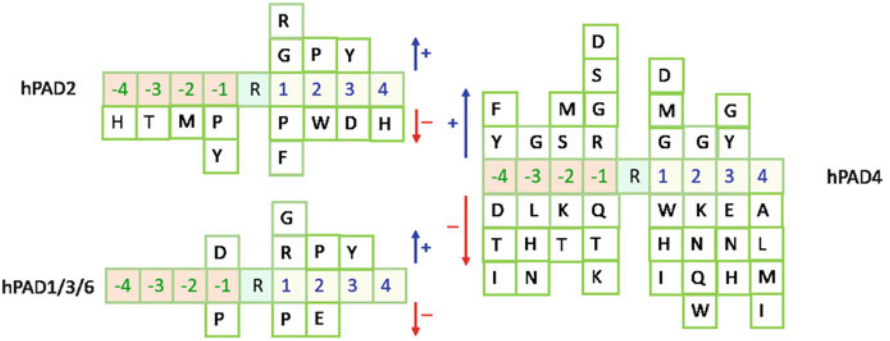


**Fig. 7** Graphical illustration of the influence of the surrounding residues of arginine on human peptidylarginine deiminase catalysis. Naturally occurring/substituted amino acids, flanking targeted arginine, influence its susceptibility to citrullination by peptidylarginine deiminases. Promulgated positive and negative influences of amino acids on substrate specificity of human deiminase isoforms are shown with blue and red arrows

**Table 2** Influence of arginine neighboring residues and protein secondary structure on peptidylarginine deiminase catalysis

| Arg and other residues | Enzyme catalysis | Ref. |
|---|---|---|
| Arg[a] near to N-terminus | Slow citrullination | [83] |
| Arg near to C-terminus | Slow citrullination except for MBP | [30, 170] |
| Pro-Arg-Pro | No citrullination at all | [15, 30, 171] |
| Pro-Arg-Arg-Pro | Moderate citrullination | [171] |
| Pro/Glu adjacent to Arg | Bare citrullination | [30, 83] |
| ¡Arg-Arg | Rapid citrullination at ¡Arg | [83] |
| 'N-Arg-Asp-C' | Rapid citrullination[b] | [30] |
| Gly next to Arg | Rapid citrullination | [104] |
| Tyr at +3 position to Arg | Preferred citrullination by hPAD2 and hPAD4 | [11] |
| 'N-X-X-X-Arg-Z-Z-Z-C' | Citrullination is more influenced by X amino acids compare to Z | [142, 171] |
| Secondary conformation of substrates | | |
| Alpha helix | Hardly deiminated | [30] |
| Beta turn | Rapid citrullination[c] | [30, 72] |
| Beta sheet | Data are not available | [30] |
| Disordered | Rapid citrullination[d] | [30, 72] |

[a]At position 1–3, except if preceded by carbobenzoxy or benzoyl group. 'N and C' are the N and C-termini of the substrates

[b]Up to 100% efficiency

[c]Most favorable region for citrullination; X represents any amino acid besides Arg towards N-terminal while Z illustrates any amino acid adjacent to Arg towards C-terminal

[d]Up to 95% efficiency

## 7 Peptidylarginine Deiminase Regulation

Recent developments of peptidylarginine deiminase inhibitors have enhanced the understanding of the physiological functions of deiminases, but the mechanisms that regulate their activities, under physiological and pathological conditions, are poorly known [123–125]. It has been reported that citrullination is regulated at multiple levels, including the transcription and translation of PADI genes [52], by calcium ions [41], estrogen hormone concentration [30], as well as by auto-deimination of peptidylarginine deiminase [77, 123]. The influence of calcium concentration, one of the major regulators of PAD activity, is discussed in Sect. 4.

### *7.1 Transcriptional and Translational Regulation*

Peptidylarginine deiminase type 4 is reported to be regulated at the transcriptional, translational, as well as post-translational levels [25, 126]. Mechin and colleagues observed levels of PADI1-3 mRNAs, their protein amounts, and also the activity as an effect of the differentiation to natural human keratinocytes (NHKs) [52]. The active form of vitamin $D_3$ (1,25-dihydroxy vitamin $D_3$), a known inducer of deiminase activity, can also regulate a complex differentiation network in the keratinocytes, chondrocytes, and osteoblasts [83, 127]. Upregulation of PADI1-3 mRNA was recorded with distinct kinetics upon treatment of NHKs with vitamin D, although the amount of the enzymes as well as their activities remained unchanged [52]. Increased cell density is another cellular model for differentiation induction in NHKs, which failed to affect PADI2 genes, but the mRNA and corresponding peptidylarginine deiminase of type 1 and 3 were upregulated, suggesting that PADI genes follow distinct or independent kinetics of regulation during cellular differentiation [52].

Long-range enhancers, i.e. 86 kb and 81–82 kb distant from the PADI3 promoter, are reported to regulate transcription of PADI3 genes by binding with AP-1 factors through chromatin looping events in differentiated keratinocytes [128, 129]. Moreover, Mechin and colleagues have described the post-transcriptional regulation of PADI 1–3 genes [52], like others who reported this for PADI2 and PADI4 during monocyte/macrophage differentiation and in the optic nerves [25, 130], suggesting that a long 3′-untranslated region of PADI2 mRNA plays a role in regulation of corresponding protein production.

An oocyte-specific transcriptional regulator, Nobox (Newborn ovary homeobox), is reported to regulate PAD6 activity in germ cells [80]. The presence of the Nobox DNA-binding element (NBE) in the mouse peptidylarginine deiminase type 6 promoter region suggests a direct regulation of PAD6 in oocytes by Nobox, although the specificity of Nobox on peptidylarginine deiminase type 6 regulation and its role in oocyte and germ cell development remain to be determined [80].

## 7.2 Hormonal Regulation

Peptidylarginine deiminase types 1, 2, and 4 are regulated by hormones, e.g. estrogen and/or epidermal growth factors in the uterus, pituitary, and mammary glands of female rats, mice, dogs, and humans in consonance with the estrous cycle [44]. Expression of PADs in the mouse uterus and mammary glands is highest during the estrus stage, while in canine mammary glands, estrus initiates peptidylarginine deiminase type 2 expression, which peaks during diestrus [84]. The difference may be due to the different lengths of the individual stages of the estrous cycle or peculiar hormonal levels between the species [21]. Following ovariectomy, peptidylarginine deiminase levels in the uterus, pituitary, and mammary glands dropped considerably [15], but can be restored by injection of exogenous 17$\beta$-estradiol, but not by progesterone or testosterone [131, 132]. Progesterone is reported to antagonize the estradiol-induced peptidylarginine deiminase activity in the uterus of ovariectomized mice, when injected simultaneously [83].

During pregnancy, peptidylarginine deiminase type 2 expression in the mouse uterus and pituitary gland is elevated after an initial decline [15, 133]. Studies with MCF-7 cells revealed that estrogen-induced PADI4 expression is mediated by estrogen's receptor-alpha-promoted Sp1, nuclear factor-Y, and transfactor activator protein-1 that bind with PADI4 promoter and upregulate its expression [41, 134]. As most of the tissues do not exhibit estrogen-dependent peptidylarginine deiminase expression, it is suggested that hormonal regulation of PAD expression is tissue-specific [15].

## 7.3 Auto-Citrullination

Post-translational modifications (phosphorylation, methylation, acetylation, etc.) of enzymes may regulate their interactions, catalytic activities, as well as tissue/cellular localization [123]. Likewise, it is reported that citrullination reduces the activity of the peptidylarginine deiminase [52] as a function of its regulatory mechanism [77]. An in vitro study suggested that the optimal temperature required to auto-citrullinate recombinant human peptidylarginine deiminases of types 1–3 ranges between 37°C and 50°C in a time-dependent manner [52]. Moreover, auto-citrullination is reported to occur only in the presence of calcium ions, although the presence of substrate does not change the pattern of auto-citrullination of the enzyme, as analyzed with the recombinant human peptidylarginine deiminase type 4 [77].

Loss of positive charge as a consequence of citrullination may lead to structural transformation of the target protein, and thus it was hypothesized that auto-citrullination of peptidylarginine deiminase alters its structural conformation. French researchers have demonstrated a reduced avidity of anti-peptidylarginine deiminase type 3 antibody to recognize the immunogenic peptide (49-DIYISPNMERGRERADTR-66) of human PAD3 after auto-deimination [52]. Similarly, anti-peptidylarginine deiminase type 4 antibodies against its

C-terminal epitope (amino acids 519–528) and N-terminal sequence from residues 1–15, failed to immunoprecipitate the auto-citrullinated recombinant human peptidylarginine deiminase type 4 [77], ratifying the immunogenic variations of structure and/or charge of PAD after auto-deimination. In vivo experimentation using PAD4 tagged with green fluorescent protein (GFP) demonstrated the same results [77].

A three-dimensional model of peptidylarginine deiminase type 3 was developed [52] to mimic auto-deimination in silico, using the crystal structure of deiminase type 4, in which most accessible arginine residues were replaced by citrulline. The calculated volume and surface area of the whole molecule and of the active site cleft remained unexpectedly the same to affirm that auto-citrullination does not perturb remarkably the overall structure of the enzyme. However, for the four major residues of the active site cleft, a profound conformational change was monitored (Fig. 8). The distances between the conserved active site residues (D350, D472, H470, and C646) increased after auto-deimination [52]. Consequently, reduction of the activity of the enzyme occurred as a mode of self-regulation, which may play a major role in the metabolism and rate of citrullination of filaggrin in the stratum corneum to maintain the barrier function and moisturization of skin [52].

Potential auto-deamination sites were determined by scrutinizing the trypsinized auto-citrullinated human PAD4 using linear-trap-quadrupole (LTQ) and QSTAR mass spectrometers. Among the ten identified possible citrullination sites, R372 and R374 span into the active site cleft, and play a major role in substrate recognition and were reported previously [72]. Residue R252 (position 419 when aligned) has also been reported as a possible auto-citrullination site in mouse PAD2 [15]. Thus, mutant variants of human PAD4 were expressed by replacing R372 and

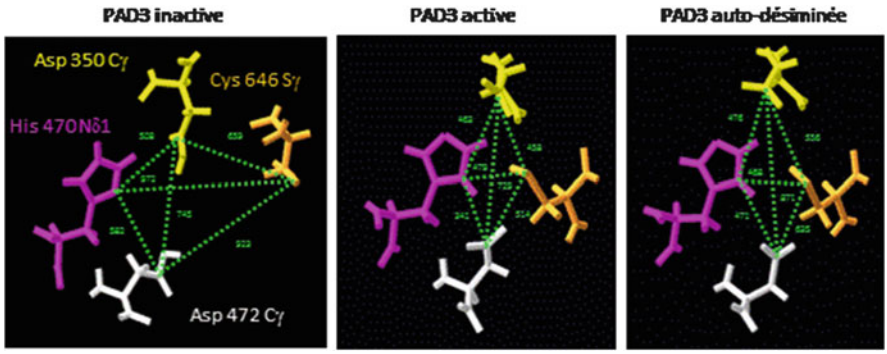


**Fig. 8** Magnification of the four major amino acids at the active site cleft of human peptidylarginine deiminase 3. Left: inter-amino acid distances of the inactive form of PAD3 in the absence of calcium ions, middle: abatement of distances in active form of PAD3 in the presence of calcium ions, and right: auto-deiminated form where more accessible arginine (accessibility to solvents ≥40%) has been replaced by citrulline. Calculated distances are indicated in picometers. Auto-deimination induces an enlargement of the active site of PAD3 in the presence of calcium ions. The increase of distances between the four amino acids D350 (Cγ yellow), D472 (Cγ white), H470 (Nδ1, pink), and C646 (Sγ orange) reduces the enzyme activity (printed with permission from Ref. [75])

R374 with L-lysine to preserve the charge, but to lack the guanidine group. A dearth of activity supported the critical interactions of arginine with the carbonyl backbones of substrates that are essential to stabilize the active site of the enzyme [72, 77].

Contrary to this, Slack and colleagues identified seven auto-deimination sites (six in vitro and two in vivo; none of which had been reported earlier) in peptidylarginine deiminase type 4 using isotopic labeling and matrix-assisted laser desorption/ionization-time-of-flight analysis [123, 125]. They further demonstrated that auto-citrullination does not alter the enzymatic activity and substrate specificity or their dependence on calcium ions, but weakens the enzyme interactions with its binding partners, e.g. citrullinated histone (Cit H3), proteinarginine methyltransferase 1 (PRMT1), and histone deacetylase 1 (HDAC1) [135]. Moreover, it was reported that histone deacetylase imposes an inhibitory effect on auto-deimination activity of human peptidylarginine deiminase type 4 [123]. The major disparities between these studies include the choice of substrates and methodologies as well as the particular detection strategies utilized.

## 8 Activity Assay for Peptidylarginine Deiminase

Conversion of arginyl to citrullyl is a regular measure of peptidylarginine deiminase activity, often known as COLDER or colorimetric assay, with $N_{\alpha}$-benzoyl-L-arginine ethyl ester (**1**) (BAEE) as a commonly used substrate [136, 137]. Zendman and colleagues have introduced an antibody-based assay to determine the PAD activity by incubating it with immobilized arginine-containing epitope sequences of filaggrin in a microtiter plate [138]. In addition to this, a monoclonal anticitrulline antibody (single chain variable fragment (scFv) RA3) was produced to detect the incipient citrulline [139]. The (scFv) RA3 antibody is reported to be reactive against up to 5 pmol filaggrin-derived citrullinated peptides, although not to endogenous ureido-containing compounds, e.g. urea, citrulline, etc. [138]. Anti-modified citrulline immunoblotting has also been reported to determine enzyme catalysis [8, 52, 77, 123–125].

Interestingly, PAD activity can also be determined using thin-layer chromatography [111], where the reaction product of the enzyme and substrate can be resolved

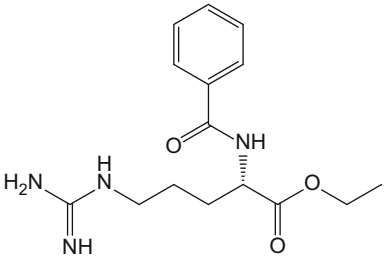


**1** ($N_{\alpha}$-benzoyl-L-arginine ethyl ester, BAEE)

on a silica gel plate in the presence of methanol and ammonium hydroxide solution. Ninhydrin was used to stain the modified arginine as a measure of enzyme activity [140]. Moreover, to monitor the release of ammonia during arginyl to citrullyl conversion there is another assay reported to determine PAD activity [141]. The authors specified their method as a "continuous spectrophotometric assay", where the ammonia released was directly coupled to α-ketoglutarate via glutamate dehydrogenase (GDH) yielding glutamate in the presence of nicotinamide adenine dinucleotide (NADH). The rate of ammonia formation is directly associated with the oxidation of NADH, which decreases the absorbance at 340 nm. This assay uses the change of absorbance as a measure of peptidylarginine deiminase activity, suitable for enzyme kinetics. However, the impedance of endogenous ammonia, NAD(P)H, and dehydrogenases reduce the usefulness of the assay, particularly for small amounts of PAD activity [104].

Chikuma and colleagues have developed a more sensitive HPLC-fluorometric assay using *N*-dansyl-glycyl-arginine as a fluorescent substrate [142]. In this assay the reaction product of PAD catalysis can be measured at 533 nm. Dansyl-glycyl-Cit is separated well from dansyl-glycyl-Arg using an acetate buffer with octane sulfonate (pH 4.0) and acetonitrile on a reversed-phase $C_{18}$ column at a retention time of 5 and 9 min, respectively. This assay is reported to have a linear response from 10 nmol to 2 pmol without any hindrance of endogenous citrulline, urea, or other ureido-containing compounds [142].

Recently, Wang and colleagues have proposed a fluorescence-based sensing strategy to monitor peptidylarginine deiminase activity [143] using a TAMRA-coupled pre-described PAD4 substrate (GRGA) [107]. Among all the commercially available dyes screened against a fluorophore-coupled substrate, acid green-27 was found to exhibit a 166-fold fluorescent readout of TAMRA-(GRGA) tetramer upon citrullination [143]. Over a decade ago, a simple fluorescence-based assay for peptidylarginine deiminase activity was also reported that exploited the substrate specificity of trypsin [144]. The fluorophore substrate was synthesized by coupling 7-amino-4-methylcoumarin (AMC) at the carboxyl side of arginine and hydrolysis of the amide by trypsin releases AMC and generates fluorescence (450 nm). Acylation of AMC on arginine reduces the fluorescence intensity up to four-fold. However, the sensitivity of the assay and its application in live-cell biology was not described [145].

## 9 Inhibitors/Inactivators of Peptidylarginine Deiminase

Diversified evidence of human peptidylarginine deiminase activity in several human diseases, e.g. rheumatoid arthritis [146–149], multiple sclerosis [19, 73, 116, 118, 150, 151], prion disease [152], Alzheimer's disease [27, 153], Crohn's disease [154], and different cancers [21, 45, 155, 156] has demonstrated their significance as therapeutic targets [11] to stop further disease progression [109]. Initially, paclitaxel (**2**) (a taxane derivative), which bears a similar functionality to

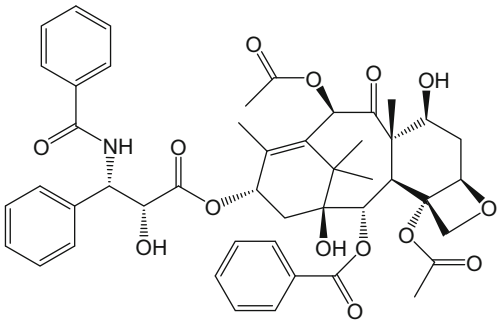


**2** (paclitaxel)

the well-known peptidylarginine deiminase substrate $N_{\alpha}$-benzoyl-L-arginine ethyl ester (**1**) (BAEE), demonstrated a complete inhibition of PAD2 activity at 12.5 m*M* concentration [157]. Later on, arginine derivatives were synthesized to examine their inhibitory activity [158], and monomethylarginine and asymmetric dimethylarginine were reported as specific peptidylarginine deiminase type 4 inhibitors [158]. Half-maximal inhibitory concentrations ($IC_{50}$) for some of the promulgated peptidylarginine deiminase inhibitors are shown in Table 3.

Halogen(acet)amidine and haloamides (mainly F- or Cl-containing) potentially inactivate peptidylarginine deiminase type 4 irreversibly by modifying C645, the active site nucleophile [159], in a time- and concentration-dependent manner [160]. In particular, 2-chloroacetamidine has been disseminated as a general pharmacophore for covalent inactivation of two diverse members of the amidinotransferase superfamily, i.e. peptidylarginine deiminase (PAD) and dimethylarginine dimethylamino hydrolase (DDAH). A possible mechanism of enzyme inactivation by 2-chloroacetamidine and 2-chloroacetamide using DDAH C249 as an active center was proposed by Stone and colleagues [160]. Also, fluoroamidine (F-amidine), a small molecule with a similar structure to benzoylated arginine, exhibited PAD4 inhibition at an $IC_{50}$ value of 22 μ*M* [161]. Due to its positive charge and two potential H-bond donors, it mimics closely the structure of arginine and binds covalently with the active site C645 for selective and irreversible inactivation following a similar mechanism proposed by Stone and coworkers in 2005 [160]. Hence, substitution of halide may occur either directly by nucleophilic attack of C645 on the methylene carbon of a halo-amidine or by the attack of the thiolate on the iminium carbon to form a tetrahedral and three-membered sulfonium ring intermediate which subsequently rearranges to form a stable thioether bond. Although the latter mechanism has a poor leaving group potential for fluoride [161, 162], it has been suggested to be the preferential mechanism of inactivation [163, 164].

Luo and colleagues tagged Cl- and F-amidines with a fluorophore, e.g. rhodamine and biotin to develop activity-based protein profiling [161, 162] reagents with a detection limit of 125 ng (or 1.7 pmol) of peptidylarginine deiminase type 4.

**Table 3** Selected inhibitors of peptidylarginine deaminases and their half-maximal inhibitory concentrations ($IC_{50}$)

| Promulgated PAD inhibitors/inactivators | Half-maximal inhibitory concentration ($IC_{50}$)/m*M* | PAD isozyme | Ref. |
|---|---|---|---|
| Paclitaxel (= taxol) (**2**) | 5-6 | Bovine PAD2 | [157] |
| Bz-$N^G$-monomethyl-Arg | | PAD4 | [158] |
| Bz-$N^G$-dimethyl-Arg (asymmetric) | 0.4 | | |
| Halo-amidine | 0.022[a], 0.0059[b] | PAD4 | [160, 161] |
| Halo-acetamidine | >0.5 | | |
| Tetracycline, chlortetracycline | 0.78, 0.1, | PAD4 | [165] |
| Minocycline, deoxycycline | 0.62, 0.86 | | |
| 5-Aminosalicylic acid, azathioprine | >10, 8.5, >10, | PAD4 | [165] |
| Azithromycin, clindamycin, leflunomide | 5.1, 2.6, >10, | | |
| Methotrexate, streptomycin, sulfamethoxazole | 1.8, >10, >10, | | |
| Sulfapyridine, trimethoprim | >10, 7.5 | | |
| Rhodamine-tagged-fluouroamidine (RFA) | 0.024 | PAD4 | [162, 164] |
| Rhodamine-tagged-chloroamidine (RCA) | 0.0074 | | |
| *o*-F-amidine | 0.0014, 0.05, 0.034, 0.0019 | PAD1-4 | [166] |
| *o*-Cl-amidine | 0.00084, 0.0062, 0.00069, 0.0022 | PAD1-4 | |
| Thr-Asp-F-amidine (TDFA) | 0.0085, 0.071, 0.026, 0.0023 | PAD1-4 | [163] |
| Thr-Asp-Cl-amidine (TDCA) | 0.0028, 0.059, 0.032, 0.0034 | | |
| YW4-03, YW3-56, YW4-15 | 0.005[c], 0.001-0.005[d] | PAD4 | [29] |
| Imidazolone derivatives designated as 10 and 11 ($H_2/H_3$-antagonists) | Comparable to Cl-amidine | PAD4 | [51] |

[a]F-amidine
[b]Cl-amidine
[c]For YW4-03
[d]For YW3-56 and YW4-15

Rhodamine-tagged-F-amidine (RFA) showed a higher selectivity, while rhodamine-tagged-Cl-amidine (RCA) inhibited peptidylarginine deiminase type 4 four-fold more potently (see Table 3). In addition, by using RFA, disease-modifying antirheumatic drugs (DMARDs) were screened for PAD4 inhibition that led to the identification of streptomycin, minocycline, and chlortetracycline as relatively weak (μ*M*) peptidylarginine deiminase inhibitors [165].

Causey and colleagues have developed a second generation of F-/Cl-amidines by side chain and backbone substitutions, e.g. *N*-α-(2-carboxyl)benzoyl-*N*5-(2-fluoro-1-iminoethyl)-L-ornithine amide (*o*-F-amidine) and $N_\alpha$-(2-carboxyl)benzoyl-*N*5-(2-chloro-1-iminoethyl)-L-ornithine amide (*o*-Cl-amidine), with improved potency and differential selectivity for peptidylarginine deiminase type 1–4 isozymes [166], as summarized in Table 3. In turn, Jones and coworkers screened a 264-membered F-acetamidine-containing peptide assembly and identified Thr-Asp-F-amidine (TDFA), an irreversible and highly potent inhibitor [163] selecting peptidylarginine deiminase type 4 ≥15-fold more when compared to peptidylarginine deiminase type 1, and ≥50-fold more than peptidylarginine deiminase types 2 and 3. It is reported that these cell-active F-, and Cl-amidines reduce the disease severity in animal models of rheumatoid arthritis (RA) [159, 161], ulcerative colitis (UC) [167], and neuron degeneration in multiple sclerosis (MS) [73] by decreasing human deiminase activity and protein citrullination [163].

Analogues of Cl-amidine, e.g. YW3-56, YW4-03, and YW4-15 [29], are reported to activate p53 target genes and inhibit mTORC1 signaling pathways that suppress the growth of cancerous cells and reduce tumor size [168, 169]. Guanidine-containing compounds [51] have also been tested against peptidylarginine deiminase type 4, but a weak or no inhibitory activity was recorded when compared to Cl-amidine except for two imidazolone derivatives (compounds 10 and 11 in Ref. [51]), where the guanidine group at the center of the molecules was suggested to react with D323 and H613, shown by docking simulations. H610 and E615 were reported to establish hydrogen bonds with the imidazolone ring while R347 at the peptidylarginine deiminase type 4-binding groove interacts with the 1,2,5-oxadiazole of compounds 10 and 11 of Ref. [51].

## 10 Conclusions

Citrullination events in the pathophysiology of trauma or brain injuries contribute to protein degradation and neurodegeneration. In this sense, PAD may facilitate the discovery of new biomarkers that could improve diagnostic and prognostic standards in clinical use. Also, peptide-based selective inhibitors for human PAD isozymes, that mimic the structure of its substrate, may help to enhance therapeutic applications. Peptidylarginine deiminase inhibitors have been demonstrated to selectively suppress colitis via cell cycle arrest in mice. Thus, it can be hypothesized that PAD inhibitors can prevent tumorigenesis and degradation of neuronal connections as well as inflammation. Detailed studies on the substrate specificity for peptidylarginine deiminase isozymes and appropriate study designs to characterize peptidylarginine deiminase-specific and closely related disorders, such as lung and heart inflammation in arthritis, neurodegenerative disorders, or dementia, are necessary. Early diagnostic markers are urgent, as these will facilitate earlier intervention for better treatment outcomes and thereby will decrease the disease burden on the population.

## References

1. Fert-Bober J, Giles JT, Holewinski RJ, Kirk JA, Uhrigshardt H, Crowgey EL, Andrade F, Bingham IIICO, Park JK, Halushka MK, Kass DA, Bathon JM, Van Eyk JE (2015) Citrullination of myofilament proteins in heart failure. Cardiovasc Res 108:232
2. Nishijyo T, Kawada A, Kanno T, Shiraiwa M, Takahara H (1997) Isolation and molecular cloning of epidermal- and hair follicle-specific peptidylarginine deiminase (type III) from rat. J Biochem 121:868

3. Asaga H, Nakashima K, Senshu T, Ishigami A, Yamada M (2001) Immunocytochemical localization of peptidylarginine deiminase in human eosinophils and neutrophils. J Leukoc Biol 70:46
4. Suzuki A, Yamada R, Yamamoto K (2007) Citrullination by peptidylarginine deiminase in rheumatoid arthritis. Ann N Y Acad Sci 1108:323
5. Rogers GE (1962) Occurrence of citrulline in proteins. Nature 194:1149
6. Rogers GE, Simmonds DH (1958) Content of citrulline and other amino-acids in a protein of hair follicles. Nature 182:186
7. Giles JT, Fert-Bober J, Park JK, Bingham CO 3rd, Andrade F, Fox-Talbot K, Pappas D, Rosen A, van Eyk J, Bathon JM, Halushka MK (2012) Myocardial citrullination in rheumatoid arthritis: a correlative histopathologic study. Arthritis Res Ther 14:R39
8. Amin B (2014) Proteomics and post-translational modification studies in patients with multiple sclerosis. PhD Thesis, University of Tuebingen, p 115
9. Acharya NK, Nagele EP, Han M, Coretti NJ, DeMarshall C, Kosciuk MC, Boulos PA, Nagele RG (2012) Neuronal PAD4 expression and protein citrullination: possible role in production of autoantibodies associated with neurodegenerative disease. J Autoimmun 38:369
10. Witalison EE, Thompson PR, Hofseth LJ (2015) Protein arginine deiminases and associated citrullination: physiological functions and diseases associated with dysregulation. Curr Drug Targets 16:700
11. Assohou-Luty C, Raijmakers R, Benckhuijsen WE, Stammen-Vogelzangs J, de Ru A, van Veelen PA, Franken KL, Drijfhout JW, Pruijn GJ (2014) The human peptidylarginine deiminases type 2 and type 4 have distinct substrate specificities. Biochim Biophys Acta 1844:829
12. Witalison EE, Cui X, Hofseth AB, Subramanian V, Causey CP, Thompson PR, Hofseth LJ (2015) Inhibiting protein arginine deiminases has antioxidant consequences. J Pharmacol Exp Ther 353:64
13. Chavanas S, Mechin MC, Takahara H, Kawada A, Nachat R, Serre G, Simon M (2004) Comparative analysis of the mouse and human peptidylarginine deiminase gene clusters reveals highly conserved non-coding segments and a new human gene, PADI6. Gene 330:19
14. Chang X, Yamada R, Suzuki A, Kochi Y, Sawada T, Yamamoto K (2005) Citrullination of fibronectin in rheumatoid arthritis synovial tissue. Rheumatology 44:1374
15. Vossenaar ER, Zendman AJ, van Venrooij WJ, Pruijn GJ (2003) PAD, a growing family of citrullinating enzymes: genes, features and involvement in disease. Bioessays 25:1106
16. McGraw WT, Potempa J, Farley D, Travis J (1999) Purification, characterization, and sequence analysis of a potential virulence factor from *Porphyromonas gingivalis*, peptidylarginine deiminase. Infect Immun 67:3248
17. Shirai H, Blundell TL, Mizuguchi K (2001) A novel superfamily of enzymes that catalyze the modification of guanidino groups. Trends Biochem Sci 26:465
18. Guerrin M, Ishigami A, Mechin MC, Nachat R, Valmary S, Sebbag M, Simon M, Senshu T, Serre G (2003) cDNA cloning, gene organization and expression analysis of human peptidylarginine deiminase type I. Biochem J 370:167
19. Lei H (2010) Protein hypercitrullination, a basic mechanism in demyelinating diseases. MSc Thesis, University of Toronto, p 115
20. Liu YL, Chiang YH, Liu GY, Hung HC (2011) Functional role of dimerization of human peptidylarginine deiminase 4 (PAD4). PLoS One 6:e21314
21. Mohanan S, Cherrington BD, Horibata S, McElwee JL, Thompson PR, Coonrod SA (2012) Potential role of peptidylarginine deiminase enzymes and protein citrullination in cancer pathogenesis. Biochem Res Int 2012:895343
22. Arita K, Hashimoto H, Shimizu T, Nakashima K, Yamada M, Sato M (2004) Structural basis for $Ca^{2+}$-induced activation of human PAD4. Nat Struct Mol Biol 11:777

23. van Beers JJ, Zendman AJ, Raijmakers R, Stammen-Vogelzangs J, Pruijn GJ (2013) Peptidylarginine deiminase expression and activity in PAD2 knock-out and PAD4-low mice. Biochimie 95:299
24. Foulquier C, Sebbag M, Clavel C, Chapuy-Regaud S, Al Badine R, Mechin MC, Vincent C, Nachat R, Yamada M, Takahara H, Simon M, Guerrin M, Serre G (2007) Peptidyl arginine deiminase type 2 (PAD-2) and PAD-4 but not PAD-1, PAD-3, and PAD-6 are expressed in rheumatoid arthritis synovium in close association with tissue inflammation. Arthritis Rheumatol 56:3541
25. Vossenaar ER, Radstake TR, van der Heijden A, van Mansum MA, Dieteren C, de Rooij DJ, Barrera P, Zendman AJ, van Venrooij WJ (2004) Expression and activity of citrullinating peptidylarginine deiminase enzymes in monocytes and macrophages. Ann Rheum Dis 63:373
26. Rus'd AA, Ikejiri Y, Ono H, Yonekawa T, Shiraiwa M, Kawada A, Takahara H (1999) Molecular cloning of cDNAs of mouse peptidylarginine deiminase type I, type III and type IV, and the expression pattern of type I in mouse. Eur J Biochem 259:660
27. Ishigami A, Maruyama N (2010) Importance of research on peptidylarginine deiminase and citrullinated proteins in age-related disease. Geriatr Gerontol Int 10(Suppl 1):S53
28. Akihito-Ishigami HA, Takako O, Kyoichi A, Naoki M (2001) Peptidylarginine deiminase type I, type II, type III and type IV are expressed in rat epidermis. Biomed Res 22:63
29. Wang Y, Li P, Wang S, Hu J, Chen XA, Wu J, Fisher M, Oshaben K, Zhao N, Gu Y, Wang D, Chen G, Wang Y (2012) Anticancer peptidylarginine deiminase (PAD) inhibitors regulate the autophagy flux and the mammalian target of rapamycin complex 1 activity. J Biol Chem 287:25941
30. Gyorgy B, Toth E, Tarcsa E, Falus A, Buzas EI (2006) Citrullination: a posttranslational modification in health and disease. Int J Biochem Cell Biol 38:1662
31. Pearton DJ, Dale BA, Presland RB (2002) Functional analysis of the profilaggrin N-terminal peptide: identification of domains that regulate nuclear and cytoplasmic distribution. J Invest Dermatol 119:661
32. Resing KA, al-Alawi N, Blomquist C, Fleckman P, Dale BA (1993) Independent regulation of two cytoplasmic processing stages of the intermediate filament-associated protein filaggrin and role of $Ca^{2+}$ in the second stage. J Biol Chem 268:25139
33. Ishida-Yamamoto A, Senshu T, Eady RA, Takahashi H, Shimizu H, Akiyama M, Iizuka H (2002) Sequential reorganization of cornified cell keratin filaments involving filaggrin-mediated compaction and keratin 1 deimination. J Invest Dermatol 118:282
34. Simon M, Haftek M, Sebbag M, Montezin M, Girbal-Neuhauser E, Schmitt D, Serre G (1996) Evidence that filaggrin is a component of cornified cell envelopes in human plantar epidermis. Biochem J 317:173
35. Mack JW, Steven AC, Steinert PM (1993) The mechanism of interaction of filaggrin with intermediate filaments. The ionic zipper hypothesis. J Mol Biol 232:50
36. Manabe M, Sanchez M, Sun TT, Dale BA (1991) Interaction of filaggrin with keratin filaments during advanced stages of normal human epidermal differentiation and in ichthyosis vulgaris. Differentiation 48:43
37. Kizawa K, Jinbo Y, Inoue T, Takahara H, Unno M, Heizmann CW, Izumi Y (2013) Human S100A3 tetramerization propagates $Ca^{2+}/Zn^{2+}$ binding states. Biochim Biophys Acta 1833:1712
38. Kizawa K, Takahara H, Troxler H, Kleinert P, Mochida U, Heizmann CW (2008) Specific citrullination causes assembly of a globular S100A3 homotetramer: a putative $Ca^{2+}$ modulator matures human hair cuticle. J Biol Chem 283:5004
39. Unno M, Kinjo S, Kizawa K, Takahara H (2013) Crystallization and preliminary X-ray crystallographic analysis of human peptidylarginine deiminase type I. Acta Crystallogr Sect F Struct Biol Cryst Commun 69:1357
40. Saijo S, Nagai A, Kinjo S, Mashimo R, Akimoto M, Kizawa K, Yabe-Wada T, Shimizu N, Takahara H, Unno M (2016) Monomeric form of peptidylarginine deiminase type I revealed by X-ray crystallography and small-angle X-ray scattering. J Mol Biol 428:3058

41. Anzilotti C, Pratesi F, Tommasi C, Migliorini P (2010) Peptidylarginine deiminase 4 and citrullination in health and disease. Autoimmun Rev 9:158
42. Rohrbach AS, Slade DJ, Thompson PR, Mowen KA (2012) Activation of PAD4 in NET formation. Front Immunol 3:360
43. Wang S, Wang Y (2013) Peptidylarginine deiminases in citrullination, gene regulation, health and pathogenesis. Biochim Biophys Acta 1829:1126
44. Cherrington BD, Morency E, Struble AM, Coonrod SA, Wakshlag JJ (2010) Potential role for peptidylarginine deiminase 2 (PAD2) in citrullination of canine mammary epithelial cell histones. PLoS One 5:e11768
45. Cherrington BD, Zhang X, McElwee JL, Morency E, Anguish LJ, Coonrod SA (2012) Potential role for PAD2 in gene regulation in breast cancer cells. PLoS One 7:e41242
46. Zhang X, Bolt M, Guertin MJ, Chen W, Zhang S, Cherrington BD, Slade DJ, Dreyton CJ, Subramanian V, Bicker KL, Thompson PR, Mancini MA, Lis JT, Coonrod SA (2012) Peptidylarginine deiminase 2-catalyzed histone H3 arginine 26 citrullination facilitates estrogen receptor alpha target gene activation. Proc Natl Acad Sci U S A 109:13331
47. Darrah E, Rosen A, Giles JT, Andrade F (2012) Peptidylarginine deiminase 2, 3 and 4 have distinct specificities against cellular substrates: novel insights into autoantigen selection in rheumatoid arthritis. Ann Rheum Dis 71:92
48. Slade DJ, Fang P, Dreyton CJ, Zhang Y, Fuhrmann J, Rempel D, Bax BD, Coonrod SA, Lewis HD, Guo M, Gross ML, Thompson PR (2015) Protein arginine deiminase 2 binds calcium in an ordered fashion: implications for inhibitor design. ACS Chem Biol 10:1043
49. Ishigami A, Ohsawa T, Asaga H, Akiyama K, Kuramoto M, Maruyama N (2002) Human peptidylarginine deiminase type II: molecular cloning, gene organization, and expression in human skin. Arch Biochem Biophys 407:25
50. Musse AA, Polverini E, Raijmakers R, Harauz G (2008) Kinetics of human peptidylarginine deiminase 2 (hPAD2)-reduction of $Ca^{2+}$ dependence by phospholipids and assessment of proposed inhibition by paclitaxel side chains. Biochem Cell Biol 86:437
51. Bozdag M, Dreker T, Henry C, Tosco P, Vallaro M, Fruttero R, Scozzafava A, Carta F, Supuran CT (2013) Novel small molecule protein arginine deiminase 4 (PAD4) inhibitors. Bioorg Med Chem Lett 23:715
52. Mechin MC, Coudane F, Adoue V, Arnaud J, Duplan H, Charveron M, Schmitt AM, Takahara H, Serre G, Simon M (2010) Deimination is regulated at multiple levels including auto-deimination of peptidylarginine deiminases. Cell Mol Life Sci 67:1491
53. Kanno T, Kawada A, Yamanouchi J, Yosida-Noro C, Yoshiki A, Shiraiwa M, Kusakabe M, Manabe M, Tezuka T, Takahara H (2000) Human peptidylarginine deiminase type III: molecular cloning and nucleotide sequence of the cDNA, properties of the recombinant enzyme, and immunohistochemical localization in human skin. J Invest Dermatol 115:813
54. Chirivi RGS, van Rosmalen JWG, Jenniskens GJ, Pruijn GJ, JMH R (2013) Citrullination: a target for disease intervention in multiple sclerosis and other inflammatory diseases? J Clin Cell Immunol 4:146
55. Rogers G, Winter B, McLaughlan C, Powell B, Nesci T (1997) Peptidylarginine deiminase of the hair follicle: characterization, localization, and function in keratinizing tissues. J Invest Dermatol 108:700
56. Raijmakers R, Zendman AJ, Egberts WV, Vossenaar ER, Raats J, Soede-Huijbregts C, Rutjes FP, van Veelen PA, Drijfhout JW, Pruijn GJ (2007) Methylation of arginine residues interferes with citrullination by peptidylarginine deiminases in vitro. J Mol Biol 367:1118
57. Lee SC, Kim IG, Marekov LN, O'Keefe EJ, Parry DA, Steinert PM (1993) The structure of human trichohyalin. Potential multiple roles as a functional EF-hand-like calcium-binding protein, a cornified cell envelope precursor, and an intermediate filament-associated (cross-linking) protein. J Biol Chem 268:12164
58. O'Keefe EJ, Hamilton EH, Lee SC, Steinert P (1993) Trichohyalin: a structural protein of hair, tongue, nail, and epidermis. J Invest Dermatol 101:65S

59. Tarcsa E, Marekov LN, Mei G, Melino G, Lee SC, Steinert PM (1996) Protein unfolding by peptidylarginine deiminase. Substrate specificity and structural relationships of the natural substrates trichohyalin and filaggrin. J Biol Chem 271:30709
60. Hsu CY, Henry J, Raymond AA, Mechin MC, Pendaries V, Nassar D, Hansmann B, Balica S, Burlet-Schiltz O, Schmitt AM, Takahara H, Paul C, Serre G, Simon M (2011) Deimination of human filaggrin-2 promotes its proteolysis by calpain 1. J Biol Chem 286:23222
61. Ying S, Simon M, Serre G, Takahara H (2012) Peptidylarginine deiminases and protein deimination in skin physiopathology. In: O'Daly J (ed) Psoriasis — a systemic disease. InTech, Rijeka, Croatia, p 117
62. Nachat R, Mechin MC, Takahara H, Chavanas S, Charveron M, Serre G, Simon M (2005) Peptidylarginine deiminase isoforms 1–3 are expressed in the epidermis and involved in the deimination of K1 and filaggrin. J Invest Dermatol 124:384
63. Mechin MC, Enji M, Nachat R, Chavanas S, Charveron M, Ishida-Yamamoto A, Serre G, Takahara H, Simon M (2005) The peptidylarginine deiminases expressed in human epidermis differ in their substrate specificities and subcellular locations. Cell Mol Life Sci 62:1984
64. Kizawa K, Takahara H, Unno M, Heizmann CW (2011) S100 and S100 fused-type protein families in epidermal maturation with special focus on S100A3 in mammalian hair cuticles. Biochimie 93:2038
65. Unno M, Kawasaki T, Takahara H, Heizmann CW, Kizawa K (2011) Refined crystal structures of human $Ca^{2+}$/$Zn^{2+}$-binding S100A3 protein characterized by two disulfide bridges. J Mol Biol 408:477
66. Unno M, Kizawa K, Ishihara M, Takahara H (2012) Crystallization and preliminary X-ray crystallographic analysis of human peptidylarginine deiminase type III. Acta Crystallogr Sect F Struct Biol Cryst Commun 68:668
67. Nakashima K, Hagiwara T, Ishigami A, Nagata S, Asaga H, Kuramoto M, Senshu T, Yamada M (1999) Molecular characterization of peptidylarginine deiminase in HL-60 cells induced by retinoic acid and 1$\alpha$,25-dihydroxyvitamin D(3). J Biol Chem 274:27786
68. Nakashima K, Hagiwara T, Yamada M (2002) Nuclear localization of peptidylarginine deiminase V and histone deimination in granulocytes. J Biol Chem 277:49562
69. Baka Z, Gyorgy B, Geher P, Buzas EI, Falus A, Nagy G (2012) Citrullination under physiological and pathological conditions. Joint Bone Spine 79:431
70. Arita K, Hashimoto H, Shimizu T, Yamada M, Sato M (2003) Crystallization and preliminary X-ray crystallographic analysis of human peptidylarginine deiminase V. Acta Crystallogr D Biol Crystallogr 59:2332
71. Hagiwara T, Nakashima K, Hirano H, Senshu T, Yamada M (2002) Deimination of arginine residues in nucleophosmin/B23 and histones in HL-60 granulocytes. Biochem Biophys Res Commun 290:979
72. Arita K, Shimizu T, Hashimoto H, Hidaka Y, Yamada M, Sato M (2006) Structural basis for histone N-terminal recognition by human peptidylarginine deiminase 4. Proc Natl Acad Sci U S A 103:5291
73. Moscarello MA, Lei H, Mastronardi FG, Winer S, Tsui H, Li Z, Ackerley C, Zhang L, Raijmakers R, Wood DD (2013) Inhibition of peptidyl-arginine deiminases reverses protein-hypercitrullination and disease in mouse models of multiple sclerosis. Dis Model Mech 6:467
74. Jones JE, Causey CP, Knuckley B, Slack-Noyes JL, Thompson PR (2009) Protein arginine deiminase 4 (PAD4): Current understanding and future therapeutic potential. Curr Opin Drug Discov Devel 12:616
75. Mechin MC, Nachat R, Coudane F, Adoue V, Arnaud J, Serre G, Simon M (2011) Deimination or citrullination, a post-translational modification with many physiological and pathophysiological facets. Med Sci (Paris) 27:49

76. Jang B, Jeon YC, Choi JK, Park M, Kim JI, Ishigami A, Maruyama N, Carp RI, Kim YS, Choi EK (2012) Peptidylarginine deiminase modulates the physiological roles of enolase via citrullination: links between altered multifunction of enolase and neurodegenerative diseases. Biochem J 445:183
77. Andrade F, Darrah E, Gucek M, Cole RN, Rosen A, Zhu X (2010) Autocitrullination of human peptidyl arginine deiminase type 4 regulates protein citrullination during cell activation. Arthritis Rheumatol 62:1630
78. Wright PW, Bolling LC, Calvert ME, Sarmento OF, Berkeley EV, Shea MC, Hao Z, Jayes FC, Bush LA, Shetty J, Shore AN, Reddi PP, Tung KS, Samy E, Allietta MM, Sherman NE, Herr JC, Coonrod SA (2003) ePAD, an oocyte and early embryo-abundant peptidylarginine deiminase-like protein that localizes to egg cytoplasmic sheets. Dev Biol 256:73
79. Coonrod SA, Naaby-Hansen S, Shetty J, Shibahara H, Chen M, White JM, Herr JC (1999) Treatment of mouse oocytes with PI-PLC releases 70-kDa (pI 5) and 35- to 45-kDa (pI 5.5) protein clusters from the egg surface and inhibits sperm-oolemma binding and fusion. Dev Biol 207:334
80. Choi M, Lee OH, Jeon S, Park M, Lee DR, Ko JJ, Yoon TK, Rajkovic A, Choi Y (2010) The oocyte-specific transcription factor, Nobox, regulates the expression of Pad6, a peptidylarginine deiminase in the oocyte. FEBS Lett 584:3629
81. Zhang J, Dai J, Zhao E, Lin Y, Zeng L, Chen J, Zheng H, Wang Y, Li X, Ying K, Xie Y, Mao Y (2004) cDNA cloning, gene organization and expression analysis of human peptidylarginine deiminase type VI. Acta Biochim Pol 51:1051
82. Liu M, Oh A, Calarco P, Yamada M, Coonrod SA, Talbot P (2005) Peptidylarginine deiminase (PAD) is a mouse cortical granule protein that plays a role in preimplantation embryonic development. Reprod Biol Endocrinol 3:42
83. Mechin MC, Sebbag M, Arnaud J, Nachat R, Foulquier C, Adoue V, Coudane F, Duplan H, Schmitt AM, Chavanas S, Guerrin M, Serre G, Simon M (2007) Update on peptidylarginine deiminases and deimination in skin physiology and severe human diseases. Int J Cosmet Sci 29:147
84. Horibata S, Coonrod SA, Cherrington BD (2012) Role for peptidylarginine deiminase enzymes in disease and female reproduction. J Reprod Dev 58:274
85. Esposito G, Vitale AM, Leijten FP, Strik AM, Koonen-Reemst AM, Yurttas P, Robben TJ, Coonrod S, Gossen JA (2007) Peptidylarginine deiminase (PAD) 6 is essential for oocyte cytoskeletal sheet formation and female fertility. Mol Cell Endocrinol 273:25
86. Yurttas P, Vitale AM, Fitzhenry RJ, Cohen-Gould L, Wu W, Gossen JA, Coonrod SA (2008) Role for PADI6 and the cytoplasmic lattices in ribosomal storage in oocytes and translational control in the early mouse embryo. Development 135:2627
87. Kan R, Yurttas P, Kim B, Jin M, Wo L, Lee B, Gosden R, Coonrod SA (2011) Regulation of mouse oocyte microtubule and organelle dynamics by PADI6 and the cytoplasmic lattices. Dev Biol 350:311
88. Rose R, Rose M, Ottmann C (2012) Identification and structural characterization of two 14-3-3 binding sites in the human peptidylarginine deiminase type VI. J Struct Biol 180:65
89. Taki HTG, Knuckley B, Thompson PR, Vugrek O, Hirata K, Miyahara T, Shinoda K, Hounoki H, Sugiyama E, Usui I, Urakaze M, Tobe K, Ishimoto T, Inoue R, Tanaka A, Mano H, Ogawa H, Mori H (2011) Purification of enzymatically inactive peptidylarginine deiminase type 6 from mouse ovary that reveals hexameric structure different from other dimeric isoform. Adv Biosci Biotechnol 2:304
90. Bridges D, Moorhead GB (2004) 14-3-3 proteins: a number of functions for a numbered protein. Sci STKE 2004(242):re10
91. Fearon WR (1939) The carbamido diacetyl reaction: a test for citrulline. Biochem J 33:902
92. Rogers GE, Harding HW, Llewellyn-Smith IJ (1977) The origin of citrulline-containing proteins in the hair follicle and the chemical nature of trichohyalin, an intracellular precursor. Biochim Biophys Acta 495:159

93. Kubilus J, Waitkus RF, Baden HP (1980) Partial purification and specificity of an arginine-converting enzyme from bovine epidermis. Biochim Biophys Acta 615:246
94. Fujisaki M, Sugawara K (1981) Properties of peptidylarginine deiminase from the epidermis of newborn rats. J Biochem 89:257
95. Sugawara K, Oikawa Y, Ouchi T (1982) Identification and properties of peptidylarginine deiminase from rabbit skeletal muscle. J Biochem 91:1065
96. Kubilus J, Baden HP (1983) Purification and properties of a brain enzyme which deiminates proteins. Biochim Biophys Acta 745:285
97. Takahara H, Okamoto H, Sugawara K (1986) Calcium-dependent properties of peptidylarginine deiminase from rabbit skeletal muscle. Agric Biol Chem 50:2899
98. Watanabe K, Akiyama K, Hikichi K, Ohtsuka R, Okuyama A, Senshu T (1988) Combined biochemical and immunochemical comparison of peptidylarginine deiminases present in various tissues. Biochim Biophys Acta 966:375
99. Terakawa H, Takahara H, Sugawara K (1991) Three types of mouse peptidylarginine deiminase: characterization and tissue distribution. J Biochem 110:661
100. Takahara H, Tsuchida M, Kusubata M, Akutsu K, Tagami S, Sugawara K (1989) Peptidylarginine deiminase of the mouse. Distribution, properties, and immunocytochemical localization. J Biol Chem 264:13361
101. Watanabe K, Senshu T (1989) Isolation and characterization of cDNA clones encoding rat skeletal muscle peptidylarginine deiminase. J Biol Chem 264:15255
102. Senshu T, Akiyama K, Nagata S, Watanabe K, Hikichi K (1989) Peptidylarginine deiminase in rat pituitary: sex difference, estrous cycle-related changes, and estrogen dependence. Endocrinology 124:2666
103. Asaga H, Yamada M, Senshu T (1998) Selective deimination of vimentin in calcium ionophore-induced apoptosis of mouse peritoneal macrophages. Biochem Biophys Res Commun 243:641
104. Hensen SM, Pruijn GJ (2014) Methods for the detection of peptidylarginine deiminase (PAD) activity and protein citrullination. Mol Cell Proteomics 13:388
105. Kearney PL, Bhatia M, Jones NG, Yuan L, Glascock MC, Catchings KL, Yamada M, Thompson PR (2005) Kinetic characterization of protein arginine deiminase 4: a transcriptional corepressor implicated in the onset and progression of rheumatoid arthritis. Biochemistry 44:10570
106. Bicker KL, Subramanian V, Chumanevich AA, Hofseth LJ, Thompson PR (2012) Seeing citrulline: development of a phenylglyoxal-based probe to visualize protein citrullination. J Am Chem Soc 134:17015
107. Knuckley B, Causey CP, Jones JE, Bhatia M, Dreyton CJ, Osborne TC, Takahara H, Thompson PR (2010) Substrate specificity and kinetic studies of PADs 1, 3, and 4 identify potent and selective inhibitors of protein arginine deiminase 3. Biochemistry 49:4852
108. Takahara H, Oikawa Y, Sugawara K (1983) Purification and characterization of peptidylarginine deiminase from rabbit skeletal muscle. J Biochem 94:1945
109. Knuckley B, Bhatia M, Thompson PR (2007) Protein arginine deiminase 4: evidence for a reverse protonation mechanism. Biochemistry 46:6578
110. Smith BC, Denu JM (2009) Chemical mechanisms of histone lysine and arginine modifications. Biochim Biophys Acta 1789:45
111. Rodriguez SB, Stitt BL, Ash DE (2009) Expression of peptidylarginine deiminase from *Porphyromonas gingivalis* in *Escherichia coli*: enzyme purification and characterization. Arch Biochem Biophys 488:14
112. Ke Z, Wang S, Xie D, Zhang Y (2009) Born-Oppenheimer ab initio QM/MM molecular dynamics simulations of the hydrolysis reaction catalyzed by protein arginine deiminase 4. J Phys Chem B 113:16705

113. Galkin A, Lu X, Dunaway-Mariano D, Herzberg O (2005) Crystal structures representing the Michaelis complex and the thiouronium reaction intermediate of *Pseudomonas aeruginosa* arginine deiminase. J Biol Chem 280:34080
114. Van Steendam K, Tilleman K, De Ceuleneer M, De Keyser F, Elewaut D, Deforce D (2010) Citrullinated vimentin as an important antigen in immune complexes from synovial fluid of rheumatoid arthritis patients with antibodies against citrullinated proteins. Arthritis Res Ther 12:R132
115. Nicholas AP, Sambandam T, Echols JD, Tourtellotte WW (2004) Increased citrullinated glial fibrillary acidic protein in secondary progressive multiple sclerosis. J Comp Neurol 473:128
116. Boggs JM, Rangaraj G, Koshy KM, Ackerley C, Wood DD, Moscarello MA (1999) Highly deiminated isoform of myelin basic protein from multiple sclerosis brain causes fragmentation of lipid vesicles. J Neurosci Res 57:529
117. Senshu T, Kan S, Ogawa H, Manabe M, Asaga H (1996) Preferential deimination of keratin K1 and filaggrin during the terminal differentiation of human epidermis. Biochem Biophys Res Commun 225:712
118. Mastronardi FG, Wood DD, Mei J, Raijmakers R, Tseveleki V, Dosch HM, Probert L, Casaccia-Bonnefil P, Moscarello MA (2006) Increased citrullination of histone H3 in multiple sclerosis brain and animal models of demyelination: a role for tumor necrosis factor-induced peptidylarginine deiminase 4 translocation. J Neurosci 26:11387
119. Ishigami A, Ohsawa T, Hiratsuka M, Taguchi H, Kobayashi S, Saito Y, Murayama S, Asaga H, Toda T, Kimura N, Maruyama N (2005) Abnormal accumulation of citrullinated proteins catalyzed by peptidylarginine deiminase in hippocampal extracts from patients with Alzheimer's disease. J Neurosci Res 80:120
120. Hermansson M, Artemenko K, Ossipova E, Eriksson H, Lengqvist J, Makrygiannakis D, Catrina AI, Nicholas AP, Klareskog L, Savitski M, Zubarev RA, Jakobsson PJ (2010) MS analysis of rheumatoid arthritic synovial tissue identifies specific citrullination sites on fibrinogen. Proteomics Clin Appl 4:511
121. Stensland M, Holm A, Kiehne A, Fleckenstein B (2009) Targeted analysis of protein citrullination using chemical modification and tandem mass spectrometry. Rapid Commun Mass Spectrom 23:2754
122. Nakayama-Hamada M, Suzuki A, Kubota K, Takazawa T, Ohsaka M, Kawaida R, Ono M, Kasuya A, Furukawa H, Yamada R, Yamamoto K (2005) Comparison of enzymatic properties between hPADI2 and hPADI4. Biochem Biophys Res Commun 327:192
123. Slack JL, Jones LE, Jr., Bhatia MM, Thompson PR (2011) Autodeimination of protein arginine deiminase 4 alters protein-protein interactions but not activity. Biochemistry 50:3997
124. Slack JL, Causey CP, Thompson PR (2011) Protein arginine deiminase 4: a target for an epigenetic cancer therapy. Cell Mol Life Sci 68:709
125. Slack JL, Causey CP, Luo Y, Thompson PR (2011) Development and use of clickable activity based protein profiling agents for protein arginine deiminase 4. ACS Chem Biol 6:466
126. Suzuki A, Yamada R, Chang X, Tokuhiro S, Sawada T, Suzuki M, Nagasaki M, Nakayama-Hamada M, Kawaida R, Ono M, Ohtsuki M, Furukawa H, Yoshino S, Yukioka M, Tohma S, Matsubara T, Wakitani S, Teshima R, Nishioka Y, Sekine A, Iida A, Takahashi A, Tsunoda T, Nakamura Y, Yamamoto K (2003) Functional haplotypes of PADI4, encoding citrullinating enzyme peptidylarginine deiminase 4, are associated with rheumatoid arthritis. Nat Genet 34:395
127. Lu J, Goldstein KM, Chen P, Huang S, Gelbert LM, Nagpal S (2005) Transcriptional profiling of keratinocytes reveals a vitamin D-regulated epidermal differentiation network. J Invest Dermatol 124:778
128. Chavanas S, Adoue V, Mechin MC, Ying S, Dong S, Duplan H, Charveron M, Takahara H, Serre G, Simon M (2008) Long-range enhancer associated with chromatin looping allows AP-1 regulation of the peptidylarginine deiminase 3 gene in differentiated keratinocyte. PLoS One 3:e3408

129. Adoue V, Chavanas S, Coudane F, Mechin MC, Caubet C, Ying S, Dong S, Duplan H, Charveron M, Takahara H, Serre G, Simon M (2008) Long-range enhancer differentially regulated by c-Jun and JunD controls peptidylarginine deiminase-3 gene in keratinocytes. J Mol Biol 384:1048
130. Bhattacharya SK, Crabb JS, Bonilha VL, Gu X, Takahara H, Crabb JW (2006) Proteomics implicates peptidyl arginine deiminase 2 and optic nerve citrullination in glaucoma pathogenesis. Invest Ophthalmol Vis Sci 47:2508
131. Nagata S, Uehara T, Inoue K, Senshu T (1992) Increased peptidylarginine deiminase expression during induction of prolactin biosynthesis in a growth-hormone-producing rat pituitary cell line, MtT/S. J Cell Physiol 150:426
132. Takahara H, Kusubata M, Tsuchida M, Kohsaka T, Tagami S, Sugawara K (1992) Expression of peptidylarginine deiminase in the uterine epithelial cells of mouse is dependent on estrogen. J Biol Chem 267:520
133. Arai T, Kusubata M, Kohsaka T, Shiraiwa M, Sugawara K, Takahara H (1995) Mouse uterus peptidylarginine deiminase is expressed in decidual cells during pregnancy. J Cell Biochem 58:269
134. Dong S, Zhang Z, Takahara H (2007) Estrogen-enhanced peptidylarginine deiminase type IV gene (PADI4) expression in MCF-7 cells is mediated by estrogen receptor-alpha-promoted transfactors activator protein-1, nuclear factor-Y, and Sp1. Mol Endocrinol 21:1617
135. Denis H, Deplus R, Putmans P, Yamada M, Metivier R, Fuks F (2009) Functional connection between deimination and deacetylation of histones. Mol Cell Biol 29:4982
136. Knipp M, Vasak M (2000) A colorimetric 96-well microtiter plate assay for the determination of enzymatically formed citrulline. Anal Biochem 286:257
137. Rahmatullah M, Boyde TR (1980) Improvements in the determination of urea using diacetyl monoxime; methods with and without deproteinisation. Clin Chim Acta 107:3
138. Zendman AJ, Raijmakers R, Nijenhuis S, Vossenaar ER, Tillaart M, Chirivi RG, Raats JM, van Venrooij WJ, Drijfhout JW, Pruijn GJ (2007) ABAP: antibody-based assay for peptidylarginine deiminase activity. Anal Biochem 369:232
139. Raats JM, Wijnen EM, Pruijn GJ, van den Hoogen FH, van Venrooij WJ (2003) Recombinant human monoclonal autoantibodies specific for citrulline-containing peptides from phage display libraries derived from patients with rheumatoid arthritis. J Rheumatol 30:1696
140. Deraos G, Chatzantoni K, Matsoukas MT, Tselios T, Deraos S, Katsara M, Papathanasopoulos P, Vynios D, Apostolopoulos V, Mouzaki A, Matsoukas J (2008) Citrullination of linear and cyclic altered peptide ligands from myelin basic protein (MBP (87-99)) epitope elicits a Th1 polarized response by T cells isolated from multiple sclerosis patients: implications in triggering disease. J Med Chem 51:7834
141. Liao YF, Hsieh HC, Liu GY, Hung HC (2005) A continuous spectrophotometric assay method for peptidylarginine deiminase type 4 activity. Anal Biochem 347:176
142. Chikuma T, Yamada M, Tsuda A, Yamamoto M, Nakashima K, Yajima R, Kato T (2000) A highly sensitive high-performance liquid chromatography-fluorometric method for the assay of peptidylarginine deiminase activity. Anal Biochem 285:230
143. Wang Q, Priestman MA, Lawrence DS (2013) Monitoring of protein arginine deiminase activity by using fluorescence quenching: multicolor visualization of citrullination. Angew Chem Int Ed Engl 52:2323
144. Zhang J, Goodlett DR, Quinn JF, Peskind E, Kaye JA, Zhou Y, Pan C, Yi E, Eng J, Wang Q, Aebersold RH, Montine TJ (2005) Quantitative proteomics of cerebrospinal fluid from patients with Alzheimer's disease. J Alzheimers Dis 7:125
145. Wildeman E, Pires MM (2013) Facile fluorescence-based detection of PAD4-mediated citrullination. Chembiochem 14:963
146. Shelef MA, Sokolove J, Lahey LJ, Wagner CA, Sackmann EK, Warner TF, Wang Y, Beebe DJ, Robinson WH, Huttenlocher A (2014) Peptidylarginine deiminase 4 contributes to tumor necrosis factor alpha-induced inflammatory arthritis. Arthritis Rheumatol 66:1482

147. Bawadekar M, Gendron-Fitzpatrick A, Rebernick R, Shim D, Warner TF, Nicholas AP, Lundblad LK, Thompson PR, Shelef MA (2016) Tumor necrosis factor alpha, citrullination, and peptidylarginine deiminase 4 in lung and joint inflammation. Arthritis Res Ther 18:173
148. Guo Q, Fast W (2011) Citrullination of inhibitor of growth 4 (ING4) by peptidylarginine deminase 4 (PAD4) disrupts the interaction between ING4 and p53. J Biol Chem 286:17069
149. Guo J, Qian L, Li XP, Li XM, Wang GS, Fang X (2013) Peptidyl arginine deiminase 4 participates in the pathogenesis of rheumatoid arthritis by influencing histone methylation. Zhonghua Nei Ke Za Zhi 52:928
150. Bates IR, Libich DS, Wood DD, Moscarello MA, Harauz G (2002) An Arg/Lys→Gln mutant of recombinant murine myelin basic protein as a mimic of the deiminated form implicated in multiple sclerosis. Protein Expr Purif 25:330
151. Calabrese R, Zampieri M, Mechelli R, Annibali V, Guastafierro T, Ciccarone F, Coarelli G, Umeton R, Salvetti M, Caiafa P (2012) Methylation-dependent PAD2 upregulation in multiple sclerosis peripheral blood. Mult Scler 18:299
152. Jang B, Ishigami A, Maruyama N, Carp RI, Kim YS, Choi EK (2013) Peptidylarginine deiminase and protein citrullination in prion diseases: strong evidence of neurodegeneration. Prion 7:42
153. Ishigami A, Masutomi H, Handa S, Nakamura M, Nakaya S, Uchida Y, Saito Y, Murayama S, Jang B, Jeon YC, Choi EK, Kim YS, Kasahara Y, Maruyama N, Toda T (2015) Mass spectrometric identification of citrullination sites and immunohistochemical detection of citrullinated glial fibrillary acidic protein in Alzheimer's disease brains. J Neurosci Res 93:1664
154. Struyf S, Noppen S, Loos T, Mortier A, Gouwy M, Verbeke H, Huskens D, Luangsay S, Parmentier M, Geboes K, Schols D, Van Damme J, Proost P (2009) Citrullination of CXCL12 differentially reduces CXCR4 and CXCR7 binding with loss of inflammatory and anti-HIV-1 activity via CXCR4. J Immunol 182:666
155. McElwee JL, Mohanan S, Griffith OL, Breuer HC, Anguish LJ, Cherrington BD, Palmer AM, Howe LR, Subramanian V, Causey CP, Thompson PR, Gray JW, Coonrod SA (2012) Identification of PADI2 as a potential breast cancer biomarker and therapeutic target. BMC Cancer 12:500
156. Ulivi P, Mercatali L, Casoni GL, Scarpi E, Bucchi L, Silvestrini R, Sanna S, Monteverde M, Amadori D, Poletti V, Zoli W (2013) Multiple marker detection in peripheral blood for NSCLC diagnosis. PLoS One 8:e57401
157. Pritzker LB, Moscarello MA (1998) A novel microtubule independent effect of paclitaxel: the inhibition of peptidylarginine deiminase from bovine brain. Biochim Biophys Acta 1388:154
158. Hidaka Y, Hagiwara T, Yamada M (2005) Methylation of the guanidino group of arginine residues prevents citrullination by peptidylarginine deiminase IV. FEBS Lett 579:4088
159. Luo Y, Arita K, Bhatia M, Knuckley B, Lee YH, Stallcup MR, Sato M, Thompson PR (2006) Inhibitors and inactivators of protein arginine deiminase 4: functional and structural characterization. Biochemistry 45:11727
160. Stone EM, Schaller TH, Bianchi H, Person MD, Fast W (2005) Inactivation of two diverse enzymes in the amidinotransferase superfamily by 2-chloroacetamidine: dimethylargininase and peptidylarginine deiminase. Biochemistry 44:13744
161. Luo Y, Knuckley B, Lee YH, Stallcup MR, Thompson PR (2006) A fluoroacetamidine-based inactivator of protein arginine deiminase 4: design, synthesis, and in vitro and in vivo evaluation. J Am Chem Soc 128:1092
162. Luo Y, Knuckley B, Bhatia M, Pellechia PJ, Thompson PR (2006) Activity-based protein profiling reagents for protein arginine deiminase 4 (PAD4): synthesis and in vitro evaluation of a fluorescently labeled probe. J Am Chem Soc 128:14468
163. Jones JE, Slack JL, Fang P, Zhang X, Subramanian V, Causey CP, Coonrod SA, Guo M, Thompson PR (2012) Synthesis and screening of a haloacetamidine containing library to identify PAD4 selective inhibitors. ACS Chem Biol 7:160

164. Dreyton CJ, Jones JE, Knuckley BA, Subramanian V, Anderson ED, Brown SJ, Fernandez-Vega V, Eberhart C, Spicer T, Zuhl AM, Ferguson J, Speers AE, Wang C, Boger DL, Thompson P, Cravatt BF, Hodder P, Rosen H (2010) Optimization and characterization of a pan protein arginine deiminase (PAD) inhibitor. In: Probe Reports from the NIH Molecular Libraries Program. Bethesda, MD, USA
165. Knuckley B, Luo Y, Thompson PR (2008) Profiling Protein Arginine Deiminase 4 (PAD4): a novel screen to identify PAD4 inhibitors. Bioorg Med Chem 16:739
166. Causey CP, Jones JE, Slack JL, Kamei D, Jones LE, Subramanian V, Knuckley B, Ebrahimi P, Chumanevich AA, Luo Y, Hashimoto H, Sato M, Hofseth LJ, Thompson PR (2011) The development of *N*-alpha-(2-carboxyl)benzoyl-*N*(5)-(2-fluoro-1-iminoethyl)-l-ornithine amide (*o*-F-amidine) and *N*-alpha-(2-carboxyl)benzoyl-*N*(5)-(2-chloro-1-iminoethyl)-l-ornithine amide (*o*-Cl-amidine) as second generation protein arginine deiminase (PAD) inhibitors. J Med Chem 54:6919
167. Witalison EE, Cui X, Causey CP, Thompson PR, Hofseth LJ (2015) Molecular targeting of protein arginine deiminases to suppress colitis and prevent colon cancer. Oncotarget 6:36053
168. Wang H, Xu B, Zhang X, Zheng Y, Zhao Y, Chang X (2016) PADI2 gene confers susceptibility to breast cancer and plays tumorigenic role via ACSL4, BINC3 and CA9 signaling. Cancer Cell Int 16:61
169. Mohanan S, Horibata S, McElwee JL, Dannenberg AJ, Coonrod SA (2013) Identification of macrophage extracellular trap-like structures in mammary gland adipose tissue: a preliminary study. Front Immunol 4:67
170. Wood DD, Moscarello MA (1989) The isolation, characterization, and lipid-aggregating properties of a citrulline containing myelin basic protein. J Biol Chem 264:5121
171. Nomura K (1992) Specificity and mode of action of the muscle-type protein-arginine deiminase. Arch Biochem Biophys 293:362

**Bushra Amin** has completed her Ph.D. degree in Biochemistry from the University of Tübingen in Germany. Currently, she is working as an analytical chemist at the University of Pittsburgh, and is exploring the following topics: (1) Post-translational modifications that impose critical influences on structure and functions of proteins and play a central role in the pathogenesis of neurodegenerative and autoimmune diseases; (2) development of labile chemical, isotopic, and peptide labels to improve the quantification of proteins by mass spectrometry; (3) enhanced sample multiplexing/hyperplexing approaches to enable the analysis of $\geq$96 different samples simultaneously, and (4) the development of sensitive and reliable methodologies to untangle the challenges of higher-order multiplexing to achieve maximum information hidden in complex biological mixtures.

**Wolfgang Voelter** was born on October 20, 1936, in Ludwigsburg, Baden-Württemberg, Germany, as the second son of the textile store owners Theodor and Henriette Voelter. In 1956, he received an Abitur diploma from Friedrich-Schiller-Gymnasium in Luwigsburg and started studies in chemistry and medicine at the universities of Tübingen and Erlangen, leading to the completion of the Diploma in Chemistry (1963, University of Tübingen), Dr. rer. nat. (1966, University of Tübingen; Prof. Ernst Bayer), and Physikum (1966, University of Erlangen) degrees. From 1966–1967, he worked as a Research Associate in the Laboratory of Prof. Carl Djerassi at Stanford University on steroid modifications and the structure investigation of organic molecules using mass spectrometry, nuclear magnetic resonance spectroscopy, circular dichroism, and magnetic circular dichroism. Based on structure determination rules he developed for investigations of mainly terpenes, steroids, carbohydrates, and peptides by $^{13}$C NMR and $^{19}$F NMR spectroscopy and by circular dichroism, the *venia legendi* was awarded in 1970 to Prof. Voelter for work in organic chemistry and biochemistry from the University of Tübingen.

As University Professor (1973), Vice Director of the Chemisches Zentralinstitut (1976), Vice Dean of the Fakultät für Chemie und Pharmazie (1976), Head of the Abteilung für Phsikalische Biochemie (1979), and Head of the Institute of Scientific Cooperation (1985) in Tübingen, Prof. Voelter started to cooperate with research groups based at institutions in tropical or subtropical areas to discover bioactive materials from the flora and fauna of these regions. Starting from the Philippines in the east to Chile in the west and South Africa in the south, numerous new natural compounds inclusive of alkaloids, terpenoids, and withanolides were isolated and structurally determined collaboratively. Among the plants that have been studied are *Buxus papillosa*, *Cassia absus*, *Colchicum ritchii*, *Delphinium fissum*, *Discaria febrifuga*, *Euphorbia lactea*, *Inula viscosa*, *Melia azadirachta*, *Nepeta hindustana*, *Primula denticulata*, *Rauvolfia vomitoria*, and *Withania coagulans*.

Prof. Voelter's group has used unsaturated and epoxy sugars as synthons for amino, azido, halo, cyclopropanated sugars, chiral polysubstituted butanolides, and muramyl dipeptide derivatives, and has synthesized natural constituents like D-forosamine, D-ossamine, D-tolyposamine, argentilactones, massoilactone, osmundolactone, and canadensolide. To improve chemical peptide/protein synthesis, new α-amino protecting groups (Adpoc, *t*-Bumeoc), side-chain protecting groups for arginine, cysteine, asparagine, glutamine, and anchor groups for peptide amide synthesis, were developed.

Prof. Voelter has applied in his work sophisticated separation techniques, in addition to structure determination methods, like high-field NMR spectroscopy, mass spectrometric techniques of different modes, X-ray crystallography, circular dichroism, and Edman degradation. He has also developed specific immunoassays in combination with epitope mapping and chromogenic substrates, and has synthesized both the partial and total sequences of natural peptides/proteins. In particular, he has made contributions to the structures and bioactivities of the hypothalamus hormones, prothymosin alpha, parathymosin alpha, beta thymosins (related to the phylogenetic tree from man to sea urchin), relaxin, hemocyanins, macrophage migration inhibiting factor, amyloidogenesis, and lung surfactant proteins.

For his work and worldwide scientific interactions, Prof. Voelter has received numerous honors, including the Sebastian Kneipp Award for the structure determination of natural products, the Erich Krieg Award for metabolism studies of drugs, the Japan Society for the Promotion of Science Award, and the University Award of Tübingen University. He received honorary doctorates from the University of Karachi and Hamdard University. In 2016, the Prof. Wolfgang Voelter Laboratories Complex was dedicated at the University of Karachi.

# Progress in the Chemistry of Naturally Occurring Coumarins

**Satyajit D. Sarker and Lutfun Nahar**

## Contents



## 1 Introduction

Coumarins are the largest class of 1-benzopyran derivatives, and coumarin (**1**) (2*H*-1-benzopyran-2-one) (Fig. 1), a fragrant colorless compound isolated from the tonka bean (*Dipteryx odorata*; family Fabaceae; Plate 1) in 1820, was the initial member of this class of compounds. The name coumarin comes from the French

S.D. Sarker (✉) • L. Nahar
Medicinal Chemistry and Natural Products Research Group, School of Pharmacy and Biomolecular Sciences, Faculty of Science, Liverpool John Moores University, Byrom Street, Liverpool L3 3AF, UK
e-mail: S.Sarker@ljmu.ac.uk; L.Nahar@ljmu.ac.uk



A.D. Kinghorn, H. Falk, S. Gibbons, J. Kobayashi (eds.), *Progress in the Chemistry of Organic Natural Products*, *Vol. 106,* DOI 10.1007/978-3-319-59542-9_3

**Fig. 1** Coumarin (**1**) and its numbering system

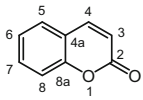


**1** (coumarin)

**Plate 1** *Dipteryx odorata* (tonka bean), the source of the first coumarin. Photograph courtesy of http://www.kladovayalesa.ru/archives/5732

**Fig. 2** Umbelliferone (**2**) and bruceol (**3**)

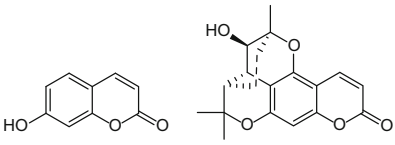


**2** (umbelliferone) **3** (bruceol)

term for the tonka bean, "coumarou". Since the discovery of coumarin (**1**), several of its derivatives have been isolated from various natural sources, especially from higher plants. Major detailed and comprehensive accounts of the chemistry and biochemistry of coumarins have been provided by Murray in this book series up to 2002 [1–4].

Most of the plant-derived coumarins are oxygenated at C-7, and the intitial such member is umbelliferone (**2**), which was first isolated from the family Umbelliferae (syn. Apiaceae). Umbelliferone (**2**) (Fig. 2), also known as 7-hydroxycoumarin, hydrangine, or skimmetine, is considered biosynthetically as the parent compound for other highly oxygenated, prenylated, geranylated, farnesylated, and more complex forms of coumarin derivatives (e.g. bruceol, **3**, isolated from *Eriostemon brucei*). The prenyl groups found in coumarins undergo various biogenetic modifications to form dihydrofuran, dihydropyran, furan, and pyran ring systems. Similarly, various biogenetic processes produce monoterpenyl- and sesquiterpenyl-coumarins, respectively, from geranyl- and farnesyl-substituted coumarins. The plant families Apiaceae, Asteraceae, and Rutaceae are the three major sources of coumarins [5].

The biosynthesis of most of the naturally occurring coumarins starts from (*E*)-4-hydroxycinnamic acid (**4**, also known as *p*-coumaric acid) (Scheme 1). An enzyme-

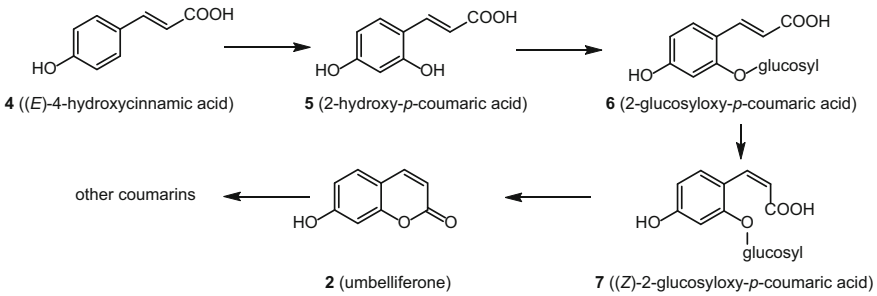


**Scheme 1** Biosynthesis of umbelliferone (**2**)

mediated oxidation of this starting compound **4** produces 2-hydroxy-*p*-coumaric acid (**5**) followed by the formation of its 2-glucoside **6** [5]. This glucoside (**6**) undergoes isomerization to produce its (*Z*)-diastereomer (**7**). Umbelliferone (**2**) is formed through ring closure of compound **7**.

Generally, coumarins can be structurally classified into simple, simple prenylated, simple geranylated, furano, pyrano, sesquiterpenyl, and oligomeric coumarins [5]. Using this standard classification, this chapter presents a snapshot of the advances of the chemistry of naturally occurring coumarins reported recently (within the period 2014–2015) in the literature.

## 2 Naturally Occurring Coumarins Recently Reported

A significant body of literature has become available on the extraction, isolation, identification, and assessment of biological activities of naturally occurring coumarins in recent years. Several new coumarins together with various known coumarins were reported from known or new plant sources. Although the main focus of this chapter is on new analogs that have contributed to the discovery of new coumarin chemistry, some of the known coumarins, which have been re-isolated as bioactive components or reported from new sources, have also been incorporated into this chapter.

### *2.1 Simple Coumarins*

Most of the recently reported simple coumarins (Fig. 3) are known compounds, with some of them from new plant sources, and others re-isolated as part of bioassay-guided isolation processes. However, there has been also a number of new simple coumarins reported recently. The occurrence of simple coumarins is quite widespread in the plant kingdom. However, most of the recently reported coumarins are mainly from the families Apiaceae, Asteraceae, and Rutaceae, with

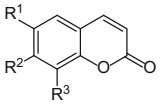


| | $R^1$ | $R^2$ | $R^3$ | |
|---|---|---|---|---|
| **8** | OH | OH | H | (aesculetin) |
| **9** | O-$\beta$-D-glucopyranosyl | OH | H | (aesculin) |
| **10** | H | $OCH_3$ | H | (ayapanin) |
| **11** | $CO_2H$ | OH | H | (6-carboxy-umbelliferone) |
| **12** | OH | O-$\beta$-D-glucopyranosyl | H | (chicoriin) |
| **13** | OH | H | OH | (6,8-dihydroxycoumarin) |
| **14** | H | H | OH | (7,8-dihydroxycoumarin) |
| **15** | $OCH_3$ | O-$\beta$-D-glucopyranosyl | $OCH_3$ | (eleutheroside B1) |
| **16** | $OCH_3$ | OH | OH | (fraxetin) |
| **17** | $OCH_3$ | $OCH_3$ | OH | (fraxidin) |
| **18** | $OCH_3$ | OH | *O*-$\beta$-D-glucopyranosyl (fraxin) | |
| **19** | OH | H | H | (6-hydroxycoumarin) |
| **20** | H | $OCH_3$ | OH | (daphnetin-7-methyl ether) |
| **21** | H | OH | $OCH_3$ | (7-hydroxy-8-methoxycoumarin) |
| **22** | $OCH_3$ | OH | $OCH_3$ | (isofraxidin or phytodolor) |
| **23** | OH | $OCH_3$ | H | (isoscopoletin) |
| **24** | H | $OCH_3$ | CHO | (7-methoxy-8-formylcoumarin) |
| **25** | H | $OCH_3$ | $CH_3$ | (7-methoxy-8-methylcoumarin) |
| **26** | H | $OCH_3$ | $CH_2CH_2OH$ | (7-*O*-methylphellodenol B) |
| **27** | $CO_2CH_3$ | OH | H | (officinalin) |
| **28** | $OCH_3$ | $OCH_3$ | H | (scoparone) |
| **29** | $OCH_3$ | OH | H | (scopoletin) |
| **30** | $OCH_3$ | O-$\beta$-D-glucopyranosyl | H | (scopolin) |
| **31** | O-$\beta$-D-glucopyranosyl | H | H | (skimmin) |
| **32** | $OCH_3$ | $OCH_3$ | $OCH_3$ | (6,7,8-trimethoxycoumarin) |

**Fig. 3** Simple coumarins **8**–**32**

the other reported sources from the families Aceraceae, Apocynaceae, Araliaceae, Caryophyllaceae, Convolvulaceae, Dryopteridaceae, Gomphidiaceae, Guttiferae, Lamiaceae, Lauraceae, Malvaceae, Meliaceae, Moraceae, Oleaceae, Rosaceae, Rubiaceae, Salvadoraceae, Saxifragaceae, Simaroubaceae, Solanaceae, and Thymelaeaceae.

Aesculetin (**8**), aesculin (**9**), chicoriin (**12**), scopoletin (**29**), and umbelliferone (**2**) were isolated from an aqueous ethanolic extract of the leaves of *Calendula officinalis* (Asteraceae) (Plate 2) [6]. Among these, **8** showed amylase inhibitory activity at concentrations ranging from 1.02 to 2.64 μg/cm$^3$. Scopoletin (**29**) and its glucoside, scopolin (**30**), were identified as part of a quality control assessment of bark samples of *Lycium chinense* and *L. barbarum* (Solanaceae) using a validated LC-MS/MS method [7]. Coumarin (**2**) was also identified from *Salvadora indica* (Salvadoraceae) as an antihyperlipidemic and antitumor principle [8]. Isofraxidin (**22**) and eleutheroside B1 (**15**) were purified and analyzed by UPLC/DAD/qTOF-MS from the Tibetan herbal medicine *Carduus acanthoides* (Asteraceae), which is well known for the treatment of hematemesis, hematuria, and menorrhagia [9]. A phytochemical investigation on the aerial parts of the Chinese medicinal plant *Gerbera piloselloides* (Asteraceae) afforded 7,8-dihydroxycoumarin (**14**), which is also known as daphnetin [10]. A coumarin ester, officinalin (**27**), was found in the aerial parts of *Opopanax hispidus* (Apiaceae) [11].

**Plate 2** *Calendula officinalis* (pot marigold). Photograph courtesy of KENPEI, Creative Commons

**Plate 3** *Solanum indicum* (Indian nightshade), flower. Photograph courtesy of Vinayaraj, Creative Commons

Scopoletin (**29**), isolated from *Artemisia roxburghiana* (Asteraceae), was utilized for the preparation of an anti-inflammatory nanoconjugate [12]. A phytochemical study on the seeds of *Solanum indicum* (Solanaceae) (Plate 3) afforded fraxetin (**16**) and **22**, as well as a new 3-substituted coumarin, 7-hydroxy-6,8-dimethoxy-3-(4′-hydroxy-3′-methoxyphenyl)-coumarin (**33**) [13]. While isoscopoletin (**23**) was found in the twigs of *Micromelum integerrimum* (Rutaceae) [14], scoparone (**28**) and **29** were isolated from the fruit pulp of *Acanthopanax senticosus* (Araliaceae) [15]. Coumarin **28** was also found in *Ferula oopoda* (Apiaceae) [16]. Ayapanin (**10**) was reported recently from the leaves of *Murraya alata* (Rutaceae) [17].

The simple coumarins, **2**, **8**, **9**, **16**, fraxidin (**17**), **22**, **28**–**30**, skimmin (**31**), 6,7,8-trimethoxycoumarin (**32**), and 6-hydroxy-5,7-dimethoxycoumarin (**36**), were reported from the fruits of *Chroogomphus rutilus* (Gomphidiaceae) [18] (Fig. 4;

**Fig. 4** Simple coumarins **33–42**

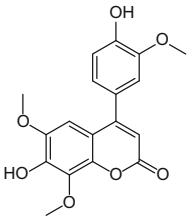

**33** (7-hydroxy-6,8-dimethoxy-3-(4'-hydroxy-3'-methoxyphenyl)-coumarin)

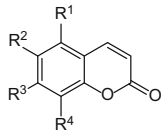

| | $R^1$ | $R^2$ | $R^3$ | $R^4$ |
|---|---|---|---|---|
| **34** | OH | H | OH | H |
| **35** | $OCH_3$ | H | $OCH_3$ | H |
| **36** | $OCH_3$ | OH | $OCH_3$ | H |
| **37** | OH | H | H | H |
| **38** | $OCH_3$ | H | $OCH_3$ | $OCH_3$ |

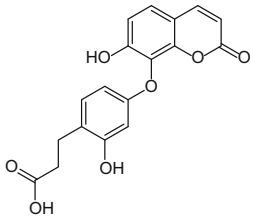

**39** (edgeworic acid)

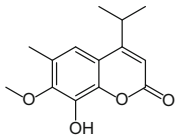

**40** (dryofracoumarin A)

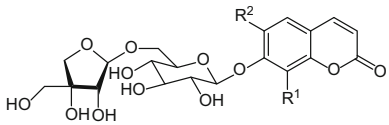

**41** $R^1$ = H, $R^2$ = $OCH_3$ (hymexelsin)
**42** $R^1$ = $OCH_3$, $R^2$ = H (xanthoxyloside)

Plate 4). Coumarins **2** and **29** were also present in the roots of *Saposhnikovia divaricata* (Apiaceae) [19], and **28** and **29** were isolated from the stem bark of *Zanthoxylum avicennae* (Plate 5) [20], and from the roots of *Bunium incrassatum* (Apiaceae) [21].

Coumarins **29** and **36** were found in the bark of *Entandrophragma congoense* (Meliaceae) [22]. A new simple coumarin, edgeworic acid (**39**), together with 5,7-dihydroxycoumarin (**34**) and **2**, were obtained from the flower buds of *Edgeworthia chrysantha* (Plate 6) (Thymelaeaceae) [23].

Coumarins **2**, **8**, **9**, and **28–30** occur very widely in the plant kingdom [24–36]. Scopolin (**30**) was purified from the roots of *Angelica dahurica* (Apiaceae) [34] and *Lindera reflexa* (Lauraceae) [35]. Coumarins **29** and **30** were also isolated from

**Plate 4** *Chroogomphus rutilus* (brown slimecap), Ehingen, Germany. Photograph courtesy of H. Krisp, Creative Commons


**Plate 5** *Zanthoxylum avicennae*, Hong Kong Zoological and Botanical Gardens. Photograph courtesy of Daderot, Public Domain

*Micromelum integerrimum* (Rutaceae) [32]. A phytochemical and chemotaxonomic investigation on *Ficus tsiangii* (Moraceae) afforded **1**, **2**, **8**, **29**, and 6-carboxy-umbelliferone (**11**) [37]. Coumarins with a carboxylic acid functionality, such as in **11**, are not very common in Nature.

**Plate 6** *Edgeworthia chrysantha* (oriental paperbush, mitsumata). Photograph courtesy of peganum, Creative Commons

**Plate 7** *Cnidium monnieri*. Photograph courtesy of Henry Qin, Linkedin

A new coumarin with an alkyl substituent at C-8, named 7-*O*-methylphellodenol B (**26**), was purified from the fruits of *Cnidium monnieri* (Apiaceae) (Plate 7) [38]. In addition, 7-methoxy-8-formylcoumarin (**24**) was reported. Dryofracoumarin A (**40**), a new 4-substituted simple coumarin, along with **8** and isoscopoletin (**23**), were isolated as cytotoxic components of a hydro-ethanolic extract of the whole plant of *Dryopteris fragrans* (Dryopteridaceae) [39]. While coumarins **2**, **29**, and 8-hydroxy-7-methoxycoumarin (**20**) were identified in the twigs of *Feroniella lucida* (Rutaceae) (Plate 8) [40], **17** and **29** were reported as NF-κB inhibitors from a methanolic extract of the roots of *Eurycoma longifolia* (Simaroubaceae) [41]. Hymexelsin (**41**) and **29** were isolated from the stem bark of *Pauridiantha callicarpoides* (Rubiaceae) [24].


**Plate 8** *Feroniella lucida*, grown as bonsai, Vietnam. Photograph courtesy of Nguyen Thanh Quang, Creative Commons

7-Methoxy-8-methyl-coumarin (**25**) was isolated from the fruits of *Micromelum minutum* (Rutaceae) [42], and toddalenone (**43**) and 5,7,8-trimethoxycoumarin (**38**) were obtained from the roots of *Toddalia asiatica* (Rutaceae) [43]. From the same family, **43** was also purified from the aerial parts of *Murraya tetramera* [44], and from the leaves of *M. alata* [17]. Two new isomeric (*erythro* and *threo*) coumarin glycosides **44** and **45** (Fig. 5) possessing hepatoprotective properties were obtained from the stems of *Hydrangea paniculata* (Saxifragaceae), and named hydrangeside C (*erythro* form, **44**) and hydrangeside D (*threo* form, **45**) [45]. Li et al. reported the isolation of several simple coumarins and coumarin glycosides from the stems of *Zanthoxylum schinifolium* (Rutaceae) [46]; those were hymexelsin (**41**), daphnetin 7-methyl ether (**20**), phytodolor (**22**), **28**–**30** and xanthoxyloside (**42**). A new coumarin glycoside, isoscopoletin (6-(6-*O*-*β*-apiofuranosyl-*β*-glucopyranoside)) (**46**), similar to xanthoxyloside (**42**), was isolated from the stems of *Morus alba* (Moraceae), by centrifugal partition chromatography [47].

Dracunculin (**47**), a simple coumarin that contains a methylenedioxy functionality, and **29** were purified from an ethanolic extract of the aerial parts of *Artemisia elegantissima* (Asteraceae) [48]. Dracunculin (**47**) was also isolated from *Artemisia indica* (Asteraceae) as a potential antitumor agent [49].

The coumarinolignan cleomiscosin A (**48**), a simple coumarin with a substituted ethylenedioxy functionality (Fig. 5), was reported from the aerial parts of *Melochia umbellata* (Malvaceae) (Plate 9) [50]. This compound is in fact a dimer between a coumarin and a phenylpropanoid moiety, and can also be placed under the class of miscellaneous coumarins as shown near the end of this chapter. Two similar

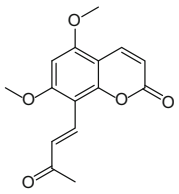

**43** (toddalenone)

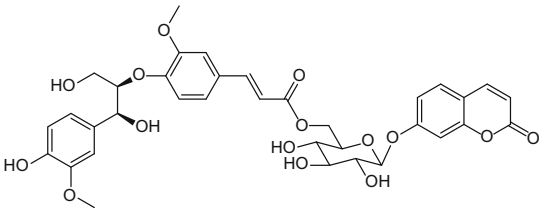

**44** (hydrangeside C, *erythro* form)

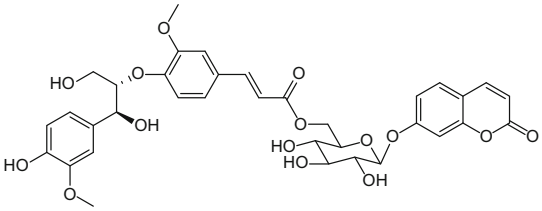

**45** (hydrangeside D, *threo* form)

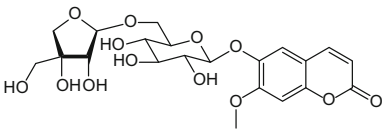

**46** (isoscopoletin-6-(6-*O*-apiofuranosyl-glucopyranoside)

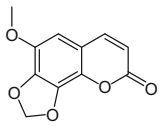

**47** (dracunculin)

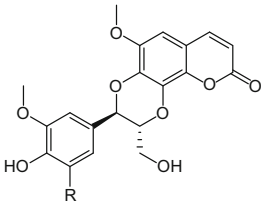

R

**48** H (cleomiscosin A)

**49** $OCH_3$ (cleomiscosin C)

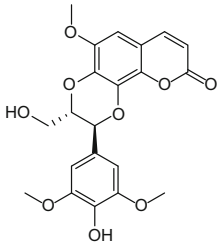

**50** (cleomiscosin D)

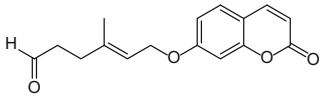

**51** ((*E*)-4-methyl-6-(coumarin-7'-yloxy)hex-4-enal)

**Fig. 5** Simple coumarins **43**–**51**

coumarinolignans, cleomiscosins C (**49**) and D (**50**), together with **29**, were identified from *Acer mono* (Aceraceae) [51]. Coumarins **8**, **16** and their glucosides, **9** and **18**, were found in *Fraxinus chinensis* (Oleaceae) [52].

**Plate 9** *Melochia umbellata*, Keaukaha, Hawaii. Photograph courtesy of Forest & Kim Starr, Creative Commons

The occurrence of 6-hydroxycoumarin (**19**), reported from *Prangos pabularia* (Apiaceae), is rare, as 7-hydroxylation (as in **2**) is biogenetically more favored in plants [27]. A simple coumarin with eight carbon atoms containing a formyl side chain, (*E*)-4-methyl-6-(coumarin-7′-yloxy)hex-4-enal (**51**), was reported from the leaves of *Zanthoxylum schinifolium* (Rutaceae) [53]. Two new methoxylated simple coumarins, muralatins G (**52**) and H (**53**) (Fig. 6), were detected in the leaves of *Murraya alata* (Rutaceae) [17]. A new ester of 7-hydroxycoumarin, 7-*O*-(4,8,12-trihydroxy-4,8,12-trimethyl-tridecanoyl)-coumarin, named ferulone C (**54**), was purified from the aerial parts of *Ferula persica* (Apiaceae) [54]. A phytochemical study on an infusion prepared from the stem bark of *Exostema caribaeum* (Rubiaceae) afforded the new 4-phenylcoumarin glycosides **55**–**61** [55].

Glucose is the most common sugar unit found in the coumarin glycosides reported recently. Two 4-substituted simple coumarins, isopedilanthocoumarin B (**62**) and pedilanthocoumarin B (**63**), with the former being a new coumarin, were reported from a dichloromethane extract of the bark of *Mammea neurophylla* (Caryophyllaceae) [56].

A new 3-substituted simple coumarin, 6-hydroxy-3-(4-hydroxyphenyl)-7-methoxy-2*H*-chromen-2-one (**64**), which showed anti-tobacco mosaic virus activity, was isolated from the roots and stems of flue-cured *Nicotiana tabacum* (Solanaceae) [57]. 7,7′-Dimethoxy-6,6′-biscoumarin (**65**), an unusual 6-substituted coumarin (Fig. 7), was identified from a methanolic extract of the stem bark of *Hypericum riparium* (Guttiferae) [58]. Two new isomeric 3-substituted simple coumarins, talacoumarins A (**66**) and B (**67**), were purified from the wetland soil-derived fungus *Talaromyces flavus* [59]. None of these coumarins has the usual oxygenation at C-7. The new coumarins, cashmins A (**68**) and B (**69**), were reported from *Sorbus cashmiriana* (Rosaceae) (Plate 10) [60], and they also lack any oxygenation at C-7. A glycoside of a 3-substitued coumarin, gerberinside (**70**), was isolated from the whole plant of *Ainsliaea fragrans* (Asteraceae) [61] and this coumarin glucoside also does not have any oxygenation at C-7.

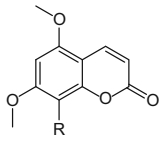

R

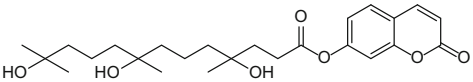

**54** (ferulone C)

**52**  (muralatin G)

**53**  (muralatin H)

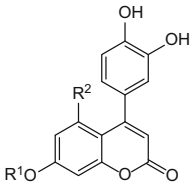

| | $R^1$ | $R^2$ |
|---|---|---|
| **55** | H | 5-*O*-[*β*-D-xylopyranosyl-(1-6)-*β*-D-glucopyranosyl] |
| **56** | H | 5-*O*-*β*-D-glucopyranosyl |
| **57** | $CH_3$ | 5-*O*-[*β*-D-xylopyranosyl-(1-6)-*β*-D-glucopyranosyl] |
| **58** | $CH_3$ | 5-*O* *β*-D-galactopyranosyl |
| **59** | $CH_3$ | 5-*O*-*β*-D-glucopyranosyl |
| **60** | H | 6''-*O*-acetyl-5-*O*-*β*-D-glucopyranosyl |
| **61** | $CH_3$ | 6''-*O*-acetyl-5-*O*-*β*-D-galactopyranosyl |

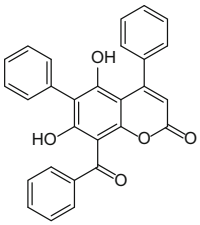

**62** (isopedilanthocoumarin B)

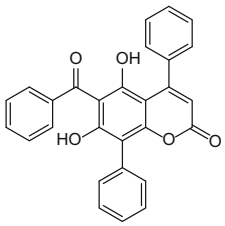

**63** (pedilanthocoumarin B)

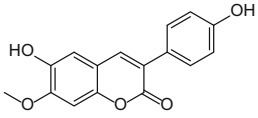

**64** (6-hydroxy-3-(4-hydroxyphenyl)-7-methoxy-2*H*-chromen-2-one)

**Fig. 6** Simple coumarins **52**–**64**

A new unusual coumarin, where both the 3- and 4-positions are substituted, was isolated from the roots of *Sideritis pullulans* (Lamiaceae) and named 7-demethyl-8-methoxycoumarsabin (**72**) [62]. Another new simple coumarin derivative with similar structural features, 3,8-dihydroxy-4-(4-hydroxyphenyl)-6-methylcoumarin

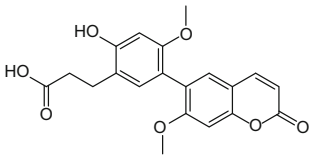

**65** (7,7'-dimethoxy-6,6'-biscoumarin)

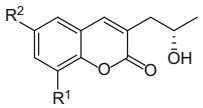

**66** $R^1$ = OH, $R^2$ = $OCH_3$ (talacoumarin A)
**67** $R^1$ = $OCH_3$, $R^2$ = OH (talacoumarin B)

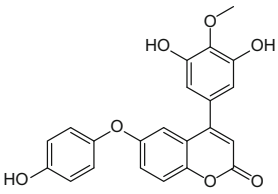

**68** (cashmin A)

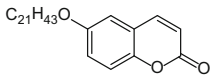

**69** (cashmin B)

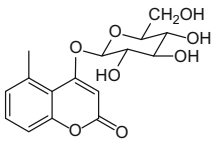

**70** (gerberinside)

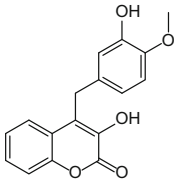

**71** (alyterinin)

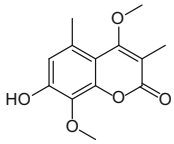

**72** (7-demethyl-8-methoxycoumarsabin)

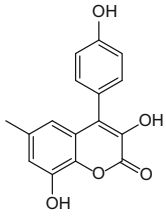

**73** (3,8-dihydroxy-4-(4-hydroxyphenyl)-6-methylcoumarin))

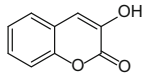

**74** (3-hydroxycoumarin)

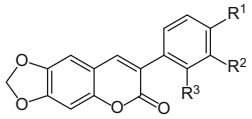

**75** $R^1$ = OH, $R^2$ = H, $R^3$ = H (7-(4-hydroxyphenyl)-6*H*-[1,3]dioxolo[4,5-*g*]chromen-6-one)
**76** $R^1$ = $OCH_3$, $R^2$ = $OCH_3$, $R^3$ = OH (7-(2-hydroxy-3,4-dimethoxyphenyl)-6*H*-[1,3]dioxolo[4,5-*g*]chromen-6-one)

**Fig. 7** Simple coumarins **65**–**76**

(**73**), was isolated from the endolichenic fungus, *Tolypocladium cylindrosporum* [63]. This coumarin is also rather unusual in the sense that it does not have any 7-oxygenation. The extraction of the stems of *Alyxia schlechteri* (Apocynaceae) followed by chromatographic separation and recrystallization afforded a new

**Plate 10** *Sorbus cashmiriana* (Kashmir rowan), Botanical Garden Zielona Góra, Poland. Photograph courtesy of Krzysztof Ziarnek, Creative Commons

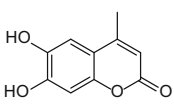


**77** (4-methyl-6,7-dihydroxycoumarin)

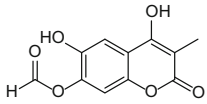


**78** (4,6-dihydroxy-7-formyl-3-methylcoumarin)

**Fig. 8** Simple coumarins **77**–**78**

benzyl coumarin derivative, alyterinin (**71**), which also does not possess oxygenation at C-7 [64]. This plant also produces coumarin (**1**), 6,8-dihydroxycoumarin (**13**), 3-hydroxycoumarin (**74**), 5-hydroxycoumarin (**37**), and 7-hydroxy-8-methoxycoumarin (**21**) [64].

Several 3- and 4-substituted simple coumarins were obtained from the flue-cured roots and stems of *Nicotiana tabacum* (Solanaceae) [65]. Among them, the 3-substitued coumarins, 7-(4-hydroxyphenyl)-6*H*-[1,3]dioxolo[4,5-*g*]chromen-6-one (**75**) and 7-(2-hydroxy-3,4-dimethoxyphenyl)-6*H*-[1,3]dioxolo[4,5-*g*]chromen-6-one (**76**), were identified as new natural products, and the other known compounds detected were **8**, **16**, **29**, **30**, and 4-methyl-6,7-dihydroxycoumarin (**77**) (Fig. 8). Coumarins **22** and **29** were found in the vines of *Prevostea ferruginea* (Convolvulaceae) [66]. A new coumarin, 4,6-dihydroxy-7-formyl-3-methylcoumarin (**78**), was reported from the broth extract of the plant endophytic fungus *Pestalotiopsis versicolor* [67].

## *2.2 Simple Prenylated Coumarins*

Plants often produce coumarins with one or more prenyl (3-methyl-but-2-en-1-yl or dimethylallyl) or modified prenyl groups attached to them. Prenyl transferases are

involved in the biosynthesis of prenylated simple coumarins. In addition to known simple prenylated coumarins, such as meranzin (**117**), osthol (**160**), and osthenol (**159**), several new coumarins of this class, including hydramicromelin D (**85**), integerrimelin (**113**), and 6-(3′-methyl-l′-oxobuty1)-7-hydroxycoumarin (**87**), were reported from various plant sources, with most of them being from the Apiaceae and the Rutaceae plant families (Figs. 9, 10, 11, 12, 13, 14, 15, 16, 17 and 18). However, prenylated coumarins were also reported recently from some

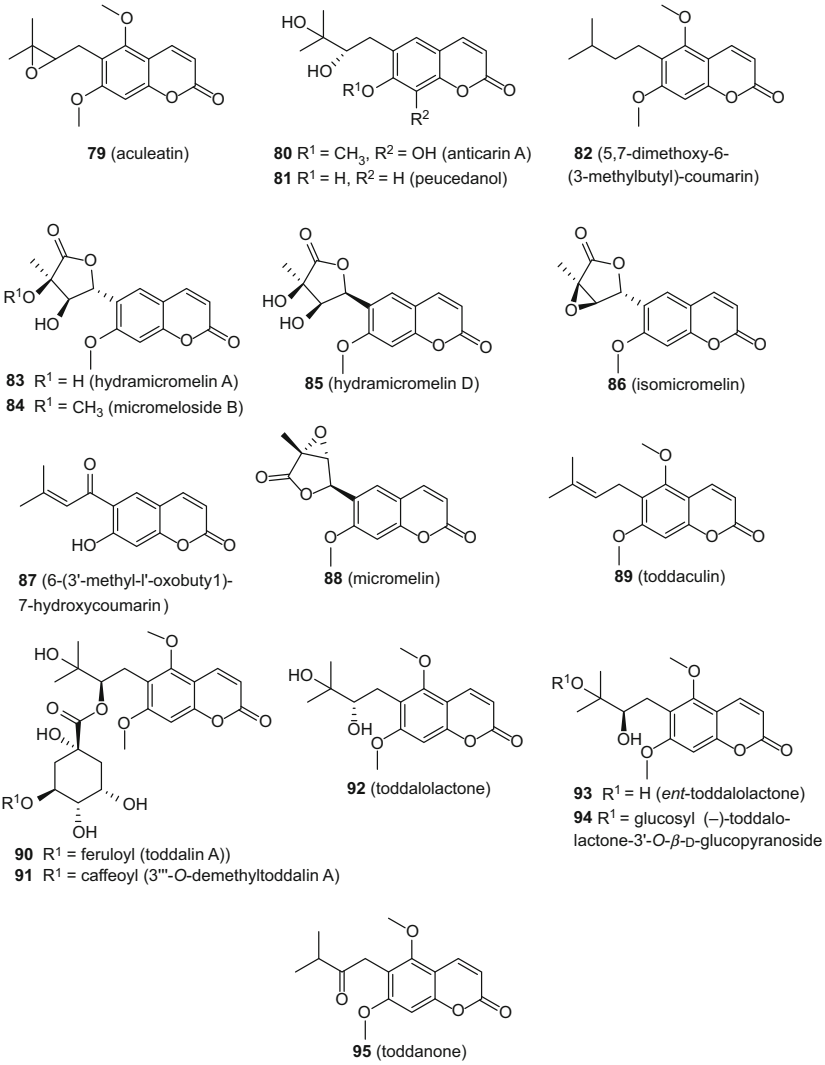


**Fig. 9** Simple prenylated coumarins **79–95**

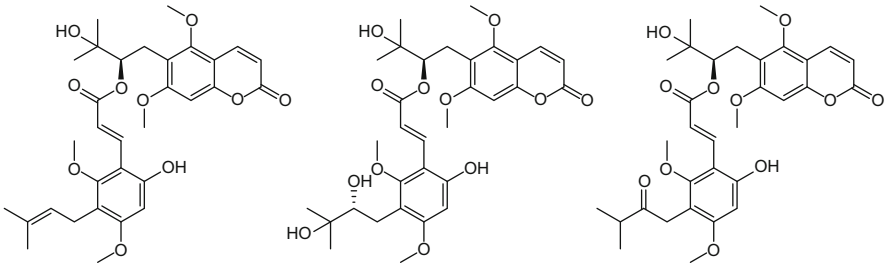


**Fig. 10** Simple prenylated coumarins **96–98**

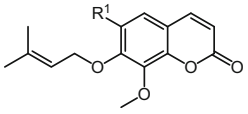


**Fig. 11** Simple prenylated coumarins **99–100**

other families, including Calophyllaceae, Caryophyllaceae, Clusiaceae, Fabaceae, and Moraceae. Most of these coumarins have C- or O-prenylation at C-6 (**79–98**) (Figs. 9 and 10) and C-8 (**101–165**) (Figs. 12–16).

Only one coumarin with prenylation at both the C-6 and C-8 positions (**166**) (Fig. 17) was described recently. In some cases, in addition to prenylations and other usual substitutions on aromatic carbons, there are substitutions at C-3, C-4, or at both (**167–180**) (Fig. 18). Two 7-*O*-prenylated coumarins, **99** and **100** (Fig. 11), were also reported.

Meranzin (**117**, also known as aurapten), a 8-*C*-prenylated coumarin, was reported from the fruits of *Citrus tangerina* (Rutaceae) (Plate 11) [68]. It was also found in *Prangos pabularia* (Apiaceae), which also provided osthol (**160**) [27].

Osthol (**160**) was also isolated from the roots of *Prangos ferulacea* [69]. The 6-*C*-prenylated and 3,4-substituted coumarin, glycyrurol (**169**), was purified as a neuroprotective principle from an herbal remedy containing *Glycyrrhiza* species (Fabaceae) [70]. Daud et al. [71] isolated a new prenylated coumarin with a pentyl group at C-3 on the coumarin nucleus, named hoseimarin (**170**), from the stem bark of *Calophyllum hosei* (Clusiaceae). 6-(3′-Methyl-l′-oxobutyl)-7-hydroxycoumarin (**87**), a new coumarin, was obtained from a non-polar extract of the aerial parts of *Apium graveolens* (Apiaceae) [72]. Phakhodee et al. [14] purified the new coumarins hydramicromelin D (**85**) and integerrimelin (**113**), together with hydramicromelin A (**83**), 7-hydroxy-8-(2′,3′-dihydroxy-3′-methylbutyl)-coumarin (**111**), micromelin (**88**), murrangatin (**151**), murralogin (**148**), and tortuoside (**112**) from the twigs of *Micromelum integerrimum* (Rutaceae).

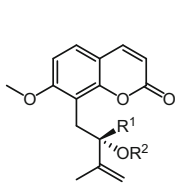

**101** $R^1$ = Me, $R^2$ = H (auraptenol)
**102** $R^1$ = $R^2$ = H (demethylauraptenol)
**103** $R^1$ = Me, $R^2$ = OH (peroxyauraptenol)

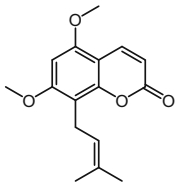

**104** (coumurrayin)

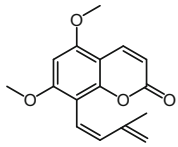

**105** ((*Z*)-dehydrocoumurrayin)

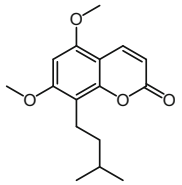

**106** (5,7-dimethoxy-8-(3-methylbutyl)-coumarin

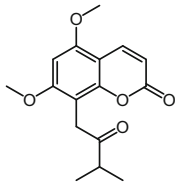

**107** (5,7-dimethoxy-8-(3-methyl-2-oxo-butyl)-coumarin

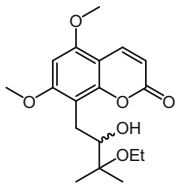

**108** (8-(3-ethoxy-2-hydroxy-3-methylbutyl)-5,7-dimethoxycoumarin)

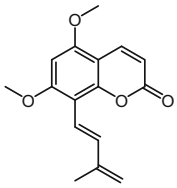

**109** (gleinadiene)

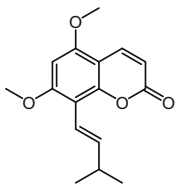

**110** (gleinene)

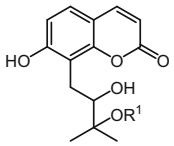

**111** $R^1$= H (7-hydroxy-8-(2',3'-dihydroxy-3'-methylbutyl)-coumarin)
**112** $R^1$= *β*-D-glucopyranosyl (7-hydroxy-8-(2'-hydroxy-3'-*β*-D-glucopyranosyl-3'-methylbutyl)-coumarin)

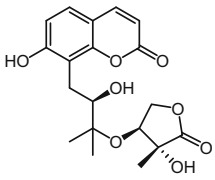

**113** (integerrimelin)

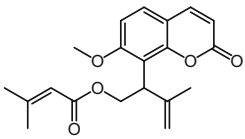

**114** (isomurraloginol senecioate)

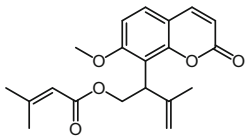

**115** (isomurraloginoic acid)

**Fig. 12** Simple prenylated coumarins **101**–**115**

The new coumarins, isomurralonginoic acid (**115**), isomurralonginol senecioate (**114**), meranzin hydrate 2′-palmitate (**119**), and murrangatin 2′-formate (**153**), were isolated from the vegetative branches of *Murraya exotica* (Rutaceae) [73]. Glycyrin (**166**), glycycoumarin (**167**), and glycyrol (**168**) were purified as antihepatitis C viral compounds from *Glycyrrhiza* species, as exemplified by *G. uralensis* (Plate 12) [74].

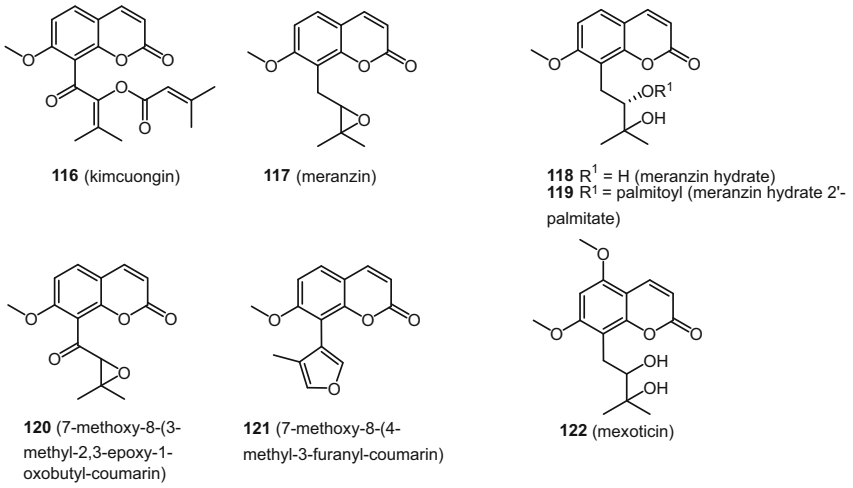


**Fig. 13** Simple prenylated coumarins **116**–**122**

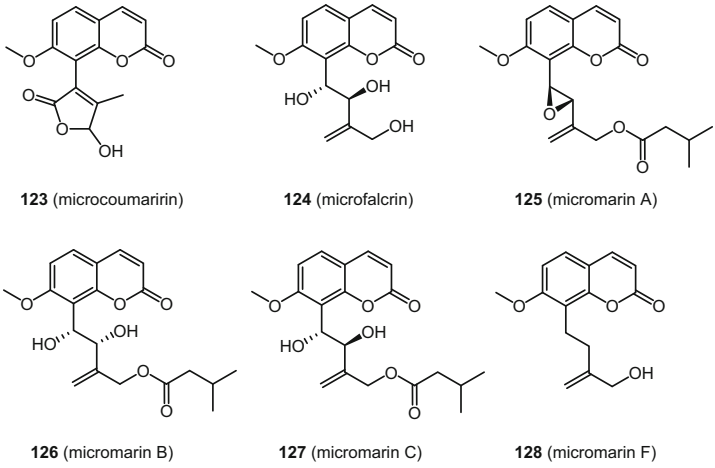


**Fig. 14** Simple prenylated coumarins **123**–**128**

Anticarin A (**80**), a new 6-prenylated coumarin, together with peucedanol (**81**), was purified from the trunk bark of *Antiaris toxicana* (Moraceae) [75] (Fig. 9). A chromatographic analysis of the chloroform fraction of the methanol extract of the leaves of *Murraya paniculata* (Rutaceae) provided a new coumarin, kimcuongin (**116**), together with murracarpin (**139**), with vasorelaxant activity [76]. Lin et al. [43] isolated seven new prenylated coumarins from an ethanolic extract of the roots of *Toddalia asiatica* (Rutaceae), a well-known component of Traditional Chinese Medicine (TCM) preparations used for the treatment of rheumatic arthritis, injuries and infections. Those coumarins were named

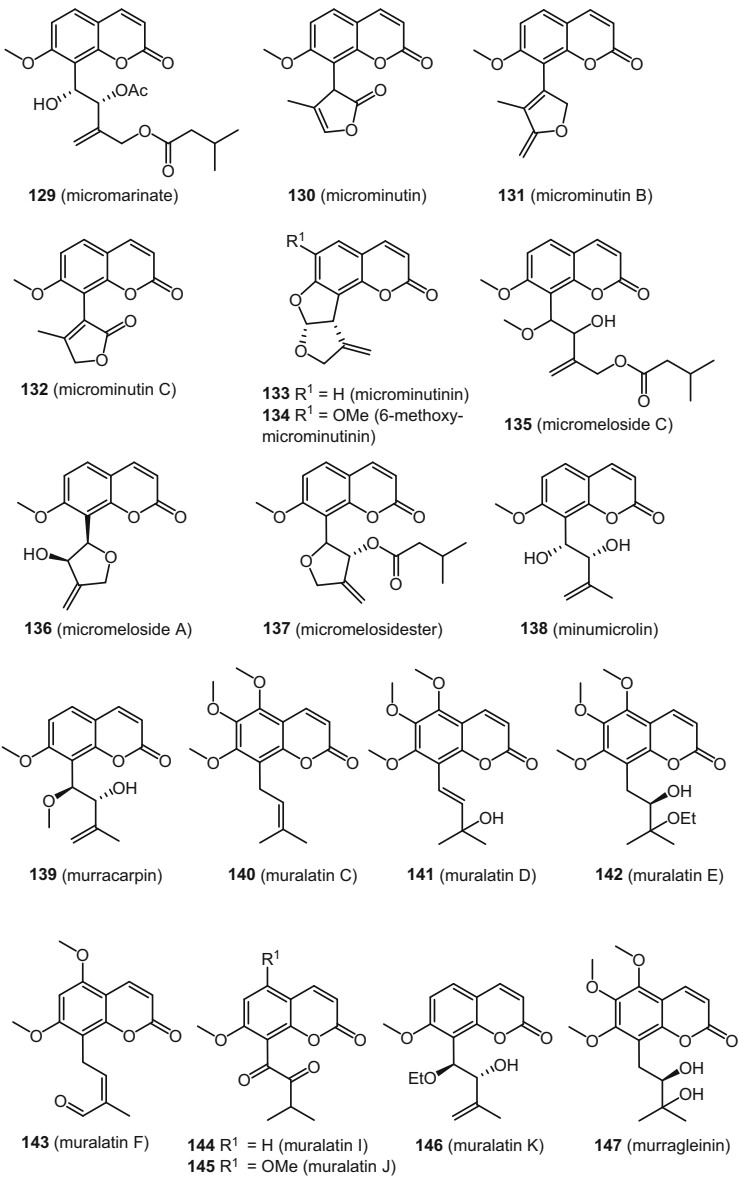


**Fig. 15** Simple prenylated coumarins **129**–**147**

3‴-*O*-demethyltoddalin A (**91**), toddalins A–D (**90**, **96**–**98**) (Fig. 10), *ent*-toddalolactone (**93**), and (–)-toddalolactone 3′-*O*-*β*-D-glucopyranoside (**94**). In addition, coumurrayin (**104**), (*Z*)-dehydrocoumurrayin (**105**), 5,7-dimethoxy-6-(3-methylbutyl)-coumarin (**82**), 5,7-dimethoxy-8-(3-methylbutyl)-coumarin (**106**), gleinadiene (**109**), toddaculin (**89**), toddalolactone (**92**), and toddanone (**95**) were

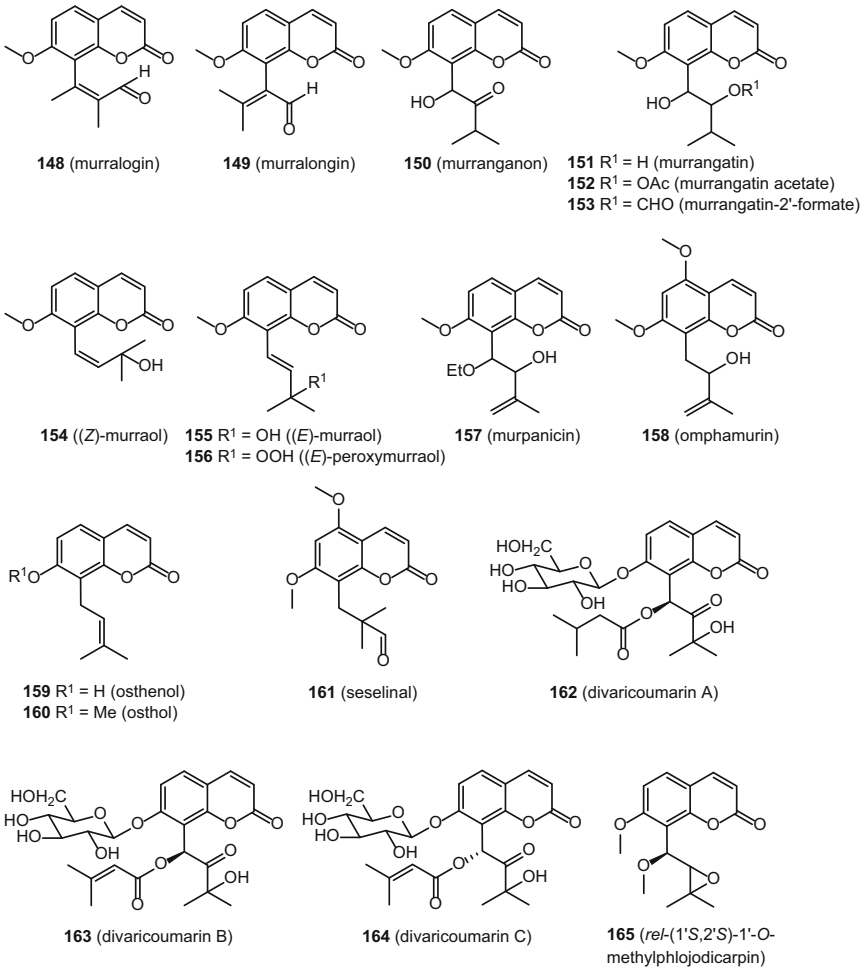


**Fig. 16** Simple prenylated coumarins **148**–**165**

obtained from this plant. Toddaculin (**89**), isolated from the stem of this plant, was found recently to inhibit osteoclastogenesis in RAW 264 cells and enhanced osteoblastogenesis in MC3T3-E1 cells [77].

Two 7-*O*-prenylated simple coumarins, lacinartin (**99**) and puberulin (**100**) (Fig. 11), were isolated from the stems of *Zanthoxylum schinifolium* (Rutaceae) [46].

A new antioxidative coumarin with a prenyl substituent at C-8, named 7-methoxy-8-(3-methyl-2,3-epoxy-1-oxobutyl)chromen-2-one (**120**), was purified from the fruits of *Cnidium monnieri* (Apiaceae) (Plate 7) [78]. In addition, the known dihydrofuranocoumarins (*Z*)- and (*E*)-murraol (**154** and **155**) and micromarin F (**128**), with cytoprotective properties, were also isolated. Several antifungal prenylated coumarins were obtained from the fruits of *Micromelum*

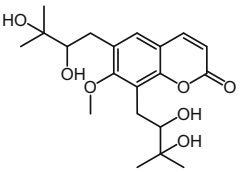

**166** (7-methoxy-6,8-bis-(2,3-dihydroxy-3-methylbutyl)-coumarin)

**Fig. 17** Simple prenylated coumarin **166**

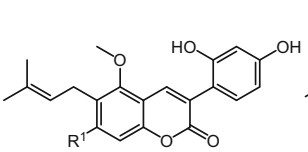

**167** $R^1$ = OMe (glycyrin)
**168** $R^1$ = OH (glycycoumarin)

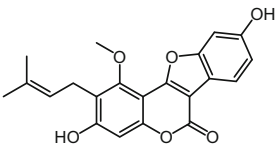

**169** (glycyrol)

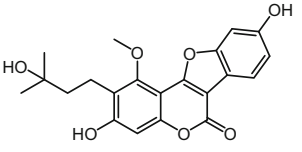

**170** (glycyrurol)

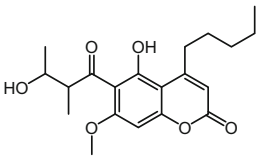

**171** (hoseimarin)

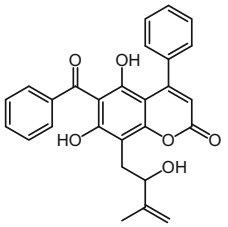

**172** (neurophyllol C)

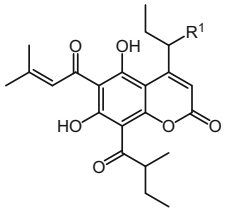

**173** $R^1$ = H (mammea B/BB)
**174** $R^1$ = OAc (mammea E/BB)

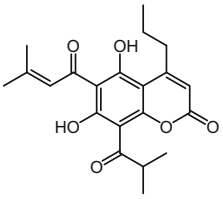

**175** (mammea B/BD)

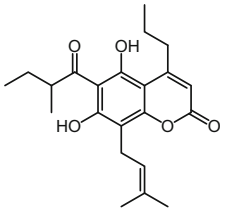

**176** (mammea B/AD)

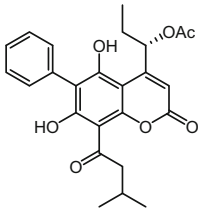

**177** (mammea E/BA)

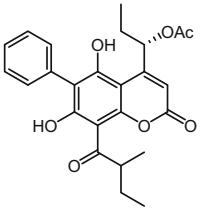

**178** (mammea E/EB)

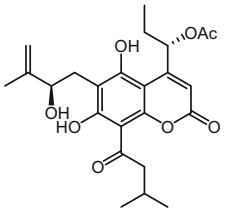

**179** (neurophyllol A)

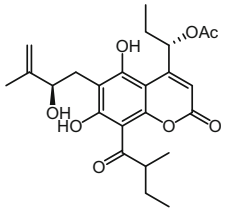

**180** (neurophyllol B)

**Fig. 18** Simple prenylated coumarins **167**–**180**

**Plate 11** *Citrus tangerina* (tangerine), Portugal. Photograph courtesy of Gold Bernard, Creative Commons

**Plate 12** *Glycyrrhiza uralensis* (Chinese licorice), San Diego Botanic Garden, Encinitas, California, USA. Photograph courtesy of Stickpen, Public Domain

*minutum* (Rutaceae), mainly by repeated preparative-thin layer chromatography (prep-TLC) and open column chromatography (CC) on silica gel. Among those coumarins, micromarinate (**129**), microminutins B and C (**131** and **132**) (Fig. 15) are new coumarins with prenylation at C-8. Hydramicromelin A (**83**), isomicromelin (**86**), 6-methoxy-microminutinin (**134**), 7-methoxy-8-(4′-methyl-3′-furanyl)coumarin (**121**), micromarins A-C (**125-127**), micromelosides A–C (**136**, **84** and **135**),

**Plate 13** *Clausena lansium* (wampee), Hong Kong. Photograph courtesy of WingkLEE, Public Domain

microminutin (**130**), microminutinin (**133**), minumicrolin (**138**), and murralongin (**149**) are known coumarins that were isolated during this study [42].

A method using off-line two-dimensional high-performance liquid chromatography coupled with electrospray tandem mass spectrometry (off-line 2D-HPLC-ESI/$MS^n$) was developed to identify coumarins in the roots of *Angelica dahurica* (Apiaceae), and, among the identified coumarins, osthenol (**159**) was the only simple prenylated coumarin [34], which was also isolated from the roots of *Clausena lansium* (Rutaceae) (Plate 13) [79]. Two new prenylated coumarins, 3′-*O*-methylmurraol (the 3′-methyl ether of **155**) and *rel*-(1′*S*,2′*S*)-1′-*O*-methylphlojodicarpin (**165**), together with auraptenol (**101**), demethylauraptenol (**102**), meranzin hydrate (**118**), (*E*)-murraol (**155**), osthol (**160**), osthenol (**159**), peroxyauraptenol (**103**), and peroxymurraol (**156**), were purified from the fruits of *Cnidium monnieri* (Apiaceae) (Plate 7) [78]. Osthol (**160**) was also found in an acetone extract of the roots of *Clausena guillauminii* (Rutaceae) [80].

7-Methoxycoumarins with various forms of prenylation patterns microcoumaririn (**123**), microfalcrin (**124**), micromarin B (**126**), micromelin (**88**), micromelosidester (**137**), micromeloside A (**136**), microminutin (**130**), and micromarin A (**125**), were isolated from *Micromelum falcatum* [81]. Microcoumaririn (**123**), microfalcrin (**124**), and micromelosidester (**137**) are new natural products (Figs. 14 and 15). A phytochemical investigation on the aerial parts of *Murraya tetramera* (Rutaceae) afforded 5,7-dimethoxy-8-[(*Z*)-3′-methylbutan-1′,3′-dienyl]coumarin (**105**) (also known as (*Z*)-dehydrocoumurrayin), 5,7-dimethoxy-8-(3-methyl-2-oxo-butyl)coumarin (**107**), and murrangatin acetate (**152**) [44].

The 6-prenylated 5,7-dimethoxycoumarins, aculeatin (**79**), toddalolactone (**92**), and toddaculin (**89**), were isolated from *Toddalia asiatica* (Rutaceae) [82], and **79** was shown to enhance differentiation and lipolysis of adipocytes. The new 8-prenylated and methoxylated simple coumarins, muralatins C–F (**140–143**) and I–K (**144–146**), were reported from the leaves of *Murraya alata* (Rutaceae) (Fig. 15) [17]. Several known 8-prenylated coumarins, coumurrayin (**104**), 5,7-dimethoxy-8-[(*Z*)-3-methylbut-1,3-dienyl]-coumarin (**105**) (also known as (*Z*)-dehydrocoumurrayin), 5,7-dimethoxy-8-(3-methyl-2-oxo-butyl)-coumarin (**107**), 8-(3-ethoxy-2-hydroxy-3-methylbutyl)-5,7-dimethoxycoumarin (**108**), gleinene (**110**), gleinadiene (**109**), mexoticin (**122**), murralongin (**149**), murranganon (**150**), murrangatin (**151**), murragleinin (**147**), murraol (**155**), murpanicin (**157**), omphamurin (**158**), osthol (**160**), peroxyauraptenol (**103**), and seselinal (**161**), were also isolated from this plant. Three new coumarins, divaricoumarins A–C (**162–164**), were purified from a methanolic extract of the roots of *Saposhnikovia divaricata* (Apiaceae) [19].

A new di-C-prenylated simple coumarin, 7-methoxy-6,8-bis-(2,3-dihydroxy-3-methylbutyl)-coumarin (**166**), was recently isolated from the leaves of *Sophora interrupta* (Fabaceae) (Fig. 17) [83].

Among the mammea-type coumarins isolated from the stem bark of *Mammea usambarensis* (Clusiaceae), four were simple prenylated coumarins, mammea B/BB (**173**), mammea E/BB (**174**), mammea B/BD (**175**), and mammea B/AB (**176**) (Fig. 18) [84]. The mammea coumarins are isoprenylated 4-alkyl or 4-phenylcoumarins, which are generally distributed exclusively in three Clusiaceae/Calophyllaceae genera [85]. A series of 4-substituted prenylated simple coumarins (Fig. 18), mammea E/BA (**177**), mammea E/EB (**178**), neurophyllols A (**179**), B (**180**), and C (**172**), was obtained from a dichloromethane extract of the bark of *Mammea neurophylla* (Caryophyllaceae) [56, 85]. Of these compounds, coumarin **172** is a new natural product.

## 2.3 Simple Geranylated Coumarins

Geranylated coumarins (**181–196**) are actually monoterpenyl coumarins containing a ten-carbon monoterpenyl unit linked to the coumarin nucleus (Figs. 19 and 20). The Rutaceae family appears to be the major source of geranylated coumarins that have been reported recently, but such coumarins were also documented from the families Apiaceae, Asteraceae, Cucurbitaceae, and Gomphidiaceae. Geranylation of coumarin is facilitated by the geranyl transferase enzyme, which utilizes geranyl diphosphate as the substrate.

Auraptene (**181**) was isolated from the fruits of *Chroogomphus rutilus* (Gomphidiaceae) [18]. Three 7-*O*-geranylated simple coumarins, collinin (**184**), 8-methoxyabisocoumarin H (**186**), and acetoxyschinifolin (**183**), were obtained from the stems of *Zanthoxylum schinifolium* (Rutaceae) [46]. Jeong et al. [53]

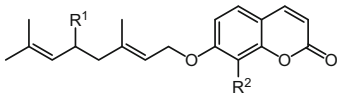

**181** $R^1 = R^2 = H$ (auraptene)
**182** $R^1 = AcO$, $R^2 = H$ (5'-acetoxyauraptene)
**183** $R^1 = AcO$, $R^2 = OMe$ (acetoxyschinifolin)
**184** $R^1 = H$, $R^2 = OMe$ (collinin)
**185** $R^1 = OH$, $R^2 = H$ (5'-hydroxyauraptene)
**186** $R^1 = OH$, $R^2 = OMe$ (8-methoxyabisocoumarin H)

**Fig. 19** Simple geranylated coumarins **181**–**186**

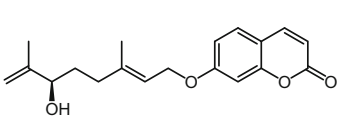

**187** (7-(6'*R*)-hydroxy-3',7'-dimethylocta-2',7'-dienyloxy)-coumarin)

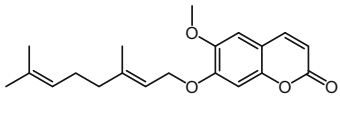

**188** (7-*O*-geranyl-6-methoxycoumarin)

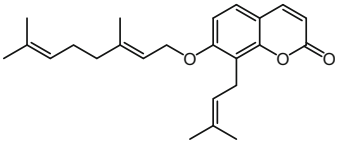

**189** (7-*O*-geranyl-osthenol)

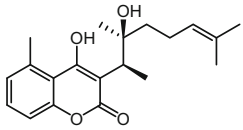

**190** (ainsliaeasin A1)

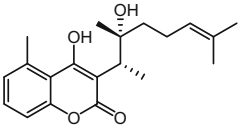

**191** (ainsliaeasin A2)

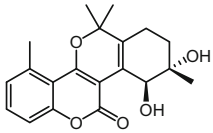

**192** (ainsliaeasin B1)

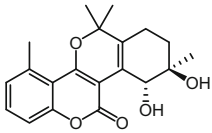

**193** (ainsliaeasin B2)

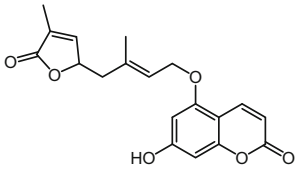

**194** (clausenalansimin B)

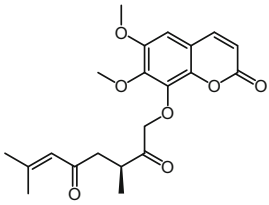

**195** (tricanguina A)

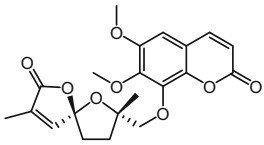

**196** (tricanguina B)

**Fig. 20** Simple geranylated coumarins **187**–**196**

reported collinin (**184**), 8-methoxyabisocoumarin H (**186**), and 7-((6′*R*)-hydroxy-3′,7′-dimethylocta-2′,7′-dienyloxy)-coumarin (**187**) as a result of their search for bioactive constituents from the leaves of *Z. schinifolium*. A modified geranyl (monoterpenyl) substituted simple coumarin, clausenalansimin B (**194**), was

isolated from the peels of *Clausena lansium* (Rutaceae) (Plate 13) [86]. While 7-*O*-geranyl-osthenol (**189**) was purified from *Rauia nodosa* (Rutaceae) [87], 7-*O*-geranyl-6-methoxycoumarin (**188**) was found in the aerial parts of *Murraya tetramera* of the same family [44]. In the search for acetylcholinesterase inhibitors, in addition to **2** and a few sesquiterpenyl coumarins, three geranylated coumarins, auraptene (**181**), 5′-acetoxyauraptene (**182**), and 5′-hydroxyauraptene (**185**), were isolated from the oleogum resin of *Ferula gummosa* (Apiaceae) [88]. The monoterpenyl simple coumarins tricanguinas A (**195**) and B (**196**) were obtained from the aerial parts of *Trichosanthes anguina* (Cucurbitaceae) [89]. Four rather unusual new coumarins, ainsliaeasins A1 (**190**) and A2 (**191**), and ainsliaeasins B1 (**192**) and B2 (**193**) were reported from the whole plant of *Ainsliaea fragrans* (Asteraceae) [61].

## 2.4 Furanocoumarins

Furanocoumarins (also known as furocoumarins) possess a furan (or dihydrofuran) ring fused with the coumarin skeleton, e.g., psoralen (**198**) (Scheme 2).

**Scheme 2** Biosynthesis of furanocoumarins

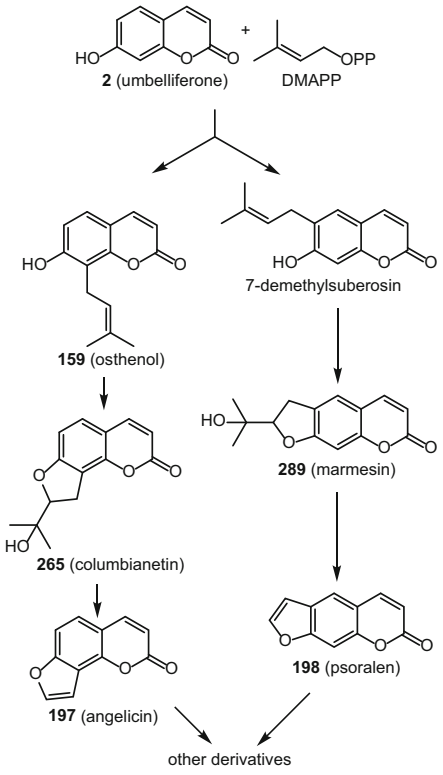

These two rings are fused in different ways to produce various angular (e.g. angelicin (**197**)) and linear (e.g. psoralen (**198**)) furanocoumarins. They are generally biosynthesized involving two pathways, the phenylpropanoid and the mevalonic acid pathways, by a coupling of dimethylallyl pyrophosphate (DMAPP) and umbelliferone (**2**), and through the formation of a prenylated simple coumarin intermediate (Scheme 2). The Apiaceae and the Rutaceae are the main sources of furanocoumarins, with the families Asteraceae, Caryophyllaceae, Fabaceae, Moraceae, and Salvadoraceae, having also been shown to produce these compounds in recent studies. Furanocoumarins (including dihydrofuranocoumarins) can broadly be classified into angular and linear furanocoumarins, and furanocoumarins reported recently are discussed under these classes below.

### 2.4.1 Angular Furanocoumarins

There are not many angular furanocoumarins (Fig. 21) found in plants, and even recent work has only revealed known compounds of this class. The simplest angular furanocoumarin, isopsoralen (**197**), (also known as angelicin), was reported from the seeds of *Psoralea corylifolia* (Fabaceae) (Plate 14) and found to possess antidiabetic potential [90]. A bioassay-guided isolation of antimicrobial coumarins from the fruits of *Heracleum mantegazzianum* (Apiaceae) (Plate 15) by high-performance counter-current chromatography afforded **197** and pimpinellin (**199**) (Fig. 9) [91].

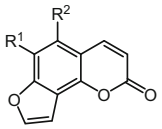


**197** $R^1 = R^2 = H$ (isopsoralen/angelicin)
**199** $R^1 = R^2 = OMe$ (pimpinellin)

**Fig. 21** Angular furanocoumarins **197** and **199**

**Plate 14** *Psoralea corylifolia* (babchi), The Agri-Horticultural Society of India, Alipore, Kolkata, India. Photograph courtesy of Biswarup Ganguly, Creative Commons

**Plate 15** *Heracleum mantegazzianum* (giant hogweed), National Botanic Garden of Belgium. Photograph courtesy of Jean-Pol Grandmont, Creative Commons

### 2.4.2 Linear Furanocoumarins

No new simple linear furanocoumarins, which do not have any prenylation or geranylation, were recently reported; all reported coumarins of this category (Fig. 22) are known natural products.

Bergapten (**200**), isopimpinellin (**204**), and xanthotoxin (**205**), together with the prenylated furanocoumarin imperatorin (**212**), were isolated from the roots of *Heracleum dissectum* (Apiaceae) [92]. Furanocoumarins **200** and **205** were also found in a water extract of *Peucedanum praeruptorum* (Apiaceae) [30]. Xanthotoxin (**205**) was purified from an ethanolic extract of the stems of *Salvadora indica* (Salvadoraceae) by flash chromatography, and showed considerable antihyperlipidemic and antitumor activities [7]. Psoralen (**198**) was one of the active components with antidiabetic potential in the seeds of *Psoralea corylifolia* (Fabaceae) (Plate 14) [90]. Coumarins **198**, **204**, and **205** were identified as a result of GC-MS analysis of the extract of the Bulgarian celeriac, *Apium graveolens* var. *rapaceum* (Apiaceae) [72]. Xanthotoxin (**205**) was again isolated as an anticonvulsant agent from the fruits of *Pastinaca sativa* (Apiaceae) [93], and also from *Gerbera anandria* (Asteraceae) [94], and the whole plant of *Ainsliaea fragrans* (Asteraceae) [61]. The aerial parts of *Prangos pabularia* (Apiaceae) were found to produce **205** and xanthotoxol (**206**) [27]. The methoxylated furanocoumarin, isopimpinellin (**204**), which is a linear version of pimpinellin (**199**), was purified from the roots of *Angelica nitida* (Apiaceae) [95]. A bioassay-guided isolation procedure of antimicrobial coumarins from the fruits of *Heracleum mantegazzianum* (Apiaceae) (Plate 15) led to the identification of **200**, **204**, and **205** [91]. While xanthotoxol-8-*O*-*β*-D-glucopyranoside (**207**) was isolated from

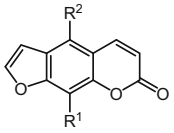


**Fig. 22** Simple linear furanocoumarins **200**–**207**

**200** $R^1$ = H, $R^2$ = OMe (bergapten)
**201** $R^1$ = H, $R^2$ = OH (bergaptol)
**202** $R^1$ = OMe, $R^2$ = OH (5-hydroxy-xanthotoxin)
**203** $R^1$ = OH, $R^2$ = OMe (5-hydroxy-8-methoxy-psoralen)
**204** $R^1$ = OMe, $R^2$ = OMe (isopimpinellin)
**205** $R^1$ = OMe, $R^2$ = H (xanthotoxin)
**206** $R^1$ = OH, $R^2$ = H (xanthotoxol)
**207** $R^1$ = glucosyloxy, $R^2$ = H (xanthotoxol-8-*O*-*β*-D-glucopyranoside)

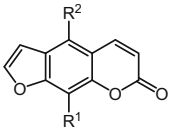


**Fig. 23** Simple prenylated linear furanocoumarins **208**–**214**

**208** $R^1$ = 3-methyl-2-butenyl, $R^2$ = OH (alloimperatorin)
**209** $R^1$ = OH, $R^2$ = 3-methyl-2-butenyl (alloisoimperatorin)
**210** $R^1$ = 3-methyl-2-butenyloxy, $R^2$ = 3-methyl-2-butenyloxy (cnidicin)
**211** $R^1$ = OMe, $R^2$ = 3-methyl-2-butenyloxy (cnidilin)
**212** $R^1$ = 3-methyl-2-butenyloxy, $R^2$ = H (imperatorin)
**213** $R^1$ = H, $R^2$ = 3-methyl-2-butenyloxy (isoimperatorin)
**214** $R^1$ = 3-methyl-2-butenyloxy, $R^2$ = OMe (phellopterin)

*Clausena lansium* (Rutaceae) (Plate 13) [96], **200**, bergaptol (**201**), **204**, 5-methoxy-8-hydroxy-psoralen (**205**), and 5-hydroxy-8-methoxy-psoralen (**203**) were reported from *Angelica dahurica* (Apiaceae) [34].

Among the recently reported furanocoumarins, prenylated linear furanocoumarins (Figs. 23 and 24) form one of the largest groups of furanocoumarins, but most have been known natural products. Both C- and O-prenylations are common in these compounds. The *O*-prenylated furanocoumarins, byakangelicin (**218**), cnidilin (**211**), imperatorin (**212**), isobyakangelicin (**224**), isoimperatorin (**213**), and phellopterin (**214**), were obtained from the roots of *Angelica nitida* (Apiaceae) [95]. Heraclenol (**219**), heraclenol-glycoside (**220**), oxypeucedanin hydrate (**225**), a demethoxy derivative of isobyakangelicin (**224**), oxypeucedanin hydrate monoacetate (**226**), pabulenol (**236**), and **212** were isolated from the aerial parts of *Prangos pabularia* (Apiaceae) [27]. A bioassay-guided isolation of antimicrobial coumarins from the fruits of *Heracleum mantegazzianum* (Apiaceae) (Plate 15) afforded **212** and **214** [91]. Coumarin **225** was also isolated from the trunk bark of *Antiaris toxicaria* (Moraceae) [75], and from a methanolic extract of the roots of *Saposhnikovia divaricata* (Apiaceae) [36]. Several furanocoumarins, **212**–**214**, demethylfuropinarine (**222**), and isodemethylfuropinarine (**230**) (Fig. 25) were identified from the roots of *Angelica dahurica* var. *formosana* cv. Chuanbaizhi (Apiaceae) [97]. Chalepensin (**221**), which is a 3-prenylated linear furanocoumarin, together with **200**, was isolated from the leaves of *Esenbeckia alata* (Rutaceae) [98].

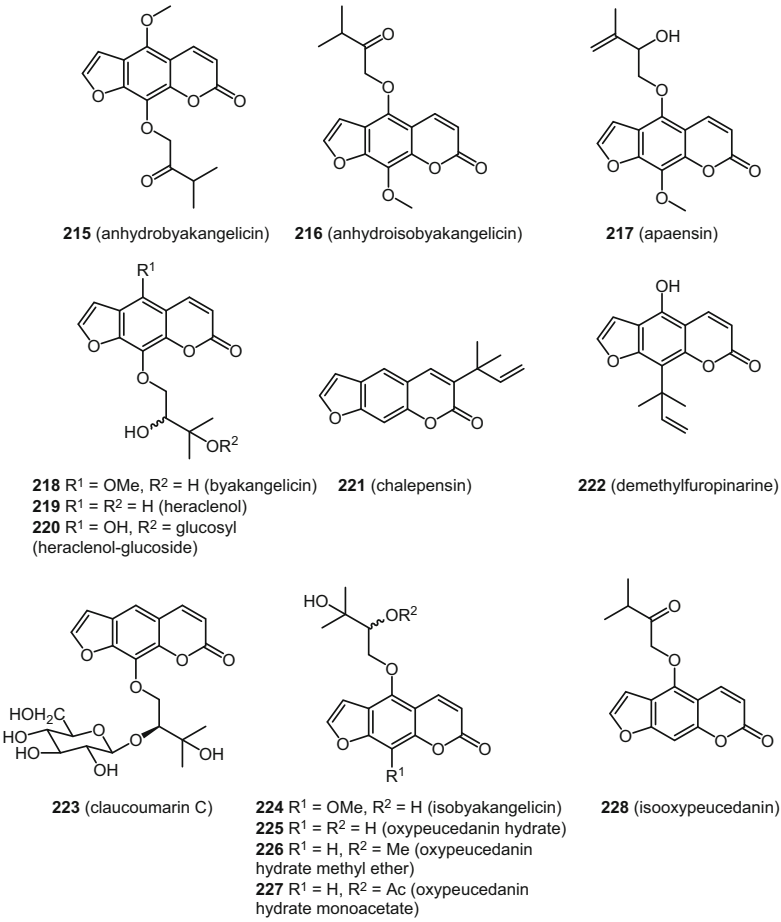


**Fig. 24** Simple prenylated linear furanocoumarins **215**–**228**

A method using off-line two-dimensional high-performance liquid chromatography coupled with electrospray tandem mass spectrometry (off-line 2D-HPLC-ESI/$MS^n$) was developed to identify linear furanocoumarins in the roots of *Angelica dahurica* (Apiaceae), and several of these compounds were prenylated furanocoumarins, e.g. **211**–**214**, **224**, **225**, alloimperatorin (**208**), alloisoimperatorin (**209**), anhydrobyakangelicin (**215**), anhydroisobyakangelicin (**216**), apaensisn (**217**), byakangelicin (**218**), isobyakangelicol (**229**), isogospherol (**231**), isooxypeucedanin (**228**), neobyakangelicol (**232**), oxypeucedanin (**234**), pabulenol (**236**), and pabularinone (**235**) [34]. Similar known coumarins were isolated from the aerial parts of the Bhutanese medicinal plant *Pleurospermum amabile* (Apiaceae) as antibacterial compounds, namely, **198**, **200**, **204**, **213**, **225**, and oxypeucedanin methanolate (**226**) [99]. Imperatorin (**212**) was also reported from the flowers of *Ferula lutea* (Apiaceae) [33, 100]. While **204** was recently isolated

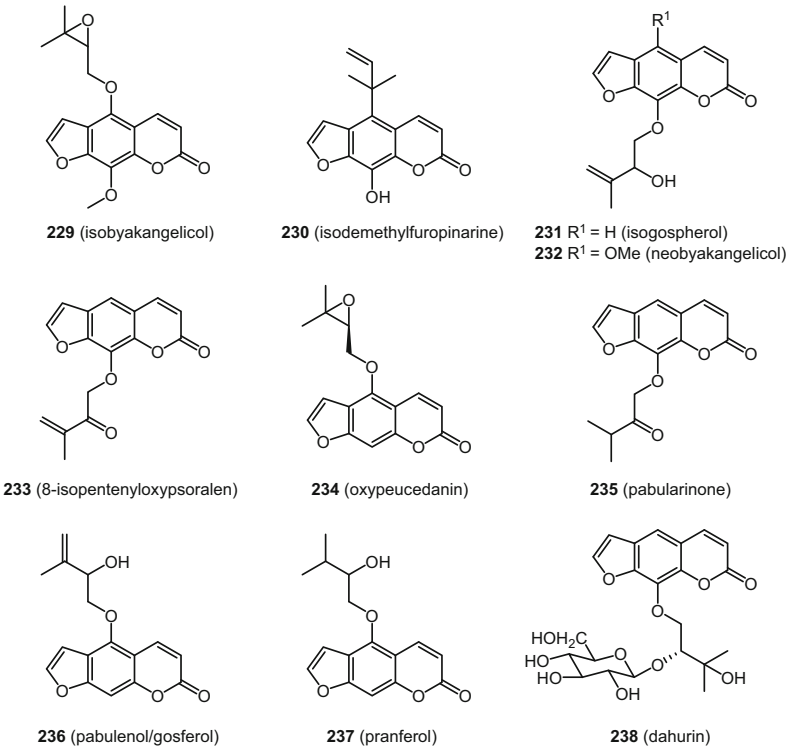


**Fig. 25** Simple prenylated linear furanocoumarins **229**–**238**

from the leaves of *Sophora interrupta* (Fabaceae) [83], oxypeucedanin (**234**), which is conspicuous in the genus *Ferulago*, has been found in *Ferulago angulata* (Apiaceae) [101].

Lee et al. [78] purified **200**, **204**, **205**, **206**, and **212** from the fruits of *Cnidium monnieri* (Apiaceae) (Plate 7). Shokoohinia et al. [69] isolated the antiviral and cytotoxic furanocoumarins, **198**, **213**, **225**, **226**, **234**, **236**, and **237** from the roots of *Prangos ferulacea* (Apiaceae).

In recent years, several geranylated linear furanocoumarins were isolated from various species, mainly of the families Apiaceae and Rutaceae (Figs. 26 and 27), and some of these are new natural products, e.g. clausemarins A–D (**248**–**251**). A phytochemical study on the twigs of *Feroniella lucida* (Plate 8) afforded several coumarins of this category, such as anisolactone (**239**), bergamottin (**240**), 2′,3′-epoxyanisalactone (**243**), lucidafuranolactone B (**246**), and notoptol (**247**) [40]. Bergamottin (**240**) and 8-geranyloxypsoralen (**244**) were identified from the roots of *Angelica dahurica* (Apiaceae) [34]. Clausemarins A–D (**248**–**251**), the new coumarins referred to above, were obtained from the roots of *Clausena lansium* (Rutaceae) (Plate 13) [79]. In all of these new compounds, a monoterpene unit is linked to the furanocoumarin skeleton. The known geranylated compounds from

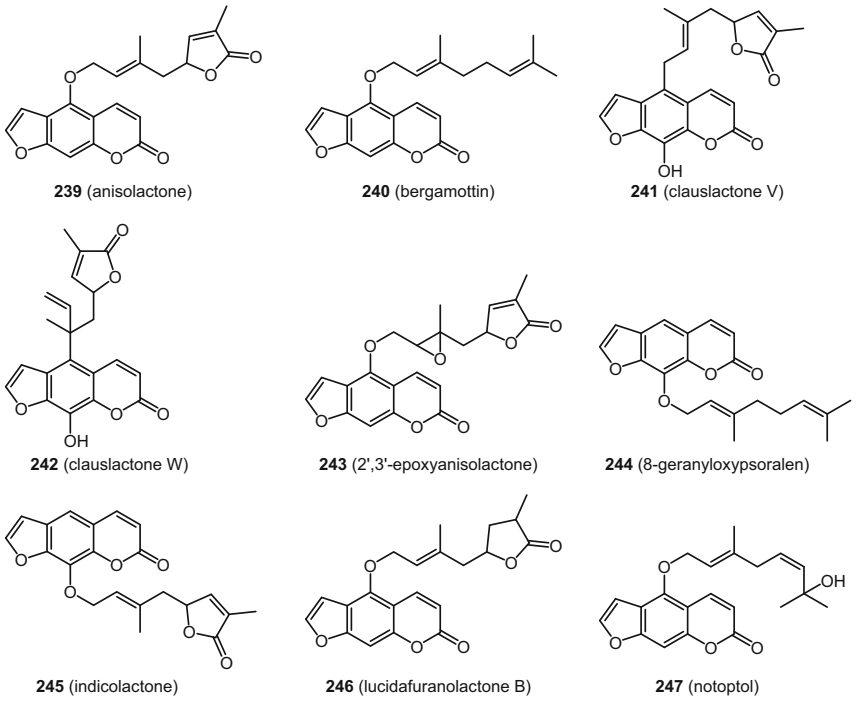


**Fig. 26** Geranylated linear furanocoumarins **239**–**247**

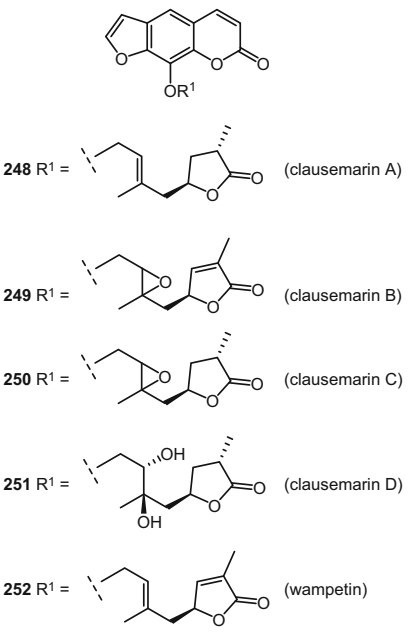


**Fig. 27** Geranylated linear furanocoumarins **248**–**252**

this plant are **244** and wampetin (**252**), together with known prenylated compounds **212** and **213**. Clauslactone V (**241**) and clauslactone W (**242**), together with **239** and **252**, were isolated from the peel of *C. lansium* (Plate 13) [86, 102].

A new monoterpenyl furanocoumarin, 9-[3-methyl-4-(4-methyl-5-oxo-tetrahydro-furan-2-yl)-but-2-enyloxy]-furo[3,2-*g*]chromen-7-one (**253**) (Fig. 28), quite similar to the clausemarins (**248**–**251**), was identified from the stems of *Clausena lansium* (Rutaceae) (Plate 13) [102]. Pabularinone (**235**) was also found in this plant. While Xu et al. [103] isolated **206** and indicolactone (**245**) from the

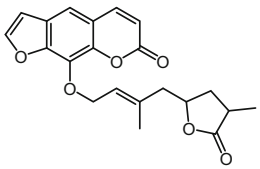

**253** (9-[3-methyl-4-(4-methyl-5-oxo-tetrahydrofuran-2-yl)-but-2-enyloxy]-furo[3,2- *g*]chromen-7-one)

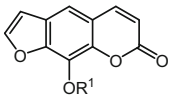

**254** $R^1$ = 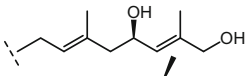 (claucoumarin A)

**255** $R^1$ = 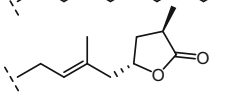 (claucoumarin B)

**256** $R^1$ = 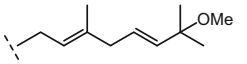 (claucoumarin D)

**257** $R^1$ = 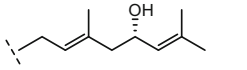 (clausenalansimin A)

**258** $R^1$ = 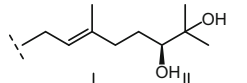 ((*E*)-9-((6,7-dihydroxy-3,7-dimethyloct-2-en-1-yl)oxy)-7*H*-furo[3,2-*g*]chromen-7-one

**259** $R^1$ = 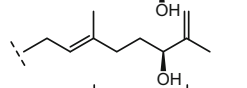 (lansiumarin C)

**260** $R^1$ = 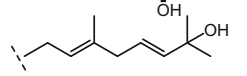 ((*E*,*E*)-8-((7-hydroxy-3,7-dimethyloct-2,5-dienyl)oxy)-psoralen)

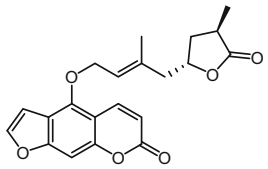

**261**

**Fig. 28** Geranylated linear furanocoumarins **253**–**261**

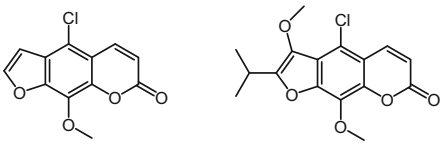


**262** (5-chloro-8-methoxy-psoralen) **263** (peucedanin)

**Fig. 29** Linear furanocoumarins with unusual substitutions **262** and **263**

fresh ripe fruits, Liu et al. [96] obtained 17 furanocoumarins including some geranylated representatives from the stems of the same plant. The stem-derived coumarins were alloisoimperatorin (**209**), anisolactone (**239**), clausenalansimin A (**257**), claucoumarins A–D (**254**, **255**, **223**, and **256**, which are new natural products), dahurin (**238**), (*E*)-9-(6,7-dihydroxy-3,7-dimethyloct-2-en-1-yl)oxy)-7*H*-furo[3,2-*g*]chromen-7-one (**258**), (*E*,*E*)-8-(7-hydroxy-3,7-dimethylocta-2,5-dimethoxy)-psoralen (**260**), imperatorin (**212**), 8-isopentonyloxypsoralen (**234**), lansiumarin C (**259**), 5-{[(*E*)-3-methyl-4-(2*S*,4*R*)-4-methyl-5-oxotetrahydrofuran-2-yl)but-2-en-1-yl]oxy}-psoralen (**261**), wampetin (**252**), xanthotoxol (**206**), and xanthotoxol-8-*O*-*β*-D-glucopyranoside (**207**). However, claucoumarin B (**255**) and 9-[3-methyl-4-(4-methyl-5-oxo-tetrapydrofuran-2-yl)-but-2-enyloxy]-furo[3,2-*g*] chromen-7-one (**253**) are the same compound, with the only difference being that in **255**, the relative configuration was defined.

A new chlorinated furanocoumarin, 5-chloro-8-methoxy-psoralen (**262**), together with **204** and **205**, were isolated by Severino et al. as a mixture from the aerial parts (branches) of *Hortia superba* (Rutaceae) (Fig. 29) [105]. Halogenated coumarins like **262** are rare in the plant kingdom, and as often in similar occurrences, the possibility that these compounds might be extraction artefacts cannot be rouled out convincingly.

The same group reported **200** and two angular pyranocoumarins from this same plant in the following year [106]. Compound **200**, together with **204**, were isolated as phytotoxic agents from the roots and rhizomes of Notopterygii (*Notopterygium incisum*) of the family Apiaceae [106]. Peucedanin (**263**), where substitutions are on the furan ring, was found in the aerial parts of *Opopanax hispidus* [11].

### 2.4.3 Angular Dihydrofuranocoumarins

Only a handful of angular dihydrofuranocoumarins were reported recently (Fig. 30). 3-*O*-Methylvaginol (**268**) (also described as (1′*S*,2′*S*)-1′-*O*-methylvaginol, a new angular dihydrofuranocoumarin), was isolated from the fruits of *Cnidium monnieri* (Apiaceae) [78]. Apterin (**265**), a dihydrofuranocoumarin glucoside, was purified from the roots of *Heracleum dissectum* (Apiaceae) [92]. An unusual angular dihydrofuranocoumarin, (2*S**,3*R**)-2-[(3*E*)-4,8-dimethylnona-3,7-dien-1-yl]-2,3-dihydro-7-hydroxy-2,3-dimethylfuro[3,2*c*]coumarin (**269**), and its stereoisomer, (2*R**,3*R**)-2-[(3*E*)-4,8-dimethylnona-3,7-dien-1-yl]-2,3-dihydro-7-hydroxy-2,3-dimethylfuro[3,2*c*]coumarin (**270**), were isolated from a chloroform

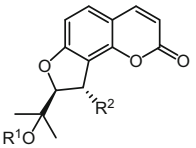

**264** $R^1$ = glucosyl, $R^2$ = H (apterin)
**265** $R^1$ = $R^2$ = H (2′*S*-columbianetin)
**266** $R^1$ = Ac, $R^2$ = H ((2′*S*)-columbianetin acetate)
**267** $R^1$ = glucosyl, $R^2$ = H ((2′*S*)-columbianetin glucoside)
**268** $R^1$ = H, $R^2$ = OMe (3-*O*-methylvaginol)

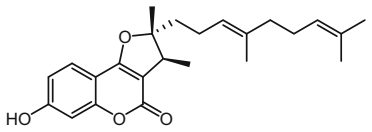

**269** ((2*S**,3*S**)-2-[(3*E*)-4,8-dimethylnona-3,7-dien-1-yl]-2,3-dihydro-7-hydroxy-2,3-dimethylfuro[3,2*c*]coumarin)

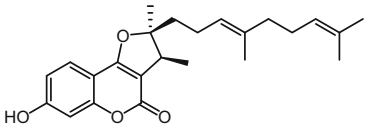

**270** ((2*R**,3*R**)-2-[(3*E*)-4,8-dimethylnona-3,7-dien-1-yl]-2,3-dihydro-7-hydroxy-2,3-dimethylfuro[3,2*c*]coumarin)

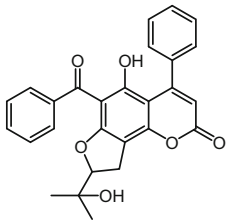

**271** (6-benzoyl-5-hydroxy-4-phenylcolumbianelin)

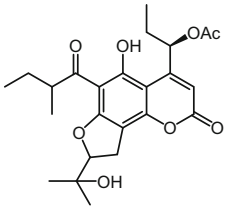

**272** (ochrocarpin F)

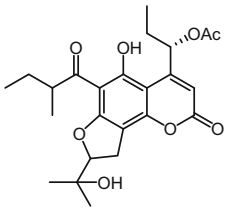

**273** (ochrocarpin G)

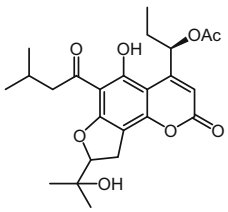

**274** (ochrocarpin H)

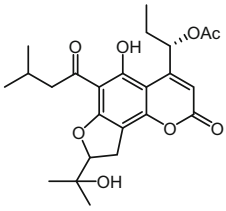

**275** (ochrocarpin I)

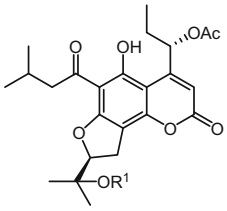

**276** $R^1$ = propanoyl ((2′*S*)-columbianetin-3′-propanoate)
**277** $R^1$ = $SO_3H$ ((2′*S*)-columbianetin-3′-sulfate)
**278** $R^1$ = (2*S*)-methylbutanoate ((2′*S*)-columbianetin-3′-isopentanoate)

**Fig. 30** Angular dihydrofuranocoumarins **264**–**278**

extract of the underground parts of *Ferula heuffelii* (Apiaceae) [107]. Both new compounds can also be classified as sesquiterpenyl coumarins.

Six coumarins of this same category, possessing antioxidant properties, were obtained from the salt marsh plant *Corydalis heterocarpa* [108]; these were (2′*S*)-columbianetin (**265**), (2′*S*)-columbianetin 3′-acetate (**266**), (2′*S*)-columbianetin 3′-glucoside (**267**), (2′*S*)-columbianetin 3′-propanoate (**276**), (2′*S*)-columbianetin

3′-sulfate (**277**), and (2′*S*)-columbianetin 3′-isopentanoate (**278**). The 4-substituted angular dihydrocoumarins, 6-benzoyl-5-hydroxy-4-phenylcolumbianelin (**271**), isopedilanthocoumarin B (**62**), and ochrocarpins F–I (**272**–**275**), were purified from a dichloromethane extract of the bark of *Mammea neurophylla* (Calophyllaceae) [56, 85].

### 2.4.4 Linear Dihydrofuranocoumarins

A number of linear dihydrofuranocoumarins, with most of them are known compounds, were reported recently (Fig. 31). Marmesinin (**290**), a glucoside of marmesin (**289**), was isolated from the aerial parts of *Gerbera piloselloides*

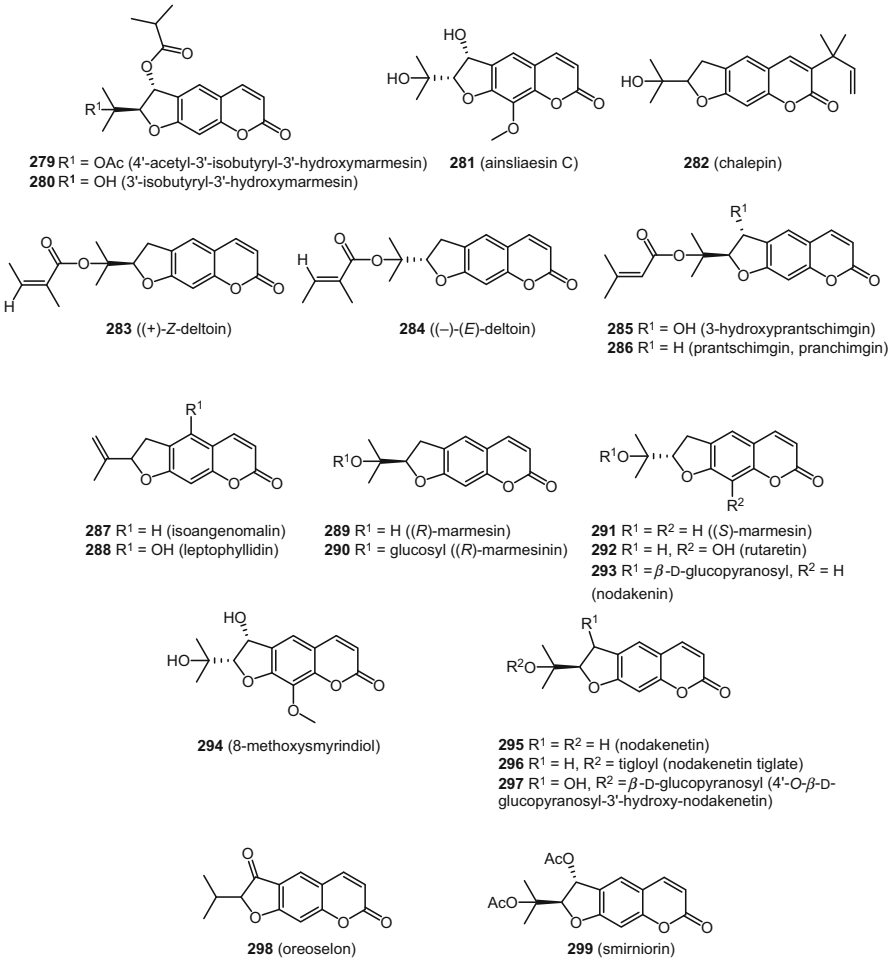


**Fig. 31** Linear dihydrofuranocoumarins **279**–**299**

[10]. Several acylated marmesin derivatives, smirniorin (**299**), 3-hydroxyprantschimgin (**285**), 4′-acetyl-3′-isobutyryl-3′-hydroxymarmesin (**279**), and 3′-isobutyryl-3′-hydroxymarmesin (**280**), with the latter being a new coumarin, were purified from the aerial parts of *Opopanax hispidus* [11]. A 3′-oxo dihydrofuranocoumarin, oreoselon (**298**), was also found in this plant.

While (*S*)-marmesin (**291**) was isolated from the twigs of *Feroniella lucida* (Plate 8) [40] and the flowers of *Ferula lutea* (Apiaceae) [100], (*R*)-marmesin (**289**) was reported from the trunk bark of *Antiaris toxicaria* (Moraceae) [75]. Imperatorin (**212**) was also found in *Ferula lutea* (Apiaceae). Isoangenomalin (**287**), nodakenetin (**295**) and 4′-*O*-*β*-D-glucopyranosyl-3′-hydroxy-nodakenetin (**296**) were identified from *Ficus tsiangii* (Moraceae) [37]. Chalepin (**282**), a 3-prenylated dihydrofuranocoumarin from *Ruta angustifolia* (Rutaceae) (Plate 16), was isolated as a bioactive compound that was found to inhibit hepatitis C virus replication [109]. Nodakenetin (**295**), nodakenetin tiglate (**296**), and rutaretin (**292**) were obtained from a water extract of *Peucedanum praeruptorum* (Apiaceae) [26]. Prantschimgin (**286**) (also known as pranchimgin) was obtained from *Ferulago angulata* (Apiaceae) [101], and this compound is also distributed in other species of the genus *Ferulago*. While isoangenomilin (**287**) and leptophyllidin (**288**) were obtained from the woody stems of *Esenbeckia alata* (Rutaceae) [98], a phytochemical study of the flowers of *Ferula lutea* (Apiaceae) revealed the presence of (+)-(*Z*)-deltoin (**283**) and (–)-(*E*)-deltoin (**284**) [33, 100]. A new linear dihydrofuranocoumarin, 8-methoxysmyrindiol (**294**), was isolated from *Gerbera anandria* (Asteraceae), and was found to possess antibacterial and antitumor properties [94]. Ainsliaeasin C (**281**), a stereoisomer of 8-methoxysmyrindiol (**294**), which is a new natural product, together with (*S*)-marmesin (**291**) and nodakenin (**293**), were reported from the whole plants of *Ainsliaea fragrans* (Asteraceae) [61].

**Plate 16** *Ruta angustifolia* (rue) Torà, 575 m, Segarra-Catalunya, Spain. Photograph courtesy of Isedre Blanc, Creative Commons

## 2.5 *Pyranocoumarins*

Pyranocoumarins possess a pyran (or dihydropyran) ring usually fused with the aromatic ring of the coumarin skeleton, as e.g. in xanthyletin (**322**). These two rings are fused in different ways to produce various angular (e.g. seselin (**312**)) and linear (e.g. xanthyletin (**322**)) pyranocoumarins. The biosynthesis pathway for pyranocoumarins is quite similar to that of furanocoumarins, and starts from a coupling of dimethylallyl pyrophosphate (DMAPP) and umbelliferone (**2**), and proceeds through the formation of a prenylated simple coumarin intermediate (Scheme 3). The only difference is in the ring formation from the prenyl group to a pyran ring, not to a furan (Scheme 2).

Most of the pyranocoumarins reported recently are from the Rutaceae, but plants from other families, such as Apiaceae, Asteraceae, Calophyllaceae, Clusiaceae, Fabaceae, and Malvaceae, were also shown to produce this class of compounds. Like furanocoumarins (including dihydrofuranocoumarins), pyranocoumarins can also be classified into angular and linear pyranocoumarins, and pyranocoumarins recently reported are discussed under these classes below.

### 2.5.1 Angular Pyranocoumarins

Angular pyranocoumarins are generally formed involving either C-5 and C-6 of a coumarin nucleus resulting in the alloxanthoxyletin-type (**300**) angular pyranocoumarins (Fig. 32), or C-7 and C-8 leading to the seselin-type (**312**)

**Scheme 3** Biosynthesis of pyranocoumarins

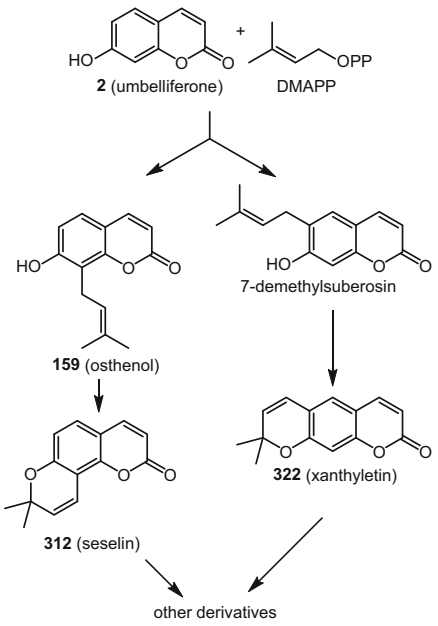

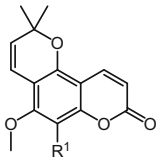

**300** $R^1$ = H (alloxanthoxyletin)
**301** $R^1$ = CHO (8-formylalloxanthoxyletin)

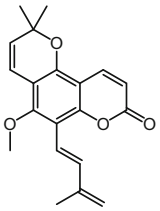

**302** (avicennin)

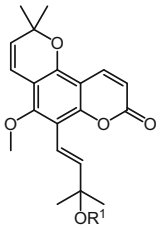

**303** $R^1$ = OH (avicennol)
**304** $R^1$ = OMe (avicennol methyl ether)

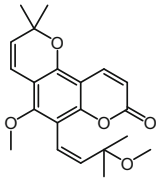

**305** ((*Z*)-avicennol methyl ether)

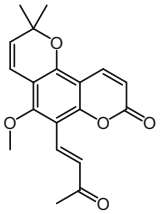

**306** (avicennone)

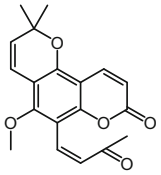

**307** ((*Z*)-avicennone)

**Fig. 32** Angular pyranocoumarins **300–307** involving C-5 and C-6

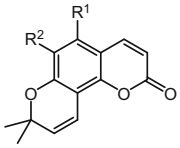

**308** $R^1$ = H, $R^2$ = OMe (braylin)
**309** $R^1$ = H, $R^2$ = 3,3-dimethylallyl (6-(3,3-dimethylallyl)seselin)
**310** $R^1$ = OMe, $R^2$ = H (5-methoxyseselin)
**311** $R^1$ = H, $R^2$ = OH (norbraylin)
**312** $R^1$ = H, $R^2$ = H (seselin)

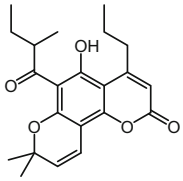

**313** (mammaea B/AB cyclo D)

**Fig. 33** Angular pyranocoumarins **308–313** involving C-7 and C-8

(Fig. 33) pyranocoumarins. In recent years, a good number of angular pyranocoumarins, many of them with prenylations (e.g. avicennol (**303**)), were reported. Avicennin (**302**), a prenylated angular pyranocoumarin, was isolated from the roots and stems of *Zanthoxylum avicennae* (Rutaceae) [110]. Three new coumarins, 8-formylalloxanthoxyletin (**301**), avicennone (**306**), and (*Z*)-avicennone (**307**), as well as alloxanthoxyletin (**300**), avicennin (**302**), avicennol (**303**), avicennol methyl ether (**304**), and (*Z*)-avicennol methyl ether (**305**) were purified from the stem bark of the same plant [20]. Alloxanthoxyletin (**300**) was also procured from the roots of *Hibiscus vitifolius* (Malvaceae) [111].

Braylin (**308**), 5-methoxyseselin (**310**), and norbraylin (**311**) were isolated from a 95% ethanolic extract of the roots of *Toddalia asiatica* (Rutaceae) [43]. 5-Methoxyseselin (**310**), together with 6-(3,3-dimethylallyl)seselin (**309**), was

obtained from the leaves of *Murraya alata* (Rutaceae) [17]. While a 3-substituted angular pyranocoumarin, called mammaea B/AB cyclo D (**313**), was found in the stem bark of *Mammea usambarensis* (Clusiaceae) [84], the simplest compounds of this class, seselin (**312**) and 5-methoxyseselin (**310**), were identified from *Hortia superba* (Rutaceae) [104, 105].

The 3-phenyl-substituted angular pyranocoumarins, 11,12-anhydroionophyllum A (**314**), calophyllolide (**315**), inophyllum A (**316**), inophyllum C (**317**), and inophyllum E (**318**), were isolated from the fruits of *Calophyllum inophyllum* (Calophyllaceae) (Plate 17) [112] (Fig. 34).

**Plate 17** *Calophyllum inophyllum* (Alexandrian laurel), Maui Nui Botanical Garden. Photograph courtesy of Forest & Kim Starr, Creative Commons

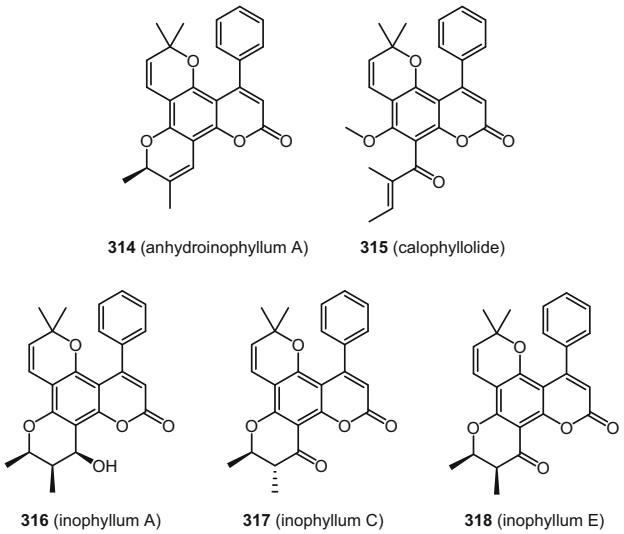


**314** (anhydroinophyllum A) **315** (calophyllolide)

**316** (inophyllum A) **317** (inophyllum C) **318** (inophyllum E)

**Fig. 34** 3-Phenyl substituted angular pyranocoumarins **314–318**

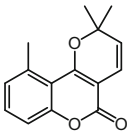

**319** (bothrioclinin)

**Fig. 35** An unusual angular pyranocoumarin **319** involving C-3 and C-4

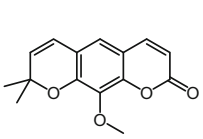

**320** (luvangetin)

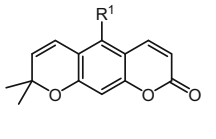

**321** $R^1$ = OMe (xanthoxyletin)
**322** $R^1$ = H (xanthyletin)

**Fig. 36** Linear pyranocoumarins **320**–**322**

An unusual angular pyranocoumarin (Fig. 35), bothrioclinin (**319**), where the pyran ring formation involves oxygenation at C-4 and prenylation at C-3 of the coumarin nucleus, was reported from the whole plant of *Ainsliaea fragrans* (Asteraceae) [61]. This compound is also unusual in the sense that, unlike most other plant-derived coumarins, it does not have any oxygenation at C-7.

### 2.5.2 Linear Pyranocoumarins

The roots and stems of *Zanthoxylum avicennae* (Rutaceae) afforded a well-known linear pyranocoumarin (Fig. 36), xanthoxyletin (**321**), as well as its isomer, luvangetin (**320**) [20, 111], with the latter also isolated from the stem bark of *Zanthoxylum ailanthoides* by centrifugal partition chromatography [113]. Xanthoxyletin (**321**) and xanthyletin (**322**) were found in *Hibiscus vitifolius* (Malvaceae) [107]. An acetone extract of the roots of *Clausena guillauminii* (Rutaceae) produced **321** [80], which was also purified from *Ficus tsiangii* (Moraceae) [37].

### 2.5.3 Angular Dihydropyranocoumarins

Angular dihydropyranocoumarins, formed involving C-7 and C-8 of the coumarin nucleus (Figs. 37 and 38), are the major group of pyranocoumarins reported recently. Most of these have further substitutions, predominantly prenylations. Many of them are (–)-(*Z*)-khellactone (**340**) derivatives. A new angular dihydropyranocoumarin glycoside, anticarin B (**324**), was reported from the trunk bark of *Antiaris toxicaria* (Moraceae) [75]. 3′,4′-Dihydrobraylin (**325**) and 5-methoxydihydroseselin (**326**) were isolated from a 95% ethanolic extract of the roots of *Toddalia asiatica* (Rutaceae) [43].

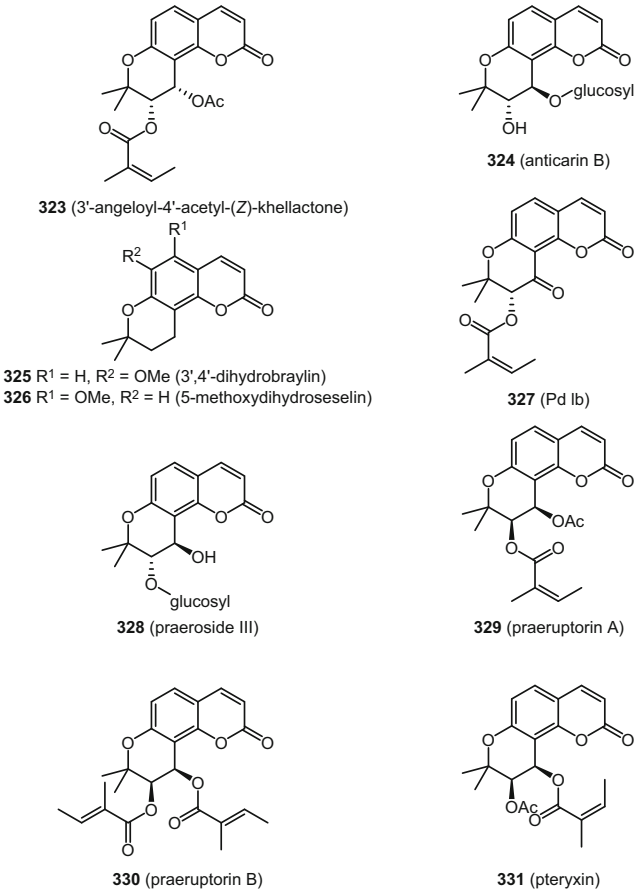


**323** (3'-angeloyl-4'-acetyl-(*Z*)-khellactone)

**324** (anticarin B)

**325** $R^1$ = H, $R^2$ = OMe (3',4'-dihydrobraylin)
**326** $R^1$ = OMe, $R^2$ = H (5-methoxydihydroseselin)

**327** (Pd Ib)

**328** (praeroside III)

**329** (praeruptorin A)

**330** (praeruptorin B)

**331** (pteryxin)

**Fig. 37** Angular dihydropyranocoumarins **323–331**

Praeruptorins A (**329**) and B (**330**) were detected in the wood bark of *Peucedanum praeruptorum* (Apiaceae), commonly known as Peucedani Radix (Chinese: "Qian-hu") [114]. Additional prenylation is present in both compounds. Another plant from the same genus, *P. japonicum,* afforded an angular dihydropyranocoumarin with potential antiobesity activity, called pteryxin (**331**) [115]. A stereoisomer of praeruptorin A (**329**), namely, 3′-angeloyl-4′-acetyl-(*Z*)-khellactone (**323**), was purified from an ethanolic extract of the root bark of *Oplopanax horridus* (Araliaceae) [28]. Corymbocoumarin (**334**), (–)-(*Z*)-khellactone (**340**), *d*-laserpitin (**341**), praeroside III (**328**), Pd-lb (**327**), praeruptorins A (**329**), B (**330**), praeruptorin E (**342**), and qiamhucoumarin (**333**) were obtained from an aqueous extract of *Peucedanum praeruptorum* (Apiaceae) [30].

Six angular dihydropyranocoumarins were isolated from the aerial parts of *Glehnia littoralis* (Apiaceae) (Plate 18) and shown to inhibit lipopolysaccharide-induced nitric oxide (NO) production in RAW 264.7 macrophage cells [116].

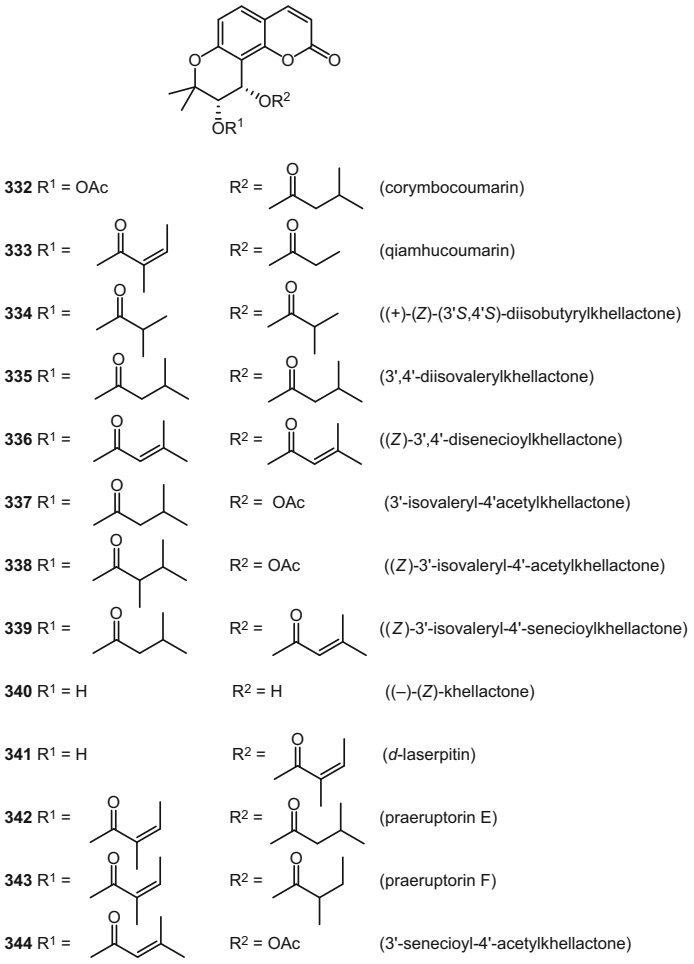


**Fig. 38** Angular dihydropyranocoumarins **332**–**344**

(+)-(*Z*)-(3′*S*,4′*S*)-Diisobutyrylkhellactone (**334**) was identified as a new natural product, and 3′-senecioyl-4′-acetylkhellactone (**344**), 3′-isovaleryl-4′-acetylkhellactone (**337**), 3′,4′-disenecioylkhellactone (**336**), 3′-isovaleryl-4′-senecioylkhellactone (**339**), and 3′,4′-diisovalerylkhellactone (**335**) are known angular dihydropyranocoumarins. (*Z*)-3′,4′-disenecioylkhellactone (**336**) (*Z*)-3′-isovaleryl-4′-acetylkellactone (**338**), (*Z*)-3′-isovaleryl-4′-senecioylkhellactone (**339**), (–)-(*Z*)-khellactone (**340**), and praeruptorins B (**330**) and F (**343**) were purified from a methanolic extract of the roots of *Saposhnikovia divaricata* (Apiaceae) [19] (Fig. 38).

**Plate 18** *Glehnia littoralis* (American silvertop), Syonai area, Japan. Photograph courtesy of Qwert1234, Creative Commons

### 2.5.4 Linear Dihydropyranocoumarins

Only a few linear dihydropyranocoumarins were reported recently (Fig. 39). Licopyranocoumarin (**351**) was isolated from an herbal medicine composed mainly of *Glycyrrhiza* species (Fabaceae) as a potential neuroprotective agent for the treatment of Parkinson's disease [70].

Dihydrozanthyletin (**347**) was purified from *Ficus tsiangii* (Moraceae) [37], and (–)-decursinol (**345**) was found in the fruits of *Micromelum minutum* (Rutaceae) [42] as well as in a methanolic extract of the roots of *Saposhnikovia divaricata* (Apiaceae) [19]. An angeloyl derivative of decursinol (**345**), decursinol angelate (**346**), was isolated from a water extract of *Peucedanum praeruptorum* (Apiaceae) [30]. A new linear dihydropyranocoumarin, (−)-hydroxydecursinol (**349**), together with (+)-decursinol (**348**), was reported from the roots of *Angelica dahurica* var. *formosana* cv. Chuanbaizhi [97].

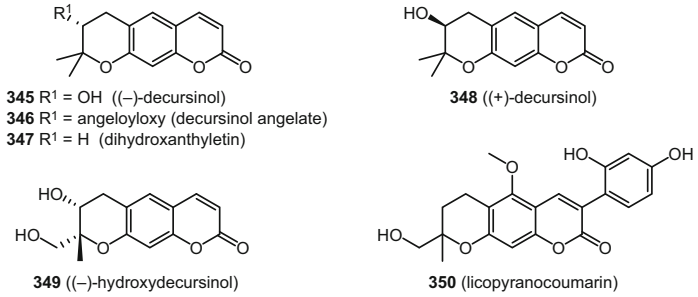


**Fig. 39** Linear dihydropyranocoumarins **345**–**350**

## 2.6 *Sesquiterpenyl Coumarins*

Sesquiterpenyl coumarins are formed via conjugation between a farnesyl (or substituted farnesyl) unit or a sesquiterpene unit and a coumarin nucleus. The conjugation can be either through C or O. In recent years, several sesquiterpenyl coumarins were reported, including some new natural products (Figs. 40, 41, 42, 43 and 44). All of these compounds have been obtained exclusively from species in the Apiaceae. Umbelliprenin (**351**) (Fig. 40) is the simplest member of this group of compounds, where a farnesyl moiety is linked through an oxygen bridge involving C-7 of the coumarin nucleus. These sesquiterpenyl coumarins, almost exclusively, have been reported from various species of the genus *Ferula* of the family Apiaceae.

The sesquiterpene coumarins, badrakemin acetate (**352**), kellerin (**357**), and a samarkandin diastereomer (**380**), were isolated from the gum resin of *Ferula assa-foetida* (Apiaceae) (Plate 19), employed as an herbal medicine used traditionally for the treatment of microbial, protozoal and viral infections [117]. A phytochemical investigation of a dichloromethane extract of the fruits of *Ferula gummosa* afforded three drimane-sesquiterpene coumarins, conferone (**355**), feselol (**368**), and mogoltacin (**378**), which were shown to enhance doxorubicin uptake by a

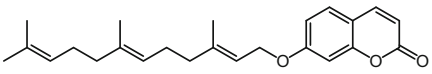

**351** (umbelliprenin)

**Fig. 40** Umbelliprenin (**351**), the simplest member of the sesquiterpenyl coumarins

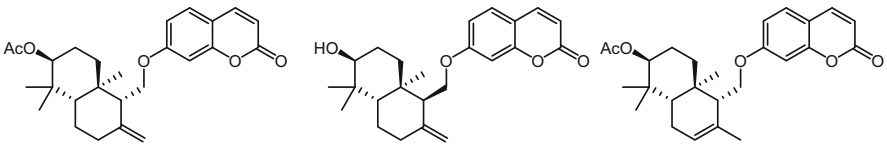


**352** (badrakemin acetate) **353** (colladonin) **354** (conferol)

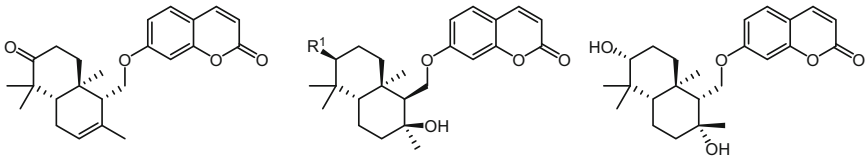


**355** (conferone) **356** $R^1$ = OH (deacetylkellerin) **358** (episamarcandin)
**357** $R^1$ = OAc (kellerin)

**Fig. 41** Sesquiterpenyl coumarins **352–358**

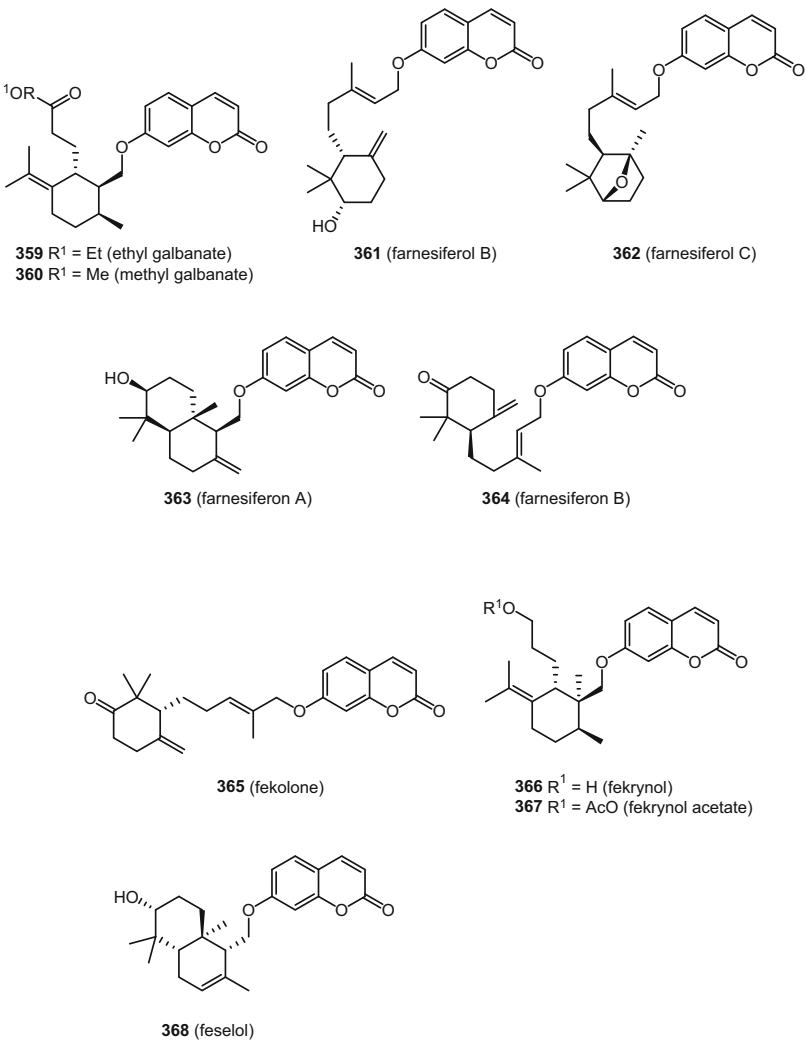


**Fig. 42** Sesquiterpenyl coumarins **359**–**368**

doxorubicin-resistant human breast cancer cell line (MCF-7/Dox) [118]. The new sesquiterpene coumarins, fnarthexone (**371**) and fnarthexol (**370**), along with conferol (**355**), conferone (**356**), and **2**, were isolated from *Ferula narthex* (Apiaceae) [26].

Samarkandin acetate (**379**) was found in the underground parts of *Ferula heuffelii* [107]. In a search for acetylcholinesterase inhibitors, in addition to **2** and a few geranylated coumarins, the sesquiterpenyl coumarins deacetylkellerin (**356**), farnesiferol B (**361**), farnesiferol C (**362**), and kellerin (**357**), were purified from the oleogum resin of *Ferula gummosa* [88, 130]. A new sesquiterpene coumarin with a

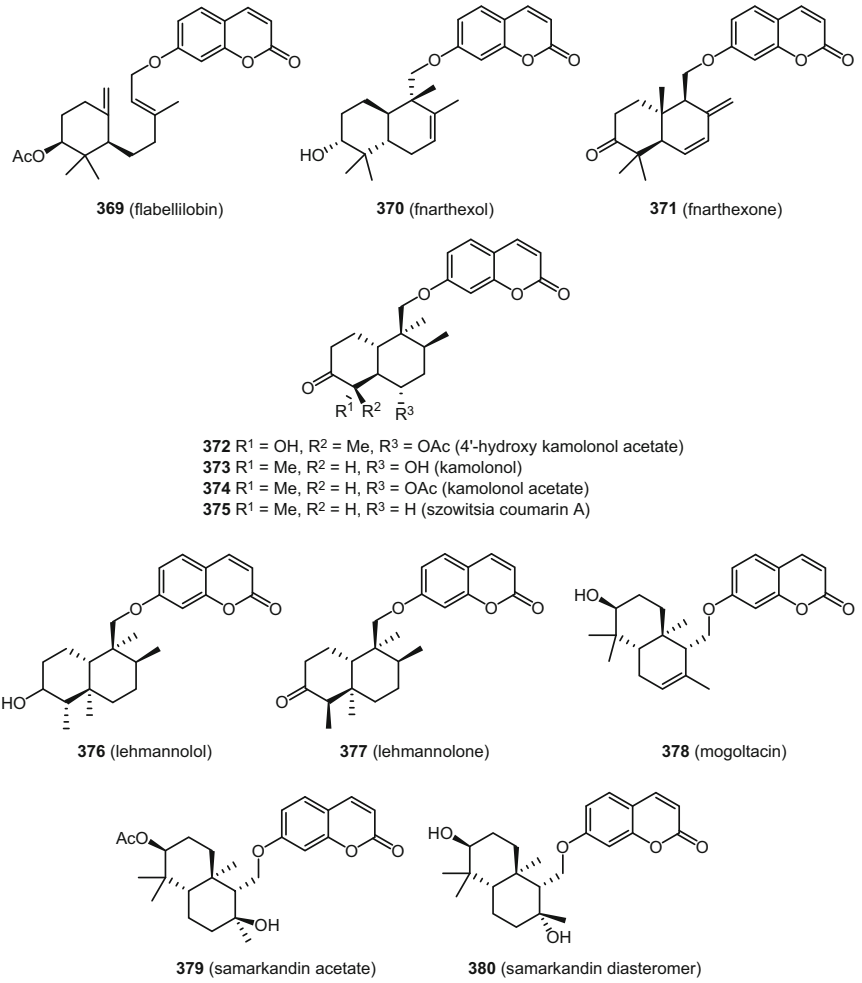


**369** (flabellilobin)
**370** (fnarthexol)
**371** (fnarthexone)

**372** $R^1$ = OH, $R^2$ = Me, $R^3$ = OAc (4'-hydroxy kamolonol acetate)
**373** $R^1$ = Me, $R^2$ = H, $R^3$ = OH (kamolonol)
**374** $R^1$ = Me, $R^2$ = H, $R^3$ = OAc (kamolonol acetate)
**375** $R^1$ = Me, $R^2$ = H, $R^3$ = H (szowitsia coumarin A)

**376** (lehmannolol)
**377** (lehmannolone)
**378** (mogoltacin)
**379** (samarkandin acetate)
**380** (samarkandin diasteromer)

**Fig. 43** Sesquiterpenyl coumarins **369–380**

novel sesquiterpene carbon framework, sinkiangenorin D (**382**), and lehmannolol (**376**), lehmannolone (**377**), episamarcandin (**358**), colladonin (**353**), sinkianone (**383**), fekrynol (**366**), fekolone (**365**), feselol (**368**), and the simple farnesyloxycoumarin, umbelliprenin (**351**), were reported from the seeds of *Ferula sinkiangensis* (Apiaceae) [119]. Their cytotoxic activity for a small panel of cancer cells was also investigated.

The first ever reported disesquiterpenyl coumarin, sanandajin (**381**), together with methyl galbanate (**360**), ethyl galbanate (**359**), fekrynol acetate (**367**), farnesiferol B (**361**), and kamonolol (**373**), was isolated from the roots of *Ferula pseudalliacea* [120, 121].

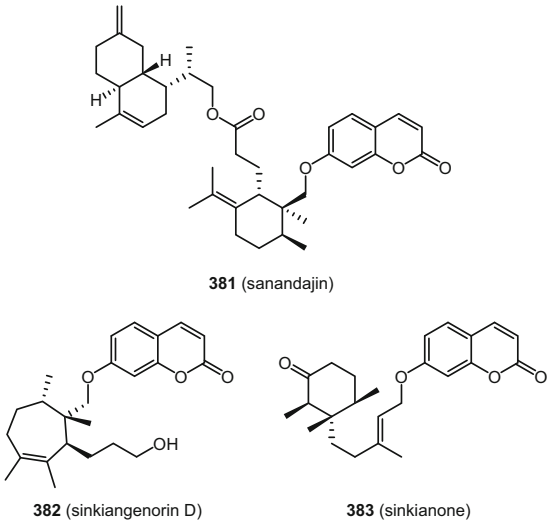


**381** (sanandajin)

**382** (sinkiangenorin D)

**383** (sinkianone)

**Fig. 44** Sesquiterpenyl coumarins **381**–**383**

**Plate 19** *Ferula assa-foetida* (asant), Ayaz Kala, Kyzyl Kum desert, Uzbekistan. Photograph courtesy of V. Fassiaux, Public Domain

All of these coumarins showed considerable phyto- and cytotoxicity. The same research group also reported further sesquiterpene coumarins (Fig. 43) from the roots of the same plant, namely, 4′-hydroxy-kamolonol acetate (**372**), kamolonol (**373**), szowitsia-coumarin A (**375**), farnesiferon B (**364**), farnesiferol C (**362**), and flabellilobin A (**369**). 4′-Hydroxy-kamolonol acetate (**372**) was considered as a new natural product [120, 121].

## 2.7 *Oligomeric Coumarins*

Oligomeric coumarins (Figs. 45, 46, 47, 48, 49 and 50), predominantly coumarin dimers, have been appearing more and more in the literature in recent years,

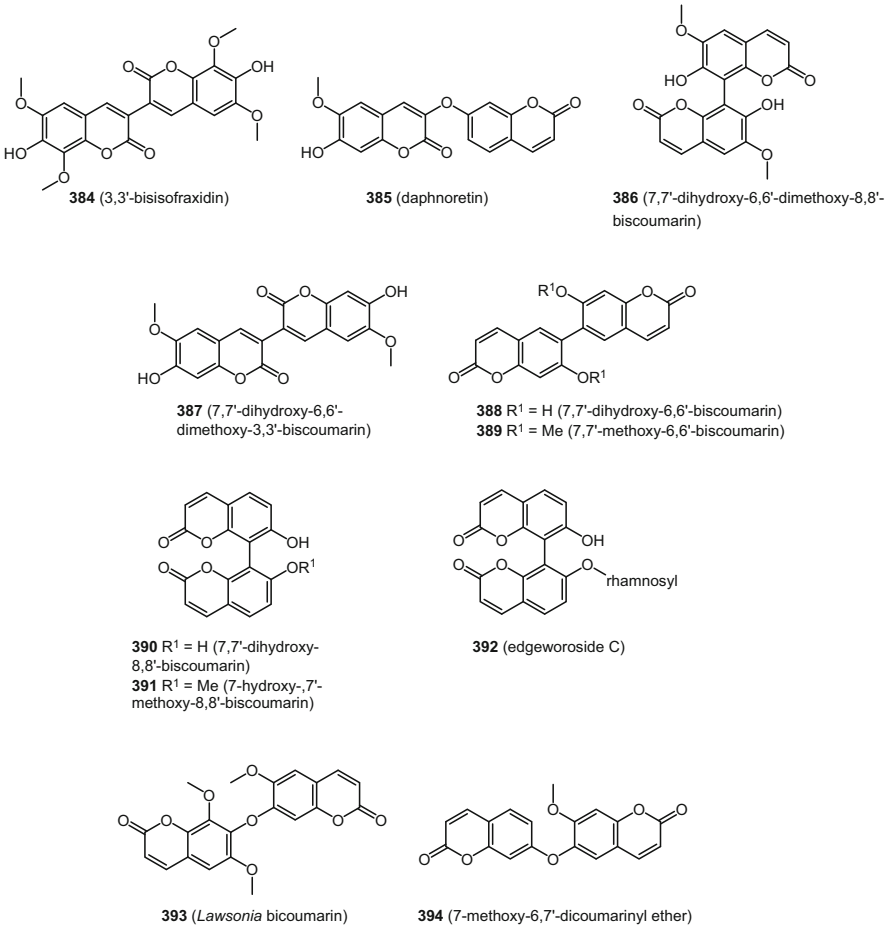


**Fig. 45** Dimeric coumarins **384–394**

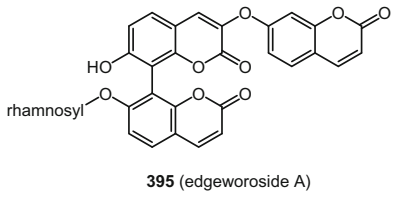


**Fig. 46** The coumarin trimer edgeworoside A (**395**)

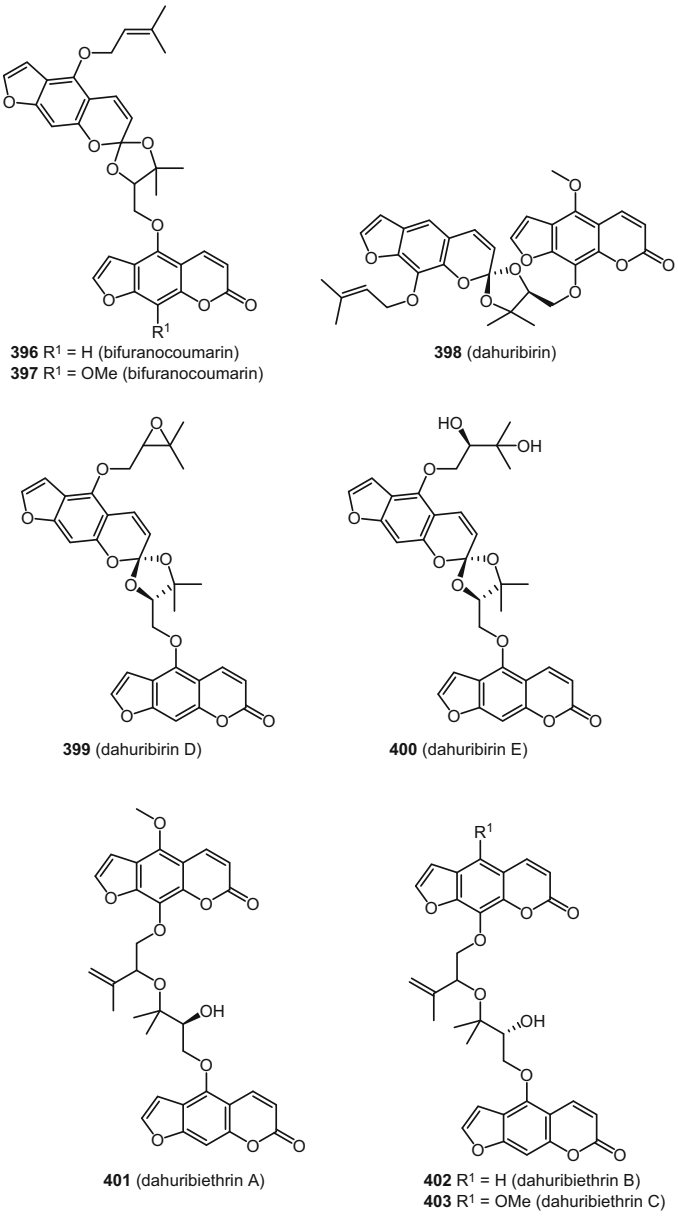


**Fig. 47** Dimeric coumarins **396**–**403** with a spacer group

probably because of significant advances in separation and identification techniques, which have made it much easier to isolate and characterize structurally such compounds with greater confidence. Most of these oligomers are predominantly from plants in the Apiaceae and the Thymelaeaceae, and a few from species

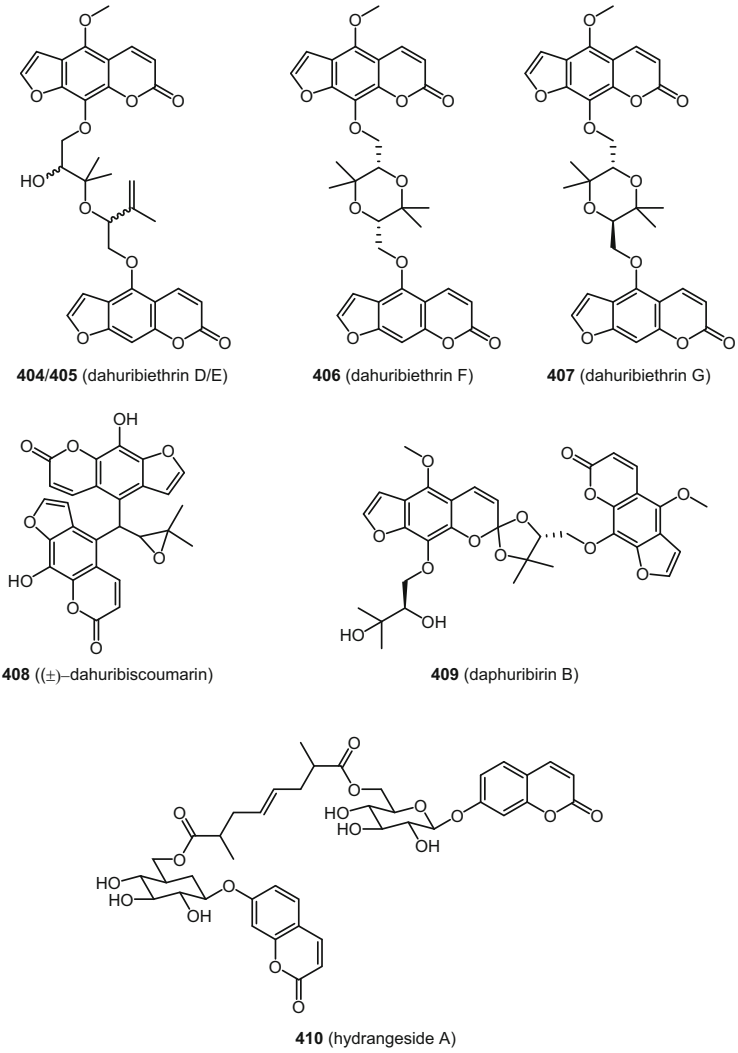


**Fig. 48** Dimeric coumarins **404**–**410** with a spacer group

in the other families, Asteraceae, Guttiferae, Lythraceae, Rubiaceae, Rutaceae, and Saxifragaceae. Many of the recently reported oligomeric coumarins are new natural products.

A dimeric coumarin, 3,3′-bisisofraxidin (**384**), was purified from a Tibetan traditional medicine based on *Carduus acanthoides* (Asteraceae) (Fig. 45) [9]. Ghanem et al. [122] isolated daphnoretin (**385**), a 3,7′-dimer through an ether linkage, from the aerial parts of *Thymelaea microphylla* (Thymelaeaceae);

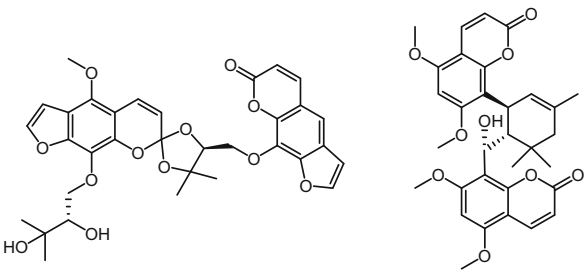


**411** (rivulobrin D) **412** (toddalosin)

**Fig. 49** Dimeric coumarins **411**–**412** with a spacer group

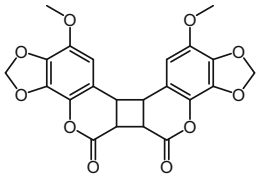

**413** (bis-dracunculin)

**Fig. 50** Bis-dracunculin (**413**)

compound **385**, together with a rhamnoside of a 8,8′-coumarin dimer, edgeworoside C (**392**), was also obtained from *Edgeworthia chrysantha* (Thymelaeaceae) [23].

Rajachan et al. [25] isolated daphnoretin (**387**) from the roots of *Enkleia siamensis* of the same family. 7,7′-Dihydroxy-6,6′-dimethoxy-8,8′-biscoumarin (**386**) and 7,7′-dihydroxy-6,6′-dimethoxy-3,3′-biscoumarin (**387**) were obtained from the stem bark of *Pauridiantha callicarpoides* (Rubiaceae) [24]. 7,7′-Dihydroxy-6,6′-biscoumarin (**388**), 7,7′-dihydroxy-8,8′-biscoumarin (**390**), 7,7′-dimethoxy-6,6′-biscoumarin (**389**), and 7-methoxy-6,7′-dicoumarinyl ether (**394**) were isolated from a methanolic extract of the stem bark of *Hypericum riparium* (Guttiferae) [58]. 7-Hydroxy-7-′-methoxy-8,8′-biscoumarin (**391**) was found in *Thymelaea microphylla* (Thymelaeaceae) [23, 123]. A new bicoumarin, *Lawsonia* bicoumarin A (**393**), was identified from a dichloromethane extract of the flowers of *Lawsonia inermis* (Lythraceae), through repeated column chromatography on silica gel, as well as reversed-phase semi-preparative HPLC [122]. A trimeric coumarin glycoside, edgeworoside A (**395**), was identified as a constituent of the flower buds of *Edgeworthia chrysantha* (Fig. 46) [23].

The formation of coumarin dimers through spacer groups, normally a prenyl or a terpenyl group, has added to interest in coumarin chemistry. A new biscoumarin, (±)-dahuribiscoumarin (**408**), formed through dimerization between two linear furanocoumarins units, involving a prenyl derived spacer group, was purified from the roots of *Angelica dahurica* var. *formosana* cv. Chianbaixhi (Apiaceae) [97]. A method using off-line two-dimensional HPLC coupled with electrospray

tandem mass spectrometry afforded two new bifuranocoumarins **396** and **397** (Fig. 47), as well as dahuribirin A (**398**), dahuribirin D (**399**), dahuribirin E (**400**), daphuribirin B (**409**), and rivulobirin D (**411**) (Fig. 48), in the roots of *Angelica dahurica* (Apiaceae) [34, 131].

All of these dimers have a spacer group formed from their prenyl side chains. The new furanocoumarin dimers, dahuribiethrins A–G (**401**–**407**), formed through prenyl spacers, were reported from the roots of *Angelica dahurica* (Apiaceae) [125], and all of these coumarins possess anti-inflammatory properties as demonstrated in an assay using the murine RAW 264.7 macrophage cell line.

Toddalosin (**412**) (Fig. 49) was isolated from an ethanolic extract of the roots of *Toddalia asiatica* (Rutaceae) [43]. It is a dimer formed through a monoterpenyl spacer group. A dimeric simple coumarin, hydrangeside A (**410**), with an extensive spacer group, possessing hepatoprotective properties, was purified from the stems of *Hydrangea paniculata* (Saxifragaceae) [45].

An unusual simple coumarin dimer, bis-dracunculin (Fig. 50) (**413**), was purified from an ethanolic extract of the aerial parts of *Artemisia elegantissima* (Asteraceae) [48]. Two dracunculin (**47**) units form *bis*-dracunculin (**413**), a symmetrical dimer, through dimerization involving 3,3′ and 4,4′ carbons, leading to a cyclobutane ring system.

## *2.8 Miscellaneous Coumarins*

Approximately a dozen unusual coumarin derivatives, which may not be placed under any of the above classifications, have also been reported recently (Fig. 51). Two anti-inflammatory coumarinolignans of previously known structure, cleomiscosin A (**414**) and cleomiscosin E (**415**), were isolated from the seeds of *Brucea javanica* (Simaroubaceae) [126]. Compounds **414** and **415** might, however, also be regarded as simple coumarins. Cleomiscosin A (**414**) was also found in the stem bark of *Pentas schimperi* (Rubiaceae) [127]. A new coumarinolignan (**416**), a unique coumarin-lignan adduct that possesses anti-HBV activity against HBeAg and HBsAg, and moderate antifibrotic and neuroprotective properties, was reported from the stems of *Kadsura heteroclita* (Schisandraceae) [128]. An unusual coumarin, 10-methoxy-7-methyl-2*H*-benzo[*g*]chromen-2-one (**423**), was purified from the aerial parts of *Murraya tetramera* (Rutaceae) and shown to possess cytotoxicity against a small panel of cancer cell lines [44].

Two new rather rare coumarins, muralatins A (**424**) and B (**425**), were isolated from the leaves of another species of the same genus, *Murraya alata* (Rutaceae) [17]. Muralatin A (**424**) is an angular version of 10-methoxy-7-methyl-2*H*-benzo[*g*] chromen-2-one (**423**). Two new unusual coumarins, herpetosperins A (**421**) and B (**422**), and a known analog, herpetolide A (**421**), were found in the seeds of *Herpetospermum caudigerum* (Cucurbitaceae) [129]. A new isocoumarin, ethyl

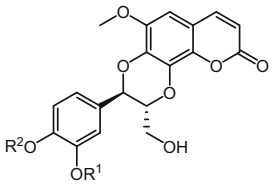

**414** $R^1$ = Me, $R^2$ = H (cleomiscosin A)
**415** $R^1$ = H, $R^2$ = Me (cleomiscosin E)

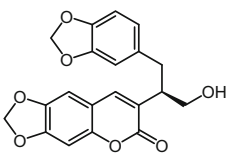

**416** (new coumarinolagnan)

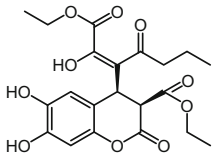

**417** (ethyl (*E*)-3-((3*S*,4*S*)-3-butyryl-6,7-dihydroxy-2-oxochroman-4-yl)-2-hydroxy-4-oxohept-2-enoate)

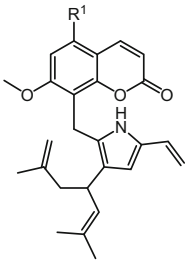

**418** $R^1$ = H (exotine A)
**419** $R^1$ = OMe (exotine B)

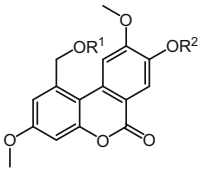

**420** $R^1$ = $R^2$ = H (herpetolide A)
**421** $R^1$ = H, $R^2$ = $\beta$-D-glucopyranosyl (herpetosperim A)
**422** $R^1$ = $\beta$-D-glucopyranosyl , $R^2$ = H (herpetosperim B)

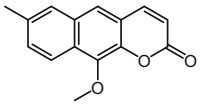

**423** (10-methoxy-7-methyl-2*H*-benzo[*g*]chromen-2-one)

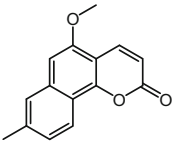

**424** (muralatin A)

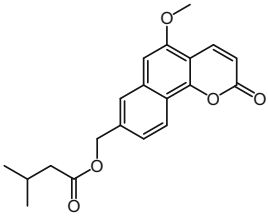

**425** (muralatin B)

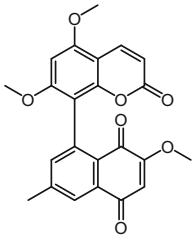

**426** (toddacoumaquinone)

**Fig. 51** Miscellaneous coumarins **414**–**426**

(*E*)-3-((3*S*,4*S*)-3-butyryl-6,7-dihydroxy-2-oxochroman-4-yl)-2-hydroxy-4-oxohept-2-enoate (**417**), was obtained from the whole plants of *Euphorbia wallichii* (Euphorbiaceae) (Plate 20) [130]. The occurrence of coumarins or isocoumarins in the genus *Euphorbia* is rare, and is limited to a few species, e.g., *E. lunulata, E. quinquecostata, E. lagascae*, and *E. portlandica.*

Exotines A (**418**) and B (**419**), two isopentenyl-substituted indole-coumarin adducts, where the indolyl moiety is linked to C-8 of the coumarin nucleus, were isolated from the roots of *Murraya exotica* (Rutaceae) [131]. Toddacoumaquinone (**426**) is a coumarin-quinone adduct formed via a C–C link directly between a coumarin and a quinone, and was isolated from the roots of *Toddalia asiatica* [43].

**Plate 20** *Euphorbia wallichii* (Wallich spurge), Real Jardín Botánico, Madrid, Spain. Photograph courtesy of A. Barra, Creative Commons

## 3 Conclusions

Well over 400 coumarin isolations were reported in the years 2014 and 2015, with many of these being re-isolations of previously known compounds from new or known sources, most often associated with some type of biological activity. However, an appreciable number of compounds based on new coumarin skeletons, especially various coumarin dimers, prenylated furanocoumarins, sesquiterpenyl coumarins, and some unusual coumarins, were reported during this period. Coumarin chemistry is still one of the major interest areas for phytochemists, especially because of their quite versatile bioactivities and potential medicinal properties, as exemplified by substances showing analgesic, anticoagulant, anti-HIV, anti-inflammatory, antimicrobial, antioxidant, cytotoxic, and immune-modulation effects. Coumarins as a group remain of strong interest because of their interesting structural diversity. While there have been significant advancements recently in the extraction, isolation, structure elucidation, and bioactivity testing of naturally occurring coumarins, only a marginal advancement is an apparent in relation to the study of their biosynthesis.

## References


1. Murray RDH (1978) Naturally occurring plant coumarins. Prog Chem Org Nat Prod 35:199
2. Murray RDH (1991) Naturally occurring plant coumarins. Prog Chem Org Nat Prod 59:1
3. Murray RDH (1997) Naturally occurring plant coumarins. Prog Chem Org Nat Prod 72:121
4. Murray RDH (2002) Naturally occurring coumarins. Prog Chem Org Nat Prod 83:1
5. Sarker SD, Nahar L (2007) Chemistry for pharmacy students: general, organic and natural product chemistry. Wiley, London
6. Olennikov SN, Kashchenko NI (2014) Componential profile and amylase inhibiting activity of phenolic compounds from *Calendula officinalis* L. leaves. Scientific World J 2014:1
7. Li Y-Y, Di E, Baibado JT, Cheng Y-S, Huang Y-Q, Sun H, Cheung H-Y (2014) Identification of kukoamines as the novel markers for quality assessment of Lycii Cortex. Food Res Int 55:373
8. Iyer D, Patil UK (2014) Evaluation of antihyperlipidemic and antitumor activities of isolated coumarins from *Salvadora indica*. Pharm Biol 52:78
9. Li R, Liu S-K, Song W, Wang Y, Li Y-J, Qiao X, Liang H, Ye M (2014) Chemical analysis of the Tibetan herbal medicine *Carduus acanthoides* by UPLC/DAD/qTOF-MS and simultaneous determination of nine major compounds. Anal Methods 6:7161
10. Wang J, Petrova V, S-B W, Zhu M, Kennelly EJ, Long C (2014) Antioxidants from *Gerbera piloselloides*: an ethnomedicinal plant from southwestern China. Nat Prod Res 28:2072
11. Ghasemi S, Habibi Z (2014) A new dihydrofuranocoumarin from *Opopanax hispidus* (Friv.) Griseb. Nat Prod Res 21:1808
12. Shah MR, Shamim A, White LS, Bertino MF, Mes MA, Soomo S (2014) The anti-inflammatory properties of Au-scopoletin nanoconjugates. New J Chem 38:5566
13. Yin HL, Li JH, Li B, Chen L, Li J, Tian Y, Liu SJ, Zhao YK, Xiao YH, Dong JX (2015) Two new coumarins from the seeds of *Solanum indicum*. J Asian Nat Prod Res 16:153
14. Phakhodee W, Pattarawarapan M, Pongpam P, Laphookhieo S (2014) Naturally occurring prenylated coumarins from *Micromelum integerrimum* twigs. Phytochem Lett 7:165
15. Yan ZW, Liu JP, Lu D, Narlawar R, Groundwater P, Li PY (2014) Two new ceramides from the fruit pulp of *Acanthopanax senticosus* (Rupr. et Maxim.) Harms. Nat Prod Res 28:144
16. Kasaian J, Iranshahy M, Masullo M, Poacente S, Ebrahimi F, Iranshahi M (2014) Sesquiterpene lactones from *Ferula oopoda* and their cytotoxic properties. J Asian Nat Prod Res 16:248
17. Lv H-N, Wang S, Zeng K-W, Li J, Guo X-Y, Ferreira D, Zjawiony JK, Tu P-F, Jiang Y (2015) Anti-inflammatory coumarin and benzocoumarin derivatives from *Murraya alata*. J Nat Prod 78:279
18. Luo J, Zhou W, Cao S, Zhu H, Zhang C, Jin M, Li G (2015) Chemical constituents of *Chroogomphus rutilus* (Schaeff.) O.K. Mill. Biochem Syst Ecol 61:203
19. Yang J-L, Dhodary B, Ha TKQ, Kim J, Kim E, Oh WK (2015) Three new coumarins from *Saposhnikovia divaricata* and their porcine epidemic diarrhea virus (PEDV) inhibitory activity. Tetrahedron 71:4651
20. Chen J-J, Yang C-K, Kuo Y-H, Hwang T-L, Kuo W-L, Lim Y-P, Sung P-J, Chang T-H, Cheng M-J (2015) New coumarin derivatives and other constituents from the stem bark of *Zanthoxylum avicennae*: effects on neutrophil pro-inflammatory responses. Int J Mol Sci 16:9719
21. Bousetla A, Zellagui A, Derouiche K, Rhouati S (2015) Chemical constituents of the roots of Algerian *Bunium incrassatum* and evaluation of its antimicrobial activity. Arabian J Chem 8:313
22. Happi GM, Kouam SF, Yalontsi FM, Zuhlke S, Lamshoft M, Spiteller M (2015) Minor secondary metabolites from the bark of *Entandrophragma congoense* (Meliaceae). Fitoterapia 102:35
23. Li X-N, Tong S-Q, Cheng D-P, Li Q-Y, Yan J-Z (2014) Coumarins from *Edgeworthia chrysantha*. Molecules 19:2042

24. Tatuedom OK, Kouam SF, Yapna DB, Ngadjui BT, Green IR, Choudhary MI, Lantovololona JER, Spiteller M (2014) Spiroalkaloids and coumarins from the stem bark of *Pauridiantha callicarpoides*. Z Naturforsch B 69:747
25. Rajachan OA, Kanokmedhakul S, Nasomjai P, Kanokmedhakul K (2014) Chemical constituents and biological activities from roots of *Enkleia siamensis*. Nat Prod Res 28:268
26. Bashir S, Alam M, Adhikari A, Shrestha RL, Yousuf S, Ahmad B, Parveen S, Aman A, Choudhary MI (2014) New antileishmanial sesquiterpene coumarins from *Ferula narthex* Boiss. Phytochem Lett 9:46
27. Shakeel-ur-Rahman FS, Dangroo NA, Priya D, Banday JA, Sangwan PL, Qurishi MA, Koul S, Saxena AK (2014) Isolation, cytotoxicity evaluation and HPLC-quantification of the chemical constituents from *Prangos pabularia*. PLoS One 9:e108703
28. Huang W-H, Luo W, Wang C-Z, Yuan C-S, Nie M-K, Shi S-Y, Zhou H-H, Ouyang D-S (2014) Phenolic constituents from *Oplopanax horridus*. China J Chin Mat Med 39:1852
29. Kang YF, Liu CM, Kao CL, Chen CY (2014) Antioxidant and anticancer constituents from the leaves of *Liriodendron tulipifera*. Molecules 19:4234
30. Liu JL, Wang XY, Zhang LL, Fang MJ, YL W, Wu Z, Qiu YK (2014) Two-dimensional countercurrent chromatography x high performance liquid chromatography with heart-cutting and stop-and-go techniques for preparative isolation of coumarin derivatives from *Peucedanum praeruptorum* Dunn. J Chromatogr A 1374:156
31. Silva FL, Moreno PRH, Braz R, Tavares JF, Barbosa JM (2014) Chemical constituents of *Cardiospermum corindum* and their distribution in Sapindaceae. Biochem Syst Ecol 57:137
32. Wang ZY, He WJ, Zhou WB, Zeng GZ, Yin ZQ, Zhao SX, Tan NH (2014) Two phenylpropanoids from *Micromelum integerrimum*. Chin J Nat Med 12:619
33. Znati M, Ben Jannet H, Cazaux S, Bouajila J (2014) Chemical composition, biological activities of plant extracts and compounds isolated from *Ferula lutea*. Molecules 19:2733
34. Li B, Zhang X, Wang J, Zhang L, Gao BW, Shi SP, Wang XH, Li J, Tu PH (2014) Simultaneous characterisation of fifty coumarins from the roots of *Angelica dahurica* by off-line two dimensional high-performance liquid chromatography coupled with electrospray ionisation tandem mass spectrometry. Phytochem Anal 25:229
35. Chen SQ, Wang LL, Zhang WQ, Wei YL (2015) Secondary metabolites from the root of *Lindera reflexa* Hemsl. Fitoterapia 105:222
36. Yang XL, Huang L, Li HY, Yang DF, Li ZZ (2015) Two compounds from the plant endophytic fungus *Pestalotiopsis versicolor*. J Asian Nat Prod Res 17:333
37. Wang Y, Liang H, Zhang Q, Cheng W, Sirong Y (2014) Phytochemical and chemotaxonomic study on *Ficus tsiangii* Merr. ex Corner. Biochem Syst Ecol 57:210
38. Chang C-I, Hu W-C, Shen C-P, Hsu B-D, Lin W-Y, Sung P-J, Wang W-H, J-B W, Kuo Y-H (2014) 8-Alkylcoumarins from the fruits of *Cnidium monierri* protect against hydrogen peroxide induced oxidative stress damage. Int J Mol Sci 15:4608
39. Zhao D-D, Zhao Q-S, Liu L, Chen Z-Q, Zeng W-M, Lei H, Zhang Y-L (2014) Compounds from *Dryopteris fragrans* (L.) Schott with cytotoxic activity. Molecules 19:3345
40. Sruyatep T, Chakthong S, Leejae S, Voravuthikunchai SP (2014) Two lignans, one alkaloid, and flavone from the twigs of *Feroniella lucida*. Tetrahedron 70:1773
41. Tran TVA, Malainer IC, Schwaiger S, Atanasov AG, Heiss EH, Dirsch VM, Stuppner H (2014) NF-κB inhibitors from *Eurycoma longifolia*. J Nat Prod 77:483
42. Suthiwong J, Sriphana U, Thongsri Y, Promswan P, Prariyachatigul C, Yenjai C (2014) Coumarinoids from the fruits of *Micromelum falcatum*. Fitoterapia 94:134
43. Lin T-T, Huang Y-Y, Tang G-H, Cheng Z-B, Liu X, Luo H-B, Yin S (2014) Prenylated coumarins: natural phosphodiesterase-5 inhibitors from *Toddalia asiatica*. J Nat Prod 77:955
44. You X-X, Yang K, Wang C-F, Zhang W-J, Wang Y, Han J, Fan L, Du S-S, Geng Z-F, Deng Z-W (2014) Cytotoxic compounds isolated from *Murraya tetramera* Huang. Molecules 19:13225
45. Shi J, Li C-J, Yang J-Z, Ma J, Wang C, Tang J, Li Y, Chen H, Zhang D-M (2014) Hepatoprotective coumarins and secoiridoids from *Hydrangea paniculata*. Fitoterapia 96:138

46. Li W, Zhou W, Shim SH, Kim YH (2014) Chemical constituents of *Zanthoxylum schinifolium* (Rutaceae). Biochem Syst Ecol 55:60
47. Rivere C, Krisa S, Pechamat L, Nassra M, Delaunay J-C, Marchal A, Badoc A, Waffo-Teguo P, Merillon J-M (2014) Polyphenols from the stems of *Morus alba* and their inhibitory activity against nitric oxide production by lipolysaccharide activated microglia. Phytochemistry 97:253
48. Mamoon-ur-Rashid, Ali S, Alamzeb M, Igoli J, Clements C, Shah SQ, Ferro VA, Gray AI, Khan MR (2014) Phytochemical and antitrypanosomal investigation of the compounds isolated from *Artemisia elegantissima*. Pharm Biol 52:983
49. Zeng YT, Jiang JM, Lao HY, Guo JW, Lun YN, Yang M (2015) Antitumor and apoptotic activities of the chemical constituents from the ethyl acetate extract of *Artemisia indica*. Mol Med Rep 11:2234
50. Erwin NA, Soekamto NH, Altena IV, Syah YM (2014) Waltherione C and cleomiscosin from *Melochia umbellata* var. *degrabrata* K. (Malvaceae), biosynthetic and chemotaxonomic significance. Biochem Syst Ecol 55:358
51. Yim S-H, Jung D-W, Williams DR, Geckeler KE, Kim KK, Shin BA, Lee I-S, Kim HJ (2015) Antiproliferative effects of β-cyclodextrin inclusion complexes with coumarinolignans from *Acer mono*. Korean J Pharmacog 46:133
52. Yu M, Sun A, Zhang Y, Liu R (2014) Purification of coumarins from Cortex Fraxinus by adsorption chromatography. J Chromatogr Sci 52:1033
53. Jeong SY, Nguyen PH, Zhao BT, Min BS, Ma ES, Woo MH (2015) Bioactive constituents from the leaves of *Zanthoxylum schinifolium*. Nat Prod Sci 21:1
54. Razavi SM, Janani M (2015) A new ester coumarin from *Ferula persica* Wild. indigenous to Iran. Nat Prod Res 29:717
55. Perez-Vasquez A, Castillejos-Ramirez E, Cristian S, Mata R (2014) Develoment of a UHPLC-PDA method for the simultaneous quantification of 4-phenylcoumarins and chlorogenic acid in *Exostema caribaeum* stem bark. J Nat Prod 77:516
56. Dang BT, Rouger C, Litaudon M, Richomme P, Seraphim D, Derbre S (2015) Identification of minor benzoylated 4-phenylcoumarins from a *Mammea neurophylla* bark extract. Molecules 20:17735
57. Liu W, Wu J, Wang SJ, Kong WS, Qin YH, Yang GY, Chen YK (2014) A new coumarin from roots and stems of flue-cured tobacco and its anti-tobacco mosaic virus activity. Asian J Chem 26:2820
58. Tanemossu SAF, Franke K, Arnold N, Schmidt J, Wabo HK, Tane P, Wessjohann LA (2014) Rare biscoumarin derivatives and flavonoids from *Hypericum riparium*. Phytochemistry 105:171
59. He J-W, Qin D-P, Gao H, Kuang R-Q, Yu Y, Liu X-Z, Yao X-S (2014) Two new coumarins from *Talaromyces flavus*. Molecules 19:20880
60. Khan S, Fatima I, Kazmi MH, Malik A, Afza N, Iqbal L, Latif M (2015) Cashmins A and B, potent antioxidant coumarins from *Sorbus cashmiriana*. Chem Nat Compd 51:626
61. Lei L, Xue Y-B, Liu Z, Peng S-S, He Y, Zhang Y, Fang R, Wang J-P, Luo Z-W, Yao G-M, Zhang J-W, Zhang G, Song H-P, Zhang Y-H (2015) Coumarin derivatives from *Ainsliaea fragrans* and their anticoagulant activity. Sci Rep 5:13544
62. Faeilla L, Piaz FD, Bader A, Bracca A (2014) Diterpenes and phenolic compounds from *Sideritis pullulans*. Phytochemistry 106:164
63. Li X-B, Li L, Zhu R-X, Chang W-Q, Zhang L-L, Wang X-N, Zhao Z-T, Lou H-X (2015) Tetramic acids and pyridone alkaloids from the endolichenic fungus *Tolypocladium cylindrosporum*. J Nat Prod 78:2155
64. Sribuhom T, Sriphana U, Thongsri Y, Yenjao C (2015) Chemical constituents from the stems of *Alyxia schlechteri*. Phytochem Lett 11:80
65. Lei C, Xu W, Wu J, Wang S, Sun J-Q, Chen Z, Yang G (2015) Coumarins from the roots and stems of *Nicotiana tabacum* and their anti-tobacco mosaic virus activity. Chem Nat Compd 51:43

66. Lopes EV, Dias HB, Torres ZES, Chaves FCM, Siani AC, Pohlit AM (2015) Coumarins, triterpenes and a hemiterpene from *Bonamia ferruginea* (Choisy) Hallier f. Biochem Syst Ecol 61:67
67. Yang XL, Huang L, Li HY, Yang DF, Li ZZ (2015) Two compounds from the plant endophytic fungus *Pestalotiopsis versicolor*. J Asian Nat Prod Res 17:333
68. EA Y, Kim G-S, Jeong SW, Park S, Lee SJ, Kim JH, Lee WS, Bark K-M, Jin JS, Shin SC (2014) Flavonoid profile and biological activity of Korean citrus varieties (II): Pyunkuul (*Citrus tangerina* Hort. ex Tanaka) and overall contribution of its flavonoids to antioxidant effect. J Funct Foods 6:637
69. Shokoohinia Y, Sajjadi SE, Gholamzade S, Fattahi A, Behbahani M (2014) Antiviral and cytotoxic evaluation of coumarins from *Prangos ferulacea*. Pharm Biol 52:1543
70. Fujimaki T, Saiki S, Tashiro E, Yamada D, Kitagawa M, Hattori N, Imoto M (2014) Identification of licopyranocoumarin and glycyruril from herbal medicies as neuroprotective compounds for Parkinsons's disease. PLoS One 9:e100395
71. Daud S-B, Ee GCL, Malek EA, Teh SS, See I (2014) A new coumarin from *Calophyllum hosei*. Nat Prod Res 28:1534
72. Popova M, Stoyanova A, Valyovska-Popova N, Bankova V, Peev D (2014) A new coumarin and total phenolic and flavonoids content of Bulgarian celeriac. Bulg Chem Commun 46:88
73. Negi N, Abou-Dough AM, Kurosawa M, Kitaji Y, Saito K, Ochi A, Ushijima K, Kusakabe E, Kitaguchi Y, JGJ Y (2015) Coumarins from *Murraya exotica* collected in Egypt. Nat Prod Commun 10:617
74. Adianti M, Aoki C, Komoto M, Deng L, Shoji I, Wahyuni TS, Lusida MI, Soetjipto A, Fuchino H, Kawahara N (2014) Anti-hepatitis C virus compounds obtained from *Glycyrrhiza uralensis* and other *Glycyrrhiza* species. Microbiol Immunol 58:180
75. Shi L-S, Kuo S-C, Sun H-D, Morris-Natschke SL, Lee K-H, Wu R-S (2014) Cytotoxic cardiac glycosides and coumarins from *Antiaris toxicaria*. Bioorg Med Chem 22:1889
76. Cuong NM, Khanh PN, Duc HV, Huong TT, Tai BH, Binh NQ, Durante M, Fusi F (2014) Vasorelaxing activity of two coumarins from *Murraya paniculata* leaves. Biol Pharm Bull 37:694
77. Watanabe A, Kumagai M, Mishima T, Ito J, Otoki Y, Harada T, Kato T, Yoshida M, Suzuki M, Yoshida I, Fujita K, Watai M, Nakagawa K, Miyazawa T (2015) Toddaculin, isolated from *Toddalia asiatica* (L.) Lam., inhibited osteoclastogenesis in RAW 264 cells and enhanced osteoblastogenesis in MC3T3-E1 cells. PLoS One 10:e127158
78. Lee T-H, Chen Y-C, Hwang T-L, Shu C-W, Sung P-J, Lim Y-P, Kuo W-L, Chen J-J (2014) New coumarins and anti-inflammatory constituents from the fruits of *Cnidium monnieri*. Int J Mol Sci 15:9566
79. Shen DY, Chan YY, Hwang TL, Juang SH, Huang SC, Kuo PC, Thang TD, Lee EJ, Damu AG, Wu TS (2014) Constituents of the roots of *Clausena lansium* and their potential anti-inflammatory activity. J Nat Prod 77:1215
80. Auranwiwat C, Laphookhieo S, Trisuwan K, Pyne SG, Ritthiwigrom T (2014) Carbazole alkaloids and coumarins from the roots of *Clausena guillauminii*. Phytochem Lett 8:113
81. Kouloura E, Danika E, Kim S, Hoerle M, Cuendet M, Halabalaki M, Skaltsounis LA (2014) Rapid identification of coumarins from *Micromelum falcatum* by UPLC-HRMS/MS and targeted isolation of three new derivatives. Molecules 19:15042
82. Watanabe A, Kato T, Ito Y, Yoshida I, Harada T, Mishima T, Fujita K, Watai M, Nakagawa K, Miyazawa T (2014) Aculeatin, a coumarin derived from *Toddalia asiatica* (L.) Lam., enhances differentiation and lipolysis of 3T3-L1 adipocytes. Biochem Biophys Res Commun 452:787
83. Rammohan A, Munikishore R, Gunasekar D, Deville A, Bodo B (2015) A new di-*C*-prenylated coumarin from *Sophora interrupta*. Nat Prod Res 29:82
84. Magadula JJ, Masimba PJ, Tarimo RB, Msengwa Z, Mbwambo ZH, Heydenreich M, Breard D, Richomme P (2014) Mammaea-type coumarins from *Mammaea usambarensis* Verdc. Biochem Syst Ecol 56:65

85. Dang BT, Guitton Y, Freuze I, Grovel O, Litaudon M, Derbre S, Seraphin D, Derbre S (2015) Dereplication of *Mammea neurophylla* metabolites to isolate original 4-phenylcoumarins. Phytochem Lett 11:61
86. Deng H-D, Mei W-L, Guo Z-K, Liu S, Zuo W-J, Dong W-H, Li S-P, Dai H-F (2014) Monoterpenyl coumarins from the peels of *Clausena lansium*. Planta Med 80:955
87. Rocha MRE, de Souza JJ, Barcellos LT, Sant'Anna CMR, Braz-Filho R, Vieira IJC (2014) A novel 3,9-(1,2,3-trioxocine)-type steroid of *Rauia nodosa* (Rutaceae). Molecules 19:14637
88. Adhami H-R, Fitz V, Lubich A, Kaehlig H, Zehl M, Krenn L (2014) Acetylcholinesterase inhibitors from galbanum, the oleogum resin of *Ferula gummosa* Boiss. Phytochem Lett 10: lxxxii
89. Nhiem NX, Yen HT, Kiem PV, Minh CV, Tai BH, Anh HLT, Park S, Kim N, Kim SH (2015) $^{1}H$ and $^{13}C$ NMR assignments of tricanguinas A and B, coumarin monoterpenes from *Trichosanthes anguina* L. Magn Reson Chem 53:178
90. Lee SE, Lee EK, Chun CS, Lee K-H, Jun M-Y, Sook H (2014) *Psoralea corylifolia* L. seed extract ameliorates streptozotocin-induced diabetes in mice by inhibition of oxidative stress. Oxid Med Cell Longev 2014:897296
91. Walasek M, Grzegorczyk A, Malm A, Skalicka-Wozniak K (2015) Bioactivity-guided isolation of antimicrobial coumarins from *Heracleum mantegazzianum* Sommier & Levier (Apiaceae) fruits by high-performance counter-current chromatography. Food Chem 186:133
92. Gao Y, Liu Y, Wang ZG, Zhang HL (2014) Chemical constituents of *Heracleum dissectum* and their cytotoxic activity. Phytochem Lett 10:276
93. Skalicka-Wozniak K, Zagaia M, Glowniak K, Liszczki JJ (2014) Purification and anticonvulsant activity of xanthotoxin (8-methoxypsoralen). Cent Eur J Biol 9:43
94. He F, Wang M, Gao M, Zhao M, Bai Y, Zhao C (2014) Chemical composition and biological activities of *Gerbera anandria*. Molecules 19:4046
95. Song P-P, Ly Y, Xu Z-L, Wang Q, Wang N-H (2014) Chemical constituents of *Angelica nitida* roots. J Chin Med Mat 37:55
96. Liu H, Li F, Li C-J, Yang J-Z, Li L, Chen N-H, Zhang D-M (2014) Bioactive furanocoumarins from stems of *Clausena lansium*. Phytochemistry 107:141
97. Deng G-G, Wei W, Yang X-W, Zhang Y-B, Xu W, Gong N-B, Lu Y, Wang F-F (2015) New coumarins from the roots of *Angelica dahurica var. formosana* cv. Chianbaixhi and their inhibition on NO production in LPS-activated RAW 264.7 cells. Fitoterapia 101:194
98. Garcia-Beltran O, Areche C, Cassels BK, Suarez LEC (2014) Coumarins isolated from *Esenbeckia alata* (Rutaceae). Biochem Syst Ecol 52:38
99. Wanchuk P, Pyne SG, Keller PA, Taweechotipatr M, Kamchonwongpaisam S (2014) Phenylpropanoids and furanocoumarins as antibacterial and antimalarial constituents of the Bhutanese medicinal plant *Pleurospermum amabile*. Nat Prod Commun 9:957
100. Znati M, Ben Jannet H, Cazaux S, Souchard JP, Skhiri FH, Bouajila J (2014) Antioxidant, 5-lipoxygenase inhibitory and cytotoxic activities of compounds isolated from the *Ferula lutea* flowers. Molecules 19:16959
101. Razavi SM, Ravansalar A, Mirinejad S (2015) The investigation on phytochemicals from *Ferulago angulata* (Schlecht) Boiss. indigenous to central parts of Iran. Nat Prod Res 29:2037
102. Jiang HY, Zhang WJ, You CX, Yang K, Fan L, Feng JB, Chen J, Yang YJ, Wang CF, Deng ZW, Yin H-B, Du S-S (2014) Two new cytotoxic constituents from *Clausena lansium* (Lour.) Skeels. Phytochem Lett 9:92
103. Xu XY, Xie HH, Wei XY (2014) Jasmonoid glucosides, sesquiterpenes and coumarins from the fruit of *Clausena lansium*. LWT-Food Sci Technol 59:65
104. Severino VGP, de Freitas SDL, Braga PAC, Forim MR, da Silva MFGF, Fernandes JB, Vieira PC, Venacio T (2014) New limonoids from *Hortia oreadica* and unexpected coumarin from *H. superba* using chromatography over cleaning Sephadex with sodium hypochlorite. Molecules 19:1203

105. Severino VGP, Monteiro AF, da Silva MFDF, Luxarini R, Martins CHG (2015) Chemical study of *Hortia superba* (Rutaceae) and investigation of the antimyxobacterial activity of crude extracts and constituents isolated from *Hortia* species. Quim Nova 38:42
106. Hu F, Wang LF, Zhou XM, Luo K, Bai LY (2015) Two coumarins with safer activity from Rhizoma et Radix Notopterygii. Weed Technol 29:161
107. Pavlovic I, Krunic A, Nikolic D, Radenkovic M, Brankovic S, Niketic M, Petrovic S (2014) Chloroform extract of underground parts of *Ferula heuffelii*: secondary metabolites and spasmolytic activity. Chem Biodiversity 11:1417
108. Kim AH, Lee JI, Kong C-S, Choe JC, Oh K-S, Seo Y (2014) Antioxidant activity of dihydrofuranocoumarins from *Corydalis heterocarpa*. Biotechnol Bioprocess Eng 19:771
109. Wahyuni TS, Widyawaruyanti A, Lusida MI, Fuad A, Soetjipto, Fuchino H, Kawahara N, Hayashi Y, Aoki C, Hotta H (2014) Inhibition of hepatitis C virus replication by chalepin and pseudane IX isolated from *Ruta angustifolia* leaves. Fitoterapia 99:276
110. Guo T, Tang XF, Zhang JB, Wei JQ, Wang Y, Li YH, Zhang Z (2014) Chemical constituents from the root and stem of *Zanthoxylum avicennae*. In: Materials, machines and development of technologies for industrial production, Vol 618. Trans Tech Zurich, p 428
111. Ramasamy D, Saraswathy A (2014) Vitiquinolone – a quinolone alkaloid from *Hibiscus vitifolius* Linn. Food Chem 145:970
112. Bin Zakaria M, Vijayasekaran A, Ilham Z, Muhammad NA (2014) Anti-inflammatory activity of *Calophyllum inophyllum* fruit extracts. Procedia Chem 13:218
113. Bai G, Xu J, Cao XL, Pei HR (2014) Preparative separation of luvangetin from *Zanthoxylum ailanthoides* Sieb. & Zucc. by centrifugal partition chromatography. J Liq Chromatogr Relat Technol 37:1819
114. Song YL, Jing WH, Chen YG, Yuan YF, Yan R, Wang YT (2014) H-1 nuclear magnetic resonance based-metabolomic characterisation of Peucedani Radix and simultaneous determination of praeruptorin A and praeruptorin B. J Pharm Biomed Anal 93:86
115. Nugara RN, Inafuku M, Takara K, Iwasaki H, Oku H (2014) Pteryxin: a coumarin in *Peucedanum japonicum* Thunb. leaves exerts antiobesity activity through modulation of adipogenic gene network. Nutrition 30:1177
116. Lee JW, Lee C, Jin Q, Yeon TE, Lee D, Kim S-Y, Han SB, Hong JT, Lee MK, Hwang BY (2014) Pyranocoumarins from *Glenhia littoralis* inhibit the LPS-induced NO production in macrophage RAW 264.7 cells. Bioorg Med Chem Lett 24:2717
117. Ghannadi A, Fattahian K, Shokoohinia Y, Behbahani M, Shahnoush A (2014) Anti-viral evaluation of sesquiterpene coumarins from *Ferula assa-foetida* against HSV-1. Iran J Pharm Res 13:523
118. Iranshahi M, Barthomeuf C, Bayet-Robert M, Chollet P, Davoodi D, Piacente S, Rezaee R, Aahebkar A (2014) Drimane-type sesquiterpene coumarins from *Ferula gummosa* fruits enhance doxorubicin uptake in doxorubicin-resistant human breast cancer cell line. J Tradit Complement Med 4:118
119. Li G, Li X, Li C, Zhang L, Shen L, Zhu J, Wang J, Si J (2015) Sesquiterpene coumarins from seeds of *Ferula sinkiangensis*. Fitoterapia 103:222
120. Dastan D, Salehi P, Ghanati F, Gohari AR (2014) Phytotoxicity and cytotoxicity of disesquiterpene and sesquiterpene coumarins from *Ferula pseudalliacea*. Ind Crops Prod 55:43
121. Dastan D, Salehi P, Gohari AR, Ebrahami SN, Aliahmadi A, Hamburger M (2014) Bioactive sesquiterpene coumarins from *Ferula pseudalliacea*. Planta Med 80:1118
122. Ghanem H, Haba H, Marcourt L, Benkhaled M, Wolfender JL (2014) Microphynolides A and B, new spiro-γ-lactone glycosides from *Thymelaea microphylla*. Nat Prod Res 28:1732
123. Kerbab K, Mekhelfi T, Zaiter L, Benayache S, Benayache F, Picerno P, Mencherini T, Sansone F, Aquino RP, Rastrelli L (2015) Chemical composition and antioxidant activity of a polar extract of *Thymelaea microphylla* Coss. et Dur. Nat Prod Res 29:671
124. Li Q, Gao W, Cao J, Bi X, Chen C, Zhang X, Xia X, Zhao Y (2014) New cytotoxic compounds from flowers of *Lawsonia inermis* L. Fitoterapia 94:148

125. Yang WQ, Song YL, Zhu ZX, Su C, Zhang X, Wang J, Shi SP, Tu PF (2015) Anti-inflammatory dimeric furanocoumarins from the roots of *Angelica dahurica*. Fitoterapia 105:187
126. Yang JH, Liu WY, Li SC, Ye HY, Tang H, Chen LJ, Peng AH (2014) Coumarinolignans isolated from the seeds of *Brucea javanica*. Helv Chim Acta 97:278
127. Donfack ARN, Tala MF, Wabo HK, Jerz G, Zeng GZ, Winterhalter P, Tan NH, Tane P (2014) Two new anthraquinone dimers from the stem bark of *Pentas schimperi* (Rubiaceae). Phytochem Lett 8:55
128. Su W, Zhao JP, Yang M, Yan HW, Pang T, Chen SH, Huang HY, Zhang SH, Ma XC, Guo DA (2015) A coumarin lignanoid from the stems of *Kadsura heteroclita*. Bioorg Med Chem Lett 25:1506
129. Xu B, Liu S, Fan X-D, Deng L-Q, Ma W-H, Chen M (2015) Two new coumarin glycosides from *Herpetospermum caudigerum*. J Asian Nat Prod Res 17:738
130. Xu W-H, Shen Y-H, Liang Q, Zhao P (2015) New coumarin derivative from *Euphorbia wallichii*. Nat Prod Res 29:1860
131. Liu B-Y, Zhang C, Zeng K-W, Li J, Guo X-Y, Zhao M-B, Tu P-F, Jiang Y (2015) Exotines A and B, two heterodimers of isopentenyl-substituted indole and coumarin derivatives from *Murraya exotica*. Org Lett 17:4380

**Satyajit Dey Sarker** is Professor of Pharmacy and the Director of the School of Pharmacy and Biomolecular Sciences, Liverpool John Moores University, Liverpool, UK. He received his B.Pharm. (Hons.) and M.Pharm. degrees from Dhaka University, Bangladesh, and a Ph.D. degree in Phytochemistry from the University of Strathclyde, Glasgow, Scotland, UK. Prior to assuming his current position, he worked as Professor of Pharmacy, Deputy Head of the School of Pharmacy, and Pharmacy Research Group Leader at the University of Wolverhampton, during the period 2008–2013. Earlier, he also held various academic and research positions including Reader in Pharmacy (University of Ulster), Lecturer in Pharmaceutical Sciences (The Robert Gordon University), Senior Natural Products Scientist and Head of the Spectroscopy Group (the Institute of Grassland and Environmental Research), BBSRC Postdoctoral Fellow (Exeter University), and Lecturer in Pharmacy and Research Fellow in Pharmacy (Dhaka University). Professor Sarker has served as a Visiting Professor at the University of Technology Malaysia, Stamford University, Tripoli University, North-South University, and the University of Dammam. He is an international advisor to the State University of Bangladesh. His research focuses on purified compounds from higher plants with potential analgesic, anticancer, anti-inflammatory, antimalarial, antimicrobial, antioxidant, cancer chemopreventive, and wound-healing properties, as well as bioactive novel synthetic organic compounds.

Professor Sarker is the Editor-in-Chief of "Phytochemical Analysis" and serves on the editorial advisory board of several other journals, and regularly reviews articles for more than 70 journals. He co-authored the popular textbook, "Chemistry for Pharmacy Students: General, Organic, and Natural Products Chemistry", published by John Wiley and Sons in 2007 (subsequently, this book was translated into the Japanese, Greek and Portuguese languages), and a book on steroid dimers (2012), also published by John Wiley and Sons. In addition, he co-edited both the second and the third editions of the book, "Natural Products Isolation", published by Humana Press/Springer-Verlag, in 2005 and 2012. He has co-authored a total of 22 book chapters to date, in addition to about 400 other publications. Prof. Sarker has been a member of the Phytochemical Society of Europe since 1991, and served as the Treasurer of this society during 2008–2013, and has been Vice-President since June 2016. His scientific profile has been published in "Marquis Who's Who in the World" since 2010.

**Lutfun Nahar** is a synthesis-oriented Organic Medicinal Chemist. She received her B.Sc. (Hons.) in Chemistry from Exeter University, England, UK and a Ph.D. in Synthetic Organic Medicinal Chemistry from Aberdeen University, Scotland, UK. Currently, she has been working as a medicinal chemist in the Faculty of Science, Liverpool John Moores University. Prior to this current position, she worked as a Senior Lecturer in Pharmaceutical and Medicinal Chemistry, and coordinated the Drug Discovery and Design Research Division within the Pharmacy Research Group at the University of Wolverhampton (2008–2011).

Dr. Nahar is the Managing Editor of "Phytochemical Analysis", and is on the editorial advisory board of several other journals, and regularly reviews articles for more than 20 journals. She co-authored the popular textbook, "Chemistry for Pharmacy Students: General, Organic, and Natural Products Chemistry", published by John Wiley and Sons in 2007, and translated into Portuguese (2009), Japanese (2012) and Greek (2015). Currently, she has been working on the second edition of this textbook. Dr. Najar also co-edited the 3rd edition of the book, "Natural Products Isolation", published by Humana Press/Springer-Verlag in 2012, and

co-authored the book, “Steroid Dimers: Chemistry and Applications in Drug Design and Delivery”, published by John Wiley and Sons in 2012. She has co-authored a total of 15 book chapters to date, along with approximately 200 other publications. Her scientific profile has been published in “Marquis Who’s Who in the World” since 2009 and “Who’s Who in Science and Engineering” since 2010.